ISSN 0021-9673

VOL. 474 NO. 1 JULY 14, 1989

5th Symp. on LC–MS, SFC–MS and MS–MS
Freiburg i.Br., November 2–4, 1988

JOURNAL OF CHROMATOGRAPHY

INTERNATIONAL JOURNAL ON CHROMATOGRAPHY, ELECTROPHORESIS AND RELATED METHODS

ELSEVIER

JOURNAL OF CHROMATOGRAPHY

Scope. The *Journal of Chromatography* publishes papers on all aspects of chromatography, electrophoresis and related methods. Contributions consist mainly of research papers dealing with chromatographic theory, instrumental development and their applications. The section *Biomedical Applications*, which is under separate editorship, deals with the following aspects: developments in and applications of chromatographic and electrophoretic techniques related to clinical diagnosis or alterations during medical treatment; screening and profiling of body fluids or tissues with special reference to metabolic disorders; results from basic medical research with direct consequences in clinical practice; drug level monitoring and pharmacokinetic studies; clinical toxicology; analytical studies in occupational medicine.

Submission of Papers. Papers in English, French and German may be submitted, in three copies. Manuscripts should be submitted to: The Editor of *Journal of Chromatography*, P.O. Box 681, 1000 AR Amsterdam, The Netherlands, or to: The Editor of *Journal of Chromatography, Biomedical Applications*, P.O. Box 681, 1000 AR Amsterdam, The Netherlands. Review articles are invited or proposed by letter to the Editors. An outline of the proposed review should first be forwarded to the Editors for preliminary discussion prior to preparation. Submission of an article is understood to imply that the article is original and unpublished and is not being considered for publication elsewhere. For copyright regulations, see below.

Subscription Orders. Subscription orders should be sent to: Elsevier Science Publishers B.V., P.O. Box 211, 1000 AE Amsterdam, The Netherlands, Tel. 5803 911, Telex 18582 ESPA NL. The *Journal of Chromatography* and the *Biomedical Applications* section can be subscribed to separately.

Publication. The *Journal of Chromatography* (incl. *Biomedical Applications*) has 37 volumes in 1989. The subscription prices for 1989 are:

J. Chromatogr. + *Biomed. Appl.* (Vols. 461–497):
Dfl. 6475.00 plus Dfl. 999.00 (p.p.h.) (total *ca.* US$ 3737.00)

J. Chromatogr. only (Vols. 461–486):
Dfl. 5200.00 plus Dfl. 702.00 (p.p.h.) (total *ca.* US$ 2951.00)

Biomed. Appl. only (Vols. 487–497):
Dfl. 2200.00 plus Dfl. 297.00 (p.p.h.) (total *ca.* US$ 1248.50).

Our p.p.h. (postage, package and handling) charge includes surface delivery of all issues, except to subscribers in Argentina, Australia, Brasil, Canada, China, Hong Kong, India, Israel, Malaysia, Mexico, New Zealand, Pakistan, Singapore, South Africa, South Korea, Taiwan, Thailand and the U.S.A. who receive all issues by air delivery (S.A.L. — Surface Air Lifted) at no extra cost. For Japan, air delivery requires 50% additional charge; for all other countries airmail and S.A.L. charges are available upon request. Back volumes of the *Journal of Chromatography* (Vols. 1–460)are available at Dfl. 195.00 (plus postage). Claims for missing issues will be honoured, free of charge, within three months after publication of the issue. Customers in the U.S.A. and Canada wishing information on this and other Elsevier journals, please contact Journal Information Center, Elsevier Science Publishing Co. Inc., 655 Avenue of the Americas, New York, NY 10010. Tel. (212) 633-3750.

Abstracts/Contents Lists published in Analytical Abstracts, ASCA, Biochemical Abstracts, Biological Abstracts, Chemical Abstracts, Chemical Titles, Chromatography Abstracts, Current Contents/Physical, Chemical & Earth Sciences, Current Contents/Life Sciences, Deep-Sea Research/Part B: Oceanographic Literature Review, Excerpta Medica, Index Medicus, Mass Spectrometry Bulletin, PASCAL-CNRS, Referativnyi Zhurnal and Science Citation Index.

See inside back cover for Publication Schedule, Information for Authors and information on Advertisements.

0021-9673/89/$03.50

This issue is printed on acid-free paper.

Printed in The Netherlands

For contents see p. VII

JOURNAL OF CHROMATOGRAPHY

VOL. 474 (1989)

JOURNAL
of
CHROMATOGRAPHY

INTERNATIONAL JOURNAL ON CHROMATOGRAPHY,
ELECTROPHORESIS AND RELATED METHODS

ELSEVIER
AMSTERDAM — OXFORD — NEW YORK — TOKYO

J. Chromatogr., Vol. 474 (1989)

0021-9673/89/$03.50

SPECIAL ISSUE

FIFTH (MONTREUX) SYMPOSIUM ON LIQUID CHROMATOGRAPHY–MASS SPECTROMETRY, SUPERCRITICAL FLUID CHROMATOGRAPHY–MASS SPECTROMETRY AND TANDEM MASS SPECTROMETRY

Freiburg i.Br. (F.R.G.), November 2–4, 1988

Guest Editors

R. W. FREI†
(Amsterdam)

J. VAN DER GREEF
(Leiden and Zeist)

CONTENTS

5TH SYMPOSIUM ON LIQUID CHROMATOGRAPHY–MASS SPECTROMETRY, SUPERCRITICAL FLUID CHROMATOGRAPHY–MASS SPECTROMETRY AND TANDEM MASS SPECTROMETRY, FREIBURG I. BR., NOVEMBER 2–4, 1989

In articles with more than one author, the name of the author to whom correspondence should be addressed is indicated in the article heading by a 6-pointed asterisk (*)

Journal of Chromatography, 474 (1989) 1–2
Elsevier Science Publishers B.V., Amsterdam — Printed in The Netherlands

ROLAND W. FREI (1937–1989)

On January 29, 1989, Professor Roland W. Frei died in a hospital in his hometown Allschwil near Basle (Switzerland), after a courageous fight of several months against his fatal illness. A few days later he was laid to rest in the presence of his family and relatives, and many of his friends.

Roland Frei started his career by obtaining a degree in chemistry from a Swiss technical college. He then worked as a chemical engineer with Union Carbide in Geneva, before enrolling at the University of Hawaii as a Ph.D. candidate, where he got his degree in analytical chemistry in 1964. He worked as an instructor of physical science and chemistry in Tokyo and on the island of Samoa and, in July 1966, was appointed as Assistant (later: Associate) Professor of Analytical Chemistry at Dalhousie University (Halifax, Canada). In this early part of his scientific career, much of his research activity was directed to the study of reflectance spectroscopy and its use for the determination of both metal ions and organic compounds in thin-layer chromatography (TLC). In 1970 Roland Frei was appointed Editor-in-Chief of the *International Journal of Environmental Analytical Chemistry* and, together with a number of co-workers, he started to publish papers on the fluorigenic labelling of analytes for improved detection performance in TLC.

Two rather dramatic changes occurred in 1972. Roland Frei left Canada for Europe to become head of the Department of Analytical Research at Sandoz (Basle), and he published his first papers on high-performance liquid chromatography (HPLC). In his Swiss period, papers on TLC and HPLC, fluorigenic labelling and derivatization —techniques which were applied to both environmental pollutants and pharmaceutical preparations— illustrated his many-sided interest in analytical chemistry and, especially, in separation techniques. At this time of his life, he also became active as an organizer of symposia, chairing the Fourth Symposium on the Analytical Chemistry of Pollutants (Basle, 1974) and co-chairing the sixth one in Vienna (1976).

Having already selected HPLC as the method of separation he loved best, in 1977 Roland Frei came to The Netherlands to become Professor of Analytical Chemistry at the Free University (*Vrije Universiteit*) in Amsterdam. He rapidly felt at home in The Netherlands, especially appreciating the informal atmosphere in Amsterdam. Learning another language did not present a real problem and, almost from the start, he gave courses and seminars in Dutch. With regard to his professional career, in the decade he worked in Amsterdam he succeeded in bringing his plans to fruition. Together with his colleagues in the *vakgroep* of General and Analytical Chemistry and an increasing number of collaborators, he published a long list of scientific and review papers. Two separate topics were easily recognizable: pre-column technology and post-column reaction detection.

On-line pre-column technology for the clean-up of samples and the enrichment of trace-level analytes was developed from a crude manual technique into a sophisticated and fully automated procedure, sometimes involving the use of two or even three pre-columns in series. Post-column reaction detection nicely showed the versatility which the clever combination of instrumental analysis and wet chemistry can offer. Open-tubular, segmented-stream and (active) packed-bed reactors were studied in detail, and new tee-pieces and phase separators were designed, successfully applied and, at a later stage, miniaturized. Fluorescence monitoring always remained the

primary means of detection, but alternatives such as chemiluminescence, phosphorescence, electroanalytical or radiochemical detection were not neglected. Method development frequently led to routine applications in industrial laboratories, and many visiting scientists were attracted by the group's performance.

Roland Frei was an enthusiastic and industrious worker. He was (co)author of several hundreds of papers, edited some ten books and served on the editorial or advisory boards of many internationally known chromatographic journals. In 1987 he was appointed as one of the new Associate Editors of the *Journal of Chromatography*, with a view to becoming an Editor in May 1989. This was also, tragically, not to be. As president of the International Association of Environmental Analytical Chemistry, he laid the basis for successful symposia series such as the "Liquid Chromatography–Mass Spectrometry", "Sample Handling" and "Analytical Chemistry of Pollutants" series. Actually, it was during the nineteenth of this last series, in September 1988 in Barcelona, that he displayed his many talents and his charm for the last time at a scientific meeting.

A great traveller and a good lecturer, Roland Frei liked to see foreign countries, to attend symposia and visit industrial or university laboratories. In 1987, he was invited to lecture at the École Supérieure de Physique et de Chimie in Paris. About a year ago, he was awarded the prestigious Scheele Medal by the Swedish Academy of Pharmaceutical Sciences. During 1988, new plans were being discussed in the *vakgroep*, several post-docs arrived, and Roland Frei was as eager as ever to participate in new activities. We all know what happened then. Two major operations and a four-month struggle did not bring the ardently hoped-for recovery. On the contrary, on January 29, 1989, we all lost a gifted colleague and good friend, whose voice, face and contributions to chemistry will long be remembered by those who wrote these pages.

Amsterdam (The Netherlands) U. A. Th. BRINKMAN
N. H. VELTHORST

Journal of Chromatography, 474 (1989) 3–4
Elsevier Science Publishers B.V., Amsterdam — Printed in The Netherlands

PREFACE

The *Fifth (Montreux) International Symposium on Liquid Chromatography–Mass Spectrometry, Supercritical Fluid Chromatography–Mass Spectrometry and Tandem Mass Spectrometry* held in Freiburg, November 2–4, 1988, was once more a clear reflection of the growing interest in this topic and the enthusiasm for this symposium series. However, the illness of Roland Frei at that time cast a shadow over this meeting. The news of his decease the following January was a terrible shock to all of us who knew him personally.

Roland Frei's broad interest not only in science itself but also in the persons practising it, as well as his ability to communicate this interest, resulted in a series of successful activities. Many of them, for example the successful "Montreux" symposia, have been mentioned on the preceding pages. The ability to discover challenging new research fields combined with a skill at bringing different research fields together, prompted Roland Frei to organize the first symposium in 1981. The utmost importance of bringing mass spectrometrists and chromatographers together was stressed by him during this event and although the techniques of liquid chromatography (LC) and mass spectrometry (MS) were seemingly incompatible, optimism was sensed.

One year later, during the second symposium, despite an atmosphere of scepticism and uncertainty the discussion on the optimal way of interfacing obtained more depth. Roland Frei concluded that the dominant techniques at that time (moving belt and direct liquid introduction) were more complementary than competitive, thereby bringing the two camps closer together. The third symposium was expanded to three days in order to cope with the growing interest and it was clear that LC–MS and MS–MS would become established in the analytical field and LC–MS–MS showed considerable promise.

Roland Frei's ability to grasp the potential of new techniques was demonstrated by his statement in 1984 that not only thermospray but also electrospray could be a future alternative, which became very clear to us last year. Coupling of supercritical fluid chromatography (SFC) was the subject of a half-day session during the fourth symposium, by which time LC–MS was firmly established, and the dynamic developments in this field resulted in the incorporation of SFC–MS in the title of the fifth symposium. Chemistry, sample handling and miniaturization were incorporated into the programme in a stimulating way, which encouraged several researchers to explore these fields in LC–MS.

In the preparation of the scientific programme for the fifth symposium other new developments were evaluated and I remember Roland Frei's enthusiasm for the possibilities of coupling capillary zone electrophoresis with mass spectrometry. Unfortunately, he could not experience the exciting scientific level of this last symposium, which reflected the broad activities in both the fundamental and application fields. The important trends noted were the renaissance of electron impact [besides the moving-belt interface also the use of electron impact in monodisperse aerosol generation interface (MAGIC) and SFC–MS], the analysis of high-molecular-weight biomolecules, multidimensional approaches (coupled column chromatography–tandem mass spectrometry), coupling of capillary zone electrophoresis and isotachophoresis with MS and significant modifications and improvements to all interfaces (thermospray, direct liquid introduction, continuous-flow fast atom bombardment,

moving belt, atmospheric pressure ionization, MAGIC and electrospray/ionspray).

The rapid developments in the "hyphenated" MS research field prompted Roland Frei to extend the biannual European tradition of the symposium series by holding every alternate meeting in the U.S.A. The first one, the sixth (Montreux) Symposium on LC–MS, SFC–MS, CZE–MS and MS–MS, July 19–21, 1989 in Ithaca, will be organized by Jack Henion. It will be preceded by the traditionally successful two-days LC–MS course.

Roland Frei's outstanding vision in this field stimulated many of his friends and, especially, newcomers to the field. The scientific community has been deprived of his valuable activities but above all we will miss Roland as a good friend.

JAN VAN DER GREEF

Journal of Chromatography, 474 (1989) 5–19
Elsevier Science Publishers B.V., Amsterdam — Printed in The Netherlands

CHROM. 21 424

LIQUID CHROMATOGRAPHY–MASS SPECTROMETRY

THE NEED FOR A MULTIDIMENSIONAL APPROACH

J. VAN DER GREEF

TNO-CIVO Institutes, Section of Instrumental Analysis, P.O. Box 360, 3700 AJ Zeist (The Netherlands) and Division of Analytical Chemistry, Center for Bio-Pharmaceutical Sciences, University of Leiden, P.O. Box 9502, 2300 RA Leiden (The Netherlands)

and

W. M. A. NIESSEN* and U. R. TJADEN

Division of Analytical Chemistry, Center for Bio-Pharmaceutical Sciences, University of Leiden, P.O. Box 9502, 2300 RA Leiden (The Netherlands)

SUMMARY

Combined liquid chromatography–mass spectrometry is now used routinely in both qualitative and quantitative analysis. Therefore, it is important to consider the integration of this method in the whole analytical procedure. Attention has to be paid to other topics than interface technology. This paper deals with some of those aspects, especially with those important in target compound analysis. Strategies are outlined and discussed in the tuning of the selectivity of the method, in improving the compatibility of the liquid chromatography, the interface and mass spectrometry, in enhancing the detectability, and with respect to pre- and post-column derivatization techniques.

INTRODUCTION

The successful development of various interface methods for coupling liquid chromatography with mass spectrometry (LC–MS) has made this method an important analytical tool in many laboratories. However, if a method reaches the stage of being used in daily practice for both qualitative and quantitative analysis it becomes very important to achieve an integration within the whole analytical procedure. In particular, for trace analysis each method consists of an interplay between the four basic building blocks: sample pretreatment, separation, detection and data handling.

LC–MS research has been focused strongly on the interface technology. The input has come mainly from the MS side and not from the chromatography side, despite some excellent and stimulating reviews on the chromatographic side of LC–MS[1,2]. This situation is clearly illustrated by the LC–MS presentations in 1988 on the two major annual meetings in both areas, *i.e.* the American Society for Mass Spectrometry (ASMS)[3] and the HPLC 88 meeting[4]. Approximately 13% and 1% of

0021-9673/89/$03.50

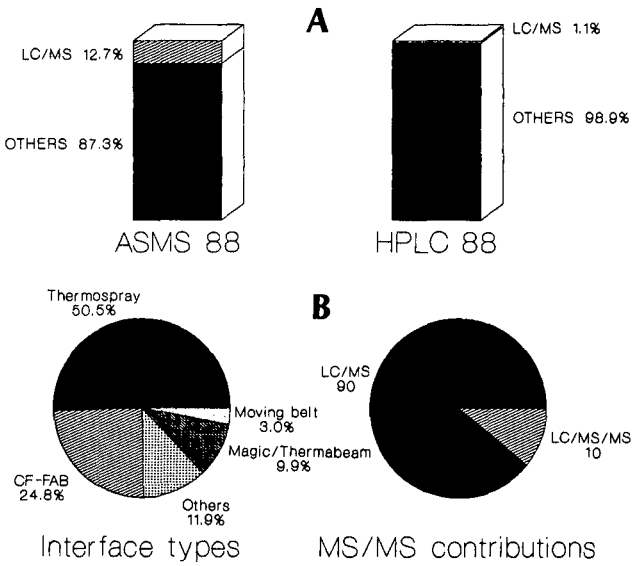

Fig. 1. Summary of presentations on LC–MS at the ASMS 88 and HPLC 88 meetings (A) and the contributions on different interfaces and MS–MS at the ASMS 88 meeting (B).

the presentations at the ASMS and HPLC 88 meetings, respectively, were on LC–MS, as shown in Fig. 1A. This somewhat unbalanced situation is an enormous challenge and, because of the impressive results of today's LC–MS, despite this indicated weakness, it also holds out promise for the near future. An increase in the availability of lower cost instrumentation will certainly be helpful for many chromatographers to overcome the threshold of applying MS detection.

The optimum conditions for coupling chromatography with mass spectrometry are strongly dependent on the type of interface used, since each interface is characterized by quite different values for parameters such as flow-rate and mobile phase composition. The most widely applied interfaces, as indicated in Fig. 1B, are thermospray (TSP), continuous-flow fast atom bombardment (CF-FAB), and particle beam approaches (MAGIC, Thermabeam); some others, such as the moving belt and direct liquid introduction (DLI) methods and the very promising electrospray and the related ionspray techniques, are also used by several groups[5]. The different characteristics can be illustrated by the preference for flow-rates of *ca.* 1.5 ml/min for TSP and of *ca.* 5–10 μl/min for CF-FAB, while the optimum mobile phase for TSP and CF-FAB is more compatible with reversed-phase chromatography than in general for the moving-belt interface.

The use of soft ionization methods in LC–MS has laid more emphasis on the generation of structural information. Tandem mass spectrometry (MS–MS) is an attractive approach, although identification is not always straightforward. The same is true for the fragmentation induced in TSP by variation of the repeller voltage or by applying a discharge electrode[6]. Electron impact (EI) remains of interest in this respect, and the moving belt and the particle beam approaches offer this attractive possibility. In the interfacing of supercritical fluid chromatography with mass

spectrometry (SFC–MS) structurally informative EI spectra can be generated by capillary SFC via direct coupling[7] or by packed-column SFC with a moving belt[8] or via charge exchange using CO_2 in the direct coupling[9]. About 10% of all LC–MS presentations at the ASMS meeting were on LC–MS–MS, with a strong accent however on the increase of selectivity in target compound analysis using selected reaction monitoring.

In this paper three important aspects of LC–MS are discussed, with emphasis on target compound analysis and special attention to the chromatographic side: the tuning of the overall selectivity, the improvement of the compatibility and the enhancement of the detectability. Furthermore, attention is paid to the importance of chemistry, such as derivatization procedures, in both pre- and post-column modes.

SELECTIVITY TUNING

One of the attractive features of the mass spectrometer as a detector is the possibility of using either the universal mode (scanning conditions) for identification purposes or the selective mode (single or multiple ion detection) for target compound analysis. Numerous examples have been presented to illustrate this, but the lack of sufficient selectivity has also been shown in complex problems or in cases of trace analysis. Fig. 2 schematically illustrates several ways to increase the selectivity, such as by applying LC–MS–MS or by using coupled column chromatography (CCC) combined with MS or MS–MS.

LC–MS–MS has been extensively demonstrated and thus will not be discussed here. However, it is important to point out that high selectivities have been demonstrated, although this does not mean that the method is guaranteed to be robust. Often severe contamination of the mass spectrometer will influence even the short-term stability of the procedure, and in those cases the overall selectivity has to be readdressed by improving the sample pretreatment and the chromatography.

Hardly any work has been published on LC–LC–MS and LC–LC–MS–MS, despite the fact that CCC has become a routine technique in many bioanalytical laboratories[10]. Edholm *et al.*[11] have investigated the effect of using CCC in LC–MS to increase the overall selectivity for the determination of terbutaline enantiomers in plasma. In this study the LC–MS results, using a β-cyclodextrin column, were

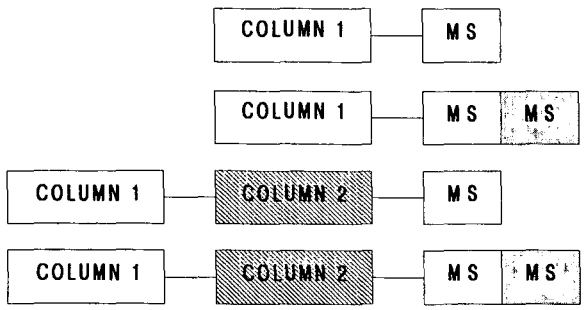

Fig. 2. Schematic diagrams showing different ways of increasing the LC–MS selectivity by applying coupled column chromatography, tandem mass spectrometry or a combination of both.

promising but the limit of determination was mainly set by a rather high background. Using a CCC system in an off-line mode, the selectivity was improved, but the main benefit appeared to be the improvement in the stability of the method.

In principle, one has to distinguish the different components in the background if the selecivity is to be improved. If the sample gives the main contribution to the background, CCC is of great help, but if the background comes predominantly from the LC system itself (*e.g.* mobile phase constituents or impurities) tandem MS is the obvious choice. An important aspect is the fact, that minimum sample loss takes place in the CCC approach, whereas in MS–MS the reduction in the signal is considerable, typically a factor of ten, but depending on the fragmentation pathway selected for monitoring. Thus, in that case the benefit is only due to the strong decrease in the noise yielding an increase in the signal-to-noise ratio[12]. In practical situations a combination of both contributions is encountered, and by removing one of them the other becomes the limiting factor so both have to be dealt with when the aim is to measure low levels. However, not only MS–MS but also high resolution MS, or a combination of the two can be attractive, especially when the analyte under investigation can be resolved at medium resolution, as is often the case with halogen-containing compounds. Effective reduction of the background has been demonstrated in measuring bromazapam and clopentixol in human plasma[13,14] and for the analysis of diuron in *post-mortem* body fluids with LC–MS using the moving-belt interface[15].

The power of CCC–MS–MS has been demonstrated by Edlund and Henion[16] for the determination of dianabol and metabolites in equine urine using an atmospheric ionization (API) source combined with either a heated pneumatic nebulizer or an ionspray interface. Comparison of LC–UV, LC–LC–UV, LC–LC–MS and LC–LC–MS–MS illustrated clearly the effects described above, while in this case the coupled column system appeared to be mandatory to obtain an effective separation of the isomers.

These results reflect the importance of carefully tuning the different building blocks of the overall system to construct a balanced procedure. A consequence of the high selectivity and the rather low contamination of the system is the possibility of increasing the speed of the method considerably, which becomes important if extensive series have to be analysed.

COMPATIBILITY IMPROVEMENT

Although the developed LC–MS interfaces have quite different characteristics they have one thing in common: the incompatibility with mobile phases containing high concentrations of non-volatile additives. On-line extraction has been developed to overcome this problem, as well as to switch from highly aqueous phases to organic phases, which are more compatible with moving-belt interfaces[17–19] and the DLI interfaces using gas nebulization[20]. For the latter also a miniaturized membrane separator has been used for microbore LC–MS[21].

A strategy has been reported based on the use of mixed-mode columns[22]. With a mixed-mode hydrophobic ion-exchange column, compounds that are normally chromatographed by ion-pair LC could be separated and detected by TSP LC–MS. A mobile phase consisting of ammonium trifluoroacetate (1 *M*, pH 2.5) and methanol (75:25) gave good results but, in order to avoid clogging, the flow-rate was limited to 0.5 ml/min.

As outlined in the previous selectivity considerations, the overall selectivity can be very high in CCC–MS–MS. Since this is not always necessary in its extreme form, we started to investigate whether in such cases CCC systems can be developed with additional features to improve the overall performance. Two factors were optimized in one setup: compatibility improvement and detectability enhancement. Simple CCC systems were studied with the configuration shown in Fig. 3. The precolumn configuration has been used extensively for trace enrichment in LC and has been shown[23] to be effective in DLI LC–MS as well, but it is of course interface-independent. The setup is also an elegant way to meet the requirements for injecting aqueous samples in SFC[24] and SFC–MS systems[25], which is important in bioanalysis. The other system, which consisted of a post-column (referred to as a trapping column) following the analytical column, also provides various attractive characteristics. The combination of various precolumns in such a system has been suggested for DLI LC–MS by McKellop *et al.*[26].

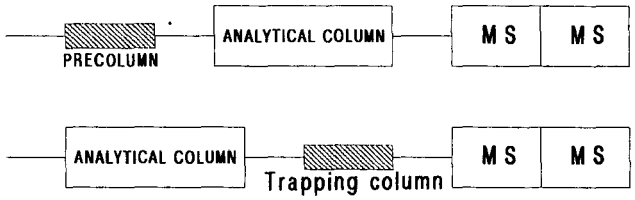

Fig. 3. Schematic diagrams of simplified coupled column systems coupled with tandem mass spectrometry.

Our approach has been to improve the compatibility for LC–MS coupling for different types of interface. The concept is based on "phase-system switching" (PSS)[27]: the experimental setup and the principle[28] are outlined in Fig. 4. After injection into the LC system, chromatography is performed without any restrictions on the mobile phase; for instance, ion-pairing reagents and/or phosphate buffers can be used. Via heart-cutting the analyte is trapped on the trapping column, which can be achieved by selection of the appropriate stationary phase or by changing the mobile phase after the analytical column. In the next step, washing and (often) drying of the trapping column is performed to remove non-volatile materials and, if necessary, the residual water from the washing step. In the last step, desorption of the analyte is effected by the optimum mobile phase for the interface used. Typical mobile phases used are 100% methanol or acetonitrile for the moving belt, 20% methanol in 50 m*M* ammonium acetate for thermospray or glycerol–acetonitrile–water (10:30:60) for CF-FAB. In this way the optimum mobile phase and flow-rate can be used for both the LC and the MS parts. The combination with MS–MS is needed because in most cases the desorbed background might interfere at lower levels. The system has been used for the analysis of mitomycin C[28] with a moving belt using a 50 m*M* phosphate buffer as mobile phase in the LC system. Furthermore, the concept can be extended for two analytes, using two trapping columns, as demonstrated for the determination of metoprolol enantiomers by TSP LC–MS[29].

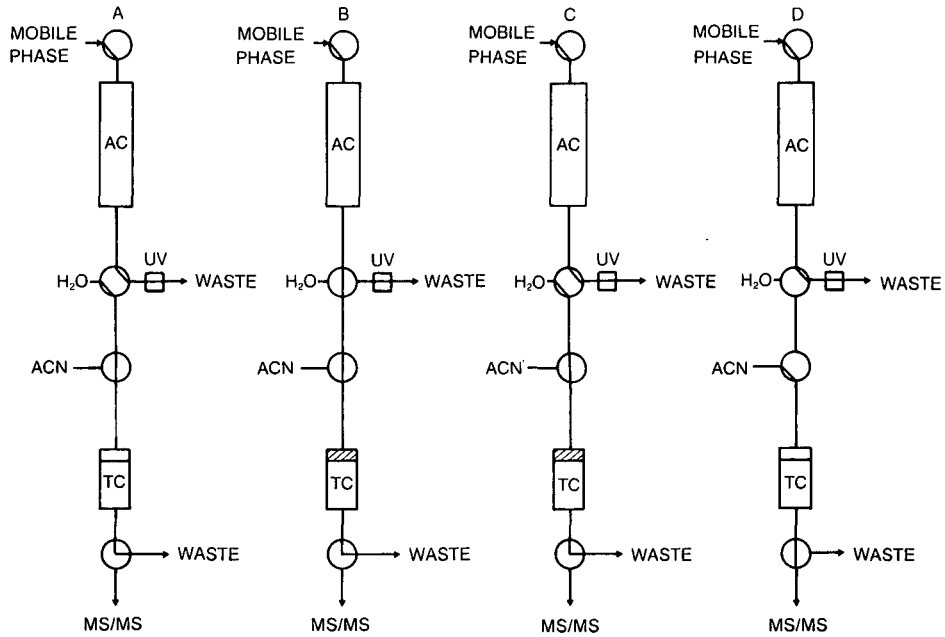

Fig. 4. Principle of the "phase-system switching" approach. After (A) injection of the sample, (B) trapping is achieved and (C) after washing (D) desorption and MS–MS analysis are performed.

DETECTIBILITY ENHANCEMENT

The PSS concept is also very attractive in improving the detection and determination limits, since an important aspect not mentioned so far is the peak compression achieved via the trapping procedure[28]. For the experimental setup in Fig. 4, an estimation of the conditions for obtaining peak compression can be made by considering that the mass spectrometer is a mass-flow-sensitive detector, which means that the signal $U(t)$ is proportional to the mass-flow, $\mathrm{d}m/\mathrm{d}t$:

$$U(t) = \tau \, \mathrm{d}m/\mathrm{d}t \tag{1}$$

where τ is a proportionality factor, usually called the transfer factor. The transfer factor is the sensitivity of the detector, as it is the slope of the line correlating the signal and the mass introduced. The mass-flow can be written as:

$$\mathrm{d}m/\mathrm{d}t = C(t)F \tag{2}$$

where $C(t)$ is the concentration of the analyte after the chromatography, and F the flow-rate of the mobile phase. The concentration at the peak maximum at the end of the column can be written as:

$$C_m = \frac{4m\sqrt{N}}{\sqrt{2\pi}\,\pi d_c^2 L\,\varepsilon\,(1 + k')} \tag{3}$$

where m is the injected amount, N the plate number, d_c the column diameter, L the column length, ε the column porosity and k' the capacity ratio.

A combination of both formulae gives a rough estimate of the attainable peak compression, defined as G:

$$G = \frac{(\mathrm{d}m/\mathrm{d}t)_{TC}}{(\mathrm{d}m/dt)_{AC}} = \frac{C_{m,TC} \cdot F_{TC}}{C_{m,AC} \cdot F_{AC}} \tag{4}$$

where F_{TC} is the desorption flow-rate through the trapping column, F_{AC} is the flow-rate through the analytical column, and $C_{m,TC}$ and $C_{m,AC}$ are the maximum concentrations of the peak at the ends of the trapping and the analytical columns, respectively. An accurate estimation of $C_{m,TC}$ is hampered by the fact that desorption from the trapping column is generally performed in the backflush mode, in contrast to what is shown in the schematic diagram in Fig. 4. However, it is clear from this last equation that the design characteristics of the trapping column are very important. A compromise between miniaturization of the trapping column and external peak-broadening have to be realized. The capacity ratio of the analyte on the trapping column, k'_{TC}, is the most important parameter. Trapping is possible if:

$$x\sigma_{v,AC} < (1 + k'_{TC})V_{0,TC} \tag{5}$$

in which, $\sigma_{v,AC}$ is the peak standard deviation of the analytical column and $V_{0,TC}$ is the void volume of the trapping column. The factor x determines the total trapping volume: in order to trap a complete chromatographic peak, x must be no less than 6. Rearrangment leads to the following formula, by which the necessary capacity ratio of the analyte on the trapping column can be estimated:

$$k'_{TC} > \frac{x d_{AC}^2 L_{AC}(1 + k'_{AC})}{d_{TC}^2 L_{TC} \sqrt{N_{AC}}} - 1 \tag{6}$$

where d_{AC} and L_{AC}, and d_{TC} and L_{TC} are the I.D. and length of the analytical column and the trapping column, respectively. Equal column porosities are assumed. Aspects with respect to the optimization of the dimensions of analytical and trapping columns, *e.g.* the use of a miniaturized trapping column in line with a conventional LC column, will be discussed in detail elsewhere.

Considerable improvements in detection limits are also possible in CF-FAB, since the flow-rate adjustment by PSS avoids splitting and combines a conventional LC system with a high loadability with an on-line miniaturization to meet the interface requirements of a 5–10 μl/min flow-rate[30]. Direct coupling of miniaturized LC systems with CF-FAB also reduces the split ratio, or even avoids the splitting, but in practical applications this does not mean an improvement in concentration detection limits since the injection volume is correspondingly decreased, as outlined in Table I. Only if the sample size is the limiting factor does miniaturization give significant improvement. Also, if a given mass is injected into miniaturized systems, the increase in the concentration of the analyte is balanced by the reduced flow-rate, as pointed out before[2].

TABLE I

SOME TYPICAL VALUES IMPORTANT IN COUPLING DIFFERENT FORMS OF HPLC WITH CONTINUOUS-FLOW FAB

	Injection volume (μl)	*Flow-rate (μl/min)*	*Split ratio*
Conventional HPLC	100	1000	1:200
Microbore HPLC	5	50	1:10
Packed fused-silica micro-LC	0.5	5	No split
Open tubular HPLC	0.001	0.01	Make-up flow

In LC concentration-sensitive detectors are generally used, therefore most of the effort has gone into those compression techniques that result in an increased concentration of the analyte in the detector. For MS detection the effect of the flow-rate is also worth considering.

Several approaches are possible: *e.g.* the technique of belt-speed programming[31] using the moving-belt interface. The basic concept is extremely simple. The analyte is deposited on to the belt at a low belt speed and desorbed from the belt not at the same belt speed, as is usually done, but at an increased belt speed. This results in a higher mass-flow given by:

$$dm/dt = m'V_2/V_1 \tag{7}$$

where m' is the mass-flow without belt-speed programming, and V_1 and V_2 are the belt speeds for depositing and desorption, respectively. An example of the belt-speed programming approach is given in Fig. 5, comparing peaks obtained with either a constant belt speed or by means of belt-speed programming from 1.6 to 3.6 cm/s after

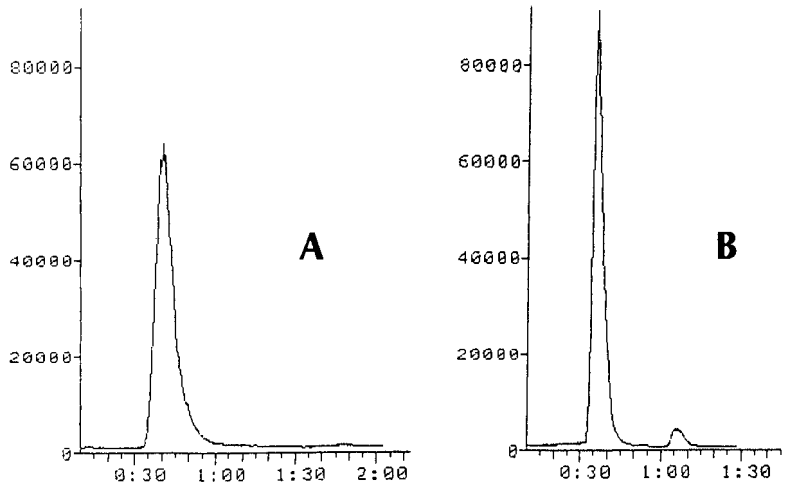

Fig. 5. Belt-speed programming with diuron, with (A) the normal situation with a constant belt speed, and (B) the peak compression achieved by increasing the belt speed after deposition on the belt.

deposition. The increased mass-flow of a factor of *ca.* 2 is reflected by an corresponding increase in peak height and decrease in peak width. A limitation is the reduced maximum flow-rate for deposition as a consequence of the lower applied belt speed. This restricts the attainable benefit from the approach in conventional LC systems, but this is not the case in SFC–MS using the moving-belt interface, as has been demonstrated[31], or if for sample size requirements miniaturized LC systems are used, for instance packed fused-silica columns in combination with the moving belt, as demonstrated by Barefoot and Reiser[32]. Furthermore, the temperature of the sample evaporator must be set at a low value, suitable for the low belt speed, but too low for the high belt speed[31].

Another approach in increasing the mass-flow by flow-rate programming is possible for miniaturized LC systems. With those systems a post-column increase of the flow-rate will result in an increased mass-flow. Flow-rate programming in the usual way is rather limited with respect to the attainable flow-rate range, therefore the possibilities of analyte trapping were studied, not on a precolumn as before in the PSS approach but in a storage loop that can be switched into a high flow-rate system as used for the TSP analysis. The general setup for such an experiment is given in Fig. 6. The results of a preliminary experiment are given in Fig. 7. A peak for metoprolol is produced at a flow-rate of 10 μl/min, which is a typical value for packed fused-silica columns of 0.32 mm I.D. After storage the analyte is measured by TSP LC–MS at a flow-rate of 1.5 ml/min. The increase in mass-flow is now given by:

$$dm/dt = m'F_2/F_1 \tag{8}$$

where m' is the mass-flow without flow-rate programming, and F_1 and F_2 are the flow-rates in the micro-LC and the TSP systems, respectively. Theoretically, a peak

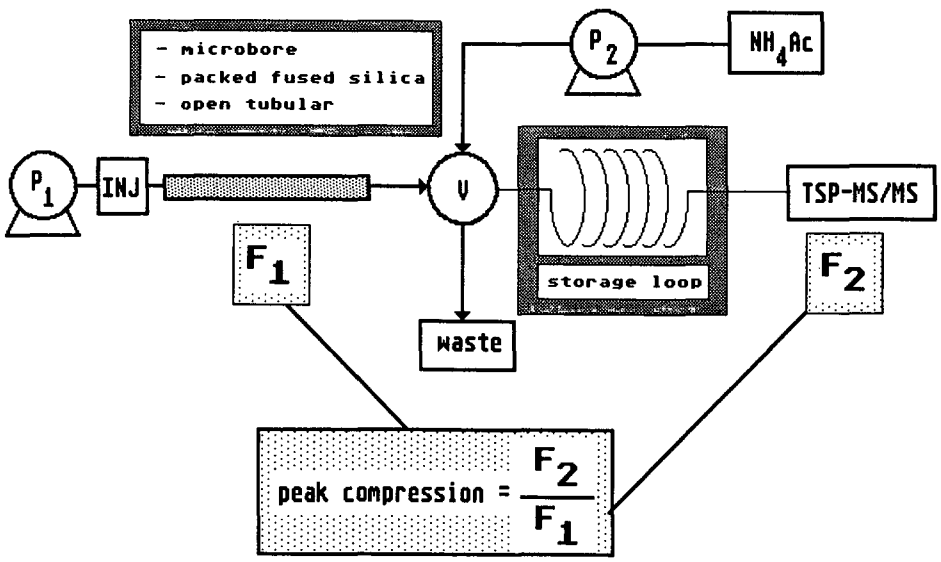

Fig. 6. Schematic diagram of mass-flow programming by trapping of an analyte from a miniaturized LC system via a storage loop and analysis by TSP LC–MS using a high flow-rate.

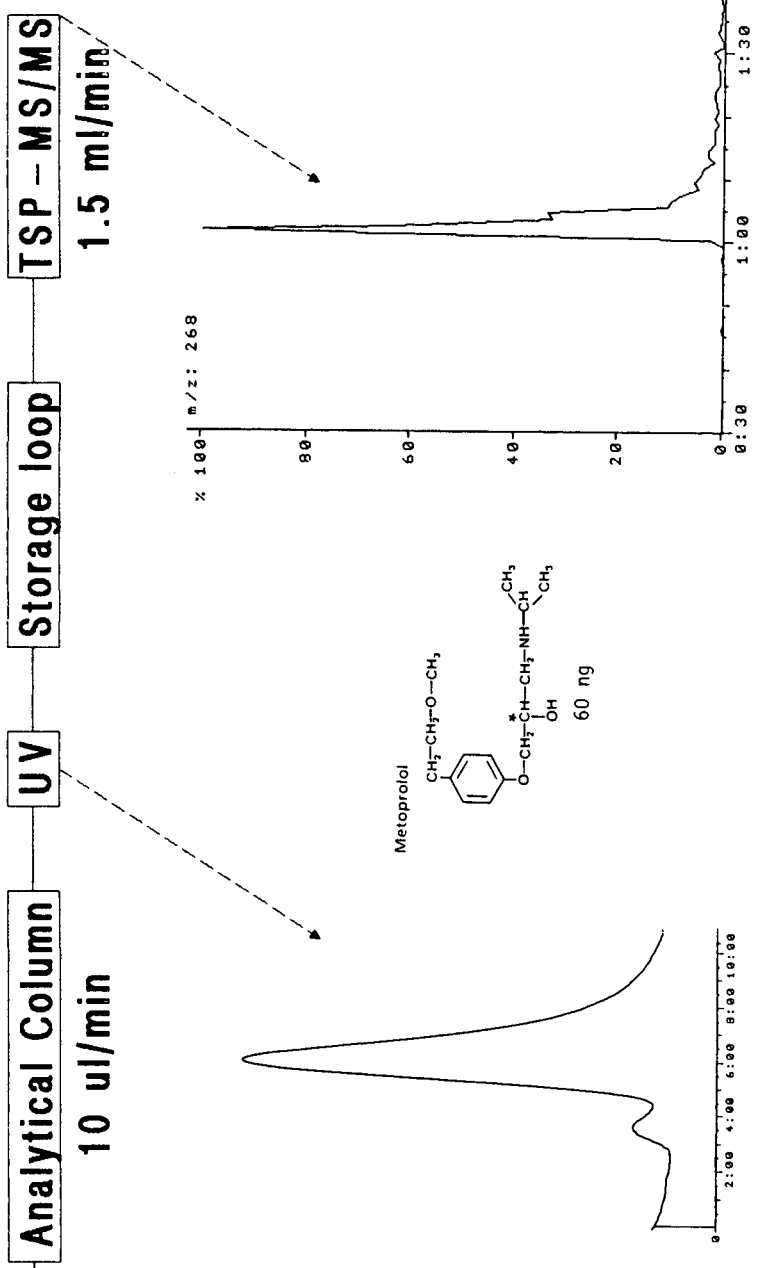

Fig. 7. Mass-flow programming experiment by trapping of metoprolol in a storage loop at a low flow-rate and analysis at a high flow-rate using TSP LC–MS. Peak compression of *ca.* 40-fold is achieved. A schematic diagram of the experimental setup is in Fig. 6.

compression of 1500/10 = 150 should be possible in this case. A factor of *ca.* 40 is measured, which is considerable but still much less than theoretically achievable. This can be explained by the fact that the dimensions of the various system components and the appropriate time windows for switching had not yet been optimized in this preliminary experiment. Nevertheless, such a compression factor could be obtained in a straightforward way. This approach is of course only of value if miniaturized LC systems are needed as outlined above.

DERIVATIZATION IN LC–MS

The role of chemistry in LC–MS has been small and is generally neglected, since often as a primary goal of LC–MS coupling it is formulated that analysis can be performed without the need to perform the kind of chemical modifications which are often necessary in gas chromatography (GC)–MS[33]. However, some of the interfaces strongly rely on chemistry in their LC–MS operation, such as DLI, TSP and CF-FAB, and it is clear that the detection can be improved considerably if the chemistry is tuned properly. This has been pointed out by Vouros *et al.*[34]. In particular, derivatization procedures are of importance and will be discussed, although other forms of incorporating chemical interactions, electrochemistry or biochemistry, are attractive. For instance, mobile phase additives can enhance detection in DLI in the negative ion CI mode[35–37], the use of a TSP interface as a flow reactor[38], electrochemistry in combination with TSP–MS[39] or TSP–MS–MS[40] or the elegant approach of combining LC columns and various columns containing immobilized enzymes for rapid protein sequencing[41,42].

In LC, derivatization is widely used to improve the detection properties. The scarce attention to this method in LC–MS can be partly explained again by the low input from the chromatographic side in this area. Furthermore, the combination of derivatization and detection makes other (selective) detection methods, *e.g.* fluorescence, competitive with LC–MS. The incorporation of selective derivatization reactions is in general only applicable in target compound analysis.

In pre-column derivatization the chemistry influences the chromatographic, the interface and the MS detection properties, whereas in post-column mode only the latter two are affected, with the additional problem of the high concentrations of derivatization reagent in the mobile phase. To improve the MS detection the approaches well known in GC–MS can be used, such as increasing the molecular weight to enhance the selectivity, volatility enhancement, the introduction of electrophoric groups for negative ion chemical ionization, and increasing the stability of the molecular-weight-related ions.

Pre-column derivatization

Several papers have appeared describing the analysis of derivatized compounds but without a clear strategy for LC–MS analysis, so they will not be discussed.

Silylation has been applied by Quilliam and Yaraskavitch[43] for the analysis of fatty acids for similar reasons as in GC–MS, namely to increase the volatility and to broaden the range of compounds to be analysed by the moving-belt interface. The reduced polarity also allows the choice of less polar mobile phases for the chromatography, which is advantageous for this interface type. *tert.*-Butyldimethyl-

silyl derivatives were preferred for stability reasons, and provided both molecular weight and structure information in the EI mode. Anthryl esters of fatty acids were used in another study[44] using a non-aqueous reversed-phase system.

Separation of enantiomeric amphetamines and detection with a moving-belt interface combined with EI has been performed[45] after derivatization with N-(trifluoroacetyl)-1-propyl chloride to form the diastereoisomers, which could be separated by a chiral column. Derivatization was applied to achieve the separation but the label might be attractive to enhance to detection in negative ion chemical ionization (CI) mode as well.

Amino acids, peptides and oligopeptides have been studied by several approaches. Yu *et al.*[46] used a moving belt to study the behaviour of N-acetyl-N,O,S-permethylated derivatives of oligopeptides. CI with isobutane as the reagent gas yielded sequence information, while the chromatographic integrity of the gradient system was maintained by using a heated-gas nebulizer for effluent deposition on the belt. DLI LC–MS for N-acetyl-O-methylester derivatives of oligopeptides were presented by Arpino and McLafferty[47]. Studies on derivatized amino acids have been published for LC–MS using atmospheric pressure ionization[48], DLI[49], the moving belt and TSP[50]. For the latter two a comparative study revealed that underivatized amino acids decompose to some extent at low concentrations on the moving-belt system and to a lesser extent in thermospray, although one compound could not be detected. Phenylthiohydantoin-amino acids gave satisfactory results on the belt system.

Derivatization of carbonyl compounds with 2,4-dinitrophenylhydrazine yields informative spectra in positive and negative ion CI in combination with the moving belt[51]. Aldehydes and ketones can be distinguished in the negative ion mode, and low-molecular-weight compounds became sufficiently involatile to be analysed by LC–MS.

The negative ion behaviour of pentafluorobenzyl (PFB) esters of hydroxylated metabolites of docosahexanoic acid in TSP[52] with the auxiliary filament on was used to confirm the molecular weight observed in the positive ion mode. An abundant $[M-PFB]^-$ ion, as normally observed under electron-capture conditions, was obtained for various metabolites present in a rat brain incubate.

Voyksner *et al.*[53] showed that the sensitivity for prostaglandins and thromboxane B_2 in TSP was limited by the low proton affinity of the compounds. Derivatization with diethylaminoethyl chloride (or bromide) increased the proton affinity, which was reflected in a considerable improvement in the detection limit. The positive ion mode was more sensitive than the negative ion mode, but an improvement by a factor of 2–3 was still observed for the latter technique. Detection of a prostaglandin metabolite in plasma at a level of 30 ppb was shown after including the derivatization step.

Derivatization to improve the detectability in CF-FAB seems to be straightforward, since considerable work has been performed for conventional FAB[33]. The derivatization to form charged derivatives or preformed ions, for instance by Girard's P or T, will increase the sensitivity as observed by us for progesterone in FIA in the CF-FAB mode. However, if derivatization is performed in pre-column mode the chromatography for the ionic compounds, will be less compatible with on-line LC–MS.

Post-column derivatization

The extraction device developed for the moving belt enabled Karger and co-workers[17,18] to perform on-line ion-pair extraction and to study the MS behaviour of the ion-pairs formed. The volatilization of ionic compounds using this method has been studied[54,55], and alkylsulphonates and sulphates were studied as counter-ions in both EI and CI modes. The flash evaporation induces thermal degradation, yielding for instance an alkene, sulphuric acid and an amine in the case of sulphate–amine ion-pairs. This ion-pair concept was further evaluated to a derivatization system based on the alkylation of analytes during flash evaporation. In this case trimethylanilinium hydroxide was used as the ion-pairing reagent[34], and a complete conversion of stearic acid into methylstearate was shown. Furthermore, volatile carboxylic acids were analysed by this approach with tetra-*n*-butylammonium hydroxide[56] as well as derivatization of primary amines with carbon disulphide to form isothiocyanates[57].

In TSP, post-column derivatization of prostaglandins was achieved by forming methyl esters[58] with tetra-*n*-butylammonium hydroxide as the reagent and the TSP vaporizer and the ion source as the reaction chamber. The yield of the methyl esters was maximized by setting the optimal temperatures of both the vaporizer and the ion source. A gain in the ion current of a factor of 3–6 has been reported.

CONCLUSIONS

LC–MS extended by multidimensional approaches in both LC and MS opens new research areas, which allow the improvement of the compatibility of the LC and MS parts, the optimal tuning of the overall selectivity and the enhancement of the detectability. These items will become even more important because of the successful development of new interface types that have special characteristics, such as low flow-rate requirements or extremely good sensitivity for ionic compounds, which can be applied successfully only if the chromatographic part is carefully optimized as well.

The role of chemistry is becoming more important since many interfaces are linked with ionization conditions possessing an important chemistry component. Derivatization, although not often applied in LC–MS, can be used successfully but a better understanding of the ionization mechanisms involved will be of great help in this area.

The present state of the art of LC–MS makes the method a powerful tool for an analytical laboratory and, because of the rapid developments in the field, much more can be expected in the near future.

REFERENCES

1 G. Guiochon and P. J. Arpino, *J. Chromatogr.*, 271 (1983) 13.
2 B. L. Karger and P. Vouros, *J. Chromatogr.*, 323 (1985) 13.
3 *The 36th American Society for Mass Spectrometry meeting on Mass Spectrometry and Allied Topics, June 5–10, San Francisco, CA, 1988.*
4 *The 12th International Symposium on Column Liquid Chromatography, Washington, DC, June 20–24, 1988.*
5 T. R. Covey, E. D. Lee, A. P. Bruins and J. D. Henion, *Anal. Chem.*, 58 (1986) 1451A.
6 W. H. McFadden and S. A. Lammert, *J. Chromatogr.*, 385 (1987) 201.
7 R. D. Smith, H. T. Kalinoski and H. R. Udseth, *Mass Spectrom. Rev.*, 6 (1987) 445.
8 A. J. Berry, D. E. Games and J. R. Perkins, *J. Chromatogr.*, 363 (1986) 147.

9 D. E. Games, A. J. Berry, I. M. Mylchreest, J. R. Perkins and S. Pleasance, *Eur. Chrom. News*, 1 (1987) 10.
10 L.-E. Edholm and L. E. Ogren, in I. Wainer (Editor), *Liquid Chromatography in Pharmaceutical Development*, Aster, Springfield, OR, 1986, p. 345.
11 L.-E. Edholm, C. Lindberg, J. Paulson and A. Walhagen, *J. Chromatogr.*, 424 (1988) 61.
12 J. V. Johnson and R. A. Yost, *Anal. Chem.*, 57 (1985) 759A.
13 A. C. Tas, J. van der Greef, M. C. ten Noever de Brauw, T. A. Plomp, R. A. A. Maes, M. Hoehn and U. Rapp, *J. Anal. Toxicol.*, 10 (1986) 46.
14 J. van der Greef, A. C. Tas, M. C. ten Noever de Brauw, M. Hohn, G. Meyerhoff and U. Rapp, *Adv. Mass Spectrom.*, 10 (1986) 587.
15 E. R. Verhey, G. F. LaVos, W. van de Pol, W. M. A. Niessen and J. van der Greef, *J. Anal. Toxicol.*, 13 (1989) 8.
16 P. O. Edlund and J. Henion, presented at the *36th ASMS Conference on Mass Spectrometry and Allied Topics, June 5–10, San Francisco, CA*, p. 1095.
17 B. L. Karger, D. P. Kirby, P. Vouros, R. L. Foltz and B. Hidy, *Anal. Chem.*, 51 (1979) 2324.
18 B. L. Karger, D. P. Kirby and P. Vouros, *J. Chromatogr. Sci.*, 18 (1980) 111.
19 D. P. Kirby, P. Vouros, B. L. Karger, B. Hidy and B. Petersen, *J. Chromatogr.*, 203 (1981) 139.
20 J. A. Apffel, U. A. Th. Brinkman, R. W. Frei and E. A. I. M. Evers, *Anal. Chem.*, 55 (1983) 2280.
21 J. A. Apffel, U. A. Th. Brinkman and R. W. Frei, *J. Chromatogr.*, 312 (1984) 153.
22 J. R. Lloyd, M. L. Cotter, D. Ohori and A. R. Oyler, *Anal. Chem.*, 59 (1987) 2534.
23 F. A. Maris, R. B. Geerdink, R. W. Frei and U. A. Th. Brinkman, *J. Chromatogr.*, 323 (1985) 113.
24 W. M. A. Niessen, P. J. M. Bergers, U. R. Tjaden and J. van der Greef, *J. Chromatogr.*, 454 (1988) 243.
25 W. M. A. Niessen, M. A. G. de Kraa, E. R. Verhey, P. J. M. Bergers, G. F. LaVos, U. R. Tjaden and J. van der Greef, *Rapid Commun. Mass Spectrom.*, 3 (1989) 1.
26 K. McKellop, G. Hansen and F. Hatch, presented at the *33rd ASMS Meeting, San Diego, CA, May 26–31, 1985*, p. 765.
27 J. van der Greef, W. M. A. Niessen and U. R. Tjaden, *J. Pharm. Biomed. Anal.*, 6 (1988) 565.
28 E. R. Verhey, H. J. E. M. Reeuwijk, G. F. LaVos, W. M. A. Niessen, U. R. Tjaden and J. van der Greef, *Biomed. Environ. Mass Spectrom.*, 16 (1988) 393.
29 A. Walhagen, L.-E. Edholm, C. E. M. Heeremans, R. A. M. van der Hoeven, W. M. A. Niessen, U. R. Tjaden and J. van der Greef, *J. Chromatogr.*, 474 (1989) 257.
30 P. Kokkonen, W. M. A. Niessen, U. R. Tjaden and J. van der Greef, *J. Chromatogr.*, 474 (1989) 59.
31 E. R. Verhey, G. F. LaVos, W. M. A. Niessen, U. R. Tjaden and J. van der Greef, *J. Chromatogr.*, 474 (1989) 275.
32 A. C. Barefoot and R. W. Reiser, *J. Chromatogr.*, 398 (1987) 217.
33 R. J. Anderegg, *Mass Spectrom. Rev.*, 7 (1988) 395.
34 P. Vouros, E. P. Lankmayr, M. J. Hayes, B. L. Karger and J. M. McGuire, *J. Chromatogr.*, 251 (1982) 175.
35 C. E. Parker, K. Yamaguchi, D. J. Harvan, R. W. Smith and J. R. Hass, *J. Chromatogr.*, 319 (1985) 273.
36 R. D. Geerdink, F. A. Maris, G. J. de Jong, R. W. Frei and U. A. Th. Brinkman, *J. Chromatogr.*, 394 (1987) 51.
37 D. Barceló, F. A. Maris, R. B. Geerdink, R. W. Frei, G. J. de Jong and U. A. Th. Brinkman, *J. Chromatogr.*, 394 (1987) 65.
38 M. M. Siegel, R. K. Isensee and D. J. Beck, *Anal. Chem.*, 59 (1987) 989.
39 G. Hambitzer and J. Heitbaum, *Anal. Chem.*, 58 (1986) 1067.
40 K. J. Volk, M. S. Lee, R. A. Yost and A. Brajter-Toth, *Anal. Chem.*, 60 (1988) 722.
41 H. Y. Kim, D. Pilosof, D. F. Dyckes and M. L. Vestal, *J. Am. Chem. Soc.*, 106 (1984) 7304.
42 K. Stachowiak, C. Wilder, M. L. Vestal and D. F. Dyckes, *J. Am. Chem. Soc.*, 110 (1988) 1758.
43 M. A. Quilliam and J. M. Yaraskavitch, *J. Liq. Chromatogr.*, 8 (1985) 449.
44 J. D. Baty, R. G. Willis and R. Tavendale, *Biomed. Mass Spectrom.*, 12 (1985) 565.
45 S. M. Hayes, R. H. Lin, W.-S. Tsang, M. G. Legendre, R. J. Berni, D. J. Pillion, S. Barnes and M. H. Cho, *J. Chromatogr.*, 398 (1987) 239.
46 T. J. Yu, H. A. Schwartz, S. A. Cohen, P. Vouros and B. L. Karger, *J. Chromatogr.*, 301 (1984) 425.
47 P. J. Arpino and F. W. McLafferty, in F. C. Nachod, J. J. Ackermann and E. W. Randall (Editors), *Determination of Organic Structures by Physical Methods*, Academic Press, New York, 1976, Vol. 6, p. 1.
48 E. C. Horning, D. I. Caroll, I. Dzidic, K. D. Haegele, M. G. Horning and R. N. Stillwell, *J. Chromatogr.*, 99 (1974) 13.

49 D. J. Dixon, *Analusis*, 10 (1982) 343.
50 D. E. Games and E. D. Ramsey, *J. Chromatogr.*, 323 (1985) 67.
51 K. L. Olsen and S. J. Swarin, *J. Chromatogr.*, 333 (1985) 337.
52 J. A. Yergey, H.-Y. Kim and N. Salem, Jr., *Anal. Chem.*, 58 (1986) 1344.
53 R. D. Voyksner, E. D. Bush and D. Brent, *Biomed. Environ. Mass Spectrom.*, 14 (1987) 523.
54 D. P. Kirby, P. Vouros and B. L. Karger, *Science (Washington, DC)*, 209 (1980) 495.
55 D. P. Kirby, P. Vouros, B. L. Karger, B. Hidy and B. Petersen, *J. Chromatogr.*, 203 (1981) 139.
56 C.-P. Tsai, A. Sahil, J. M. McGuire, B. L. Karger and P. Vouros, *Anal. Chem.*, 58 (1986) 2.
57 P. Vouros, A. Sahil, C.-P. Tsai and B. L. Karger, presented at the *33rd ASMS Meeting on Mass Spectrometry and Allied Topics, San Diego, CA, May 26–31, 1985*, p. 379.
58 R. D. Voyksner and E. D. Bush, *Biomed. Environ. Mass Spectrom.*, 14 (1987) 213.

Journal of Chromatography, 474 (1989) 21–37
Elsevier Science Publishers B.V., Amsterdam — Printed in The Netherlands

CHROM. 21 558

CAPILLARY ELECTROPHORESIS–ELECTROSPRAY IONIZATION-MASS SPECTROMETRY

C. G. EDMONDS, J. A. LOO, C. J. BARINAGA, H. R. UDSETH and R. D. SMITH*
Chemical Methods and Separations Group, Chemical Sciences Department, Pacific Northwest Laboratory, P.O. Box 999, Richland, WA 99352 (U.S.A.)

SUMMARY

New developments are described in the area of capillary electrophoresis combined with electrospray ionization-mass spectrometry (CE–ESI-MS), a promising new method for the separation and mass spectrometric characterization of labile, polar or ionic constituents of biological mixtures. The various experimental modes of capillary electrophoresis are reviewed. The ESI-MS technique is described and the significance of its combination with capillary electrophoresis is illustrated by MS analysis of large biomolecules. The design and performance optimization of a new ESI interface are discussed, including the influence of electrophoretic and MS operating parameters. Various examples from our laboratory illustrating the range of present application of this interface and direction of future development are presented. These include negative ion electrospray mass spectra of nucleotide co-enzymes, nucleotide mono-, di- and triphosphates and positive ion spectra of biologically important oligopeptides and proteins of $M_r > 75$ kilodaltons.

INTRODUCTION

The development of analytical methodology for the identification and characterization of biopolymers and their constituents is of broad significance in biochemistry, molecular biology and biotechnology. The important characteristics of high selectivity and high sensitivity offered by mass spectrometry (MS) are inherently advantageous in these areas of research. The electrospray ionization (ESI) method is applicable to broad classes of involatile and labile compounds. Coupled with capillary electrophoresis (CE), an ionic separation method of high efficiency, flexibility and speed, electrospray ionization-mass spectrometry (ESI-MS) is a potentially powerful tool for biomolecular analysis.

Electrophoresis, based on the separation of charged species in a background medium under the influence of an applied electric field, is probably the oldest differential migration technique, due originally to Wiedeman in 1856[1]. Since the introduction of discrete "band" separation of solutes by paper electrophoresis in 1937[2], the method has been extensively elaborated and applied, and is currently the classical method for the separation of biopolymers. Separation may be on the basis of molec-

0021-9673/89/$03.50

ular charge and/or size (when using an appropriate gel medium) and is especially useful for the analysis of complex protein mixtures and in DNA sequencing. Electrophoresis forms a family of related techniques including electrophoresis (polyacrylamide, agarose, etc.), isotachophoresis, gel electrofocusing (*i.e.*, isoelectric focusing) and free zone electrophoresis.

Analytical separation techniques based on these electrophoretic principles in the capillary format can be divided into four types: capillary zone electrophoresis (CZE), capillary gel electrophoresis (CGE), capillary isotachophoresis (CITP) and capillary isoelectric focusing (CIEF). Our present research efforts have focused on CZE and CITP development and application. In principle, all techniques may be carried out with the same type of electrophoretic equipment, providing considerable instrumental flexibility. Capillary electrophoresis methods present an opportunity for greatly enhanced separation speeds, improved automation and (potentially) greater sensitivity and compatibility with alternative detection methods.

CZE

In zone electrophoresis, a column is filled with a single electrolyte having a specific conductivity. The mixture of substances to be separated is applied as a narrow band to the head of a buffer filled column in a band whose width is much less than the length of the column and at a concentration ideally too low to affect the buffer conductivity. An electric field is then applied across the length of the column and the individual substances migrate and separate according to their net electrophoretic velocities. Zone electrophoresis carried out in small diameter (< 100 μm) fused-silica capillaries is a relatively new approach to the high-resolution separation of aqueous samples[3–5]. An important physical effect of the high electric field on any surface having a net charge (*e.g.*, fused silica) is the formation of an electric double layer[6]. Such a layer for the fused silica–water system results from exposed silanol groups, which acquire a net negative charge while the bulk solution remains neutral. The immediate neighborhood of the glass surface acquires a corresponding net positive charge which extends for a short distance into the fluid. Under the influence of an external electric field the ions of the diffusive part of the electrical double layer move toward the oppositely charged electrode and a flow originates near the wall. Viscous forces then drag the rest of the solution in the capillary creating a flat flow profile, in contrast to the parabolic flow profile of hydrodynamic flow[7]. The width of the double layer, dependent on ionic strength, is typically a few nanometers and steady state flow is reached almost immediately in a 100 μm I.D. (typical for CZE) capillary when the field is applied[3]. A substantial electric double layer (strong zeta potential at the silica surface) results in a strong electroosmotic flow and rapid analysis times (5–30 min) for typical capillary lengths (100 cm) and voltages (30 kV). The electroosmotic flow-rate is proportional to the applied voltage for the field gradients typically used. In addition to the bulk flow of the electrolyte, charged species in solution will migrate under the influence of the external field. This velocity is proportional to the applied field and separations are due to differences in electrophoretic mobility among species. Differences in the velocity of migration may be established, as in the case of electrokinetic chromatography, by secondary means utilizing partitioning with a counter-migrating charged micellar phase[8].

The most important contributions to band spread in CZE are molecular diffu-

sion (which is inherent and unavoidable), adsorption on capillary surfaces, and effects due to heating (*e.g.* convection driven by thermal gradients[9–13]). In CZE the effects of molecular diffusion can only be countered by minimizing the separation time (*i.e.*, using higher voltages). The effects due to Joule heating of the capillary are generally responsible for the greatest loss of separation efficiency and must be minimized. Small diameter columns reduce the resistance to heat transfer, minimize the radial temperature differential and have wall effects which act to suppress convection. Typically, molecular diffusion rates in liquids are quite small (10^{-6}–10^{-8} cm^2/s) and the ultimate efficiency of electrophoretic separations can be very high ($> 10^6$ plates). Since maximum separation efficiencies are defined by molecular diffusion, increased molecular weights should, in principle, afford better separations.

Amino acids and small peptides are well-separated by CZE in untreated glass or fused-silica capillaries[3]. Capillary electrophoresis has been particularly effective in the analysis of fluorescently labelled amino acids[14–16]. Separation of fluorescently labelled tryptic peptides have also been reported[17,18]. Free zone separations of protein mixtures in the capillary format have been reported with high efficiencies[19–22]. Fluorescence detection of myoglobin with detection limits in the attomol (10^{-18} mol) range has been achieved[21] by CZE. Surface adsorption may be avoided by raising the pH of the buffer solution above the isoelectric point of the sample proteins, by dynamic modification of the buffer–silica wall interfacial double layer[20] or by covalent modification of the silica wall[22]. Nucleic acid constituents may be separated by CZE as nucleobases, nucleosides[23] and nucleotides[24,25]. The addition of detergent micelles with complexing metal ions allows improved separations of these analytes by differential complexation and good separations of small oligonucleotides are obtained.[26].

CITP

In isotachophoresis (sometimes called displacement electrophoresis) all analytes progress through the separating medium at the same final velocity[27]. Isotachophoresis, though utilizing similar equipment and principles as zone electrophoresis, can accommodate larger samples and may actually result in an *increase* in the concentration of the material being separated. In CITP the column is initially filled with an electrolyte (*i.e.*, leading electrolyte) which contains ions with a mobility higher than that of any ions in the sample mixture (and, ions of opposite polarity having a useful buffering capacity). The solutes are then loaded on the column as a second band. The head of the column is placed in an electrolyte solution which contains ions with an effective mobility lower than any in the sample mixture (*i.e.*, terminating electrolyte). On application of an electric field the lead electrolyte will attempt to "pull away" from the analyte ions. This results in a gap where the conductivity is dropping (the solvent having no significant conductivity) and the electric field is rising. The increased field will "pull" the analyte ions along until they catch up to the lead electrolyte, with the highest mobility analyte ion arriving first. This "pulling along" effect will continue as the analyte bands arrange in order of decreasing mobilities until finally the trailing electrolyte, which has the lowest mobility, is reached. Eventually a steady state will be reached in which each solute is isolated in its own band, and all bands are moving at the same velocity.

The steady state concentration of the analyte in CITP is largely determined by the leading electrolyte concentration. Accordingly, if the analyte is more dilute than

the leading ion concentration, the analyte will often be *concentrated* as it separates into its own band. In a fully developed separation the ionic concentration of each band is equivalent and the relative abundance of the analyte (and thus the sample concentration) is proportional to the length of the band. Thus, CITP offers the potential for higher sample loading than CZE (and increased *molar* sensitivity), and can provide (in many cases) actual concentration of separated sample bands. We have recently shown that the CITP–MS combination has advantages for certain trace analyses and is capable of providing high resolution separations[28,29].

Amino acids and small peptides can be easily separated by capillary isotachophoresis[27], usually as anions, provided suitable leading and terminating electrolytes are chosen. Recently, Stover has described the cationic CITP separations of proteins with average molecular weights of 13–35 kilodaltons[30].

ESI and CE–MS-ESI

Electrospray ionization, pioneered by the early work of Dole *et al.*[31], is a soft ionization method capable of producing gaseous ions of ionic molecules from highly charged evaporating liquid droplets. Fenn and co-workers[32–34] have further developed the technique as a means of ionizing charged, labile and involatile samples in solution for MS analysis, including nucleotide mono- and diphosphates. ESI generally provides production of multiply charged ions of large molecules and allows mass spectrometers with moderate mass/charge limit (*e.g.*, conventional quadrupole mass filters) to analyze macromolecules with dramatically higher molecular weights. For example, a net charge of 23+ (multiply sodiated) has been observed on a polyethylene glycol oligomer of nominal molecular weight 17 500 daltons[35]. Mass spectra have been obtained on peptides up to 40 000 daltons using a quadrupole mass spectrometer of m/z 1600 limit[36]. A nebulizer assisted variation of this technique is also described[37].

We have recently described the on-line combination of CZE based upon ESI-MS[38–40], the first direct combination of any electrophoretic separation technique in dynamic (*i.e.*, "on-line") combination with MS. This development was based upon the recognition that it is not necessary for both ends of the CZE capillary to be immersed in buffer reservoirs, as conventionally practiced. Thus, with an appropriately designed electrode MS detection is possible at the capillary terminus utilizing an ESI source. The interface allows compatibility with the low (approximately 0–1 μl/min) electroosmotic flow-rates of CE and provides for ion production at atmospheric pressure from the electrically induced nebulization process. Because CE relies on analyte charge in solution, and the ESI process appears to function most effectively for ionic species, the CE–ESI-MS combination is highly complementary. We have reported the analysis by CZE–ESI-MS of a mixture of quaternary ammonium compounds[38] obtaining a separation efficiency of over 330 000 theoretical plates, an order of magnitude better than obtainable by liquid chromatography in similar time. For scanning MS sample sizes in the femtomole range were required; however detection limits of *ca.* 10 attomol were obtainable using single ion detection. Thus, the CZE–ESI-MS approach offers previously unobtainable separation efficiencies (for the combination with MS) as well as significantly enhanced sensitivity. Further instrumentation development should provide even better detection limits.

CITP has also been evaluated as an alternative mode of electrophoretic sep-

aration with ESI-MS detection[28,29]. CITP is an attractive complement to CZE and is near ideally suited for combination with MS. Sample sizes which can be introduced in CITP are much greater (>100 fold) than CZE. Additionally, as discussed above, CITP may result in concentration of analyte bands, which is in contrast to the inherent dilution obtained in CZE. Samples elute in CITP ideally as broad, flat-topped bands, well suited to sensitive analysis with long integration times and the slow scan speed of the mass spectrometer, particularly for tandem MS detection. High-sensitivity and high-resolution separations for quaternary phosphonium and ammonium salts, amino acids and catacholamines have been demonstrated by CITP–ESI-MS[29]. Vinyltriphenyl and ethyltriphenyl phosphonium ions are well separated by this combined method, in contrast to previous CZE–ESI-MS results. CITP–ESI-MS is complementary to CZE–ESI-MS in many ways. The CZE column is easily overloaded, whereas CITP tolerates very high loading. Thus, larger injection volumes (0.1–1.0 μl) of extremely dilute sample solutions may be analyzed. Detection limits of approximately 10^{-11} *M* have been demonstrated for quaternary phosphonium salts[29] and substantial improvements appears feasible. CITP is well suited to low concentration samples where the amount of solution is relatively large whereas CZE is ideal for the analysis of minute quantities of solution.

This paper reports further results obtained by ESI-MS employing an atmospheric pressure interface adapted for combination with CZE for biomolecule analyses.

EXPERIMENTAL

The instrumentation developed at our laboratory has been elsewhere described in detail[38–40]. Fig. 1 shows the detailed construction of the interface. In earlier versions of the CZE–ESI interface the electrospray ionization was accomplished from an electrodeposited metal contact established at the end of the CZE capillary[38,39]. The most recent design employs a flowing liquid sheath electrode interface which allows the composition of the electrosprayed liquid to be controlled independently of the CZE buffer (which is desirable since high-percentage aqueous and high-ionic-strength buffers useful for CZE are not well tolerated by ESI)[40]. The electrical contact is through a conductive liquid sheath (typically methanol, acetonitrile, acetone or isopropanol). With this arrangement no significant additional mixing volume (< 10 nl) is produced and analyte contact with metal surfaces is avoided. This interface provides greatly improved performance and flexibility and is adaptable to other forms of CE. For direct ESI-MS experiments, syringe pumps control the flow of analyte solution and liquid sheath at 1 μl/min and 3 μl/min, respectively. CZE–ESI-MS experiments were conducted in untreated fused-silica capillaries using methods which have been described previously[28,38–40].

The ESI source consists of a 50 or 100 μm I.D. fused-silica capillary (which can be the CZE capillary) that protrudes 0.2–0.4 mm from a tubular stainless-steel electrode. High voltage, generally +5 kV for positive ions and − 5 kV for negative ions, is applied to this electrode. The ESI source tip is mounted 1.5 cm from the ion sampling nozzle of the ion sampling orifice (nozzle) of the quadrupole mass spectrometer. A 3–6 l/min counter-current flow of warm (80°C) nitrogen gas is used between the nozzle and source to aid desolvation of the highly charged droplets and to mini-

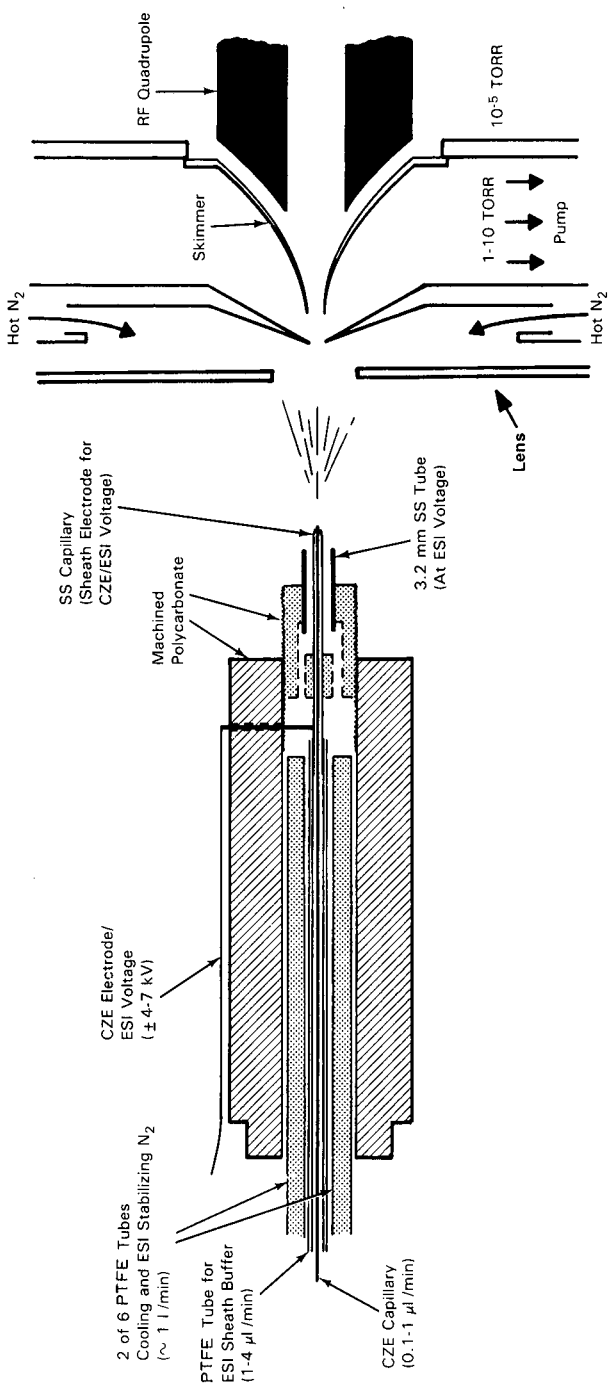

Fig. 1. Detailed schematic drawing of sheath electrode electrospray ionization interface and atmospheric pressure focusing and sampling region of the mass spectrometer entrance. SS = stainless steel.

mize solvent cluster formation during expansion into the vacuum chamber. Analyte clustering is further minimized by the mutual repulsion of highly charged ions and droplets (which, in contrast to the thermospray ionization, all have the same polarity). A lens placed in front of the sampling nozzle is used to help focus the ions or electrospray droplets to the point of ion sampling. Ions are sampled through the 1-mm diameter nozzle to a 2-mm skimmer directly in front of the radio frequency (RF) focusing quadrupole lens (Fig. 1). Typically, +350–500 V is applied to the focussing lens and +200 V to the nozzle (V_n), while the skimmer potential is at ground. A single-stage roots blower pumps the nozzle–skimmer region to 1–10 Torr. The cryopumped RF focusing region typically reaches pressures on the order of 10^{-6} Torr, while analysis quadrupole housing is maintained at 10^{-7} Torr with a turbomolecular pump (500 l/s). The analysis quadrupole (Extrel, Pittsburgh, PA, U.S.A.) has an upper m/z limit of 1700.

Biochemical samples were purchased from Sigma (St. Louis, MO, U.S.A.) except bovine apotransferin (Calbiochem, San Diego, CA, U.S.A.) and were used without further purification. Sample solutions were prepared in distilled water with varying ratios of acetonitrile —100% water to water–acetonitrile (20:80)]. For protein solutions, 1–5% glacial acetic acid was added.

RESULTS AND DISCUSSION

Preliminary studies with ESI have shown it to be a useful technique for ionization of nucleotides[34], especially in the negative ion mode. In the experiments which follow sample solutions were delivered directly to the ESI interface. Spectra are recorded over 1–2 min intervals requiring approximately 1–100 pmol of sample. Fig. 2 shows an ESI negative ion mass spectrum from an equimolar mixture of adenosine mono-, di- and triphosphate (sodium salt). We observe decreasing abundance of molecular ions with increasing phosphorylation. The molecular anion $(M-H)^-$ and

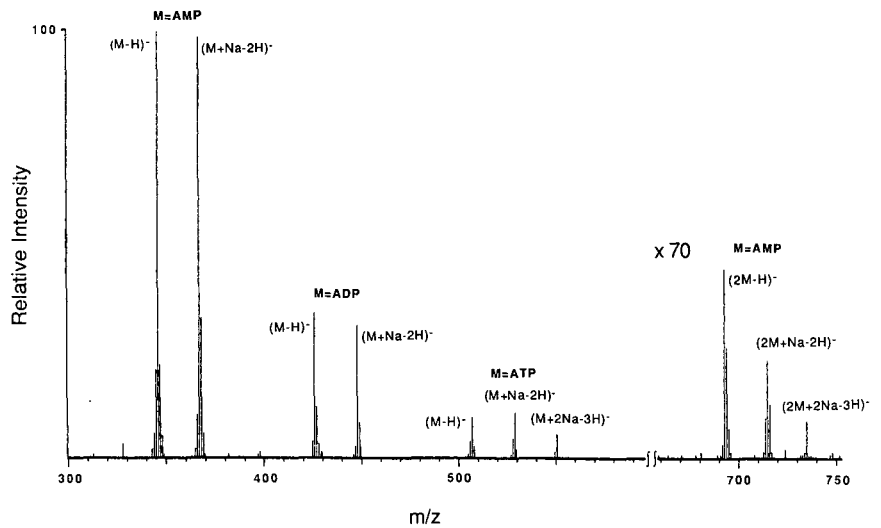

Fig. 2. Negative ion ESI mass spectrum of an equimolar mixture of AMP, ADP and ATP.

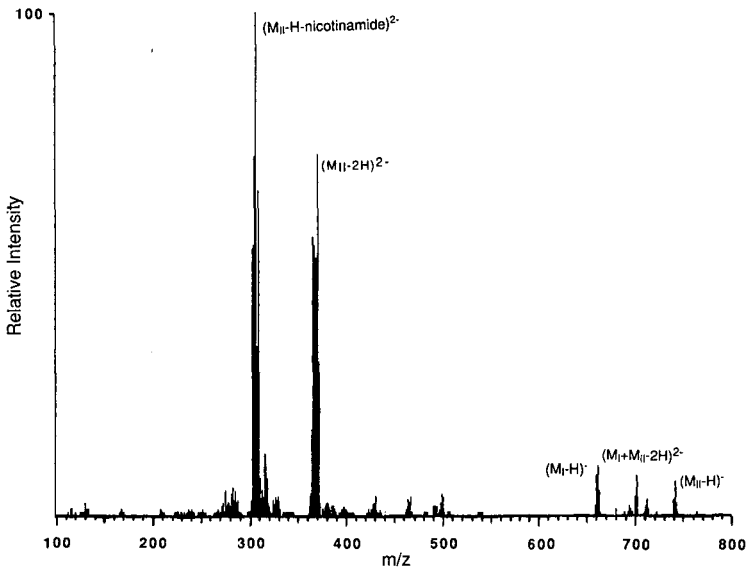

Fig. 3. Negative ion ESI mass spectrum of an equimolar mixture of β-NAD (I) and β-NADP (II).

the sodiated molecular anion $(M+Na-2H)^-$ are of approximately equal relative abundance for AMP, ADP and ATP. In the case of ATP a disodiated molecular anion is also abundant. Some solute clustering is evident in the spectrum, as demonstrated by the appearance of the AMP dimeric species $(2M-H)^-$, $(2M+Na-2H)^-$ and $(2M+2Na-3H)^-$ at approximately 1% relative abundance compared to the molecular anion. No ions of higher m/z were observed. We tentatively attribute such dimer species to self association in solution, since recombination after desorption is unlikely. For dinucleotides, such as β-nicotinamide-adenine dinucleotide and its phosphate analogue (β-NAD and βNADP), as shown in Fig. 3, we observe large signals for the negative ion molecular species for β-NAD and β-NADP, as well as the doubly charged molecular anion for β-NADP. A fragment ion, tentatively the loss of the nictinamide moiety from β-NADP, forms the base peak of the spectrum. A mixed dimeric dianion is also observed which implies contributions of the unmixed dianion dimers. No ions of higher m/z were observed. Multiple charging is also demonstrated in ESI mass spectra of larger oligonucleotides[41].

The positive ion ESI mass spectra of small peptides are dominated by molecular ions (*i.e.*, protonated or cation adducts) which can be either singly or multiply charged. The extent of multiple charging increases as the number of basic amino acids (*i.e.*, arginine, lysine, histidine, etc.) present in the peptide sequence increases. As demonstrated in Fig. 4 for bradykinin ($M_r = 1060$), ESI is a soft ionization technique with little fragmentation evident. The triply protonated molecule is observed, arising from ionization of two basic arginine residues and the N-terminus. The doubly protonated molecular ion constitutes the base peak of the spectrum. A similar spectrum is generated for gramicidin S (Fig. 5), a cyclic decapeptide ($M_r = 1141$) containing two basic ornithine residues.

The extent of multiple charging by ESI can be influenced by the composition of

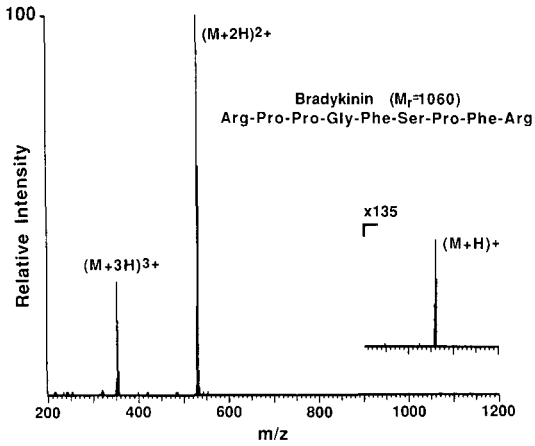

Fig. 4. Positive ion ESI mass spectrum of bradykinin.

the liquid sheath electrode[42] (*i.e.*, the charge distribution is shifted toward lower m/z values with solvents of greater surface tension and/or dielectric constant) as illustrated in a study on gramacidin S with various sheath liquids shown in Fig. 6. For example, the $(M+2H)^{2+}$ to $(M+H)^{+}$ ratio increases by a factor greater than 5 by changing the sheath liquid from isopropanol to methanol. Up to a factor of ten loss in sensitivity, in addition to an increase in the amount of analyte–solvent clustering, results with the use of an isopropanol sheath. The nature of the solvent association

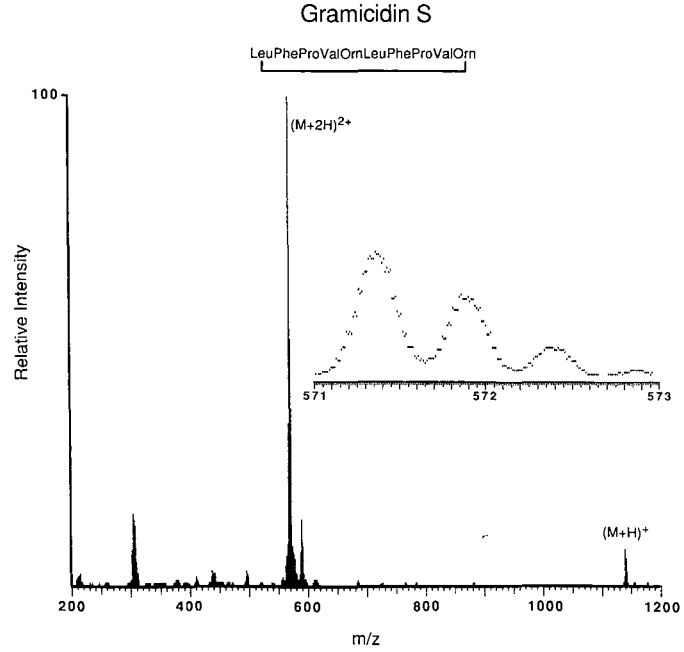

Fig. 5. Positive ion ESI mass spectrum of gramicidin S. Inset shows profile on the $(M+2H)^{2+}$ ion.

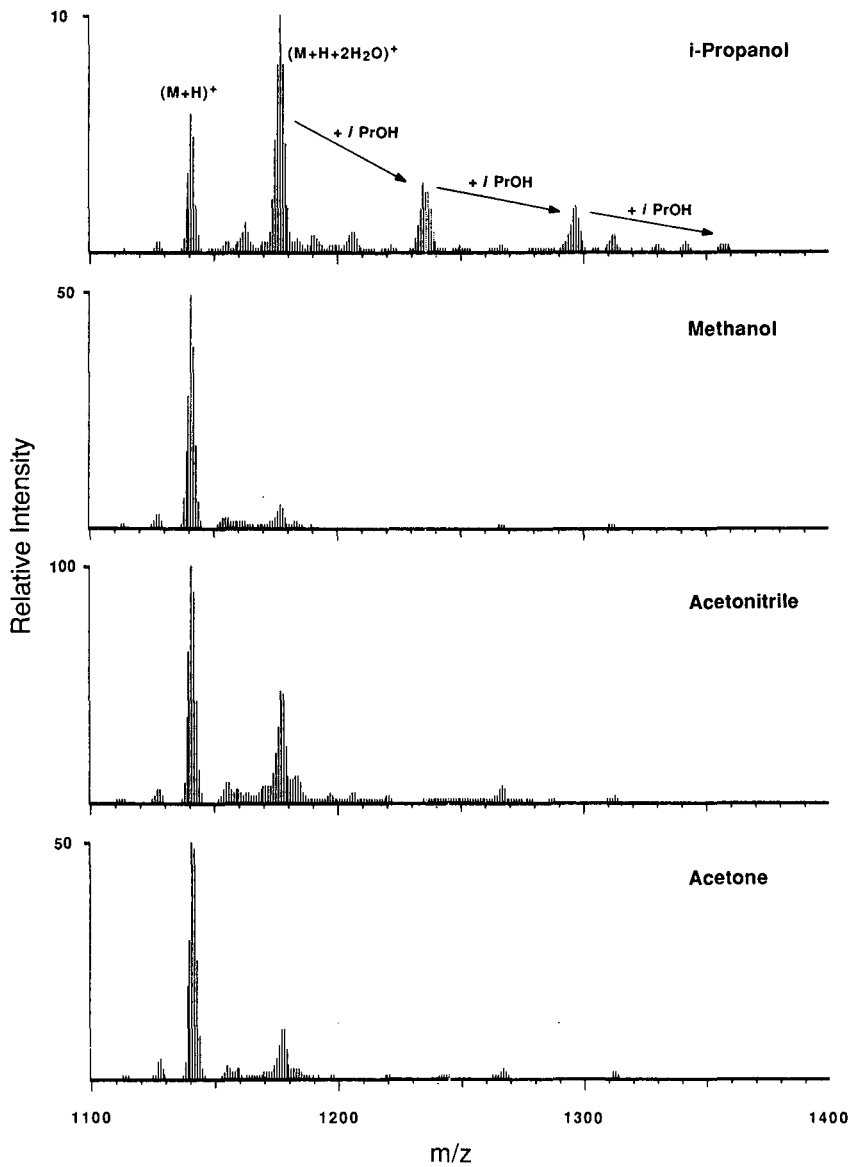

Fig. 6. Positive ion ESI $(M+H)^+$ ion region for gramicidin S with liquid sheath compositions as indicated. For this experiment the mass spectrometer was tuned at substantially less than unit mass resolution.

remains uncertain, but a number of isopropanol ions clearly can become somewhat more strongly associated with the molecular species than generally observed for other solvents.

As molecular weight increases with increasing numbers of basic amino acid residues, the ESI mass spectrum remains within the m/z 1700 range of our quadrupole mass spectrometer. Typical positive ion mass spectra for picomole amounts of pep-

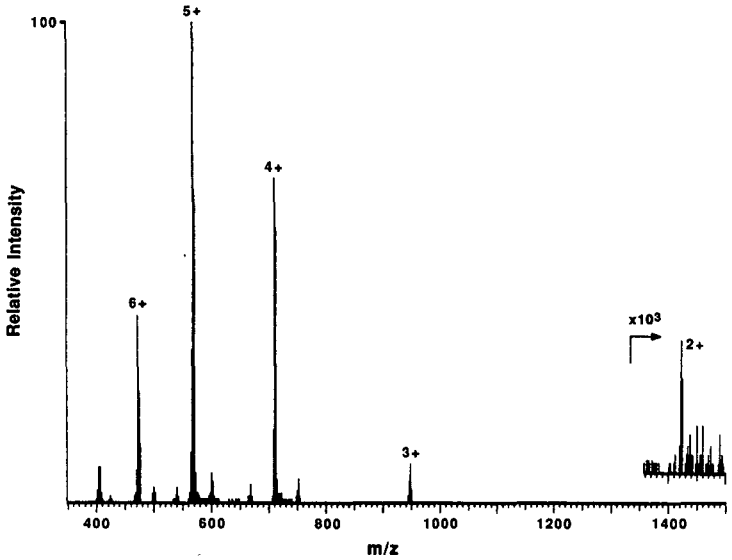

Fig. 7. Positive ion ESI mass spectrum of melittin ($M_r = 2845$).

tides are shown in Figs. 7 and 8 for melittin, a water-soluble 26-residue polypeptide ($M_r = 2845$), and an equimolar mixture of bovine ($M_r = 5734$) and porcine ($M_r = 5778$) insulin, respectively.

For larger protein molecules, a bell-shaped distribution of multiply charged molecular ions dominates the ESI mass spectrum with the distribution maxima gener-

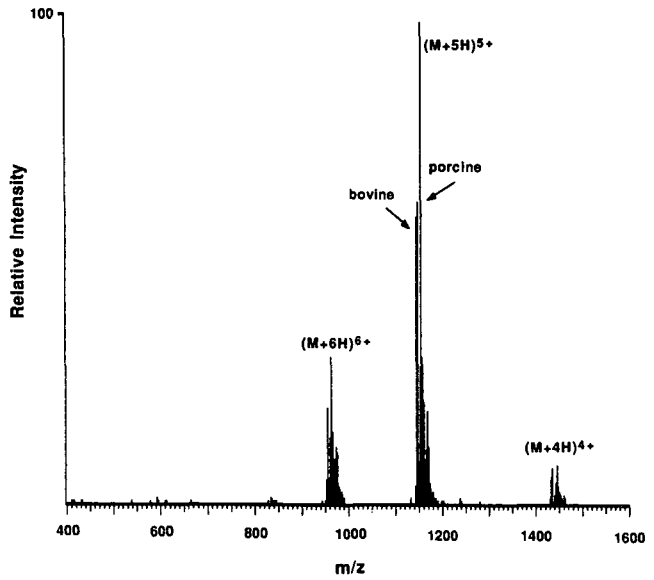

Fig. 8. Positive ion ESI mass spectrum of an equimolar mixture of bovine ($M_r = 5734$) and porcine insulin ($M_r = 5778$).

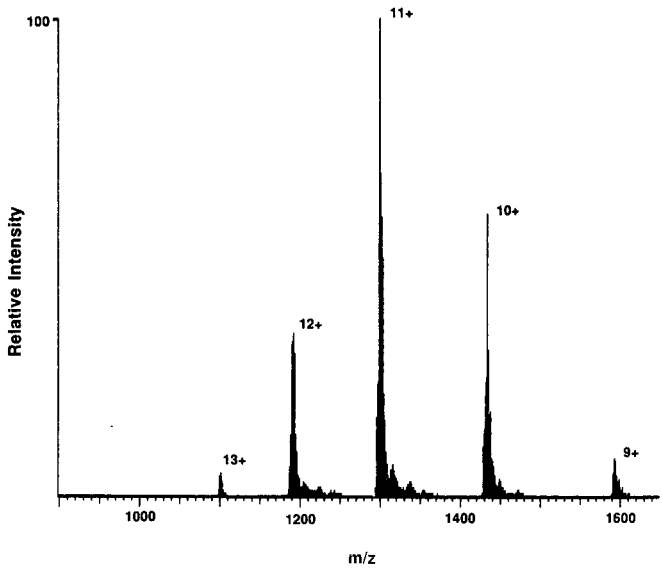

Fig. 9. Positive ion ESI mass spectrum of hen egg lysozye ($M_r = 14\,300$).

ally observed between m/z 500 and 1500, as evident in the mass spectra for hen egg lysozyme ($M_r \approx 14\,300$) and equine heart myoglobin ($M_r \approx 17\,600$), shown in Figs. 9 and 10, respectively. With increasing molecular weight and extent of multiple charging the broadening due to the unresolved isotopic envelope is balanced by the charge

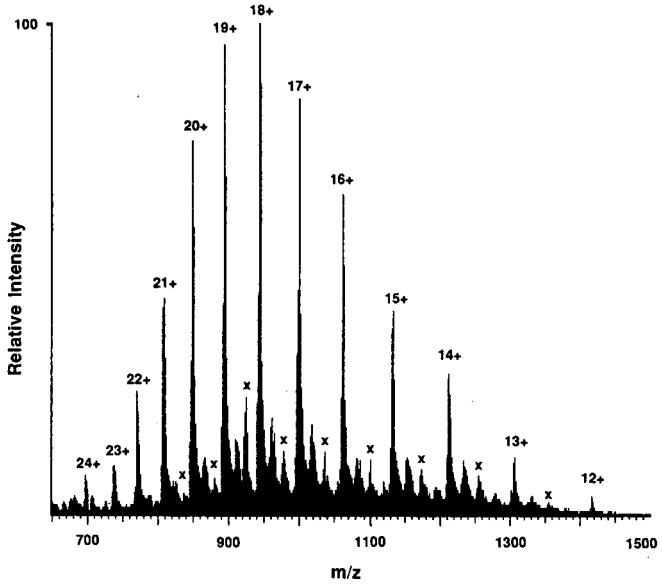

Fig. 10. Positive ion ESI mass spectrum of horse heart myoglobin ($M_r = 17\,600$). Principal ions represent the protein portion ($M_r = 16\,950$) of the molecule with loss of the heme moiety. Ions arising from the intact molecule were marked (X).

state (at a given m/z) to maintain similar peak widths for members of the distribution. Additional small contributions are often evident arising from cationization and solvent association. The latter effects may be minimized by adjustment of temperature and flow-rate of drying nitrogen gas in the ESI interface and increased collison energy (warming) in the interface provided by the nozzle–skimmer bias voltage. While such steps may not always be fully effective, as observed in the electrospray mass spectra of hen egg lysozyme (Fig. 9), in general we operate under conditions such that only strongly associated adducts and actual chemical heterogeneity contribute to the spectra[40]. Myoglobin is composed of a single 153 amino acid polypeptide chain (globin) bound to an iron–heme unit. Multiply charged ions are indicated for both the globin portion and the intact myoglobin molecule in Fig. 10. Over 65+ charges are detected by ESI-MS for a sample of bovine apotransferrin (Fig. 11). The spectrum shows a series of doublets indicating two species present with average molecular weights approximately 76 750 and 77 000 daltons. Elsewhere we have presented ESI mass spectra for proteins exceeding 130 000 daltons[43].

The charge distributions for large molecules are also sensitive to the nozzle–skimmer bias voltage[44], indicating that highly efficient collisionally activated dissociation processes may be occurring for these highly charged molecules in a manner which discriminates on the basis of the charge state of the molecule. More highly charged species (at lower m/z values) are more susceptible to collisional activation, as evident by their apparent dissociation at lower collision energy. For example, melittin yields multiply charged ions up to the 6+ species with the nozzle potential (V_n) below +200 V (Fig. 7) but disappears above this potential. Similarly the $(M+5H)^{5+}$ abundance drops below background at nozzle voltages greater than +370 V. Additional evidence of this effect is seen in the ESI mass spectrum of bovine hemoglobin ($M_r \approx 65\,000$) (Fig. 12). At $V_n = +200$ V the spectrum is dominated by multiply charged ions up to the $(M+25H)^{25+}$ species due to the α- and β-polypeptide chains. Increasing V_n to +300 V causes the multiply charged ions with charges 21+ to 25+ to disappear, shifting the distribution to lower charge state (higher m/z and revealing

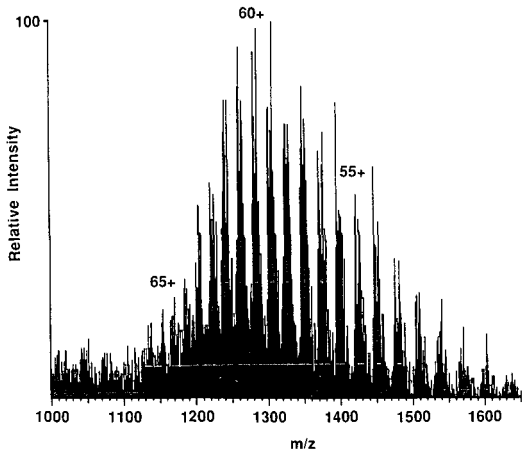

Fig. 11. Positive ion ESI mass spectrum of bovine apotransferrin. Two closely spaced series of multiply charged ions are consistent with a binary mixture of $M_r = 77\,000$ and $M_r = 76\,750$ proteins.

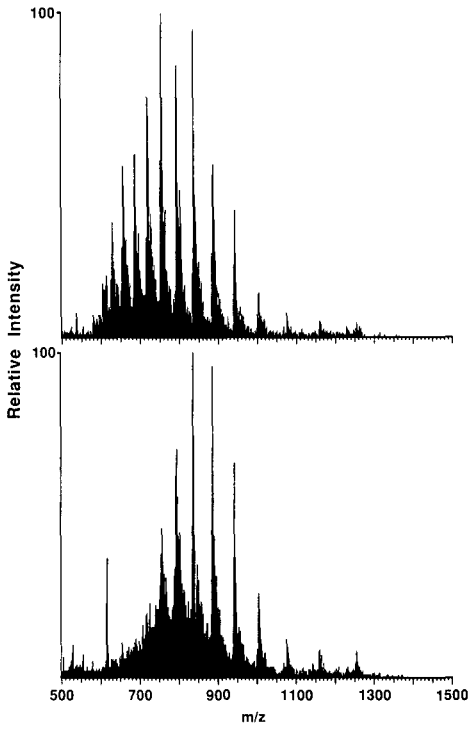

Fig. 12. ESI–MS of bovine hemoglobin ($M_r = 65\,000$) with nozzle potential (top) +200 V and (bottom) +300 V. α = 15 000; β = 15 970.

an ion which may be ascribed to the iron–heme unit at m/z 617. For small peptides such as angiotensin I ($M_r = 1296$) and melittin, singly and multiply charged fragment ions (generally A, B and Y type sequence ions) are clearly evident with V_n above +200 V[44]. The potential for tandem mass spectrometry (MS–MS)[45] with collisionally activated dissociation of multiply charged molecular ions from large proteins is an exciting prospect for structural elucidation. Initial results on the MS–MS of multiply charged ions produced by ESI are presented elsewhere[46].

An example of a preliminary attempt at CZE–MS of peptides and proteins is shown in Fig. 13. Previous studies of CZE of proteins in untreated fused silica capillaries (with UV detection) have resulted in broad, tailing peaks due to protein adsorption on active sites of the negatively charged silica wall[3]. However, as demonstrated by Lauer and McManigill[20], using buffered solutions with the pH above the isoelectric point of the peptides and proteins allows both the sample and the capillary wall to be negatively charged and mutually repulsive. The 2 pmol per component separation shown in Fig. 13 was performed with a 0.01 *M* sodium phosphate–sodium hydroxide buffer (pH 11). CZE–MS separations of proteins as large as myoglobin have been demonstrated in our laboratory[43]. Although improved sensitivity and resolution are desired, these CZE–MS results are encouraging initial steps for the electrophoretic separation and mass spectrometric detection of large biomolecules.

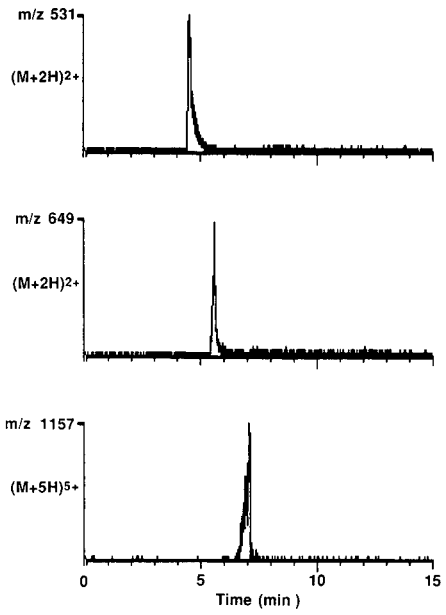

Fig. 13. Single ion electropherograms for a CZE–MS separation of a synthetic mixture of bradykinin ($M_r = 1060$), angiotensin I ($M_r = 1296$) and porcine insulin ($M_r = 5778$) with use of a 0.6 m × 100 μm I.D. fused-silica capillary at 15 kV.

CONCLUSIONS

The ability to ionize molecules of high molecular weight has opened new applications of MS in the biological sciences. The production of multiply charged molecular ions by ESI increases the detectable mass range by a factor equal to the number of charges. The effect of this is to bring into the mass range (mass/charge) of conventional mass spectrometers macromolecules whose relative mass approaches or exceeds the limits of any current high MS technique while solving the major problem associated with such applications by providing efficient ionization, detection, and (possibly) collisionally activated dissociation.

In many cases, molecular weight information on large molecules provided by MS may be sufficient to solve a problem[47]. Alternatively, however, collisionally activated dissociation of large multiply charged ions is an exciting approach that may lead to more efficient fragmentation and provide a route to obtaining structural information. Preliminary results show that the high charge state of ESI produced ions allows the extension of MS–MS methods to much larger compounds than previously tractable[48].

The speed and reliability of capillary electrophoretic methods have allowed peptide and protein separation and characterization to be nearly routine. Although CZE–MS is a promising methodology, the related technique of CE–MS should also be practical and provides an attractive combination for biomolecule analysis. High-resolution CGE[49] and CIEF[50] with ESI-MS should also be viable and feasible in the near future.

As stated in a recent review article[51], "mass spectrometry is on the verge of becoming a primary research tool in the biological sciences". Coupled with high-resolution separation techniques, the ability of CE–MS and CE–MS–MS to provide structure determination of larger and larger biomolecules is expected to become of premier importance to the biological science community.

ACKNOWLEDGEMENTS

The research was supported by the U.S. Department of Energy, Office of Health and Environmental Research, under Contract DE-AC06-76RLO 1830. Pacific Northwest Laboratory is operated by Battelle Memorial Institute. The authors also thank H. K. Jones for assistance in the CZE–MS experiments.

REFERENCES

1 G. Wiedeman, *Pogg. Ann.*, 99 (1856) 197.
2 P. Koenig, *Actas III Congr. Sundam. Chim.*, 2 (1937) 334.
3 J. W. Jorgenson and K. D. Lukacs, *Science (Washington D.C.)*, 222 (1983) 266.
4 F. E. P. Mikkers, F. M. Everaerts and Th. P. E. M. Verhegge, *J. Chromatogr.*, 169 (1979) 11.
5 J. W. Jorgenson and K. D. Lukacs, *Anal. Chem.*, 53 (1981) 1298.
6 A. W. Adamson, *Physical Chemistry of Surfaces*, Wiley, New York, 1976.
7 V. Pretorius, B. J. Hopkins and J. D. Schieke, *J. Chromatogr.*, 99 (1974) 23.
8 P. A. David, P. J. Pellechia and D. L. Manning, *Anal. Chem.*, 58 (1986) 166.
9 K. D. Lukacs and J. W. Jorgenson, *J. High Resolut. Chromatogr. Chromatogr. Commun.*, 8 (1985) 407.
10 M. Martin and G. Guiochon, *Anal. Chem.*, 56 (1984) 614.
11 S. Hjertén, *J. Chromatogr.*, 347 (1985) 191.
12 S. Hjertén, K. Elenbring, F. Kilar, J. Liliao, A. J. C. Chen, C. J. Siebert and M. Deshu, *J. Chromatogr.*, 403 (1987) 47.
13 H. K. Jones and R. D. Smith, *J. Chromatogr.*, submitted for publication.
14 Y.-F. Cheng and N. J. Dovichi, *Science (Washington, D.C.)*, 242 (1988) 562.
15 M. Yu and N. J. Dolvichi, *Anal. Chem.*, 61 (1989) 37.
16 S. L. Pentoney, Jr., X. Huang, D. S. Burgi and R. N. Zare, *Anal. Chem.*, 60 (1988) 2625.
17 J. W. Jorgenson and K. D. Lukas, *J. Chromatogr.*, 218 (1981) 209.
18 J. S. Green and J. W. Jorgenson, *J. High Resolut. Chromatogr. Chromatogr. Commun.*, 7 (1984) 529.
19 Y. Walbroehl and J. W. Jorgensen, *J. Chromatogr.*, 315 (1984) 135.
20 H. H. Lauer and D. McManigill, *Anal. Chem.*, 58 (1986) 166.
21 D. J. Rose, Jr., and J. W. Jorgenson, *J. Chromatogr.*, 447 (1988) 117.
22 R. M. McCormick, *Anal. Chem.*, 60 (1988) 2322.
23 A. S. Cohen, A. Paulus and B. L. Karger, *Chromatographia*, 24 (1987) 15.
24 T. Tsuda, G. Nakagawa, M. Sato and K. Yagi, *J. Appl. Biochem.*, 5 (1983) 330.
25 W. G. Kuhr and E. S. Yeung, *Anal. Chem.*, 60 (1988) 2642.
26 A. S. Cohen, S. Terabe, J. A. Smith and B. L. Karger, *Anal. Chem.*, 59 (1987) 1021.
27 F. M. Everaerts, J. L. Beckers and Th. P. E. M. Verheggen, *Isotachophoresis: Theory, Instrumentation and Applications (Journal of Chromatography Library*, Vol. 6), Elsevier, Amsterdam, 1976.
28 R. D. Smith, H. R. Udseth, J. A. Loo, B. W. Wright an G. A. Ross, *Talanta*, 36 (1989) 161.
29 H. R. Udseth, J. A. Loo and R. D. Smith, *Anal. Chem*, 61 (1989) 228.
30 F. S. Stover, *J. Chromatogr.*, 445 (1988) 417.
31 M. Dole, L. L. Mack, R. L. Hines, R. C. Mobley, L. D. Ferguson and M. B. Alice, *J. Chem. Phys.*, 49 (1968) 2240.
32 M. Yamashita and J. B. Fenn, *J. Phys. Chem.*, 88 (1984) 4451.
33 M. Yamashita and J. B. Fenn, *J. Phys. Chem.*, 88 (1984) 4671.
34 C. M. Whitehouse, R. N. Dreyer, M. Yamashita and J. B. Fenn, *Anal. Chem.*, 57 (1985) 675.
35 S. F. Wong, C. K. Meng and J. B. Fenn, *J. Phys. Chem.*, 92 (1988) 546.
36 C. K. Meng, M. Mann and J. B. Fenn, *Z. Phys. D, Atoms, Molecules and Clusters*, 10 (1988) 361.

37 E. D. Lee, W. Mück, J. D. Henion and T. R. Covey, *J. Chromatogr.*, 458 (1988) 313.
38 J. A. Olivares, N. T. Nguyen, C. R. Yonker and R. D. Smith, *Anal. Chem.*, 59 (1987) 1230.
39 R. D. Smith, J. A. Olivares, N. T. Nguyen and H. R. Udseth, *Anal. Chem.*, 60 (1988) 436.
40 R. D. Smith, C. J. Barinaga and H. R. Udseth, *Anal. Chem.*, 60 (1988) 1948.
41 C. G. Edmonds, J. A. Loo, H. R. Udseth and R. D. Smith, in preparation.
42 J. A. Loo, H. R. Udseth and R. D. Smith, *Biomed. Environ. Mass Spectrom.*, 17 (1988) 411.
43 J. A. Loo, H. R. Udseth and R. D. Smith, *Anal. Biochem.*, in press.
44 J. A. Loo, H. R. Udseth and R. D. Smith, *Rapid Commun. Mass Spectrom.*, 2 (1988) 207.
45 F. W. McLafferty (Editor), *Tandem Mass Spectrometry*, Wiley, New York, 1983.
46 C. J. Barinaga, H. R. Udseth and R. D. Smith, *Rapid Commun. Mass Spectrom.*, in press.
47 R. J. Cotter, *Anal. Chem*, 60 (1988) 781A.
48 R. D. Smith, C. J. Barinage and H. R. Udseth, *J. Phys. Chem.*, in press.
49 A. S. Cohen and B. L. Karger, *J. Chromatogr.*, 397 (1987) 409.
50 S. Hjerten and M.-D. Zhu, *J. Chromatogr.*, 346 (1985) 265.
51 A. L. Burlingame, D. Maltby, D. H. Russel and P. T. Holland, *Anal. Chem.*, 60 (1988) 294R.

Journal of Chromatography, 474 (1989) 39–50
Elsevier Science Publishers B.V., Amsterdam — Printed in The Netherlands

CHROM. 21 204

MICROCOLUMN LIQUID CHROMATOGRAPHY–MASS SPECTROMETRY USING MOVING BELT AND CONTINUOUS FLOW FAST ATOM BOMBARDMENT INTERFACES

A. C. BAREFOOT and R. W. REISER*
E. I. du Pont de Nemours and Co., Agricultural Products Department, Experimental Station, Wilmington, DE 19880-0402 (U.S.A.)
and
S. A. COUSINS
E. I. du Pont de Nemours and Co., Engineering Department, Engineering Development Lab., Wilmington, DE 19898 (U.S.A.)

SUMMARY

Packed fused-silica liquid chromatographic columns were interfaced to a magnetic mass spectrometer using a commercially available moving belt interface to obtain electron ionization and chemical ionization mass spectra, and a continuous flow fast atom bombardment interface built in our laboratories to obtain fast atom bombardment mass spectra. Good quality spectra were obtained on 0.1-μg samples injected into the liquid chromatographic column with all three ionization techniques. Examples showing the utility of these techniques for the identification of herbicides and their plant metabolites are presented.

INTRODUCTION

In our work on the identification of pesticide metabolites isolated from plants, animals, soil or water, we frequently have very small quantities of sample to work with. Typically, the total amount of metabolite isolated is 1 μg or less. These samples often contain impurities which preclude their analyses by mass spectral probe techniques. Most of these metabolites are too polar or thermally labile for direct gas chromatographic–mass spectrometric (GC–MS) analysis, and many cannot be derivatized for GC–MS, therefore liquid chromatography (LC)–MS is the method of choice for their identification.

Miniaturization of the LC column has allowed us to obtain improved performance of the moving belt interface with reversed-phase columns using aqueous mobile phases[1,2]. The moving belt interface allows one to obtain electron ionization (EI) spectra for structural information and library searching, and chemical ionization (CI) spectra with a choice of reagent gases[3,4]. LC-fast atom bombardment (FAB)–MS with a moving belt interface has been reported in the literature[3,5], but the sensitivity is poor, possibly due to the short residence time of the sample in the ion source. With the

0021-9673/89/$03.50

continuous flow FAB interface[6], the sample remains on the FAB target until it is ionized, vaporized or sputtered away. Continuous flow FAB has been interfaced to a conventional bore LC column[7]; however the column effluent was split and only about 1% was introduced into the mass spectrometer. Recent work in several laboratories[8,9] has shown the potential of interfacing packed fused-silica capillary LC columns with continuous flow FAB, where the entire sample is introduced to the mass spectrometer.

We have designed and constructed a continuous flow FAB (CFF) interface which is interchangeable with the moving belt interface. This paper reviews the performance of the CFF interface, and demonstrates the utility of the LC–MS in the EI, CI and FAB modes for the identification of herbicides and their plant metabolites.

EXPERIMENTAL

The 0.25-mm I.D. fused-silica columns (J&W Scientific, Folsom, CA, U.S.A.) were slurry packed with 3-μm Nucleosil ODS (Macherey-Nagel, Duren, F.R.G.), as described in ref. 1. A 0.05-mm I.D. fused-silica (SGE, Austin, TX, U.S.A.) transfer line of approximately 70 cm length was epoxy bonded into the column.

A Beckman Model 114M LC pump was used for both packing columns and LC–MS analyses. For LC–MS, the constant pressure mode was used. Typical pressures for a 30-cm column were 140–190 bar to obtain flow-rates from 1 to 3 μl/min.

A Valco (Houston, TX, U.S.A.) Model C14W submicroliter injection valve with a 0.1-μl rotor was used. The analysis of dilute solutions was accomplished by removing the rotor and slowly depositing 1–5 μl of the sample dissolved in a volatile solvent, such as methanol or acetonitrile, while allowing the solvent to evaporate[1,2]. The rotor was replaced, flow restored, and the sample was injected by turning the valve to the "inject" position for 10 s.

A Finnigan MAT Model 8230 magnetic-sector mass spectrometer equipped with a moving belt interface[3,4] was used. A schematic diagram of this interface is

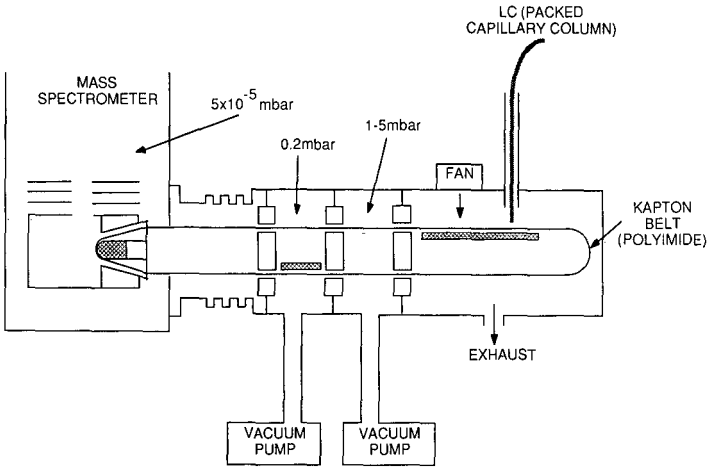

Fig. 1. Schematic diagram of moving belt interface.

shown in Fig. 1. The 0.05-mm I.D. fused-silica transfer line was fed through stainless-steel capillary tubing and adjusted so it just touched the center of the moving belt. The following interface settings were used: belt speed, 3 cm/s; solvent evaporator temperature, 100°C; vaporizer tip set at 5 W; cleanup heater set at 80% (approximately 250°C). Typical MS conditions were: ion source temperature, 200°C; ionizing voltage, 70 eV in EI and 200 eV in CI; CI source pressure using ammonia as reagent gas, 0.5 Torr (source ion gauge reading $5 \cdot 10^{-4}$); resolution, 1000; scan rate, 2 s per decade.

A CFF probe was designed and constructed to be interchangeable with the moving belt interface, since the alignment of the moving belt with the hole in the ion source is very critical, and it is desirable not to dismount the hardware once it is aligned. Fig. 2 shows a schematic diagram of the CFF probe. The internal moving belt unit was removed, then the first chamber (atmospheric pressure chamber) was removed prior to inserting the CFF probe.

For CFF, the LC parameters were the same as described above. An Ion Tech FAB gun was used with xenon gas, at 8 kV anode voltage, 1–2 A discharge current and 0.4 mA monitor current. The ion source temperature was held at 200°C to provide heat to the capillary tip to prevent freezing of the LC solvent as it evaporates. The source ion gauge reading was $3 \cdot 10^{-4}$–$5 \cdot 10^{-4}$ mm during operation.

RESULTS AND DISCUSSION

CFF interface

The FAB target is heated by radiation from the ion source. With the source at 200°C, the target temperature is 45–50°C, which is about optimum for CFF[6]. A benefit of keeping the source at 200°C, rather than the normal low temperature commonly used for conventional FAB (used to prevent the matrix compound from evaporating from the target too fast), is less contamination/less frequent source cleaning.

The 0.05-mm I.D. fused-silica transfer line was fed through the center of the probe and adjusted so the end was flush with the stainless-steel FAB target. The hole in the target was obtained by wire electric discharge machining drilling, and was made slightly larger than the O.D. of the fused-silica tubing to obtain a snug fit. The snug fit

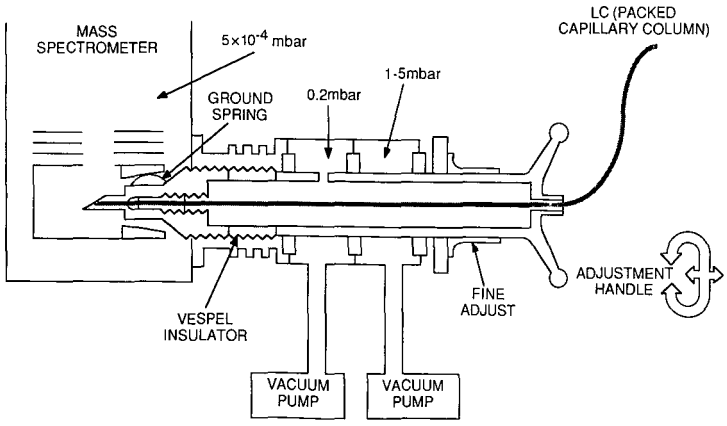

Fig. 2. Schematic diagram of continuous flow FAB interface.

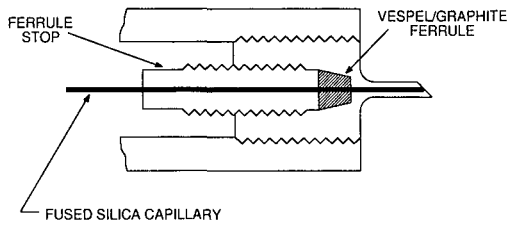

Fig. 3. Schematic diagram of threaded FAB target.

and a Vespel/graphite ferrule incorporated into the threaded FAB target, as shown on Fig. 3, prevent backflow of liquid into the probe.

Glycerol was added to the LC mobile phase at the 10% level. With acetonitrile–water mobile phases, addition of 10% glycerol caused the formation of two phases if the acetonitrile concentration was increased above 50%. We found acetonitrile–water–glycerol (50:40:10) to be a good general purpose mobile phase. If a stronger mobile phase is needed, methanol–water can be used, such as: methanol–water–glycerol (80:10:10). The mobile phase was degassed in an ultrasonic bath for 10 min to eliminate air bubbles which give an unstable vacuum. Mobile phase was prepared fresh weekly since aged mobile phase appeared to cause an unsteady vacuum, possibly due to bacterial action generating carbon dioxide. Typically a steady vacuum and matrix ion current was obtained about 30 min after start of operation.

With CFF we obtained a ten-fold increase in sensitivity over that obtained with the conventional FAB probe, likely due to increased sample concentration in the glycerol matrix since a much thinner film of glycerol is obtained with the continuous flow probe. Good quality FAB spectra were obtained on 0.1-μg quantities injected into the LC.

Fig. 4 shows a separation obtained on a mixture of four sulfonylurea herbicides

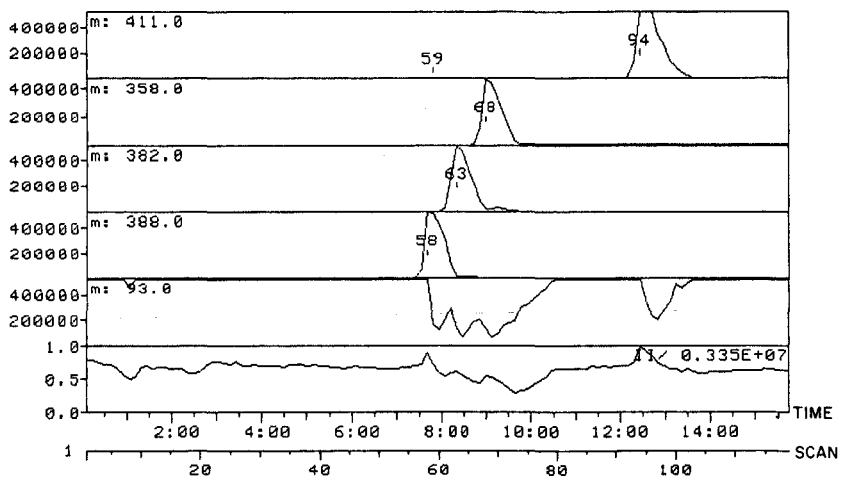

Fig. 4. Separation of four sulfonylurea herbicides, the active ingredients in: Harmony® (M + 1 at 388), Ally® (M + 1 at 382), Glean® (M + 1 at 358) and Londax® (M + 1 at 411), using LC–FAB-MS. Column: 30 cm × 0.25 mm I.D. Nucleosil ODS. Mobile phase: acetonitrile–glycerol–water (pH 3, formic acid) (50:10:40).

at the 0.1 μg/component level. The mass range scanned was 45–650, therefore the glycerol matrix ions were acquired by the data system. Since the glycerol ions were more intense than the sample ions, the LC peaks were not observed in the total ion plot (bottom trace). We have used two techniques to locate the LC peaks: (1) use the data system to re-plot the chromatogram using the high mass ions, *e.g.* *m/z* 300–650, (2) examine the plot of the protonated glycerol ion, *m/z* 93, which is often suppressed during elution of the LC peak as shown on Fig. 4. This suppression suggests a CI process is occurring, where the sample molecule is protonated by the glycerol ion.

Analysis of sulfometuron methyl and plant metabolites

An example showing the complementary data obtained on sulfometuron methyl, a sulfonylurea herbicide, and two plant metabolites using LC–MS in the EI, CI and FAB modes is presented. Fig. 5 shows the LC–EI-MS chromatogram obtained using the moving belt interface. The three components were readily separated by the reversed-phase LC column. The EI mass spectrum of the parent compound (sulfometuron methyl, the active ingredient in Oust® herbicide) is shown in Fig. 6. As with most sulfonylurea herbicides, a molecular ion is not obtained in the EI mass spectrum. However, a lot of structural information is obtained from the fragment ions, as shown in Fig. 6. Major fragment ions are obtained by cleavage on both sides of the carbonyl, which can allow one to deduce the molecular weight and assign a structure. The identity of the parent compound was confirmed by library search. The EI spectrum of the hydroxylated metabolite (Fig. 7) also gives a lot of structural information. The pyrimidine amine and isocyanate fragment ion are shifted sixteen mass units higher, showing that hydroxylation occurred on this side of the molecule. The EI mass spectrum of the glucose conjugate (Fig. 8) shows fragment ions from the sulfonyl isocyanate portion of the molecule, but is of minimum value for structure determination.

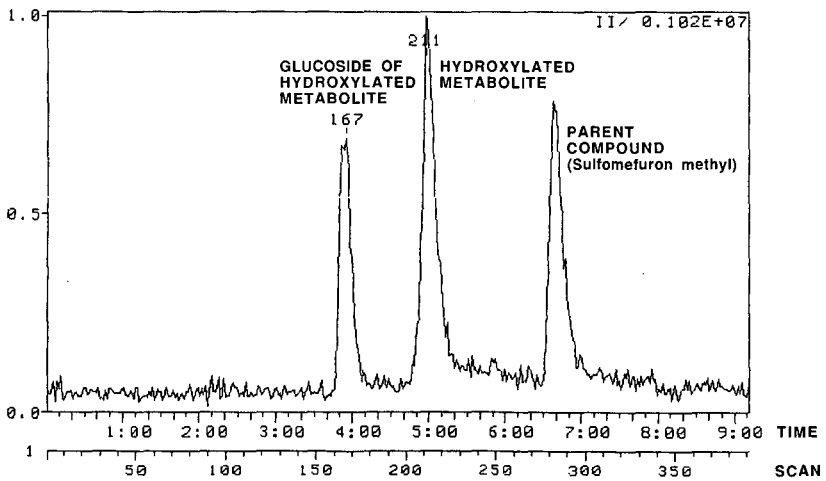

Fig. 5. Separation of sulfometuron methyl and two plant metabolites using LC–EI-MS. Column as in Fig. 1. Mobile phase: acetonitrile–water (60:40) (pH 3, formic acid).

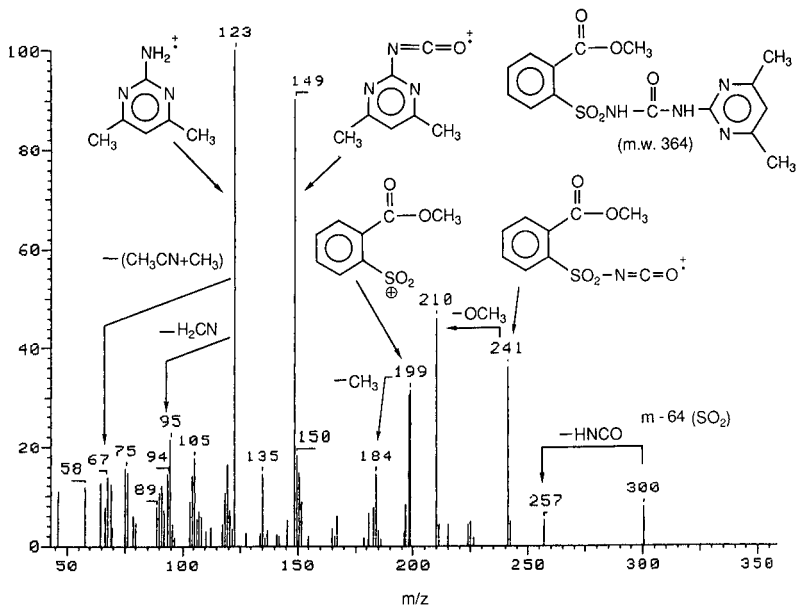

Fig. 6. EI mass spectrum of sulfometuron methyl.

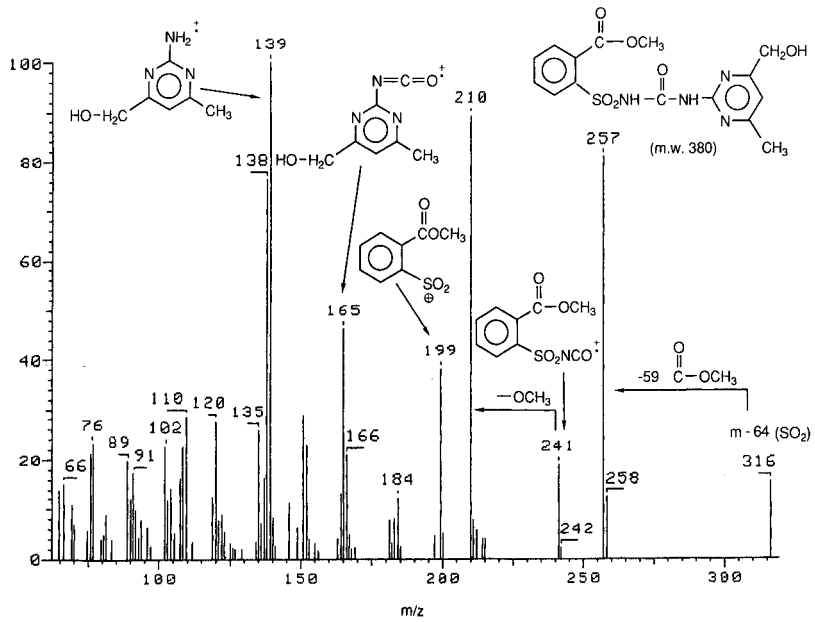

Fig. 7. EI mass spectrum of hydroxylated metabolite of sulfometuron methyl.

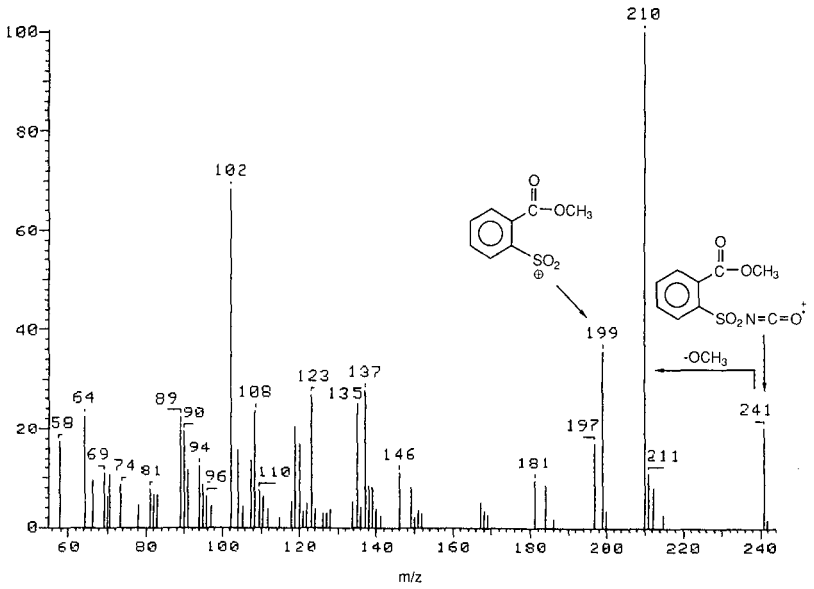

Fig. 8. EI mass spectrum of glucoside of hydroxylated sulfometuron methyl.

LC–MS using ammonia CI gave protonated molecular ions in the mass spectra of the parent compound and the hydroxylated metabolite, and structurally useful fragment ions due to cleavage on both sides of the carbonyl. The ammonia CI mass spectrum of the glucoside does not include molecular weight related ions, but does give structural information, as shown in Fig. 9. The thermospray mass spectrum of the

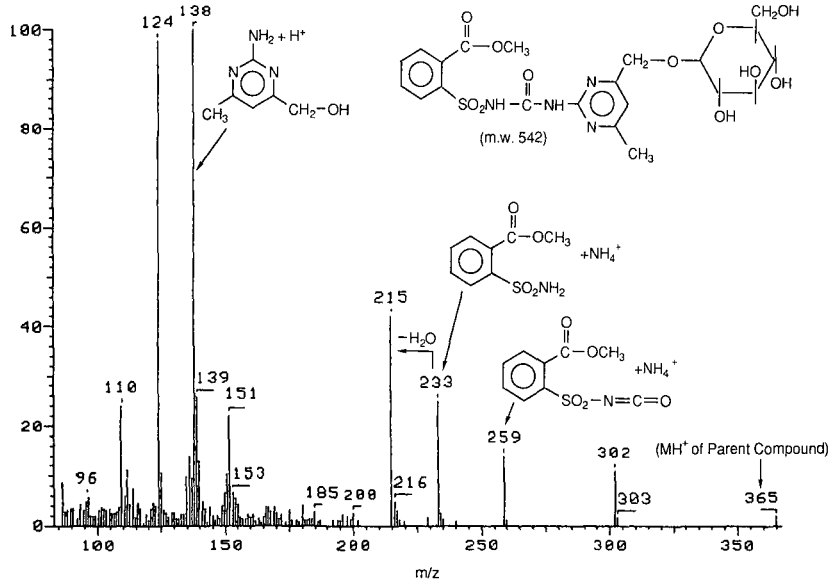

Fig. 9. Ammonia CI mass spectrum of glucoside of hydroxylated sulfometuron methyl.

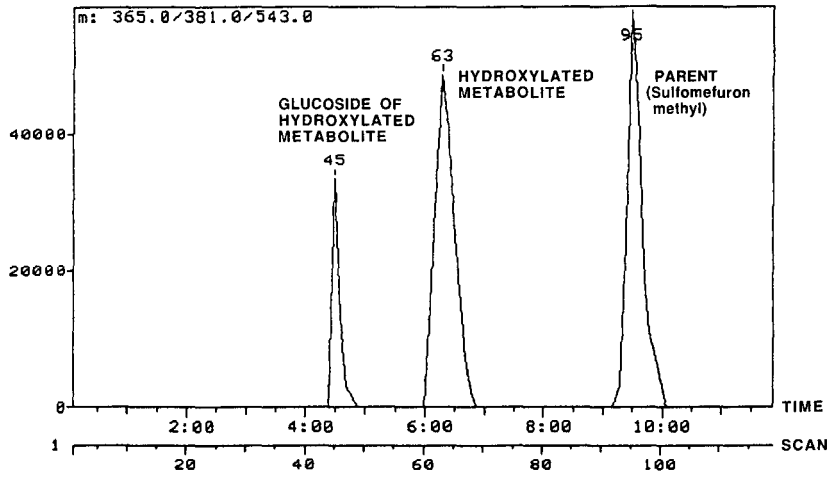

Fig. 10. Separation of sulfometuron methyl and two plant metabolites using LC–FAB-MS. Column and mobile phase as in Fig. 4.

glucoside was similar to the ammonia CI spectrum obtained with the moving belt interface, and also did not show molecular weight related ions[10].

The LC–FAB-MS chromatogram obtained by plotting the sum of the protonated molecular ion intensity for each component is shown on Fig. 10, and the background subtracted FAB spectra obtained are shown in Figs. 11–13. The glycerol matrix ions can easily be subtracted out of the spectra. The protonated molecular ion is the base peak in the FAB spectra of all three components. This is a particularly

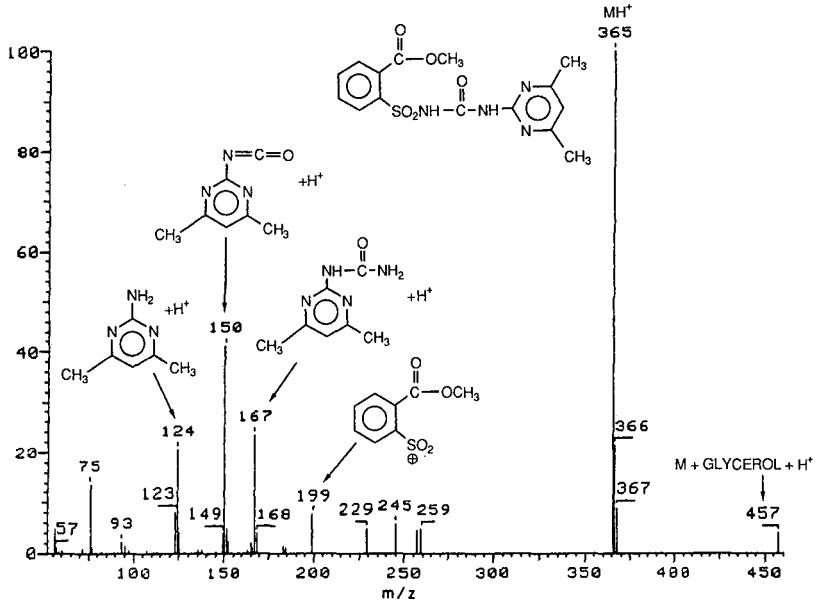

Fig. 11. FAB mass spectrum of sulfometuron methyl.

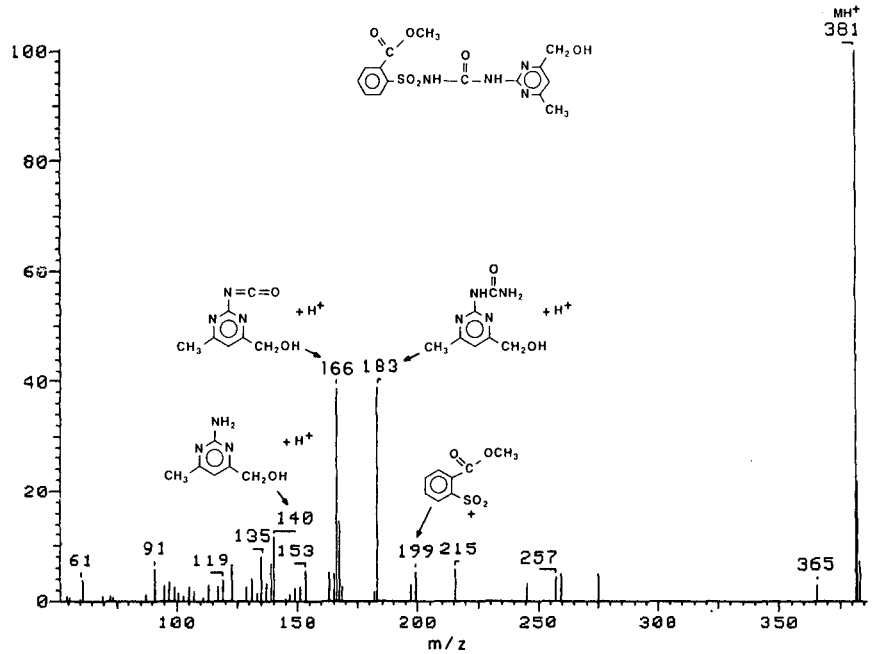

Fig. 12. FAB mass spectrum of hydroxylated sulfometuron methyl.

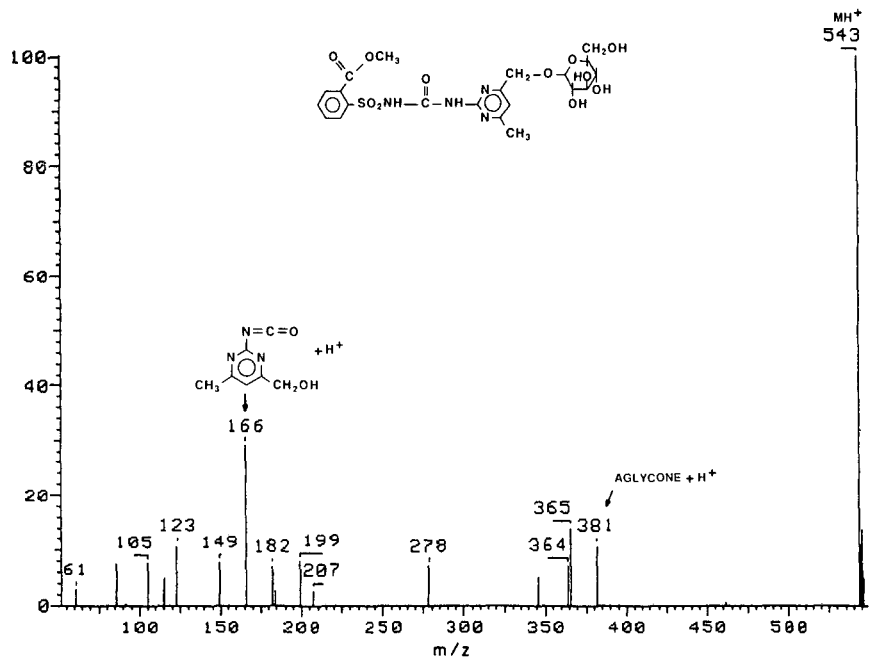

Fig. 13. FAB mass spectrum of glucoside of hydroxylated sulfometuron methyl.

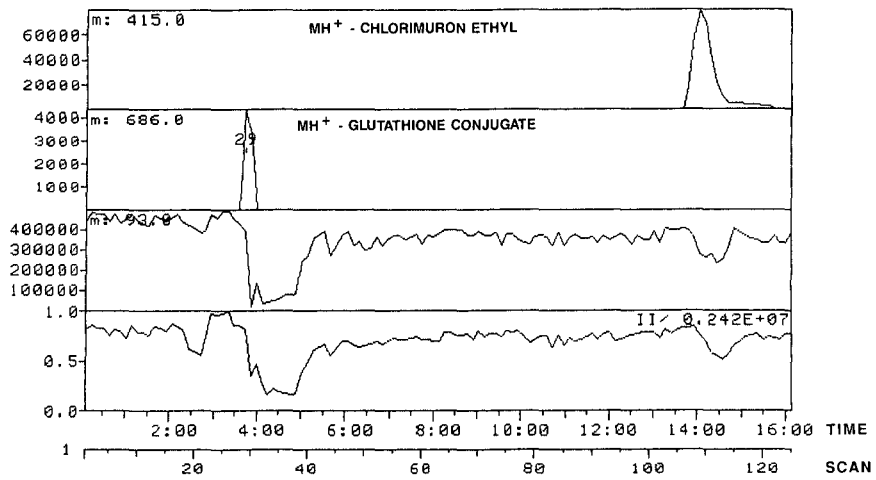

Fig. 14. Separation of chlorimuron ethyl and its glutathione conjugate using LC–FAB-MS. Column: 15 cm × 0.25 mm I.D. Nucleosil ODS. Mobile phase as in Fig. 4.

impressive result for the glucoside metabolite, since this is very polar and extremely thermally labile, and molecular ions were not obtained with ammonia CI or thermospray ionization. The FAB spectra also give some structural information, with fragment ions due to the protonated pyrimidine amine, isocyanate and urea and a weak fragment at *m/z* 199 due to the methyl benzoate sulfonyl ion, as shown in Figs. 11–13.

Analysis of chlorimuron ethyl and plant metabolite

Chlorimuron ethyl, the active ingredient in Classic® herbicide, forms a glutathione conjugate in plants through displacement of the chlorine atom. The LC–FAB-MS chromatographic data obtained on a mixture of chlorimuron ethyl and its glutathione conjugate are shown in Fig. 14, and the background subtracted FAB spectra are shown in Figs. 15 and 16. The spectra show prominent protonated molecular ions and [M + Na^+] adducts, and characteristic fragment ions. The glutathione conjugate did not show molecular ion adducts by LC–CI-MS or thermospray ionization[10], again showing the value of LC–FAB-MS for identification of polar conjugates.

CONCLUSIONS

The LC–EI-MS, LC–CI-MS and LC–FAB-MS techniques described in this paper have provided the high sensitivity and specificity needed for the identification of unknown metabolites obtained in environmental studies of agricultural chemicals. LC–FAB-MS is particularly valuable for obtaining molecular weights of highly polar metabolites that cannot be obtained by EI, CI or thermospray ionization techniques. We are using these techniques daily to identify unknown metabolites obtained in environmental studies of agricultural chemicals.

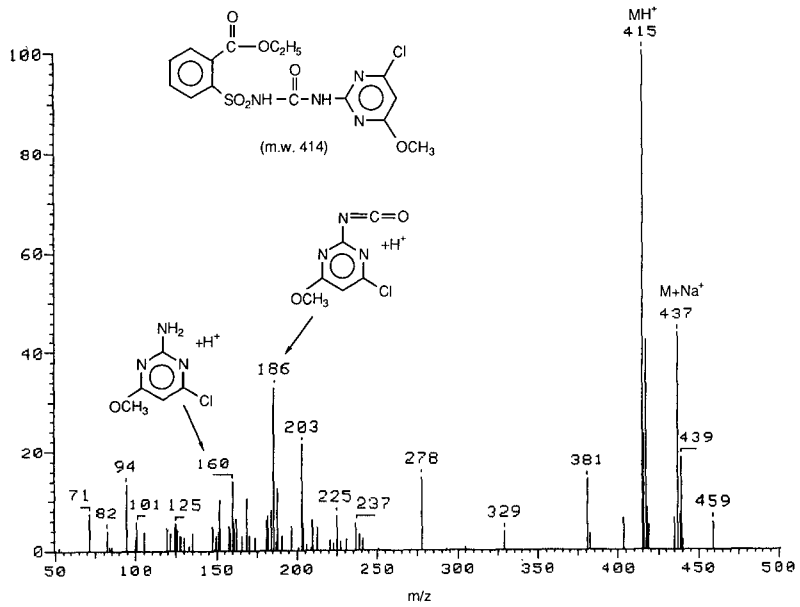

Fig. 15. FAB mass spectrum of chlorimuron ethyl.

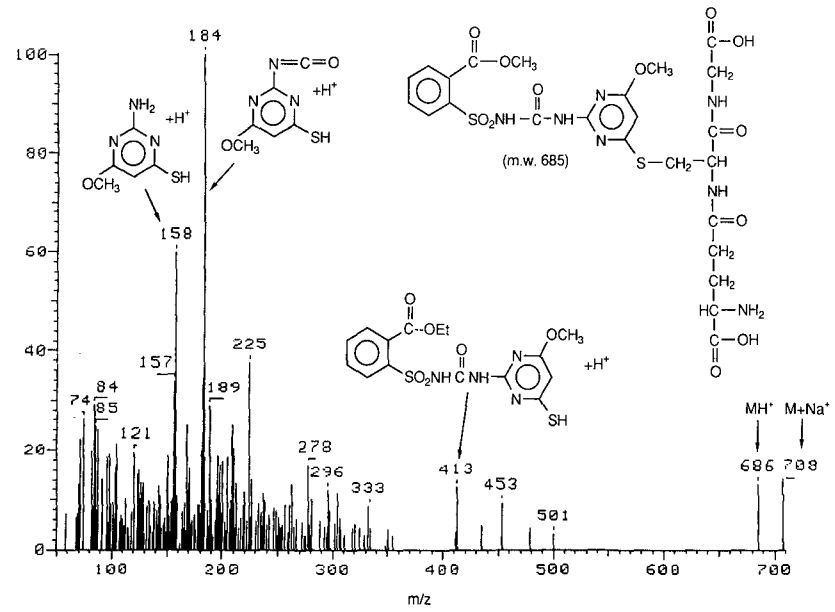

Fig. 16. FAB mass spectrum of glutathione conjugate of chlorimuron ethyl.

ACKNOWLEDGEMENT

We thank W. R. Johnson who carried out much of the LC–MS experimental work.

REFERENCES

1 A. C. Barefoot and R. W. Reiser, *J. Chromatogr.*, 398 (1987) 217.
2 A. C. Barefoot and R. W. Reiser, *Biomed. Environ. Mass Spectrom.*, 18 (1988) 77.
3 P. Doberstein, E. Korte, G. Meyerhoff and R. Pesh, *Int. J. Mass Spectrom. Ion Phys.*, 46 (1983) 185.
4 D. E. Games, M. A. McDowall, K. Levsen, K. H. Schafer, P. Doberstein and J. L. Gower, *Biomed. Mass Spectrom.*, 11 (1984) 87.
5 J. G. Stroh, J. C. Cook, R. M. Millberg, L. Brayton, T. Kihara, Z. Huang and K. L. Rinehart, Jr., *Anal. Chem.*, 57 (1985) 985.
6 R. M. Caprioli, T. Fan and J. S. Cottrell, *Anal. Chem.*, 58 (1986) 2949.
7 D. E. Games, S. Pleasance, E. D. Ramsey and M. A. McDowall, *Biomed. Environ. Mass Spectrom.*, 15 (1988) 179.
8 T. Takeuchi, S. Watanabe, N. Kondo, D. Ishii and M. Goto, *J. Chromatogr.*, 435 (1988) 482.
9 R. M. Caprioli, W. T. Moore, B. DaGue and M. Martin, *J. Chromatogr.*, 443 (1988) 355.
10 L. M. Shalaby, private communication.

Journal of Chromatography, 474 (1989) 51–58
Elsevier Science Publishers B.V., Amsterdam — Printed in The Netherlands

CHROM. 21 548

OPTIMISATION OF CONTINUOUS FLOW FAST ATOM BOMBARDMENT MASS SPECTROMETRY FOR BIOANALYSIS

J. A. PAGE* and M. T. BEER
Shell Research Limited, Sittingbourne Research Centre, Sittingbourne, Kent ME9 8AG (U.K.)
and
R. LAUBER
Department of Chemistry, University of Warwick, Coventry CV4 7AL (U.K.)

SUMMARY

Fast atom bombardment mass spectrometry (FAB-MS) has been employed very successfully over the last seven years for the analysis of polar and thermally-labile compounds which are frequently encountered in bioanalysis. The recently developed method of continuous flow FAB-MS (CF-FAB) as a liquid chromatography–MS interface and ionization method has opened up a new area of research in the analysis of biomolecules such as peptides and proteins. Ion suppression effects observed in standard FAB analysis seem to be reduced, and increased signal-to-noise gives better sensitivity for quantification. The optimisation of CF-FAB on the MAT90 magnetic sector mass spectrometer will be discussed. Applications in bioanalysis, *e.g.*, peptide analysis in conjunction with linked scan techniques, will also be reported.

INTRODUCTION

Fast atom bombardment mass spectrometry (FAB-MS) has been employed very successfully over the last seven years for the analysis of polar and thermally labile compounds[1] which are frequently encountered in bioanalysis. The recently developed method of continuous flow FAB-MS[2] (CF-FAB) offers a number of advantages over conventional FAB-MS, especially in the analysis of peptides and protein digests[3,4]. These are: more rapid analysis, the ability to monitor processes such as enzyme digestions and increased signal-to-noise ratio giving better sensitivity for quantification[5].

Potential applications for CF-FAB at Sittingbourne Research Centre (SRC) include directly coupled liquid chromatograpy (LC)–CF-FAB-MS of polar metabolites, antibiotics from fermentation broths, biosurfactant and peptide analysis. The analysis of peptide and protein digests by CF-FAB will allow enzyme digestions to be followed in real time with prior on-line reversed-phase high-performance liquid chromatographic (HPLC) separation of components[6].

0021-9673/89/$03.50

The CF-FAB probe was installed on the Finnigan MAT90 magnetic sector spectrometer in August, 1988. The initial aims were to optimise the performance of the CF-FAB method as follows. (i) To make the technique viable for peptide analysis with picomole sensitivity. (ii) To examine the feasibility of obtaining sequence information from peptides run by CF-FAB using linked scanning techniques on the MAT90 instrument.

The CF-FAB probe for the MAT90 instrument at SRC was the first delivered by Finnigan in Europe, with the exception of two prototype probes under development in collaboration with Finnigan MAT. The MAT90 is an ideal instrument on which to install the device because it is fully microprocessor controlled, facilitating easy programming of a sequence of scanning modes *i.e.*, normal spectrum acquisition followed by B/E linked scans [keeping the ratio of magnet to electric sector (B/E) constant] of the parent ions.

A number of features were critical in optimising the conditions for a stable flow and good sensitivity in the CF-FAB technique. These were (i) wettability of the probe tip; (ii) temperature of the probe tip; (iii) flow-rate of the solvent; (iv) solvent composition.

These important factors and their interrelations were examined using model peptides, and are discussed in this report.

EXPERIMENTAL

Design and operation of the CF-FAB probe

The probe, shown in Fig. 1, consists of a hollow shaft that is capped with an angled probe tip, through which a 0.7 m × 0.075 mm I.D. fused-silica capillary is passed. This is allowed to protrude by approximately 0.2 mm beyond the tip. The tip

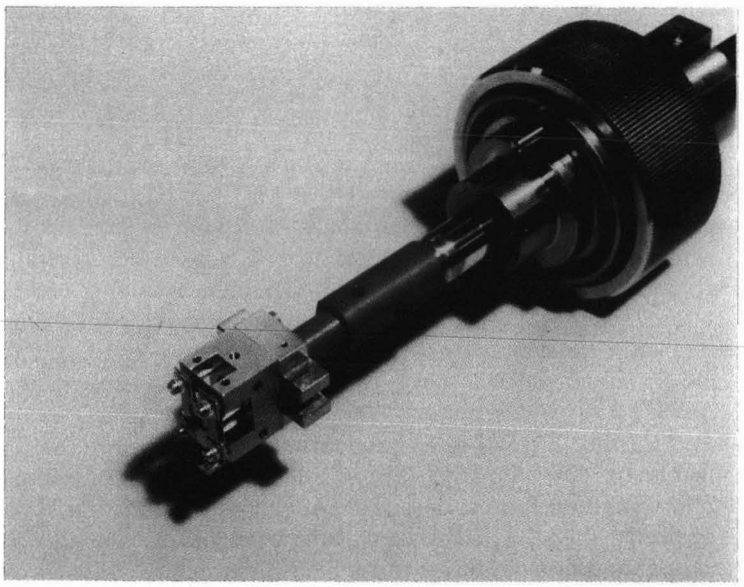

Fig. 1. Continuous flow FAB probe for the Finnigan MAT90 spectrometer.

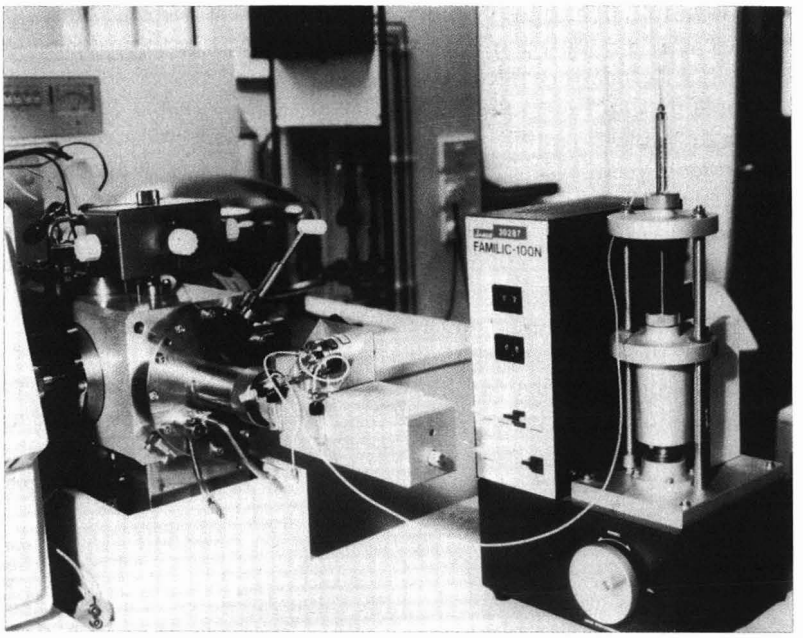

Fig. 2. CF-FAB probe in position on the MAT90 instrument.

is in contact with a paper wick, which is located inside the source ion volume directly below the probe tip. The capillary is connected to a Rheodyne injection valve (Model 7410) for injection of 0.5-μl amounts. The continuous flow solvent is provided by a suitable pump (a Jasco Famlic–100N) normally operated at 2–5 μl/min as shown in Fig. 2.

The FAB gun is operated at 8 keV and 1 mA current with Xenon bombarding gas, as with conventional FAB.

The two novel design features of the Finnigan MAT CF-FAB probe are (i) a paper wick below the probe tip to soak up the excess solvent running down the probe; (ii) an adjustment screw at the base of the probe to alter the position of the capillary tip in-situ (Fig. 2).

Reagents

Bradykinin, bradykinin potentiator B and renin substrate tetradecapeptide were obtained from Sigma. The samples were dissolved in the same solvent mixture as used for the continuous flow carrier solvent *i.e.,* typically glycerol–water–methanol–trifluoracetic acid (10:45:45:0.2, v/v).

RESULTS

Stability

Stable operation of the probe can be defined as the condition where a constant ion current is obtained from ions sputtering from the tip under steady solvent flow conditions, *i.e.,* 2–5 μl/min. This is achieved when the rate of evaporation of the

solvent from the probe tip is in balance with the pumping speed of the MS source. If this is not the case, boiling/bubbling of solvent occurs, giving rise to peak height fluctuations. It has been generally agreed[7] that fluctuations in peak heights within $\pm 10\%$ are acceptable, but that most CF-FAB systems take approximately half an hour to settle down to this level. Stable operation was very difficult to obtain on the MAT90 system and reproducible response for repeat 50-ng injections of undecanoic acid was poor as shown in Fig. 3. The upper trace represents the selected mass trace for the $[M - H]^-$ ion, showing variation in peak height of $\pm 50\%$. The lower trace represents the total ion current trace and indicates the instability. The mass spectrum obtained, however, shows good signal-to-noise ratio. Repeat injections could be made every 2–3 min with no significant memory effects with dilute solutions, although with sample quantities in excess of 100 ng slight memory effects become apparent.

The Rheodyne injector supplied had a fixed internal loop of nominal volume 0.5 μl. Use of 1-, 2- and 5-μl sample volumes to fill this internal loop gave inconsistent results. Only with sample volumes >10 μl were reproducible ion current traces obtained. It was concluded, therefore, that dead volumes within the valve precluded its use with <10 μl sample volumes.

Modifications

Two modifications were made, which radically enhanced the performance and stability of the CF-FAB probe. (i) The Rheodyne valve supplied by Finnigan MAT was replaced by a Model 7125 with a 10-μl external loop. A better model, the 8125 with lower dead volumes, is to be ordered. (ii) The length of capillary within the probe was increased to 1.1 m of 0.05 mm I.D. This may have acted as a flow restrictor applying a back pressure to the pump and greatly increased stability.

The effect of the above allowed stability to $\pm 10\%$ for full day operation.

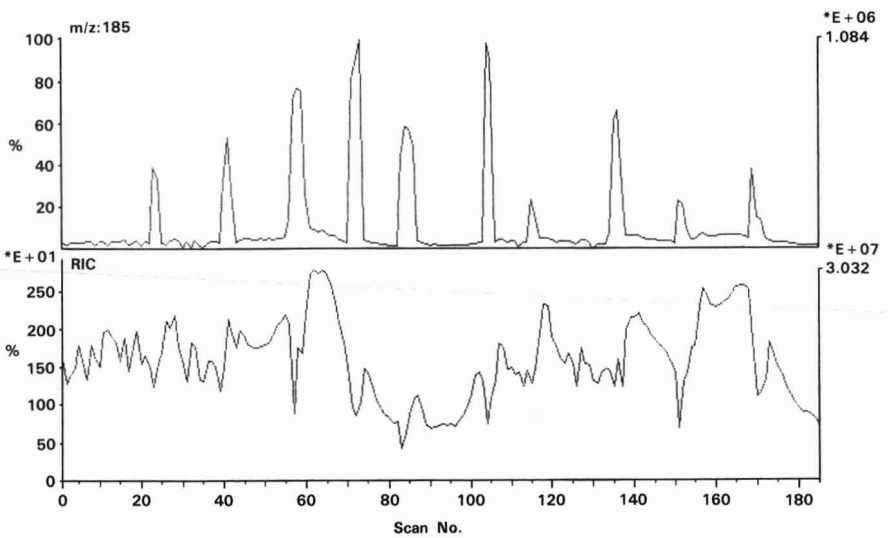

Fig. 3. Repeat injection of 50 ng of undecanoic acid.

Wettability of the probe tip

Even coating of solvent from the capillary onto the probe tip was critical. Acid etching of the surface was found most effective. Wettability varied with solvent composition, methanol–water mixtures being better than water or water–acetonitrile.

Role of the wick

The wick, situated below and in contact with the probe tip, consists of a wad of compressed filter paper approximately 6 mm diameter and 3 mm depth. The role of this wick is to ensure an even thin film of solvent across the probe reducing the formation of droplets thus stabilising the ion current produced. In addition, evaporation takes place from the flow of solvent rather than on the end of the capillary, therefore reducing sample memory effects. A deterioration in stability was observed when the wick was omitted. The wick was replaced when saturated with solvent. In practice this depended upon solvent composition and flow-rate and more critically upon the glycerol content. Using 10% glycerol in the solvent the wick was replaced daily.

Probe tip temperature

The probe tip is heated indirectly from the source. Its temperature was not easy to control. A temperature of approximately 40°C at the tip was required to avoid freezing of the solvent within the capillary tip. The design of this could be improved to allow direct heating and faster response to changes. Lower probe temperatures resulted in decreased ion currents and reduced stability. Reoptimisation was necessary with changes in solvent composition, however, adjustment of capillary position had a greater effect than change in probe temperature.

Solvent flow-rates

Flow-rates of 1–7 μl/min were evaluated. 5 μl/min and above led to sputtering of the liquid surface formed on the tip, giving rise to unsteady ion currents and very high source pressures $> 10^{-3}$ Torr. Low flow-rates led to a diffusion of sample and broad peak shape. 3–4 μl/min was found optimum for most solvent systems.

Solvent composition

Initial solvents of water, water–methanol, acetonitrile–water were made up with 20% glycerol. It was desirable to reduce the glycerol content to make the solvent more suitable for HPLC columns. A reduction to 10% glycerol was tolerated with no reduction in sensitivity. Optimising the capillary position for different solvent compositions was essential to retain a wet film of solvent on the probe tip at the position where the atom beam impinges. This could be easily carried out on this probe design.

Model peptides

A range of peptides *i.e.*, bradykinin, bradykinin potentiator B, renin substrate in the 1000–2000 dalton molecular weight range could be run by CF-FAB at the 1–2-pmol level. Fig. 4 shows the $[M + H]^+$ of bradykinin for 2 pmol injected. For comparable spectra from the conventional FAB probe nanomol of sample are required. Mixtures of three peptides all at the 40-pmol level gave very similar responses, unlike conventional FAB where suppression effects are known to occur.

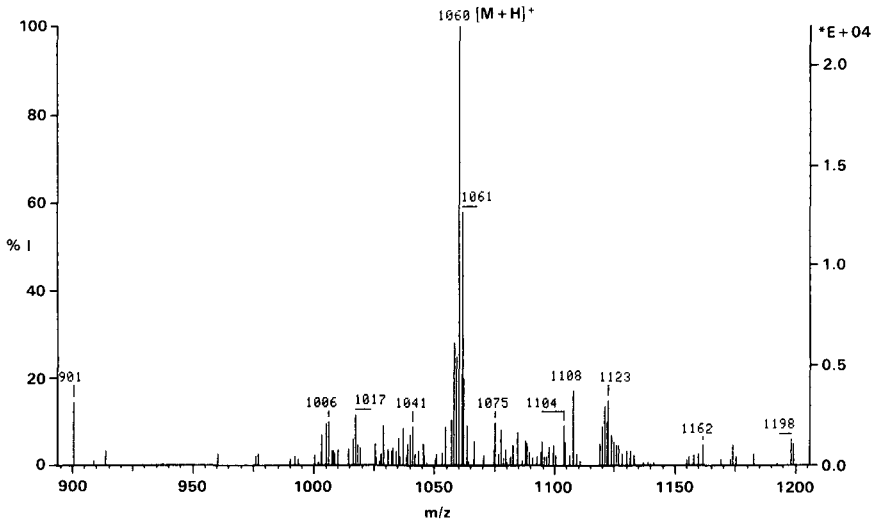

Fig. 4. CF-FAB spectrum of bradykinin (2 pmol).

Linked scans

Collision-induced fragmentation could be obtained on the peptide molecular ions, by the introduction of helium into the first field free region gas cell (between the source and the magnetic sector). Daughter or fragment ions formed could be analysed by a B/E constant scan from the parent ion. This was done from the conventional FAB probe (Fig. 5) and from the CF-FAB probe (Fig. 6). 100 pmol of sample was utilised for the CF-FAB, whereas approximately 10 nmol was required for the conventional FAB analysis to give comparable signal-to-noise ratios. Comparing the B/E spectra of bradykinin potentiator B run under conventional FAB conditions (Fig. 5)

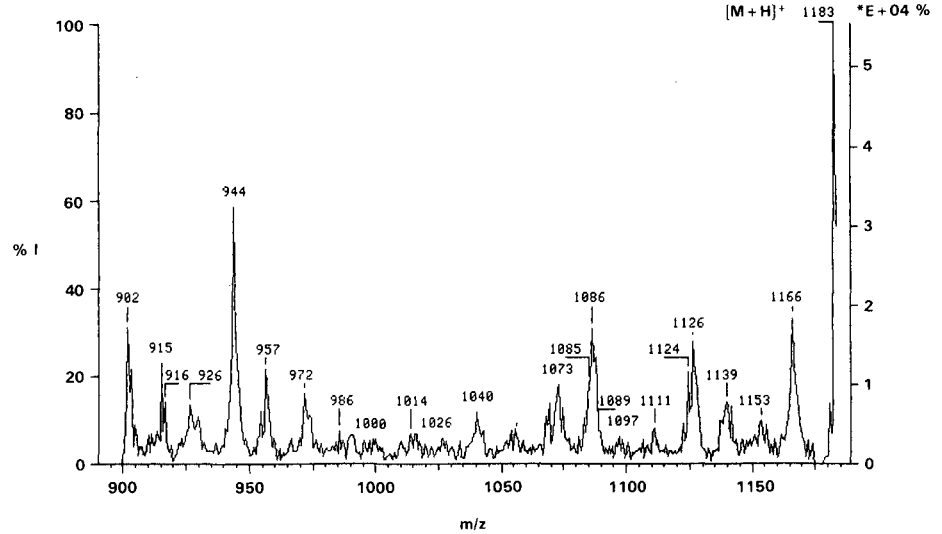

Fig. 5. B/E linked scan of bradykinin potentiator B from conventional FAB probe (10 nmol).

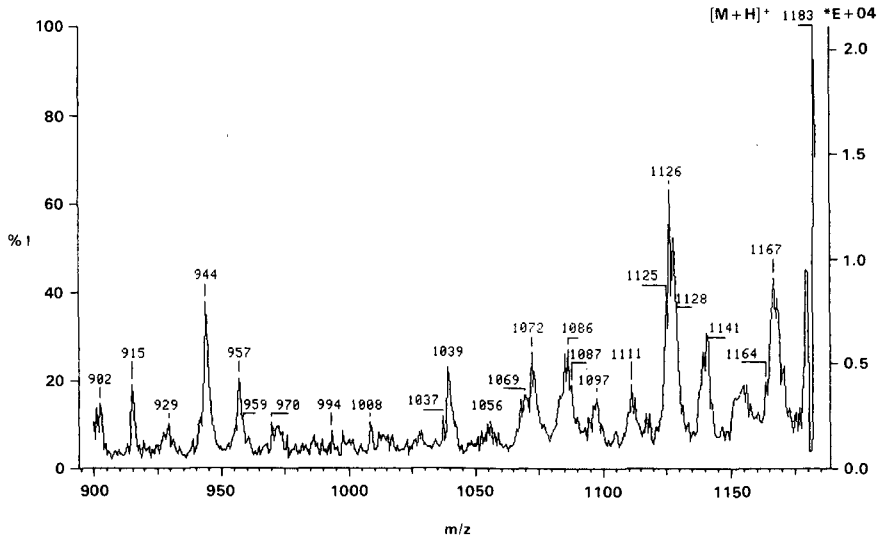

Fig. 6. B/E linked scan of bradykinin potentiator B from CF-FAB probe (100 pmol).

and from the CF-FAB (Fig. 6) the same daughter ions are present, however, intensities do vary. Significant fragment ions could be rationalised by amino acid cleavages from N- or C-termini, and according to fragmentation behaviour of peptides in collision dissociation mode[8–10]. Some assumptions have been made about amino acid side chain losses. Table I lists the peaks observed and assignment has been made with the Roepstorff and Fohlman nomenclature[11].

TABLE I

FAB B/E LINKED SCAN ANALYSIS OF BRADYKININ POTENTIATOR B (900 > 1183 μ)

pGlu-Gly-Leu-Pro-Pro-Arg-Pro-Lys-Ile-Pro-Pro.

m/z	*Assignment*[a]
1183	$[M + H]^+$ or protonated molecular ion
1166	B11
1139	MH − Arg side chain
1138	A11
1126	MH − Leu side chain
1086	C10
1073	Y10
1069	B10
1040	A10
972	B9
957	MH − Leu, Arg, Lys side chain
944	A9
902	Y8

[a] Using Roepstorff and Fohlman nomenclature.

DISCUSSION

These initial results indicate that CF-FAB can be used to analyse polar and thermally labile compounds encountered in bioanalysis and the following preliminary conclusions can be drawn. (i) It can be 100 times more sensitive than conventional FAB; (ii) may be used with a range of solvents compatible with HPLC systems; (iii) provides a rapid method for analysis of samples injected via a loop into the solvent flow; (iv) is compatible with linked scanning techniques.

Further work is continuing with on-line coupling to HPLC, linked scanning techniques and optimisation of performance for a wider range of compounds.

ACKNOWLEDGEMENTS

We would like to thank Dr. Rolf Lauber, a post doctoral research fellow (Warwick University), for his major contributions in establishing the flow FAB technique at SRC, and Professor K. Jennings (Warwick University) for useful discussions.

REFERENCES

1 J. A. Page, in C. S. Creaser and A. M. C. Davies (Editors), *Analytical Applications of Spectroscopy*, Royal Society of Chemistry, London, 1988, p. 274.
2 R. M. Caprioli, T. Fan and J. S. Cottrell, *Anal. Chem.*, 58 (1986) 2949.
3 A. E. Ashcroft, J. R. Chapman and J. S. Cottrell, *J. Chromatogr.*, 394 (1987) 15.
4 A. E. Ashcroft, *Org. Mass Spectrom.*, 22 (1987) 754.
5 R. M. Caprioli, W. T. Moore and T. Fan, *Rapid Commun. Mass Spectrom.*, 1 (1987) 15.
6 D. W. Hutchinson, A. R. Woolfitt and A. E. Ashcroft, *Org. Mass Spectrom.*, 22 (1987) 304.
7 R. M. Caprioli, presented at the *36th Annual Conference on Mass Spectrometry and Allied Topics, San Francisco, CA, 1988.*
8 W. Herma, J. P. Kamerling, A. J. Slotboom and G. J. M. van Scharrenburg, *Biomed. Mass Spectrom.*, 10 (1983) 13.
9 D. L. Lippstreu-Fisher and M. L. Gross, *Anal. Chem.*, 57 (1985) 1174.
10 D. M. Desiderio, *Int. J. Mass Spectrom. Ion Proc.*, 74 (1986) 217.
11 P. Roepstorff and J. Fohlman, *Biomed. Mass Spectrom.*, 11 (1984) 601.

Journal of Chromatography, 474 (1989) 59–68
Elsevier Science Publishers B.V., Amsterdam — Printed in The Netherlands

CHROM. 21 378

APPLICABILITY OF CONTINUOUS-FLOW FAST ATOM BOMBARDMENT LIQUID CHROMATOGRAPHY–MASS SPECTROMETRY IN BIOANALYSIS

DEXTROMETHORPHAN IN PLASMA

P. KOKKONEN

TNO-CIVO Institutes, P.O. Box 360, 3700 AJ Zeist (The Netherlands) and Division of Analytical Chemistry, Center for Bio-Pharmaceutical Sciences, Gorlaeus Laboratories, P.O. Box 9502, 2300 RA Leiden (The Netherlands)

W. M. A. NIESSEN* and U. R. TJADEN

Division of Analytical Chemistry, Center for Bio-Pharmaceutical Sciences, Gorlaeus Laboratories, P.O. Box 9502, 2300 RA Leiden (The Netherlands)

and

J. VAN DER GREEF

TNO-CIVO Institutes, P.O. Box 360, 3700 AJ Zeist (The Netherlands) and Division of Analytical Chemistry, Center for Bio-Pharmaceutical Sciences, Gorlaeus Laboratories, P.O. Box 9502, 2300 RA Leiden (The Netherlands)

SUMMARY

Continuous-flow fast atom bombardment (CF-FAB) is an interface for combined liquid chromatography–mass spectrometry using FAB as the ionization method. The applicability of CF-FAB for quantitative bioanalysis was studied for a model compound, dextromethorphan, in plasma samples using conventional high-performance liquid chromatography. The flow-rate reduction was achieved either by splitting or by the phase-system switching approach. The features of both systems are discussed.

INTRODUCTION

In recent years various liquid chromatography–mass spectrometry (LC–MS) interfaces have been developed and successfully applied in bioanalysis[1]. Despite the fast progress, a number of difficulties still exist in daily practice strongly depending on the interface type used. Many of the interfaces have limitations in the handling of very polar and thermally labile compounds frequently encountered in bioanalysis. In this respect the recently introduced method of continuous-flow fast atom bombardment (CF-FAB)[2,3] has opened up new possibilities. The CF-FAB technique has been used for the analysis of peptides[3–11], dansylated amino acids[6], antibiotics[7,12], bile acids[2,13] and oligosaccharides[14].

CF-FAB has so far mainly been applied in qualitative analysis using either flow injection analysis[2–4,6–9,12–14] or micro high-performance liquid chromatography

0021-9673/89/$03.50

(HPLC)[2,5–14]. Advantages of CF-FAB over conventional FAB are the fact that ion-suppression effects are reduced considerably and the determination limits are improved[3,4]. Therefore, it is interesting to explore the potential of CF-FAB in quantitative analysis.

Dextromethorphan, (+)-3-methoxy-17-methylmorphinan, was selected as the model compound, because of its solubility and high stability in water and its good FAB sensitivity, especially in acidic solutions. Methods for the determination of dextromethorphan and its metabolites in human plasma[15,16] and urine[15] have been reported using conventional HPLC with fluorescence detection. Typical concentration levels of dextromethorphan in plasma are less than 10 ng/ml after a single dose of 60 mg of dextromethorphan hydrobromide[15,17]. The applicability of the CF-FAB method for quantitative bioanalysis was studied by analysing dextromethorphan in plasma. Because conventional HPLC is used in most bioanalytical studies, the possibilities of conventional HPLC coupled with CF-FAB were investigated. Flow-rate reduction is achieved by using a splitter between the HPLC apparatus and the CF-FAB interface.

EXPERIMENTAL

Equipment

The two different experimental set-ups that have been used are referred in the text as system I and system II. The most important differences between those two systems are summarized in Table I.

The HPLC system consisted of either a Pharmacia P-3500 pump (Uppsala, Sweden) or an LKB 2150 pump (Bromma, Sweden), a Rheodyne 7125 injector (20 μl, Berkeley, CA, U.S.A.) and a Techopak reversed-phase C_{18} column (15 cm × 3.9 mm I.D., packed with 10 μm material, HPLC Technology, Cheshire, U.K.). The temperature of the column and the stainless steel capillaries was kept at 56°C in order to reduce the viscosity of the mobile phase. The column effluent was directed to a splitter (see below), which was connected to a Finnigan MAT prototype CF-FAB

TABLE I

SYSTEM DESCRIPTIONS

	System I	*System II*
Pump	Pharmacia	LKB
Mobile phase[a]	TFA–Gly–ACN–H_2O	TFA–Gly–ACN–H_2O
Composition (w/w%)	0.25-10-30-59.75	0.25-9.9-29.8-60.05
HPLC flow-rate	1.0 ml/min	1.2 ml/min
Split capillary	19 cm × 200 μm I.D.	44 cm × 150 μm I.D.
CF-FAB capillary	85 cm × 75 μm I.D.	75 cm × 75 μm I.D.
Split ratio	1:200	1:170
Split flow-rate	5 μl/min	7 μl/min
Mass spectrometer	MAT 8200	MAT 90
Data system	SS300	ICIS
Source temperature	40°C	60°C
Source pressure	*ca.* 0.1 Pa	*ca.* 0.01 Pa

[a] TFA = trifluoroacetic acid; Gly = glycerol; ACN = acetonitrile.

probe (Bremen, F.R.G.) with a stainless steel target. The CF-FAB probe was fitted on to either a Finnigan MAT 8200 or Finnigan MAT 90 double-focusing mass spectrometer, operated at 3 kV and 5 kV, respectively. Both instruments were equipped with a FAB gun (Ion Tech, Teddington, U.K.) using xenon and producing a beam of neutral atoms of 6 kV energy.

In the Finnigan MAT 90 instrument (system II) an exchangeable ion volume with a wick was applied. The wick was prepared from compressed paper and positioned at the bottom of the ion volume. Additional vacuum pumping at the ion source housing was obtained by a liquid nitrogen trap. In the Finnigan MAT 8200 instrument (system I) there was no possibility to use an exchangeable ion volume, a wick or a cold trap.

A schematic diagram of the laboratory-made splitter is given in Fig. 1. The HPLC column was connected to a zero dead volume stainless-steel union-T (TEE.020″, Upchurch Scientific, Washington, U.S.A.) by means of a short stainless-steel capillary (1/16 in. O.D., 0.5 mm I.D.) in which the 75 μm I.D. fused-silica capillary (SGE, Melbourne, Australia) going to the CF-FAB probe is inserted to a position as close as possible to the column end. The split ratio was determined by the length and internal diameter of the fused-silica capillaries, the actual dimensions of which are given in Table I. The flow-rates stated in Table I were measured by weighing the effluents.

Reagents

Dextromethorphan hydrobromide was obtained from the Research Center of Orion Pharmaceutica (Espoo, Finland). Trifluoroacetic acid and hexane were purchased from E, Merck (Darmstadt, F.R.G.). Glycerol (98% chem. pure) was supplied by Lamers & Pleuger ('s Hertogenbosch, The Netherlands), acetonitrile (ChromAR) by Promochem (Wesel, F.R.G.), sodium carbonate (AnalaR) by BDH (Poole, U.K.) and triethylamine by Pierce (Rockford, IL, U.S.A.). Water was distilled before use.

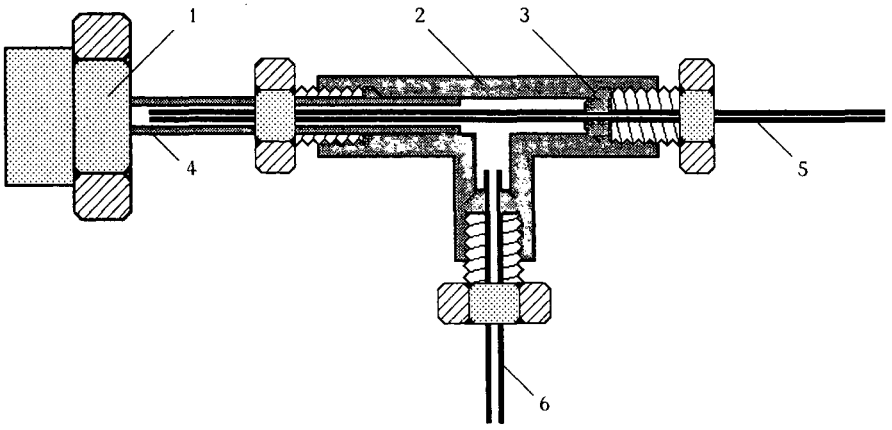

Fig. 1. Schematic diagram of the CF-FAB splitter. 1 = LC column; 2 = union-T; 3 = vespel ferrule; 4 = stainless-steel capillary; 5 = CF-FAB capillary (75 μm I.D.); 6 = split capillary (200 μm I.D.).

The mobile phase was prepared daily in order to avoid bacterial growth and mould formation. Before use it was filtered and degassed ultrasonically. The mobile phase reservoir was flushed with helium during the experiments.

Sample preparation

Stock solutions containing 15 mg of dextromethorphan hydrobromide were prepared in 10 ml of water. Plasma samples containing 0.11, 0.22, 0.44, 0.88, 1.75, 3.5, 7.0, 14.0 and 28.0 μg/ml of dextromethorphan were prepared by adding the appropriate amount of dextromethorphan in 50 μl of water to 2.0 ml of blank human plasma. A mixture of 0.5 ml of saturated sodium carbonate in water and 5 ml of 0.1% (v/v) of triethylamine in hexane was added to the plasma. The tubes were gently shaken on a horizontal shaker for 20 min. After centrifugation for 5 min at 1000 *g*, 4.0 ml of the organic layer were separated and evaporated to dryness in a gentle stream of helium at 40°C. The residue was dissolved in 50 μl of the mobile phase. An aliquot of 20 μl was injected on to the HPLC column. This procedure is a modification of the method described by East and Dye[15]. Recoveries of *ca.* 96% have been reported for the original procedure[15].

RESULTS AND DISCUSSION

System description

In most bioanalytical applications conventional bore columns are used. With several LC–MS interfaces, miniaturized HPLC columns are applied to achieve flow-rate reduction in order to avoid large split ratios. It is important to realize that no significant improvements in concentration detection limits are to be expected from the use of microbore columns since the advantage of reducing the split ratio is balanced by the necessary reduction in injection volume[18].

In the case of CF-FAB the optimum flow-rate is *ca.* 5 μl/min. For coupling with conventional HPLC columns with typical flow-rates of 1 ml/min a considerable split of 1:200 is necessary. For microbore columns the typical flow-rates are about an order of magnitude lower, resulting in a split of 1:10, but also the maximum injection volume is diminished by at least a factor of 10. Therefore, similar concentration detection limits will be obtained in both cases. Only if the sample size is limited does miniaturization become attractive. In most cases conventional HPLC columns are also preferred in bioanalysis for their high sample loadability. Moreover, miniaturization of sample pretreatment procedures is rather difficult. Because of these arguments, coupling of conventional HPLC with CF-FAB was investigated for bioanalysis and a splitter was designed for this purpose.

Several types of flow splitter for use in CF-FAB experiments have been described: a commercially available pneumatic splitter[19] and a splitter with a needle valve[11]. Fig. 1 gives a schematic diagram of a low-cost laboratory-made splitting device, used in the experiments described here. With certain precautions this splitter is very easy to handle. The split ratio is determined by the length and the internal diameter of the fused-silica capillaries. It is important to wash the splitter with water daily after use to prevent bacterial growth and mould formation. No additional peak broadening due to the splitter has been observed. Day-to-day variation of the split ratio is smaller than 10%. When one of the fused-silica capillaries accidentally becomes clogged it can be easily replaced.

In FAB, glycerol is generally used as the matrix. In CF-FAB glycerol can be added to the mobile phase of the HPLC system either in pre-column[1–10,12–14] or post-column[11] mode. In the pre-column mode glycerol is mixed with the mobile phase. Unfortunately, a mobile phase containing 10% of glycerol has a much higher viscosity than the corresponding conventional mobile phase, resulting in an increased pressure drop over the column. A higher temperature of the mobile phase is needed to decrease the viscosity. In that case it must be taken into account that the increased temperature and the polarity of glycerol influences the chromatography. When glycerol is added in post-column mode, the chromatography is not affected. However, adequate post-column mixing of pure glycerol with the column effluent is rather difficult. Post-column addition of glycerol can only be achieved by adding a solvent mixture containing glycerol, resulting in dilution and peak broadening. In this study pre-column addition of glycerol was used. The increased temperature (56°C) not only decreased the viscosity of the mobile phase but also improved the chromatography of dextromethorphan.

Analysis of plasma samples

The applicability of the CF-FAB method for quantitative bioanalysis was studied by determining dextromethorphan in plasma samples. Total ion current chromatograms of a blank plasma sample and a spiked plasma sample are shown in Fig. 2. The sample has been spiked with 28 μg/ml of dextromethorphan, which corresponds to 85 ng introduced into the mass spectrometer. No interfering background peaks were observed in the chromatogram of the blank plasma sample. The CF-FAB LC–MS spectrum of dextromethorphan taken from the chromatogram in Fig. 2B is given in Fig. 3 without background subtraction. Compared with conventional FAB the background of glycerol clusters is considerably reduced. Only the protonated glycerol clusters at *m/z* 93 and 185 can be seen. The protonated molecule of dextromethorphan at *m/z* 272 and the protonated glycerol cluster at *m/z* 277, although of very low abundance, are used in selected-ion monitoring.

Analytical data

The within-run precision of the method was studied by analysing spiked plasma samples containing 1.8 or 28 μg/ml of dextromethorphan using a stainless steel target. Table II summarizes the coefficients of variation (C.V.) of the peak areas and peak heights. The data in Table II were acquired under various conditions. With system I an untreated stainless steel target was used, whereas with system II results are given for an acid-treated stainless steel target. No significant differences in the precision of the method were observed at the two plasma levels investigated. The acid treatment roughens the surface of the target and hence enhances the wettability[20]. The use of the wick together with the acid-treated target improves the liquid film properties of the target, resulting in an improved stability of the baseline[20] and precision of the method. The cold trap, which is used to increase the pumping capacity of the mass spectrometer at the ion source housing, also improves the baseline stability, partly because pressure fluctuations influence the stability of the FAB gun. Application of the wick, the acid-treated stainless-steel target and cold trap improves the C.V. of the peak heights and areas. A typical series of peaks for plasma samples containing 1.75 μg/ml of dextromethorphan as obtained with the latter system is given in Fig. 4. The glycerol

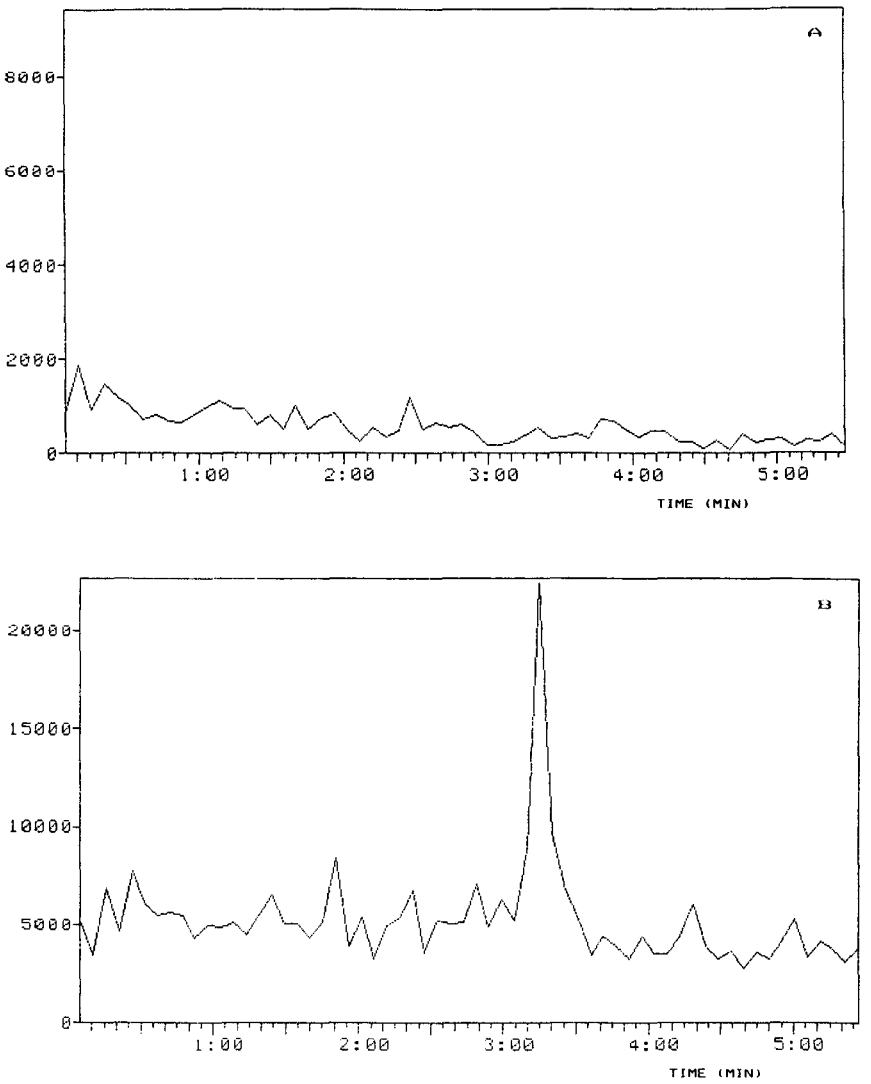

Fig. 2. Total ion current chromatograms of human plasma extracts. (A) Blank plasma sample. (B) Spiked plasma sample containing 28 μg/ml of dextromethorphan (retention time 3 min 15 s). System I (see Table I) with an untreated stainless-steel target.

background was monitored to check the conditions of the system during the run. By using a labelled internal standard the precision of the method can be improved further, and the effect of occasional instabilities as well as effects of the changes in the conditions (*e.g.* properties of the liquid film, pressure and temperature of the ion source) are avoided.

The recovery of the extraction method was found to be *ca.* 80% at the 1.76 μg/ml level by comparing the peak areas as obtained from extracted spiked plasma samples and extracted blank samples, to which dextromethorphan was added after extraction.

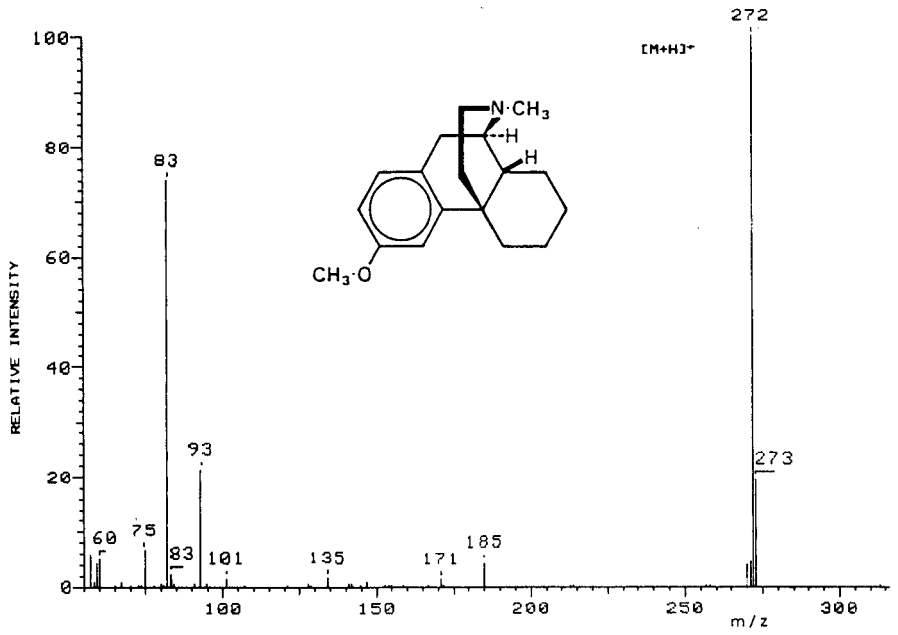

Fig. 3. The LC-FAB mass spectrum of dextromethorphan (MW 271) taken from the analysis shown in Fig. 2B. System I (see Table I) with an untreated stainless-steel target.

The linearity (peak area *vs.* concentration) of the method was checked in the range 0.11–28.0 μg/ml dextromethorphan in plasma. The calibration curve is linear (correlation coefficient, $r = 0.995$) over the range 1.75–14.0 μg/ml corresponding to 7–53 ng of dextromethorphan introduced into the mass spectrometer. The calibration samples containing 0.11–0.88 μg/ml were measured separately. Day-to-day reproducibility of the absolute peak areas is not very good: peak-area ratios up to 10 were found between two successive days. Daily calibration is therefore necessary, and an isotopically labelled internal standard would certainly improve the overall performance.

The determination limit with a signal-to-noise ratio of 10 in selected-ion monitoring is *ca.* 1 μg/ml, when system I is used. With system II the determination limit is 110 ng/ml, corresponding to 400 pg introduced into the spectrometer.

TABLE II

WITHIN-RUN PRECISION OF THE PEAK AREAS AND PEAK HEIGHTS FOR DETERMINATION OF DEXTROMETHORPHAN IN HUMAN PLASMA BY MEANS OF CF-FAB LC–MS WITH A STAINLESS-STEEL TARGET

Target	*Conc. (μg/ml)*	*N*	*C.V. (%)*		*Conditions*
			Area	*Height*	
Untreated	28	4	22	29	System I
	1.8	5	24	28	System I
Acid-treated	1.8	6	15	16	System II

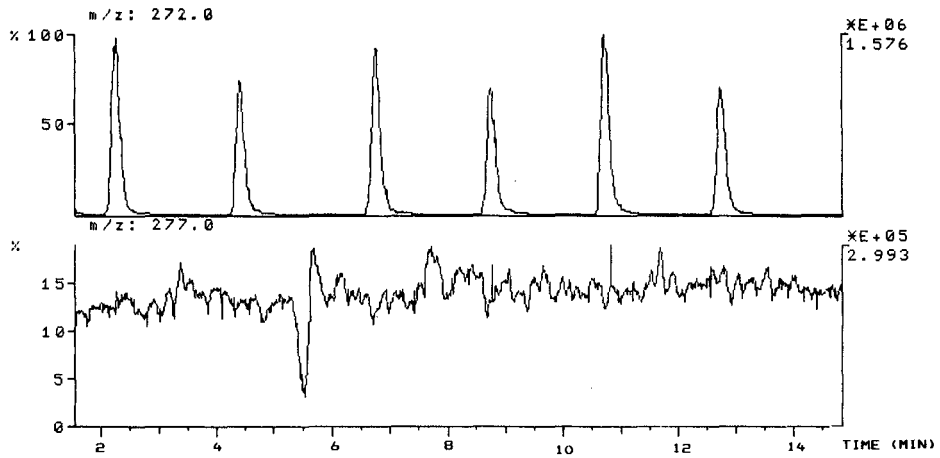

Fig. 4. Multiple ion monitoring chromatograms of the protonated dextromethorphan (upper trace, *m/z* 272) and the $[3M + H]^+$ of glycerol (lower trace, *m/z* 277). Plasma spiked with 1.75 μg/ml of dextromethorphan, corresponding to 7 ng into the spectrometer. System II (see Table I) with an acid-treated stainless-steel target.

Phase-system switching

The mandatory splitting ratio of 1 to 200 considerably restricts the determination limits of the method. Plasma levels of dextromethorphan below 10 ng/ml, which are found in practice, cannot be determined. The use of microbore LC columns in stead of conventional columns gives no significant advantages in this respect, because the lower injection volume balances the reduced splitting ratio. Preliminary experiments indicate that splitting can be avoided completely by the use of the phase-system switching (PSS) approach[21,22]. This approach, which is based on valve-switching techniques, was originally designed for solving mobile phase incompatibilities in target compound analysis with LC–MS, but it has several additional features, such as the

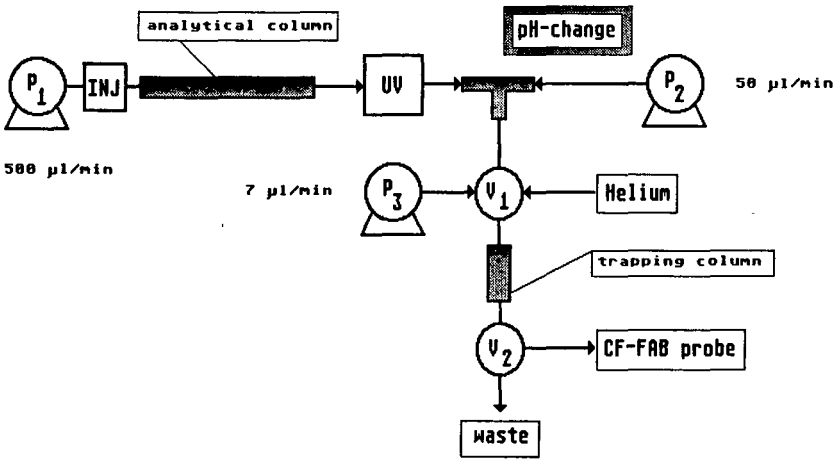

Fig. 5. Schematic diagram of the phase-system switching.

possibility of peak compression and of changing the flow-rate into the spectrometer. In PSS the compound of interest is trapped after the analytical separation on to a short trapping column, from which after washing and drying of the column it is eluted in an appropriate solvent and at a flow-rate favourable to the LC–MS interface applied. The applicability of this approach has been demonstrated for both the moving-belt interface and the thermospray interface[21–23]. If the appropriate trapping column dimensions are chosen, the PSS approach can also be used for the flow-rate reduction necessary in CF-FAB and for the post-column addition of glycerol. In the PSS system illustrated schematically in Fig. 5, an RP-2 analytical column (100 mm × 3.0 mm I.D.) is used at a flow-rate of 1.0 ml/min in combination with a XAD-2 trapping column of 50 mm × 1.0 mm I.D. In order to make trapping of dextromethorphan possible, a pH change after the analytical column is necessary. The optimization of the conditions (the trapping column dimensions, the washing and drying steps and the minimization of the dead volume of the system) is presently under investigation and will be reported together with quantitative analysis of dextromethorphan with the PSS system.

CONCLUSION

The CF-FAB method can be used in quantitative bioanalysis of very polar and thermally labile compounds. The analytical performance of the method is sufficient for most bioanalytical applications concerning determination of plasma levels. A system equipped with a wick, a cold trap and surface-treated targets shows a better stability, which is reflected in the precision of the method. At present the quantitation levels are restricted by the mandatory splitting. However, preliminary results from the use of the phase-system switching approach, in which the necessary flow-rate reduction is realized without splitting, indicate that these problems can probably be solved as well.

ACKNOWLEDGEMENT

One of the authors (P.K.) thanks Orion Pharmaceutica and the Finnish Academy of Sciences for the support of this project.

REFERENCES

1 T. R. Covey, E. D. Lee, A. P. Bruins and J. D. Henion, *Anal. Chem.*, 58 (1986) 1451A.
2 Y. Ito, T. Takeuchi, D. Ishii and M. Goto, *J. Chromatogr.*, 346 (1985) 161.
3 R. M. Caprioli, T. Fan and J. S. Cottrell, *Anal. Chem.*, 58 (1986) 2949.
4 R. M. Caprioli, W. T. Moore and T. Fan, *Rapid Commun. Mass Spectrom.*, 1 (1987) 15.
5 D. W. Hutchinson, A. R. Woolfitt and A. E. Ashcroft, *Org. Mass Spectrom.*, 22 (1987) 304.
6 A. E. Ashcroft, J. R. Chapman and J. S. Cottrell, *J. Chromatogr.*, 394 (1987) 15.
7 A. E. Ashcroft, *Org. Mass Spectrom.*, 22 (1987) 754.
8 D. W. Hutchinson, A. R. Woolfitt and A. E. Ashcroft, *Org. Mass Spectrom.*, 23 (1988) 59.
9 R. M. Caprioli, *Trends Anal. Chem.*, 7 (1988) 328.
10 R. M. Caprioli, W. T. Moore, B. DaGue and M. Martin, *J. Chromatogr.*, 443 (1988) 355.
11 D. E. Games, S. Pleasance, E. D. Ramsey and M. A. McDowall, *Biomed. Environ. Mass Spectrom.*, 15 (1988) 179.
12 T. Takeuchi, S. Watanabe, N. Kondo, D. Ishii and M. Goto, *J. Chromatogr.*, 435 (1988) 482.
13 Y. Ito, T. Takeuchi, D. Ishii, M. Goto and T. Mizuno, *J. Chromatogr.*, 358 (1986) 201.
14 Y. Ito, T. Takeuchi, D. Ishii, M. Goto and T. Mizuno, *J. Chromatogr.*, 391 (1987) 296.
15 T. East and D. Dye, *J. Chromatogr.*, 338 (1985) 99.

16 M. Johansson and C. Svensson, *J. Pharm. Biomed. Anal.*, 6 (1988) 211.
17 M. Silvasti, P. Karttunen, H. Tukiainen, P. Kokkonen, U. Hänninen and S. Nykänen, *Int. J. Clin. Pharm. Ther. Tox.*, 25 (1987) 493.
18 J. van der Greef, W. M. A. Niessen and U. R. Tjaden, *J. Chromatogr.*, 474 (1989) 5.
19 T. Kobayashi, K. Matsuura, K. Otsuka, E. Kubota, Y. Itagaki, B. D. Musselman and T. Higuchi, *"New Design of a Splitter for Frit-FAB LC-MS and Batch Liquid Inlet System"*, presented at the *36th ASMS Conference on Mass Spectrometry and Allied Topics, June 5–10, 1988, San Francisco, CA*, p. 1249.
20 P. Kokkonen, W. M. A. Niessen, U. R. Tjaden and J. van der Greef, in preparation.
21 J. van der Greef, W. M. A. Niessen and U. R. Tjaden, *J. Pharm. Biomed. Anal.*, 6 (1988) 565.
22 E. R. Verheij, H. J. E. M. Reeuwijk, G. F. Lavos, W. M. A. Niessen, U. R. Tjaden and J. van der Greef, *Biomed. Environ. Mass Spectrom.*, 16 (1988) 393.
23 A. Walhagen, L. E. Edholm, C. E. M. Heeremans, R. A. M. van der Hoeven, W. M. A. Niessen, U. R. Tjaden and J. van der Greef, *J. Chromatogr.*, 474 (1989) 257.

Journal of Chromatography, 474 (1989) 69–82
Elsevier Science Publishers B.V., Amsterdam — Printed in The Netherlands

CHROM. 21 259

DESIGN AND INDUSTRIAL APPLICATIONS OF A REMOVABLE PROBE INTERFACE FOR DIRECT CAPILLARY SUPERCRITICAL-FLUID CHROMATOGRAPHY–MASS SPECTROMETRY

HENRY T. KALINOSKI* and LEONARD O. HARGISS
Unilever Research U.S., Inc., 45 River Road, Edgewater, NJ 07020 (U.S.A.)

SUMMARY

An interface coupling capillary supercritical-fluid chromatography (SFC) with a commercial quadrupole mass spectrometer has been assembled and utilized to investigate problems involving separation and identification in the consumer products industry. The design of the interface allowed positive and negative ion chemical ionization mass spectra to be obtained on a Hewlett-Packard 5985 gas chromatograph–mass spectrometer without instrumental modification. Changeover from gas chromatography–mass spectrometry (GC–MS) to SFC–MS was accomplished in minutes without the need to remove chromatographic columns or vent the vacuum system. The interface included provisions for maintaining SFC oven temperature to the ion source region and for independent heating of the flow restrictor terminus. The system allowed for choices of restrictor design, column flow-rate and chemical ionization reagent gas. Chromatographic conditions developed using SFC with flame ionization detection were readily transferred to the SFC–MS system with only a small change in chromatographic efficiency. No compromises to MS operating parameters were required. Examples of the evaluation and use of the SFC–MS system on samples and problems of concern in the consumer products industry are described.

INTRODUCTION

Supercritical-fluid chromatography (SFC) has developed as an important separation technique for problems not amenable to gas chromatography (GC) and liquid chromatography (LC). As with these other chromatographic techniques, the use of mass spectrometry (MS) is recognized as one of the most versatile detection methods available for SFC[1,2]. The interface of SFC with MS has now left the research phase of development and is being applied to a wide range of analytical problems[1–12]. These applications have been facilitated by the numerous interfaces developed for coupling SFC to a wide variety of commercial GC–MS and LC–MS systems[1,3–12]. Many of these instruments require the mass spectrometer to be dedicated for an extended period of time to SFC–MS operation. For many laboratories, such dedication of the mass spectrometer to one operating mode is not always practical and it is preferable to have a system which can convert from one operational mode to another with a

0021-9673/89/$03.50

minimum of down-time. It is also advantageous to have a means to test the performance of an SFC–MS interface with relation to other modes of introduction or detection.

An interface has been developed, based on the capillary–direct injection method pioneered by Smith and co-workers[1,2], for coupling a commercial capillary SFC system with a Hewlett-Packard 5985 GC–MS system. The design permits positive ion (PICI) and negative ion chemical ionization (NICI) mass spectra to be obtained on a range of analytes, using a wide variety of CI reagent gases. No modification of the mass spectrometer or chromatograph was required. The interface incorporates an independently heatable region for the SFC flow restrictor and allows coaxial introduction of CI reagent gas. A number of the current SFC flow restrictor designs can be accommodated. Conversion from GC–MS or direct insertion probe (DIP)–MS operational modes to SFC–MS or from SFC with flame ionization detection (FID) to SFC–MS can be accomplished in a matter of minutes. This flexibility permits a wide range of independent or interrelated experiments to be run on the two instruments, permitting evaluation of the performance of SFC–MS with respect to GC–MS, DIP–MS or SFC–FID.

Efforts to couple SFC to the HP5985 mass spectrometer first required considering designs previously developed in other laboratories. Henion *et al.*[3] interfaced an HP5985 with packed column SFC using a momentum separator. The underlying reason for this approach was the desire to produce electron impact (EI) ionization mass spectra. Refinements of this and of the MAGIC LC–MS interface of Willoughby and Browner[13] have led to commercial momentum–separator interfaces for LC–MS and SFC–MS. This design was not pursued because there was no specific need for EI spectra, and this approach required additional pumping and dedication of the instrument to SFC–MS. The use of open-tubular column SFC minimizes the gas load on the vacuum system, so additional pumping to reduce the load is not warranted.

Attempts to replicate the efforts of Hawthorne and Miller[4–6] by simply guiding the SFC flow restrictor through a capillary direct interface (used for GC) into the ion source were unsuccessful. With the HP5985 such an approach requires the vacuum system of the mass spectrometer to be vented to replace a capillary GC column with the SFC restrictor. The later works by this group[5,6] did use the newer HP5988 instrument which eliminated the need to vent the vacuum chamber. This method, wherein the GC/SFC–MS interface region is maintained about 100°C above column temperature to help heat the restrictor tip[4], was found workable at high SFC column velocities (4–10 times higher than used for other interface designs) and with the more volatile and lower-molecular-weight materials. This was the case with both polished and frit-type restrictors. High volumetric flow-rates led to excessive gas loads in the ion source chamber and the inability to operate the SFC through the practical density range of carbon dioxide. The use of higher temperatures in the interface block did not improve the performance of this approach. The inability to transport higher-molecular-weight and lower volatility analytes was reason to abandon this approach.

The use of Smith's capillary–direct approach with an HP5985 was recently reported by Owens *et al.*[7]. In that effort the interface used a 6.4 mm O.D. × 4.8 mm I.D. stainless-steel probe and a custom machined vacuum seal. The design incorporated a 20-mm heated region for the restrictor and experiments utilized tapered restrictors. The vacuum system of the mass spectrometer was equipped with a cryogenic

pumping system but still operated with a partial pressure of $1.0 \cdot 10^{-4}$–$1.5 \cdot 10^{-4}$ Torr carbon dioxide in the ion source chamber. This was due to use of restrictor aperatures much larger than were used for SFC–FID[7]. Finally, the system was run at low MS resolution and high detector voltages to increase system sensitivity[7].

Details of the SFC separation process, the direct injection process for SFC–MS and the advantages of SFC–MS have been fully described elsewhere[1]. This report focuses on the design, construction and evaluation of the probe-mounted interface. Application of the system to selected analytical problems from the consumer products industry are also addressed. A brief comparison of the parameters required for operation in SFC–FID *versus* SFC–MS, and the relative efficiency of SFC–MS separations will be made and the effects of using the mass spectrometer in a direct injection mode for SFC–MS will be described.

EXPERIMENTAL

Chromatography

All work was conducted on the Model 602 SFC–GC system (Lee Scientific, Salt Lake City, UT, U.S.A.) which consisted of a computer-controlled syringe pump for delivery of supercritical carbon dioxide (AGL, Clifton, NJ, U.S.A.), a Model 7526 helium-actuated HPLC-type injector (Rheodyne, Cotati, CA, U.S.A.) with a 0.5-μl internal volume, a gas chromatograph oven capable of isothermal or temperature-programmed operation and a GC-type flame ionization detector. The Lee Scientific computer and software (Ver. 2.0) enabled either pressure or density programming of the mobile phase. All injections were made at ambient temperature and split using the "T" supplied by the manufacturer[14]. The split ratio, usually about 50:1, was controlled by the flow through a length (50–60 mm) of 10 μm I.D. fused-silica capillary tubing. Chromatography was conducted at 100°C, isothermal, using a fluid density ramp on a 10 m × 50 μm I.D. fused-silica open-tubular column coated with a 30% biphenyl–70% methyl polysiloxane (SB-Biphenyl-30) stationary phase from Lee Scientific. Three types of SFC flow (pressure) restrictor were used, the "frit" restrictor from Lee Scientific[1], both a shorter length supplied for FID use and the longer "MS-frit", where the frit material is at the end of a 1-m length of deactivated 50-μm fused-silica tubing, the polished "Guthrie" type[1,15] and the tapered[1,16], both fabricated from deactivated 50-μm fused-silica tubing. A detailed comparison of the various restrictor designs was beyond the scope of the current work. In all cases the restrictor was attached to the column terminus using a zero-dead-volume union (MVSU/003; SGE, Austin, TX, U.S.A.). The restrictor terminus was kept flush with the interface probe exit. Efforts were made to keep the mobile phase linear velocity between 2 and 2.5 cm/s, or a volumetric flow-rate of about 4 μl/s, measured at a density of 0.2 g/ml.

Samples were obtained from numerous sources and used in solution in dichloromethane or chloroform (certified ACS grade, Fisher Scientific, Fair Lawn, NJ, U.S.A.). Sample preparation involved dissolving a weighed amount of sample in appropriate solvent and diluting to the working concentration. Concentrations used for more complex mixtures, such as nonionic surfactants, were 1–10% by weight and 1 to 5 mg/ml for single compounds or simple mixtures.

Mass spectrometry

MS was conducted on a Hewlett-Packard (Palo Alto, CA, U.S.A.) Model 5985B GC–MS system operated in both positive and negative chemical ionization modes. The MS system was comprised of a convertible EI/CI ion source and a single quadrupole mass analyzer. Ion source chamber pumping was accomplished using a 680 l/s (air) diffusion pump, which cannot be valved off from the vacuum chamber. Any interface design that would require venting the vacuum system to atmosphere would need 4–8 h to cycle from shut-down to start-up. The ion source chamber was equipped with a vacuum interlock for insertion of the tuning probe or the direct insertion probe. The tuning probe or DIP mates with a tapered port on the source, so the source volume is relatively well confined, with respect to the GC–EI-MS configuration, when solid samples are introduced or for operation in CI mode. The system was controlled by an HP-1000 E series computer system. Ion source temperature, for both PICI and NICI was 200°C with a starting ion source pressure, measured on the ion source chamber vacuum gauge, of $1.2 \cdot 10^{-4}$ Torr. The ion gauge, calibrated for nitrogen, was not corrected for the various gases present. This pressure value is what is routinely used for GC–CI-MS and DIP–CI-MS. Depending on the flow restrictor used for SFC, the ion source chamber pressure would range from $2.0 \cdot 10^{-4}$ to $4.5 \cdot 10^{-4}$ Torr at the end of the density programmed SFC–MS separation (410 bar, 0.765 g/ml). No effort was made to maintain a constant carbon dioxide/reagent gas ratio. Methane, isobutane, ammonia, 1% ammonia in methane, argon and Freon-12 were used as reagent gases for CI. All gases were of the highest available purity and obtained from AGL. Electron multiplier voltages used for PICI and NICI were similar to those used for GC–MS and DIP–MS. The mass range scanned depended on the sample being analyzed. The mass spectrometer was tuned using the Hewlett-Packard computer-controller tuning procedures. The system was always operated at unit mass resolution to m/z 614 (from perfluorotributylamine).

Interface probe design

The SFC–MS interface probe was assembled using a 1.27 cm O.D. × 0.85 cm I.D. leak probe (HP part No. 05985-20585), the same type of probe used for the tuning probe. This permitted use of the vacuum interlock and proper mating with the ion source without modification. A 35 cm length of 0.16 cm O.D. stainless-steel

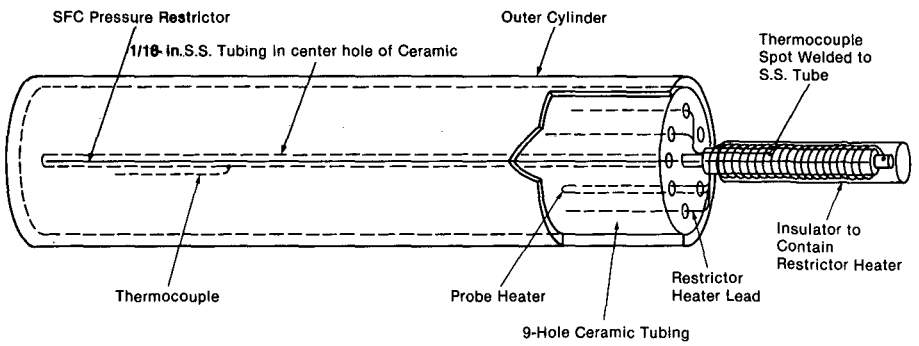

Fig. 1. Schematic diagram of the mass spectrometer end of the probe-mounted SFC–MS interface detailing the ceramic tube support and restrictor heater. S.S. = stainless steel.

tubing was used to contain the fused-silica flow restrictors and to supply CI reagent gas. This tube was supported in the probe inside a 22 cm length of nine hole ceramic tubing. A schematic diagram of the MS end of the interface probe is given in Fig. 1, illustrating the stainless-steel and ceramic tubes. The ceramic tube also provided a means of heating the interface probe, as a nichrome wire was passed through two of the holes and used as a heater. A thermocouple, silver-soldered to the tube containing the restrictor, was used to monitor temperature in the probe. The steel tube exited the leak probe to the SFC oven via a reducing tube fitting. This allowed a tube fitting "T" to be used to supply the CI reagent gas. CI reagent gases were metered through a fine metering valve. The flow restrictor was held in the "T" using a graphite-filled vespel ferrule (GVF/003, SGE) which provided a vacuum seal. The region external to the SFC oven and MS interlock was wrapped with heating tape and insulator to maintain oven temperature. The Model 602 SFC system was supplied with holes pre-cut in the oven wall and access panels in the cabinet to facilitate interface of the oven with an MS system. This feature allowed the SFC column to remain in the oven and reduced the need for externally heated zones in the interface. The mass spectrometer end of the interface probe (Fig. 1) was fitted with a nichrome wire wrapped around an insulator, sheathing the end of the stainless-steel tube. A second insulator covered the nichrome wire. A thermocouple, silver-soldered to the steel tube inside the insulator, enabled the temperature on the steel tube to be monitored. This heater was capable of temperatures of about 500°C, and heated on a 30–35 mm length of the end of the flow restrictor. This is approximately equal to the length in the heated zone in the Lee Scientific flame ionization detector. The electrical and thermocouple leads were admitted through holes in the ceramic tube. There was no vacuum seal on the MS end of the probe; all seals were made with tube fittings external to the vacuum system. The restrictor heater fits the ion source mating fitting in a manner analogous to the tip of the direct insertion probe, placing the restrictor terminus within 5 mm of the CI source volume entrance. An early version of the interface did not include the extra restrictor heater and relied on the ion source block to heat the restrictor. As the interface utilized the probe obtained from the instrument manufacturer, a tight fit to the CI source was assured. The interface probe was operated at SFC oven temperature and the restrictor heater temperature was varied between 100°C and 400°C.

RESULTS AND DISCUSSION

Supercritical-fluid chromatography

The first effort at a probe-mounted interface did not incorporate a restrictor heater, which permitted evaluation of the need for a restrictor heater in addition to heat from the ion source block. The ability of the vacuum system of the mass spectrometer to operate under SFC–MS conditions was also evaluated with the early interface version. Fig. 2A shows the carbon dioxide SFC–MS total ion chromatogram, positive ion CI-MS, for the separation of a poly(ethylene glycol) methyl ether [$HO(CH_2CH_2O)_nCH_3$] sample, average molecular weight ($\overline{MW}$) 550 daltons. The mass spectrometer was scanned from 130 to 750 daltons at 6 s/scan. The chromatogram shown was not background subtracted. Without an external heater, the restrictor sheath was between column temperature (100°C) and ion source temperature (200°C). Reasonably good separation, defined as narrow peak widths (approx. 30 s

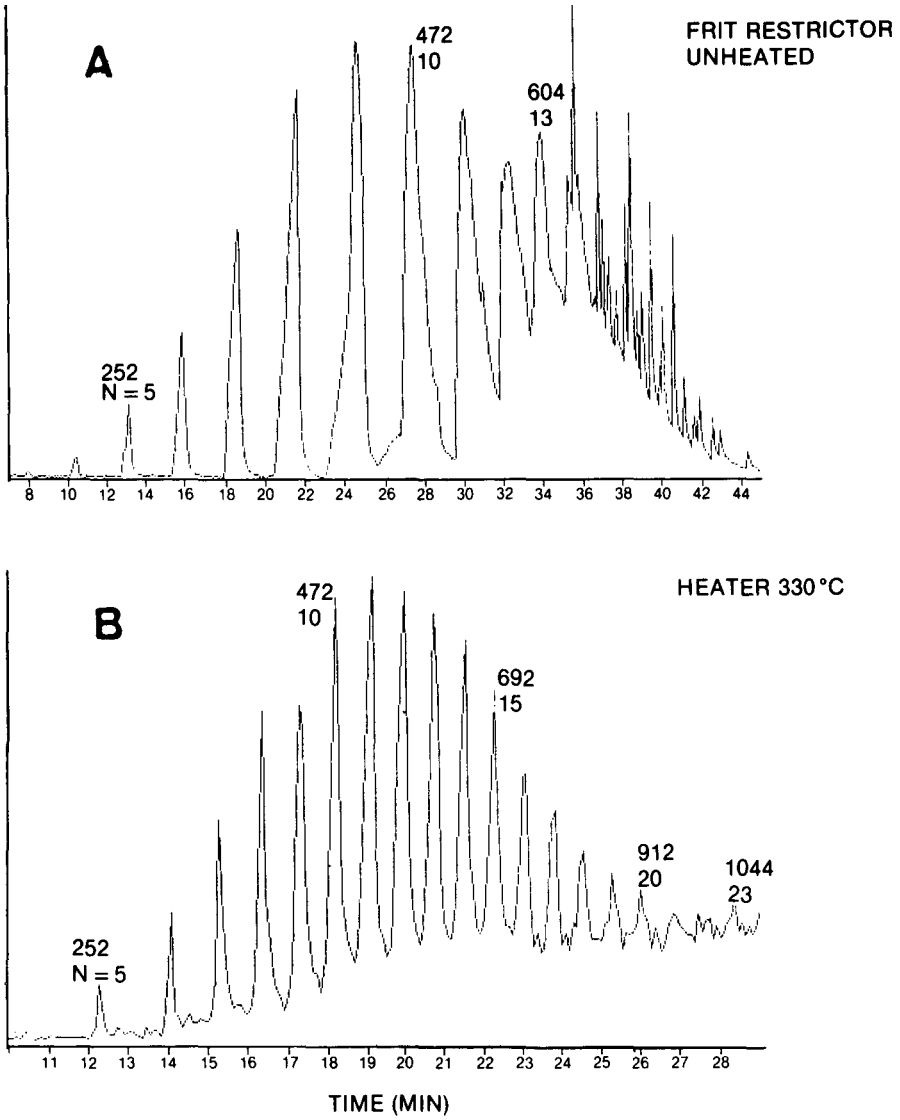

Fig. 2. Total ion chromatograms from the carbon dioxide capillary SFC–MS separations of poly(ethylene glycol) methyl ether (average mol.wt. 550) samples. Methane positive ion chemical ionization was employed for both samples, one obtained without additional flow restrictor heating (A) and one with a restrictor heater operated at 330°C (B).

full width at half hight) and baseline resolution, was achieved for early eluting components (up to $n = 8$) but higher-molecular-weight components could not be successfully transported and ionized. Mass spectra of components up to $n = 13$, 604 daltons, contained protonated molecules $(M + H)^+$ and structurally significant fragment ions. SFC with FID of this sample, as well as $\overline{MW}$ 750, under similar chromatograph-

ic conditions gave baseline separation of telomers up to $n = 20$ for $\overline{MW}$ 550 and $n = 26$ for $\overline{MW}$ 750 with no detector spiking or apparent discrimination against higher-molecular-weight components. For FID experiments the detector was operated at 395°C with the frit restrictor.

Fig. 2B shows the same poly(ethylene glycol) methyl ether sample separated using carbon dioxide SFC–MS and the interface incorporating the restrictor heater. In this example a frit restrictor was used and the restrictor heater operated at 330°C. All of the telomers found with SFC–FID were eluted and ionized, with peak shape and peak widths directly comparable to SFC–FID. The example illustrates the value of the added heated region in aiding transport of higher-molecular-weight analytes

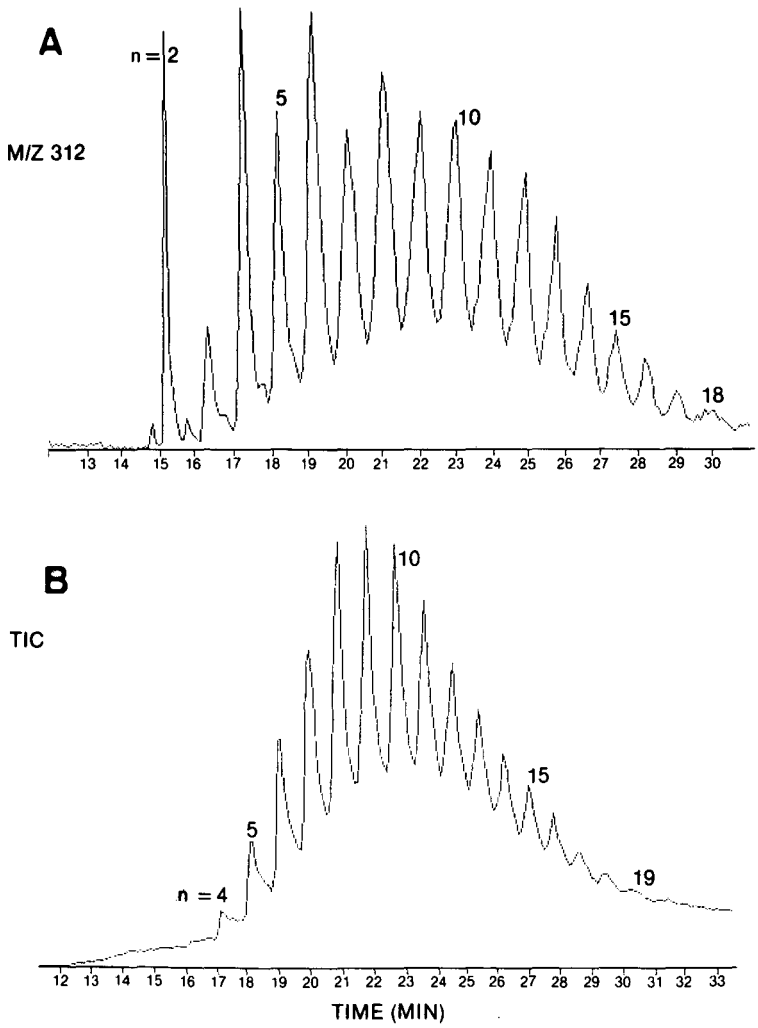

Fig. 3. Chromatograms from the capillary carbon dioxide SFC–MS separations of the ethoxylated surfactant Triton X-100. (A) *m/z* 312 selected ion chromatogram obtained in positive ion ammonia chemical ionization; (B) total chromatogram (TIC) obtained in methane negative ion chemical ionization.

for SFC–MS and the ability of the mass spectrometer to operate across the practical density range of carbon dioxide.

Although the ability to controllably heat the SFC flow restrictor aids the analysis of less volatile analytes, the current design does not display the marked effects of restrictor heater temperature found with the previously described interface[7]. Fig. 3 shows the SFC–MS chromatograms of Triton X-100, octylphenol ethoxylate with an average of about 10 moles ethylene oxide. This sample was analyzed as it is often used as a test mixture for SFC and to compare SFC with other techniques, many previous separations had been performed on this particular batch using SFC–FID and previous efforts[7] demonstrated restrictor heater temperature effects using this surfactant. Carbon dioxide SFC–FID with a frit restrictor had shown all telomers to $n = 19$ reproducibly eluted at restrictor heater temperatures from 300°C to 400°C, with expected small shifts in retention times due to variations in mobile phase viscosity and flow-rate at the restrictor. The same chromatographic conditions, including restrictor heater temperature, developed for SFC–FID were used for SFC–MS to produce the separations shown in Fig. 3. Variations in restrictor heater temperature of 50–75°C, shown in other interfaces to drastically alter the appearance of the SFC–MS reconstructed total ion chromatogram[7], did not show such profound effects here. This probe-mounted SFC–MS interface succeeds in duplicating nearly all the conditions found in the SFC–FID system, such that parameters developed for SFC–FID can be directly transferred to SFC–MS. Although not demonstrated here, SFC–MS extends the utility of SFC through the use of mobile phases not amenable to SFC–FID[1].

Mass spectra

Information on analyte identification, in the form of mass spectra, is the most tangible benefit of SFC–MS. Capillary-direct SFC–MS allows for use of any CI reagent gas in both positive and negative ion modes. Figs. 4 and 5 show the PICI mass

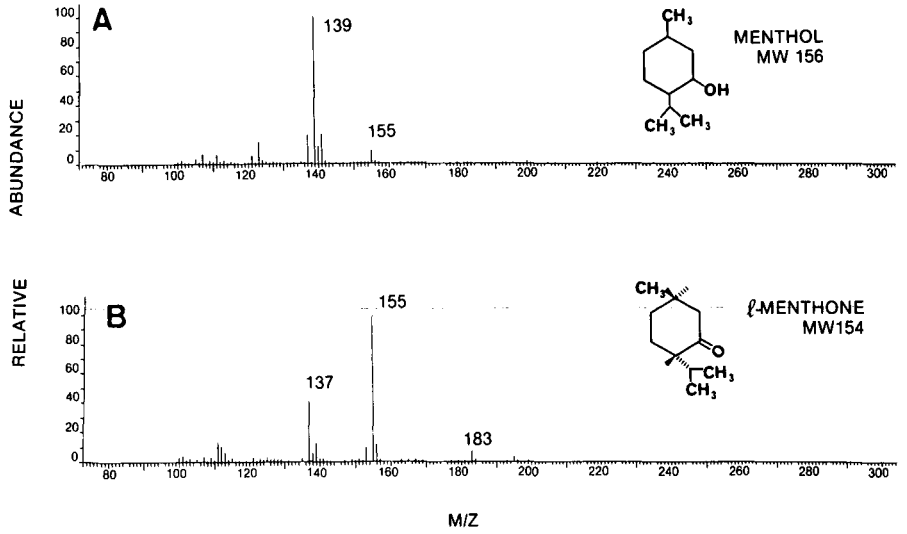

Fig. 4. Methane positive ion chemical ionization mass spectra of (A) menthol and (B) *l*-menthone, obtained following carbon dioxide SFC.

spectra of two flavor/fragrance compounds, menthol (Figs. 4A and 5B, MW = 156) and *l*-menthone (Figs. 4B, 5A and 5C, MW = 154), obtained following carbon dioxide SFC, using a variety of CI reagent gases. Irrespective of the fact that these particular compounds are amenable to GC–MS, many flavor and fragrance components do exhibit thermal lability and low temperature separations are obviously preferable for such samples. These two compounds highlight a common problem in flavor/fragrance analysis, very similar mass spectra from closely related structures. With the more energetic methane CI-MS both compounds show an ion at *m/z* 155. This is the protonated molecule $(M + H)^+$ for menthone (Fig. 4B) but corresponds to the loss of molecular hydrogen from the protonated molecule of menthol $(M + H - H_2)^+$. This type of loss is common in CI mass spectra of alkanes and alkanols. Common fragment ions are found at *m/z* 137 and *m/z* 139. The use of a mild CI

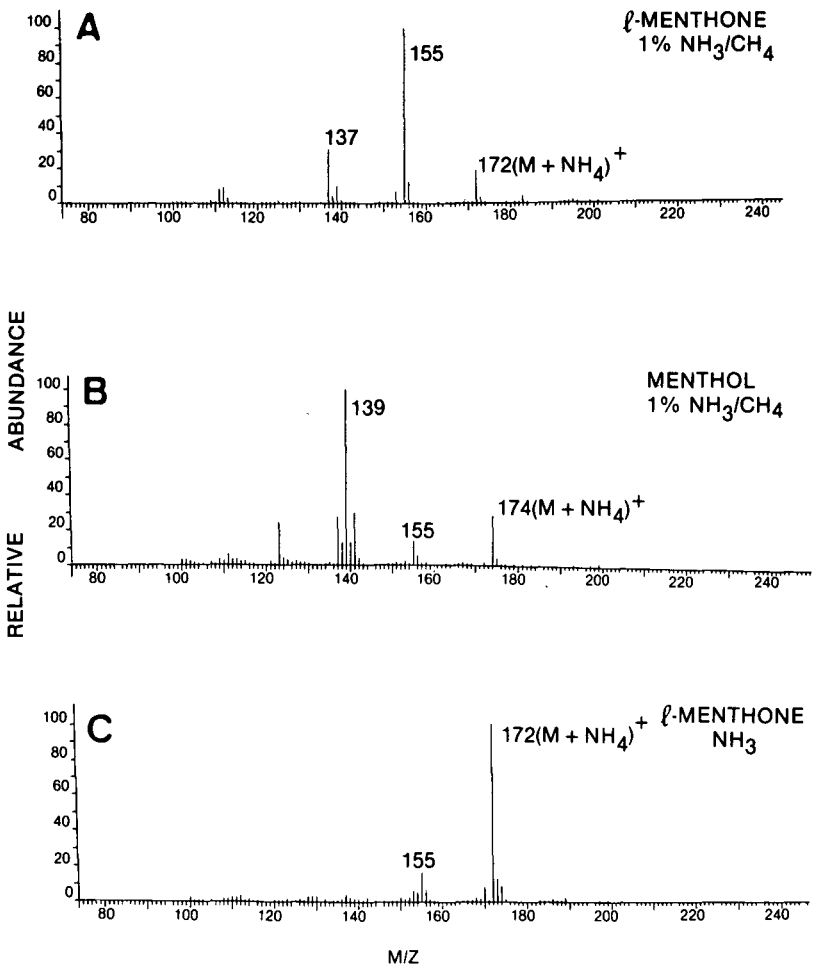

Fig. 5. Positive ion chemical ionization mass spectra of *l*-menthone and menthol obtained following capillary carbon dioxide SFC separation using 1% ammonia mixed in methane (A and B) and ammonia (C) as the reagent gases.

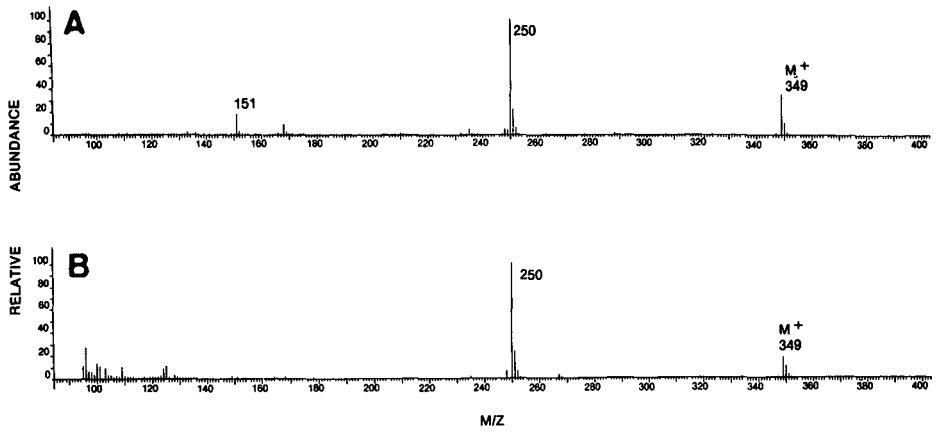

Fig. 6. Probe inlet 70 eV electron ionization (A) and 180 eV charge exchange CO_2–Ar chemical ionization mass spectra (B) of a sample of chromium(III) acetyl acetonate. The sample for CE ionization was introduced using carbon dioxide SFC.

reagent, ammonia (Fig. 5C) clearly gives weight information, in the form of ammonium adduct ions $(M + NH_4)^+$. The use of a mixed reagent gas, in this case 1% ammonia in methane, produces both molecular weight and useful structural information.

Fig. 6 gives a comparison of charge exchange CI and EI ionization to obtain similar information from a sample[17]. Again, the analyte is amenable to GC–MS, but in this example there needs to be an independent means of sample introduction for EI. The analyte, chromium(III) acetyl acetonate used as a spin-relaxation reagent for ^{13}C NMR, may be present in samples submitted for SFC analysis. Charge exchange (CE) CI mass spectra were obtained using the carbon dioxide mobile phase and an additional amount of argon to maintain ion source pressure at about $1.2 \cdot 10^{-4}$ Torr. Methane and isobutane CI mass spectra of metal acetyl acetonates produced on this instrument generally show extensive fragmentation and little to no parent ion production. Metal acetyl acetonates are quite amenable to EI, yielding molecular ions M^+, m/z 349 in Fig. 6A, and ions due to the loss of one and two ligands with reduction of the charge on the metal. The same types of ions are found with argon–carbon dioxide charge exchange with the exception of the m/z 350 ion $(M + H)^+$ being of greater relative abundance in the CE mass spectrum. In contrast to the intentional use of the carbon dioxide mobile phase as the CI reagent gas, the occurrence of CE ionization by carbon dioxide (as evidenced by M^+ ions) when other reagent gases were used was not found to be significant.

Industrial application

Analysis of ethoxylate alcohol (non-ionic) surfactants is one application for which SFC is particularly well-suited[18,19]. Usually the samples, although complex, are composed only of the starting alcohol and telomers of the surfactant of the structure $R–O–(CH_2CH_2O)_n–H$, (n = 1–100 or more). In such instances characterization, comprised of R group identification, average molecular weight calculation and ethoxylate distribution, can be accomplished by SFC–FID[18,19]. Samples can, at

times, contain additional components and FID offers no means of identification. Other methods of characterization which do not contain a separation step may not reveal the additional materials[19,20]. The coupled SFC–MS technique is invaluable for such samples. Fig. 7 shows the total ion chromatogram of a carbon dioxide SFC–MS separation of an ethoxylated stearyl alcohol with an average of 13 moles of ethylene oxide. Telomers of up to 1238 daltons (n = 22) are illustrated here (the MS data system was filled to capacity and ceased acquisition) which directly compares with SFC–FID results of this sample[19]. Such an example illustrates the ability of the interface to transport and ionize materials of higher molecular weight (greater than the mass range of the mass spectrometer, in fact) and lower volatility.

A reportedly similar ethoxylated alcohol was found to contain a second distribution of components centered between the n = 4 and 5 telomers of the alcohol ethoxylate[19]. Positive ion chemical ionization mass spectra of these components, obtained during the carbon dioxide SFC–MS separation of the mixture, are shown in Fig. 8. The mass spectra indicate the identity of the second distribution to be poly (ethylene glycol), at times present in ethoxylated surfactants. The mass spectra are characterized by abundant protonated molecules of the oligomers and characteristic fragment ions, at m/z 133 and m/z 177. SFC–FID and SFC–MS of standard poly (ethylene glycol) samples confirmed the identification of the second distribution and aided in an average molecular weight calculation[19]. The separation power of SFC combined with the ability to obtain molecular weight and structural information through MS is shown to provide a fast, efficient means of identifying unknown materials.

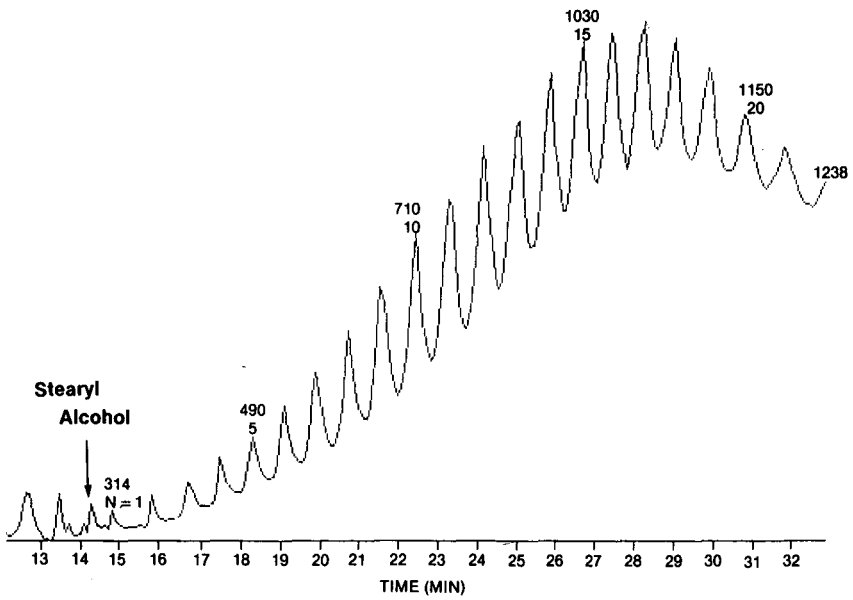

Fig. 7. Total ion chromatogram of the capillary SFC–MS separation of a sample of stearyl alcohol ethoxylate obtained using methane negative ion chemical ionization. The data system ceased acquiring at just under 33 min (prior to the end of sample elution).

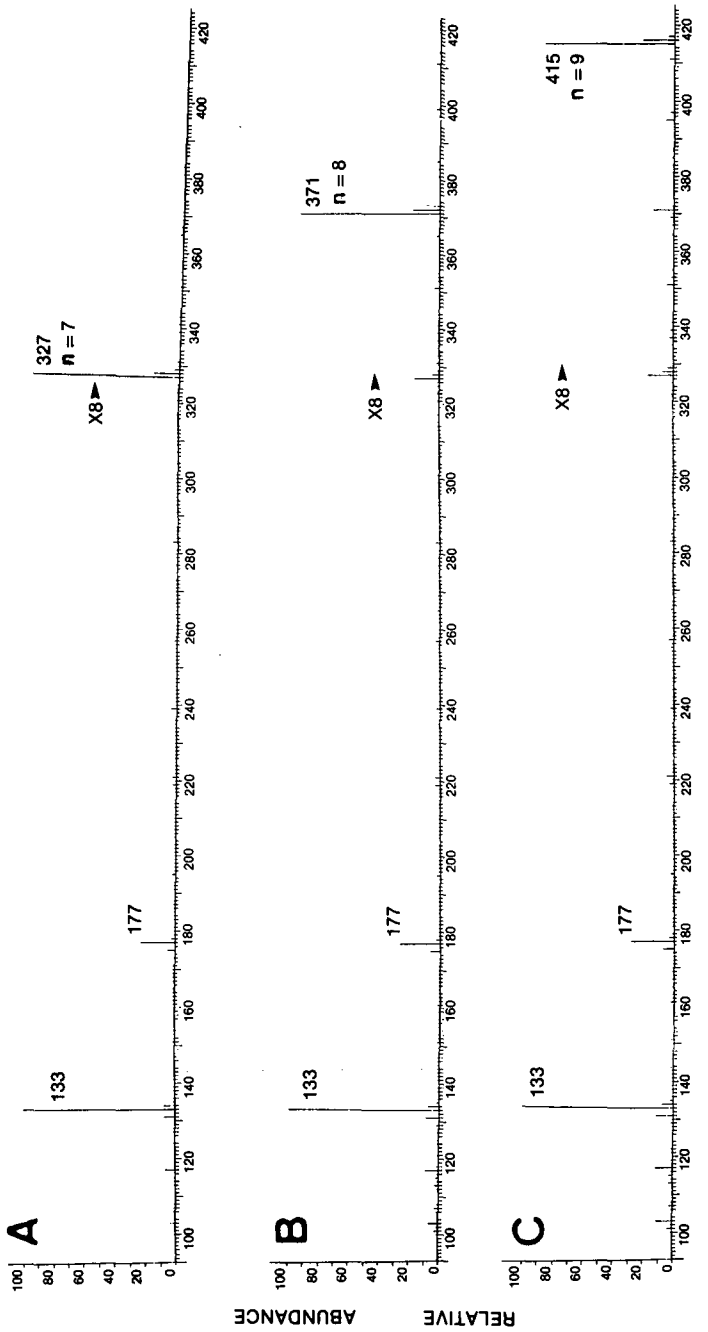

Fig. 8. Methane positive ion chemical ionization mass spectra of the $n = 7$, 8 and 9 oligomers of poly(ethylene glycol) obtained during the carbon dioxide capillary SFC–MS separation of a stearyl alcohol ethoxylate sample found to contain a second distribution of components.

CONCLUSION

A probe-mounted, capillary-direct interface has been assembled to allow a commercial GC–MS system to operate in the SFC–MS mode. The design required no custom machining and no modifications to either the chromatograph or the mass spectrometer. The design incorporated a heated zone for the SFC flow restrictor and three of the most widely applied types of SFC flow restrictor were used with comparable ease. All components and conditions used for SFC–FID were directly transferable to the SFC–MS system. This permitted separations to be optimized using SFC–FID with a rapid change to SFC–MS for complete analyte characterization, including abundant structural information. Changeover from GC–MS (or DIP–MS) to SFC–MS required only a few minutes. This permitted the system to be tuned and calibrated using the procedures applied for GC–MS or for direct comparison of SFC–MS introduction with other forms of sample introduction. Chromatographic performance of the SFC–MS system was only slightly less efficient than SFC–FID. This comparison was made using the identical column, splitter, restrictor and conditions and results obtained without compromising the MS system operating parameters. The one sacrifice from standard GC–MS capabilities made was the loss of electron ionization, but information usually contained in EI spectra was available through charge exchange chemical ionization. SFC has previously been shown to be broadly applicable in consumer products research and SFC–MS augments and extends the utility of SFC for solving analytical problems in this industry.

ACKNOWLEDGEMENT

The authors thank Dr. R. W. R. Humphreys and Dr. K. Slatkavitz (Unilever Research U.S., Inc.) for their support and assistance, the members of the K. L. Busch group (Indiana University) for their assistance in the assembly of the interface probe and M. P. Kieselbach for typing the manuscript.

REFERENCES

1 R. D. Smith, H. T. Kalinoski and H. R. Udseth, *Mass Spectrom. Rev.*, 6 (1987) 445–496.
2 R. D. Smith, W. D. Felix, J. C. Fjeldsted and M. L. Lee, *Anal. Chem.*, 54 (1982) 1883–1885.
3 J. D. Henion, P. O. Edlund, E. D. Lee and L. McLaughlin, *Proceedings of the 36th ASMS Conference on Mass Spectrometry and Allied Topics, San Francisco, CA, June 5–10, 1988.*
4 S. B. Hawthorne and D. J. Miller, *J. Chromatogr.*, 388 (1987) 397–409.
5 S. B. Hawthorne and D. J. Miller, *Proceedings of the 36th ASMS Conference on Mass Spectrometry and Allied Topics, San Francisco, CA, June 5–10, 1988.*
6 S. B. Hawthorne and D. J. Miller, *Fresenius Z. Anal. Chem.*, 330 (1988) 235–236.
7 G. D. Owens, L. J. Burkes, J. D. Pinkston, T. Keough, J. R. Simms and M. P. Lacey, in B. A. Charpentier and M. R. Sevenants (Editors), *Supercritical Fluid Extraction and Chromatography (ACS Symposium Series,* No. 366), American Chemical Society, Washington, DC, 1988, pp. 191–207.
8 N. M. Frew, C. G. Johnson and R. H. Bromund, in B. A. Charpentier and M. R. Sevenants (Editors), *Supercritical Fluid Extraction and Chromatography (ACS Symposium Series,* No. 366), American Chemical Society, Washington, DC, 1988, pp. 208–228.
9 H. T. Kalinoski, H. R. Udseth, E. K. Chess and R. D. Smith, *J. Chromatogr.*, 394 (1987) 3–14.
10 E. D. Huang, B. J. Jackson, K. E. Markides and M. L. Lee, *Chromatographia*, 25 (1988) 51–54.
11 J. D. Pinkston, G. D. Owens, L. J. Burkes, T. E. Delaney, D. S. Millington and D. A. Maltby, *Anal. Chem.*, 60 (1988) 962–966.

12 E. D. Lee, J. D. Henion, R. B. Cody and J. A. Kinsinger, *Anal. Chem.*, 59 (1987) 1309–1312.
13 R. D. Willoughby and R. F. Browner, *Anal. Chem.*, 56 (1984) 2623–2631.
14 B. E. Richter, D. E. Knowles, M. R. Andersen, N. L. Porter, E. R. Campbell and D. W. Later, *J. High Resolut. Chromatogr. Chromatogr. Commun.*, 11 (1988) 29–32.
15 E. J. Guthrie and H. E. Schwartz, *J. Chromatogr. Sci.*, 24 (1986) 236–241.
16 T. L. Chester, D. P. Innes and G. D. Owens, *Anal. Chem.*, 57 (1985) 2243–2247.
17 D. F. Hunt and J. P. Gale, *Anal. Chem.*, 56 (1984) 1111–1114.
18 D. E. Knowles, L. Nixon, E. R. Campbell, D. W. Later and B. E. Richter, *Fresenius Z. Anal. Chem.*, 330 (1988) 225–228.
19 H. T. Kalinoski and A. Jensen, *J. Am. Oil Chem. Soc.*, submitted for publication.
20 G. Carminati, L. Cavalli and F. Buosi, *J. Am. Oil Chem. Soc.*, 65 (1988) 669–677.

Journal of Chromatography, 474 (1989) 83–96
Elsevier Science Publishers B.V., Amsterdam — Printed in The Netherlands

CHROM. 21 465

SUPERCRITICAL-FLUID CHROMATOGRAPHY–MASS SPECTROMETRY OF HIGH-MOLECULAR-WEIGHT BIOPOLYMERS

INSTRUMENTAL CONSIDERATIONS AND RECENT PROGRESS

DOUGLAS M. SHEELEY and VERNON N. REINHOLD*
Division of Biological Sciences, Department of Nutrition, Harvard School of Public Health, Boston, MA 02115 (U.S.A.)

SUMMARY

Interest in supercritical-fluid chromatography (SFC) of biological samples has recently increased. The following is a summary of recent progress in SFC–mass spectrometry interfacing and its application to the analysis of high-molecular-weight biopolymers. The approaches taken in several interface designs and results obtained with each are presented and compared. Areas which are of special concern in working with high mass, thermally labile, or polar analytes include interface heating and flow restrictor design. These topics are discussed in light of previous work, and directions for further study are suggested.

INTRODUCTION

The structural analysis of biopolymers has been advanced considerably in recent years by the introduction of newer instrumental methods for their characterization. One approach of considerable importance has been the mass spectrometer, using a "soft" ionization technique called fast atom bombardment (FAB)[1]. This ionization method has extended structural understanding to samples of greater polarity and higher molecular weight, and application to post-translationally modified peptides has been most important. For these materials and related biopolymers, other soft ionization techniques[2–4], such as direct chemical ionization (DCI)[5] and laser desorption (LD)[6–8], have also contributed to sensitive methods for understanding sample molecular weights and oligomer sequence. To capitalize on this progress, mass spectroscopists have focused considerable effort on the interfacing of existing liquid chromatographic (LC) systems that resolve these polar and/or higher-molecular-weight biopolymers. Most successful in this regard has been the technique of "flow" or "dynamic" FAB[9].

As important as these LC systems are in biological research, their mass spectrometric (MS) interfacing imposes serious instrumental constraints, especially when coupled with FAB desorption. As a method for ion generation, FAB is a very selective technique, a problem very apparent when analyzing samples composed of mixtures. With these samples, product ions are usually a function of surface activity

0021-9673/89/$03.50

not sample concentration, and when compared to other ionization techniques, FAB remains insensitive. For most lipophilic samples, FAB is a very ineffective method of ionization, and frequently unsuccessful. These problems can be related, in large part, to the desorption matrix which causes a biased presentation of the sample. The problems are minimized in "flow FAB" by dynamic surface motion and a lower concentration of matrix[10]. The problem is also diminished in FAB desorption from a polyimide belt[11] which does not require an applied matrix and appears to avoid sample suppression. But this high-performance liquid chromatographic (HPLC) belt interface is expensive, appears to have high mass limitations, and is technically demanding. DCI, as an alternative approach, does not require a desorption matrix and samples are always detected. However, heat-initiated desorption causes pyrolysis of many highermolecular-weight and non-volatile materials, which limits its applicability in these areas.

A separations technique that has received relatively little attention for the analysis of biopolymers has been supercritical-fluid chromatography (SFC). This approach, combined with the low flow-rates of capillary columns[12–14] and the ease of solvent elimination provides features most appropriate for MS interfacing[15–17]. Specifically, these factors are: (a) the utilization of column efficiencies provided by enhanced analyte diffusion coefficients, (b) a smaller volume of mobile phase that is more effectively pumped, (c) the avoidance of high temperatures and thermal limits experienced with gas–liquid chromatography (GLC) and some LC–MS interfaces; and, probably the most important, (d) a possibility for capturing the extreme sensitivities of negative-ion chemical ionization by utilizing derivatization protocols developed in GLC–MS.

Most applications of SFC–MS have been limited to non-polar analytes of low mass. Higher-molecular-weight samples of limited polarity, such as fatty alcohols, ethoxylated alcohols[18,19], and mono- and diglycerides[18,20], however, have provided most interesting results. Unfortunately, the poor solubility of peptides, nucleotides, and oligosaccharides in CO_2 has precluded a direct application of SFC to these important biomolecules. Derivatization has been used in GC to overcome sample polarity, and enhance volatility and thermal stability. Similarly, for SFC, analyte derivatization has served to increase solute miscibility[22]. Using this strategy, researchers have reported success in the study of sucrose polyesters[22], glycosphingolipids[23] and N-linked glycans from glycoproteins[24], as well as SFC–MS of glucose homopolymers in excess of 5 kD[25]. Two cyclic peptides also have been studied by SFC–MS; these samples, however, were not derivatized[26,27].

The study of biopolymers by SFC has been very limited, and derivatization schemes to broaden the application are not usually considered. Thus, applications are limited to those analytes that are miscible in the more convenient mobile phases; a feature constrained by the relatively few gases possessing critical points in a workable temperature-pressure range.

Considering the advantages SFC can bring to biopolymer separations, the structural insight provided by SFC–MS, and with the expectation of improved selectivity and sensitivity; we would suggest applications to problems in biomedical research and molcular biology to be well served. In this regard we have discussed some of the critical aspects of SFC and MS interfacing, the limitations, current progress, and perceived advantages, in the hope others may share their problems and progress.

INSTRUMENTAL CONSIDERATIONS

An excellent review discussing the basic principles of SFC–MS interfacing has recently been published[28]. This summary is therefore focused on those features particularly significant to the characterization of high-molecular-weight samples, a focus that relates immediately to the design and fabrication of flow restrictors. In previous MS interfacing an assortment of designs have been used (Fig. 1), varying principally in the shape and length of the restricting region. The simplest restrictors are fabricated from deactivated capillary tubing and coupled with a zero dead volume union to the unmodified column tip. The volume of effluent passing through the restrictor is proportional to its length and internal diameter. The platinium–irridium crimped tube is an example of a simple restrictor which can be effective but is limited with problems of reproducibility. Laser-drilled disks are easy to prepare, but this device is more technically demanding because of the difficulty in mounting and alignment. Considering the several types of restrictors that have been employed, three are most commonly used: the multipath frit[29], the robot-pulled tapered restrictor[22], and the integral restrictor[30]. Both the frit and tapered restrictors are relatively long, while the integral and laser-drilled disk restrictors are short. This design aspect has significant bearing on sample transmission and ionization, for it relates directly to mobile phase density and analyte solubilities.

These features can be appreciated better by considering the principles of hydrolics and the equation of continuity (Fig. 2A). From these relationships it can be expected that as a conduit is restricted, the velocity of a passing fluid must increase to maintain a constant flow. Under such circumstances, Bernoulli's law requires that this increase in flow velocity must result in decreased pressure at this point (Venturi effect, Fig. 2B). This pressure decrease is important because the solvating power of a supercritical fluid is dependent on density and therefore pressure. With pressure decreasing through a finite restrictor, this presents an opportunity for analyte nucleation (*e.g.*, association and/or precipitation), to occur previous to orifice exit and

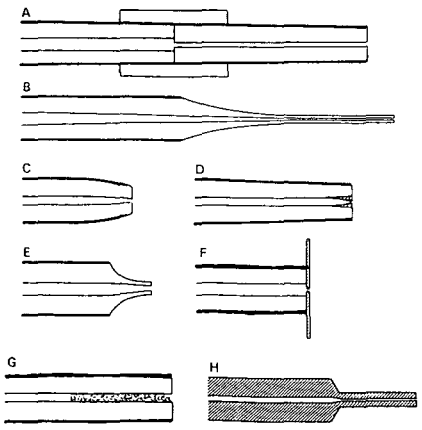

Fig. 1. Examples of flow restrictors used for SFC. (A) Straight capillary, (B) robot-pulled tapered capillary, (C) Guthrie and (D) deposition integral restrictors, (E) quick-drawn capillary, (F) laser-drilled pinhole, (G) multipath frit, (H) pinched tube. Reprinted with permission from ref. 28.

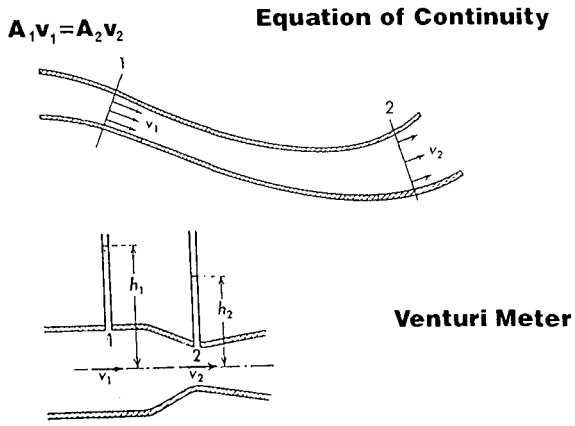

Fig. 2. (A) Schematic of a restricted conduit, showing that as diameter decreases, velocity of the moving fluid must increase. (B) Venturi meter, demonstrating Bernoulli's principle, that as velocity of a fluid increases, its pressure decreases.

analyte desolvation. Analyte solubility, transit time in the restrictor, desolvation characteristics, and the methods used for eluant measurement make this area very difficult to approach on first principles. However, some indications of nucleation may have been observed experimentally by flame ionization detector (FID) spiking when using different restrictors, pressures, and temperatures[31]. The relationship of restrictor design, analyte solubility and nucleation to the observed experimental factors of FID spiking, restrictor plugging, and losses in sensitivity may not be as clear as one would wish. But, from the above, it does suggest that transmission and ionization at high mass may be directly related to mobile phase density, which can change markedly in restrictors.

APPLICATIONS

Previous reports of high-molecular-weight SFC–MS transmission have utilized different samples, restrictors, and diverse strategies for interface and restrictor heating. Thus, it is difficult to make direct comparisons and draw solid conclusions about the selective advantages of each. Additional differences lie in the variety of mass spectrometers utilized and the degree of instrumental modification required. In the work summarized below, some of these differences have been mentioned.

In a study of peptide SFC–MS, Huang *et al.*[27], working with a double focusing instrument (Finnigan-MAT Model 8430), have recently presented chemical ionization (CI) data for valinomycin, a cyclic peptide in excess of 1100 a.m.u. (Fig. 3). This spectrum was obtained in the negative-ion mode, using methane as reagent gas. When additional amounts of CO_2 were added to the reagent gas, greater structural detail was obtained due to charge exchange fragmentation[32]. These data were obtained using a multipath frit restrictor, maintained at 350°C, and a source temperature of 280°C. In this interface the high-temperature region (350°C) was limited to the frit portion of the restrictor. A diagram of the SFC–MS interface is presented in Fig. 4.

Additional cyclic peptide data has been presented by Kalinosky *et al.*[26] utilizing

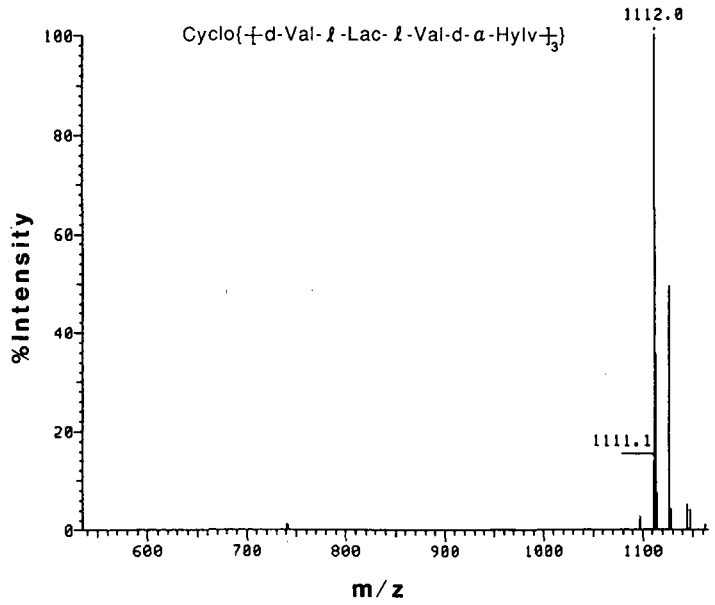

Fig. 3. The methane CI mass spectrum of valinomycin, obtained by SFC–MS, using a multipath frit restrictor maintained at 350°C. Reprinted with permission from ref. 27.

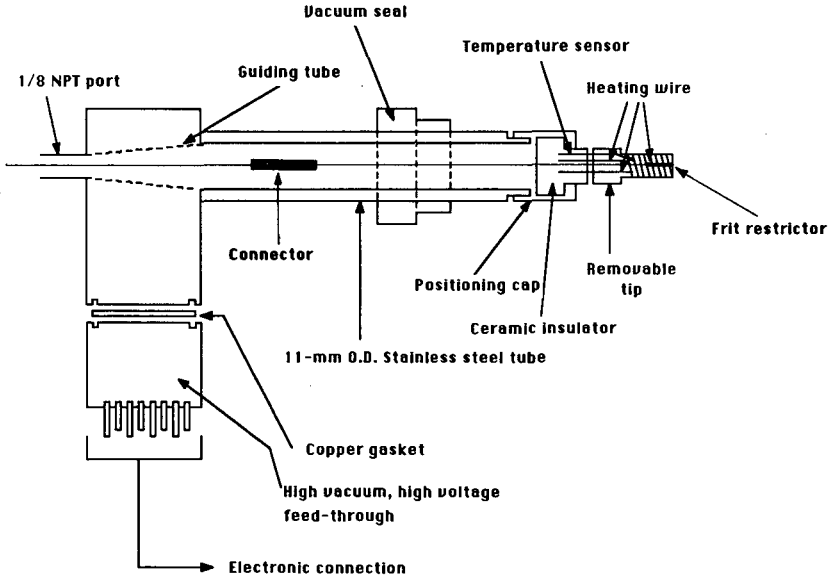

Fig. 4. Schematic diagram of the SFC–MS interface used by Huang *et al*[27]. The column is maintained at oven temperature up to the restrictor region, which is heated separately. Reprinted with permission from ref. 27.

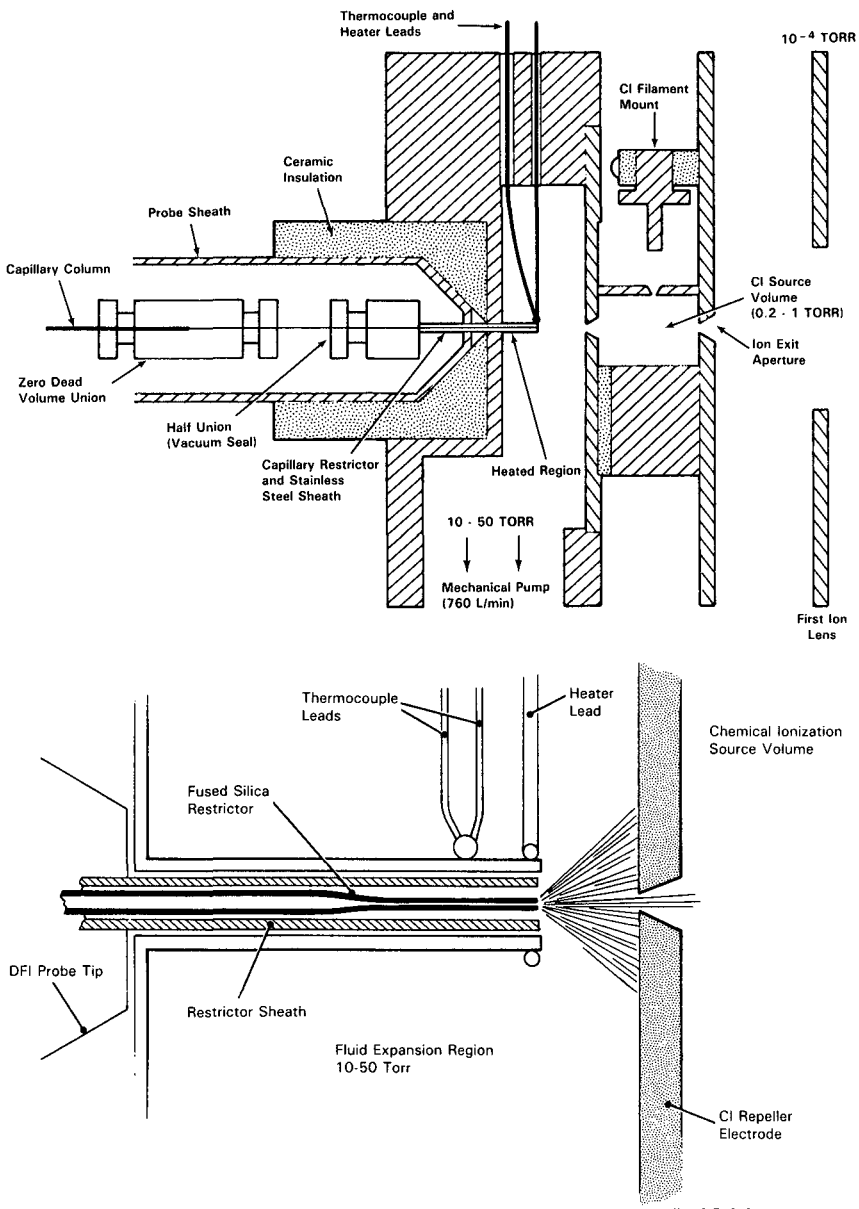

Fig. 5. Schematic of the "high-flow-rate" interface of Smith and Udseth[21]. The source is differentially pumped to accomodate the high flow-rates of packed-column SFC. Restrictor heating occurs in the last 7 mm. Reprinted with permission from ref. 21.

packed SFC columns and a "high flow-rate" interface[21] (Fig. 5). This interface, designed to accomodate the faster flow-rates of packed columns, was combined with an integral restrictor and heated along the last 7 mm of the restrictor to about 145°C. The peptide, cyclosporin, was chromatographed in a CO_2 mobile phase doped with

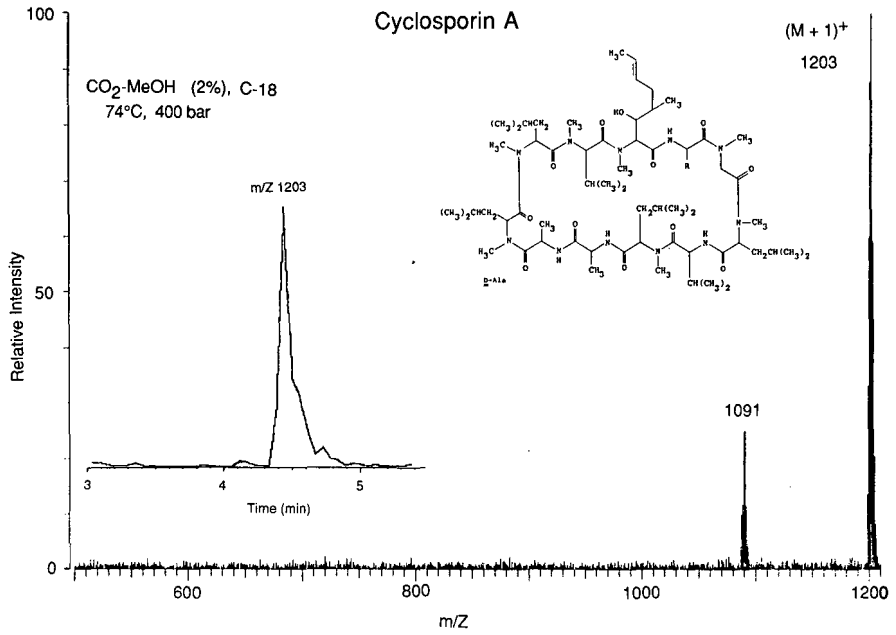

Fig. 6. Selected ion chromatogram and CI mass spectrum of cyclosporin A obtained using the "high-flow-rate" interface with an integral restrictor heated to 145°C. Reprinted with permission from ref. 26.

2% methanol and analyzed by CI-MS. The selected ion chromatogram $(MH)^+$ and the mass spectrum are presented in Fig. 6. A notable difference between this interface, (integral restrictor), and the previous frit restrictor[32] is the lower temperature requirements for molecules of similar structure. Higher flow-rates, however, would be expected to improve transmission and thereby demand less thermal assistance.

Methanol was used as a modifier in the latter case and also served as a convenient CI reagent gas, providing abundant protonated molecular ions, $[M+H]^+$, while still showing adequate fragmentation to study molecular detail.

High-molecular-weight waxes have been analyzed by SFC–MS utilizing an unmodified GC transfer line (Hewlett-Packard Model 5985B GC–MS system)[34]. These authors have demonstrated transmission and characterization of components weighing about 950 dalton. An integral restrictor fabricated directly on the column end was inserted through the transfer line, and heated to one hundred degrees above column temperature, which for the separations demonstrated, was 125°C (interface temperature 225°C). Fig. 7 is the mass spectrum obtained from a component detected in beeswax by methane chemical ionization. The authors have tentatively identified the sample as a dipalmitoyl ester of a C_{24} diol.

Chester and Innis[33] and Pinkston et al.[35] have extended high-molecular-weight studies to carbohydrates using trimethylsilylation to block the polar hydroxyl groups. This relatively simple method of depolarization also insures mobile phase solubility. SFC–MS of a series of glucose polymers prepared in this manner has extended high mass transmission and detection to approximately 3000 Dalton. CI spectra were obtained with a quadrupole (VG 30-250, VG Masslab) instrument using ammonia as

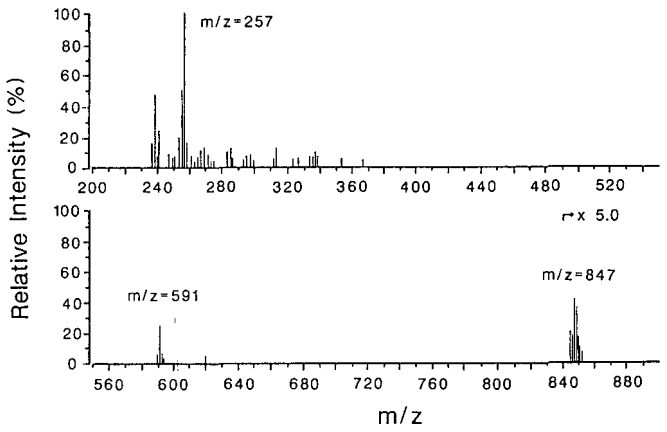

Fig. 7. Mass spectrum of a component from beeswax, obtained using an HP 5985B GC–MS, with an integral restrictor introduced through the normal GC inlet, heated to 225°C. Reprinted with permission from ref. 34.

the reagent gas[35]. The $[M+NH_4]^+$ ions were detected up to *m/z* 2830 which was the expected ion for $(Glc)_7$ of this homopolymer series (Fig. 8). This mass range approximates the detection limits of the quadrupole mass spectrometer and is not a constraint imposed by the interface. For these studies, a robot pulled tapered restrictor, fabricated on site, was used. This interface (Fig. 9), was designed to maintain temperatures equal to that of the column in one zone and heated to 350°C in a second zone for a length of about 4 cm where restriction occurs.

As an extension of the study by Pinkston *et al.*[35], we wished to evaluate two major points using a high voltage magnetic instrument: (i) were there mass limitations to sample desolvation and ionization; and, (ii) what were the temperature requirements for the interface and restrictor. Imposed on these primary concerns were additional points that for successful application to biopolymers, both processes should be demonstrated on thermally labile and high-molecular-weight samples at sensitivities comparable, at least, to that realized by FAB.

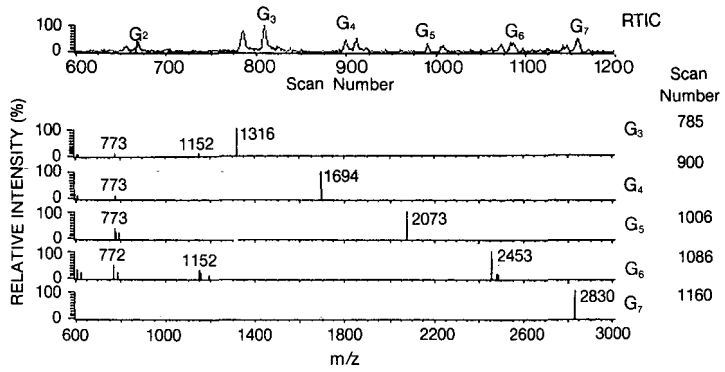

Fig. 8. Total ion chromatogram and selected ammonia CI mass spectra of a pertrimethylsilylated glucose homopolymer mixture. A robot-pulled tapered restrictor was used, at a temperature of 350°C. Reprinted with permission from ref. 35.

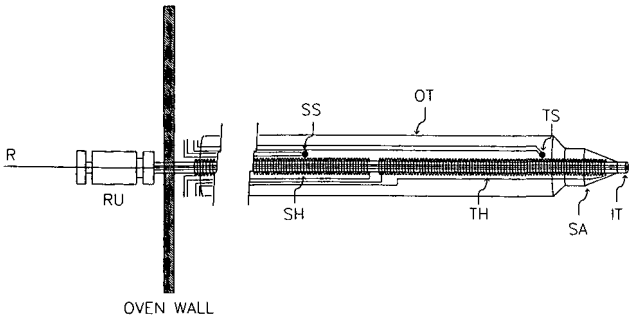

Fig. 9. Diagram of the interface used by Pinkton *et al.*[35]. Reprinted with permission from ref. 35.

For this work[25] a high-performance mass spectrometer was used (VG ZAB-SE, VG Analytical), operating at an ion source potential of 8 kV. Presented in Fig. 10 is a drawing of the standard DCI probe modified with an additional ceramic feed to accept the SFC capillary column. A platinum heating wire of the same type used in the standard probe is wrapped in a coil directly around the column end. Heating was necessary and supplied to the last millimeter of column, corresponding to the length of the integral restrictor fabricated at that point. In this design restrictors may be changed without disruption of the heating wire. The precise temperature at the restrictor tip has been difficult to assess because of the extremely small area of the heated region, but the platinum wire temperature under normal operating conditions was estimated to be 280°C based on its length, resistance, and the current supplied by the DCI control unit. Lower currents resulted in tip plugging and the operating current was set slightly above this point. Over a rather broad range above this temperature, no discernible effect on the eluting spectra was detected, although excessive heating currents were not

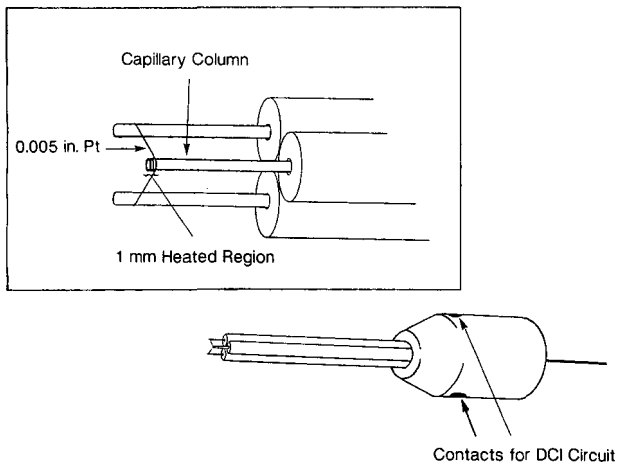

Fig. 10. Diagram of the SFC–MS probe from ref. 25. The standard DCI probe tip is configured with additional ceramic feed to accomodate the SFC column. Contact points privide electrical coupling to tabs on the side of the ion source to control temperature. The inset shows the enlarged tip with the capillary column and heating wire.

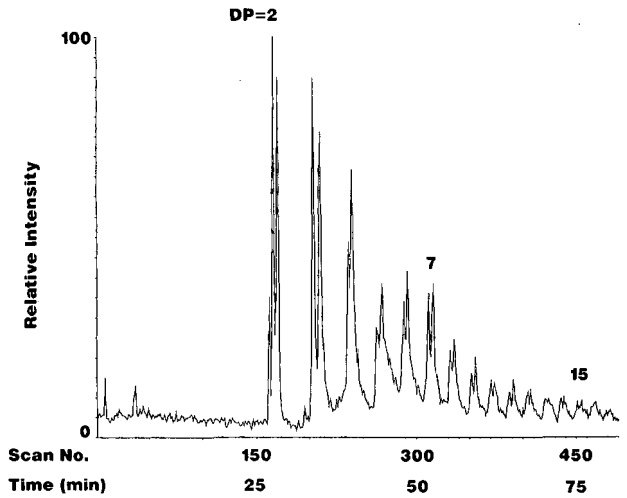

Fig. 11. Total ionization plot of pertrimethylsilylated glucose polymers. Reprinted with permission from ref. 25.

evaluated. The temperature experienced by analytes on passing the restrictor zone must be somewhat lower than that calculated above, due to insulation by the column wall and tip cooling contributed by mobile phase vaporization.

To assess the effectiveness of this restrictor for analyte transmission and ionization, the same glucose homopolymer described previously[35] was prepared and analyzed by SFC and SFC–MS (Fig. 11). A comparison of total ionization plots with FID signal suggests that sample transmission and ionization efficiency is maintained from the low to high mass oligomers. Profiles of individual products in the homopolymer series, $[M + NH_4]^+$, for this sample are presented in Fig. 12 which shows normalized adduct ions from DP2 to DP15. The chromatographic fidelity is very apparent with anomer separation still observable at DP15. Fig. 13 is the mass spectrum for DP15.

The overall sensitivity of this interface was studied by use of known concentrations of cyclodextrin which have been permethylated previous to analysis. Shown at

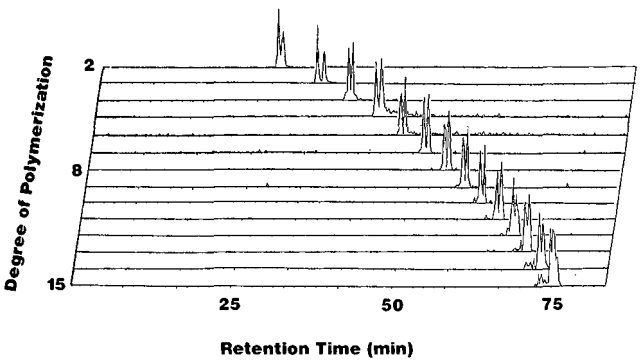

Fig. 12. Selected ion profile of trimethylsilylated glucose polymers. Reprinted with permission from ref. 25.

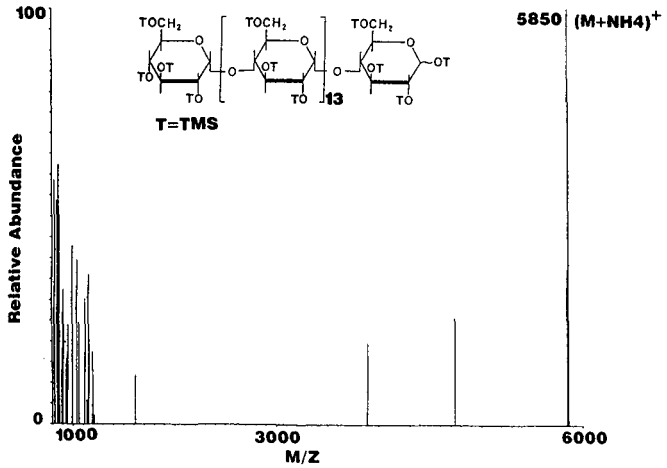

Fig. 13. Mass spectrum of trimethylsilylated glucose oligomer, DP15. Reprinted with permission from ref. 25.

the top of Fig. 14 is the total ion profile (TIP) of 100 ρmol of cyclodextrin. Panel 14B is the ammonium adduct ion profile, m/z 1446 $[M + NH_4]^+$, for that sample. The limits of detectability appear to approach 2 picomol. At this concentration no peaks were detected in the TIP although the ion was easily detected at this concentration (Fig. 14C).

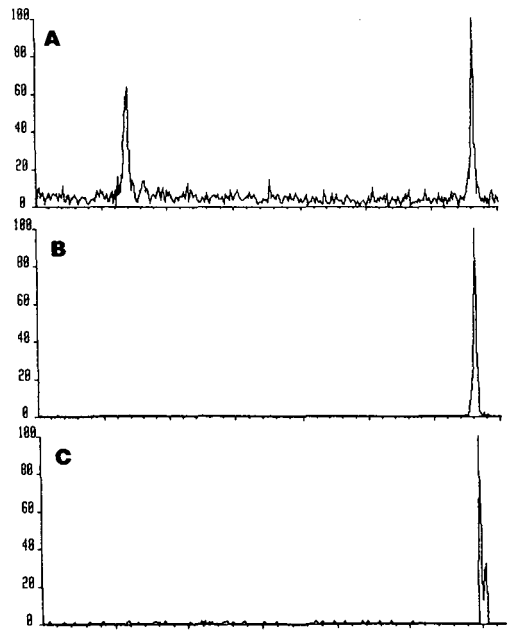

Fig. 14. SFC–MS: (A) total ionization plot for an injection of 150 ng permethylated β-cyclodextrin; (B) Selected ion chromatogram for molecular ion adduct $[M+NH_4]^+$, m/z 1446, for the above injection; (C) selected ion plot of molecular ion adduct $[M+NH_4]^+$ for a 3-ng injection. Reprinted with permission from ref. 25.

DISCUSSION

A practical observation of MS interface operation, that increased restrictor temperatures improve sample detection (up to a limit), suggests that nucleation is occuring. For those compounds that are thermally stable, heating would enhance analyte volatility and thus restrictor transmission. Extensive restrictor heating, however, circumvents one of the advantages offered by SFC, and more importantly, would be self-limiting with thermally labile and/or polar materials which potentially could be chromatographed in more polar mobile phases. In the current context, it would seem that the lower temperature requirements of the integral or disk restrictors, (the shortest of the three), bears out this reasoning. Since abrupt restriction is desirable, (in order to minimize solute precipitation and the necessity for extensive heating), the laser drilled disk would appear to be an ideal restrictor[36], although difficult to fabricate. Subsequently, we have made extensive use of the integral restrictor as the "next best thing" for high mass transmission during SFC–MS interfacing.

Much of the earlier work in SFC–MS has been carried out with low-voltage quadrupole instruments[25,35,36] and from these reports it was not clear whether there were high-mass limitations to detection. Another concern related to high-molecular-weight studies and SFC interfacing was the use of high-voltage sector instruments and the possibility of extensive arcing of the ion source. Two recent reports of interfaces with sector instruments, one operating at 8 kV[25,27] have provided some assurance that this is not a problem.

One of the most obvious features of CI spectra obtained by SFC–MS is their strong molecular ions, with little or no fragmentation. There are a variety of alternatives for developing structural information from these systems, and one's choice would depend largely on its appropriateness for particular classes of compounds. Charge exchange from CO_2 has already been mentioned as a useful tool for obtaining structural detail, and seems to parallel electron impact ionization in the fragmentations it induces[37]. Use of other appropriate CI reagents has potential for providing greater structural detail as well. Work in this laboratory with glycosphingolipids has indicated that while ammonia CI provides molecular ions, with little fragmentation, use of a mixture of CO_2 and methanol as CI reagent can induce very informative fragmentations in this particular class of molecules. Certainly there is much to be done in this area.

Another approach to eliciting structural detail from SFC–MS is through collisionally induced dissociation (CID) of molecular ions. In this case, fragmentation in the ion source is not desirable, because a strong signal for the parent ion is necessary for CID. Here an interesting question is whether CID can be performed on transient CI product ions, and whether collisions in a low-voltage cell would be more desirable than collisions at high energy. Addressing the first question, Hurst[38] has performed MS–MS experiments on SFC–CI-MS generated ions using a TSQ 70 quadrupole, and in preliminary experiments in this laboratory, using direct chemical ionization, metastable ion kinetic energy spectra (MIKES) have been obtained for ammoniated molecular ions of 3500 daltons[39]. The second question, about the informativeness of various collision processes, is more complex, but there are certainly advantages to use of lower collision energies and even chemically reactive reagents in the collision cell.

Obviously, SFC–MS has not caught up with GC–MS or even LC–MS, but it has great potential in its application to biological research problems; an area in great need of all the analytical assistance it can receive. There appear to be no significant mass limitations, at least up to 6000 dalton, and most current difficulties are purely technical and will, more than likely, be resolved. One important area in need of work is in the design of an effective restrictor, which should require far less heating. This could improve SFC–MS both by making the interface design simpler, and by providing broader applicability to materials of biological interest.

REFERENCES

1 M. Barber, R. S. Bordoli, R. D. Sedgwick and A. N. J. Tyler, *Chem. Soc., Chem. Commun.*, 213 (1981) 1497–1501.
2 K. Biemann and H. A. Scoble, *Science (Washington, D.C.)*, 237 (1987) 992–998.
3 K. Biemann, *Anal. Chem.*, 58 (1986) A1288–A1305.
4 V. N. Reinhold and S. A. Carr, *Mass Spectrom. Rev.*, 2 (1983) 153–221.
5 V. N. Reinhold, in S. J. Gaskell (Editor), *Mass Spectrometry in Biomedical Research*, Wiley, New York, 1986, pp. 181–213.
6 A. Dell, *Adv. Carbohydr. Chem. Biochem.*, 45 (1987) 17–72.
7 V. N. Reinhold, in V. Ginsburg (Editor), *Oligosaccharide Chemical Ionization, Methods in Enzymology, Complex Carbohydrates, Part E. Vol. 138*, Academic Press, New York, 1987, pp. 59–84.
8 M. L. Coates and C. L. Wilkins, *Anal. Chem.*, 59 (1987) 197–200.
9 R. M. Caprioli, T. Fan and J. S. Cottrell, *Anal. Chem.*, 58 (1986) 2949.
10 R. M. Caprioli, W. T. Moore and T. Fan, *Rapid Commun. Mass Spectrom.*, 1 (1987) 15–18.
11 S. Santikarn, G. R. Her and V. N. Reinhold, *Carbohydr. Chem.*, 6 (1987) 129–139.
12 M. Novotny, S. R. Springston, P. A. Peadon, J. C. Fjeldsted and M. L. Lee, *Anal. Chem.*, 53 (1981) 407A–414A.
13 J. C. Fjeldsted and M. L. Lee, *Anal. Chem.*, 56 (1984) 619A–628A.
14 J. C. Fjeldsted, R. C. Kong and M. L. Lee, *J. Chromatogr.*, 279 (1983) 449–455.
15 R. D. Smith, J. C. Fjeldsted and M. L. Lee, *J. Chromatogr.*, 247 (1982) 231–243.
16 R. D. Smith and H. R. Udseth, *Anal. Chem.*, 55 (1983) 2266–2272.
17 B. W. Wright, H. R. Udseth, R. D. Smith and R. N. Hazlett, *J. Chromatogr.*, 314 (1984) 253–262.
18 T. L. Chester, *J. Chromatogr.*, 299 (1984) 424–431.
19 C. M. White, C. P. Wagner, R. M. Ravey and R. K. Houck, presented at the *190th ACS National Meeting, September 8–13, Chicago, IL*, paper ANYL48.
20 C. M. White and R. K. Houck, *J. High. Res. Chromatogr. Chromatogr. Commun.*, 8 (1985) 293–296.
21 R. D. Smith and H. R. Udseth, *Anal. Chem.*, 59 (1987) 13–22.
22 T. L. Chester, D. P. Innis and G. D. Owens, *Anal. Chem.*, 57 (1985) 2243–2247.
23 J. C. H. Kuei, G. R. Her and V. N. Reinhold, *Anal. Biochem.*, 172 (1988) 228–234.
24 D. M. Sheeley and V. N. Reinhold, *Anal. Biochem.*, submitted for publication.
25 V. N. Reinhold, D. M. Sheeley, J. C. Kuei and G. R. Her, *Anal. Chem.*, 60 (1988) 2719–2722.
26 H. T. Kalinosky, B. W. Wright and R. D. Smith, *Biomed. Environ. Mass Spectrom.*, 15 (1988) 239.
27 E. C. Huang, B. J. Jackson, K. E. Markides and M. L. Lee, *Anal. Chem.*, 60 (1988) 2715–2719.
28 R. D. Smith, H. T. Kalinoski and H. R. Udseth, *Mass Spectrom. Rev.*, 6 (1987) 445–496.
29 K. E. Markides, S. M. Fields and M. L. Lee, *J. Chromatogr. Sci.*, 24 (1986) 254–257.
30 E. J. Guthrie and H. E. Schwartz, *J. Chromatogr. Sci.*, 24 (1986) 236–240.
31 R. D. Smith, J. L. Fulton, R. C. Peterson, A. J. Kopriva and B. W. Wright, *Anal. Chem.*, 58 (1986) 2057–2064.
32 E. Huang and M. L. Lee, *SFC Applications*, published in conjunction with the *1988 Workshop on Supercritical Fluid Chromatography, Park City, Utah, January 12–14, 1988*, BYU Press, 1988, pp. 169–172.
33 T. L. Chester and D. P. Innis, *J. High Resolut. Chromatogr. Chromatogr. Commun.*, 9 (1986) 178–181.
34 S. B. Hawthorne and D. J. Miller, *J. Chromatogr.*, 388 (1987) 397–409.
35 J. D. Pinkston, G. D. Owens, D. S. Millington, L. J. Burkes and T. E. Delaney, *Anal. Chem.*, 60 (1988) 962–966.

36 S. Santikarn and V. N. Reinhold, Proceedings of the *33rd Annual Conference on Mass Spectrometry and Allied Topics, San Diego, CA, May 26–31, 1985*, pp. 218–219.
37 E. D. Lee, S. H. Hsu and J. D. Henion, *Anal. Chem.*, 60 (1988) 1990–1993.
38 J. Hurst, *TSP Report: Technologies and Applications of LC/MS*, 2 (1988) 1.
39 V. N. Reinhold, D. M. Sheeley and G. R. Her, unpublished results.

Journal of Chromatography, 474 (1989) 97–111
Elsevier Science Publishers B.V., Amsterdam — Printed in The Netherlands

CHROM. 21 507

INDUSTRIAL APPLICATIONS OF SUPERCRITICAL-FLUID CHROMATOGRAPHY–MASS SPECTROMETRY INVOLVING OLIGOMERIC MATERIALS OF LOW VOLATILITY AND THERMALLY LABILE MATERIALS

J. DAVID PINKSTON*, DONALD J. BOWLING and THOMAS E. DELANEY
The Procter & Gamble Company, Research and Development Department, Corporate Research Division, Miami Valley Laboratories, P.O. Box 398707, Cincinnati, OH 45239-8707 (U.S.A.)

SUMMARY

Three recent applications of supercritical-fluid chromatography with flame ionization (SFC–FID) and with mass spectrometric (SFC–MS) detection are discussed. These applications involve thermally labile and/or relatively non-volatile materials. Specifically, they involve ethoxylated alcohols, inositol triphosphate and peroxides. Ammonia chemical ionization (CI) and methane CI SFC–MS were used to deconvolute complex chromatograms and to confirm postulated identities. The SFC–MS "electron ionization like" spectrum of the trimethylsilyl (TMS) derivative of inositol triphosphate was shown to be very similar to the library electron ionization spectrum of TMS-inositol diphosphate. SFC–MS was shown to be particularly suitable for the analysis of thermally labile peroxides using ammonia CI SFC–MS. All three applications discussed here would have been difficult, if not impossible, by traditional gas or liquid chromatographic methods.

INTRODUCTION

Industrial analytical chemists encounter separation problems involving widely differing types of materials. It is not uncommon that these problems are difficult to address by traditional methods such as gas chromatography (GC) and high-performance liquid chromatography (HPLC). This is the case when the mixture in question contains components which are too low in volatility or thermal stability for GC, and which simultaneously lack a good functional group for sensitive HPLC detection or are members of a mixture too complex for traditional HPLC separation[1].

Capillary supercritical-fluid chromatography (SFC) has experienced widespread growth and commercialization since it was reported in 1981[2,3]. Though it has been proposed as a general screening tool for non-polar samples[4], most SFC work has served to fill the "gap" between GC and HPLC described above. Applications involving thermally labile compounds, such as azo-compounds[5,6], and complex mixtures of low volatility, such as oligosaccharides[7], have been reported. Mass spectrometry (MS) has been shown to provide sensitive, universal, and specific detection for SFC[8–15]. Though our laboratory has been involved in supercritical-fluid

0021-9673/89/$03.50

chromatography–mass spectrometry (SFC–MS) for a number of years[16,17], we only recently acquired a mass spectrometer dedicated to SFC detection. This report discusses three of our first applications using this dedicated instrument. They involve ethoxylated alcohol mixtures, inositol triphosphate, and peroxides. In their own way, each is a good illustration of how SFC and SFC–MS can be used to solve problems which are difficult to address by traditional GC and HPLC.

EXPERIMENTAL

The SFC system is identical to that previously described[17] except for the incorporation of a stainless-steel tubing 10 cm × 0.127 mm (0.005 in.) I.D. × 1.6 mm (0.063 in.) O.D. just before the Valco injection valve in the carbon dioxide line from the syringe pump. This small addition dramatically reduced the solvent front tail in the direct (on-column) injection mode used in all the SFC–MS work.

Other modifications include the use of an Upchurch (Oak Harbor, WA, U.S.A.) fitting with an F226 fused-silica adapter and F140 nut to link the 1 m × 50 μm I.D. retention gap directly to the injection valve. SGE MVSU-004 zero dead volume unions (Scientific Glass Engineering, Austin, TX, U.S.A.) were used to link the retention gap to the column and the column to the restrictor. A fused-silica capillary sleeve (Polymicro Technologies, Phoenix, AZ, U.S.A.) with an O.D. of 375 μm and an I.D. of 200 μm was inserted into each SGE union to reduce the inner diameter. The column was a 10 m × 50 μm I.D. SB-Methyl 100 (Lee Scientific, Salt Lake City, UT, U.S.A.) with a 0.5-μm film thickness. The tapered-flow restrictor was fashioned from a 50 cm × 50 μm I.D. 180 μm O.D. fused-silica tubing (Polymicro Technologies) in the manner previously described[18]. It tapered to an aperture of approximately 3 μm over a 3.2-cm length.

The SFC–MS interface probe houses the flow restrictor and is similar to one previously described[17]. The tip of the interface probe was machined to fit the rear of the ion source ion volume of a Finnigan-MAT TSQ-70 triple quadrupole mass spectrometer (Finnigan-MAT, San Jose, CA, U.S.A.). The aperture of the flow restrictor was positioned just inside the interface probe tip, as described previously[17]. The probe stem was held at the same temperature as was the SFC oven, and the probe tip was held at roughly 300°C, unless otherwise indicated.

The first and third quadrupoles (Q1 and Q3, respectively) of the TSQ-70 were operated in the "low-mass-range mode" (m/z 4–2000) with Q1 and Q2 transmitting all ions. Q3 was used as the mass filter. The instrument was tuned and calibrated using perfluorotributylamine and tris(perfluorononyl)-s-triazine (PCR Research Chemicals, Gainsville, FL, U.S.A.) with automatic tuning software in the customary manner. The ion source temperature was held at 150°C unless otherwise indicated and the analyzer manifold was held at 70°C. Ammonia chemical ionization (CI) was performed with 1% ammonia in methanol ("Matheson" purity, 99.99% minimum, Matheson Gas Products, Dayton. OH, U.S.A.). Matheson purity methane was used for methane CI (Matheson). Isobutane CI was performed with "Instrument Grade" isobutane (99.5% minimum, Matheson). The indicated "ion source" pressure required to achieve proper CI conditions was approximately 1.3 kPa (10 Torr) for both ammonia and methane CI, and approximately 360 Pa (2.7 Torr) for isobutane CI. However, these measurements are performed using an uncalibrated Pirani gauge in the

CI reagent gas supply line and do not provide an accurate measurement of the actual ion source pressure. Electron ionization (EI) (with possible contribution from EI-like carbon dioxide charge exchange ionization) was performed by simply exchanging the "CI probe" ion source ion volume for the "EI probe" volume. Electron energy and emission current were held at 70 eV and 200 μA, respectively. The electron multiplier was operated at −1500 V with an electrometer gain of 10^{-7} A/V.

All the Neodol samples but Neodol 23-3 were commercial samples obtained from the Shell Chemical Co. (Houston, TX, U.S.A.). Neodol 23-3 was obtained courtesy of W. R. West (Shell Development, Houston, TX, U.S.A.). Approximately 2% (w/v) solutions of the Neodol samples were prepared in dichloromethane (American Burdick & Jackson, Muskegon, MI, U.S.A.) and injected without further preparation. The 1-pentaethoxy tetradecanol was synthesized and purified in house. Retention standards were obtained from PolyScience Corp. (Niles, IL, U.S.A.).

The Neodol samples were also analyzed by SFC–flame ionization detection (FID) using a Lee Scientific Model 622 SFC–GC system. The capillary column was a 10 m × 50 μm I.D. DB-1 (J&W Scientific, Folsom, CA, U.S.A.) with a 0.2-μm film thickness. The flow restrictor was a 50-μm I.D. ceramic frit (Lee Scientific). Injection was performed using a 0.2-μl internal loop (Valco, Houston, TX, U.S.A.) and flow splitting with a rougly 10:1 split ratio. The oven temperature was 120°C while the detector was held at 300°C. The mobile phase in all the work described in this publication was unmodified, SFC-grade carbon dioxide (Scott Specialty Gases, Plumsteadville, PA, U.S.A.). In the SFC–FID runs of the Neodol samples, the mobile phase pressure was held at 10.1 MPa (100 atm) for 5 min and then ramped to 35.5 MPa (350 atm) over 50 min. In the SFC–MS runs the SFC oven and interface probe stem were held at 100°C. The mobile phase pressure was held at 9.1 MPa (90 atm) for 8 min after the direct injection and then ramped at 0.5 MPa/min (5 atm/min) to 34.5 MPa (340 atm) during the methane CI runs. A slight modification of this pressure program was used in later ammonia CI work. The injection was performed at 7.1 MPa (70 atm). After 5 min at 7.1 MPa the pressure was stepped to 10.1 MPa (100 atm). The pressure was then ramped at 0.5 MPa/min (5 atm/min) to 35.5 MPa (350 atm). The mass spectrometer was scanned from m/z 100 to 1200 every second for Neodol 91-6, from m/z 100 to 1000 every 1.5 s for Neodol 45-7T, and from m/z 100 to 900 every 1.5 s for Neodol 23-3.

Inositol triphosphate was obtained from W. R. Sherman (Washington University School of Medicine, St. Louis, MO, U.S.A.). The sample was silylated as described in ref. 19. The solution injected had a concentration of 4.1 mg/ml of the trimethylsilyl ester/ether of inositol trophosphate. The SFC oven temperature was held at 150°C while the mobile phase pressure was held at 12.2 MPa (120 atm) for 4 min and then ramped to 32.4 MPa (320 atm) at 1.0 MPa/min (10 atm/min). The mass spectrometer was scanned from m/z 300 to 1200 in the CI mode and from m/z 100 to 1200 in the EI-like mode, both with a cycle time of 2 s. During EI-like ionization, at a mobile phase pressure of 27.4 MPa (270 atm) [approximately 2.0 MPa (20 atm) above the elution pressure of the analyte], the "ion source" pressure (as previously described) was 26 mTorr. Under these same EI-like conditions the analyzer pressure was $1.1 \cdot 10^{-5}$ Torr, as measured with an uncalibrated Bayert–Alpert ion gauge.

Benzoyl peroxide was obtained from Aldrich (Milwaukee, WI, U.S.A.). Terpineol succinate peroxide was synthesized in-house. The former was dissolved in

dichloromethane (American Burdick & Jackson) to a concentration of 0.5 μg/μl, while the latter was dissolved in acetone (American Burdick & Jackson) at the same concentration. The mass spectrometer was scanned from *m/z* 100 to 300 with a cycle time of 1 s for benzoyl peroxide. The scan range for terpineol succinate peroxide was *m/z* 100 to 550, also with a 1-s cycle time. A variety of component temperatures were used during the benzoyl peroxide runs, but the spectrum presented in the following section was obtained with an SFC oven and interface probe stem temperature of 80°C, a probe-tip temperature of roughly 120°C, and an ion source temperature of 150°C. Temperatures for the terpineal succinate peroxide run presented in the following section were: oven and probe-stem at 40°C, probe-tip at 100°C, and source at 85°C. The mobile phase pressure was held at 7.1 MPa (70 atm) for 2 min and then ramped to 27.4 MPa (270 atm) at 1.0 MPa/min (10 atm/min) for both peroxides.

RESULTS AND DISCUSSION

Ethoxylated surfactant

Neodol (Scheme 1) is a trade name for ethoxylated alcohols, an important class of non-ionic surfactants. They are generally named Neodol xx-z, where "xx" indicates a range of *n* values and "z" is an average *m* value. For example, Neodol 45-7 indicates that the starting alcohols were 14 and 15 carbon alcohols and that the average ethoxylate value is 7. The average length and range of the alkyl and ethoxylate chains determine the properties of each mixture. Neodols are used in a wide variety of industrial and household products. Yet they are difficult to analyze using traditional chromatographic methods. Many Neodols contain components which are too low in volatility for traditional GC analysis. Ethoxylated alcohols lack a good chromophore or other functionality for HPLC detection, and are thus difficult to analyze with good sensitivity by HPLC. In addition, they are often the product of the ethoxylation of a mixture of alcohols. It is difficult to resolve the various components of such a complicated mixture using traditional HPLC, especially if the chosen detector requires isocratic elution. We have found that SFC using carbon dioxide and FID is an excellent tool for analyzing Neodol samples. SFC–MS has been used to identify unknown components of the ethoxylated mixtures and to confirm postulated peak identities.

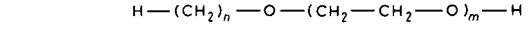

Scheme 1. Structure of neodol.

Fig. 1 shows an SFC–FID trace of Neodol 45-7T ("T" stands for "topped", meaning that the concentration of the lower oligomers in the mixture has been reduced) to which 1-tetradecanol and 1-pentadecanol have been added. The two straight-chain alcohols co-elute with the first members of each ethoxylated series allowing one to postulate identities for the other members of the series by simply counting from the unethoxylated peak (E_0). Postulating peak identities in this manner was straightforward for the chromatograms of most Neodol mixtures. Fig. 2 shows the chromatogram of Neodol 45-8NRE, where NRE stands for "narrow

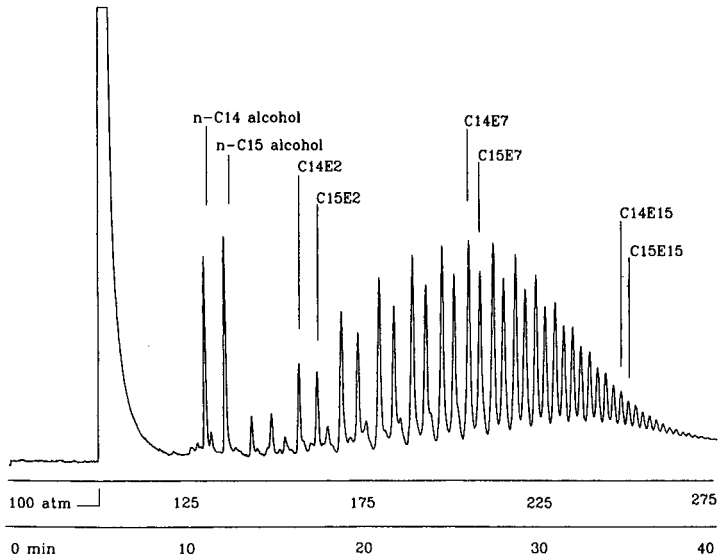

Fig. 1. SFC–FID chromatogram of Neodol 45-7T with straight-chain C_{14} and C_{15} alcohols "spiked" as retention standards.

range ethoxylate". It is obvious from the chromatograms that the second sample does indeed have a tighter ethoxylate distribution than does the Neodol 45-7T, Table I summarizes the results of the analysis of a number of Neodol samples. These results assume that the FID response factor is constant during the chromatographic run, in spite of the increase in carbon dioxide flow into the flame due to pressure programming. Our results agree well with the expected composition of the mixtures.

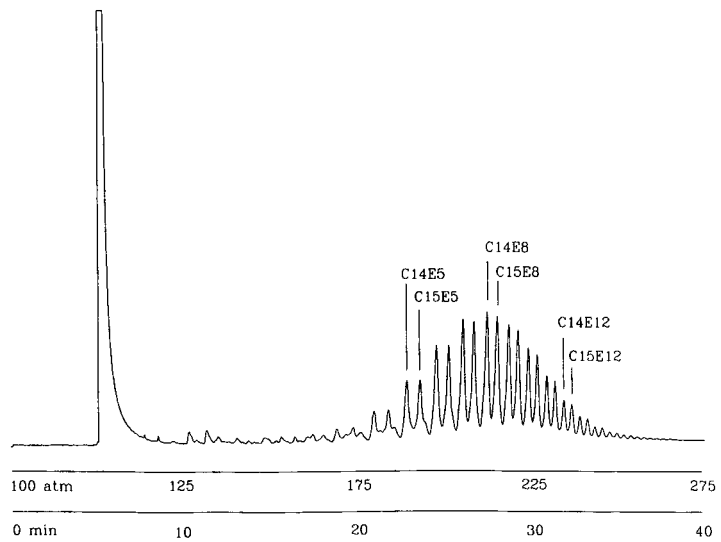

Fig. 2. SFC–FID chromatogram of Neodol 45-8NRE.

TABLE I

SUMMARY OF SFC–FID ANALYSIS OF NEODOL SAMPLES

Neodol sample	*Average ethoxylate number*	*Detectable ethoxylate range*	*Ethoxylate range carrying 68.3% mass*	*Average alkyl chain length*
23.3	3.1	0–15	0–3	12.5
45-7T	7.4	0–21	3–9	14.5
45-8NRE	8.1	1–18	6–10	14.5
91-6	6.8	0–22	3–10	10.2
91-6NRE	6.7	3–19	5–8	10.2

The postulated peak identities of the Neodol samples were confirmed by SFC–MS. Some controversy exists in the literature concerning the CI of ethoxylated alcohols. Stephanou[20] discusses spectra exhibiting the ammonium adduct ion as the base peak, a protonated molecule with a relative abundance of 3–17% depending on the length of the ethoxylate chain, and many structurally significant fragment ions of relative abundance generally 3–18%. On the other hand, spectra discussed in the work of Rudewicz and Munson[21] are much simpler, showing primarily the ammonium adduct ion, a protonated molecule with less than 2% relative abundance, and even lower levels of fragment ions. These results were obtained with either pure ammonia or 1% ammonia in methane as reagent gas. Fig. 3 shows the ammonia CI SFC–MS spectrum of an ethoxylated alcohol standard, 1-pentaethoxy tetradecanol. The base peak of the spectrum in Fig. 3 corresponds in mass to the ammonium adduct ion. The next most abundant ion corresponds to the protonated molecule. The other major peaks in the spectrum correspond in mass to logical fragments of the ethoxylated standard that would be expected based on Stephanou's work[20]. Ions at $[M + 32]^+$ and at $[M + 46]^+$ may be due to the addition of $[CH_3–NH_3]^+$ and of $[C_2H_5–NH_3]^+$, produced in the 1% ammonia in methane CI plasma, to the ethoxylated standard.

Mass chromatograms of the ammonium adduct ions of a number of components of a typical Neodol sample, Neodol 23-3, are shown in Fig. 4. Under the conditions of

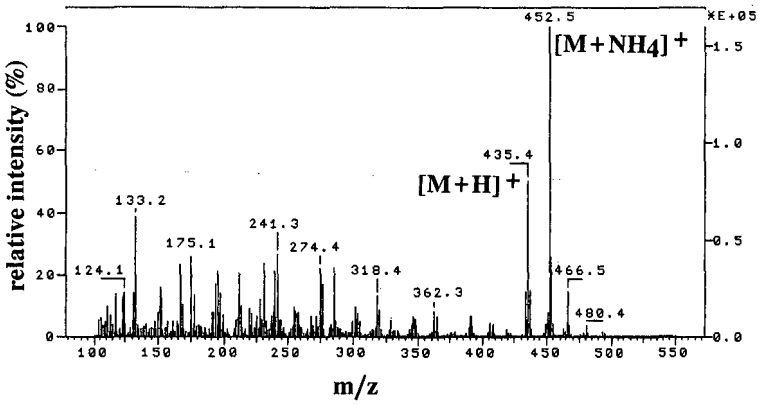

Fig. 3. Ammonia CI SFC–MS spectrum of 1-pentaethoxy tetradecanol.

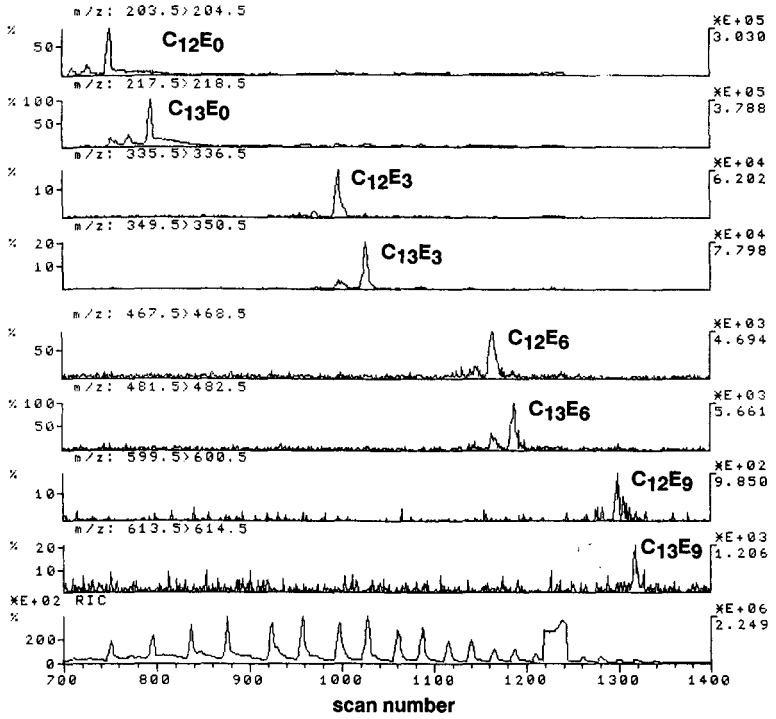

Fig. 4. Ammonia CI SFC–MS run of Neodol 23-3 showing a portion of the reconstructed total ion current chromatogram (bottom) and representative ammonium adduct mass chromatograms.

this run ethoxylated, branched-chain alcohols would elute before their straight-chain isomers[22]. Small amounts of branched-chain alcohols are known to be present in the starting alcohols used in this type of ethoxylation reaction[23]. Thus small peaks eluting before the major peak in each mass chromatogram are probably due to branched-chain isomers of the starting alcohols. The shift in baseline in the reconstructed total ion current chromatogram is due to rezeroing the electrometer during the run.

Fig. 5 shows the SFC–FID chromatogram of Neodol 91-6. We could not unambiguously assign structures to the peak series using coinjection of retention standards due to the complexity of the mixture. Fig. 6 illustrates mass chromatograms and the reconstructed total ion current chromatogram from a methane CI SFC–MS run of Neodol 91-6. Using the data from this run we were able to quickly and unambiguously assign the peak identities shown in Fig. 5. The chromatographic resolution is lower in the SFC–MS runs than in the SFC–FID runs. This has been observed and discussed in previous work[17]. It is most likely due to the use of direct injection in SFC–MS instead of flow-splitting injection, as well as column overload.

The analysis of non-ionic, ethoxylated surfactants such as Neodols by SFC–FID and SFC–MS is straightforward. These data illustrate why we feel that SFC is the most appropriate separation technique for dealing with problems which involve surfactants such as these. Some problems involving Neodol mixtures may be solved more rapidly using Rudewicz and Munson's probe distillation/CI MS method[21]. This method,

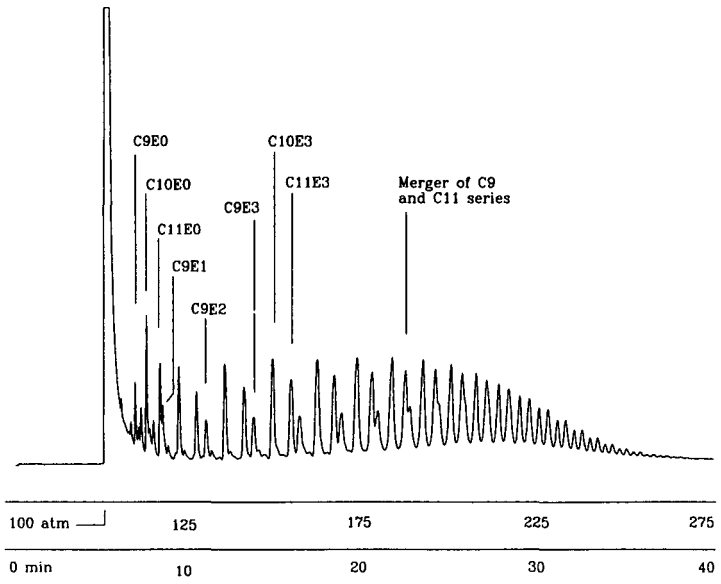

Fig. 5. SFC–FID chromatogram of Neodol 91-6.

however, would not be suitable for very complex Neodol mixtures, especially those where information about isomers was desired, or for Neodol mixtures containing components of interest too low in volatility to be desorbed from the distillation probe. Finally, the method would be difficult if ionization conditions producing the very simple spectra reported by Rudewicz and Munson[21] were not achieved (as in our work).

Thermospray LC–MS has recently been shown to be a viable alternative for the analysis of non-ionic ethoxylated surfactants[24]. Thermospray LC–MS does suffer from at least two disadvantages when compared to SFC–MS in this type of analytical

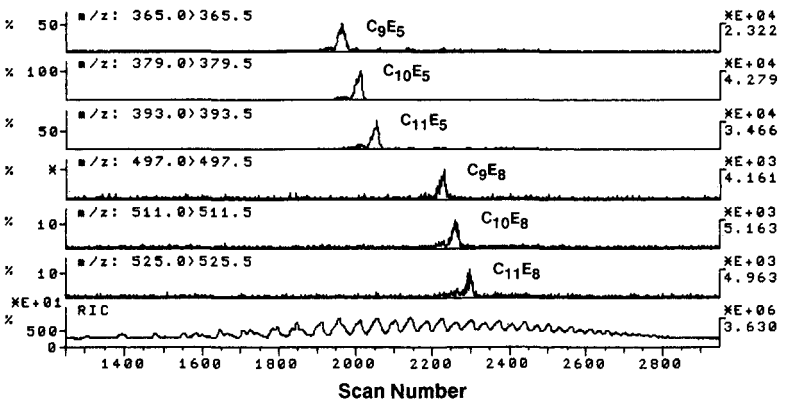

Fig. 6. Methane CI SFC–MS run of Neodol 91-6 showing a portion of the reconstructed total ion current chromatogram (bottom) and mass chromatograms of the protonated molecules of representative components.

challenge, however. Chromatographic efficiency per unit time on a given column is inherently lower with a liquid mobile phase than with a supercritical mobile phase[1]. Thermospray LC–MS is often performed with packed columns, while our results were obtained using capillary columns. Thus the results reported in ref. 24 cannot be directly compared with our results. However, individual oligomers and their isomers in each ethoxylated series are better resolved by capillary SFC–MS than by thermospray LC–MS[24]. Secondly, and perhaps more importantly, most traditional CI and even EI (see below) ionization methods are available in capillary SFC–MS, which is not the case with thermospray LC–MS.

Inositol triphosphate

The phosphorylated inositols are important in many biological systems (for a review see refs. 25 and 26). Certain isomers are involved in cellular stimulus-response coupling via calcium mobilization[25–27], and it's been postulated that lithium treatment of manic illness acts on an enzymatic pathway involving phosphorylated inositols[28]. The more highly phosphorylated inositols (*i.e.*, pentakis- and hexakis-phosphates) are commonly found in grains, seeds, soils, and sediments.

The chromatographic analysis of the members of this series with higher degrees of phosphorylation is difficult using conventional chromatographic methods. Significant losses due to adsorption during GC analysis are apparent with the TMS and methyl esters of the di- and triphosphates[29,30]. The lack of a sensitive method of detection and adsorption of the more highly phosphorylated inositols are the obstacles in HPLC analysis[30,31]. Capillary SFC has relatively inert instrumental components and is able to elute low volatility solutes at comparatively low temperatures. We have found that capillary SFC is well suited for analyzing the TMS derivatives of inositol phosphates[19]. Isobutane CI SFC–MS was used to confirm the identity of the TMS derivative of inositol triphosphate[19]. The base peak of the spectrum is at *m/z* 1069, corresponding in mass to the protonated molecule.

We have extended this work by running TMS-inositol triphosphate derivative by EI or, more appropriately, "EI-like" ionization. At least a portion of the ionization is probably due to carbon dioxide charge exchange[32,33]. The spectrum obtained from this EI run is shown in Fig. 7. The spectrum is indeed EI-like. The base peak at *m/z* 299,

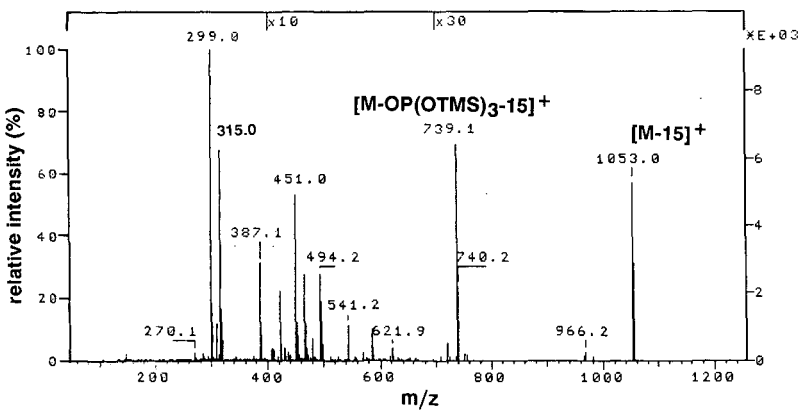

Fig. 7. EI-like SFC–MS mass spectrum of the TMS derivative of inositol triphosphate.

$[OP(OSi(CH_3)_2)\ (OTMS)_2]^+$, is a common base peak in the EI spectra of TMS derivatives of phosphate-bearing molecules. The ion of highest mass in the spectrum is the $[M - CH_3]^+$ peak at *m/z* 1053. The ion at *m/z* 739 corresponds in mass to $[M - OP(OTMS)_3 - 15]^+$. Most of the other major ions in the spectrum correspond in mass to fragments containing portions of the phosphate group. For example, *m/z* 315 corresponds to $[HO\text{–}P(OTMS)_3]^+$, *m/z* 387 to $[P(OTMS)_4]^+$, and *m/z* 451 to $[H(OP(OTMS)_2)_2]^+$.

A library search of the EI spectrum of the TMS derivative of inositol triphosphate against the NBS/EPA library of EI spectra as supplied with the TSQ-70 yields the spectrum of the TMS derivative of inositol diphosphate as the highest match (the spectrum of the TMS derivative of inositol triphosphate is not in the library). Ions at *m/z* 299, 315 and 387 are the most abundant in both spectra and have similar relative intensities. This is not surprising since these are low mass ions related to the TMS derivative of the phosphate group.

Peroxides

The use of organic peroxides as polymerization initiators, bleaching agents and oxidizing agents is widespread. They are also involved in many biochemical processes[34]. Success in the separation of mixtures of peroxides by HPLC has been reported[35–38], though evidence of decomposition was observed under certain conditions[37]. All but the smallest peroxides are difficult to analyze by traditional GC methods due to their lability[39]. Since the critical temperature of carbon dioxide is just 31°C, SFC with carbon dioxide can be performed at temperatures just above room temperature if necessary. In addition, the components of a capillary SFC system are relatively inert. SFC with FID, nitrogen–phosphorus, and ultraviolet detection has been used to analyze thermally labile materials such as peroxides[40] and azo-compounds[5,6]. We wanted to further investigate the use of SFC in the analysis of peroxides. As part of this investigation we decided to use SFC–MS to confirm that the "peroxide" peak seen by SFC–FID was indeed the intact peroxide and not a degradation product. Earlier work with a different SFC–MS system[16] yielded

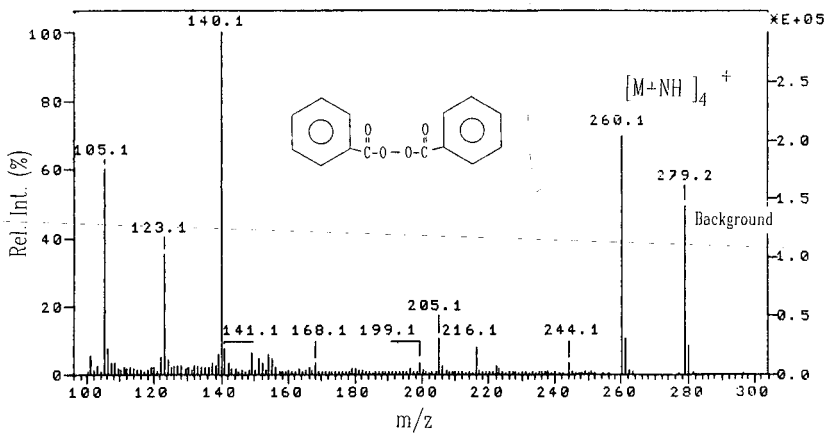

Fig. 8. Ammonia CI SFC–MS spectrum of benzoyl peroxide. Ions at *m/z* 205 and *m/z* 279 are background ions.

a single, sharp chromatographic peak for benzoyl peroxide. The major ions in the isobutane and ammonia CI spectra of this peak were related to decompensation products of benzoyl peroxide.

We recently undertook a study of the effects of the temperatures of various components of the SFC–MS system on the spectrum of benzoyl peroxide. We varied the temperatures of the mass spectrometer ion source, the SFC–MS interface probe-tip, the SFC column oven and the interface probe-stem. We also investigated the use of ammonia (1% in methane) and isobutane CI gases. Fig. 8 illustrates one result of our investigations, an ammonia CI SFC–MS spectrum of benzoyl peroxide with a large ion at *m/z* 260 corresponding to the ammonium adduct of intact benzoyl peroxide. Other major ions correspond in mass to expected thermal degradation products of benzoyl peroxide. The ammonium adduct of benzoic acid anhydride has a *m/z* of 244. Ions at *m/z* 216, 199, 140 and 123 correspond to the ammonium adducts and the protonated molecules of the phenyl ester of benzoic acid and of benzoic itself. Fig. 9 shows mass chromatograms of the ammonium adducts of intact benzoyl peroxide, benzoic acid anhydride, and benzoic acid, as well as the reconstructed total ion current chromatogram. The decomposition products co-elute with the intact peroxide in sharp, clean peaks. These results and our SFC–FID work strengthen our previous belief[16] that this peroxide is migrating through the SFC system with minimal degradation until it reaches the interface probe-tip and ion source where some degradation does occur.

We found that the temperature of the SFC–MS interface probe-tip was crucial in determining the degree of peroxide decomposition observed. The lowest probe-tip temperature where noise from sputtering and spiking of the restrictor was not a problem (100–120°C) gave the most abundant ammonium adduct of the intact peroxide. A change in the column oven temperature from 40 to 80°C and a change in the ion source temperature from 80 to 150°C did not have a significant effect on the spectrum. We did not determine the probe-tip temperature at which the adduct of the intact peroxide disappears, but it is two orders of magnitude less intense at our

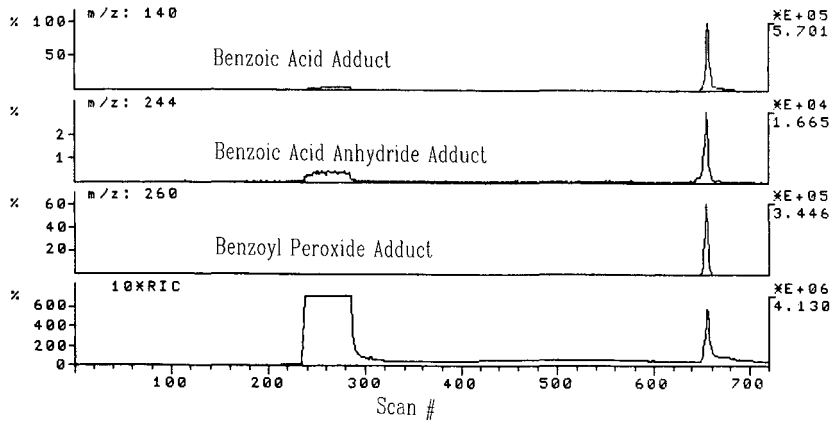

Fig. 9. Reconstructed total ion current chromatogram (bottom) and mass chromatograms of the ammonium adducts of benzoyl peroxide and of some of its degradation products from the ammonia CI SFC–MS run of benzoyl peroxide.

customary operating temperature of 300 than at 100°C. Isobutane CI did not yield the protonated molecule of the peroxide. Only two major ions were observed in the isobutane CI spectra from duplicate SFC–MS runs of benzoyl peroxide: the base peak at *m/z* 123, corresponding to protonated benzoic acid, and an ion of 20% relative abundance at *m/z* 105, corresponding to $[C_7H_5O]^+$. These isobutane CI results are consistent with the previously described behaviour of peroxides under isobutane CI conditions[41].

Armed with the knowledge gained during our work with benzoyl peroxide, we decided to attempt to confirm the molecular weight of the terpineol succinate peroxide whose postulated structure is shown in Scheme 2. MS analysis using direct-probe introduction revealed no ions related to the expected intact peroxide.

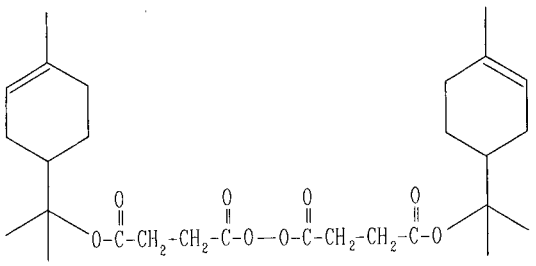

Scheme 2. Postulated structure of terpineol succinate peroxide.

Fig. 10 shows the ammonia CI SFC–MS spectrum of the terpineol succinate peroxide. The ion at *m/z* 524 corresponds in mass to the ammonium adduct of the expected peroxide, thus confirming its molecular weight of 506. As with benzoyl peroxide, the interface probe-tip temperature was crucial. The adduct ion was most intense near the lowest possible interface probe-tip temperature, in this case 100°C.

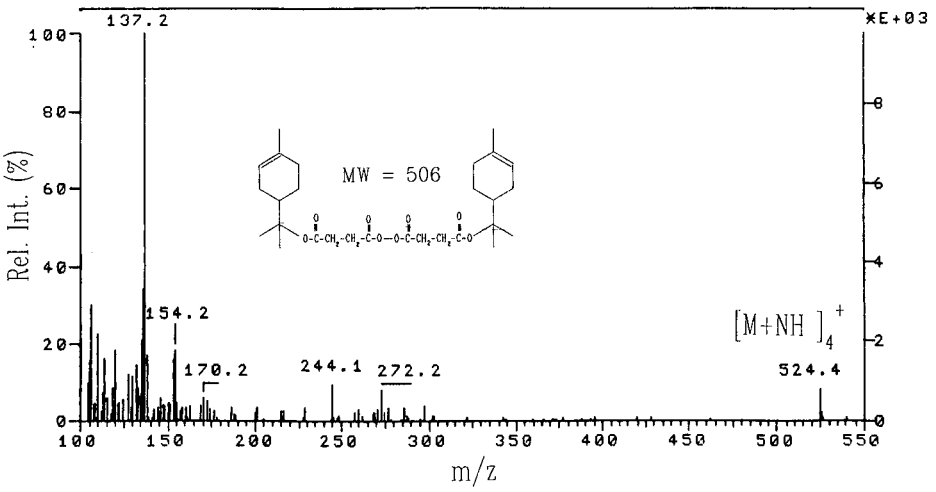

Fig. 10. Ammonia CI SFC–MS spectrum of terpineol succinate peroxide.

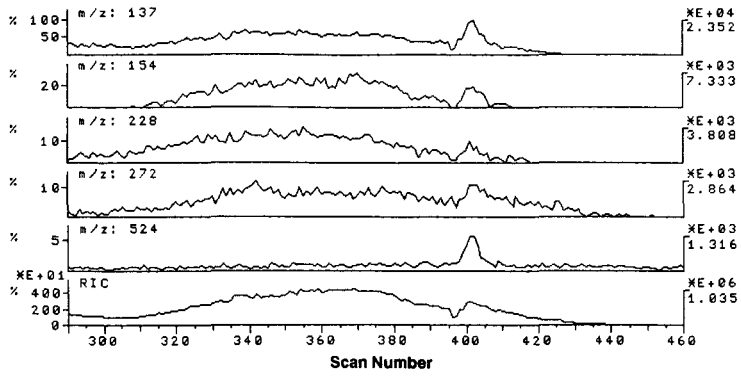

Fig. 11. Reconstructed total ion current chromatogram (bottom) and mass chromatograms of the protonated molecules and/or of the ammonium adducts of terpineol succinate peroxide and of some of its degradation products from the ammonia CI SFC–MS run of terpineol succinate peroxide.

Other temperatures were kept as low as possible and the pressure program was relatively fast, as listed in the Experimental section. Certain ions in the spectrum correspond to probable thermal degradation products of the peroxide. The ion at *m/z* 272 corresponds to the ammonium adduct of terpineol succinate monoester/free acid. The ammonium adduct of terpineol propionate has an *m/z* ratio of 228. The base peak at *m/z* 137 and the ion at *m/z* 154 correspond to the protonated molecule and the ammonium adduct of limonene. Mass chromatograms of these ions are shown in Fig. 11. While the intact peroxide (Scheme 2) elutes in a single peak less than 10 s wide, the ions related to the peroxide's thermal degradation products elute in broad "humps". This probably indictes that a significant portion of this peroxide decomposes as it travels through the SFC column. In spite of this degradation, we were able to quickly and easily confirm the postulated molecular weight of this peroxide by SFC–MS. As with benzoyl peroxide, no ions related to the intact peroxide were observed when using isobutane CI.

CONCLUSION

These three recent applications illustrate the use of SFC and of SFC–MS in the analysis of relatively non-volatile or thermally labile materials. In all three cases the analysis would have been difficult by traditional GC or HPLC. Elution and detection by SFC–FID and SFC–MS were straightforward. Inositol triphosphate did require derivatization, but this derivative was easily prepared and appeared stable under the SFC conditions used. SFC–MS was invaluable in quickly confirming the structures of the eluted species.

ACKNOWLEDGEMENTS

We gratefully acknowledge the contributions of T. L. Chester. The authors would like to thank R. L. Jacobsen and S. L. Daniel for providing the commercial Neodol samples, W. R. West for furnishing the Neodol 23-3 sample, W. R. Sherman

for providing the derivatized inositol triphosphate, and R. L. Binder for furnishing the commercial benzoyl peroxide. We gratefully acknowledge the help of J. E. Thompson and H. L. Vaughn who synthesized the 1-pentaethoxy tetradecanol and of R. V. Burkes and J. M. Gardlik who synthesized the terpineol succinate peroxide. Direct probe introduction mass spectrometry of this peroxide was performed by M. P. Lacey.

REFERENCES

1 T. L. Chester, *J. Chromatogr. Sci.*, 24 (1986) 226.
2 M. Novotny, S. R. Springston, P. A. Peaden, J. C. Fjeldsted and M. L. Lee, *Anal. Chem.*, 53 (1981) 407A.
3 M. L. Lee and K. E. Markides, *Science (Washington, D.C.)*, 235 (1987) 1342.
4 T. L. Chester, L. J. Burkes, T. E. Delaney, D. P. Innis, G. D. Owens and J. D. Pinkston, in B. A. Charpentier and M. R. Sevenants (Editors), *Supercritical Fluid Extraction and Chromatography, Techniques and Applications (ACS Symposium Series,* Vol. 366). American Chemical Society, Washington, DC, 1988, Ch. 8, p. 144.
5 J. C. Fjeldsted, R. C. Kong and M. L. Lee, *J. Chromatogr.*, 279 (1983) 449.
6 J. M. Levy and W. M. Ritchey, *J. Chromatogr. Sci.*, 24 (1986) 242.
7 T. L. Chester and D. P. Innis, *J. High Resolut. Chromatogr. Chromatogr. Commun.*, 9 (1986) 209.
8 T. H. Gouw, R. E. Jentoft and E. J. Gallegos, *J. High Pressure Sci. Technol. AIRAPT Conf. 6th,* (1979) 583.
9 R. D. Smith, W. D. Felix, J. C. Fjeldsted and M. L. Lee, *Anal. Chem.*, 54 (1982) 1883.
10 B. W. Wright, H. T. Kalinoski, H. R. Udseth and R. D. Smith, *J. High Resolut. Chromatogr. Chromatogr. Commun.*, 9 (1986) 145.
11 E. D. Lee and J. D. Henion, *J. High Resolut. Chromatogr. Chromatogr. Commun.*, 9 (1986) 172.
12 G. Holzer, S. Deluca and K. J. Voorhees, *J. High Resolut. Chromatogr. Chromatogr. Commun.*, 8 (1985) 528.
13 A. J. Berry, D. E. Games and J. R. Perkins, *Anal. Proc.*, 23 (1986) 451.
14 K. Matsumoto, S. Tsuge and Y. Hirata, *Chromatographia*, 21 (1986) 617.
15 R. D. Smith, H. T. Kalinoski and H. R. Udseth, *Mass Spectrom. Rev.*, 6 (1987) 445.
16 G. D. Owens, L. J. Burkes, J. D. Pinkston, T. Keough, J. R. Simms and M. P. Lacey, in B. A. Charpentier and M. R. Sevenants (Editors). *Supercritical Fluid Extraction and Chromatography, Techniques and Applications (ACS Symposium Series*, Vol. 366), American Chemical Society, Washington, DC, 1988, Ch. 11, p. 191.
17 J. D. Pinkston, G. D. Owens, L. J. Burkes, T. E. Delaney, D. S. Millington and D. A. Maltby, *Anal. Chem.*, 60 (1988) 962.
18 T. L. Chester, D. P. Innis and G. D. Owens, *Anal. Chem.*, 57 (1985) 2243.
19 T. L. Chester, J. D. Pinkston, D. P. Innis and D. J. Bowling, *Journal of Microcolumn Separations*, in preparation.
20 E. Stephanou, *Org. Mass Spectrom.*, 19 (1984) 510.
21 P. Rudewicz and B. Munson, *Anal. Chem.*, 58 (1986) 674.
22 J. D. Pinkston and T. E. Delaney (Procter & Gamble Co., Cincinnati, OH, U.S.A.), unpublished results.
23 W. R. West (Shell Development Co., Houston, Tx, U.S.A.), personal communication.
24 R. E. A. Escott and D. W. Chandler, *J. Chromatogr. Sci.*, 27 (1989) 134.
25 M. J. Berridge and R. F. Irvine, *Nature (London)*, 312 (1984) 315.
26 D. J. Cosgrove and G. C. J. Irving, *Inositol Phosphates*, Elsevier, Amsterdam, New York, 1980.
27 J. P. Heslop, R. F. Irvine, A. H. Tashjian, Jr. and M. J. Berridge, *J. Exp. Biol.*, 119 (1985) 395.
28 W. R. Sherman, A. L. Leavitt, M. P. Honchar, L. M. Hallcher and B. E. Phillips, *J. Neurochem.*, 36 (1981) 1947.
29 W. R. Sherman, K. E. Ackermann, R. A. Berger, B. G. Gish and M. Zinbo, *Biomed. Environ. Mass Spectrom.*, 13 (1986) 333.
30 W. R. Sherman (Washington University School of Medicine, St. Louis, MO, U.S.A.), personal communication.
31 F. F. Hsu, H. D. Goldman and W. R. Sherman, presented at the *36th ASMS Conference on Mass Spectrometry and Allied Topics, June 5–10, 1988, San Francisco, CA.*
32 R. D. Smith, H. R. Udseth and H. T. Kalinoski, *Anal. Chem.*, 56 (1984) 2971.
33 E. D. Lee, S. H. Hsu and J. D. Henion, *Anal. Chem.*, 60 (1988) 1990.

34 B. Samuelsson, *Science (Washington, D.C.)*, 220 (1983) 568.
35 L. A. Cornish, R. Ferrie and J. E. Paterson, *J. Chromatogr. Sci.*, 19 (1981) 85.
36 F. R. Sugnaux and C. Djerassi, *J. Chromatogr.*, 251 (1982) 189.
37 N. Gaddipati, F. Volpe and G. Anthony, *J. Pharm. Sci..*, 72 (1983) 1398.
38 M. O. Funk, Jr. and W. J. Baker, *J. Liq. Chromatogr.*, 8 (1985) 663.
39 G. T. Cairns, R. Ruiz Diaz, K. Selby and D. J. Waddington, *J. Chromatogr.*, 103 (1975) 381.
40 J. C. Fjeldsted and M. L. Lee (Brigham Young University, Provo, UT, U.S.A.), unpublished results.
41 T. Keough and A. J. DeStefano, *Spectra*, 8 (1982) 7.

Journal of Chromatography, 474 (1989) 113–122
Elsevier Science Publishers B.V., Amsterdam — Printed in The Netherlands

CHROM. 21 333

REPELLER EFFECTS IN DISCHARGE IONIZATION IN COMBINED LIQUID OR SUPERCRITICAL-FLUID CHROMATOGRAPHY–MASS SPECTROMETRY USING A THERMOSPRAY INTERFACE

I. CHANGES IN THE REAGENT GAS SPECTRUM

W. M. A. NIESSEN*, R. A. M. VAN DER HOEVEN, M. A. G. DE KRAA, C. E. M. HEEREMANS, U. R. TJADEN and J. VAN DER GREEF

Division of Analytical Chemistry, Center for Bio-Pharmaceutical Sciences, Gorlaeus Laboratories, P.O. Box 9502, 2300 RA Leiden (The Netherlands)

SUMMARY

The effects of the repeller voltage on the discharge-on mass spectra of the reagent gas and of analytes has been investigated systematically. This first part describes in detail the influence on the reagent gas spectra produced from methanol–water mixtures in liquid chromatography–mass spectrometry and from methanol–carbon dioxide mixtures in supercritical-fluid chromatography–mass spectrometry. Significant changes in the reagent gas spectra are observed as a function of the repeller voltage, especially in supercritical-fluid chromatography–mass spectrometry, where the most abundant species are protonated methanol (clusters), protonated carbon dioxide, or carbon dioxide molecular ions. This in principle offers the opportunity to select the ionization conditions by setting an appropriate repeller voltage.

INTRODUCTION

The thermospray interface and ion source for combined liquid chromatography–mass spectrometry (LC–MS) were introduced by Blakley and Vestal in 1983[1]. The system is now widely available from several instrument manufacturers. Several hardware changes have been made to the initial source design. The most important changes are the addition of a filament, a discharge electrode, and a repeller or retarding electrode.

The discharge electrode, like the rhenium filament, has been added to the thermospray source to induce ionization when the thermospray buffer ionization is ineffective, *e.g.* with non-aqueous solvents or when no buffer salts are present in the mobile phase[2,3]. A repeller electrode was initially introduced to increase the sampling efficiency of the ion source[4,5], resulting in better detection limits. It is placed either slightly downstream (retarding electrode)[4] or directly opposite to the sampling cone (repeller electrode)[5]. The influence of the repeller voltage, placed opposite to the ion sampling cone, in thermospray ionization of some model compounds has been studied

0021-9673/89/$03.50

systematically by Lindberg and Paulson[6] in order to optimize the sensitivity, and by Robins and Crow[7] in order to improve the high-mass sensitivity and the ion current stability. The influence of the voltage of a retarding electrode, placed slightly downstream, has been studied systematically by Bencsath and Field[8]. In general, it appears that similar effects can be observed with a repeller electrode and with a retarding electrode, although a particular effect is observed at lower voltages for a repeller electrode than for a retarding electrode. Surprisingly, little systematic research has been performed on the influence of the voltage of repeller or retarding electrode in the other thermospray modes, *i.e.* filament-on and discharge-on[9]. The repeller electrode used at higher voltages in the discharge-on mode has been claimed to induce fragmentation comparable with collisionally induced dissociation (CID), the so-called repeller-CID effect[2,10].

This paper describes the influence of the repeller voltage on the reagent gas spectrum both in LC–MS using methanol in water as mobile phase and in supercritical-fluid chromatography–mass spectrometry (SFC–MS) using methanol in carbon dioxide as mobile phase. The use of the discharge-on mode in SFC–MS has only recently been described, but without demonstrating repeller effects[11]. The results of the investigations reported in this paper indicate that the explanation of the repeller effects in analyte spectra as given by McFadden and Lammert[10] is not the main process.

EXPERIMENTAL

Equipment

(Tandem) mass spectrometry was performed on a Finnigan MAT TSQ-70 instrument (San José, CA, U.S.A.), equipped with a Finnigan MAT thermospray interface. The discharge voltage was set at values between 800 and 1200 V. In the LC–MS experiments the vaporizer tube was treated as usual, while in the SFC–MS experiments the vaporizer capillary must act as the restrictor; this was achieved by pinching the last 2 mm of the tube until a stable back-pressure of typically 30–36 MPa was achieved.

The LC–MS experiments were performed in the flow-injection analysis (FIA) mode with 20–80% of methanol in water at a flow-rate of 1–1.5 ml/min. The solvent was delivered with two Model 2150 LC pumps (LKB, Bromma, Sweden) controlled by a Model 2152 LC controller (LKB). A block temperature of 200°C and a vaporizer temperature of 90–110°C, depending on the solvent composition, were used.

The packed column SFC–MS experiments were performed on a laboratory-built instrument consisting of slightly modified commercially available modules. The system is described in detail elsewhere[12]. The mobile phase was carbon dioxide modified with 0–15% of methanol at a flow-rate of 1.5–2 ml/min. The laboratory-packed column (150 mm × 4.6 mm I.D.) was filled with either Nucleosil C_{18} material (5 μm, Macherey-Nagel, Düren, F.R.G.), or Rosil aminopropyl material (7 μm, Alltech, Deerfield, IL, U.S.A.). The block temperature was kept at 150°C, and the vaporizer temperature was 50°C unless stated otherwise.

In order to study systematically the influence of the repeller voltage on the reagent gas spectra a procedure was written in the Instrument Control Language of the TSQ-70, which automatically starts data collection, increase the repeller voltage from

0 up to 195 V in 10-V steps every 10 scans, and stops data acquisition after completion of the successive steps. The reconstructed total ion current (RIC) and (relative) intensity values reported here are averaged values of the scans 3 to 8 at each repeller voltage.

RESULTS

Liquid chromatography–mass spectrometry

In the source design used in the experiments described here the repeller electrode is placed opposite to the sampling cone. With all mobile phases used so far in both thermospray buffer ionization and filament-on and discharge-on ionization modes, a distinct influence of the repeller voltage on the intensity and the appearance of the reagent gas spectrum is observed. An automatic procedure in which the repeller voltage is varied from 0 to 200 V (in positive ion mode) and the resulting mass spectra are acquired, is used as a diagnostic tool to ascertain good performance of the interface and ion source[13]. Investigation of the repeller effect is also helpful in optimizing the sensitivity in particular applications, and may help in the understanding of the mechanisms of thermospray ionization. In this paper the effects of the repeller voltage on the reagent gas mass spectra obtained in the discharge-on mode are described.

The intensities of the most abundant ions in the reagent gas spectrum resulting from 20% methanol in water are plotted as a function of the repeller voltage in Fig. 1. The plot in Fig. 1 is a profile that can be shifted along the repeller voltage axis as a result of various experimental parameters, which are discussed below. The mass spectrum at low repeller voltages is dominated by protonated methanol clusters (ions of the type $[xCH_3OH + H]^+$ with $x = 1, 2, 3, \ldots$), decreasing in size with increasing repeller voltages. At repeller voltages above 80 V, protonated methanol (m/z 33) is the most intense ion in the spectrum. Other abundant ions in the latter region are protonated water (m/z 19), $[CH_2=OH]^+$ at m/z 31 and $[2CH_3OH + H - H_2O]^+$ at m/z 47. The vaporizer temperature, varied between 90 and 140°C, does not influence the (relative) intensities of the various protonated clusters.

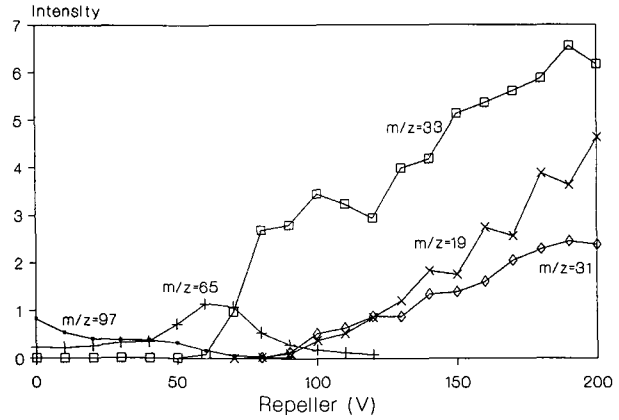

Fig. 1. Intensities (arbitrary units) of the most abundant ions in the reagent gas spectrum of 20% methanol in water in the discharge-on mode, as a function of the repeller voltage. Conditions: discharge, 1000 V; vaporizer temperature, 110°C; flow-rate, 1.2 ml/min; for other conditions see text.

A closer look at the mass spectra obtained at lower repeller voltages reveals the presence of several series of protonated clusters from water, methanol, and combinations of water and methanol with a general formula $[xCH_3OH + yH_2O + H]^+$. The various ions observed in the reagent gas spectrum of 20% methanol in water are given in Table I. Most of the protonated clusters are found with low intensity, *i.e.* below 1% of the intensity of the base peak. Several other species are also observed. Clusters with the general formula $[xCH_3OH - H_2O + H]^+$ with $x = 1, 2$ and 3 are observed at m/z 15, 47 and 79, respectively.

The reagent gas spectra of methanol–water mixtures in discharge-on mode have been studied over a broad range of solvent compositions. Increasing the percentage of methanol in the mobile phase results in a gradual shift of the profile given in Fig. 1 (for 20% of methanol in water) towards higher repeller voltage. The intensity of the protonated clusters containing water molecules decreases with decreasing water content of the mobile phase, while the protonated methanol clusters become more dominant.

Supercritical-fluid chromatography–mass spectrometry

Discharge-on ionization is also possible in high-pressure ion sources in combined packed-column SFC–MS with either pure carbon dioxide or a few percent of methanol in carbon dioxide as the mobile phase. As in LC–MS, the discharge potential has no influence on the total ion current of the reagent gas spectrum above the onset value of a stable discharge, which lies at *ca.* 700 V in the experiments reported here. Discharge potentials between 800 and 1200 V are used in practice.

In the reagent gas spectrum of pure carbon dioxide the two most intense ions are observed at m/z 44, corresponding to the carbon dioxide molecular ion, and at m/z 88, corresponding to the carbon dioxide cluster ion. The latter ion is observed only at repeller voltages below 40 V, and is the base peak of the reagent gas spectrum at repeller voltages below 20 V. The repeller voltage also exerts a marked influence on the RIC of the reagent gas spectrum: an eight-fold increase in the RIC is observed when the repeller voltage is increased from 30 to 120 V. The molecular ion of carbon dioxide has also been observed by others[14,15], working with either packed or capillary column SFC. At high pressures the carbon dioxide molecular ion becomes involved in charge-

TABLE I

THE m/z VALUES OF THE PROTONATED METHANOL–WATER CLUSTERS OBSERVED IN THE DISCHARGE-ON MASS SPECTRA OF 20% METHANOL IN WATER AT LOW REPELLER VOLTAGES

x	*y*					
	0	*1*	*2*	*3*	*4*	*5*
0	–	19	37	55	73	91
1	33	51	69	87		
2	65	83	101	119		
3	97	115				
4	129					

exchange processes. For many analytes the observed charge-exchange mass spectrum closely resembles the electron impact (EI) spectrum.

An overall ten-fold increase in the RIC is observed when carbon dioxide modified with a low percentage of methanol is used. The influence of the repeller voltage on the RIC and on the appearance of the reagent gas spectrum has been investigated in detail for a mobile phase consisting of 2% of methanol in carbon dioxide. Fig. 2 shows the intensities of the most abundant ions in the reagent gas spectrum as a function of the repeller voltage. The plot in Fig. 2 is a profile that can be shifted along the repeller voltage axis as a result of various experimental parameters, which are discussed below. Three regions based on the most intense ions can be distinguished. At low repeller voltages the reagent gas spectrum is determined by protonated methanol (clusters) of the general structural formula $[xCH_3OH + H]^+$ with $x = 1, 2, 3$ and 4. The number of methanol molecules present in the most abundant cluster decreases with increasing repeller voltages. At repeller voltages above 80 V, protonated carbon dioxide becomes the base peak, and at repeller voltages above 140 V the carbon dioxide molecular ion at m/z 44 is the base peak. Four typical reagent-gas spectra obtained with 2% of methanol in carbon dioxide at four different repeller potentials are given in Fig. 3.

The repeller voltages reported here are typical values under the conditions commonly used. However, the precise values are effected by two parameters, *i.e.* the vaporizer temperature and the degree of contamination of the ion source.

Increasing the vaporizer temperature results in a decrease of the intensities of the protonated clusters, resulting in a shift of the complete profile given in Fig. 2 to lower repeller voltages. For example, the maximum abundance of the protonated methanol cluster at m/z 65 is found at a repeller potential of 30 V at a vaporizer temperature of 50°C, but it shifts to 10 V when the vaporizer temperature is increased to 100°C.

The effect of ion-source contamination is more difficult to quantify. Increased contamination of the ion source, and especially of the repeller electrode, results in a shift of the profile of Fig. 2 to higher repeller voltages, which change can probably be

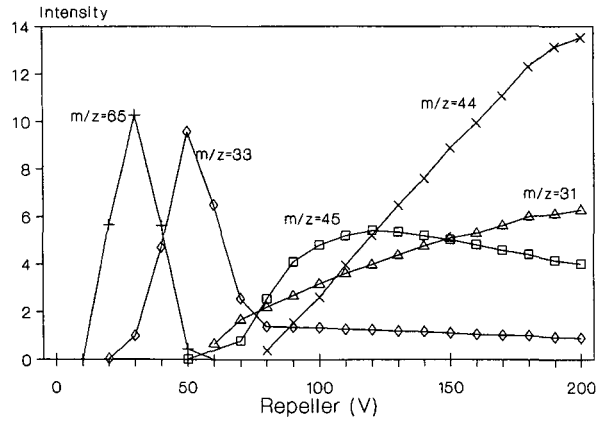

Fig. 2. Intensities (arbitrary units) of the most abundant ions in the reagent gas spectrum of 2% methanol in carbon dioxide in the discharge-on mode, as a function of the repeller voltage. Conditions: discharge, 800 V; flow-rate, 2 ml/min; for other conditions see text.

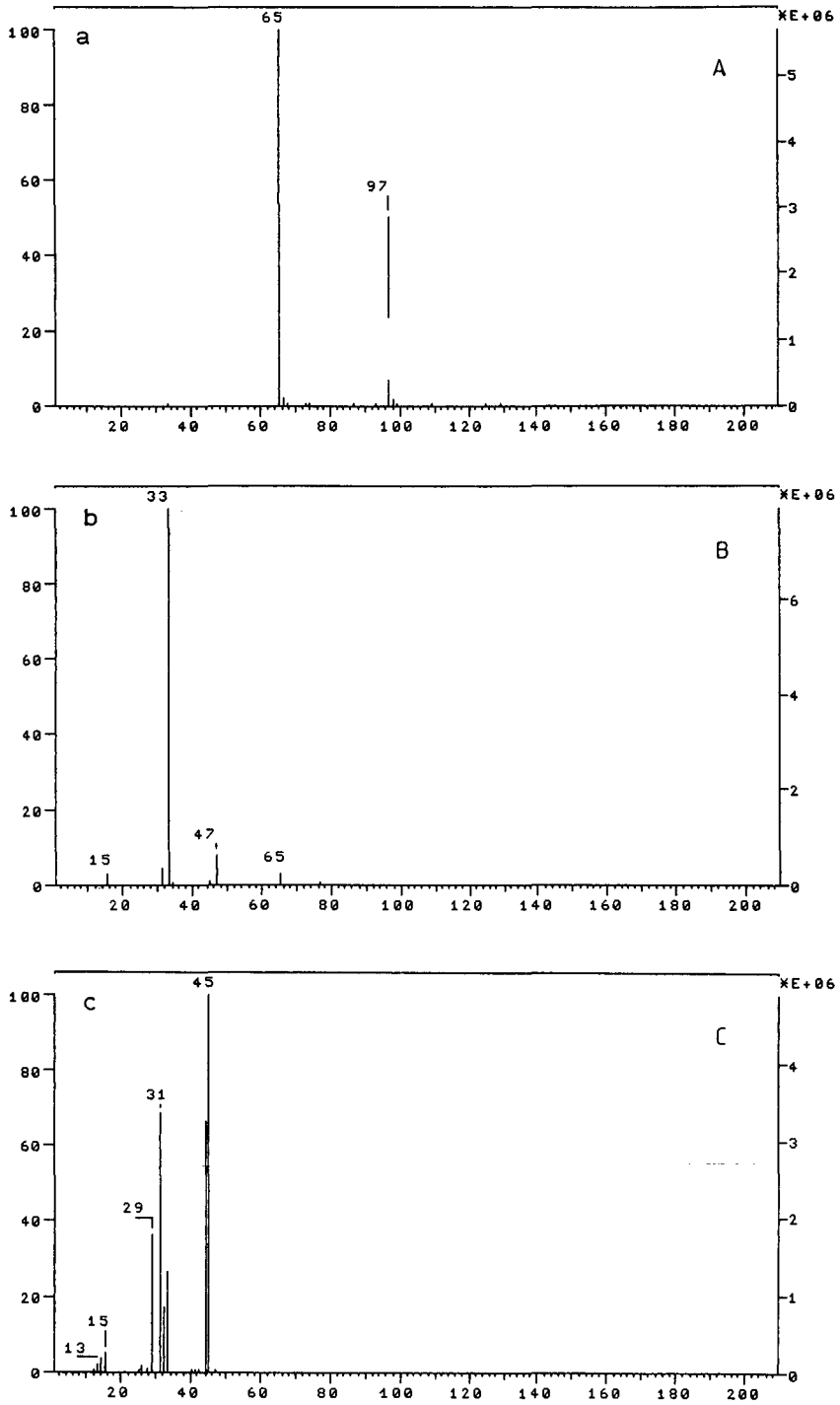

Fig. 3.

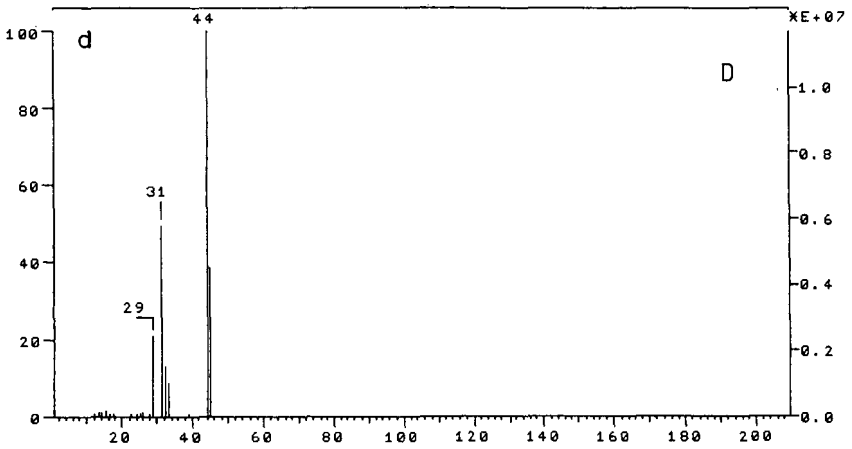

Fig. 3. Typical reagent gas spectra obtained at repeller potentials (a) 20 V, (b) 50 V, (c) 100 V, and (d) 180 V. Conditions as in Fig. 2.

attributed to changes in the effective potential of the repeller electrode. The protonated methanol cluster at *m/z* 97 appears to be an appropriate means of detecting the repeller contamination. In a clean source, the maximum abundance of the ion at *m/z* 97 is found at zero repeller potential, whereas after several days of intensive experiments, sometimes using quite high analyte concentrations, the maximum abundance of *m/z* 97 is observed at a repeller voltage of 70 V. In our experience the ion source needs cleaning after 2–3 weeks of working with either LC–MS or SFC–MS, to some extent depending on the types of sample investigated. It must be mentioned that the pressure in the ion source, which is a function of the mass-flow of mobile phase into the mass spectrometer, also influences the relative intensities of the peaks in the spectrum at a particular repeller voltage. This effect has not yet been studied systematically; preliminary experiments indicate that increasing the mass-flow results in an increase of the intensity of the protonated species relative to that of the molecular ions (comparable with a shift of the profile of Fig. 2 to higher repeller voltages).

A closer look at the reagent gas spectra obtained with 2% methanol in carbon dioxide indicates several other interesting aspects. At low repeller voltages, especially in the region 20–70 V, many protonated clusters are observed, most of which have only low intensities. Protonated clusters are observed with two general formulae, *i.e.* $[x\mathrm{CH_3OH} + z\mathrm{CO_2} + \mathrm{H}]^+$ and $[x\mathrm{CH_3OH} + z\mathrm{CO_2} - \mathrm{H_2O} + \mathrm{H}]^+$. The clusters actually observed are summarized in Table II.

Collision-induced fragmentation of some of the clusters has been performed to check the assignments. When low-energy collisions in a triple quadrupole instrument are used, it does not appear to be possible to induce complete dissociation of the clusters to protonated molecules for some of the clusters studied. The daughter spectra of two of the clusters will be discussed in more detail. In the MS–MS daughter spectrum of the protonated cluster at *m/z* 153, $[2\mathrm{CH_3OH} + 2\mathrm{CO_2} + \mathrm{H}]^+$, the successive losses of one and two methanol molecules or one and two carbon dioxide molecules are observed, resulting in either $[2\mathrm{CO_2} + \mathrm{H}]^+$ or $[2\mathrm{CH_3OH} + \mathrm{H}]^+$ at *m/z* 89

TABLE II

THE *m/z* VALUES OF THE PROTONATED METHANOL–CARBON DIOXIDE CLUSTERS AND PROTONATED DEHYDRATED METHANOL–CARBON DIOXIDE CLUSTERS OBSERVED IN THE DISCHARGE-ON MASS SPECTRA OF 2% METHANOL IN CARBON DIOXIDE

Cluster	*x*	*z*		
	0	*1*	*2*	
$[xCH_3OH + zCO_2 + H]^+$	0	–	45	89
	1	33	77	121
	2	65	109	153
	3	97	141	185
	4	129	173	
$[xCH_3OH + zCO_2 - H_2O + H]^+$	0	–	–	–
	1	15	59	103
	2	47	91	135
	3	79	123	167
	4	111	155	–

and *m/z* 65, respectively. In the daughter spectrum of *m/z* 129, corresponding to $[4CH_3OH + H]^+$, consecutive losses of methanol molecules are observed.

At high repeller voltages the reagent gas spectrum has the appearance of an EI spectrum of a mixture of carbon dioxide, with the molecular ion at *m/z* 44, and methanol, with the molecular ion at *m/z* 32, a base peak at *m/z* 31, corresponding to $[CH_2{=}\dot{O}H]^+$, and the other peaks normally present in the EI spectrum of methanol.

The reagent gas spectra have also been studied at higher percentages of methanol (7–12%) in carbon dioxide. The reagent gas spectrum of 2% of methanol in the mobile phase is dominated by protonated methanol (clusters) up to a repeller potential of 80 V (*cf.* Fig. 2), but with higher methanol contents in the mobile phase an even more predominant role of the protonated methanol (clusters) is observed. The most

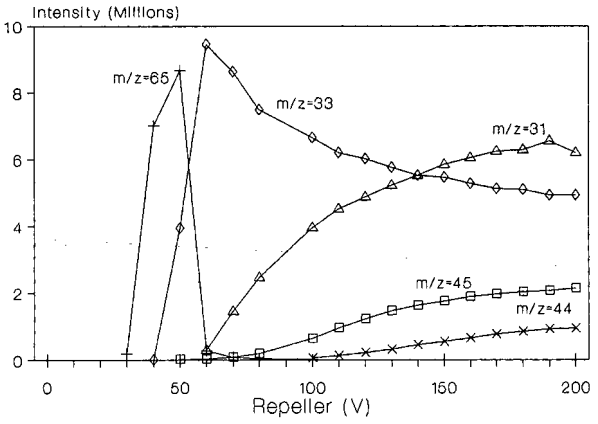

Fig. 4. Intensities (arbitrary units) of the most abundant ions in the reagent gas spectrum of 10% methanol in carbon dioxide in the discharge-on mode, as a function of the repeller voltage. Conditions: flow-rate, 1.5 ml/min; other conditions as in Fig. 2.

abundant species at various repeller voltages in the reagent gas spectra of 10% of methanol in carbon dioxide are shown in Fig. 4. At repeller potentials up to 50 V, protonated methanol clusters are the most abundant species. At repeller voltages above 150 V, the $[CH_2=OH]^+$ ion at *m/z* 31 becomes the most abundant ion, while in the intermediate region the protonated molecule at *m/z* 33 is the most intense one. The contributions of the protonated carbon dioxide ion and the carbon dioxide molecular ion to the reagent gas spectrum are greatly reduced compared with the situation at 2% methanol in carbon dioxide (*cf.* Fig. 2). There is some increase in total ion current when comparing the results from 2% and 10% of methanol. It also appears that several of the protonated methanol–carbon dioxide clusters, reported in Table II, are less abundant at 10% of methanol than at 2% of methanol.

DISCUSSION

The reagent gas spectra observed with the methanol–carbon dioxide (or water) mixtures at low repeller potentials can to some extent be predicted from the proton-transfer concepts in the theoretical description of chemical ionization[16]. Like in methanol chemical ionization, as found for instance in direct liquid introduction for LC–MS[17], the presence of methanol in the reagent gas results in protonated species due to a series of ion–molecule reactions. Methanol, being the stronger base (proton affinities are 777 kJ/mol for methanol, 727 kJ/mol for water and 541 kJ/mol for carbon dioxide), is expected to dominate the reagent gas spectrum. It is surprising that the potential of the repeller electrode can change the conditions to such an extent that protonated carbon dioxide can become the most abundant species, while the abundance of protonated methanol simultaneously decreases. At even higher repeller potentials, molecular ions and fragments of carbon dioxide and methanol are observed.

From the changes observed in the reagent gas spectra as a function of the repeller voltage in both LC–MS and SFC–MS, significant differences in the analyte mass spectra obtained at different repeller voltages can be predicted. For instance, the protonated methanol clusters are expected to have somewhat different proton affinities from that of the protonated methanol itself. The differences in the ion–molecule reactions between an analyte and protonated methanol (clusters), protonated carbon dioxide, or the carbon dioxide molecular ion and the effects on the analyte spectra, for instance with respect to the degree of fragmentation, can be easily seen. These differences will be discussed in more detail elsewhere[18].

A sound explanation for the effects observed in the reagent gas spectra cannot be easily given. The acceleration of electrons from the discharge electrode to the lower pressure region near the high voltage repeller electrode has been suggested by Coutant *et al.*[9]. Those electrons should have reached high enough energies to ionize vaporized compounds. However, the pressure in the ion source is probably too high for the electrons to travel such a large distance in the source. The ionization of analytes can be considered as a secondary ionization process in which charged species present in the reagent gas are involved in proton-transfer and/or charge-exchange reactions. Several factors are of importance in this respect. The repeller electrode can influence the appearance of the reagent gas spectrum as it effectively samples the ions of particular regions of the spray from the vaporizer into the sampling cone. Sampling takes place

from the high-pressure centre and/or the lower pressure exterior regions of the spray. Differences in the concentrations of methanol and carbon dioxide within the spray can be expected as a result of the differences in volatility and of the temperature gradient, which is also expected to be present in the spray. These effects may also influence the composition of the various regions of the spray, the cluster formation, and the types of ionization reaction involved in the secondary ionization process. Higher repeller potentials will also increase the energy of the ion–molecule collisions in the source. Collisionally induced dissociation of protonated clusters in the reagent gas is probably of great importance in the explanation of the reagent gas spectra[19].

In conclusion it can be stated that the repeller electrode can exert a strong effect on the reagent gas spectrum in the thermospray source operated under discharge-on conditions. It appears to be possible, at least in SFC–MS, to select the conditions for the ionization of the analyte by setting the potential of the repeller electrode.

REFERENCES

1 C. R. Blakley and M. L. Vestal, *Anal. Chem.*, 55 (1983) 750.
2 D. Zakett, G. J. Kallos and P. J. Savickas, presented at the *32nd Annual Conference on Mass Spectrometry and Allied Topics, San Antonio, TX, May 27–June 1, 1984*, p. 3.
3 F. Poeppel, J. Buchner, H. H. Lo and J. Dulak, presented at the *32nd Annual Conference on Mass Spectrometry and Allied Topics, San Antonio, TX, May 27–June 1, 1984*, p. 98.
4 I. A. S. Lewis, D. C. Smith and M. Veares, presented at the *32nd Annual Conference on Mass Spectrometry and Allied Topics, San Antonio, TX, May 27–June 1, 1984.*
5 W. H. McFadden and M. G. Tucker, presented at the *32nd Annual Conference on Mass Spectrometry and Allied Topics, San Antonio, TX, May 27–June 1, 1984*, p. 100.
6 C. Lindberg and J. Paulson, *J. Chromatogr.*, 394 (1987) 117.
7 R. H. Robins and F. W. Crow, *Rapid Commun. Mass Spectrom.*, 2 (1988) 30.
8 F. A. Bencsath and F. H. Field, *Anal. Chem.*, 60 (1988) 1323.
9 J. E. Coutant, B. L. Ackermann and M. L. Vestal, presented at the *35th Annual Conference on Mass Spectrometry and Allied Topics, Denver, CO, May 24–29, 1987*, p. 419.
10 W. H. McFadden and S. A. Lammert, *J. Chromatogr.*, 385 (1987) 201.
11 J. R. Chapman, *Rapid Commun. Mass Spectrom.*, 2 (1988) 6.
12 W. M. A. Niessen, P. J. M. Bergers, U. R. Tjaden and J. van der Greef, *J. Chromatogr.*, 454 (1988) 243.
13 C. E. M. Heeremans, R. A. M. van der Hoeven, W. M. A. Niessen, U. R. Tjaden and J. van der Greef, *J. Chromatogr.*, 474 (1989) 149.
14 R. D. Smith, H. T. Kalinoski and H. R. Udseth, *Mass Spectrom. Rev.*, 6 (1987) 445.
15 J. Cousin and P. J. Arpino, *J. Chromatogr.*, 398 (1987) 125.
16 A. G. Harrison, *Chemical Ionization Mass Spectrometry*, CRC Press, Boca Raton, FL, 1983.
17 W. M. A. Niessen, *Chromatographia*, 21 (1986) 342.
18 W. M. A. Niessen, R. A. M. van er Hoeven, M. A. G. de Kraa, C. E. M. Heeremans, U. R. Tjaden and J. van der Greef, *J. Chromatogr.*, submitted for publication.
19 C. E. M. Heeremans, R. A. M. van der Hoeven, W. M. A. Niessen, U. R. Tjaden, J. van der Greef and N. M. M. Nibbering, in preparation.

Journal of Chromatography, 474 (1989) 123–138
Elsevier Science Publishers B.V., Amsterdam — Printed in The Netherlands

CHROM. 21 439

APPLICATION OF THERMOSPRAY LIQUID CHROMATOGRAPHY–MASS SPECTROMETRY AND LIQUID CHROMATOGRAPHY–TANDEM MASS SPECTROMETRY FOR THE IDENTIFICATION OF CYNOMOLGUS MONKEY AND HUMAN METABOLITES OF SK&F 101468, A DOPAMINE D_2 RECEPTOR AGONIST

I. G. BEATTIE and T. J. A. BLAKE*,[a]

Department of Drug Metabolism and Pharmacokinetics, Smith Kline & French Research Ltd., The Frythe, Welwyn, Herts. AL6 9AR (U.K.)

SUMMARY

A combination of thermospray liquid chromatography–mass spectrometry (LC–MS) and LC MS–MS has allowed the structural elucidation of a number of metabolites of 4-[2-(dipropylamino)ethyl]-1,3-dihydro-2H-indol-2-one (SK&F 101468) in monkey urine. By using LC–MS–MS with the third quadrupole (Q3) set up in multiple ion detection (MID) mode, a number of metabolites were subsequently detected in the human urine and plasma samples despite very low dosing regimes. This was achieved with minimal sample preparation, *e.g.* for the urine sample centrifugation was the only preparative step, in order to remove particulate matter, prior to analysis.

The good signal-to-noise ratio obtained for the human samples, using LC–MS–MS with Q3 set up for MID, raised the possibility of a LC–MS–MS quantitative assay. As a result, the detection limit of this method for SK&F 101468 when dissolved in methanol was determined to be in the region of 20 pg on column.

INTRODUCTION

Potential drug candidates when administered to animals or humans are generally metabolised quite rapidly, producing a variety of more polar compounds that can then be eliminated from the body. This is normally achieved in the animal via a number of oxidative reactions such as hydroxylation, oxidation of alcohols, N-oxidation and N-dealkylation. These metabolites can then be excreted from the body or they can undergo further metabolism such as conjugation reactions, normally with glucuronic acid, sulphate, glutathione and in rare cases amino acids.

The oxidative reactions are normally classed as Phase I metabolism, which also includes any reductive reactions, while Phase II metabolism covers the conjugation reactions and also includes methylation and acetylation[1].

[a] Present address: Department of Drug Metabolism, Smith Kline & French Research Ltd., P.O. Box 1539, King of Prussia, PA 19406-0939, U.S.A.

0021-9673/89/$03.50

As a result of the wide range of polarities that the drug and its metabolites cover, the most widely used method for their analysis is by reversed-phase high-performance liquid chromatography (HPLC) utilising gradient elution in order to ensure good separation of all the components.

The most commonly used methods of detection for HPLC are fixed or scanning UV detectors or, if the drug is ^{14}C-labelled, a radiochemical detector. However, the information that these detectors can provide is limited with the radiochemical detector mainly being used for quantitative work. Identification of potential metabolites would therefore require isolation and analysis by NMR and mass spectrometry.

One method that can provide both structural and molecular weight information on metabolites is coupling HPLC with mass spectrometry (LC–MS). In the early days this was achieved by using a moving belt interface[2–4]. This interface enjoyed some success when used for applications that required normal-phase HPLC and where the compounds of interest were relatively volatile and thermally stable.

However, for reversed-phase HPLC systems the moving belt interface was not as successful. The major problems were associated with its inability to handle mobile phases with a high aqueous content and the vapourisation of non-volatile, thermally labile compounds. The introduction of a spray device for deposition of the HPLC eluant onto the belt largely eliminated the problem associated with high aqueous mobile phases[5–6].

Both of these problems were effectively eliminated when the thermospray LC–MS interface was introduced[7,8]. This interface was capable of handling a flow-rate of 1–2 ml min^{-1} of aqueous solvent but required a volatile buffer, normally ammonium acetate, in order to effect ionisation of the solute. This removed the requirement for an external source of ionisation, although this is now available on commercial interfaces for compounds that do not ionise under thermospray conditions.

One feature of thermospray LC–MS, is that in many cases it produces a protonated molecular ion, MH^+, as the base peak with little or no fragmentation resulting in a lack of structural information. At present there are two ways that fragment ions can be induced. One is to use an external source of ionisation which imparts more energy into the system, usually resulting in increased fragmentation. The other is to use MS–MS and collisionally activate the MH^+ ion to produce daughter ions that are structurally significant.

The objective of this paper will be to demonstrate the potential of thermospray LC–MS and LC–MS–MS for the structural analysis of drug metabolites. In addition, it will also illustrate the usefulness of LC–MS–MS with multiple ion detection (MID) for the identification of metabolites at low levels. This will be achieved by describing its application to the study of the *in vivo* metabolism of 4-[2-(dipropylamino)ethyl]-1,3-dihydro-2H-indol-2-one (SK&F 101468), a dopamine D_2 receptor agonist which has potential for the treatment of Parkinson's disease.

EXPERIMENTAL

SK&F 101468 urine and plasma samples

A male cynomolgus monkey was dosed 15 mg kg^{-1} of SK&F 101468 *per os* (p.o.) and the 0–6-h urine was collected for analysis. The human urine sample was obtained by dosing a male volunteer 640 μg of SK&F 101468 p.o. and the 0–6-h urine was collected.

Both urine samples were centrifuged at 9450 *g* for 10 min to remove particulate matter. A 50-μl volume of the monkey and 100 μl of the human supernatants were then used for the analysis.

The human plasma sample was obtained after dosing a male volunteer 1.25 mg of SK&F 101468 p.o. and taking a blood sample after 2 h. The plasma obtained from the blood was worked up prior to analysis by taking 500 μl of plasma and removing the protein by precipitation with 500 μl of acetonitrile. The protein was then removed by centrifugation at 9450 *g* for 20 min after which the supernatant was taken and the acetonitrile evaporated under a stream of nitrogen leaving a final volume of approximately 100 μl. This was then stored at −20°C prior to analysis when the whole sample was used.

High-performance liquid chromatography

HPLC was carried out on a Hewlett-Packard 1090L fitted with a filter photometric detector. The chromatographic separation was carried out on a C_{18} Hewlett-Packard 100 × 4.6 mm I.D. column packed with 5-μm sized particles which was kept at room temperature. The mobile phases used were 0.1 *M* ammonium acetate (pH unadjusted) filtered through a 0.45-μm filter and acetonitrile. The system was run at a flow-rate of 1.4 ml min^{-1}. The gradient system used to effect the separation consisted of a 3-min hold at 0% acetonitrile followed by a linear ramp up to 35% acetonitrile over 17 min with a further 3-min hold at 35%. The wavelength of the UV detector was set at 254 nm and was connected in line with the mass spectrometer in all cases.

Mass spectrometry

A Finnigan MAT TSQ 46 mass spectrometer equipped with a Nova 4X SuperIncos data system was used. The chromatograph was coupled to the mass spectrometer with a Finnigan MAT thermospray interface. The typical vapouriser temperature was 120°C with a jet temperature of 300°C.

The MS–MS was carried out using argon as the collision gas at a pressure of approximately 1.4 mTorr.

Prior to any analysis by LC–MS or LC–MS–MS the system was tuned by the continuous introduction of a solution of SK&F 101468. This was made up in 0.1 *M* ammonium acetate–acetonitrile (4:1, v/v) at an approximate concentration of 2 μg ml^{-1}. All mass spectra shown were background subtracted.

RESULTS AND DISCUSSION

Due to the relatively "soft" nature of the thermospray ionisation process, thermospray LC–MS is an analytical method that is capable of providing molecular weight information on drug metabolites in biological matrices with the minimum of sample preparation. As a result of this, the amount of structural information available in thermospray mass spectra tends to be limited due to the lack of any fragment ions. This means that the sites of any structural modifications to the parent drug cannot be readily identified. However, if the mass spectrometer has a MS–MS capability, this problem can be overcome by carrying out collisionally activated decomposition (CAD) experiments to fragment the MH^+ ion and obtain structurally meaningful

daughter ions. For the discussion a conventional mass spectrum will be termed a Q1 mass spectrum while a CAD daughter ion mass spectrum will be termed a Q3 mass spectrum.

One example where this approach was used was SK&F 101468 (Fig. 1). This compound was found to be metabolised extensively by the monkey and to a lesser extent by man. The metabolites identified by LC–MS and LC–MS–MS in the monkey and human samples are listed in Fig. 1. The results of the monkey urine analysis will be discussed initially.

The UV trace and totalled selected ion chromatogram trace obtained for the monkey urine are shown in Fig. 2. The two large peaks in Fig. 2, at scan nos. 273 and 277, are spurious peaks which were produced as a result of temporary pressure fluctuations in the ion source which artificially enhanced the sensitivity. These peaks were absent from subsequent LC–MS runs of this sample. The identities of metabolites 4, 7 and 11, SK&F 96990, 104557 and 101468, respectively, were confirmed by comparison of their mass spectra and retention times with authentic standards.

	Metabolite	Species
1.	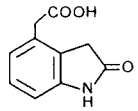	Monkey
2.	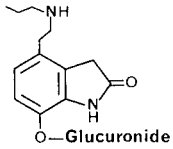	Monkey
3.	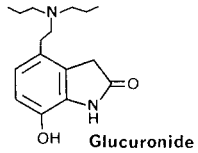	Monkey
4.	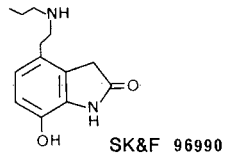	Monkey and human
5.	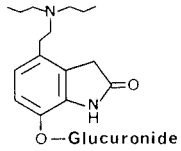	Monkey and human

Fig. 1.

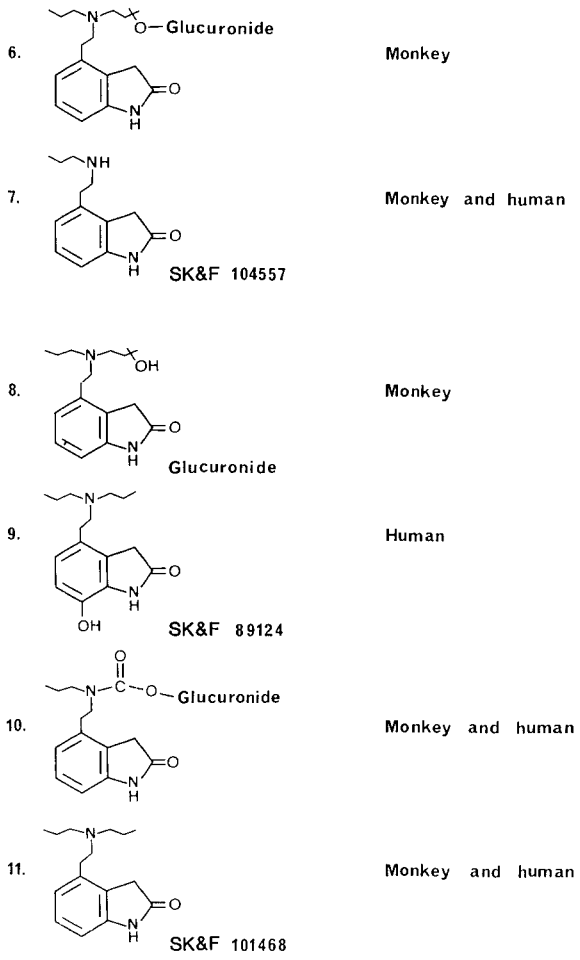

Fig. 1. Structures of SK&F 101468 and its metabolites that were found in the urine of the cynomolgus monkey and man.

The Q1 and Q3 mass spectra for metabolite 1 are shown in Fig. 3. The Q1 spectrum showed a single MH^+ ion at *m/z* 192 with no evidence of any fragmentation. However, collisional activation of *m/z* 192 resulted in the fragment ion *m/z* 146, a loss of 46 a.m.u. This corresponded to a loss of formic acid thus confirming the presence of the carboxylic acid group. This asignment was confirmed after the metabolite was isolated and analysed by NMR.

Metabolite 2 was assigned as the O-glucuronide of SK&F 96990. The presence of the glucuronide was confirmed by the ion at *m/z* 411 in the Q1 spectrum (Fig. 4a) with the aglycone ion *m/z* 235. The site of hydroxylation was narrowed down to the indolone ring system by performing CAD of *m/z* 235, (Fig. 4b), for comparison to the CAD spectrum obtained for authentic SK&F 96990.

The major fragment ions produced were *m/z* 72, 120, 148 and 176. The ion at *m/z* 72 corresponded to cleavage of the carbon–carbon bond of the ethyl link with charge

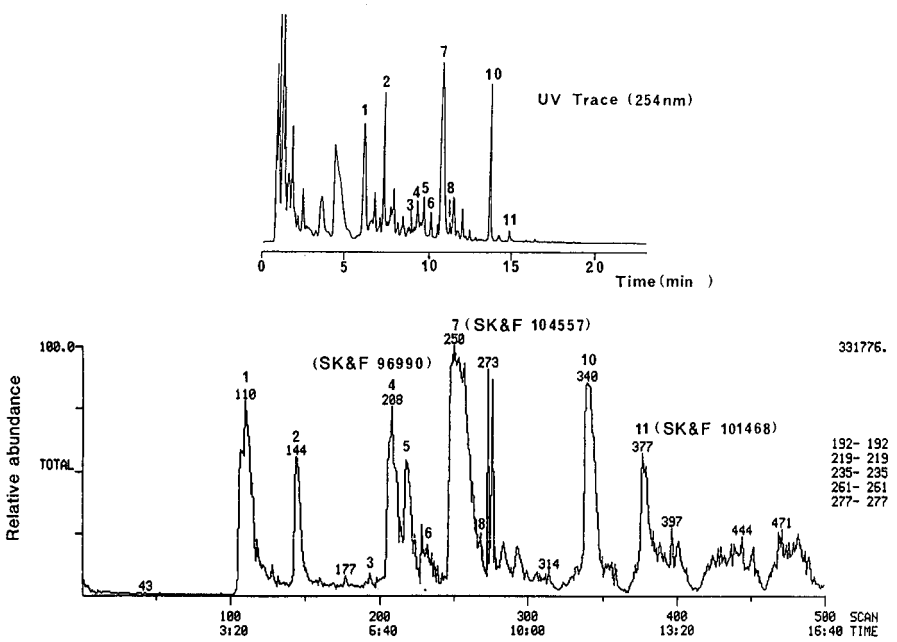

Fig. 2. UV chromatogram (254 nm) and totalled selected ion chromatogram obtained for the 0–6-h monkey urine.

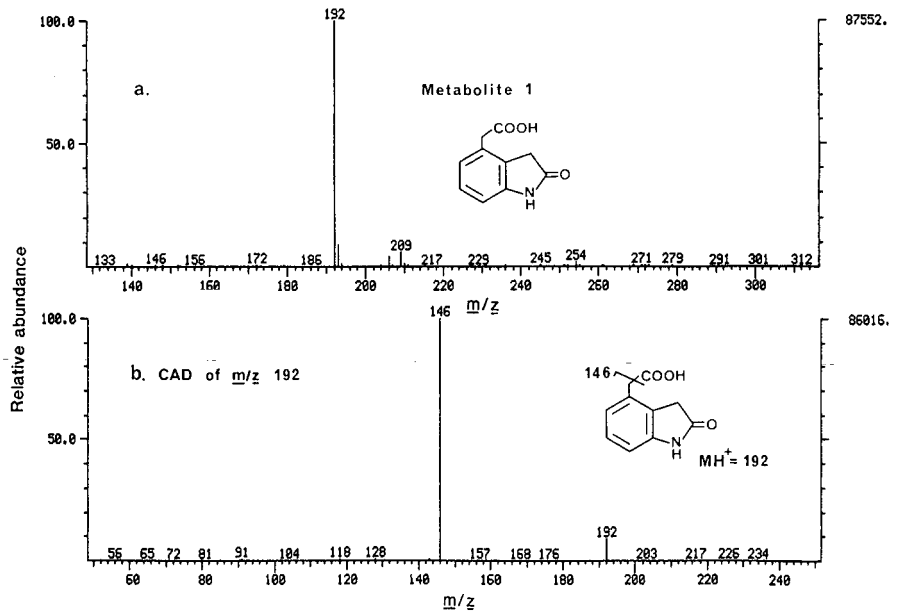

Fig. 3. (a) Thermospray Q1 mass spectrum of metabolite 1, (b) daughter ion mass spectrum of metabolite 1.

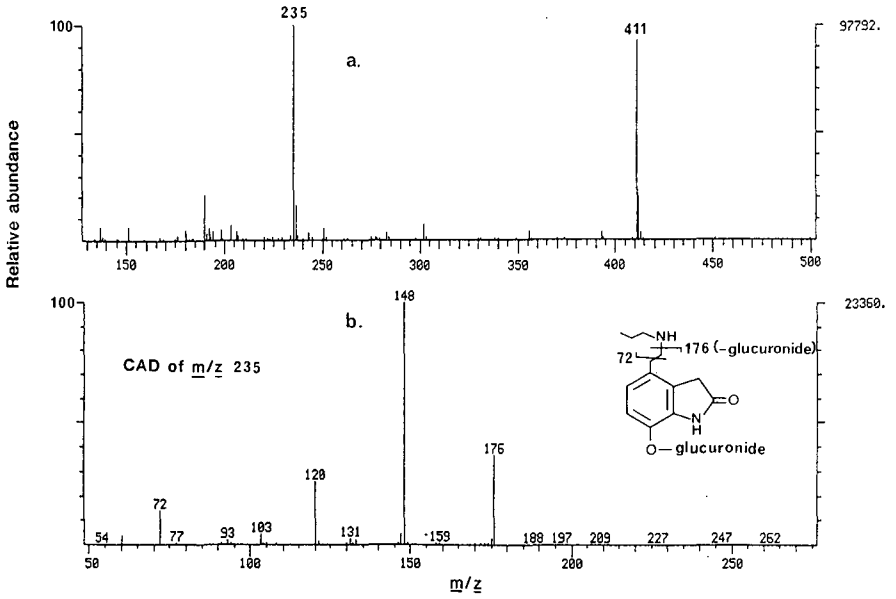

Fig. 4. (a) Thermospray Q1 mass spectrum of metabolite 2, (b) Q3 mass spectrum obtained for m/z 235, the aglycone MH^+ of metabolite 2.

retention by the propylamine fragment. Cleavage of the carbon–nitrogen bond gave rise to the ion at m/z 176 confirming that the hydroxyl group was on the indolone ring system. The two consecutive losses of 28 a.m.u. forming m/z 148 and 120 are thought to be due to successive losses of CO from the lactam and the phenolic hydroxyl group. The site of hydroxylation was assigned to position 7, as shown, for two reasons. (1) The results obtained on incubation of the sample with β-glucuronidase showed that the glucuronide peak (metabolite 2) decreased with a corresponding increase in SK&F 96990 (metabolite 4). (2) The CAD spectrum was identical to that obtained for authentic SK&F 96990.

The Q1 spectra for metabolites 3 and 5 (Fig. 5a and b) are virtually identical, with a protonated MH^+ for the glucuronide conjugate at m/z 453 with the more intense aglycone ion at m/z 277. Daughters of m/z 453 (Fig 5c and d) produced the same fragment ions although the ion ratios varied. Both metabolites produced m/z 114 and 176 which confirmed that the site of hydroxylation was on the indolone ring. This was assumed to be on position 7, as shown, for both metabolites as metabolite 5 had previously been found in rat bile, isolated and then characterised by NMR as the O-glucuronide of SK&F 89124. The site of glucuronidation for metabolite 3 is unknown.

The Q1 spectra for metabolites 6 and 8 (Fig. 6a and b) also indicated that they were both glucuronides of hydroxylated SK&F 101468. However, both compounds were able to lose water from the protonated MH^+ ion of the aglycone, m/z 277. This implied that the site of hydroxylation was on one of the aliphatic chains. This was confirmed by collisionally activating m/z 453 (spectra shown in Fig. 6c and d).

The aglycone ion, m/z 277, was the base peak which underwent loss of water to

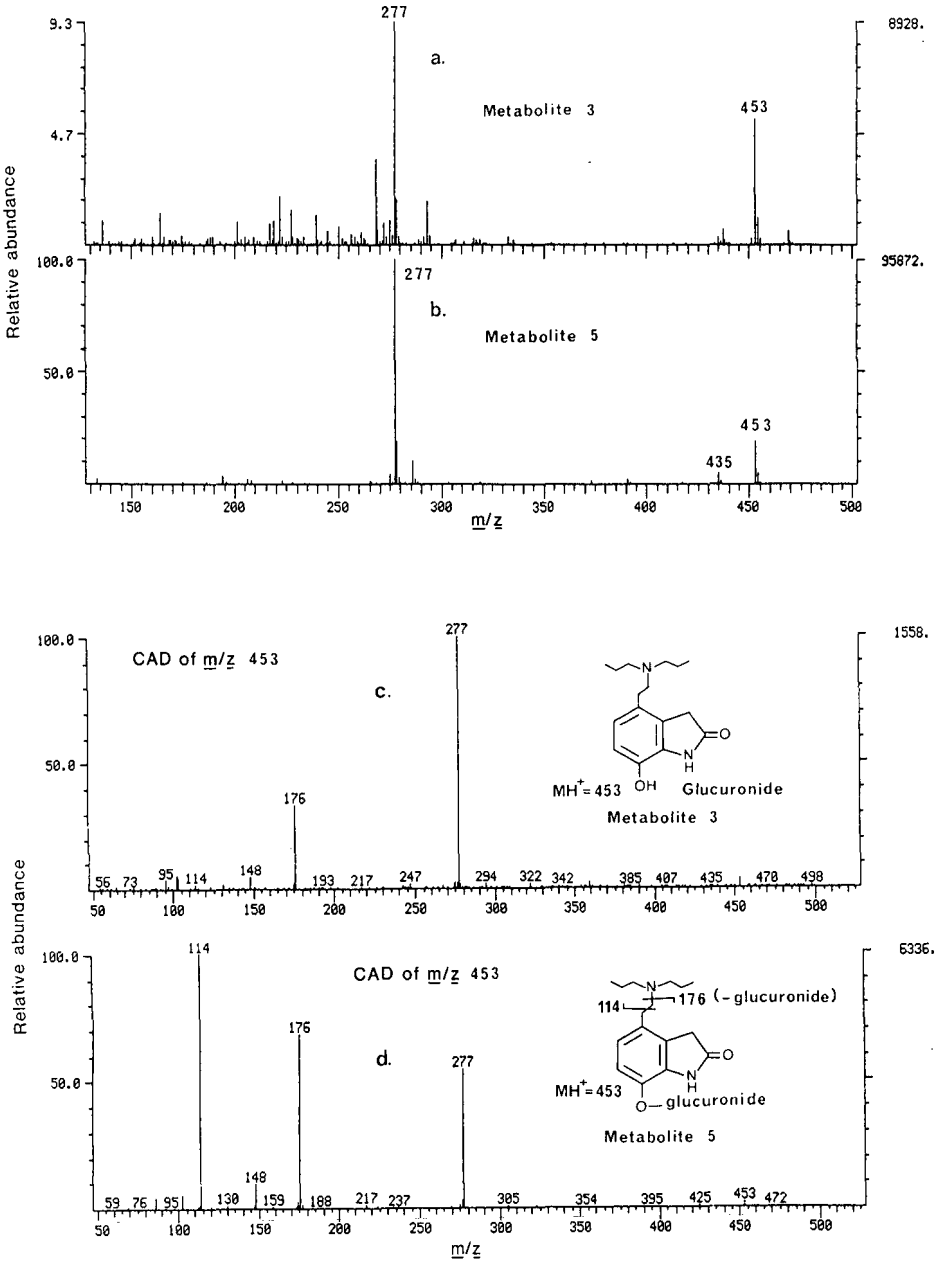

Fig. 5. (a,b) Thermospray Q1 mass spectra obtained for metabolites 3 and 5, respectively, (c,d) daughter ion mass spectra of *m/z* 453, the MH^+ ion of both metabolites 3 and 5, respectively.

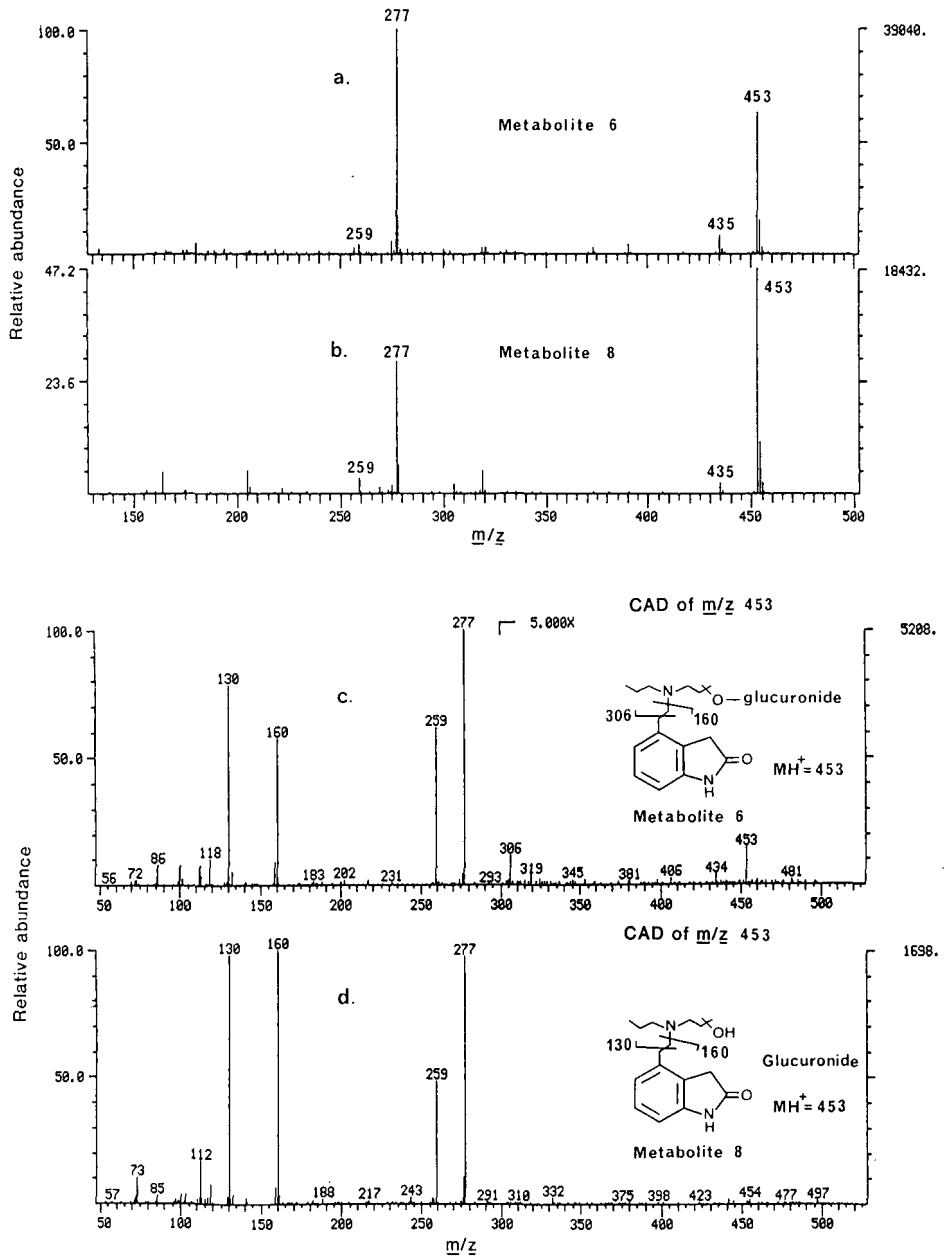

Fig. 6. (a,b) Thermospray Q1 mass spectra of metabolites 6 and 8, respectively, (c,d) Daughter ion mass spectra of *m/z* 453, the MH^+ ion of both metabolites 6 and 8, respectively.

m/z 259. The origin of the two other major fragment ions, *m/z* 130 and 160, were analogous to *m/z* 114 and 176 found for metabolites 3 and 5 with the exception that the site of hydroxylation is now on one of the propyl chains.

Metabolite 6 also produced an additional fragment ion at *m/z* 306 which represented the hydroxylated dipropylamine fragment with the glucuronide moiety still attached implying that the site of glucuronidation was on the hydroxyl group. The site of glucuronidation for metabolite 8 is unknown.

The final metabolite found in the monkey urine was metabolite 10. The Q1 spectrum (Fig. 7a) produced *m/z* 219 as the major ion which suggested a structure similar to SK&F 104557. However, two weak higher mass ions were observed at *m/z* 263 and 439. The ion at *m/z* 263 corresponded to an increase of 44 a.m.u. over *m/z* 219 and may be due to the addition of CO_2. Addition of glucuronic acid to *m/z* 263 accounted for *m/z* 439, thus confirming that the metabolite was a glucuronide conjugate.

Collisional activation of *m/z* 439 (Fig. 7b) produced the fragment ions *m/z* 263, 221, 219 and 160. Loss of the glucuronide along with proton transfer to the aglycone moiety resulted in the ion at *m/z* 263. This then demonstrated a loss of 44 a.m.u., presumably due to loss of CO_2, with concomitant proton transfer leaving the ion at *m/z* 219. The presence of the ion at *m/z* 160 confirmed that the indolone ring was present intact. The other weak fragment ion, *m/z* 221, corresponded to the glucuronide still attached to the carboxylic acid group which would suggest that the metabolite was conjugated through the acid functionality.

The metabolite was then isolated and analysed by NMR spectroscopy. It was confirmed that the substructure was SK&F 104557 and was conjugated with

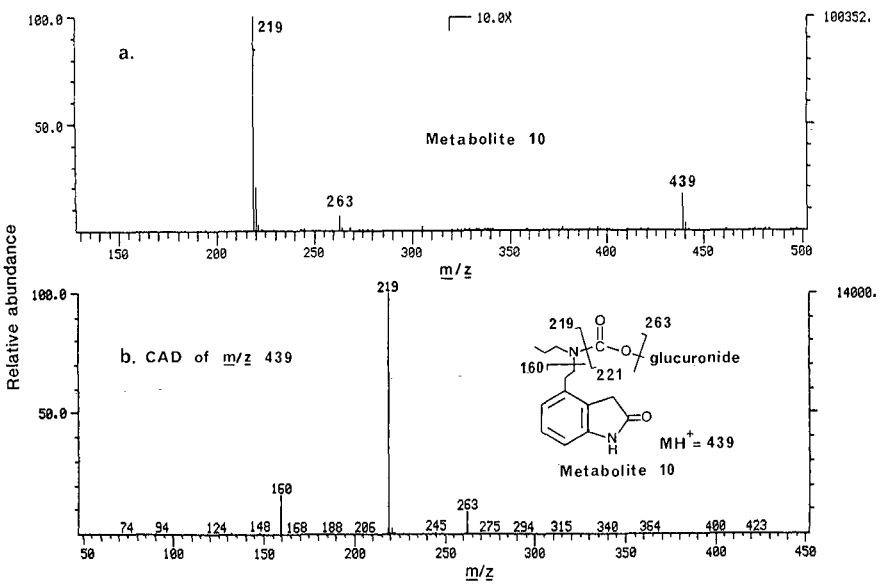

Fig. 7. (a)Thermospray Q1 mass spectrum of metabolite 10, (b) daughter ion mass spectrum obtained for *m/z* 439, the MH^+ ion of metabolite 10.

glucuronic acid. The site of the CO_2 functionality was confirmed as that shown in Fig. 1 by comparison of the chemical shifts for the α-CH_2 protons bound to nitrogen with those of SK&F 104557. The sample was also analysed by high-resolution fast atom bombardment (FAB) MS and the value for the MH^+ ion of 439.1699 corresponded well to the calculated value of 439.1717 with an error of 4.1 ppm. This confirmed that the addition of 44 a.m.u. was in fact due to CO_2.

Analysis of the human samples presented a more difficult task due to the low doses given to the human volunteers resulting in very low levels of metabolites.

The urine sample was initially analysed by LC–MS from which the selected ion traces for *m/z* 219, 235, 261 and 277 are shown in Fig. 8. By monitoring these ions all of the metabolites discussed previously, including the glucuronides, should be detected with the exception of metabolite 1 which would require a different MS–MS experiment.

From this analysis it was only possible to identify two compound related peaks, SK&F 104557 and 101468 (Fig. 8). Although there were other responses for these ions, their retention times and mass spectra did not correspond to any metabolites seen previously.

In an attempt to increase both the sensitivity and specificity it was decided to re-analyse the sample using LC–MS–MS. An experiment was created that would alternately pass *m/z* 219, 235, 261 and 277 into Q2 for collisional activation, with Q3 set for full scan to pick up the fragments.

From the MS–MS work on the monkey urine it was decided that the most important ions to look for were *m/z* 72, 160 and 176, which would identify SK&F 104557, 96990 and their conjugates, and *m/z* 114, 160 and 176 for SK&F 101468,

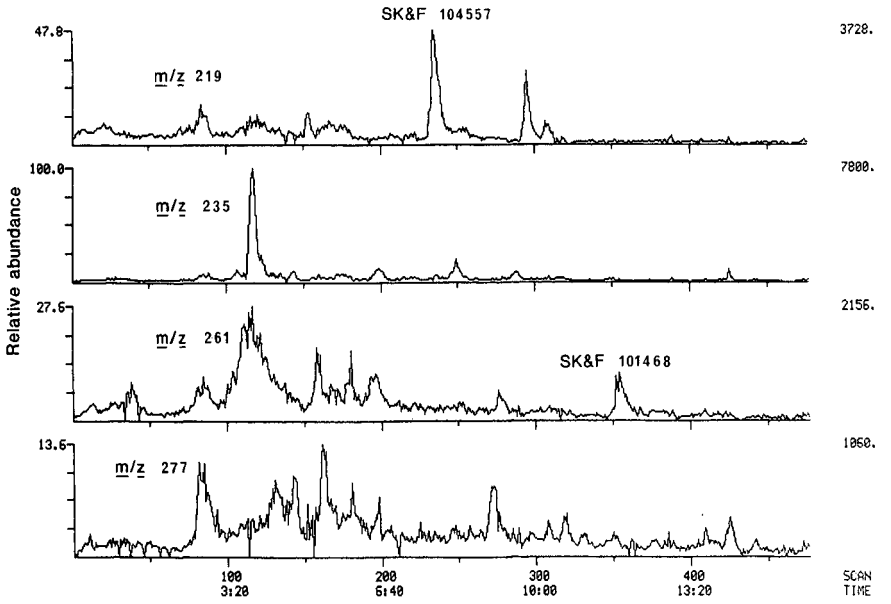

Fig. 8. Selected ion chromatogram traces of *m/z* 219, 235, 261 and 277 obtained from the LC–MS analysis of the 0–6-h human urine sample, after dosing 640 μg of SK&F 101468 p.o.

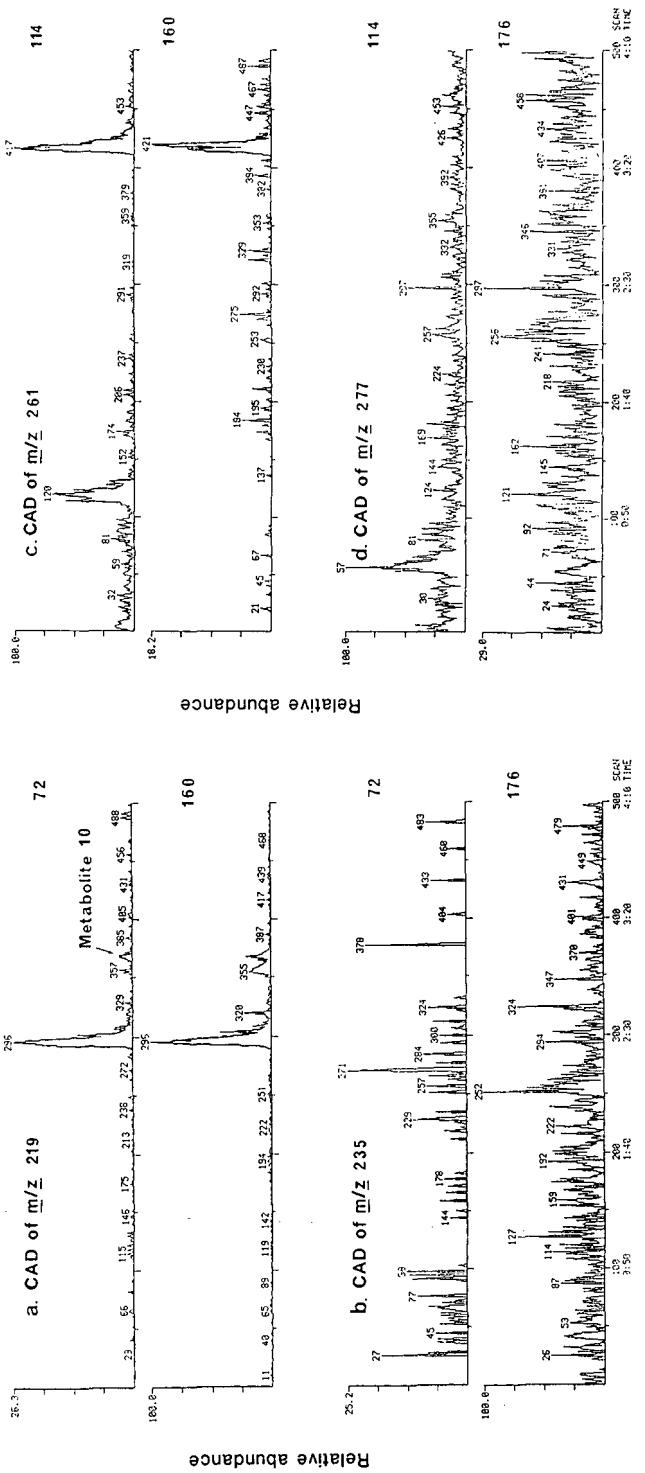

Fig. 9. Selected ion chromatogram traces obtained from the analysis of the 0–6-h human urine sample by LC–MS–MS with Q3 set for full scan, after dosing 640 μg of SK&F 101468 p.o.

SK&F 89124 and any conjugates. The results of this analysis are shown in Fig. 9. There were no responses observed for daughters of *m/z* 235 or 277 which meant that there were apparently no hydroxylated metabolites of SK&F 104557 or 101468. Two responses were observed for daughters of *m/z* 219, the major one being SK&F 104557 and the minor one corresponding to metabolite 10. There was only one response for daughters of *m/z* 261 which was attributed to SK&F 101468.

As the responses were relatively weak, an attempt was made to increase the sensitivity still further by re-analysing the sample using a similar MS–MS experiment, with the exception that Q3 was set up in MID mode to monitor the two main fragment ions of each metabolite. The results, shown in Fig. 10, were a substantial improvement over the previous results. SK&F 104557 and metabolite 10 gave a much stronger signal than before. A good response was observed for SK&F 96990 at the correct retention time. Strong responses were observed for SK&F 89124 (metabolite 9) and its O-glucuronide (metabolite 5) again at the correct retention times. There was also a substantial increase in the response for SK&F 101468 with two other possible responses which may be conjugates of SK&F 101468 which have not been seen before and their identity remains unknown. A different experiment would be required to detect metabolites 6 and 8.

The plasma sample (Fig. 11) was also analysed using this method and all of the metabolites found in the urine, were found in the plasma with the exception of metabolite 10.

CONCLUSION

The introduction of the thermospray interface has succeeded in making the coupling between HPLC and MS, in our experience, relatively routine and trouble free. It allows the direct analysis of biological samples with the minimum of sample preparation, providing structural information on drug metabolites at an early stage in the development of potential drug candidates. The technique is capable of detecting metabolites at levels of approximately 10 ng and upwards.

However, sometimes the amount of structural information obtained by thermospray LC–MS is limited as a result of the relatively "soft" nature of the ionisation method producing mainly protonated MH^+ ions. This problem can be overcome by carrying out a daughter ion MS–MS experiment in order to induce fragmentation, thus pinpointing the area of modification in the molecule.

The use of LC–MS–MS can prove invaluable for the identification of metabolites when present at levels below the detection limits of conventional LC–MS in a complex biological matrix. By switching to LC–MS–MS with Q3 on full scan the specificity of the technique is increased, as any compound related material would have to have the correct retention time, correct mass and produce structurally meaningful fragment ions. The chances of an endogenous component meeting all these requirements are remote.

However, even using this technique the sensitivity may not be sufficient, and it can be increased by setting Q3 on MID mode. The subsequent gain in sensitivity was significant and the good signal to noise ratio opened up the possibility of a quantitative LC–MS–MS assay. Although this has not yet been developed, the detection limit of the technique for SK&F 101468, when dissolved in methanol, was determined to be approximately 20 pg on column.

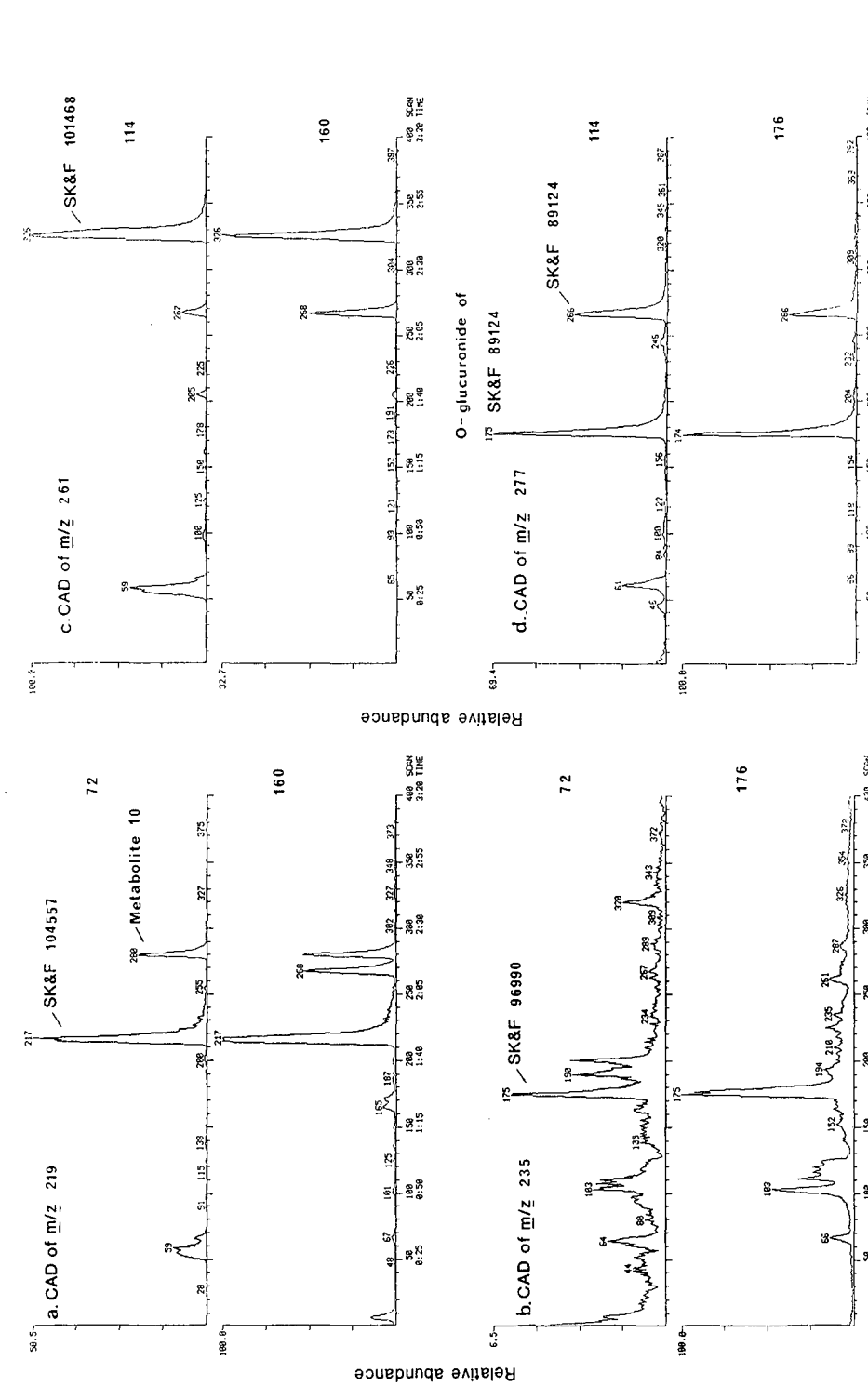

Fig. 10. Selected ion chromatogram traces obtained from the analysis of the 0–6-h human urine sample by LC–MS–MS with Q3 set for MID, after dosing 640 μg of SK&F 101468 p.o.

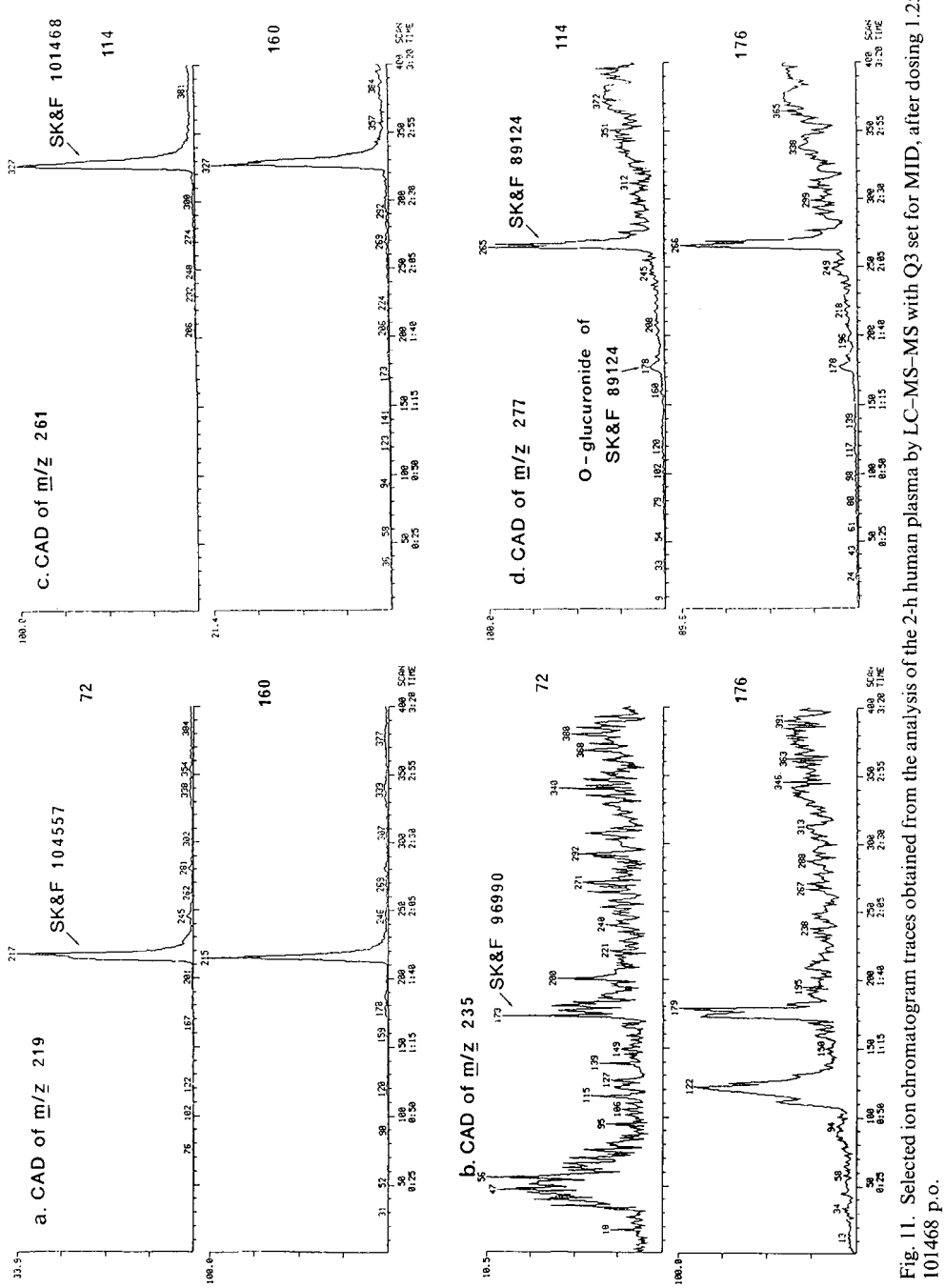

Fig. 11. Selected ion chromatogram traces obtained from the analysis of the 2-h human plasma by LC–MS–MS with Q3 set for MID, after dosing 1.25 mg of SK&F 101468 p.o.

ACKNOWLEDGEMENTS

The isolated metabolites were provided by the group of Dr. P. McWilliams of the Department of Drug Metabolism and Pharmacokinetics and the NMR analysis was performed by Mr. P. Moore of the Department of Physical Organic Chemistry.

REFERENCES

1 G. G. Gibson and P. Skett, *Introduction to Drug Metabolism*, Chapman and Hall, New York (1968).
2 R. P. W. Scott, C. G. Scott, M. Munroe and J. Hess, Jr., *J. Chromatogr.*, 99 (1974) 395.
3 W. H. McFadden, H. L. Schwartz and S. Evans, *J. Chromatogr.*, 122 (1976) 389.
4 W. H. McFadden, D. C. Bradford, D. E. Games and J. L. Gower, *Am. Lab (Fairfield, Conn.)*, 55 (1977).
5 E. P. Lankmayer, M. J. Hayes, B. L. Karger, P. Vouros and J. M. McGuire, *Int. J. Mass Spectrom. Ion Phys.*, 46 (1983) 177.
6 R. D. Smith and A. L. Johnson, *Anal. Chem.*, 53 (1981) 739.
7 C. R. Blakley and M. L. Vestal, *Anal. Chem.*, 55 (1983) 750.
8 C. R. Blakley, J. J. Carmody and M. L. Vestal, *J. Am. Chem. Soc.*, 102 (1983) 5931.

Journal of Chromatography, 474 (1989) 139–143
Elsevier Science Publishers B.V., Amsterdam — Printed in The Netherlands

CHROM. 21 502

Note

Effects of repeller position and voltage in thermospray mass spectrometry

M. E. HARRISON, G. J. LANGLEY[a] and M. A. BALDWIN*
School of Pharmacy, University of London, Brunswick Square, London WC1N 1AX (U.K.)

Chromatography coupled directly with mass spectrometry (MS) provides the analyst with a uniquely powerful combination, allowing rapid, efficient separation of complex mixtures with accurate and sensitive characterization of the individual components. Gas chromatography–mass spectrometry (GC–MS) has been in widespread use for more than two decades. It has proved so successful that GC–MS has had a major impact on mass spectrometer design and the majority of mass spectrometers are now purchased specifically for that purpose.

By contrast, and despite substantial effort by both academic and industrial researchers, the linking of high-performance liquid chromatography (HPLC) and MS has only recently become routine with the development of the thermospray ion source. Unlike most of the alternative LC–MS interfacing methods, thermospray does not compromise the chromatography significantly as it allows operation at high flow-rates (1 cm^3/min) using reversed-phase chromatography with high aqueous content mobile phases containing volatile buffers.

Thermospray provides a soft ionization method yielding predominantly protonated or other cationated molecular ions and generally giving little ion fragmentation. It involves pumping the liquid eluent through a heated capillary tube from which it sprays into a separately heated expansion chamber. This is evacuated by a high capacity mechanical pump, causing solvent molecules to evaporate rapidly, clusters of solute molecules or ions being broken up by collisions. Ion production is enhanced by the use of a buffer such as ammonium acetate. A proportion of the ions formed are drawn into the analyzing region of the mass spectrometer through an aperture in a sampling cone. This aperture is small enough to maintain differential pumping, which allows the mass spectrometer to operate effectively.

Most commercial designs incorporate a repeller electrode in the expansion chamber to enhance fragment ion production, but the precise role of the repeller has been subject to controversy, as some users report little enhancement of fragmentation. Several factors influence thermospray spectra[2], including mobile phase composition, flow-rate, nozzle temperature, chamber temperature, applied voltage on any repeller electrode, and the use of a filament or discharge as a secondary ionization method[3]. The use of a gas phase ion/molecule reaction model can explain the observ-

[a] Present address: Department of Chemistry, University of Southampton, Southampton SO9 5NH, U.K.

0021-9673/89/$03.50

ed ionization phenomena[4], whereby a basic molecule (B) in dilute aqueous ammonium acetate gives species such as $[BH]^+$ and $[BNH_4]^+$. The observation that fragment ions can be enhanced by the use of a repeller electrode down-stream of the sampling cone has been explained by collisional dissociations[5], the retarded ions being impacted by the high thermal energy molecules streaming through the expansion chamber. The effects of repeller voltage and vaporizer temperature on protonated and other cationated molecular ions as well as on fragment ion production have been described[3,6]. Lower voltages favor ammonium adduct ions, whereas intermediate voltages favor protonated molecular ions and high voltages favor fragment ions. Temperature effects are less clear-cut as they are compound-dependent, but higher temperatures discriminate against ammonium adducts compared with protonated molecular ions, and they tend to favor fragment ion production.

EXPERIMENTAL

This work was carried out on a VG 12/250 quadrupole mass spectrometer (VG MassLab, Altrincham, U.K.), operating under computer control with a standard VG thermospray source having no filament or discharge facility. The temperatures of the nozzle, the expansion chamber and the ion source were 190, 270 and 200°C respectively. The repeller electrode height was varied in the range 0–7 mm in 1-mm steps. (For simplicity the data reported here correspond only to heights of 2, 4 and 6 mm, but this is sufficient to give an accurate picture of the overall behaviour.) The height of the expansion chamber is 10 mm and the sampling cone protrudes into this by 4 mm. The repeller electrode comes into the chamber from the opposite side, so when it is at a height of 6 mm its tip is level with the aperture in the sampling cone.

At each height the voltage was varied between 0 and 340 V. The eluent was 0.1 *M* ammonium acetate (Analar BDH) in water prepared through a Milli-Q system (Millipore), delivered by a DuPont 870 pump at 1 cm^3/min. Furosemide was obtained from Hoechst and was introduced by direct injection in 0.3 m*M* aqueous solution through a Rheodyne valve with a 20-μl loop. The data presented here are averages of results obtained on two separate occasions several months apart.

RESULTS AND DISCUSSION

In this work a commercial thermospray source was used having a rod-shaped repeller electrode in the expansion chamber approximately 3 mm downstream of the sampling cone. The source design allows for easy dismantling and cleaning but the support arrangement for the repeller does not guarantee reproducibility in the repeller height settings on reassembley. It was noted that the repeller characteristics were

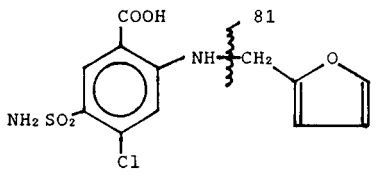

1 (M_R = 330)

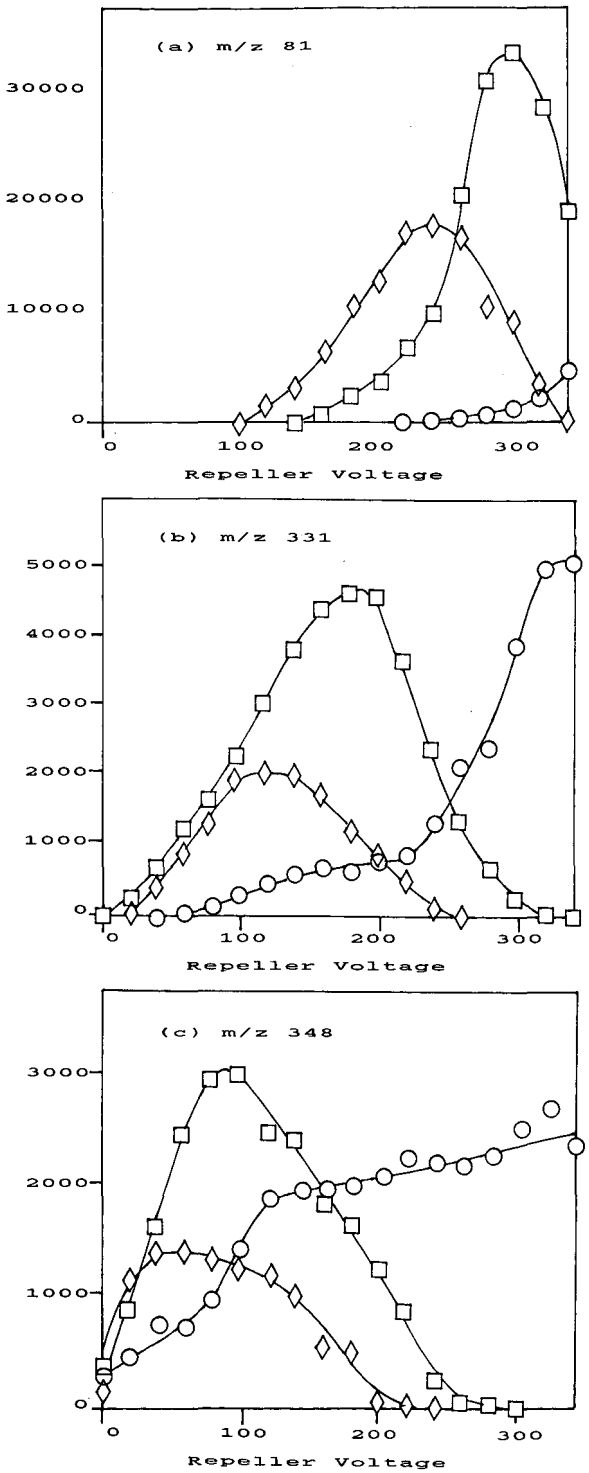

Fig. 1. Ion current (arbitrary units) *versus* repeller voltage for (a) *m/z* 81; (b) *m/z* 331; and (c) *m/z* 348 for furosemide at repeller height settings of 2 (○), 4 (□) and 6 (◇) mm.

often different after the source had been dismantled, and it was decided to investigate the effect of varying the repeller height. The diuretic drug furosemide (**1**) was used as a model compound, variations in the intensities of *m/z* 348 ($[M+NH_4]^+$), 331 ($[M+H]^+$) and *m/z* 81 (fragment ion) being monitored as functions of both height and voltage. The data are shown in Fig. 1a–c.

Fragment ion intensity

The retarding effect is at a minimum when the electrode height is only 2 mm. Under these conditions almost no fragmentation occurs to give *m/z* 81, whatever voltage is applied. At 4 mm a substantial signal is obtained for the fragment ion when a high voltage (*ca.* 300 V) is applied to the repeller, and the maximum is seen to shift to lower voltages as the height is increased to 6 mm. This behaviour is consistent with the observations of Bencsath and Field[5] and suggests that the fragmentation is not unimolecular but results from collisional activation. When the repeller height is set too low to retard the ions there is no fragmentation and whatever the height, a retarding voltage of at least 100 V is required to produce any fragmentation at all.

The origin of the *m/z* 81 ion was investigated as it could correspond either to the furfuryl group or to the protonated sulphonamide moiety. Protonation at the sulphonamide seemed unlikely as such groups are somewhat acidic whereas the secondary amine function is basic. This was confirmed by thermospray analysis from ^2H_2O: the protonated molecular ion increased in mass by 5 u and the ammonium adduct by 8 u whereas the fragment ion mass was unaltered, confirming its identity as the furfuryl cation.

Cationated molecular ions

The application of an appropriate voltage to the repeller gives increased intensity for both *m/z* 331 and 348 over the full range of repeller heights studied. At 2 mm the ion current *versus* voltage functions are still rising at the highest voltage available, 340 V, whereas the curves for 4 and 6 mm pass through maxima and the ion currents fall to zero before the maximum voltage is attained. The ion current maxima shift to lower voltages as the repeller height is increased. The ammonium adduct ion *m/z* 348 is favoured by lower voltages compared with the protonated ion *m/z* 331, which is consistent with the theory that much of the protonated molecular ion current arises through dissociation of the ammonium adduct[4].

CONCLUSION

The evidence concerning the effects of ion repeller voltage on fragmentation in thermospray spectra has frequently been contradictory. This study shows that there may indeed be little effect if the repeller is set too low, *e.g.* not even the maximum applied voltage gives significant fragmentation when the repeller height is only 2 mm.

For the particular design of source used in this work it is essential to take steps to ensure reproducibility in setting the repeller height after dismantling the source for cleaning and maintenance. Even then it may be necessary to select a height that optimises performance for a particular ion type at the expense of others; fragment ions are favoured by high repeller settings (4–6 mm) with high voltages (200–250 V) whereas these same settings will supress the ammonium adducts. It is noteworthy that

when the repeller height and voltage are optimised for fragmentation, the apparent ion current at m/z 81 is six times greater than that observed for the optimised protonated molecular ion. This casts doubt on the description of thermospray as a soft ionisation method, although as already explained most fragment ions arise by collisional dissociation and it must also be appreciated that there is significant discrimination against higher mass ions in quadrupole mass spectrometers.

REFERENCES

1 C. R. Blakley, J. J. Carmody and M. L. Vestal, *Anal. Chem.*, 52 (1980) 1636.
2 M. L. Vestal, *Science (Washington, D.C.)*, 226 (1984) 275.
3 W. H. McFadden and S. A. Lammert, *J. Chromatogr.*, 385 (1987) 201.
4 A. J. Alexander and P. Kebarle, *Anal. Chem.*, 58 (1986) 471.
5 F. A. Bencsath and F. H. Field, *Anal. Chem.*, 60 (1988) 1323.
6 C. Lindberg and J. Paulson, *J. Chromatogr.*, 394 (1987) 117.

Journal of Chromatography, 474 (1989) 145–148
Elsevier Science Publishers B.V., Amsterdam — Printed in The Netherlands

CHROM. 21 359

IMPROVING THE ION CURRENT STABILITY OF A THERMOSPRAY SOURCE BY IMPROVING THE CONTROL OF THE VAPORIZER TEMPERATURE AND SOLVENT FLOW-RATE

WIM GENUIT* and HERMAN VAN BINSBERGEN
Koninklijke/Shell-Laboratorium, Amsterdam (Shell Research B.V.), Badhuisweg 3, 1031 CM Amsterdam (The Netherlands)

SUMMARY

The original time-proportional vaporizer temperature control system of the thermospray source has been changed into a system based on phase-angle control, which enhances the vaporizer temperature stability, and hence the ion current stability of the source. When combined with a solvent pressure stabilization system, this new temperature control system stabilizes the vaporizer temperature to within 0.1°C of the set value.

INTRODUCTION

Partial evaporation and break-up of a liquid flow into small droplets, as occurs in a thermospray liquid chromatography–mass spectrometry (LC–MS) interface, inevitably involve statistical fluctuations, which affect the stability of the ion current output from the thermospray source. However, small variations in the vaporizer temperature[1] or in the LC eluent flow-rate[2] also have a large effect on ion current stability.

Conventional time-proportional control systems tend to induce variations in vaporizer temperature owing to the pulsed mode of heating, which allows the vaporizer capillary to cool between repetitive pulses, and to electrical feedback of the heating current pulses through the thermocouple spot weld. The rapid fluctuations in ion intensity resulting from these variations hamper the optimization of thermospray operating conditions, and make accurate mass calibration and quantitation from thermospray data even more problematic.

This paper deals with a temperature stabilization system based on phase-angle control, which provides a uniformly time-distributed heating power. This system yields a marked improvement in vaporizer temperature and ion-current stability, compared with the time-proportional control system. It is shown that with this new temperature control system, most of the residual temperature variation is due to LC pump pulsation and can be eliminated by stabilizing the solvent flow-rate.

0021-9673/89/$03.50

INSTRUMENTAL

A Waters Assoc. 600MS multi-solvent delivery system, provided with a flow-rate stabilization option, is used to pump a tuning solution consisting of methanol–water (1:1) with the addition of 0.05 *M* ammonium acetate buffer and 100 ppm (v/v) of polyethylene glycol PEG 400 at a flow-rate of 1.5 ml/min.

The mass spectrometer is a Finnigan 4500 TSQ quadrupole mass spectrometer equipped with a Finnigan-MAT thermospray LC–MS interface.

Initially, the interface exhibited very poor temperature stability, which was attributed to an over-dimensioned power circuit. The maximum heating power was then reduced by putting a diode into the circuit, cutting off half of each alternating current period. While this modification gave some improvement in temperature stability, rapid fluctuations of several degrees Celsius were still observed.

In the experiments described below, either the modified time-proportional control circuit, or a phase-angle control system, made up of an 818P programmable controller and a 425 phase-angle thyristor unit (both from Eurotherm, Worthing, U.K.), is used. Fig. 1 shows the two circuits with their different control characteristics. Time-proportional control varies the on/off ratio within a control cycle period which is much longer than the 10-ms power cycle period (corresponding to a 50-Hz line frequency). On a 10-ms time scale, a time-proportional system delivers its heating power in pulses. Phase-angle control varies the on/off ratio witin each power cycle period. Therefore, on the same 10-ms time scale phase-angle control provides a much more uniformly distributed heating power.

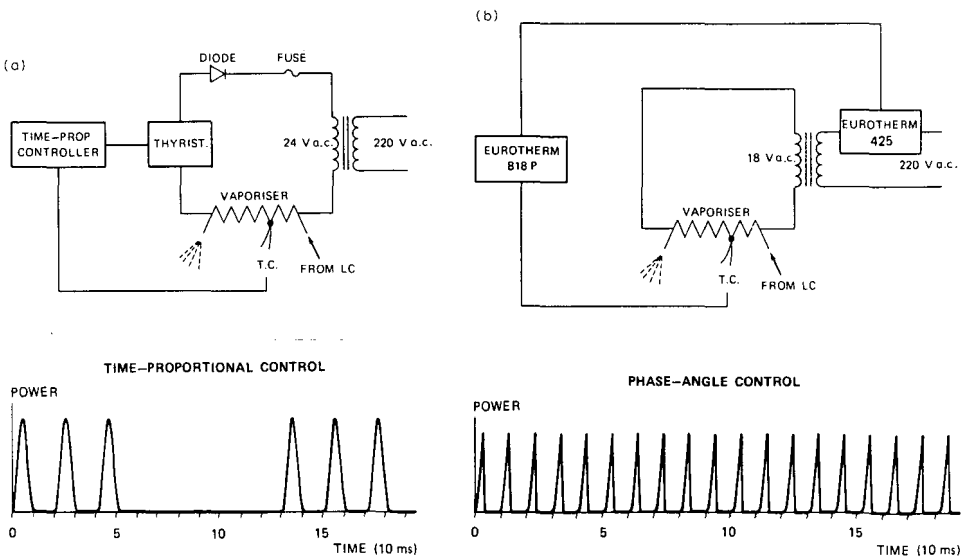

Fig. 1. (a) The modified Finnigan time-proportional vaporizer temperature control circuit. (b) The new phase-angle control circuit.

RESULTS

Fig. 2 shows the thermospray mass spectrum of the tuning solution. Ions above m/z 150 correspond to the protonated PEG oligomers (odd-numbered series) and the respective ammonium adducts (even-numbered series).

For the ion current stability tests, the quadrupole mass filter is set manually at m/z 344, and the vaporizer temperature and ion current are recorded simultaneously by a two-pen recorder. A typical result is shown in Fig. 3. The first part (A) was

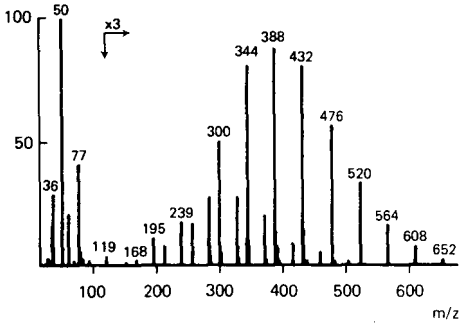

Fig. 2. Thermospray mass spectrum of the PEG 400 tuning solution.

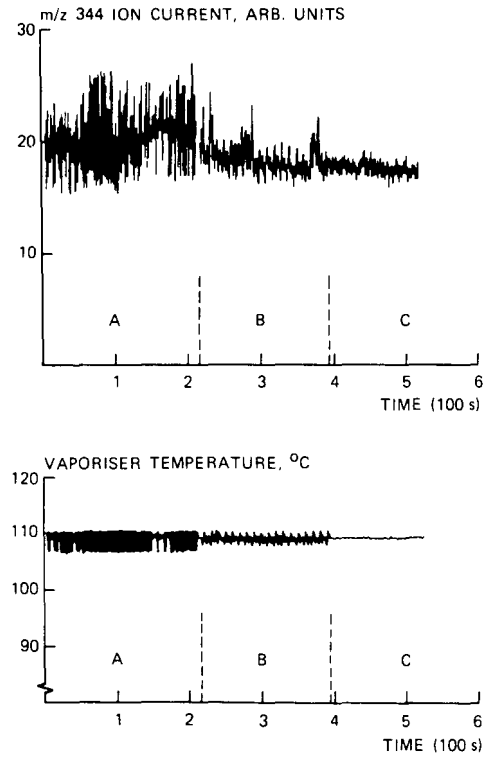

Fig. 3. Vaporizer temperature and m/z 344 ion current trace as a function of time. A, Time-proportional heating system; B, phase-angle heating system; C, phase angle heating system + flow-rate stabilization.

obtained using the time-proportional control, without flow rate stabilization. The vaporizer temperature, optimized for a maximum m/z 344 ion current, oscillates rapidly between 107 and 110°C, and the ion current trace shows corresponding fluctuations. Part B was recorded using the new phase-angle control system and without flow-rate stabilization. The high-frequency variations in temperature and ion current are largely reduced, compared with A, and the slow variations on an approximately 10-s time scale, observed in both traces, are exactly in phase with the piston movements of the solvent pump. This result illustrates the inadequately of piston pulse-damping devices in normal LC pumps for thermospray LC–MS work, at least when they are operating in the column bypass mode, or as a post-column buffer addition pump. In part C, using phase-angle temperature control combined with solvent flow-rate stabilization, this slow variation is eliminated, and the vaporizer temperature is stable to within 0.1°C of the set value. The corresponding ion current trace shows the remaining thermospray noise.

These experiments were repeated a few times with different crimped vaporizer tips. Although the vaporizer characteristics, such as optimum temperature and temperature stability, vary somewhat from one tip to another, the results are similar in that the stability is greatly enhanced by the new temperature control. Also, the vaporizer temperature is found to be much less critical, the vaporizers operating steadily in a wide temperature range.

CONCLUSIONS

Poor stabilities of vaporizer temperature and solvent flow-rate are important sources of ion current fluctuations in a thermospray LC–MS interface. Temperature stabilization by a phase-angle controlled system gives a significant stability improvement over the pulsed time-proportional systems. Temperature variations induced by pump pulsation can be eliminated by applying flow-rate stabilization.

REFERENCES

1 R. H. Robins and F. W. Grow, *Rapid Commun. Mass Spectrom.*, 2 (1988) 30.
2 M. L. Vestal and G. J. Fergusson, *Anal. Chem.*, 57 (1985) 2373.

Journal of Chromatography, 474 (1989) 149–162
Elsevier Science Publishers B.V., Amsterdam — Printed in The Netherlands

CHROM. 21 423

DEVELOPMENT OF OPTIMIZATION STRATEGIES IN THERMOSPRAY LIQUID CHROMATOGRAPHY–MASS SPECTROMETRY

C. E. M. HEEREMANS, R. A. M. VAN DER HOEVEN, W. M. A. NIESSEN*, U. R. TJADEN and J. VAN DER GREEF

Division of Analytical Chemistry, Center for Bio-Pharmaceutical Sciences, University of Leiden, P.O. Box 9502, 2300 RA Leiden (The Netherlands)

SUMMARY

In order to optimize the sensitivity and reproducibility of thermospray liquid chromatography–mass spectrometry in (bio)analytical applications, some of the experimental parameters that influence thermospray buffer ionization have been investigated systematically.

Attention was paid to the vaporizer temperature, which is especially important in the analysis of thermolabile compounds, the ammonium acetate concentration, the methanol content and the repeller potential. General optimization strategies for thermospray buffer ionization have been developed. The usefulness of extensive optimization is discussed for qualitative and quantitative analysis. In quantitative target compound analysis optimization on the analyte is necessary. In qualitative analysis, however, usually unknown compounds have to be analysed and no parent compound is available for optimization purposes.

INTRODUCTION

The thermospray interface, developed by Blakley and Vestal[1], is a valuable analytical tool, which has given a strong impetus to developments in liquid chromatography–mass spectrometry (LC–MS). In many laboratories thermospray LC–MS is now routinely used and many interesting applications have been described. In our laboratory thermospray LC–MS is applied in both qualitative and quantitative bioanalysis. In the development of bioanalytical methods, the optimization of selectivity, sensitivity and reproducibility is of utmost importance. This paper deals with the optimization of thermospray LC–MS in the buffer ionization mode. Many interdependent experimental parameters are important in this respect: the mobile phase composition (amount and type of buffer and organic modifier), the solvent flow-rate, the design and temperature of the vaporizer, the design and temperature of the ion source, and the geometry, position and potential of the repeller electrode. Other important parameters, which are difficult to adjust reproducibly, are the spray performance, the condition of the vaporizer, and the degree of contamination of the repeller electrode and the ion source. Although the thermospray interface has been

0021-9673/89/$03.50

commercially available for five years now, little attention has been paid to a systematic investigation of the influence and optimization of the various experimental parameters. Such systematic studies are hampered by the fact that there are large differences in the design and performance of the various commercially available thermospray interfaces, for instance with respect to the type of vaporizer and the temperature that has to be applied for stable spray conditions. The optimization of the temperature of the vaporizer, the type and concentration of the buffer salt, and the modifier content of the LC mobile phase has been studied by Voyksner and Haney[3] for triazine herbicides and organophosphorus pesticides. The effects of the vaporizer temperature have been investigated for some drugs by Lindberg and Paulson[4]. The influence of the potential applied to the repeller electrode, positioned either opposite to the sampling cone or slightly downstream, has been studied by Lindberg and Paulson[4] and by Bencsath and Field[5]. Various other geometries of the repeller electrode, *e.g.* a needle tip, are currently under investigation (*cf.* ref. 6). Considerable effort has been put into the improvement of the thermospray vaporizer performance, especially with respect to the reproducibility[7–12]. Both the vaporizer design[7–10] and the thermospray controller[11,12] are under investigation.

In the present paper the influence of various parameters on the eluent and analyte signals and mass spectra have been investigated systematically with a Finnigan MAT TSP interface. The results of the variation of the vaporizer temperature, the repeller potential, the ammonium acetate concentration and the methanol content of the mobile phase are reported here. From the results an optimization strategy for thermospray LC–MS studies is suggested.

EXPERIMENTAL

Thermospray mass spectrometry

The solvents were delivered by a Model 2150 high-pressure pump (LKB, Bromma, Sweden). The flow-rate was 1.2 ml/min. Thermospray MS was performed on a Finnigan MAT TSQ 70 triple quadrupole mass spectrometer equipped with a Finnigan MAT TSP interface (Finnigan MAT, San José, CA, USA). For all experiments the block temperature was kept at 200°C.

Repeller potential variation/vaporizer temperature variation

The mobile phase consisted of 50 m*M* ammonium acetate in water–methanol (80:20, v/v). For the systematic investigation of the influence of the repeller potential on the eluent background spectrum, an instrument control procedure was written, which automatically increases the repeller potential from 0 to 200 V in 10 V increments. After each potential adjustment, a stabilization time of 2 s is applied. At each repeller potential ten scans (m/z 10–100) are acquired. For investigation of the influence of the repeller potential on the analyte signal the repeller potential was increased by 10 V before every injection. These experiments were repeated at several vaporizer temperatures in order to get information about the influence of the vaporizer temperature on the eluent background, the analyte signals and mass spectra.

Methanol content variation

The mobile phase consisted of 50 m*M* ammonium acetate in water–methanol

(v/v %) mixtures. The amount of methanol was increased from 0 to 80%, in 10% increments. The vaporizer temperature was decreased with increasing methanol content (*ca.* 5°C decrease for 10% methanol content increase). At every mobile phase composition the repeller potential was varied from 0 to 200 V.

Ammonium acetate concentration variation

The concentration of ammonium acetate in water–methanol (90:10, v/v) was increased from 10^{-5} to 10^{-2} *M*. For each experiment the buffer concentration was increased by an order of magnitude. The concentration of the analyte was *ca.* $2 \cdot 10^{-4}$ *M*. In this way spectra were obtained with ammonium acetate concentrations lower than, equal to, and higher than the analyte concentration. For every mobile phase composition the repeller potential was varied from 0 to 200 V. The vaporizer temperature was 115°C.

Samples

Standard solutions of analytes, dissolved in the mobile phase used in the described experiments, were injected (*ca.* 500 ng/20 μl) in the flow-injection analysis (FIA) mode, *i.e.* direct injection into the liquid stream without a chromatographic column. The analytes were obtained from various sources.

RESULTS AND DISCUSSION

Vaporizer

In the thermospray interface used, the vaporizer is a directly heated stainless-steel capillary. After installation of a new vaporizer a good spray is produced by squeezing the end of the capillary at ambient temperature and pressure. When a proper spray is established the thermospray interface can be made operational. The spray performance obviously is one of the parameters that cannot easily be reproduced. The use of apparently more reproducible systems with replaceable fused-silica capillaries or sapphire diaphragms has been suggested recently by Vestal[10].

The degree of vaporization of the eluent is an important experimental parameter, which depends on the composition of the mobile phase, the solvent flow-rate, and the vaporizer temperature. At a constant mobile phase composition and flow-rate, relatively stable signals can be obtained within a temperature range of *ca.* 30°C. Below this temperature range the spray is too wet and unstable signals are observed; above this range a dry spray is obtained and no signals are observed at all for the compounds studied. The vaporizer temperature is typically *ca.* 110°C for 1–1.5 ml/min of water–methanol mixtures, depending on the condition of the vaporizer (*e.g.* aperture of the capillary tip after squeezing, age and history of the capillary). The vaporizer temperature has to be adjusted for each combination of the mobile phase composition and the flow-rate in order to obtain stable background signals. Within the temperature range that provides relatively stable signals, optima in absolute intensities of the eluent and the analyte can be obtained. In some cases these optima coincide, as observed by others[3,4]. However, the gain in absolute intensities that can be achieved by optimization is very compound-dependent. In favourable cases a gain of an order of magnitude can be realized. The optimum vaporizer temperature for a particular analyte also depends on the condition of the vaporizer. Vaporizer temper-

ature optimization for a particular analyte may give different results on different days. This implies a limited usefulness of reporting "optimum" vaporizer temperatures. Apparently, the vaporizer temperature has a considerable influence on the mass spectra of thermolabile compounds. At high vaporizer temperatures these compounds will tend to decompose in the eluent stream[13]. The decomposition products can also

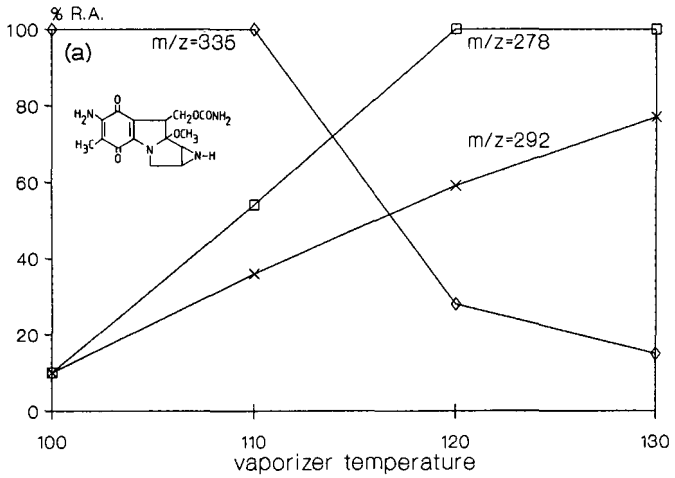

Fig. 1. Relative intensities of the protonated molecule and some fragments as a function of the vaporizer temperature (°C) for mitomycin C (MW = 334) (a) and rimexolone (MW = 370) (b). Repeller potential, 20 V; eluent, 50 m*M* ammonium acetate in water–methanol (80:20, v/v). (c) Structure of 2,7-diamino-1-hydroxy-mitosene.

be ionized in the ion source, resulting in a spectrum of both the analyte and its decomposition products. Real fragment peaks may also be observed, when such a process is thermodynamically favourable or when collisionally induced dissociation takes place in the source[14].

Fig. 1 shows the effect of the vaporizer temperature on the mass spectra of mitomycin C (MMC) and (11β,16α,17β)-11-hydroxy-16,17-dimethyl-17-(1-oxopropyl)androsta-1,4-dien-3-one (rimexolone), a thermolabile and a thermally stable compound, respectively. With increasing vaporizer temperature the relative abundance of the protonated molecule of the anti-cancer drug MMC (MW = 334) decreases compared with the fragment peaks at *m/z* 292 and 278. The peak at *m/z* 292 results from the loss of HNCO from the protonated molecule, which might take place both by thermal decomposition of the neutral and by fragmentation of the protonated molecule. The peak at *m/z* 278 is probably due to a loss of HNCO from the protonated molecule of a hydrolysis product of MMC, 2,7-diamino-1-hydroxymitosene (MW = 320, structure in Fig. 1c)[15], which is formed by cleavage of the methoxy group, resulting in an unsaturated bond and opening of the aziridine ring by addition of water. In this study, 2,7-diamino-1-hydroxymitosene obviously is a thermal hydrolysis product of MMC formed in the eluent stream, which after loss of HNCO, either by thermal decomposition of the neutral or fragmentation of the protonated species, results in a peak at *m/z* 278. In the thermospray mass spectrum of 2,7-diamino-1-hydroxymitosene, a peak at *m/z* 278, resulting from the loss of HNCO from the protonated molecule, is observed as well[6]. In the thermospray mass spectrum of MMC, a peak at *m/z* 321, due to the protonated molecule of 2,7-diamino-1-hydroxymitosene, is observed at low abundance. In the chemical ionization (CI) and desorption chemical ionization (DCI) spectra of MMC, a peak at *m/z* 292 is observed[17], whereas the peaks at *m/z* 321 and *m/z* 278 are absent. For a thermally stable compound, such as rimexolone (Fig. 1b), no influence of the vaporizer temperature is observed on the relative abundances of the protonated molecule at *m/z* 371 and the major fragment at *m/z* 353, resulting from a loss of water.

Solvent composition

Ammonium acetate concentration. The presence of a volatile buffer (50–100 m*M*), *e.g.* ammonium acetate, in the mobile phase is essential for thermospray buffer ionization[1]. The influence of the ammonium acetate concentration has been studied by Voyksner and Haney[3]. They report a strong dependence of the relative analyte signal in a concentration range between 10^{-3} and $8 \cdot 10^{-2}$ *M*, and a plateau is reached at higher concentrations. In the present experiments the buffer concentration was varied between 10^{-5} and 10^{-2} *M* in order to investigate the influence of the ammonium acetate concentration on the signal of 10^{-4} *M* of analyte. The results obtained are shown in Fig. 2 for caffeine. When the ammonium acetate concentration is ten times lower than the analyte concentration, the intensity of the protonated molecule of caffeine is very weak. Sodium and potassium cationized molecules are observed as the most intense signals. When the ammonium acetate concentration is equal to the analyte concentration, the protonated molecule becomes the most abundant peak, whereas with a buffer concentration ten times higher than the analyte concentration a large increase (three orders of magnitude) in the absolute intensity of the protonated molecule is observed. The absolute intensity of the ammoniated molecule increases by

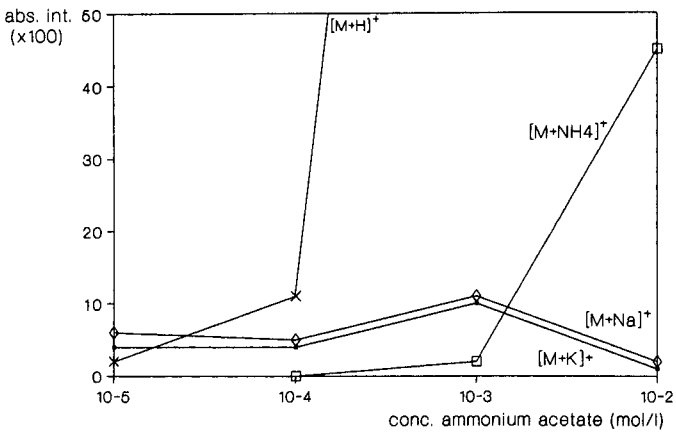

Fig. 2. Response of the protonated, ammoniated and sodium and potassium cationized molecules of caffeine ($2 \cdot 10^{-4}$ *M*) as a function of the ammonium acetate concentration. Repeller potential, 50 V; eluent, ammonium acetate in water–methanol (90:10, v/v).

two orders of magnitude in the buffer range studied, whereas the intensities of the sodium and potassium cationized molecules remain constant.

Methanol content. Because in bioanalysis gradient high-performance liquid chromatographic (HPLC) runs often have to be performed with the organic modifier content of the mobile phase changing over a wide range, *e.g.* from 0 to above 50%, the influence of the methanol content on the analyte intensities and mass spectra has been investigated. With increasing methanol content the vaporizer temperature has to be lowered to obtain similar spray conditions, because of the higher volatility of the mobile phase with increasing methanol content. When no methanol is present in the mobile phase the highest sensitivity is obtained, which is in accordance with the results, reported by others (*cf.* ref. 3). For the test compounds (adenosine, caffeine and coniferic aldehyde) a slight decrease is observed with increasing methanol content from 0 to 40%. When the methanol content exceeds 40%, the sensitivity drops significantly. External ionization sources, filament or discharge, are needed at these modifier contents.

Repeller potential

Eluent. In the thermospray source design used in these experiments, a flat circular tip repeller electrode is placed opposite to the sampling cone. Significant influence of the repeller potential on the intensity and the appearance of the mass spectrum of the eluent cluster ions has been reported[4]. The repeller potential influences both the total ion current and the abundance of the various species. The ions observed depend on the mobile phase. In Tables I and II compositions of the various ions observed with two different eluents are proposed. Fig. 3 shows the influence of the repeller potential variation on the total ion current (*m/z* 10–100) and on the intensities of some of the more abundant ions for 50 m*M* ammonium acetate in water. Similar plots for 50 m*M* ammonium acetate in water–methanol (20:80, v/v) are given in Fig. 4. The plots of the total ion current and the intensities of the various ions as a function of the repeller potential differ from the profiles reported by Lindberg and

TABLE I

COMPOSITION OF THE VARIOUS POSITIVE IONS OBSERVED IN THERMOSPRAY BUFFER IONIZATION WITH 50 m*M* AMMONIUM ACETATE IN WATER

Asterisk indicates present in the given repeller potential region.

m/z	*Composition*	*Repeller potential < 100 V*	*Repeller potential > 100 V*
15	$[CH_3]^+$		*
18	$[NH_4]^+$	*	
19	$[H_3O]^+$		*
33	$[H_2O + CH_3]^+$		*
35	$[2NH_3 + H]^+$	*	
36	$[NH_3 + H_2O + H]^+$	*	
37	$[2H_2O + H]^+$		*
43	$[CH_3CO]^+$		*
51	$[2H_2O + CH_3]^+$		*
53	$[2NH_3 + H_2O + H]^+$	*	
54	$[NH_3 + 2H_2O + H]^+$	*	
55	$[3H_2O + H]^+$		*
61	$[H_2O + CH_3CO]^+$		*
73	$[4H_2O + H]^+$		*
77	$[2NH_3 + CH_3CO]^+$	*	
78	$[NH_3 + H_2O + CH_3CO]^+$	*	
79	$[2H_2O + CH_3CO]^+$		*
95	$[2NH_3 + H_2O + CH_3CO]^+$	*	
96	$[NH_3 + 2H_2O + CH_3CO]^+$	*	
97	$[3H_2O + CH_3CO]^+$		*

Paulson[4]. The potentials at which the highest intensities for the various ions are observed are lower in our experiments. These differences cannot be attributed to the difference in solvent composition (43% methanol in ref. 4 and 20% methanol in this study).

A closer look at the various cluster ions reveals some interesting features. Clusters containing NH_3 are observed only at repeller potentials below 100 V for both mobile phases. The NH_4^+ ion (*m/z* 18) is most intense at *ca.* 100 V. Clusters containing H_2O and no NH_3 are observed only at repeller potentials above 100 V. For the mobile phase containing 20% methanol, intense methanol clusters are observed over the whole range of repeller potentials. Protonated methanol clusters ($[CH_3OH_2]^+$, $[2CH_3OH + H]^+$ and $[3CH_3OH + H]^+$) are observed at high potential. Methanol clusters containing NH_3 are observed at low potential, whereas methanol clusters containing H_2O are observed at high potential. A nice illustration of the changeover in cluster composition from NH_3-containing clusters to H_2O-containing clusters with increasing repeller potential is given in Fig. 5, where the intensities of *m/z* 77 $[2NH_3 + CH_3CO]^+$, *m/z* 78 $[NH_3 + H_2O + CH_3CO]^+$ and *m/z* 79 $[2H_2O + CH_3CO]^+$) are plotted as a function of the repeller potential. The NH_3-containing clusters at *m/z* 77 and 78 have a maximum intensity at low repeller potential, whereas the H_2O-containing cluster at *m/z* 79 is observed at high repeller potential. Similar effects have been observed for other clusters, such as *m/z* 35, 36 and 37, *m/z* 53, 54 and 55, and *m/z* 95, 96 and 97. Another interesting feature, also illustrated in Fig. 5, is observed for the

TABLE II

COMPOSITION OF THE VARIOUS POSITIVE IONS OBSERVED IN THERMOSPRAY BUFFER IONIZATION WITH 50 m*M* AMMONIUM ACETATE IN WATER–METHANOL (80:20, v/v)

Asterisk indicates present in the given repeller potential region.

m/z	*Composition*	*Repeller potential < 100 V*	*Repeller potential > 100 V*
15	$[CH_3]^+$		*
18	$[NH_4]^+$	*	
19	$[H_3O]^+$		*
31	$[CH_2{=}OH]^+$		*
33	$[CH_3OH + H]^+$		*
35	$[2NH_3 + H]^+$	*	
36	$[NH_3 + H_2O + H]^+$	*	
43	$[CH_3CO]^+$		*
47	$[CH_3{-}O{-}CH_3 + H]^+$		*
50	$[CH_3OH + NH_3 + H]^+$	*	
51	$[CH_3OH + H_2O + H]^+$		*
54	$[NH_3 + 2H_2O + H]^+$	*	
60	$[NH_3 + CH_3CO]^+$	*	
61	$[H_2O + CH_3CO]^+$		*
65	$[2CH_3OH + H]^+$		*
68	$[CH_3OH + NH_3 + H_2O + H]^+$	*	
75	$[CH_3OH + CH_3CO]^+$		*
77	$[2NH_3 + CH_3CO]^+$	*	
78	$[NH_3 + H_2O + CH_3CO]^+$	*	
79	$[2H_2O + CH_3CO]^+$ $[3CH_3OH - H_2O + H]^+$		*
82	$[2CH_3OH + NH_3 + H]^+$	*	
83	$[2CH_3OH + H_2O + H]^+$		*
96	$[NH_3 + 2H_2O + CH_3CO]^+$	*	
97	$[3H_2O + CH_3CO]^+$ $[3CH_3OH + H]^+$		*

clusters at *m/z* 43 $[CH_3CO]^+$, 61 $[H_2O + CH_3CO]^+$ and 79 $[2H_2O + CH_3CO]+$. It appears that the larger clusters fragment at higher repeller potentials. The cluster at *m/z* 79, containing two water molecules, consecutively loses the two water molecules with increasing repeller potential, resulting in clusters at *m/z* 61 and 43. More detailed discussions on these probably collisionally induced effects will be reported elsewhere[18].

The above-described instrument control procedure can also be used as a diagnostic tool to ascertain a good instrument performance. When no response of the total ion current of the solvent background is observed as a result of the increasing repeller potential, either the vaporizer spray performance has to be checked, or the repeller electrode and the ion source are seriously contaminated. Cleaning of the repeller electrode and the ion source has to be performed about every two weeks, which is obviously dependent on the nature of the samples.

The analyte. The influence of the repeller potential on the analyte signal has been investigated by means of repetitive injection at various repeller potentials between 0 and 200 V. With repeller potentials between 0 and 100 V not much influence

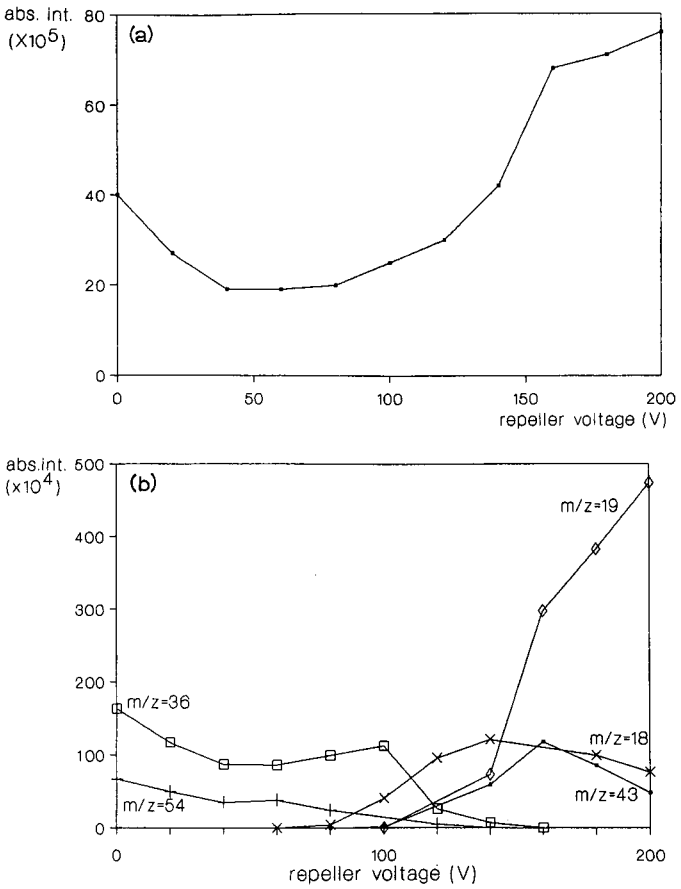

Fig. 3. Influence of the repeller potential on the total ion current (a) and on the intensities of the more abundant solvent cluster ions (*m/z* 18, 19, 36, 43, 54) (b) for 50 m*M* ammonium acetate in water. Vaporizer temperature, 120°C.

on the analyte signal is observed. Flat optima, which are to some extent compound-dependent, are found in plots of intensity *versus* repeller potential (*cf.* for instance the signal obtained for the protonated molecule of adenosine at *m/z* 268 with various repeller potentials given in Fig. 6). Above 100 V the signal drops significantly, and it decreases further with increasing potential. This repeller potential range, in which the analyte signals reach an optimum in absolute intensity, coincides with the repeller potential range in which the NH_3-containing solvent clusters have their optimum intensity. Apparently, proton transfer from the ammoniated clusters is an important contribution in the mechanism of thermospray buffer ionization. This is also in agreement with the results obtained in the studies on the influence of the ammonium acetate concentration on the analyte signals, which are described above. The potential at which the signal drops is shifted to higher repeller potential when the repeller electrode becomes contaminated. This may be attributed to changes in the effective potential. The various compounds that were investigated in these experiments, adenosine, MMC and rimexolone, reach their optimum response at similar repeller po-

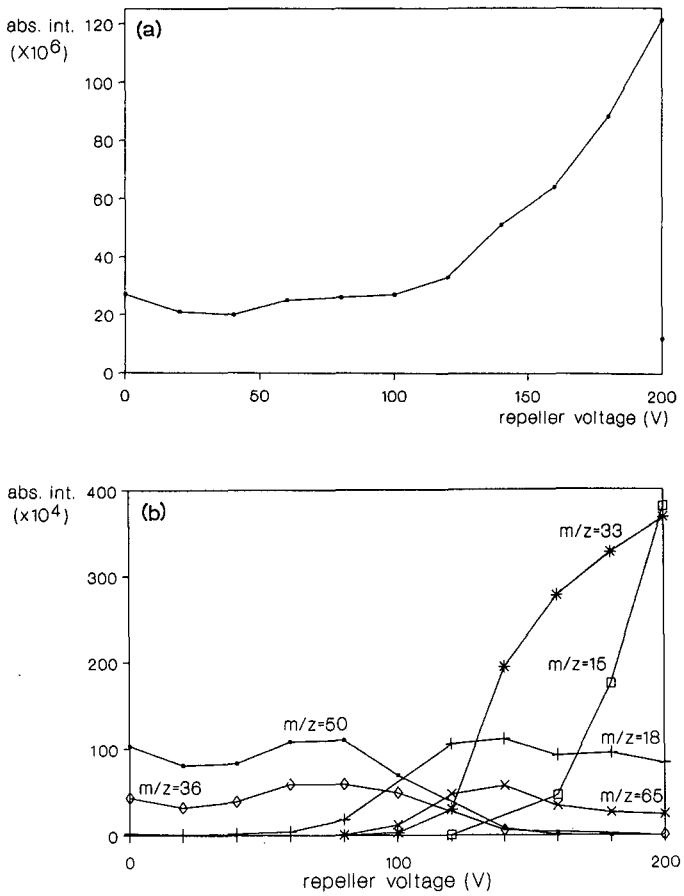

Fig. 4. Influence of the repeller potential on the total ion current (a) and on the intensities of the more abundant solvent cluster ions (*m/z* 15, 18, 33, 36, 50, 65) (b) for 50 m*M* ammonium acetate in water–methanol (20:80, v/v). Vaporizer temperature, 110°C.

tentials. This is in accordance with the results reported by Lindberg and Paulson[4]. However, the optimum repeller potentials observed in the present study are significantly lower than those reported elsewhere[4]. Thus, while the trends observed are similar, the actual potentials differ considerably between these two studies.

When the thermospray interface is used in discharge-on mode, high repeller potentials can induce significant fragmentation of the analytes[14]. Using thermospray buffer ionization these effects are usually not observed. However, for some compounds, differences in the mass spectra are observed when the repeller potential is varied. For instance for heptabarbital (Fig. 7) at low repeller potential an intense ammoniated molecule (*m/z* 268) is observed as well as a peak at *m/z* 285, which might be due to $[M + 2NH_3 + H]^+$; no fragmentation occurs. At high repeller potential the protonated molecule (*m/z* 251) becomes the base peak and an intense fragment (*m/z* 157) corresponding to the loss of the heptenyl-group is observed. Similar effects were observed by others for some other compounds (*cf.* ref. 4).

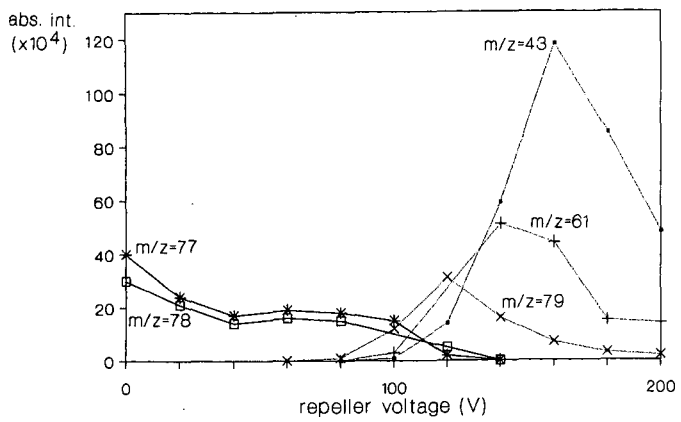

Fig. 5. Response of some solvent cluster ions (*m/z* 43, 61, 77, 78, 79) as a function of the repeller potential for 50 m*M* ammonium acetate in water. Vaporizer temperature, 120°C.

Optimization strategies

As a result of the described systematic studies, some general guidelines for optimization of thermospray buffer ionization have been developed. A clean ion source and repeller electrode are always necessary for the best results. When ammonium acetate concentrations between 50 and 100 m*M* are used, the buffer concentration generally will be higher than the analyte concentration and the highest sensitivity will be obtained. Gradient runs, with the methanol content of the mobile phase ranging from 0 to 40% for example, can easily be performed in combination with the thermospray buffer ionization mode. Above a methanol content of 40% additional sources of ionization are needed. These guidelines can be applied in both qualitative and quantitative analysis with thermospray LC–MS. In general, the usefulness of exten-

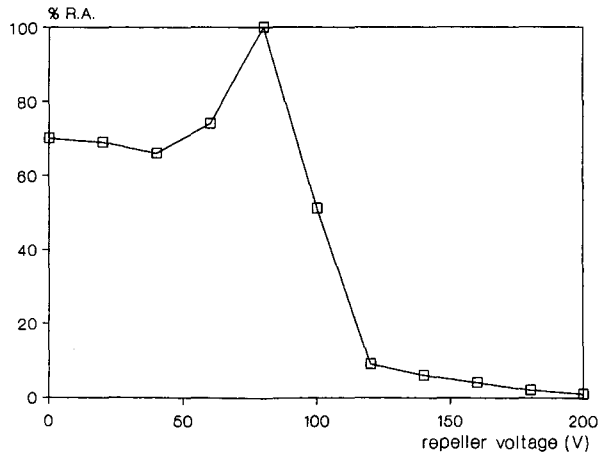

Fig. 6. Relative abundances of the protonated molecule of adenosine (MW = 267) as a function of the repeller potential obtained in the FIA mode. Vaporizer temperature, 120°C; eluent, 50 m*M* ammonium acetate in water–methanol (80:20, v/v).

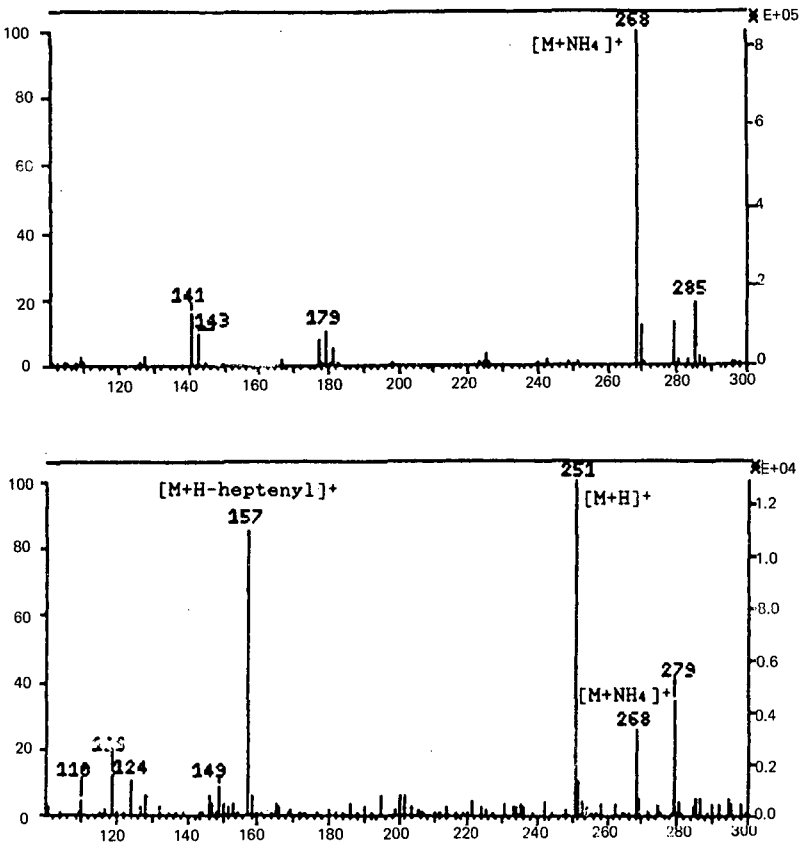

Fig. 7. Two thermospray mass spectra of heptabarbital (MW = 250) obtained at a repeller potential of 50 V (a) and 160 V (b). Vaporizer temperature, 120°C; eluent, 50 m*M* ammonium acetate in water–methanol (60:40, v/v).

sive optimization strategies for thermospray buffer ionization can be questioned. Many applications of thermospray LC–MS are concerned with qualitative analysis, *i.e.* confirmation or identification of (unknown) compounds. In some cases optimization on one of the constituents of the sample mixtures to be analysed can be useful, but in other cases the various components can show widely differing thermospray behaviour. An example of the former case is the analysis of desulphoglucosinolates, in which for example the readily available sinigrin can be used for optimization of the vaporizer temperature and the repeller potential. Other desulphoglucosinolates show similar behaviour under thermospray buffer ionization conditions, especially with respect to their thermolability[19]. An example of the latter case is the thermospray LC–MS analysis of metabolites and degradation products of mitomycin C, where the parent compound is highly sensitive to the vaporizer temperature, because of its thermolability, whereas the other products are hardly influenced at all by the vaporizer temperature[16]. In many applications, however, parent compounds are not available for optimization purposes.

The chromatographic conditions are another aspect of importance in optimiza-

tion of the analysis. Quite often the mobile phase used for the HPLC separation is not compatible with on-line thermospray LC–MS, especially because of the use of non-volatile buffers in the mobile phase. In some favourable cases the non-volatile buffers can be replaced by volatile ones without influence on the separation. In other cases the buffers are merely present for reasons of reproducibility of the retention times and can be replaced easily by volatile ones for qualitative analysis. In many applications with mixtures, correspondence of the peaks obtained with UV or fluorescence detection and the peaks observed with MS detection is obligatory. Changes in the mobile phase are not attractive in such cases. Flow-rate incompatibility, which is also encountered in practice, can be easily overcome, either by using higher flow-rates through the analytical column, which is sometimes acceptable because of the high selectivity of the mass spectrometer, or by post-column addition of buffer[20]. In general optimization for maximum intensity with direct FIA injections of (complex) mixtures can be considered as well. This approach may give some indication of the influence of the vaporizer temperature and repeller potential for some major compounds in the mixture. The highly analyte-dependent response has probably to be accepted as a fact in the analysis of complex mixtures.

The optimization strategies are more useful and applicable in quantitative analysis, especially in target compound analysis. In order to obtain the highest sensitivity and the lowest detection limits the thermospray MS system has to be optimized for each compound or group of compounds along the lines drawn in the previous sections of this paper. This optimization has to be repeated before every experimental series, because of the unpredictable influence of contamination and vaporizer condition, or even better, isotopically labelled internal standards should be used.

For some compounds the pH of the mobile phase might be an important parameter as well, because it appears that it is not only the gas-phase ion–molecule reactions that are of importance in thermospray buffer ionization but the solvent chemistry as well[21–23]. Some systematic studies on the influence of the pH of the mobile phase and the pK_a values of the analytes on the analyte signals have been described[21,24,25], but the results have been ambiguous. Systematic pH variations of the mobile phase are currently under investigation in our laboratory, and the results will be reported in due course.

CONCLUSIONS

Various experimental parameters influencing thermospray buffer ionization have been investigated systematically and as a result optimization strategies are suggested. Extensive optimization is not always very useful and in many cases, *e.g.* when dealing with unknown compounds, optimization for a certain analyte is not possible at all. For these cases some general guidelines for optimization are given.

REFERENCES

1 C. R. Blakley and M. L. Vestal, *Anal. Chem.*, 55 (1983) 750.
2 Th. R. Covey, E. D. Lee, A. P. Bruins and J. D. Henion, *Anal. Chem.*, 58 (1986) 1451A.
3 R. D. Voyksner and C. A. Haney, *Anal. Chem.*, 57 (1985) 991.
4 C. Lindberg and J. Paulson, *J. Chromatogr.*, 394 (1987) 117.
5 F. A. Bencsath and F. H. Field, *Anal. Chem.*, 60 (1988) 1323.

6 M. A. Baldwin, M. E. Harrison and G. J. Langley, presented at the *5th Symposium on Liquid Chromatography–Mass Spectrometry, Freiburg, November 2–4, 1988.*
7 R. H. Robins and F. W. Crow, *Rapid Commun. Mass Spectrom.*, 2 (1988) 30.
8 M. L. Vestal and G. J. Fergusson, *Anal. Chem.*, 57 (1985) 2373.
9 J. A. Koropchak and H. Aryamanya-Mugisha, *Anal. Chem.*, 60 (1988) 1838.
10 M. L. Vestal, presented at the *5th Symposium on Liquid Chromatography–Mass Spectrometry, Freiburg, November 2–4, 1988.*
11 C. H. Vestal, G. J. Fergusson and M. L. Vestal, *Int. J. Mass Spectrom. Ion Proc.*, 70 (1986) 185.
12 W. Genuit and H. van Binsbergen, presented at the *5th Symposium on Liquid Chromatography–Mass Spectrometry, Freiburg, November 2–4, 1988.*
13 M. M. Siegel, R. K. Isensee and D. J. Beck, *Anal. Chem.*, 59 (1987) 989.
14 W. H. McFadden and S. A. Lammert, *J. Chromatogr.*, 385 (1987) 201.
15 W. G. Taylor and W. A. Remers, *Tetrahedron Lett.*, 39 (1974) 3483.
16 C. E. M. Heeremans, R. A. M. van der Hoeven, W. M. A. Niessen, U. R. Tjaden and J. van der Greef, *Adv. Mass Spectrom.*, 11 (1989) in press.
17 C. E. M. Heeremans, R. A. M. van der Hoeven, W. M. A. Niessen, U. R. Tjaden, G. F. LaVos and J. van der Greef, *Biomed. Environ. Mass Spectrom.*, 17 (1988) 377.
18 C. E. M. Heeremans, R. A. M. van der Hoeven, W. M. A. Niessen, U. R. Tjaden, J. van der Greef and N. M. M. Nibbering, in preparation.
19 C. E. M. Heeremans, R. A. M. van der Hoeven, W. M. A. Niessen, J. Vuik, R. H. de Vos and J. van der Greef, *J. Chromatogr.*, 472 (1989) 219.
20 R. D. Voyksner, J. T. Bursey and E. P. Pellizzari, *Anal. Chem.* 56 (1984) 1507.
21 T. R. Covey, A. P. Bruins and J. D. Henion, *Org. Mass Spectrom.*, 23 (1988) 178.
22 R. D. Voyksner, *Org. Mass Spectrom.*, 22 (1987) 513.
23 M. L. Vestal, *Mass Spectrom Rev.*, 2 (1983) 447.
24 C. E. Parker, R. W. Smith, S. J. Gaskell and M. M. Bursey, *Anal. Chem.*, 58 (1986) 513.
25 R. W. Smith, C. E. Parker, D. M. Johnson and M. M. Bursey, *J. Chromatogr.*, 394 (1987) 261.

Journal of Chromatography, 474 (1989) 163–173
Elsevier Science Publishers B.V., Amsterdam — Printed in The Netherlands

CHROM. 21 326

CHARACTERIZATION OF ORGANOPHOSPHORUS COMPOUNDS AND PHENYLUREA HERBICIDES BY POSITIVE AND NEGATIVE ION THERMOSPRAY LIQUID CHROMATOGRAPHY–MASS SPECTROMETRY

D. BARCELÓ* and J. ALBAIGÉS
Environmental Chemistry Department, CID-CSIC, c/Jorge Girona Salgado, 18-26, 08034 Barcelona (Spain)

SUMMARY

Positive-ion (PI) mode and negative-ion (NI) mode thermospray liquid chromatography–mass spectrometry (LC–MS) were used to characterize three different groups of environmentally significant compounds: organophosphorus pesticides, phenylurea herbicides and trialkyl phosphates. Reversed-phase LC was performed with acetonitrile–water (25:75, 50:50 and 75:25) and methanol–water (50:50) + 0.1 *M* ammonium acetate as eluents. By employing PI thermospray LC–MS, the base peak was $[M + NH_4]^+$ for all the studied compounds when the NI mode was used, [M + acetate]$^-$ was usually obtained as base peak for organophosphorus pesticides and phenylurea herbicides. Other adduct ions obtained in the NI mode corresponded to $[M - R]^-$, $[M + Cl]^-$, $[M - H]^-$, and to large cluster ions with the eluent.

Detection limits at low nanogram level were achieved for all the studied compounds in the PI mode. Sensitivities in the NI mode were much poorer for organophosphorus pesticides and phenylurea herbicides, and trialkyl phosphates were not detectable at the nanogram level. An application of PI thermospray LC–MS is illustrated for the determination of vamidothion, paraoxon-methyl and azinphos-methyl in a sediment sample.

INTRODUCTION

The use of liquid chromatography–mass spectrometry (LC–MS) is becoming most popular with the increasing number of LC–MS interfaces commercially available: moving belt, direct liquid introduction (DLI), thermospray, plasmaspray, thermabeam and monodisperse aerosol generated interface. This technique plays an important role in environmental organic analysis and, compared with gas chromatography–mass spectrometry (GC–MS), offers major advantages for analyzing thermally labile and/or highly polar compounds[1–3]. The thermospray interfacing technique is probably the most widely used, and typically involves the use of reversed-phase columns and volatile buffers such as ammonium acetate[4].

The work described here will demonstrate the usefulness of filament-on thermospray LC–MS in combination with postive-ion and negative-ion modes (PI and NI, respectively) for the characterization of three different groups of pollutants:

0021-9673/89/$03.50

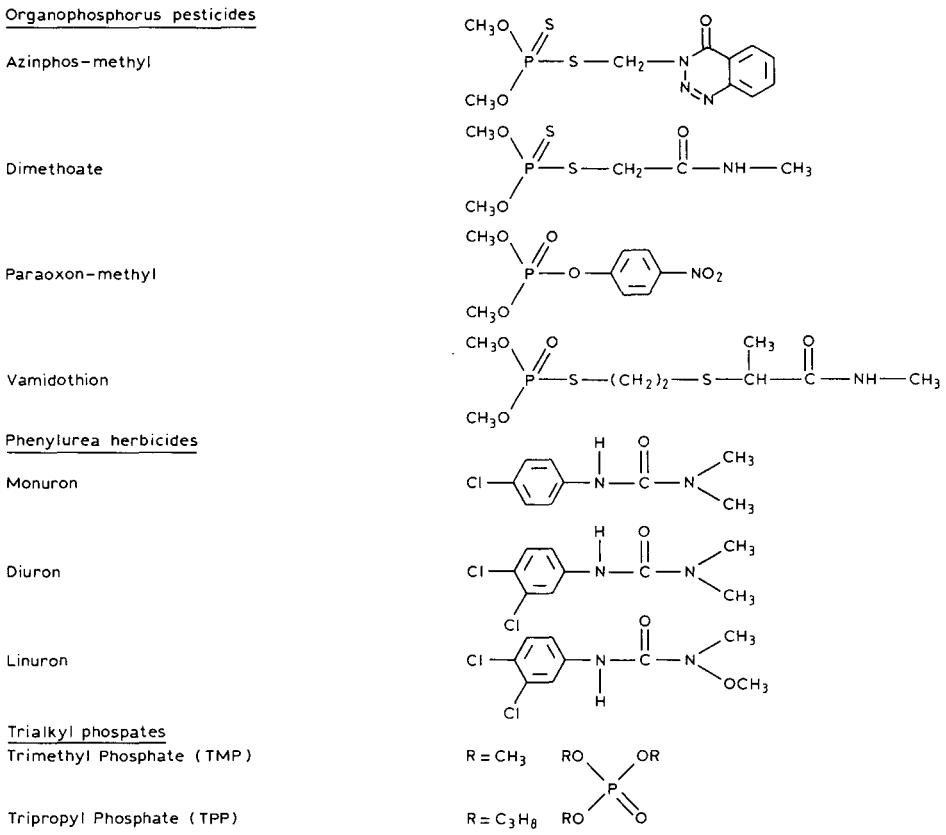

Fig. 1. Compounds analyzed.

organophosphorus pesticides, phenylurea herbicides and trialkyl phosphates (Fig. 1). Complementary information is obtained by both modes of operation. Such compounds exhibit difficulties when analysed by conventional GC because they either decompose, as do some thermally labile organophosphorus pesticides[5], or they need previous derivatization, for instance phenylurea herbicides[6].

As regards the trialkyl phosphates, although they can be analysed by GC–MS[7], there is no selective LC detector, and because of that a conventional GC thermionic detector has recently been developed[8]. The study of their fragmentation pattern is also of interest in comparison with compounds of similar structure, such as the organophosphorus pesticides, to achieve a better understanding of the thermospray LC–MS ionization behaviour.

EXPERIMENTAL

Materials

HPLC-grade water (Farmitalia Carlo Erba, Milan, Italy), methanol (Scharlau, Barcelona, Spain) and acetonitrile (Romil, Shepshed, U.K.) were passed through a 0.45-μm filter (Scharlau, Barcelona, Spain) before use. Analytical-reagent grade

ammonium acetate was obtained from Panreac (Barcelona, Spain), azinphos-methyl, dimethoate, diuron, linuron, monuron and vamidothion from Polyscience (Niles, IL, U.S.A.), paraoxon-methyl from Dr. Su. I. Ehrenstorfer (Augsburg, F.R.G.) and trimethyl phosphate (TMP) and tripropyl phosphate (TPP) from Kodak (Rochester, NY, U.S.A.).

Sample preparation

Pretreatment of a sediment sample was carried out by a method commonly used for pesticide residue analysis, and described in the literature[9]. In summary, 25 g of sediment (wet weight) after spiking with 0.2 ppm of vamidothion and azinphos-methyl and 0.1 ppm of paraoxon-methyl was placed in a Soxhlet apparatus and extracted for 4 h with 150 ml of methanol–water (9:1). Afterwards, the aqueous methanol extract was concentrated in a rotary evaporator to 2 ml.

Chromatographic conditions

Eluent delivery was provided by two Model 510 high-pressure pumps coupled with a Model 680 automated gradient controller (Waters Chromatography Division, Millipore, Bedford, MA, U.S.A.) and a Model 7125 injection valve with a 20 μl loop from Rheodyne (Cotati, CA, U.S.A.). Stainless-steel columns (30 × 0.40 cm I.D.) from Tracer Analítica (Barcelona, Spain) packed with 10-μm particle diameter Spherisorb ODS-2 (Merck, Darmstadt, F.R.G.) were used. Four different LC mobile phase compositions were tested: acetonitrile–water (25:75, 50:50 and 75:25) and methanol–water (50:50) + 0.1 *M* ammonium acetate, at flow-rates between 1 and 1.2 ml/min.

Mass spectrometric analysis

A Hewlett-Packard (Palo Alto, CA, U.S.A.) Model 5988A thermospray LC–MS quadrupole mass spectrometer and a Hewlett-Packard Model 35741B instrument for data acquisition and processing were employed. The thermospray temperatures were: stem: 100°C, tip: 178°C, vapour: 194°C and ion source 296°C, with the filament on. In all the experiments the filament-on mode (ionization by an electron beam emitted from a heated filament) was used. In this mode of operation conventional positive and negative chemical ionization can be carried out by using the vaporized mobile phase as the chemical ionization reagent gas[4].

RESULTS AND DISCUSSION

Organophosphorus pesticides

The analysed compounds were azinphos-methyl, dimethoate, paraoxon-methyl and vamidothion (Fig. 1). Mobile phase composition was generally acetonitrile–water (50:50) + 0.1 *M* ammonium acetate. In the PI mode the base peak was the $[M+NH_4]^+$ ion, which is the expected behaviour for this type of compounds in LC–MS[10] or in GC–MS with ammonia as the reagent gas[11]. The favoured formation of $[M+NH_4]^+$ indicates that the proton affinity of these compounds is slightly lower than that of ammonia (858 kJ/mol)[12]. Diazinon, with a pyrimidinyl group in its structure, has been reported as an exception to this rule, and showed $[M+H]^+$ as base peak[13]. The formation of $[M+H]^+$ reached relatively high values in some cases, up 50% for

vamidothion (see Fig. 2), which indicates an intermediate basicity for such compounds. Other adduct fragment ions are formed with the solvent, *e.g.*, $[M+(CH_3CN)NH_4]^+$ (Fig. 2).

Fragmentation for dimethoate was studied at higher water percentages in the eluent (Fig. 3). At 75% of water the base peak was still $[M+NH_4]^+$ but the intensity of $[M+H]^+$ increased up to 35%, as compared to a value of 10% when 50% of water was used[4]. It is worth mentioning that at this high water percentage the sensitivity was about 5 times higher than with the standard acetonitrile–water (50:50).

In the NI mode, similarly to a negative chemical ionization process, the ions detected are usually influenced by electron capture, dissociative electron capture and ion–molecule reactions in the source. These modes of negative ion formation can be due to impurities in the reagent gas, radical species in the ion source plasma and interactions with the ion source walls. Depending on the electron affinities, the bond strengths and the energy of the captured electron, dissociative electron capture reactions will take place together with electron capture reactions[14]. These three mechanisms have been observed for the different organophosphorus pesticides:

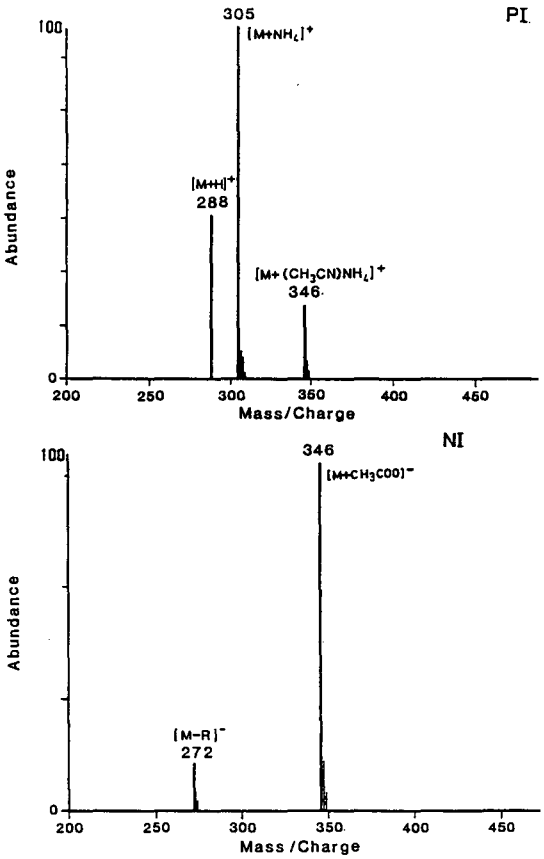

Fig. 2. Direct flow injection PI and NI thermospray MS spectra of vamidothion. Carrier stream, acetonitrile–water (50:50) + 0.1 *M* ammonium acetate; flow-rate, 1 ml/min; injection, 500 ng.

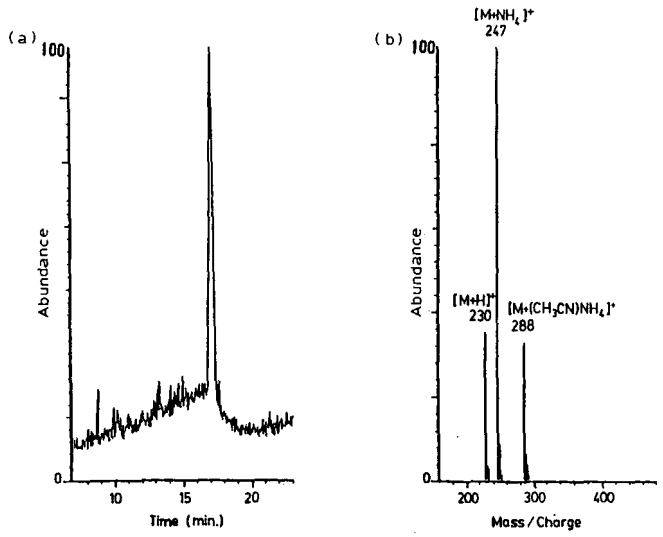

Fig. 3. (a) Reconstructed ion chromatogram and (b) mass spectrum in PI thermospray LC–MS of dimethoate. Carrier stream, acetonitrile–water (25:75) + 0.1 *M* ammonium acetate; flow-rate, 1 ml/min; injection, 500 ng.

electron capture $[M]^{\cdot-}$, dissociative electron capture $[M-R]^-$, where $R=CH_3$ or C_2H_5, and ion–molecule reactions $[M+CH_3COO]^-$ and/or $[M+Cl]^-$[4]. Formation of $[M+Cl]^-$ can be important for organophosphorus pesticides containing Cl in the molecule, such as trichlorfon[2]. The mass spectrum of vamidothion in the negative ion mode, by thermospray LC–MS, is shown in Fig. 2. The base peak corresponds to the anion attachment peak [M + acetate]$^-$, while $[M-R]^-$ is also obtained and corresponds to a typical fragment of organophosphorus pesticides as previously reported in GC–MS with negative chemical ionization[15] and in DLI LC–MS[2]. The most relevant conclusion as regards sensitivity is that the PI mode is three orders of magnitude more sensitive than the NI mode.

Phenylurea herbicides

First, it should be mentioned that in this case methanol was used in preference to acetonitrile as organic modifier because a gain of 1–2 orders of magnitude was observed when analysing compounds containing aryl halide rings[16]. Similarly to the previously mentioned compounds, the mass spectra of the studied herbicides, namely monuron and diuron, exhibit the $[M+NH_4]^+$ ion as the base peak in the PI mode (Fig. 4). Other phenylurea herbicides, *e.g.*, linuron, also exhibited the same feature[17–19], although the $[M+H]^+$ ion was the base peak for several phenylurea herbicides when volatile salt ionization (thermospray ionization) was employed[20]. Similarly to organophosphorus pesticides, the formation of $[M+NH_4]^+$ as base peak and of [M + H]$^+$, with relative intensity values close to 20%, indicates that the phenylurea herbicides containing aryl halide rings have proton affinities below that of ammonia (858 kJ/mol)[12]. When other LC–MS systems have been employed, such as DLI with a micro-LC[21], split[22] or moving belt[23], $[M+H]^+$ was always the base peak. Other fragment ions observed in Fig. 4 correspond to values higher than the molecular

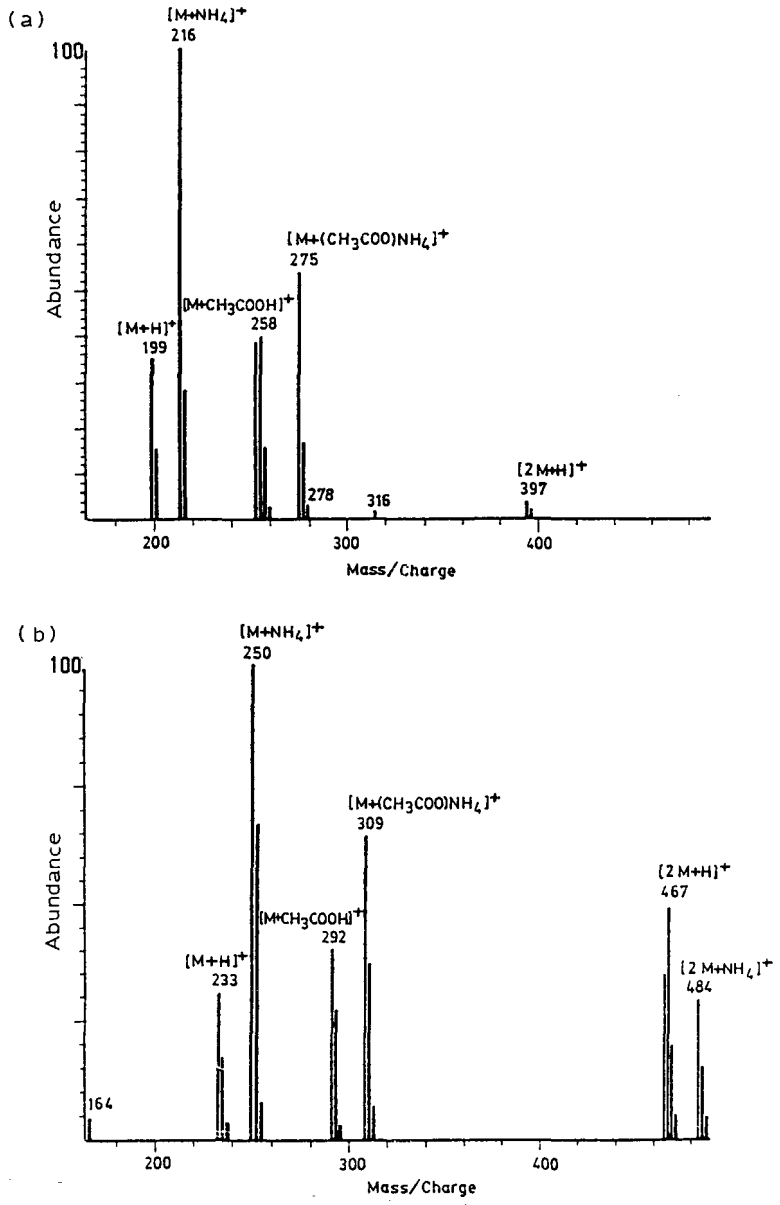

Fig. 4. Direct flow injection PI thermospray MS spectra of (a) monuron and (b) diuron. Carrier stream, methanol–water (50:50) + 0.1 *M* ammonium acetate; flow-rate, 1.2 ml/min; injection, 300 ng.

weight, and correspond to adducts with the ionizing additive, such as $[M + CH_3COOH]^+$ and $[M + (CH_3COOH)NH_4]^+$ and the dimers $[2M + H]^+$ and $[2M + NH_4]^+$.

In the NI mode, the base peak was always the anion attachment $[M + CH_3COO]^-$ ion, with a slight incidence of chloride attachment $[M + Cl]^-$ (Fig.

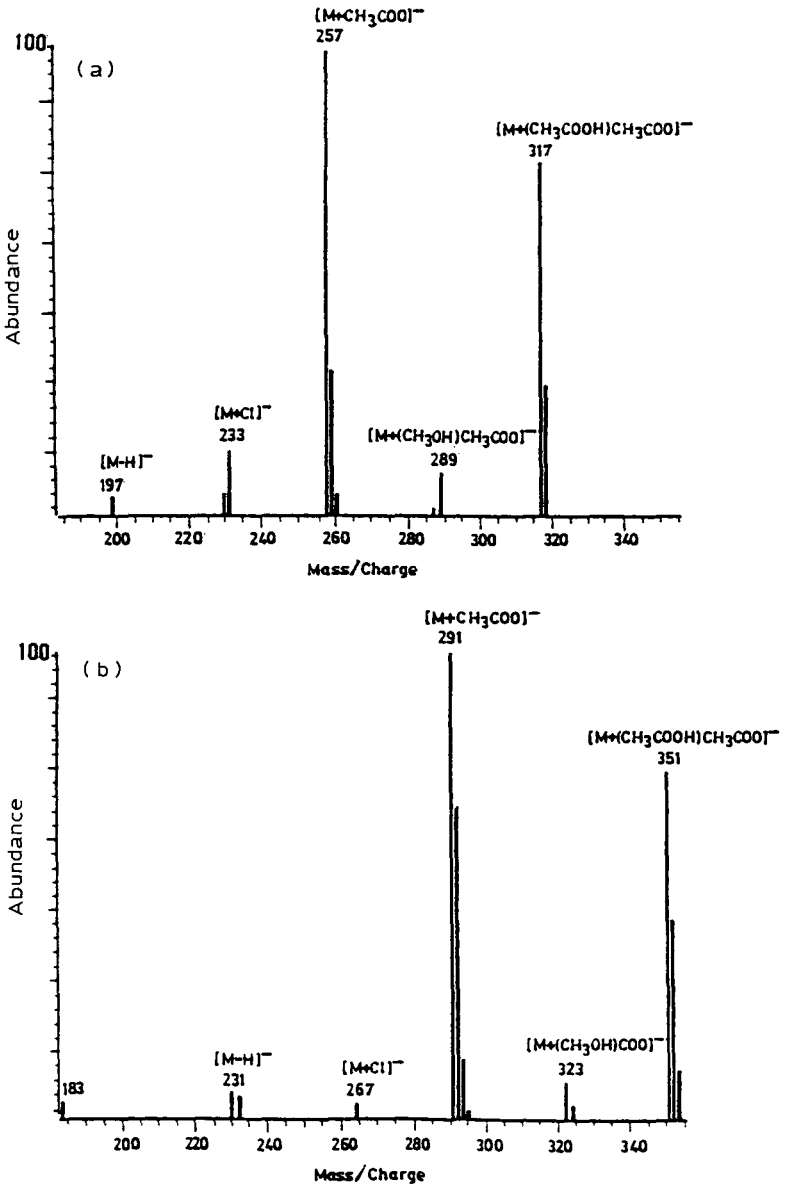

Fig. 5. Direct flow injection NI thermospray MS spectra of (a) monuron and (b) diuron under similar experimental conditions to Fig. 4.

5), as previously reported for linuron[18]. Consequently, there is no need to develop a post-column system for buffer addition in order to avoid degradation of the phenylurea herbicides[19]. To demonstrate that fact, the reconstructed ion chromatogram (RIC) in PI thermospray LC–MS for a mixture of monuron, diuron and linuron, obtained using methanol–water (50:50) + 0.1 *M* ammonium acetate, is shown in Fig.

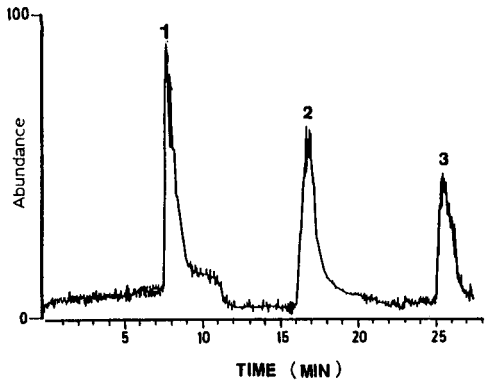

Fig. 6. Reconstructed ion chromatogram in thermospray LC–MS for a mixture of (1) monuron, (2) diuron and (3) linuron. Injected amount of each component, 300 ng. Column packing, 10 μm Spherisorb ODS-2; mobile phase, methanol–water (50:50) + 0.1 *M* ammonium acetate at a flow-rate of 1 ml/min; loop volume, 20 μl.

6. Another difference from the observations of Voyksner *et al.*[19] concerns the sensitivities in the NI mode. In our experiments, in NI thermospray LC–MS the phenylurea herbicides exhibit about 30% lower sensitivity than in the PI mode and not 4–5 orders of magnitude[19]. This large discrepancy can only be attributed to the different mode of ionization (filament-on in our experiments, *versus* filament-off ionization in their work).

Trialkyl phosphates

The PI thermospray LC–MS mass spectra of trimethyl phosphate and tripropyl phosphate obtained under conditions similar to those for organophosphorus pesticides are shown in Fig. 7. In both cases the $[M + NH_4]^+$ ion was the base peak and the $[M + H]^+$ ion was also observed. In contrast, in the literature[7] it has been reported that, when using GC–positive chemical ionization MS with ammonia as reagent gas for analyzing triethyl phosphate and tributyl phosphate, the $[M + H]^+$ ion was the base peak. This fact indicates a partial difference between ammonia chemical ionization and thermospray filament-on ionization, and conflicts with the similarities reported in the literature when comparing both ionization modes for different groups of pesticides[17]. In Fig. 7 it is also possible to observe the tendency to form adduct ions such as $[M + (CH_3CN)NH_4]^+$ and the dimer $[2M + H]^+$ ions at mass values higher than in ammonia chemical ionization.

In the NI thermospray LC–MS, the studied phosphates were not detected when 200 ng of each compound were injected. This fact could be due to their higher proton affinity than acetate ion preventing the detection by NI thermospray LC–MS[24].

Application to residue analysis

A sediment sample was spiked with three different organophosphorus pesticides: vamidothion (0.2 μg/g), azinphos-methyl (0.2 μg/g) and paraoxon-methyl (0.1 μg/g). Figure 8 shows the PI thermospray LC–MS chromatogram of the sediment after a pre-treatment procedure derived from that reported from Muir *et al.*[9]. The LC–MS

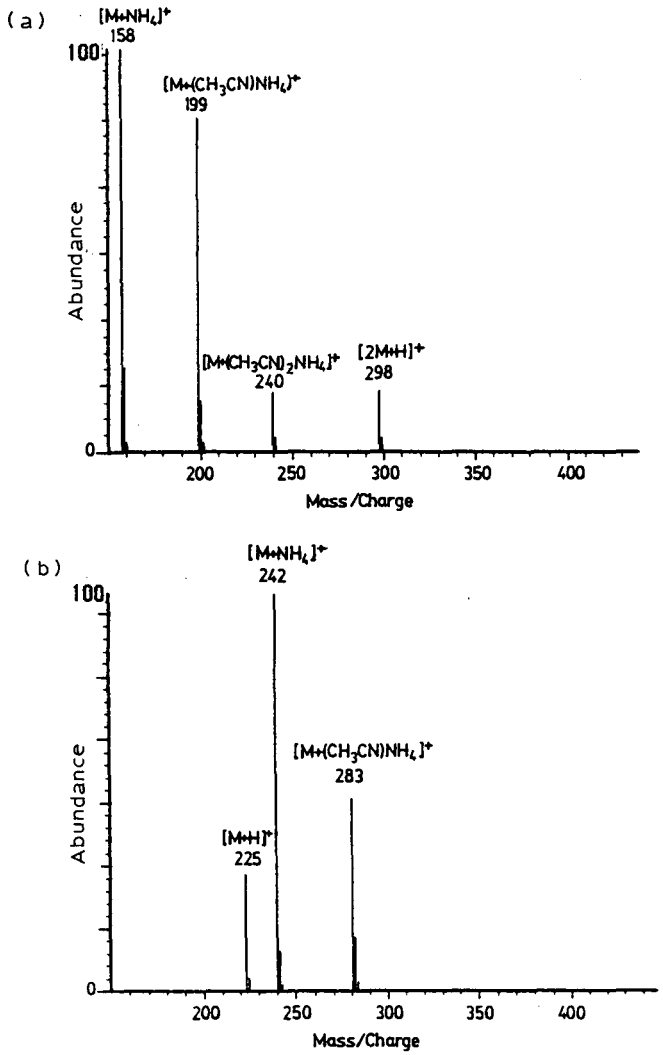

Fig. 7. Direct flow injection PI thermospray MS spectra of (a) trimethyl phosphate and (b) tripropyl phosphate under similar experimental conditions to Fig. 2.

was operated in the selected ion monitoring (SIM) mode, and three different m/z values per analyte were monitored, corresponding to the $[M + H]^+$, $[M + NH_4]^+$ and $[M + (CH_3CN)NH_4]^+$ ions. Vamidothion was monitored at m/z = 288, 305 and 346, azinphos-methyl at m/z = 318, 335 and 376, and paraoxon-methyl at m/z = 248, 265 and 306. As regards selectivity, only a small interference at the beginning of the chromatogram was noticed, and the sensitivity varied between 5 and 10 ng per compound (signal-to-noise ratio of 3–4). The thermospray LC–MS analyses were not performed in the NI mode of operation owing to its poor sensitivity as compared with the PI mode (about 3 orders of magnitude lower).

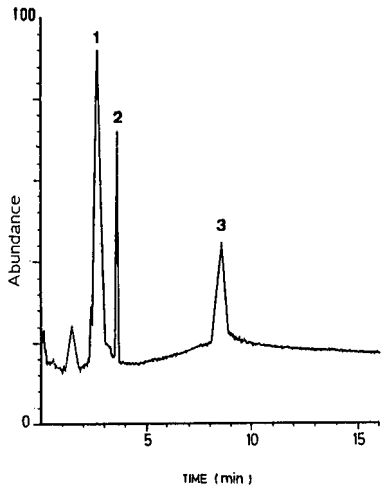

Fig. 8. Selected ion monitoring chromatogram in PI thermospray LC–MS of a sediment sample spiked with 0.2 ppm of vamidothion (peak 1), 0.1 ppm of paraoxon-methyl (peak 2) and 0.2 ppm of azinphos-methyl (peak 3). Injected amount: 5–10 ng. Column packing, 10-μm Spherisorb ODS-2; mobile phase, acetonitrile–water (75:25) + 0.1 *M* ammonium acetate at a flow-rate of 1 ml/min; loop volume, 20 μl.

CONCLUSION

The use of filament-on thermospray LC–MS in environmental analytical chemistry is a valuable technique with some points of similarity in the ionization process with other LC–MS approaches, such as DLI, and with ammonia chemical ionization GC–MS. By using two different modes of ionization in thermospray LC–MS, PI and NI modes, molecular weight information has been generally obtained with the formation of $[M+NH_4]^+$ and [M + acetate]$^-$ as base peaks, respectively. Sensitivities were always better in the PI mode than in the NI mode for the three groups of compounds studied. The lack of fragmentation is still a disadvantage in thermospray LC–MS when analyzing most environmental pollutants, for which an unequivocal identification is required.

ACKNOWLEDGEMENTS

Financial support was provided by the Consejo Superior de Investigaciones Científicas (C.S.I.C.), and Comision Asesora de Investigación Científica y Técnica (CAICYT), R. Alonso (C.S.I.C.) is thanked for technical assistance.

REFERENCES

1 K. Levsen, *Org. Mass Spectrom.*, 23 (1988) 406.
2 D. Barceló, F. A. Maris, R. B. Geerdink, R. W. Frei, G. J. De Jong and U. A. Th. Brinkman, *J. Chromatogr.*, 394 (1987) 65.
3 T. R. Covey, E. D. Lee, A. P. Bruins and J. D. Henion, *Anal. Chem.*, 58 (1986) 1441 A.
4 D. Barceló, *Biomed. Environ. Mass Spectrom.*, 17 (1988) 363.

5 S. M. Prinsloo and P. R. De Beer, *J. Assoc. Off. Anal. Chem.*, 68 (1985) 1100.
6 A. De Kok, M. Van Opstal, T. De Jong, B. Hoogcarspel, R. B. Geerdink, R. W. Frei and U. A. Th. Brinkman, *Int. J. Environ. Anal. Chem.*, 18 (1984) 101.
7 P. A. D'Agostino and L. R. Provost, *Biomed. Mass Spectrom.*, 12 (1986) 231.
8 D. Barceló, F. A. Maris, R. W. Frei, G. J. De Jong and U. A. Th. Brinkman, *Int. J. Environ. Anal. Chem.*, 30 (1987) 95.
9 D. C. G. Muir, N. P. Grift and J. Solomon, *J. Assoc. Off. Anal. Chem.*, 64 (1981) 79.
10 R. D. Voyksner and C. A. Haney, *Anal. Chem.*, 57 (1985) 991.
11 R. L. Holmstead and J. E. Casida, *J. Assoc. Off. Anal. Chem.*, 57 (1974) 1050.
12 A. G. Harrison, *Chemical Ionization Mass Spectrometry*, CRC Press, Boca Raton, FL, 1983, pp. 33–38.
13 A. Farran, J. De Pablo and D. Barceló, *J. Chromatogr.*, 455 (1988) 163.
14 E. A. Stemmler and R. A. Hites, *Biomed. Environ. Mass Spectrom.*, 17 (1988) 311.
15 H. J. Stan and G. Kellner, *Biomed. Mass Spectrom.*, 9 (1982) 483.
16 L. M. Shalaby, in J. D. Rosen (Editor), *Applications of New Mass Spectrometry Techniques in Pesticide Chemistry*, Wiley, New York, 1987, pp. 161–175.
17 R. D. Voyksner, in J. D. Rosen (Editor), *Applications of New Mass Spectrometry Techniques in Pesticide Chemistry*, Wiley, New York, 1987, pp. 146–160.
18 D. Barceló, *Chromatographia*, 25 (1988) 295.
19 R. D. Voyksner, J. T. Bursey and E. D. Pellizzari, *Anal. Chem.*, 56 (1984) 1507.
20 T. A. Bellar and W. L. Budde, *Anal. Chem.*, 60 (1988) 2076.
21 F. A. Maris, R. B. Geerdink, R. W. Frei and U. A. Th. Brinkman, *J. Chromatogr.*, 323 (1985) 113.
22 R. D. Voyksner, J. T. Bursey and E. D. Pellizzari, *J. Chromatogr.*, 312 (1984) 221.
23 T. Cairns, E. G. Siegmund and G. M. Doose, *Biomed. Mass Spectrom.*, 10 (1983) 24.
24 R. W. Smith, C. E. Parker, D. M. Johnson and M. M. Bursey, *J. Chromatogr.*, 394 (1987) 261.

Journal of Chromatography, 474 (1989) 175–180
Elsevier Science Publishers B.V., Amsterdam — Printed in The Netherlands

CHROM. 21 255

Note

Thermospray liquid chromatography–mass spectrometry of pesticides in river water using reversed-phase chromatography

I. HAMMOND*, K. MOORE, H. JAMES and C. WATTS
Water Research Centre, Henley Road, Medmenham, P.O. Box 16, Marlow, Buckinghamshire SL7 2HD (U.K.)

EEC Drinking Water Directive parameter 55, which concerns all pesticides, stipulates that individual pesticide levels in potable water must not exceed 100 ng l^{-1} and that the total level must be less than 500 ng l^{-1} [1].

By far the most highly-used class of pesticides is the herbicides in terms of both amounts applied and area treated. The two major classes of herbicides currently in use are the chlorophenoxy acids and the urons. Both classes of compound are sufficiently water-soluble and persistent to reach the aquatic environment and have been detected in surface, ground and drinking waters[2]. Chlorophenoxy acids are commonly analysed by gas chromatography–electron-capture detection (GC–ECD) or GC–mass spectrometry (MS) after derivatisation[3] but the analysis of the uron pesticides by GC–MS can be problematic in view of their thermal instability at the column temperatures typically used, and their relatively high polarity.

One potential approach to overcoming this problem whilst maintaining specificity of analysis reported the use of liquid chromatography–mass spectrometry (LC–MS) in conjunction with thermospray using a quadrupole mass spectrometer[4]. This study showed that carbamate and chlorophenoxy acid pesticides are amenable to analysis once the source conditions have been optimised and if an additional source of ionisation is used to complement the thermospray process. Spiked soil and lake water samples were analysed.

Our studies have concentrated on the use of thermospray LC–MS interfaced to a double-focusing magnetic sector instrument for the analysis of uron pesticides at environmentally-significant levels. The effects of varying source parameters have been investigated and optimised, and these conditions used to analyse a mixture of pesticides extracted from a river water sample.

EXPERIMENTAL

Mass spectra were obtained on a ZAB-1F (VG Analytical, Manchester, U.K.) mass spectrometer used in low-resolution mode for maximum sensitivity ($M/\Delta M$ typically less than 200). A 1090L liquid chromatograph (Hewlett-Packard, Winnersh, U.K.) was connected to the mass spectrometer via a thermospray interface (Vestec Corporation, Houston, TX, U.S.A.). Data was acquired into a Superincos Nova 4X data system (Finnigan MAT, Hemel Hempstead, U.K.).

0021-9673/89/$03.50

The heated thermospray source (Interion, Manchester, U.K.) was used in the discharge ionisation mode with a source block temperature of 250°C, tip temperature of 155°C and vapour temperature of 190°C. The spectrometer was scanned repetitively from *m/z* 110 to *m/z* 650 using a 2.5-s cycle time.

A mobile phase of methanol–aq. 0.1 *M* ammonium acetate (50:50, v/v) was filtered through a 2-μm membrane (Millipore, Bedford, MA, U.S.A.) and helium degassed. This mobile phase was used at a flow-rate of 0.75 ml min^{-1} during injection of the single pesticide standards.

Gradient elution for the fortified river water analyses was carried out using a linear programme of 40% methanol to 60% in 30 min and thereafter to 90% methanol in 10 min with aq. 0.1 *M* ammonium acetate as the secondary solvent system. The linear gradient programme for the water contamination analysis was from 30% methanol to 50% methanol in 5 min, held for 15 min, to 80% methanol in 15 min using the same flow-rate and secondary solvent as before. A reversed-phase S50DS1 25 cm × 0.49 cm column (Thames Chromatography, Maidenhead, U.K.) was used for all LC separations.

A standard pesticide solution was prepared containing metamitron, simazine, atrazine, chlortoluron, isoproturon and linuron at levels of 5 μg ml^{-1} in the eluent and this was used to fortify a 1-l river water sample to give a concentration of 5 μg l^{-1} per component. An unfortified sample was also collected to act as a blank.

The water samples were passed through 0.7-μm glass-fibre filters (Whatman, Maidstone, U.K.) and then C_{18} bonded-phase cartridges (Millipore). The cartridges were eluted using 2 ml of methanol (Rathburn Chemicals, Walkerburn, U.K.) and the eluate reduced to 1 ml under a stream of nitrogen. A 20-μl aliquot was injected onto the LC column, corresponding to 100 ng of each component on-column, assuming 100% recovery.

A dichloromethane extract derived from river water known to be contaminated with a uron pesticide was analysed to provide confirmation of pollutant identity. Previous work by GM–MS suggested that the pesticide was isoproturon present at a level of about 20 μg ml^{-1} in the final extract. A 20-μl aliquot was injected for analysis by thermospray LC–MS, corresponding to 400 ng of pesticide on-column.

RESULTS

The effects of changing source parameters were investigated using PEG 600. At higher block temperatures when using discharge-assisted thermospray the $[M+H]^+$ adduct was formed preferentially, as has already been shown in other laboratories[5]. Using filament-assisted thermospray the $[M+NH_4]^+$ adduct predominated. Varying the tip temperature did not change the appearance of the spectra although a temperature of 155°C gave an optimum ion yield for the chosen mobile phase composition[6].

The result of varying the amount of analyte is illustrated in Figs. 1 and 2. The spectra consist of an $[M+H]^+$ adduct (*m/z* 203) and a fragment ion due to the loss of methyl from the protonated species ($[M+H-CH_3]^+\cdot$, *m/z* 188). Such losses have been reported previously in the LC–MS analysis of explosives ($[M+NH_4-CH_3]^+\cdot$[7] and pesticides ($[M+H-CH_3]^+\cdot$[8]). We have observed fragment ions in the TSP spectra of several pesticides[6], *e.g.* loss of chlorine from atrazine ($[M+H-Cl]^+\cdot$, *m/z* 181), simazine ($[M+H-Cl]^+\cdot$, *m/z* 167) and mecoprop ($[M+NH_4-ce-Cl]^+\cdot$, *m/z* 197),

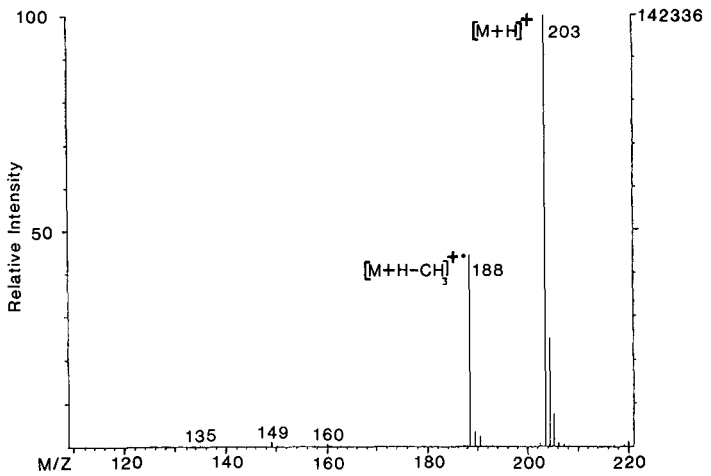

Fig. 1. Thermospray LC–MS spectrum of metamitron at 0.2 mg ml^{-1} in mobile phase (methanol–0.1 *M* ammonium acetate, 50:50 v/v,); flow-rate 0.75 ml min^{-1}; 20 μl injection.

loss of bromine from bromoxynil ($[M + NH_4 - Br]^{+\cdot}$, *m/z* 216). loss of parachlorophenate from triadimefon ($[M + H - ClPhO]^{+\cdot}$, *m/z* 167) and losses from methiocarb ($[M + NH_4 - CH_3]^{+\cdot}$, *m/z* 228; $[M + NH_4 - CH_3S]^{+\cdot}$, *m/z* 197; $[M + H - CH_3S]^{+\cdot}$, *m/z* 179).

For all pesticides investigated the relative abundances of fragment ions were greatest at the lowest concentrations of analyte. Fig. 2 illustrates that a tenfold reduction in the amount of metamitron produced a fivefold increase in the $[M + H - CH_3]^{+\cdot}/[M + H]^+$ ratio. Another typical example of this effect was observed for dicamba in which chlorine was lost from the molecular adduct ion, as has been reported previously[8]. The relative intensities observed were, for 40 μg injected:

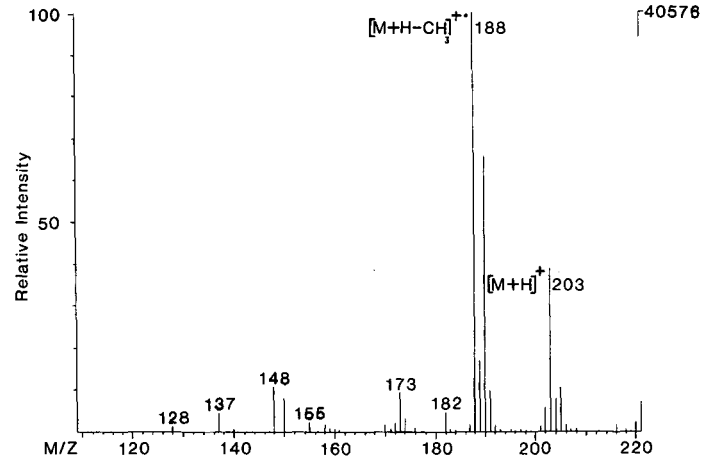

Fig. 2. Thermospray LC–MS spectrum of metamitron at 0.02 mg ml^{-1} in mobile phase, conditions as in Fig. 1.

$[M+NH_4]^+$, *m/z* 238 (60%); $[M+NH_4-Cl]^{+\cdot}$, *m/z* 203 (100%); $[M+H-Cl]^{+\cdot}$, *m/z* 186 (8%); $[M+NH_4{}^-2Cl]^+$, *m/z* 168 (19%); $[M+H-2Cl]^+$, *m/z* 151 (1%); and for 400 ng injected: $[M+NH_4]^+$ (3%); $[M+NH_4-Cl]^{+\cdot}$ (26%); $[M+NH_4-2Cl]^+$ (100%); $[M+H-2Cl]^+$ (41%). The reason for this change with changing concentration is unknown, although similar losses of chlorine have been reported to result from pyrolysis in the TSP probe[9].

Fig. 3 shows the selected mass chromatograms obtained after the injection of an extract from a spiked river water. The chromatograms correspond to metamitron ($[M+H]^+$, *m/z* 203), simazine ($[M+H]^+$, *m/z* 202; $[M+H-Cl]^{+\cdot}$, *m/z* 167), atrazine ($[M+H]^+$, *m/z* 216; $[M+H-Cl]^{+\cdot}$, *m/z* 181), chlortoluron ($[M+H]^+$, *m/z* 213, 215), isoproturon ($[M+H]^+$, *m/z* 207) and linuron ($[M+NH_4]^+$, *m/z* 266; $[M+H]^+$, *m/z* 249; *m/z* 215 uncharacterised). An unidentified component exhibiting an *m/z* 167 ion was also observed at scan 605. The spectra compared favourably with previously-reported data[9,10,11] although we did not observe solvent adduct ions.

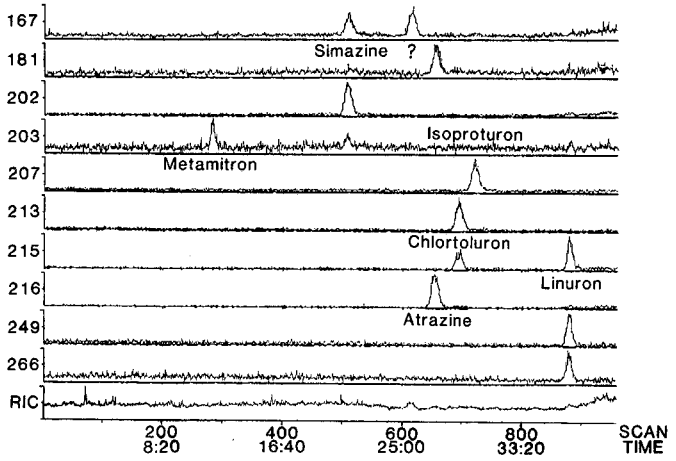

Fig. 3. Thermospray LC–MS chromatogram of 1-l river water extract spiked at 5 $\mu g\ l^{-1}$ with each pesticide component (methanol–0.1 *M* ammonium acetate (40:60) to (60:40) in 30 min to (90:10) in 10 min. Flow-rate 0.75 ml min^{-1}; 20 μl injection).

Mass chromatograms of similar intensity were obtained for the injection of the standard solution used to spike the water sample and indicated an ~80% recovery of the pesticides from the fortified water. Injection of the unfortified riverwater extract produced mass chromatograms which indicated the presence of low levels (<3 ng on-column; equivalent to about 150 ng l^{-1} in the original sample) of chlortoluron, atrazine, linuron and isoproturon although there was insufficient material to obtain recognisable full-scan spectra (approximately 20 ng on-column was necessary to achieve this).

Fig. 4 shows a mass chromatogram obtained from the analysis of a river water extract thought to contain high levels of isoproturon. The retention-time of a major peak exhibiting an ion of *m/z* 207 corresponded to that of an isoproturon standard (Greyhound Chemicals, Birkenhead, U.K.) and gave a similar mass spectrum

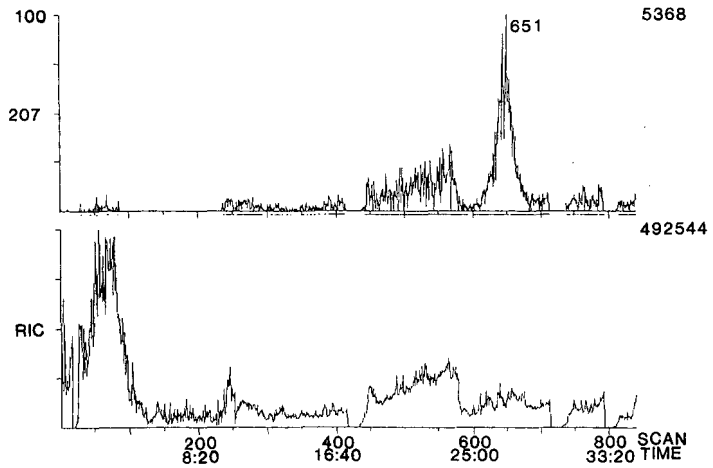

Fig. 4. Thermospray LC–MS chromatogram of 2-l river water extract in dichloromethane (methanol–0.1 *M* ammonium acetate (30:70) to (50:50) in 5 min, held 15 min, to (80:20) in 15 min; flow-rate 0.75 ml min^{-1}; 20 μl injection).

($[M + H]^+$, *m/z* 207). This provided confirmation of the suspected herbicide, isoproturon, in the river water extract.

CONCLUSIONS

The optimisation of source conditions and their effects on spectral appearance for a magnetic instrument have been found to be similar to previously published results obtained using quadrupole instruments. However, it seems unlikely that useful library searching can be performed because of the variation in relative intensities of fragments and molecular ions with analyte concentration. This has not been observed with quadrupole instruments and may be due to the high source potential involved (3 kV), partial pyrolysis of the sample, or a combination of these effects.

Application of LC–MS to analysis of riverwater extracts showed the absence of problematic interferences and allowed the detection of pesticides at levels of a few nanograms on-column. Concentration of extracts of 1-l samples to 0.1 ml and the injection of 20 μl onto the column should enable the detection of pesticides at concentrations equivalent to 10 ng l^{-1} in water samples by the use of TSP in selected-ion-monitoring mode. Due to the apparent changes in the relative intensities of TSP–MS ions with concentration, calibration curves obtained for SIM analysis will probably be non-linear leading to consequent problems with the precision of the analysis.

REFERENCES

1 *EC Directive Relating to the Quality of Water Intended for Human Consumption (80/778/EEC)*, Circular 20/82, DoE, Her Majesty's Stationary Office, London, 1982, p. 19.

2 Standing Committee of Analysts, *Chlorophenoxy Acidic Herbicides, Trichlorobenzoic Acid, Chlorophenols, Triazines and Glyphosate in Water*, Methods for the Examination of Water and Associated Materials, DoE, National Water Council, London, 1985.

3 D. Gurka, F. Shore and S. Pan, *J. Assoc. Off. Anal. Chem.*, 70 (1987) 889.
4 L. Shalaby, in J. Rosen (Editor), *Applications of New Mass Spectrometry Techniques in Pesticide Chemistry*, Wiley, New York, 1987, Ch. 12, p. 161.
5 F. Artigas and E. Gelpí, *J. Chromatogr.*, 394 (1987) 123.
6 I. Hammond, H. James and C. Watts, *The Application of Liquid Chromatography/Mass Spectrometry to the Analysis of River and Drinking Waters*, WRc Environment, Medmenham, PRU 1874-M, 1988, p. 10.
7 R. Voyksner and J. Yinon, *J. Chromatogr.*, 354 (1986) 393.
8 R. Voyksner, J. Bursey and E. Pellizzari, *J. Chromatogr.*, 312 (1984) 221.
9 D. Barceló, *Chromatographia*, 25 (1988) 295.
10 R. Voyksner, in J. Rosen (Editor), *Applications of New Mass Spectrometry Techniques in Pesticide Chemistry*, Wiley, New York, 1987, Ch. 11, p. 146.
11 R. Voyksner, W. McFadden and S. Lammert, in J. Rosen (Editor), *Applications of New Mass Spectrometry Techniques in Pesticide Chemistry*, Wiley, New York, 1987, Ch. 17, p. 247.

Journal of Chromatography, 474 (1989) 181–185
Elsevier Science Publishers B.V., Amsterdam — Printed in The Netherlands

CHROM. 21 166

Note

Thermospray liquid chromatographic–mass spectrometric analysis of *Catharanthus* alkaloids

SEPPO AURIOLA*, VELI-PEKKA RANTA, TOIVO NAARANLAHTI and SEPPO P. LAPINJOKI
Department of Pharmaceutical Chemistry, University of Kuopio, P.O. Box 6, SF-70211 Kuopio (Finland)

Catharanthus roseus (L.) G. Don is a source of the medicinally important bis-indole alkaloids vinblastine and vincristine (Fig. 1)[1]. The biosynthesis of these compounds is studied actively in order to produce them in cell or tissue cultures[2,3]. In this connection, specific and reliable analytical methods are necessary when the levels of metabolic intermediates and products are determined. High-performance liquid chromatography (HPLC) in combination with UV or fluorescence detection is widely used for this purpose[4,5], although the specificity of these techniques is often questionable. The purity of separated peaks may be evaluated by scanning their UV spectra[6,7] and mass spectral analysis of collected peaks using chemical[8] or electronic[9] ionization has been used for structure elucidation and identification.

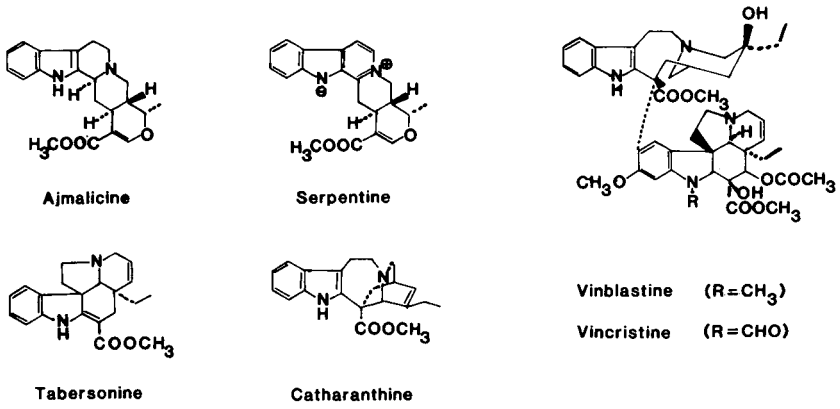

Fig. 1. Chemical structures of four monomeric and two dimeric indole alkaloids from *C. roseus*.

Thermospray liquid chromatography–mass spectrometry (LC–MS) offers a possibility to analyze non-volatile and polar compounds directly without derivatization[10–12]. In this study, this technique was utilized to check the specificity of an HPLC method in which indole alkaloids of *C. roseus* were analyzed using electrochemical and UV detection. Monitoring the MH^+ ions of tryptamine, ajmalicine, serpentine, catharanthine and tabersonine was used to reveal their presence in cell suspension samples. Thermospray mass spectral fragmentation of a bis-indole alkaloid, vinblastine, was also studied.

0021-9673/89/$03.50

EXPERIMENTAL

Chemicals

Catharanthine hydrochloride and tabersonine were generously provided by Professor W. G. W. Kurz (Plant Biotecnology Institute, National Research Council, Saskatoon, Canada). Serpentine tartrate was obtained from ICN, K&K Labs. (New York, NY, U.S.A.), ajmalicine hydrochloride and vinblastine sulphate from Sigma (St. Louis, MO, U.S.A.) and tryptamine from Aldrich Chemie (Steinheim, F.R.G.).

HPLC conditions

A Beckman 342 gradient liquid chromatograph equipped with two Beckman solvent delivery modules, a Beckman 420 controller a Beckman 165 variable-wavelength detector (at 280 nm) and an Altex 210 A injector (20-μl loop) were used. The results were recorded with a Goerz Se 120 recorder. A μBondapak C_{18} (30 cm × 3.9 mm I.D., 10 μm) reversed-phase column (Waters Assoc., Milford, MA, U.S.A.) was used. The isocratic solvent system was 0.1 *M* ammonium acetate (pH 7.2)–acetonitrile (51:49). The flow-rate was set to 1.0 ml/min.

Chromatographic conditions for thermospray LC–MS were as described above, but a Kontron 420 HPLC pump was used for solvent delivery and the samples were injected with a Rheodyne 7125 injector (loop volume 20 μl).

Mass spectrometry

The thermospray system used was a VG thermospray-plasmaspray probe coupled to a VG Trio-2 quadrupole mass spectrometer. The instrument was operated in the thermospray ionization mode. The thermospray probe temperature was 220°C, the ion source temperature was 230°C, the repeller voltage was 50 V and other ion source conditions were optimized daily.

Sample preparation

Samples from freeze-dried cell suspensions of *C. roseus* were extracted and purified as described before[7,13].

RESULTS AND DISCUSSION

A good chromatographic separation for the alkaloids of interest was achieved in 18 min with isocratic elution (Fig. 2) when 0.1 *M* ammonium acetate was used as a buffer in the mobile phase. Ammonium acetate offers the best sensitivity in acetonitrile–water and methanol–water solutions in thermospray analysis[11], and the NH_4^+ decreases polar interactions by masking free silanol groups on the bonded stationary phase[14].

The thermospray mass spectrum of ajmalicine (Fig. 3) shows MH^+ (*m/z* 353) as the base peak and no important fragment or ammonium adduct ions are present. Thermospray mass spectra of the other monomeric indole alkaloids examined were of the same type. The mass spectrum of a dimeric alkaloid, vinblastine (found only in intact plants), was more informative, containing a protonated molecular ion (*m/z* 811) and abundant fragment ions (Fig. 3). The loss of water from the parent ion gave the peak at *m/z* 793 ($MH^+ - H_2O$). Other peaks were observed at *m/z* 779 (MH^+ –

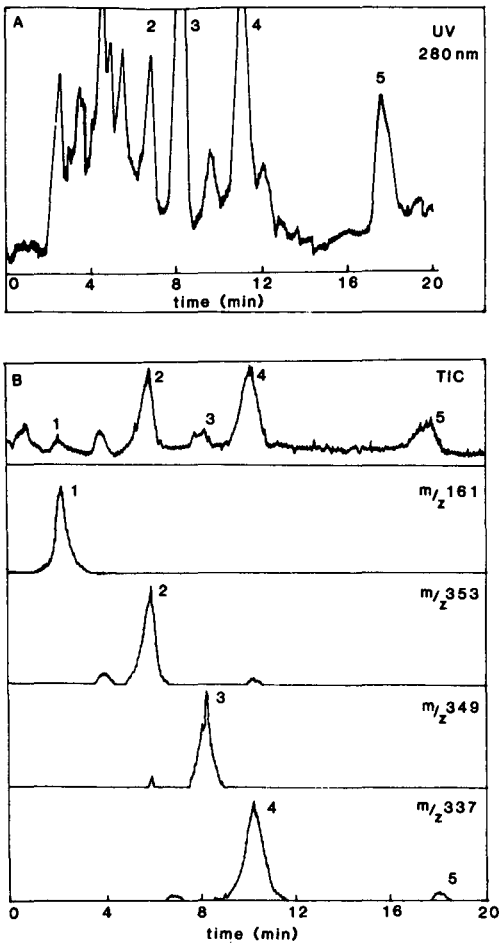

Fig. 2. HPLC UV chromatogram (A) and thermospray mass chromatograms (B) of a cell suspension sample of *C. roseus*. Compounds monitored: 1 = tryptamine; 2 = ajmalicine; 3 = serpentine; 4 = catharanthine; 5 = tabersonine. Column: 30 cm × 3.9 mm μBondapak C_{18}. Eluent: 51% acetonitrile in 0.1 *M* ammonium acetate (pH 7.2); flow-rate, 1.0 ml/min.

CH_3OH) and 753 ($MH^+ - COOCH_2$). These three fragment ions were also present in the ammonia desorption chemical ionization (DCI) spectrum published by Kuntebommanahalli *et al.*[8]. In the thermospray spectrum there also exist various other ions absent in the ammonia DCI spectrum. Of these peaks, that at *m/z* 457 might originate from the vindoline moiety (MW 456).

The peak observed at the retention time of tabersonine (18 min) with UV and electrochemical detection proved to be a mixture of two or more compounds when analyzed with thermospray LC–MS. Tabersonine was only a minor component in that peak (Fig. 2). Serpentine was not detected with electrochemical oxidation, but was easily monitored with the thermospray technique (Fig. 2).

Because of the absence of fragment ions in the thermospray mass spectra of

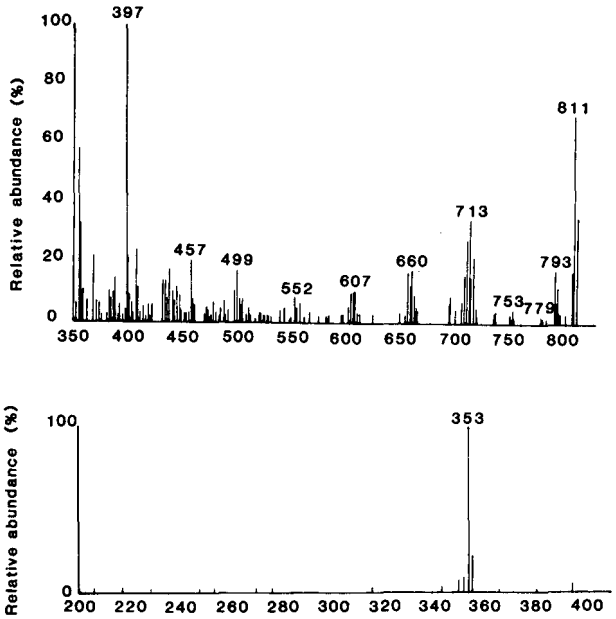

Fig. 3. Direct flow injection thermospray mass spectra of vinblastine (MH^+ 811) and ajmalicine (MH^+ 353). Eluent as in Fig. 2.

monomeric indole alkaloids, more informative ionization techniques are needed when structures of unknown compounds are elucidated. These include techniques described by McFadden and Lammert[15], *i.e.*, filament on or discharge ionization and collision-induced dissociation (CID) with the thermospray repeller or CID with MS–MS mass spectrometer.

However, single-ion monitoring of the prominent MH^+ of monomeric alkaloids is a very suitable method for screening these secondary metabolites from cultured cells of *C. roseus*. The thermospray method was more sensitive than our HPLC assay with UV detection[7], the limit of detection being 4 ng per injection for each alkaloid.

ACKNOWLEDGEMENTS

This work was supported by the Research Foundation of Kemira Oy (Helsinki, Finland), the North-Savo Cultural Foundation (Kuopio, Finland), the Association of Finnish Chemical Societies (Helsinki, Finland) and the Technology Development Centre (Helsinki, Finland). The skilful technical assistance of Mr. Jukka Knuutinen is gratefully acknowledged.

REFERENCES

1. W. I. Taylor and N. R. Farnsworth, *The Catharanthus Alkaloids: Botany, Chemistry, Pharmacology and Clinical Use*, Marcel Dekker, New York, 1975, pp. 1–323.

2 J. P. Kutney, B. Averyn, L. S. L. Choi, T. Honda, P. Kolodziejczyk, N. G. Lewis, T. Sato, S. K. Sleigh, K. L. Stuart, B. R. Worth, W. G. W. Kurz, K. B. Chatson and F. Constabel, *Tedrahedron,* 39 (1983) 3781.
3 V. DeLuca and A. J. Cutler, *Plant Physiol.,* 85 (1987) 1099.
4 J.-P. Renaudin, *Physiol. Veg.,* 23 (1985) 381.
5 W. Kohl, B. Witte and G. Höfle, *Planta Med.,* 47 (1983) 177.
6 A. F. Fell, H. P. Scott, R. Gill and A. C. Moffat, *J. Chromatogr.,* 273 (1983) 3.
7 T. Naaranlahti, M. Nordström, M. Lounasmaa and A. Huhtikangas, *J. Chromatogr.,* 410 (1987) 488.
8 N. Kuntebommanahalli, N. Thimmaiah and V. Sagar Sethi, *Cancer Res.,* 45 (1985) 5382.
9 W. Kohl, B. Witte and G. Höfle, *Z. Naturforsch., Teil B,* 36 (1981) 1153.
10 T. R. Covey, E. D. Lee, A. P. Bruins and J. D. Henion, *Anal. Chem.,* 58 (1986) 1451A.
11 R. D. Voyksner and C. A. Haney, *Anal. Chem.,* 57 (1985) 991.
12 D. A. Catlow, *J. Chromatogr.,* 323 (1985) 163.
13 P. Morris, A. H. Scragg, N. J. Smart and A. Stafford, in R. A. Dixon (Editor), *Plant Cell Culture; a Practical Approach,* IRL Press, Oxford, 1985, pp. 127–167.
14 C. K. Lim and T. J. Peters, *J. Chromatogr.,* 316 (1984) 397.
15 W. H. McFadden and S. A. Lammert, *J. Chromatogr.,* 385 (1987) 201.

Journal of Chromatography, 474 (1989) 187–195
Elsevier Science Publishers B.V., Amsterdam — Printed in The Netherlands

CHROM. 21 412

HIGH-PERFORMANCE LIQUID CHROMATOGRAPHY WITH THERMOSPRAY MASS SPECTROMETRIC DETECTION OF α-CARBOXYAMIDO AMINO ACIDS[a]

ANTHONY M. TRESTON

NCI-Navy Medical Oncology Branch, Clinical Oncology Program, Division of Cancer Therapy, National Cancer Institute, National Institutes of Health, Bethesda, MD 20892 (U.S.A.)

DOMENICK VICCHIO

Section for Metabolic Analysis and Mass Spectrometry, Laboratory of Theoretical and Physical Biology, National Institute of Child Health and Human Development, National Institutes of Health, Bethesda, MD 20892 (U.S.A.)

JAMES L. MULSHINE

NCI-Navy Medical Oncology Branch, Clinical Oncology Program, Division of Cancer Therapy, National Cancer Institute, National Institutes of Health, Bethesda, MD 20892 (U.S.A.)

and

ALFRED L. YERGEY*

Section for Metabolic Analysis and Mass Spectrometry, Laboratory of Theoretical and Physical Biology, National Institute of Child Health and Human Development, Bldg 10, Rm 6C208, National Institutes of Health, Bethesda, MD 20892 (U.S.A.)

SUMMARY

A method is described for high-performance liquid chromatographic separation of underivatized α-carboxyamido amino acids, with sensitive detection by thermospray mass spectrometry. The unit mass difference between α-carboxyamido (amidated) amino acids and their free-carboxyl analogs allows mass spectrometric detection of amidated amino acids in the presence of the usual excess of non-amidated amino acids found in samples from biological sources. Separation is carried out on an exhaustively end-capped octadecylsilyl reversed-phase support with an aqueous mobile phase containing 10 m*M* ammonium *p*-toluenesulfonate (pH 3.5) and 0–30% methanol. Using these conditions, the α-amidated amino acids are clearly separated from their analogous free-carboxyl derivatives. Ammonium formate is added post-column to provide the necessary ions for efficient thermospray detection of the eluting amino acids. Detection of the α-amidated amino acids at *ca.* 1 pmol on-column is achieved in the single ion monitoring mode. This method allows unequivocal identification of α-carboxyamido amino acids enzymatically released from amidated peptides, without the necessity for any extraction of derivatization procedures.

[a] The opinions and assertions contained herein are the private views of the authors and are not to be construed as official or reflecting the views of the Department of the Navy, the Department of Defense or the Department of Health and Human Services.

0021-9673/89/$03.50

INTRODUCTION

Many biologically active peptides, including most peptide hormones, contain amino acids which have been post-translationally modified. These modifications are often essential for complete biological activity, and it is recognized that identification of such modifications on a novel peptide suggests a hormonal function for that peptide. The most common post-translational modification of peptides is the occurrence of an α-carboxyamido moiety on the C-terminal amino acid, instead of the usual free α-carboxylic acid, *i.e.* an amidated amino acid. This modification has been identified on approximately half of the known mammalian gastrointestinal and neuroendocrine peptide hormones (*e.g.* gastrin, cholecystokinin, vasopressin and oxytocin) as well as many peptide hormones from other phyla (for instance frog bombesin, scorpion venom peptides, crustacean red pigment concentrating hormone, and insect adipokinetic hormones). Identification of peptides with C-terminal amidated amino acids has been used as a criterion for screening for novel peptide hormones[1], which has led to the discovery of novel biologically active peptides such as neuropeptide Y and pancreastatin.

The original method described for identification of amidated peptides in peptide mixtures involves enzymatic hydrolysis to liberate C-terminal amidated amino acids, unmodified amino acids, and small peptides, followed by derivatization of the mixture to yield N-dansylated derivatives, then a "specific" extraction of the dansyl α-amidated amino acids, and identification by thin-layer chromatography (TLC)[1]. This method produces a complex mixture of amino acid and peptide derivatives, which must be separated before identification of any α-amidated amino acids present. The alkaline/organic extraction method used biases the procedure towards identification of amino acid amides with non-polar side-chains, and the two-dimensional TLC detection is limited in capacity and sensitivity as well as being very labor-intensive. Modifications to the detection method using high-performance liquid chromatographic (HPLC) separation and detection have been reported, using phenylthiocarbamoyl[2,3] or dansyl[4] derivatives, but these still require extraction and derivatization steps. The problems with these methods, including inability to detect amides of polar amino acids and under- and over-derivatization, have been described[5].

The one-unit difference between the masses of an amidated amino acid ($-CONH_2$, identified here by a #) and its free-carboxyl congener (–COOH) suggests that mass spectrometry (MS) would be the ideal method for analysis of amino acid amides in the presence of non-amidated amino acids. This approach would obviate the necessity for specific extraction of amino acid amides or specific derivatization procedures. Thermospray MS is suited to identification of low-molecular-weight polar non-volatile molecules such as amino acids[6], and allows coupling to HPLC systems for separation of any compounds of the same mass (examples of such isobaric compounds include isoleucineamide and leucineamide, asparagine and aspartic acid amide, asparagineamide and leucine). Generally, MS techniques reported for amino acids are either not currently amenable to the solvent flows of HPLC (secondary-ion MS[7]), require derivatization to produce chromatographable analogues (gas chromatography–MS), or have high background at low masses and so require derivatization to produce high-mass ions for amino acids (continuous-flow fast atom bombardment MS[8]).

There are many LC and HPLC techniques reported for separation of amino acids[9,10] and amino acid amides[2–4,11]. The majority of these demand pre-column derivatization for adequate chromatography and detection, and/or use solvents containing involatile salts that are not compatible with thermospray MS. We report here a thermospray HPLC–MS method for high sensitivity analysis of amino acid α-carboxyamides that requires no extraction or derivatization procedures.

EXPERIMENTAL

Mass spectrometry

The mass spectrometer used in all these studies was a Hewlett-Packard MSD equipped with a Vestec thermospray interface (Vestec, Houston, TX, U.S.A.). The mass spectrometer was operated in the positive ion mode. Moderate probe tip (215°C), vapor (280–310°C) and block (400°C) temperatures were maintained. Data was accumulated in the single ion monitoring (SIM) mode using low resolution (± 0.45 mass units) with dwell times ranging from 200 to 500 ms/ion. Full-scan spectra were usually accumulated over mass ranges from 70 to 210 mass units, at rates of 2–4 s/scan.

High-performance liquid chromatography

A Pharmacia/LKB Model 2150 pump provided the constant solvent flow necessary for stable background ion current (Pharmacia/LKB, Piscataway, NJ, U.S.A.). A low-pressure solvent mixer and a Pharmacia/LKB Model 2152 controller were used to generate linear gradients in organic modifier content, as required, using the single pump. Mobile phase flow-rates were usually 1.0 ml/min for 4.0 and 4.6 mm (I.D.) columns. Post-column addition of ammonium formate to provide the ammonium concentration needed for efficient thermospray positive ion generation was carried out using a second Pharmacia/LKB 2150 pump and a low-volume tee joint. Post-column solvent flow-rate and concentration were adjusted to provide a final flow-rate into the thermospray source of 1.2–1.25 ml/min and an ammonium ion concentration of 0.1–0.2 *M*.

A variety of HPLC columns has been tested. The results shown here were obtained with a Beckmann 5-μm endcapped octadecylsilyl column (15.0 × 4.0 mm I.D.). Equivalent results have been obtained using a variety of octadecylsilyl columns from Pharmacia/LKB, and polymeric octadecylsilyl columns (Excellopac ODS-A from R. Gourley, Laurel, MD, U.S.A.). Column-to-column differences usually require adjustment of the organic modifier gradient to maintain adequate resolution.

Chemicals and solutions

Standard L-amino acids and L-amino acid amides were obtained from Sigma (St. Louis, MO, U.S.A.) and Bachem (Torrance, CA, U.S.A.). Lysineamide dihydrochloride was a generous gift from Dr. W. H. Simmons, Loyola University Medical Center, Maywood, IL, U.S.A. *p*-Toluenesulfonic acid was analytical-reagent grade (Eastman-Kodak, Rochester, NY, U.S.A.). The standard used, α-amino-*n*-butyric acid, was obtained from Calbiochem (San Diego, CA, U.S.A.). Water used was purified by reverse osmosis and ion exchange. Other chemicals and solvents were analytical grade.

Stock solutions of amino acids and amino acid amides were prepared in filtered

0.1 *M* ammonium acetate or 0.1 *M* ammonium formate (pH 7.0) generally at a concentration of 10 or 20 m*M*. Most solutions were found to be stable at room temperature for extended periods (up to 6 months), although some were made up more frequently, or stored in aliquots at −20°C and thawed as required. Working solutions for determining retention characteristics were diluted daily in mobile phase to a final concentration of 0.1 m*M*. Solutions for signal-to-noise determinations and standard curves ranged in concentration from 20 n*M* to 1.0 m*M*.

Solvents were prepared by dissolving the mobile phase modifier (*p*-toluenesulfonic acid, 10 m*M*) in water or water–methanol and adjusting to the desired pH with concentrated ammonium hydroxide. The solutions were then filtered (0.45 μm filter) and degassed under vacuum immediately prior to use. Stock solutions of 1.0 *M* ammonium formate were prepared and were diluted as required with water and filtered (0.45 μm) and degassed prior to use.

RESULTS

The one- and three-letter abbreviations used in the text and figures for amino acids and amino acid amides, the mass-to-charge ratio (*m/z*) of the ions used for detection and quantification, and the retention times under the conditions described in the legend to Fig. 1, are presented in Table I.

In all cases the ion used for quantification is that of the protonated monocationic molecular ion $[M+H]^+$. Most amino acids and amino acid amides had simple spectra dominated by the protonated molecular ion, although some spectra showed significant fragment ions (*e.g.* *m/z* 130 for $[Glu+H-H_2O]^+$). Arg and Arg# had complex

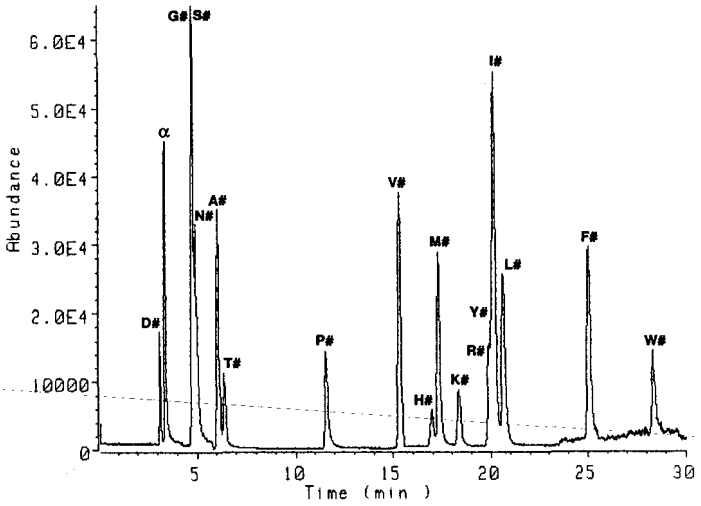

Fig. 1. Summated SIM profiles for thermospray HPLC–MS of a mixture of seventeen α-carboxyamido amino acids and α-amino-*n*-butyric acid. A 20-μl volume of a solution containing 0.1 m*M* of each compound in mobile phase was injected at 1.0 min. The mobile phase contained 10 m*M* *p*-toluenesulfonic acid, pH adjusted to 3.5 with ammonium hydroxide, and a linear gradient of methanol from 0 to 30% at 1.5%/min beginning at 5.0 min. The flow-rate through the 5-μm endcapped octadecylsilyl column (15 cm × 4.6 mm I.D.) was 1.0 ml/min, and 0.5 *M* ammonium formate at a rate of 0.25 ml/min was added post-column.

TABLE I

ABBREVIATION CODES, PROTONATED MOLECULAR ION MASSES, AND CHROMATOGRAPHIC RETENTION TIMES FOR α-AMINO-*n*-BUTYRIC ACID, THE TWENTY COMMON PROTEIC AMINO ACIDS AND SEVENTEEN AMINO ACID α-CARBOXYAMIDES

The α-carboxyamides of cysteine, glutamic acid, and glutamine were not available. α-Amino-*n*-butyric acid was used as a standard only; its α-carboxyamide is not expected to be found in any mammalian peptide.

"Parent" amino acid	*Three-letter abbrev.*[a]	*One-letter abbrev.*[a]	*Amide*		*Acid*	
			$[M+H]^+$	t_R[b]	$[M+H]^+$	t_R[b]
Alanine	Ala	A	89	5.04	90	1.80
Cysteine	Cys	C	121	–	122	1.60
Aspartic acid	Asp	D	133	2.11	134	1.47
Glutamic acid	Glu	E	147	–	148	1.76
Phenylalanine	Phe	F	165	24.05	166	17.15
Glycine	Gly	G	75	3.75	76	1.59
Histidine	His	H	155	17.35	156	6.08
Isoleucine	Ile	I	131	19.18	132	12.73
Lysine	Lys	K	146	15.94	147	4.68
Leucine	Leu	L	131	19.63	132	13.28
Methionine	Met	M	149	16.30	150	6.03
Asparagine	Asn	N	132	3.99	133	1.59
Proline	Pro	P	115	10.56	116	2.16
Glutamine	Gln	Q	146	–	147	1.90
Arginine	Arg	R	174	18.92	175	10.79
Serine	Ser	S	105	3.89	106	1.59
Threonine	Thr	T	119	5.38	120	1.76
Valine	Val	V	117	14.33	118	5.36
Tryptophan	Trp	W	204	27.33	205	23.90
Tyrosine	Tyr	Y	181	19.10	182	13.71
α-Amino-*n*-butyric acid	Aab[c]	α[c]	–	–	104	2.40

[a] The symbol used in this article to denote an α-carboxyamido amino acid is, *i.e.* asparagineamide is abbreviated to Arg# or R#.

[b] The retention time tabulated is minutes after injection, which was at 1.0 min after commencement of the run.

[c] There is no commonly accepted three- or one-letter abbreviation for α-amino-*n*-butyric acid. Aab and α are used in this text.

spectra, which showed changes that could be correlated with the cleanliness of the thermospray probe: a new probe gives spectra for Arg in which the base peak has *m/z* 115, while older probes produce *m/z* 157 (assigned to $[Arg+H-H_2O]^+$) or the molecular ion (*m/z* 175) as the base peak. This change is probably due to coating of reactive sites with a carbonized layer of organic material as the probe is used. Similar spectral changes can be deliberately induced by using non-reactive glass coatings inside the stainless-steel thermospray probe[12].

Fig. 1 shows a chromatogram of a mixture of the seventeen available amidated amino acids and the standard α-amino-*n*-butyric acid. The chromatogram has the appearance of a normal liquid chromatogram, but is actually a summation of a number of individual ion profiles. This is the reason for the sudden changes in baseline intensity, for example at 23.5 minutes. The SIM data acquisition parameters

were such that a set of two to four ions was acquired concurrently, with the start and end times of each group chosen from previous retention time determinations. The mobile phase pH and organic modifier gradient were designed to separate isobaric amidated amino acids (Ile#, Leu#) from each other, and also amidated amino acids from any isobaric amino acids (*e.g.* Asp#, Asn). Some of the amino acid amides are not totally chromatographically resolved, however the SIM profiles of the molecular ions are resolved as the overlapping peaks are not isobaric. Fig. 2 demonstrates the resolution of the individual SIM profiles for the group of amidated amino acids eluting at *ca.* 5 min after injection.

Fig. 3a shows the chromatographic profile of the set of twenty common proteic amino acids and α-amino-*n*-butyric acid under identical conditions to those shown for Fig. 1. Resolution is poor for some of the early-eluting amino acids as the chromatographic conditions were optimized for separation of the amino acid amides, as described above. The SIM parameters used for this sample are not the same as those used for detection of the amidated amino acids in Fig. 1. When the mixture of twenty amino acids and Aab was chromatographed using the SIM parameters optimized for the amidated amino acids, only three compounds were detected (Fig. 3b). These compounds are the internal standard Aab, which is present in both mixtures, and compounds having masses equivalent to Asp# and Pro#. Upon inspection of the actual retention times, the amino acids responsible for these peaks were identified as Asn and Arg, respectively. Asn and Asp# are isobaric, and Pro# is isobaric with the *m/z* 115 fragment ion of Arg described above. As shown in Fig. 3c and 3d, which are "close-up" views of the relevant sections of Figs. 1 and 3a, in both cases the interfering amino acid is resolved from the amino acid amide.

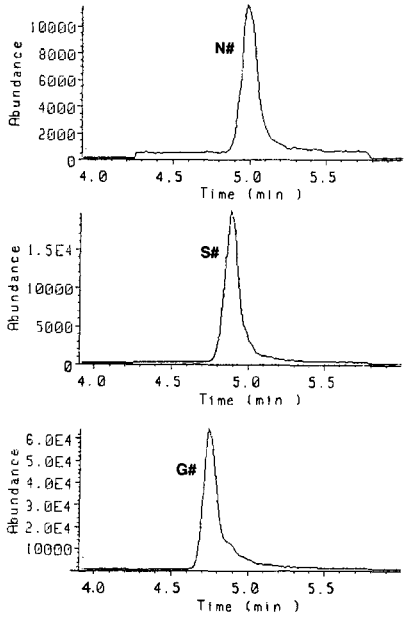

Fig. 2. Individual SIM profiles for three closely eluting amino acids amides from Fig. 1. These profiles are taken from the same data as that shown in Fig. 1, but are presented as individual profiles on an expanded scale to demonstrate the resolution of closely eluting non-isobaric compounds.

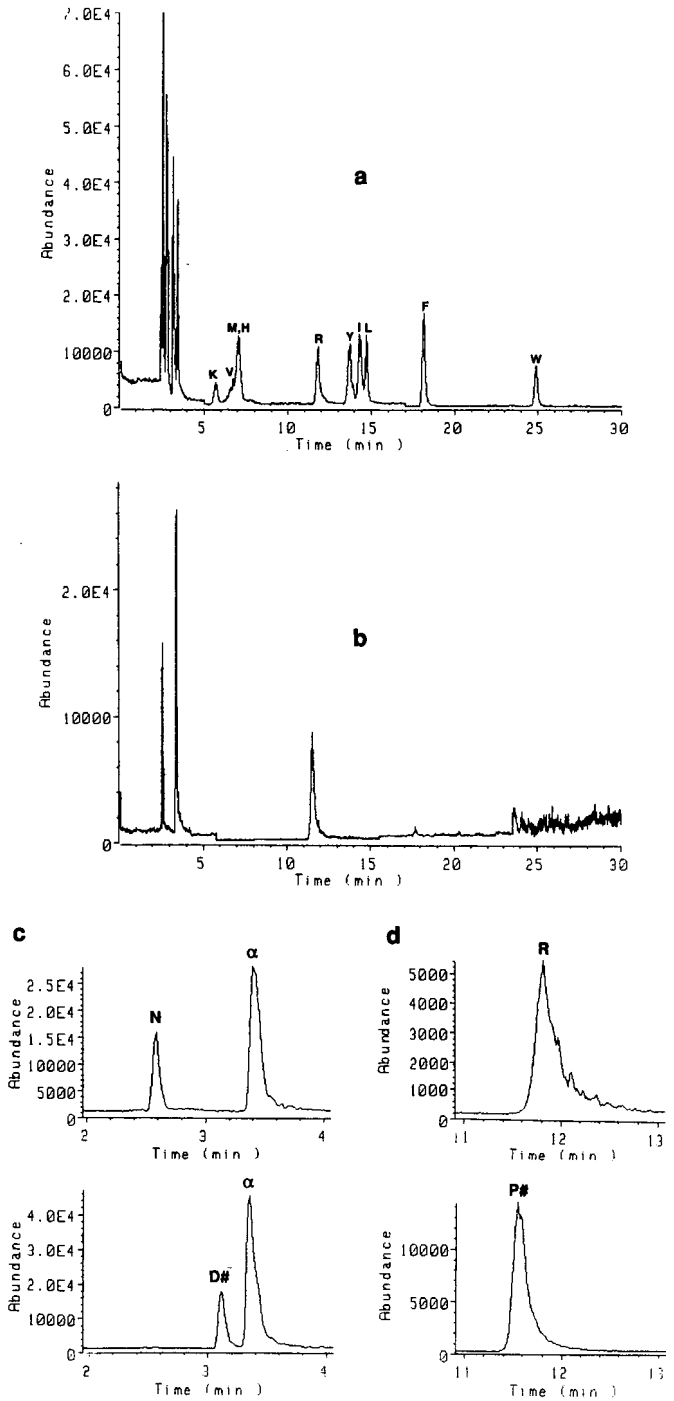

Fig. 3. Thermospray HPLC–MS profiles of amino acids. (a) Summated SIM profiles for a mixture of the twenty common amino acids and α-amino-*n*-butyric acid, chromatographed under the same conditions described in Fig. 1. As described in the text, the SIM parameters used for this sample were those optimized for the amino acids. The early-eluting group of amino acids comprised D, S, N, G, C, E, T, A, Q, P and α. (b) Summated SIM profiles for the same mixture of amino acids, chromatographed under the same conditions, but with the SIM parameters optimized for the detection of amino acid amides (*i.e.* the SIM parameters used for Fig. 1). Only two of the twenty non-amidated amino acids appear as amidated amino acids. (c) and (d) Demonstration that the amino acids seen using the SIM parameters for amidated amino acids do not co-chromatograph with the authentic amino acid amides. c shows summated SIM profiles for the relevant time period of b (upper) and Fig. 1 (lower), and d shows *m/z* 115 SIM profiles from b (upper) and Fig. 1 (lower).

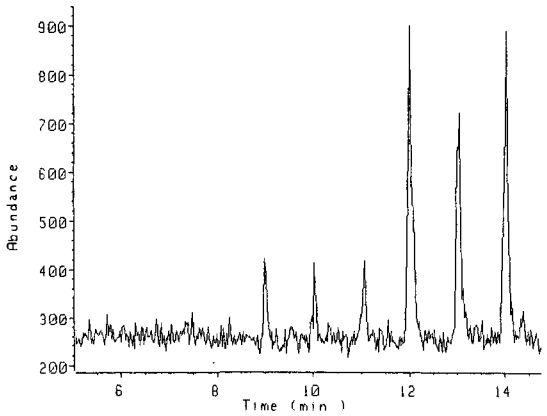

Fig. 4. Detection limit for thermospray HPLC–MS analysis of amino acids amides. SIM profile of *m/z* 89 for triplicate injections of mobile phase, 1 pmol of Ala#, and 4 pmol of Ala#. Injections were made onto the column used for Figs. 1–3, with the starting buffer only: 1.0 ml/min of 10 m*M* *p*-toluenesulfonic acid, pH 3.5 with ammonium hydroxide, no organic modifier, with 0.25 ml/min of 0.5 *M* ammonium formate added post-column. The retention time of Ala# is 5 min under these conditions, and injections were timed for elution at 6, 7 and 8 min (blank), 9, 10 and 11 min (1 pmol) and 12, 13 and 14 min (4 pmol).

As can be seen from Fig. 1, the peak-height response varies for individual amidated amino acids. The intensity of the molecular ion was not affected significantly by changes in the pH of the post-column buffer, suggesting that the variation is not primarily due to different proton affinities. To some degree the variation can be ascribed to the degree of fragmentation of the protonated molecular ion: the basic amino acid derivatives (Arg#, Lys# and His#), which have the most complex spectra, also have the lowest intensity for the parent molecular ion, while the simplest amidated amino acid, Gly#, has the highest intensity. The MS background is also not equal for all masses (*e.g.* note the noisy baseline from 23.5 to 30.0 min in Fig. 1 due to the ion *m/z* 204). The detection limits therefore vary noticeably for the different amidated amino acids. Fig. 4 shows that for a "typical" amidated amino acid, Ala#, 1 pmol on column is readily detectable, with a signal-to-noise ratio of *ca.* 2:1. As has been previously reported, amino acids and amidated amino acids (*e.g.* released by carboxypeptidase cleavage of amidated peptides) can be quantified over the picomole to nanomole range using an added internal standard, α-amino-*n*-butyric acid[11].

DISCUSSION

The method described here was developed for identification of α-carboxyamido amino acids released by enzymatic digestion of peptide mixtures. Amidated amino acids can be released from peptides by cleavage with a number of carboxypeptidase enzymes[13,14], providing a method for identification of potentially biologically active peptide hormones via detection of post-translationally modified amino acids[1,5]. We have previously presented a preliminary report describing a thermospray HPLC–MS method for analysis of amino acids and amino acid amides[11]. This paper details much-improved method utilizing endcapped octadecylsilyl HPLC columns and a low pH (pH 3.5) buffer containing *p*-toluenesulfonic acid.

Previous methods described for identification of α-carboxyamido amino acids in peptide digestion mixes have involved complicated extraction and derivatization steps[1–4]. The variation in chemical characteristics of the side-chains of the common amino acids makes it unlikely that any extraction–derivatization procedures could be specific for all possible amidated amino acids in the presence of unmodified amino acids and partially cleaved peptides. The use of a mass selective detector allows identification of α-carboxyamido amino acids in the presence of α-carboxyl amino acids due to the one-mass-unit difference between the modified and unmodified analogs. The thermospray HPLC–MS method is generally at least as sensitive as previously reported HPLC methods for amidated amino acid detection, although the sensitivity of detection for individual compounds does vary with the chemical nature of the amino acid amide and the level of background noise at each mass. However, as the thermospray HPLC–MS method requires no extraction or derivatization for detection of the α-carboxyamido amino acids, enzymatic hydrolysates of peptides can be injected directly onto the column, thereby providing a much higher overall sensitivity for detection of α-carboxyamido amino acids from hydrolyses of biological samples.

ACKNOWLEDGEMENTS

We thank Drs. F. Cuttitta, P. G. Kasprzyk and P. Smith for valuable discussions. A.M.T. is a recipient of a Hybritech Inc.–NCI Collaborative Fellowship Grant. This work was supported in part by a generous grant from the G. Harold and Leila Y. Mathers Charitable Trust.

REFERENCES

1 K. Tatemoto and V. Mutt, *Proc. Natl. Acad. Sci. U.S.A.*, 75 (1978) 4115–4119.
2 H. P. J. Bennett and S. Solomon, *J. Chromatogr.*, 359 (1986) 221–230.
3 W. E. Schmidt, J. M. Conlon, V. Mutt, M. Carlquist, B. Gallwitz and W. Creutzfeldt, *Eur. J. Biochem.*, 162 (1987) 467–472.
4 W. H. Simmons and G. Meisenberg, *J. Chromatogr.*, 266 (1983) 483–489.
5 A. M. Treston, A. Yergey, P. G. Kasprzyk, F. Cuttitta and J. L. Mulshine, in S. Rosen, J. Mulshine, F. Cuttitta and P. Abrams, *The Biology of Lung Cancer*, Marcel Dekker, New York, 1988, Ch. 4, pp. 91–119.
6 M. Vestel, A. L. Yergey, C. E. Edmonds and I. Lewis, *Liquid chromatography/mass spectrometry: Techniques and applications*, Plenum, New York, in press.
7 G. R. Pettit, G. M. Cragg, C. W. Holzapfel, A. A. Tuinman and D. P. Gieschen, *Anal. Biochem.*, 162 (1987) 236–241.
8 A. E. Ashcroft, J. R. Chapman and J. S. Cottrell, *J. Chromatogr.*, 394 (1987) 15–20.
9 R. F. Peifer and D. W. Hill, *Adv. Chromatogr.*, 22 (1983) 37–69.
10 Z. Deyl, J. Hyanek and M. Horakova, *J. Chromatogr.*, 379 (1986) 177–250.
11 A. M. Treston, A. L. Yergey, F. Cuttitta and J. L. Mulshine, *Proceedings of the 36th ASMS Conference on Mass Spectrometry and Allied Topics, June 5–10, 1988, San Francisco*, 1988, pp. 1077–1078.
12 P. C. Smith and A. L. Yergey, *Proceedings of the 36th ASMS Conference on Mass Spectrometry and Allied Topics, June 5–10, 1988, San Francisco*, 1988, pp. 1231–1232.
13 K. Breddam, *Carlsberg Res. Commun.*, 51 (1986) 83–128.
14 W. H. Simmons and R. Walter, *Biochemistry*, 19 (1980) 39–48.

Journal of Chromatography, 474 (1989) 197–207
Elsevier Science Publishers B.V., Amsterdam — Printed in The Netherlands

CHROM. 21 493

LIQUID CHROMATOGRAPHY–THERMOSPRAY MASS SPECTROMETRY OF DNA ADDUCTS FORMED WITH MITOMYCIN C, PORFIROMYCIN AND THIOTEPA

STEVEN M. MUSSER
Department of Medicinal Chemistry and Pharmacognosy, School of Pharmacy, University of Maryland at Baltimore, 20 North Pine Street, Baltimore, MD 21201 (U.S.A.)
SU-SHU PAN
University of Maryland Cancer Center, Division of Developmental Therapeutics, Baltimore, MD (U.S.A.)
and
PATRICK S. CALLERY*
Department of Medicinal Chemistry and Pharmacognosy, School of Pharmacy, University of Maryland at Baltimore, 20 North Pine Street, Baltimore, MD 21201 (U.S.A.)

SUMMARY

High-performance liquid chromatography (HPLC) and thermospray mass spectrometry were combined for the analysis of DNA adducts formed from the interaction of the anticancer drugs mitomycin C, porfiromycin and thiotepa with calf thymus DNA. The adducts formed from reaction of mitomycin C and porfiromycin with DNA were separated from unmodified nucleosides by HPLC on a C_{18} column and identified by thermospray mass spectrometry. Thiotepa DNA adducts readily depurinated from DNA and were chromatographed and identified by thermospray liquid chromatography–mass spectrometry as the modified bases without the ribose moiety attached. The utility of thermospray mass spectrometry for the identification of microgram quantities of nucleoside adducts and depurinated base adducts of these anticancer drugs was demonstrated.

INTRODUCTION

The ability to link the effluent from a high-performance liquid chromatograph to a mass spectrometer via a thermospray ionization source has proved to be very useful for the analysis of thermally labile, non-volatile compounds such as nucleotides and nucleosides[1–5]. Since the process does not require derivatization[6,7] or extensive sample workup[8,9] as required for other mass spectrometric techniques, thermospray mass spectrometry (MS) serves as an excellent method for rapid identification of nucleoside adducts observed in liquid chromatograms.

Many anticancer drugs are thought to exert their tumor cell killing potency by their ability to covalently bind to DNA forming mono and dialkylated adducts[10–12]. The identification of these adducts is important for understanding their therapeutic

0021-9673/89/$03.50

importance and designing new drugs. Since thermospray liquid chromatography (LC)–MS is well suited for nucleoside analysis it could prove to be a useful tool in determining the structures of adducts created by the alkylation of DNA with anticancer drugs.

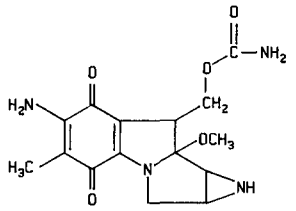

I

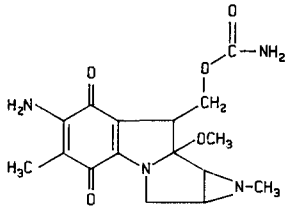

II

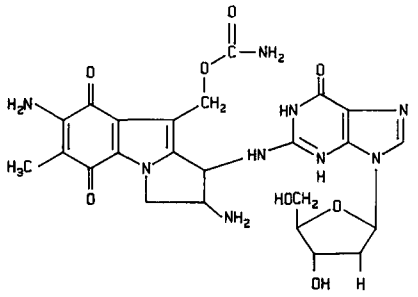

III

Mitomycin C (I) and its N-methyl analogue porfiromycin (II) are clinically effective anticancer drugs[13] that are known to alkylate DNA. The structure of the monoalkylation product formed between DNA and mitomycin C has been elucidated by Tomasz *et al.*[14] using NMR and Fourier-transform infrared (FT-IR) analysis. The alkylation product is a stable nucleoside adduct which occurs on the exocyclic N-2 position of deoxyguanosine residues (III). Porfiromycin has been shown to alkylate DNA by the same mechanism as mitomycin C, resulting in the formation of an analogous adduct[15].

Thiotepa (IV) is an anticancer drug which has been used clinically for over 30 years and has been used more aggressively in recent years in combination with autologous bone marrow transplantation[16–18]. Unlike mitomycin C, there has been little work done on the mechanism of alkylation of DNA by thiotepa. Several studies

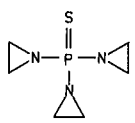

IV

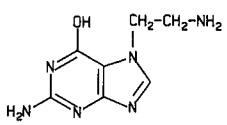

V

carried out on the alkylation of isolated nucleosides by thiotepa have suggested that alkylation occurs on the N-7 position of deoxyguanosine residues[19,20], leading to the formation of 7-(2-aminoethyl)guanine (V). Based on the instability of N-7 alkylated deoxyguanosine adducts formed by alkylation with ethylenimine or phosphoramide mustard [21,22], the adducts formed from reaction of thiotepa with DNA would also be expected to be unstable, leading to the formation of depurinated or imidazole ring opened products[21,22].

The purpose of this study was to demonstrate the utility of thermospray LC–MS for the identification of two types of drug–DNA adducts of potential clinical importance. The adducts of interest are stable nucleoside–drug adducts and adducts which cause depurination of the DNA. Since the adducts have been well defined by other methods, they should make good model compounds for comparative studies by thermospray LC–MS.

EXPERIMENTAL

Reagents and materials

Mitomycin C was provided by the Drug Development Branch, Division of Cancer Treatment, National Cancer Institute and by Dr. W. Bradner, Bristol Labs. (Syracuse, NY, U.S.A.). Porfiromycin was provided by Upjohn (Kalamazoo, MI, U.S.A.). Thiotepa was provided by Lederle Labs. (Pearl River, NY, U.S.A.). Unmodified nucleosides, calf thymus DNA, pancreatic DNAase (E.C. 3.1.4.5), snake venom phosphodiesterase (E.C. 3.1.4.1), and alkaline phosphatase (E.C. 3.1.3.1) were purchased from Sigma (St. Louis, MO, U.S.A.). Ethylenimine was prepared from the sulfate ester of ethanolamine according to the procedure of Wenker[23] and used immediately after preparation.

The water used for buffers was purified through a Milli-Q system, Millipore (Bedford, MA, U.S.A.) to give a resistivity of 18 MΩ/cm. Gold-label ammonium formate was obtained from Aldrich (St. Louis, MO, U.S.A.). HPLC grade methanol was used for all chromatography.

Preparation of mitomycin C and porfiromycin DNA adducts

Adducts were prepared by a modification of the procedure of Tomasz *et al.*[24]. In a typical experiment calf thymus DNA (1 mg) was dissolved in 1 ml of 20 m*M* Tris buffer, pH 7.4. To this solution was added approximately 300 μg of mitomycin C or porfiromycin in buffer. Nitrogen was bubbled through the solution for 1 h, after which time 100 μg of PtO_2 was added. Hydrogen gas was bubbled through the solution for 10 min, followed by nitrogen gas for 20 min, air was then bubbled through the solution for 20 min. The platinum was removed by centrifugation.

The DNA was precipitated and digested according to the procedure of Pan *et al.*[25]. The DNA was precipitated by adjusting the NaCl concentration to 0.1 m*M* and adding two volumes of cold 95% ethanol (0°C) to the DNA–mitomycin C solution. The solution was centrifuged for 5 min at 5000 *g*. The supernatant was discarded and the DNA pellet was washed with cold ethanol to remove non-covalently bound mitomycin C or porfiromycin. The DNA was resuspended in 50 m*M* Tris buffer, pH 7.4. DNAase at 200 kallikrein units per mg DNA was added to the solution and allowed to digest the DNA for 4 h at 37°C. The pH was raised to 8.5 and $MgCl_2$ was added

such that the final concentration was 5 m*M*. The DNA was digested to nucleotides with 0.05 units of phosphodiesterase per mg DNA in 4 h at 37°C. Finally, the nucleotides were digested with 3.0 units of alkaline phosphatase per mg DNA for 12 h at 37°C to yield a mixture of alkylated and non-alkylated nucleosides. This mixture was then analyzed by thermospray LC–MS. An injection of 100 μl of the digested DNA was made onto the high-performance liquid chromatographic (HPLC) column amounting to approximately 1–3 μg of adduct being directed into the thermospray interface.

Preparation of thiotepa–DNA and ethylenimine–DNA adducts

To a solution of 1 mg/ml of calf thymus DNA in 25 m*M* phosphate buffer, pH 7.4, were added aqueous buffer solutions of thiotepa (100 μg) or ethylenimine (500 μg) along with 10 μg of toluene to prevent bacterial growth. The solution was stirred at 37°C for three days in a capped test tube. At the end of the reaction the DNA was precipitated and digested as described above in the mitomycin C experiments except the supernatant from the reaction mixture was lyophilized and stored at 0°C until analysis by thermospray LC–MS. The lyophylized residue was reconstituted in 1 ml of mobile phase and 250 μl of this solution was injected onto the column, representing 20–30 μg of the guanine adduct.

HPLC instrumentation

The HPLC system consisted of two Waters Assoc. (Milford, MA, U.S.A.) Model 501 pumps, a Model 660 solvent programmer, and a Model 440 UV absorbance detector. UV data were collected and processed through a Hewlett-Packard (Palo Alto, CA, U.S.A) Model 9000 series 216 computer using a Nelson Analytical (Palo Alto, CA, U.S.A.) series A/D converter with the chromatography software package XTRA CHROM. Brownlee (Santa Clara, CA, U.S.A.) RP-18 guard columns (30 × 4.6 mm) and RP-18 analytical cartridges (5 μm diameter particles; 220 × 4.6 mm) were used for all assays.

The mobile phase used for analysis of the enzymatically hydrolyzed DNA was 0.1 *M* ammonium acetate in 5% methanol changed linearly over 30 min to 0.1 *M* ammonium acetate in 50% methanol with a flow-rate of 1.2 ml/min. The mobile phase used for analysis of the hydrolyzed supernatant from the thiotepa–DNA reaction mixture was 0.1 *M* ammonium formate adjusted to pH 4.0 with formic acid that was changed linearly over 35 min to 0.05 *M* ammonium formate, pH 4.0, in 50% methanol, with a flow-rate of 1.0 ml/min.

Thermospray mass spectrometry instrumentation

A Vestec (Houston, TX, U.S.A) thermospray interface[1,2] connected to either a Finnigan MAT (San Jose, CA, U.S.A.) Model 4500 mass spectrometer, a Hewlett-Packard mass selective detector, or a quadrupole instrument constructed in our laboratory was used. In all cases the scan range of these instruments was set between 120 and 800 a.m.u. The thermospray interface temperatures were optimized for the molecular ion of deoxyguanosine such that the ratio of molecular ion (*m/z* 268) to base peak (*m/z* 152) was greater than 10%. The optimum temperatures for the vaporizer and source block varied slightly between instruments with the optimum vaporizer temperature being 210–220°C with the block temperature set at 295°C for the Hew-

lett-Packard mass selective detector, the optimum temperature for the vaporizer was 205–215°C with source block set at 310°C on the Finnigan ion source and the optimum vaporizor temperature on the laboratory-made instrument was 220–230°C with the source block set at 300 °C. The discharge electrode was operated at 1000 V, and the filament current at 300 mA.

RESULTS AND DISCUSSION

The UV chromatogram of DNA that had been treated with mitomycin C and then enzymatically hydrolyzed (Fig. 1) showed a peak (retention time 20.1 min) corresponding to a monofunctional N-2 alkylated deoxyguanosine[14]. The UV chromatogram of the DNA treated with porfiromycin and then hydrolyzed (Fig. 1) showed an analogous peak (retention time 21.5 min) corresponding to a porfiromycin DNA adduct. The thermospray mass spectra (Fig. 2) of the adduct peaks detected in the UV chromatograms showed that the porfiromycin adduct corresponds closely to the mi-

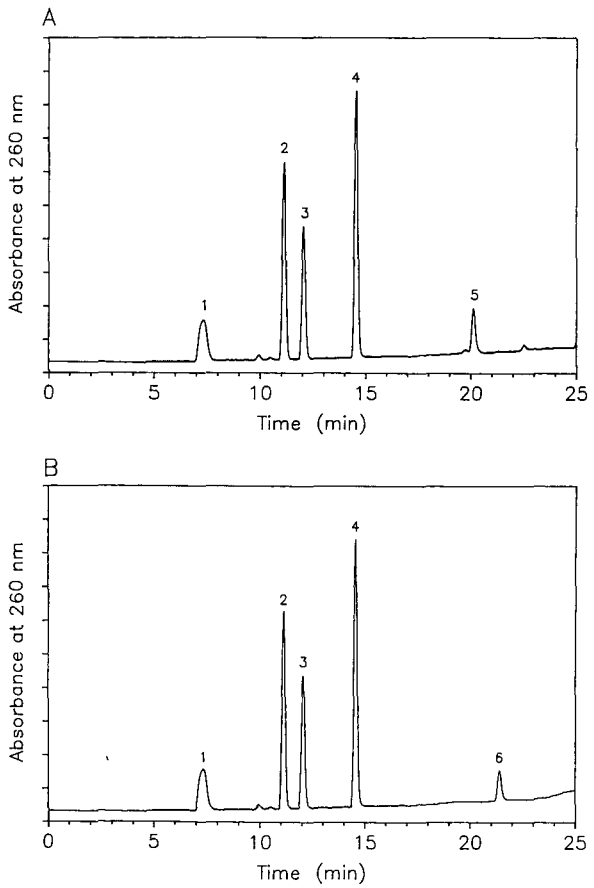

Fig. 1. UV chromatograms of DNA treated with (A) mitomycin C or (B) porfiromycin and then enzymatically digested. Peaks: 1 = deoxycytidine; 2 = deoxyguanosine; 3 = thymidine; 4 = deoxyadenosine; 5 = mitomycin C–deoxyguanosine adduct; 6 = porfiromycin–deoxyguanosine adduct.

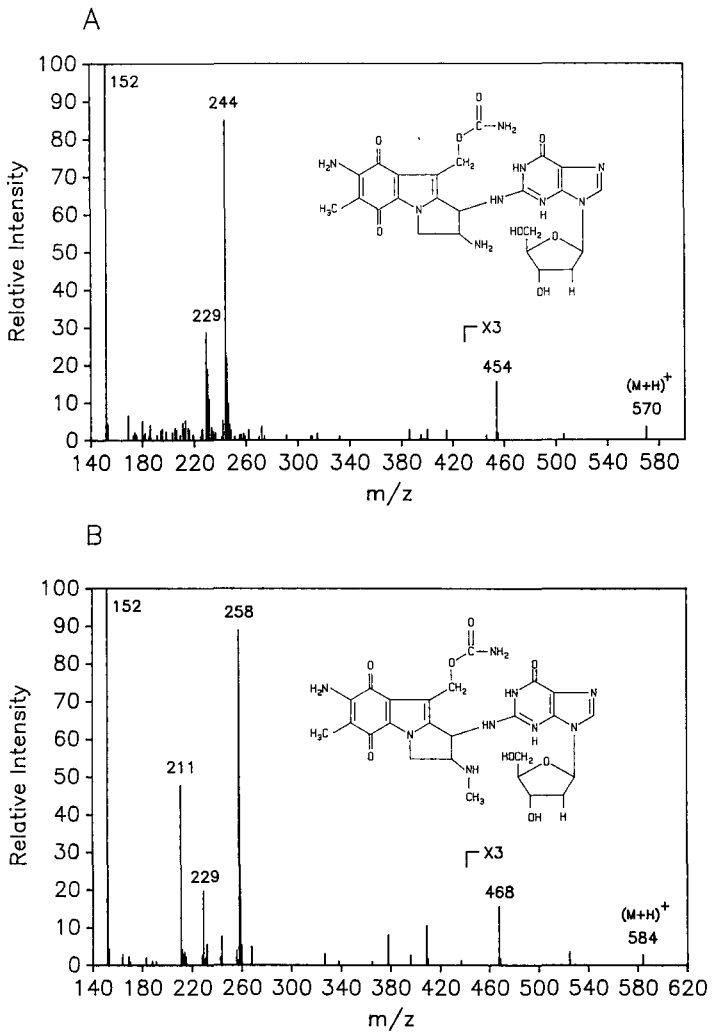

Fig. 2. Thermospray mass spectra of (A) mitomycin C–deoxyguanosine adduct and (B) porfiromycin–deoxyguanosine adduct.

tomycin C adduct except for a higher molecular weight. The difference in mass of 14 a.m.u. in the porfiromycin adduct in comparison with the mitomycin C adduct was accounted for by the presence of an N-methyl group in porfiromycin which is not present in mitomycin C.

The principal ions in the thermospray mass spectrum of the mitomycin C–deoxyguanosine adduct are the $[M+H]^+$ molecular ion at m/z 570, and the ion at m/z 244 which is proposed to be a protonated mitomycin C portion of the adduct as shown in Fig. 3.

The ion at m/z 152 was assigned as the guanine base $[B+2H]^+$, accounted for by thermal cleavage of the ribose (Fig. 3), a common fragment observed in the ther-

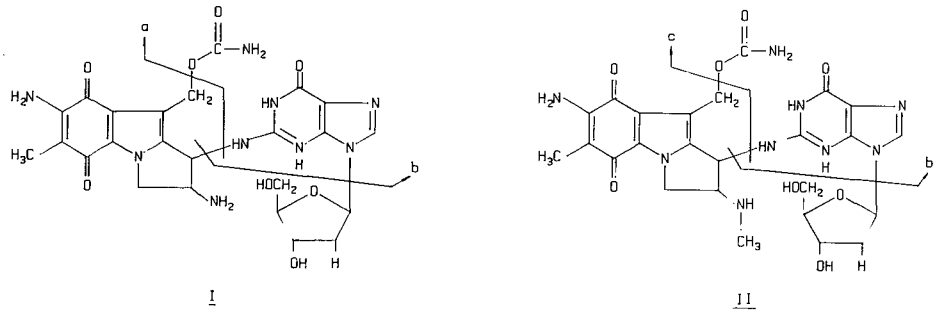

Fig. 3. Thermospray fragmentation of (I) mitomycin C adduct and (II) porfiromycin adduct. a, Protonated mitomycin C segment of the adduct, *m/z* 244; b, guanine base $[B+2H]^+$, *m/z* 152, and c, protonated porfiromycin segment of the adduct, *m/z* 258.

mospray spectrum of deoxyguanosine. The spectrum of the porfiromycin–DNA adduct is analogous to the mitomycin C adduct spectrum with an $[M+H]^+$ molecular ion at *m/z* 584, an ion at *m/z* 258 corresponding to the protonated porfiromycin segment of the adduct (Fig. 3) and the ion at 152 corresponding to the guanine base $[B+2H]^+$.

The UV chromatogram of the DNA which had been treated with thiotepa then enzymatically hydrolyzed (Fig. 4A) closely resembles that of untreated DNA (Fig. 4B), with no detectable nucleoside adduct present. However, close examination of the two chromatograms indicated that the deoxyguanosine peak was relatively smaller in the thiotepa treated DNA hydrolysate. On comparison of the peak area ratios of dG:dT and dA:dT (Table I) there is approximately a 14% reduction in the amount of deoxyguanosine and approximately 6% less deoxyadenosine found in the thiotepa treated DNA hydrolysate when compared with the untreated control.

Examination of the supernatant from the thiotepa–DNA reaction mixture showed two major peaks in both the UV chromatogram (Fig. 5A) and thermospray LC–MS total ion chromatogram (Fig. 5B). The identities of these two peaks were assigned as 7-(2-aminoethyl)guanine and 7-(2-aminoethyl)adenine since they coeluted with the adducts formed between ethylenimine and DNA (data not shown). In addition previous experiments with ethylenimine[21] and thiotepa[19] showed that the N-7 position is the preferred site of adduct formation. The thermospray mass spectra (Fig. 6A and B) consist mainly of a molecular ion at *m/z* 179 for the 7-(2-aminoethyl) adenine adduct and a molecular ion at *m/z* 195 for the 7-(2-aminoethyl)guanine adduct. Ions at *m/z* 136 for the adenine adduct and *m/z* 152 for the guanine adduct could be attributed to loss of the aminoethyl portion of the adduct. Use of the filament or discharge electrode to produce fragmentation provided no additional information.

While the lower limits of detection for the adducts were not determined, 200–300 ng of the mitomycin C or porfiromycin adducts and 50–100 ng of the thiotepa adducts produced full scan spectra. This sensitivity is comparable to that obtained by Moser and Wood[26] for non-alkylated nucleosides and nucleotides using fast atom-bombardment (FAB)–MS, although we were unsuccessful in obtaining a FAB mass spectrum of the mitomycin C adduct. Application of tandem MS with desorption chemical ionization (DCI)[27] has been shown to achieve detection of methylated nu-

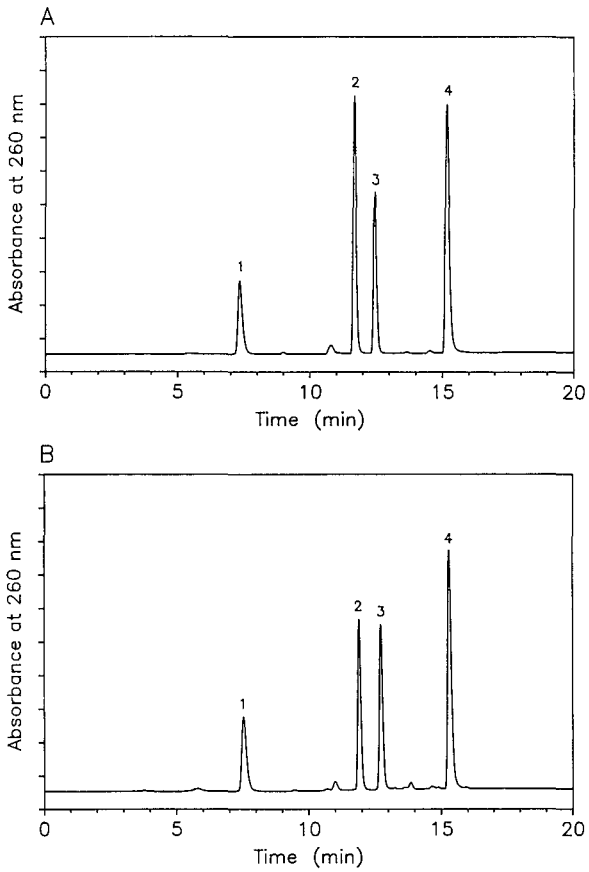

Fig. 4. UV chromatograms of (A) untreated DNA and (B) DNA which had been treated with thiotepa and then enzymatically hydrolyzed. Peaks: 1 = Deoxycytidine; 2 = deoxyguanosine; 3 = thymidine; 3 = deoxyadenosine.

TABLE I

EFFECT OF TREATMENT WITH THIOTEPA ON NUCLEOSIDE CONTENT OF DNA

dC = Deoxycytidine, T = thymidine, dG = deoxyguanosine and dA = deoxyadenosine.

	Area ratios of nucleosides		
	dC:T	*dG:T*	*dA:T*
Control DNA	0.69 ± 0.006[a]	1.61 ± 0.02	1.97 ± 0.01
Thiotepa treated DNA	0.68 ± 0.006	1.38 ± 0.01	1.88 ± 0.02

[a] Values represent the mean and the standard deviation of three runs.

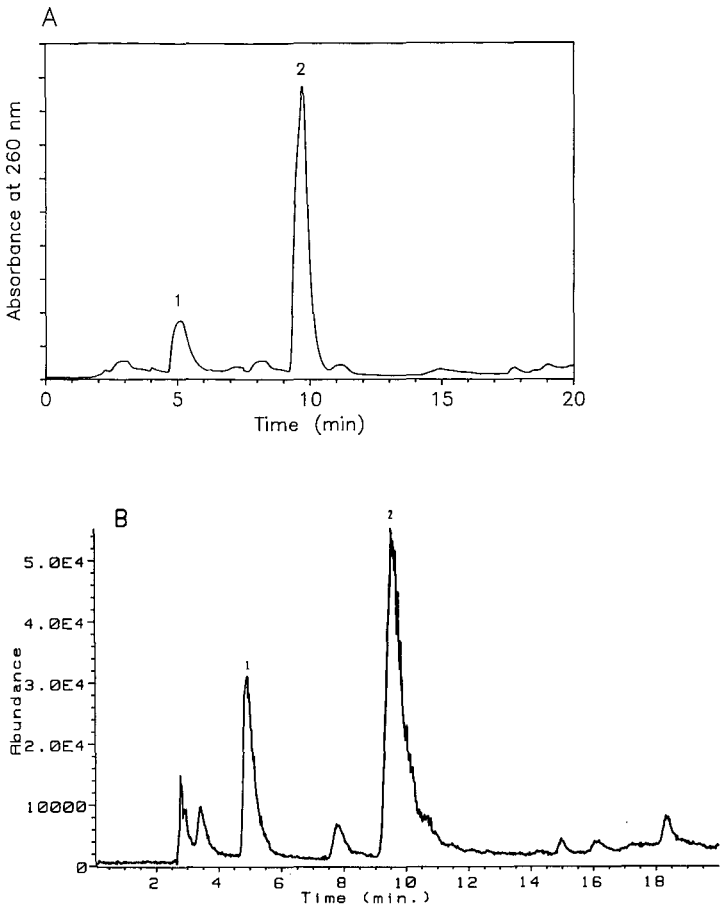

Fig. 5. (A) UV chromatogram and (B) thermospray total ion chromatogram of supernatant from DNA that had been treated with thiotepa. Peaks: 1 = 7-(2-aminoethyl)adenine, 2 = 7-(2-aminoethyl)guanine.

cleosides at a level of 1 ng, however molecular ions were not observed. Although FAB and DCI have been shown to be effective for the MS analysis of DNA adducts, thermospray provides an alternate method which is as sensitive and often produces spectra with molecular ion information not obtainable by other methods.

These results demonstrate that thermospray LC–MS is a powerful method for obtaining structural information on DNA adducts. Although thermospray yields mass spectra where molecular ions are almost always observed for nucleosides, it often fails to produce structurally important fragmentation. When fragmentation is observed, as demonstrated with the mitomycin C and porfiromycin adducts, the actual fragmentation mechanism is difficult to determine since fragments can be formed by several processes such as chemical ionization or as a result of protonating a pyrolysis product formed by the thermospray ionization process itself. Even when the fragmentation mechanism is not known this method provides useful molecular weight

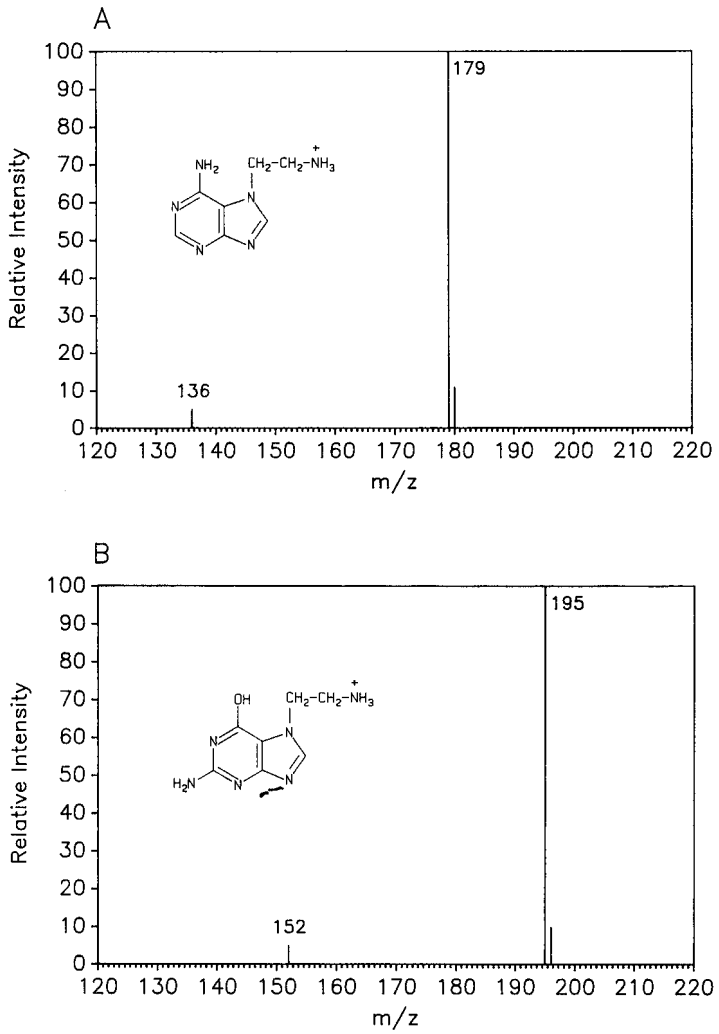

Fig. 6. Thermospray mass spectra of thiotepa DNA adducts found in the supernatant of the thiotepa–DNA reaction mixture. (A) 7-(2-aminoethyl)adenine; (B) 7-(2-aminoethyl)guanine.

information for the identification of nucleoside adducts as well as depurinated adducts resulting from the alkylation of DNA with the anticancer drugs mitomycin C, porfiromycin and thiotepa.

ACKNOWLEDGEMENTS

Supported by Hoffman-La Roche, Inc., Department of Drug Metabolism, University of Maryland Designated Research Initiative Funds, ACS grant No. IN-174D Maryland Cancer Program and ACS grant No. CH-412.

REFERENCES

1 C. R. Blakley, J. J. Carmody and M. L. Vestal, *Anal. Chem.*, 50 (1980) 1636.
2 M. L. Vestal and G. J. Fergusson, *Anal. Chem.*, 57 (1985) 2373.
3 C. G. Edmonds, M. L. Vestal and J. A. McCloskey, *Nucleic Acids Res.*, 13 (1985) 8197.
4 P. A. Blau, J. W. Hines and R. D. Voyksner, *J. Chromatogr.*, 420 (1987) 1.
5 R. D. Voyksner, *Org. Mass Spectrom.*, 22 (1987) 513.
6 M. S. Wilson and J. A. McCloskey, *J. Am. Chem. Soc.*, 97 (1975) 3436.
7 G. H. Sack, C. Fenselau, M. N. Kan and L. S. Kan, *J. Org. Chem.*, 43 (1978) 3932.
8 J. Eagles, C. Javanaud and R. Self, *Biomed. Mass Spectrom.*, 11 (1984) 41.
9 H. Moser and G. W. Wood, *Biomed. Environ. Mass Spectrom.*, 15 (1988) 547.
10 K. Hemminki and D. B. Ludlum, *J. Nat. Cancer. Inst.*, 73 (1984) 1021.
11 M. Metzler, *J. Cancer Res. Clin. Oncol.*, 112 (1986) 210.
12 P. B. Farmer, *Pharmacol. Ther.*, 35 (1987) 301.
13 L. H. Baker, R. M. Izbicki and V. K. Vaitkevicius, *Med. Ped. Onc.*, 2 (1976) 207.
14 M. Tomasz, R. Lipman, G. L. Verdine and K. Nakanishi, *Biochem.*, 25 (1986) 4337.
15 S-S. Pan and T. Iracki, *Mol. Pharmacol.*, 34 (1988) 223.
16 M. Sykes, D. Karnofsky, F. Phillips and J. Burchenal, *Cancer (Philadelphia)*, 6 (1953) 142.
17 S. F. Williams, J. D. Bitran, L. Kaminer, C. Westbrook, R. Jacobs, J. Ashenhurst, E. Robin, S. Purl, J. Beschorner, C. Schroeder and H. M. Golomb, *J. Clin. Oncol.*, 5 (1987) 260.
18 S. P. Ackland, K. E. Choi, M. J. Ratain, M. J. Egorin, S. F. Williams, J. A. Sinkule and J. D. Bitran, *J. Clin. Oncol.*, 6 (1988) 1192.
19 L. F. Sukhodub, V. S. Shelkovsky, M. V. Kosevich, T. L. Pyatigorskaya and O. Y. Zhilkova, *Biomed. Environ. Mass. Spectrom.*, 13 (1986) 167.
20 L. F. Sukhodub, V. S. Shelkovskii, M. V. Kosevich, T. L. Pyatigorskaya and O. Y. Zhilkova, *Doklady Akademii Nauk SSSR*, 283 (1985) 714.
21 K. Hemminki, *Chem.-Biol. Inter.*, 48 (1984) 249.
22 S. Kallama and K. Hemminki, *Chem. Biol. Interact.*, 57 (1986) 85.
23 H. Wenker, *J. Am. Chem. Soc.*, 69 (1935) 1540.
24 M. Tomasz, R. Lipman, J. K. Snyder and K. Nakanishi, *J. Am. Chem. Soc.*, 105 (1983) 2059.
25 S-S. Pan, T. Iracki and N. R. Bachur, *Mol. Pharmacol.*, 29 (1986) 622.
26 H. Moser and G. W. Wood, *Biomed. Environ. Mass Spectrom.*, 15 (1988) 547.
27 C-J. Chang, D. J. Ashworth, I. Isern-Flecha, X-Y. Jiang and R. G. Cooks, *Chem.-Biol. Inter.*, 57 (1986) 295.

Journal of Chromatography, 474 (1989) 209–222
Elsevier Science Publishers B.V., Amsterdam — Printed in The Netherlands

CHROM. 21 524

USE OF THERMOSPRAY LIQUID CHROMATOGRAPHY–MASS SPECTROMETRY FOR CHARACTERIZATION OF REACTIVE METABOLITES OF 3′-HYDROXYACETANILIDE, A NON-HEPATOTOXIC REGIOISOMER OF ACETAMINOPHEN

MOHAMED S. RASHED and SIDNEY D. NELSON*
Department of Medicinal Chemistry, BG-20, University of Washington, Seattle, WA 98195 (U.S.A.)

SUMMARY

3′-Hydroxyacetanilide (AMAP) is a non-hepatotoxic regioisomer of acetaminophen that nonetheless does form reactive metabolites that are trapped as glutathione thioether adducts. These reactive intermediates are, 4-acetamido-*o*-benzoquinone, 2-acetamido-*p*-benzoquinone and N-acetyl-3-methoxy-*p*-benzoquinone. Thermospray liquid chromatography–mass spectrometry (TSP LC–MS) was used to characterize products of reactions of these reactive compounds with cysteine or N-acetylcysteine. The TSP spectra of the *mono*- and *bis*-thioether adducts showed protonated molecular ions and characteristic fragmentation patterns. The chromatographic resolution together with the MS selectivity allowed for unequivocal identification of these conjugates in the urine of mice treated with AMAP.

INTRODUCTION

Thermospray liquid chromatography–mass spectrometry (TSP LC–MS) is one of several techniques developed in the last few years to overcome the inherent difficulty in interfacing the eluent of an high-performance liquid chromatograph to the source of a mass spectrometer. Since it first appeared[1] and for the last few years TSP LC–MS has proven to be a valuable technique applicable to drug metabolism studies and in routine pharmaceutical and environmental analysis[2–6]. The technique can handle normal and reversed-phase solvent systems at flow-rates of 0.5–2 ml/min and the ionization is soft, which allows for the analysis of polar, non-volatile thermally labile chemicals present in plasma or urine or other biological matrices.

Glutathione (GSH) adducts of xenobiotics and their metabolic breakdown products, namely the cysteine and N-acetylcysteine conjugates, are very polar and thermally labile compounds and therefore require softer modes of ionization such as desorption chemical ionization (DCI)[7], field desorption (FD)[8] and fast atom bombardment (FAB)[9]. More recently[10] several model compounds of this type have been studied by thermospray ionization mass spectrometry. In addition, Conchillo *et al.*[11] reported that under thermospray conditions sensitivities for GSH adducts were poor and gave unsatisfactory spectra[11]. Instead the analysis of the methyl esters of the corresponding cysteine or N-acetylcysteine derivatives afforded better spectra and

0021-9673/89/$03.50

TABLE I
STRUCTURE ABBREVIATIONS AND CHEMICAL NAMES OF COMPOUNDS MENTIONED IN THE TEXT

Structure	*Abbreviation*	*Chemical name*
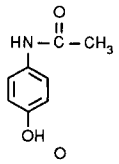	APAP	4′-Hydroxyacetanilide
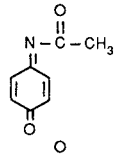	NAPQI	N-Acetyl-*p*-benzoquinone imine
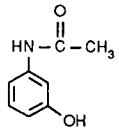	AMAP	3′-Hydroxyacetanilide
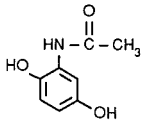	2-AcHQ	2-Acetamidohydroquinone
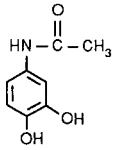	3-OH-APAP	4-Acetamido-1,2-catechol
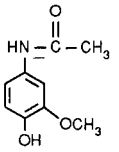	3-OMe-APAP	2-O-Methyl-4-acetamido-1,2-catechol
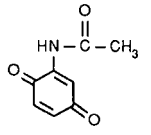	2-APBQ	2-Acetamido-*p*-benzoquinone
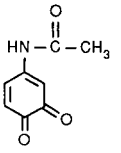	4-AOBQ	4-Acetamido-*o*-benzoquinone
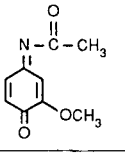	MAPQI	N-Acetyl-3-methoxy-*p*-benzoquinone imine

good sensitivity levels. Herein, we report on the use of TSP LC–MS in a drug metabolism study to detect and characterize cysteine, N-acetylcysteine and glucuronide metabolites of 3′-hydroxyacetonilide (AMAP; see Table I for structures and abbreviations).

AMAP is a non-hepatotoxic regioisomer of acetaminophen (4′-hydroxyacetanilide; APAP)[12,13]. Despite the lack of hepatotoxicity of AMAP, when equal doses of radiolabeled AMAP and APAP (400 mg/kg) were administered to hamsters, the extent of covalent binding of radioactivity to hepatic proteins was found to be nearly the same for both compounds[3]. Furthermore, NADPH-dependent covalent binding of radioactivity from [^{14}C]AMAP to microsomes from phenobarbital-pretreated mice ocurred four times faster than covalent binding of radioactivity from [^{14}C]APAP. Although the binding could be blocked by the addition of glutathione (GSH), little GSH depletion was observed after the administration of AMAP to control hamsters and mice[12,13]. Thioether adducts have been searched for, but not detected, as urinary metabolites in either animal species[14,15].

AMAP is metabolized *in vitro* to diphenolic compounds, 2-acetamidohydroquinone (2-AcHQ) and 3-hydroxyacetaminophen (3-OH-APAP)[5]. *In vivo*, 3-OH-APAP is further methylated to give 3-methoxyacetaminophen (3-OMe-APAP)[4]. 2-AcHQ is oxidized further to 2-acetamido-*p*-benzoquinone (2-APBQ) *in vitro* by mouse liver microsomes[16,17].

In a previous study[18], we presented evidence for the formation of three different reactive intermediates as a result of AMAP oxidative metabolism. Both *ortho*- and *para*-quinones are formed by further oxidation of 3-OH-APAP and 2-AcHQ. A quinone imine, N-acetyl-3-methoxy-*p*-benzoquinone imine (MAPQI) is formed by further oxidation of 3-OMe-APAP. All three intermediates form glutathione conjugates that were detected *in vitro* in mouse microsomal incubations enriched with GSH and in the bile of mice treated with AMAP.

In view of the data described above, it became necessary to study the urinary disposition of AMAP and compare it with that of APAP. This required the synthesis and characterization of several of cysteine (CYSH) and N-acetylcysteine (NACYSH) conjugates of the reactive intermediates.

MATERIALS AND METHODS

AMAP was purchased from Aldrich (Milwaukee, WI, U.S.A.) and crystallized before use from ethanol–water (1:1). CYSH, NACYSH were obtained from Sigma (St. Louis, MO, U.S.A.). An authentic sample of 3-OMe-APAP glucuronide was a generous gift from Dr. M. W. Gemborys.

Instrumentation

High-performance liquid chromatography (HPLC) was performed on an LKB Model 2152-2SD dual-pump instrument equipped with an LKB Model 2152 LC controller and an LKB Model 2151 variable-wavelength detector used at 254 nm (LKB, Bromma, Sweden). Separations were carried out on a 5-μm Ultrasphere ODS column (25 cm × 10 mm I.D.) protected with a 5-μm Ultrasphere ODS precolumn (Rainin Instruments). Mobile phase consisted of solvent A: water–acetonitrile–glacial acetic acid (96:2:2, v/v/v); solvent B: acetonitrile. A linear gradient was employed from 0% B to 20% B in 40 min with a flow-rate of 2.0 ml/min.

LC–MS spectra were generated using an LKB Model 2150 pump with an LKB Model 2152 LC controller coupled to a Vestec thermospray LC–MS Model 201 dedicated LC–MS system (Vestec, Houston, TX, U.S.A.). The separation was carried on a 5-μm Ultrasphere ODS (15 cm × 4.6 mm I.D.) protected with a 5-μm Ultrasphere ODS precolumn. The mobile phase consisted of 0.1 *M* ammonium acetate–acetonitrile (90:10, v/v) pumped isocratically at a flow-rate of 1.0 ml/min. Operating temperatures for the TSP interface were T1 (vaporizer) = 130–140°C; T2 (tip) = 250–270°C; jet (vapor) = 300–320°C; source block = 320–350°C. The system was operated in the positive ion mode with the filament off.

The thermospray interface temperature was optimized to obtain the maximum intensity for the MH^+ ion of the synthetic standards. Although a lower source temperature produced less fragmentation, the overall sensitivity was reduced significantly. Full spectra of the synthetic standards were obtained by injecting 0.5–5 μg on column. The abundance of the MH^+ ion was observed to be higher at the top end of the range.

Animals and treatments

Male Swiss-Webster mice (16–25 g) were administered sodium phenobarbital (0.1% solution) as drinking water for 5 days. Animals were fasted 12 h prior to i.p. administration of AMAP (600 mg/kg) dissolved in warm saline. Urine was collected for 24 h in cups containing ascorbic acid and immersed in dry ice/acetone. Urine was first filtered through cotton wool then through a 0.45-μm Nylon-66 filter and frozen at −20°C until analyzed.

Preparations of standards

2-AcHQ[16], 3-OH-APAP[19], 3-OMe-APAP[19], 4-acetamido-*o*-benzoquinone (4-AOBQ)[20], 2-APBQ[17] and MAPQI[18] were synthesized as previously described. The following is the general procedure used for the preparation of the thioether conjugates. In a 5-ml Reacti-vial, CYSH or NACYSH (0.12 mmol) was dissolved in 2.5 ml phosphate buffer (pH 7.4) and sealed under nitrogen. The quinone or quinone imine (0.1 mmol) was dissolved in 1 ml acetonitrile (HPLC grade) and injected gradually through the septum of the vial under nitrogen. The reaction mixture was stirred for 30 min, acidified with formic acid to pH 2.0 and the acetonitrile removed using a gentle stream of nitrogen. The aqueous solutions were frozen at −20°C until HPLC purification was performed. Following purification and lyophyllization, the powders obtained were stored at −20°C. For NMR purposes, the powders were dissolved in ^2H_2O and lyophillized once more.

RESULTS

Synthesis of the mercapturic acid conjugates of 4-AOBQ

4-AOBQ when allowed to react with NACYSH gave several products as determined by HPLC–UV analysis and LC–MS. ^1H NMR analysis (Fig. 1) of the major product purified by HPLC revealed that this material was 3-(N-acetyl-cystein-S-yl)-5-acetamidocatechol. The CYSH β-methylene protons appeared as two sets of doublets of doublets at δ 3.16 and 3.42, while the α-proton appeared as a doublet of doublets at δ 4.37. The splitting pattern for the CYSH α and β protons is

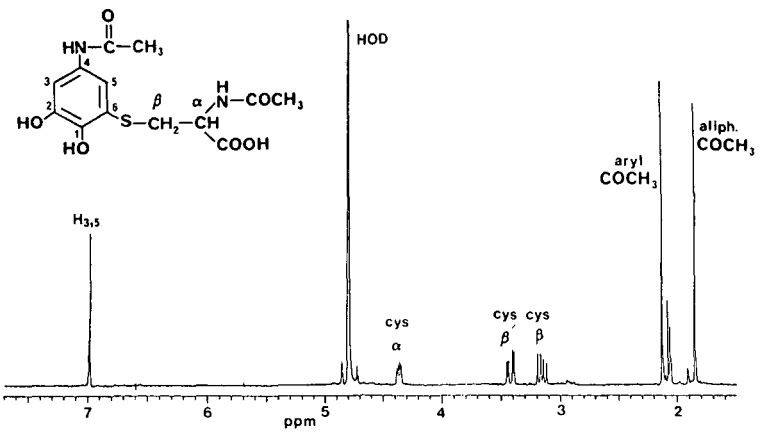

Fig. 1. ^{1}H NMR spectrum of the synthetic conjugate of 4-AOBQ.

characteristic of an ABX system. The methyl protons of the acetyl side chain of NACYSH appeared as a singlet at δ 1.85 and integrated for three protons. The methyl protons of the aryl acetamido group appeared as a singlet at δ 2.13 and integrated for three protons. The singlet at δ 6.98 integrated for two protons. These two aromatic protons were assigned to carbons 3 and 5 of the aromatic nucleus analogous to the glutathione conjugate of 4-AOBQ[18] which appear as two doublets with a coupling constant of 2.3 Hz.

The mercapturic acid conjugate was characterized further by TSP LC–MS (Fig. 2A). The spectrum showed a strong protonated molecular ion (MH^+) at *m/z* 329 and an ammonium adduct at *m/z* 346. In addition the spectrum showed several fragment ions at *m/z* 311, 287, 259, 200, 168, 147, 130. These ions are explained as follows (*m/z*): loss of H_2O (311), loss of ketene to give the CYSH conjugate (287), loss of H_2O from the CYSH conjugate (259), loss of N-acetyldehydroalanine to give the protonated catechol thiol (200), loss of N-acetyldehydrocysteine to give the protonated catechol compound (168), ammoniated N-acetyldehydroalanine (147), loss of H_2S from protonated NACYSH (130). Two other ions in the spectrum at *m/z* 217 and 182 are related to the base peak at *m/z* 200, the first being an ammonium ion adduct of the thiol compound and the other formed by elimination of water, respectively. This type of fragmentation to give the characteristic ions at *m/z* 200 and 168 have been observed previously in the spectra of the CYSH, NACYSH, and GSH conjugates of APAP (*m/z* 184, 152) under CI-MS[8] and TSP LC–MS[21] conditions. Under FAB-MS conditions, the CYSH and NACYSH conjugates of APAP essentially showed protonated molecular ions and sodiated molecular ions[9]. The fragment ion at *m/z* 287 is believed to be due to loss of ketene from the N-acetyl side chain and not from the aromatic acetamido group because the parent compound AMAP does not lose ketene to any significant extent.

A minor product of the reaction was the reduction product, 3-OH-APAP, as determined by co-chromatography with the synthetic standard and by LC–MS of the reaction mixture. Another minor product that eluted earlier on HPLC than the mercapturic acid conjugate was tentatively characterized as a *bis*-N-acetylcysteine conjugate of 4-AOBQ based on its LC–MS spectrum. The spectrum showed

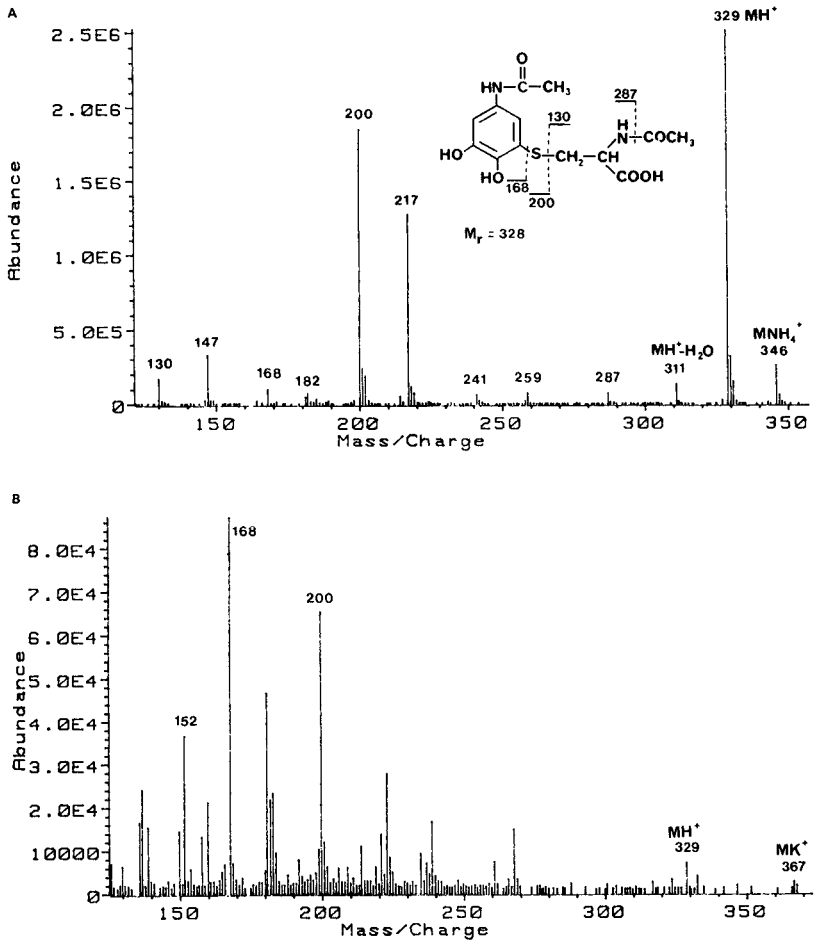

Fig. 2. (A) TSP LC–MS spectrum of the synthetic NACYSH conjugate of 4-AOBQ. (B) TSP LC–MS spectrum of the NACYSH conjugate of 4-AOBQ found in urine of mice given AMAP.

a relatively weak MH^+ at *m/z* 490 and ions at *m/z* 472 and 361 which would correspond to loss of H_2O and N-acetyldehydroalanine, respectively. Other characteristic ions were observed at *m/z* 329, 200, 182, 168, 130, the origin of which were explained above. Not enough material was on hand to rigorously characterize this compound further.

Synthesis of the cysteine conjugates of 4-AOBQ

When 4-AOBQ was allowed to react with CYSH, it gave one major adduct and a small amount of 3-OH-APAP. The reaction mixture was analyzed directly by LC–MS. The spectrum obtained for the CYSH adduct was very similar to that of the corresponding mercapturate except that the MH^+ was at *m/z* 287. Other characteristic ions were observed at *m/z* 217, 200, 168. No ions at *m/z* 146 or 130 were observed since these could only arise from the N-acetylcysteine type conjugates.

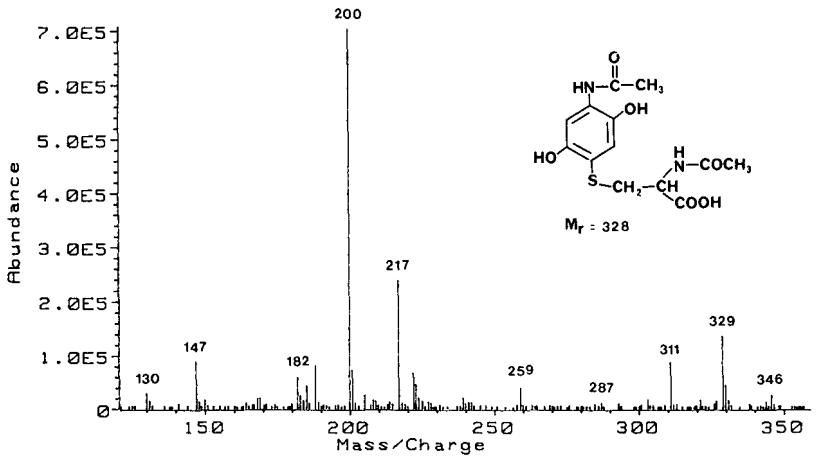

Fig. 3. TSP LC–MS spectrum of the synthetic NACYSH conjugate of 2-APBQ.

Synthesis of the mercapturic acid conjugates of 2-APBQ

When 2-APBQ was allowed to react with NACYSH, it gave several products that were characterized by LC–MS. Two major components of the reaction that were slightly resolved under the LC–MS conditions (see Experimental section) were characterized as *mono*-NACYSH conjugates of 2-APBQ. The spectrum in Fig. 3 is representative of these two compounds. Essentially the spectrum is very similar to that of the mercapturic acid conjugate of 4-AOBQ and showed the same ions discussed above. However, the 2-APBQ adduct eluted later in the chromatogram than that of the 4-AOBQ adduct. The other minor components that were observed in the analyzed mixture were the reduced quinone, 2-AcHQ, and what is tentatively characterized as a *bis*-N-acetylcysteine conjugate. This conjugate also eluted earlier than the *mono*-conjugates. The spectrum (Fig. 4) showed a MH^+ at m/z 490. Other characteristic ions

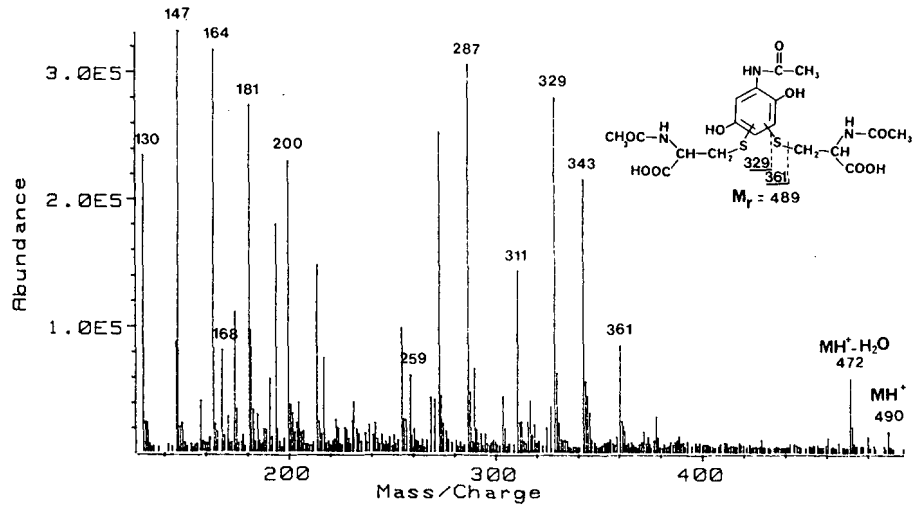

Fig. 4. TSP LC–MS spectrum of the synthetic *bis*-NACYSH conjugate of 2-APBQ.

were observed at *m/z* 472, 361, 343, 329, 311, 287, 217, 200, 168, 147, 130. Except for the ion at *m/z* 343 (loss of H_2O from ion at *m/z* 361), the origins for these ions were explained above for the 4-AOBQ *bis*-adduct. The spectrum also showed ions that would result from thermally formed NACYSH at *m/z* 181, 164, 146 which correspond to an ammonium ion adduct, protonated NACYSH, and loss of the elements of water, respectively. An authentic sample of NACYSH eluted earlier in the chromatogram, yet gave the same ions.

Synthesis of the cysteine conjugates of 2-APBQ

CYSH reacted with 2-APBQ to give the reduction product and two cysteine conjugates that were resolved under LC–MS conditions. Both conjugates gave the same ions observed for the CYSH conjugate of the regioisomer 4-AOBQ and had longer retention times.

Synthesis of the mercapturic acid conjugates of N-acetyl-3-methoxy-p-benzoquinone imine (MAPQI)

MAPQI underwent reaction with NACYSH to give two major products, 3-OMe-APAP and another product that was found to be a mercapturate following ^1H NMR and LC–MS analysis. The NMR spectrum (Fig. 5) showed three singlets at δ 1.82, 2.15, and 3.87, each integrated for three protons. These correspond to the acetyl protons of the side chain, the aryl acetamido group protons, and the 3-methoxy group protons, respectively. The CYSH β-methylene protons appeared as two sets of doublets of doublets at δ 3.12 and 3.45. The CYSH α-proton appeared as a doublet of doublets at δ 4.28. The aromatic protons appeared as two singlets at δ 7.02 and 7.11. The resonance of these protons as singlets suggests a *para* relationship. However, the broadness of the singlets suggests a small coupling which has not been observed for para protons for these type of compounds. In addition, both GSH[18] and CYSH (see below) add to MAPQI *meta* to the acetamido group, thereby giving rise to *meta* protons on carbons 2 and 6 of the conjugates. Therefore, the protons in this

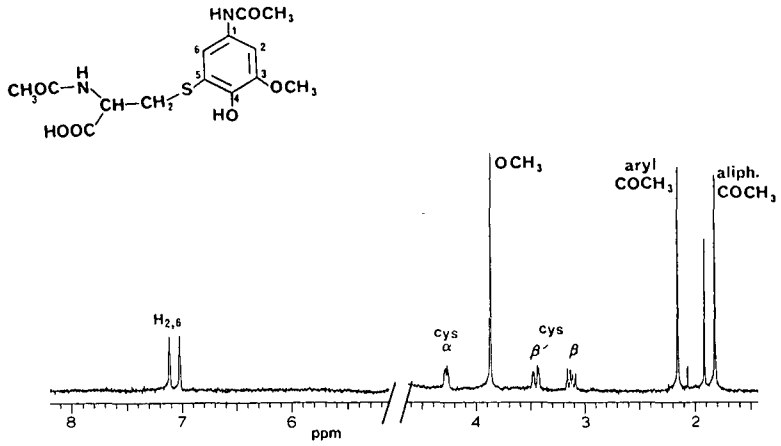

Fig. 5. ^1H NMR spectrum of the synthetic NACYSH conjugate of MAPQI.

mercapturic acid conjugate were assigned to the same carbons, and it is proposed that the compound is 3-(N-acetylcystein-S-yl)-5-methoxyacetaminophen. This compound was characterized further by LC–MS (Fig. 6A). The spectrum shows the MH^+ ion m/z 343 and other characteristic ions at m/z 301, 214, 228, 182. These correspond to losses of ketene, N-acetyldehydroalanine, N-acetyldehydroglycine, and N-acetyldehydrocysteine, respectively.

Synthesis of the cysteine conjugates of MAPQI

CYSH, when allowed to react with MAPQI also gave 3-OMe-APAP and a CYSH conjugate that was purified with HPLC. ^1H NMR (Fig. 7) indicated that this conjugate was 3-(cystein-S-yl)-5-methoxyacetaminophen. The assignement of the CYSH moiety to carbon 3 on the aromatic ring is based on the appearance of two

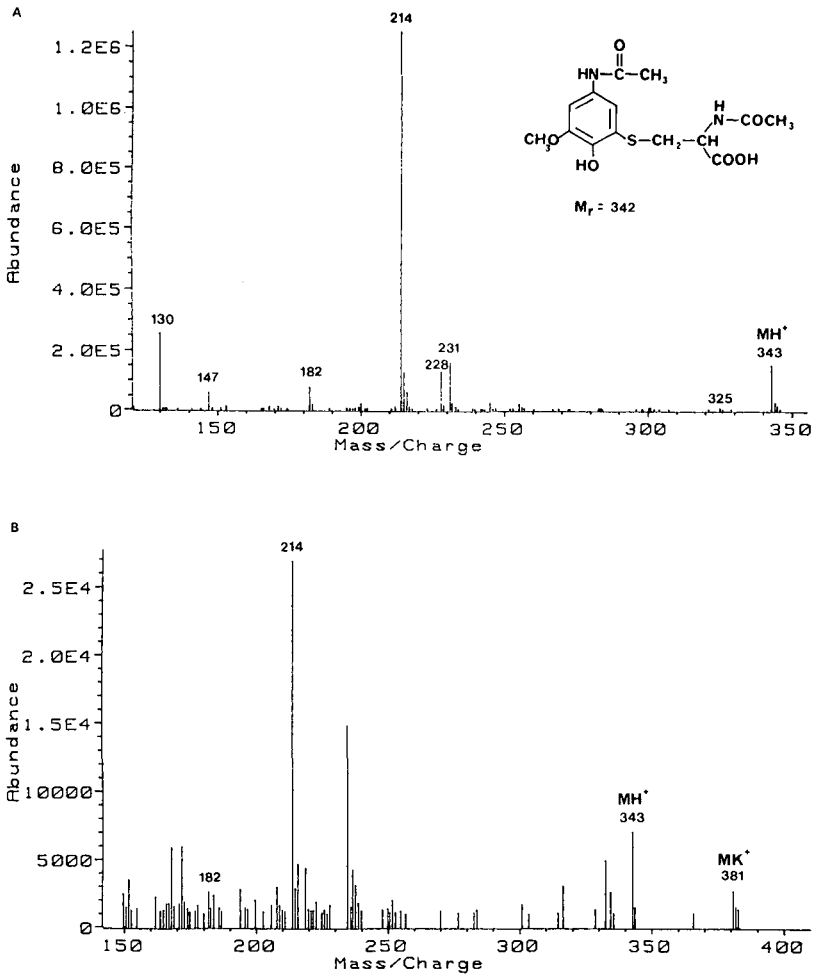

Fig. 6. (A) TSP LC–MS spectrum of the synthetic NACYSH conjugate of MAPQI. (B) TSP LC–MS spectrum of the synthetic NACYSH conjugate of MAPQI found in urine of mice given AMAP.

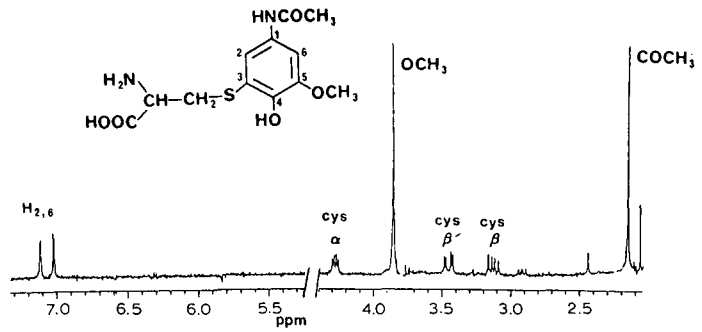

Fig. 7. ^{1}H NMR spectrum of the synthetic CYSH conjugate of MAPQI.

doublets at δ 7.02 and 7.12, each with a coupling constant of 2.3 Hz, indicating a *meta* relationship. Since the position of the 3-methoxy group is predefined, we assigned those protons to carbons 2 and 6, and hence the CYSH moiety must be attached to carbon 3. Further characterization of this compound was performed by LC–MS analysis. The spectrum of this compound exhibited an MH^+ ion at *m/z* 301 and the characteristic ions seen with the N-acetyl derivative, namely ions at *m/z* 214 and 228.

Studies in urine of mice treated with AMAP

The synthetic standards of the thioether conjugates of AMAP metabolites were used to develop an HPLC gradient elution program (see Experimental section) that gave baseline separation of these compounds as well as for AMAP, 3-OMe-APAP, 3-OH-APAP, 2-AcHQ. Table II provides the retention times for these compounds. When urine obtained from mice treated with AMAP (600 mg/kg) was analyzed under these conditions, UV peaks were observed at the retention times for the thioether adducts. Fig. 8 shows the chromatogram observed. The proposed identity of the peaks corresponding to the thioether conjugates was supported by co-chromatography with the standards.

TABLE II
HPLC RETENTION TIME DATA OF AMAP AND ITS KNOWN METABOLITES

Compound name	*Peak No.*	*Retention time (min)*
AMAP glucuronide	1	17.2
3-OMe-APAP glucuronide	2	17.5
AMAP	3	25.0
3-OMe-APAP	4	24.6
3-OH-APAP	5	15.8
2-AcHQ	6	16.3
CYCSH of AOBQ	7	19.0
NACYSH of AOBQ	8	23.5
CYSH of APBQ	9, 10	20.8, 21.8
CYSH of MAPQI	11	26.8
NACYSH of MAPQI	12	13.8

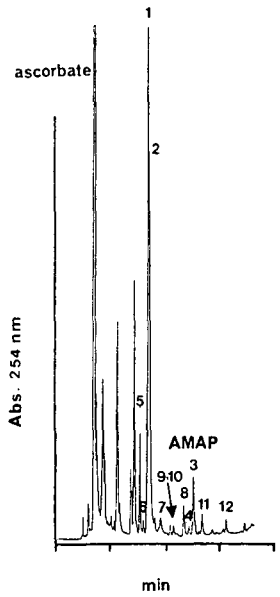

Fig. 8. HPLC analysis of urine obtained from mice treated with 600 mg/kg AMAP.

LC–MS analysis of urine

To further support conclusions described above, untreated urine was analyzed by TSP LC–MS under the same conditions used for analysis of the synthetic standards. Fig. 9 shows the total ion chromatogram (TIC) obtained. A search for the thioether adducts derived from AMAP was done by reconstructing ion chromatograms for the expected MH^+ ions and the base peak ions established for the standards. We were able to detect the NACYSH conjugate of AOBQ (Fig. 2B) and the NACYSH conjugates of MAPQI (Fig. 6B) as well as the CYSH conjugate of the latter. The major peak in the

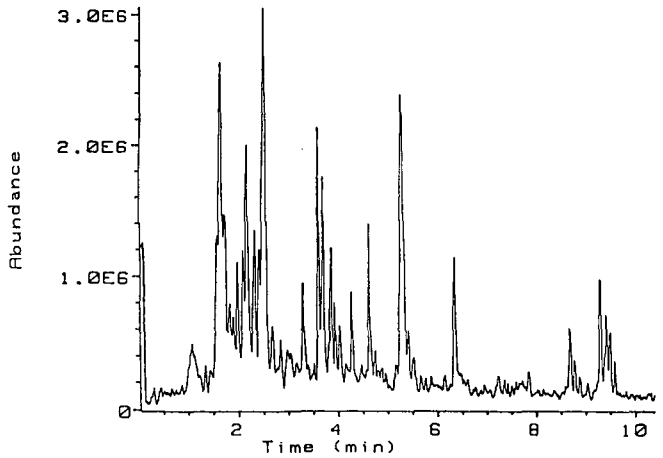

Fig. 9. Total ion chromatogram of the LC–MS analysis of urine obtained from mice treated with AMAP.

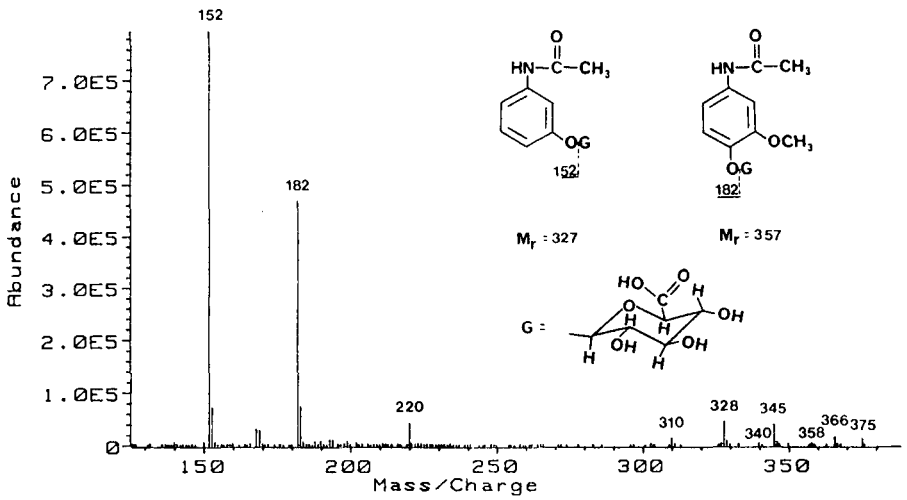

Fig. 10. TSP LC–MS spectrum of a mixture of AMAP glucuronide and 3-OMe-APAP glucuronide excreted in urine of mice given AMAP.

TIC (2.5 min) was found to correspond to a mixture of AMAP glucuronide and 3-OMe-APAP glucuronide that are co-eluting. The TSP mass spectrum of these two conjugates is shown in Fig. 10. The ions from the AMAP glucuronide were more dominant in the spectrum and they appeared at *m/z* 366 [MK^+], 350 [MNa^+], 345 [MNH_4^+], 328 [MH^+], 310 [$MH^+ - H_2O$], and 152 [MH^+ – dehydroglucuronic acid]. The ions from the 3-OMe-APAP glucuronide appeared at *m/z* 375 [MNH_4^+], 358 [MH^+], 340 [$MH^+ - H_2O$], and 182 [MH^+ – dehydroglucuronic acid]. When the authentic sample of the 3-OMe-APAP glucuronide isolated from bile of rabbits given acetaminophen was injected under the same conditions, it had the same retention time and gave the same ions observed for that present in AMAP urine. The identity of these two conjugates was also supported by their disappearance from the UV chromatograms following β-glucuronidase hydrolysis (data not shown). Glucuronide conjugates of the diphenolic metabolites of AMAP were also detected as a major component in the urine. TSP LC–MS spectrum of these components showed ions at *m/z* 382 [MK^+], 344 [MH^+], 326 [$MH^+ - H_2O$], and 168 [MH^+ – dehydroglucuronic acid]. The loss of the elements of water and that of neutral dehydroglucuronic acid (176 a.m.u.) is characteristic for this type of metabolites under TSP conditions[2,21,22].

CONCLUSION

Collectively the results presented above support previous work that indicated that AMAP is metabolized *in vivo* to three reactive intermediates, 2-APBQ, 4-AOBQ, and MAPQI. These intermediates are similar to NAPQI, the toxic metabolite from APAP, in being trapped as thioether adducts in the presence of GSH and metabolic breakdown products thereof are excreted in urine as CYSH and NACYSH adducts. Fig. 11 depicts the metabolic profile of AMAP in the mouse.

In order to investigate the importance of the reactive metabolite pathways in the

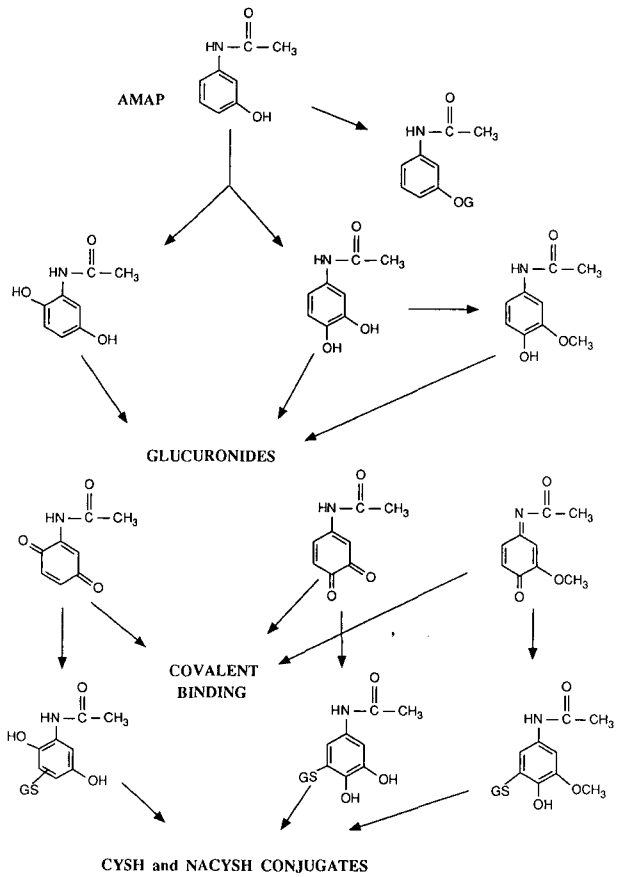

Fig. 11. Metabolic profile for the metabolism of AMAP in the mouse.

overall dispositon of AMAP, we synthesized appropiate standards, developed HPLC methods for separating the standards and utilized both NMR and MS techniques to characterize these compounds. The use of TSP LC–MS was critical in the characterization of the synthetic thioether standards because of their water solubility and their relative instability due to autooxidation especially of the hydroquinone type adducts that in some cases hampered isolation of the materials for NMR and direct mass spectral characterization by other soft ionization techniques such as FAB-MS. In addition, TSP spectra provided several characteristic fragmentation ions that aided in the unequivocal identification of the standards as well as the metabolites in urine. Work is in progress to determine the quantitative importance of the metabolic activation of AMAP in the overall disposition of AMAP.

ACKNOWLEDGEMENT

This work was supported by NIH Grant GM25418 (S.D.N.).

REFERENCES

1 C. R. Blakely, J. J. Carmody and M. L. Vestal, *J. Am. Chem. Soc.*, 102 (1980) 5931.
2 D. J. Liberato, C. C. Fenselau, M. L. Vestal and A. L. Yergey, *Anal. Chem.*, 55 (1983) 1741.
3 R. D. Voyksner and E. D. Bush, *Biomed. Environ. Mass. Spectrom.*, 14 (1987) 213.
4 T. A. Bellar and W. L. Budde, *Anal. Chem.*, 60 (1988) 2076.
5 C. E. M. Heeremans, R. A. M. van der Hoeven, W. M. A. Niessen, U. R. Tjaden, G. F. La Vos and J. van der Greef, *Biomed. Environ. Mass. Spectrom.*, 17 (1988) 377.
6 M. S. Lan, J. Oxford and L. E. Martin, *J. Chromatogr.*, 394 (1987) 223.
7 J. N. H. Meerman, F. E. Beland, B. Ketterer, S. K. S. Srai, A. P. Baruins and G. J. Mulder, *Chem. Biol. Interactions,* 39 (1982) 149.
8 S. D. Nelson, Y. Vaishnav, H. Kambara and T. A. Baillie, *Biomed. Mass. Spectrom.*, 8 (1981) 244.
9 B. L. Ackerman, J. T. Watson, J. F. Newton, Jr., J. B. Hook and W. E. Braselton, Jr., *Biomed. Environ. Mass. Spectrom.*, 11 (1984) 502.
10 C. E. Parker, J. S. M. de Wit, R. W. Smith, M. B. Gopinathan, O. Hernandez, K. B. Tomer, C. H. Vestal, J. M. Sanders and J. R. Bend, *Biomed. Environ. Mass Spectrom.*, 15 (1988) 623.
11 A. Conchillo, J. Casas, A. Messeguer and J. Abián, *Biomed. Environ. Mass Spectrom.*, 16 (1988) 339.
12 S. A. Roberts and D. J. Jollow, *Fed. Proc.*, 38 (1979) 426.
13 E. B. Nelson, *Res. Commun. Chem. Pathol. Pharmacol.*, 28 (1980) 447.
14 S. A. Roberts and D. J. Jollow, *Pharmacologist*, 2 (1978) 259.
15 M. Hamilton and P.T. Kissinger, *Drug. Metab. Dispos.*, 14 (1986) 5.
16 A. J. Streeter, S. M. Bjorge, D. B. Axworthy, S. D. Nelson and T. A. Baillie, *Drug Metab. Dispos.*, 12 (1984) 565.
17 A. J. Streeter and T. A. Baillie, *Biochem. Pharmacol.*, 34 (1985) 2871.
18 M. S. Rashed and S. D. Nelson, *Chem. Res. Toxicol.*, 2 (1989) 41.
19 A. J. Forte, J. M. Wilson, J. T. Slattery and S. D. Nelson, *Drug Metab. Dispos.*, 12 (1984) 484.
20 M. F. Ansell, A. F. Bignold, A. F. Gosden, V. J. Leslie and R. A. Murray, *J. Chem. Soc. C,* (1971) 1414.
21 L. D. Betowski, W. A. Korfmacher, J. O. Lay, Jr., D. W. Potter and J. A. Hinson, *Biomed. Environ. Mass Spectrom.*, 14 (1987) 705.
22 C. Fenselau and L. Yellet, in G. G. Paulson, J. Caldwell, D. H. Huston and J. J. Menn (Editors), *Xenobiotic Conjugation Chemistry, ACS Symp. Ser.*, 299 (1986) 159.

Journal of Chromatography, 474 (1989) 223–230
Elsevier Science Publishers B.V., Amsterdam — Printed in The Netherlands

CHROM. 21 518

APPLICATION OF THERMOSPRAY LIQUID CHROMATOGRAPHY–MASS SPECTROMETRY TO THE SIMULTANEOUS QUANTIFICATION OF TRACER CONCENTRATIONS OF ISOTOPICALLY LABELLED CARBAMAZEPINE EPOXIDE AND STEADY-STATE LEVELS OF CARBAMAZEPINE AND CARBAMAZEPINE EPOXIDE

MARKUS J. MOOR
Department of Pharmaceutics, University of Washington, Seattle, WA 98195 (U.S.A.)
MOHAMED S. RASHED
Department of Medicinal Chemistry, School of Pharmacy, BG-20, University of Washington, Seattle, WA 98195 (U.S.A.)
THOMAS F. KALHORN and RENÉ H. LEVY
Department of Pharmaceutics, University of Washington, Seattle, WA 98195 (U.S.A.)
and
WILLIAM N. HOWALD*
Department of Medicinal Chemistry, School of Pharmacy, BG-20, University of Washington, Seattle, WA 98195 (U.S.A.)

SUMMARY

A thermospray high-performance liquid chromatography–mass spectrometry method for the separation and quantification of tracer concentrations of isotopically labelled carbamazepine epoxide ([^{15}N, ^{13}C]CBZE) in the presence of steady-state levels of the anticonvulsant carbamazepine (CBZ) and its epoxide metabolite (CBZE) has been developed. The technique does not require derivatization, demonstrates little or no thermal degradation of the analytes, provides increased specificity not available from conventional high-performance liquid chromatography, and has a detection limit of 500 pg for CBZE on-column. The method, incorporating d_4-CBZ and d_4-CBZE as internal standards, allows precise and accurate determination of the analytes with good reproducibility and stability.

INTRODUCTION

The epoxide hydrolase (EH) enzyme system is mainly involved in detoxification reactions of cytotoxic and genotoxic arene oxide xenobiotic metabolites[1]. Knowledge of the overall activity of this enzyme system *in vivo* may be of clinical importance enabling the prediction of individual susceptibility to adverse drug and environmental effects.

Carbamazepine-10,11-epoxide (CBZE, Fig. 1) is one of the principle metabolites of the anticonvulsant carbamazepine (CBZ, Fig. 1). The majority of the epoxide

0021-9673/89/$03.50

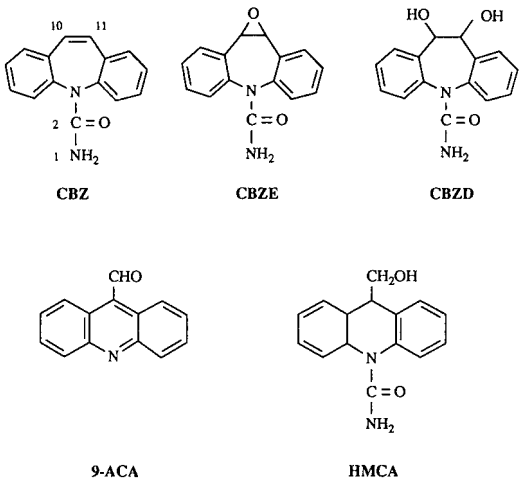

Fig. 1. Structures of Carbamazepine (CBZ); carbamazepine-10,11-epoxide (CBZE); carbamazepine-10,11-transdihydrodiol (CBZD); 9-hydroxymethyl-10-carbamoylacridan (HMCA); and 9-acridinecarboxaldehyde (9-ACA).

formed is ultimately converted to carbamazepine-10,11-transdihydrodiol (CBZD, Fig. 1) by EH. The ratio of CBZE to CBZ is reported to be higher in children than in adults, with the ratios being highest in very young children[2,3]. To examine this implied age dependent development of the EH enzyme system, CBZE pharmacokinetics must be evaluated in epileptic children on CBZ monotherapy. Such an evaluation requires an analytical method capable of distinguishing administered CBZE from the CBZE formed as a metabolite of CBZ.

Several gas chromatographic (GC) methods have been developed for the analysis of CBZ and CBZE[4,5], some of which have utilized mass spectrometric (MS) detection techniques[6,7]. However, the thermal degradation of the epoxide metabolite to 9-acridinecarboxaldehyde (9-ACA, Fig. 1) during GC analysis[8] has precluded this detection method from use with regard to isotopic labelling in the 1- and 2-positions of the molecule. High-performance liquid chromatography (HPLC) in combination with less specific detection methods, on the other hand, are routinely employed in the clinical assay of CBZ and CBZE and demonstrate no such degradation difficulties[9,10].

The thermospray liquid chromatography–mass spectrometry (TSP LC–MS) technique has proven to be a valuable and reliable tool in the routine detection and analysis of underivatized endogenous compounds that are intractable to GC–MS methods[11]. This paper describes a TSP LC–MS analytical methodology for the simultaneous determination of administered [1-^{15}N,2-^{13}C]carbamazepine epoxide ([^{15}N,^{13}C]CBZE), CBZE and CBZ in human blood utilizing stable isotope labelled internal standards and offers an assessment of the sensitivity, precision and accuracy of the technique in the quantification of these compounds.

MATERIALS AND METHODS

Reagents

Carbamazepine and 9-hydroxymethyl-10-carbamoylacridan were a generous gift from Ciba-Geigy (Summit, NJ, U.S.A.). Iminostilbene (>97% pure) and *m*-chloroperbenzoic acid (85% pure) were purchased from Fluka (Ronkonkoma, NY, U.S.A.) and used without further purification. Phosgene (^{13}C, 99%) 6.30% (w/w) in benzene, gaseous ammonia (^{15}N, 99%) and sulfuric acid ($^{2}H_2SO_4$, 99%) were supplied by Cambridge Isotope Laboratories (Woburn, MA, U.S.A.). Anhydrous ethanol (OD, 99%) was obtained from ICN Biomedicals (Cambridge, MA, U.S.A.). All solvents used in synthesis were reagent grade. Acetonitrile for HPLC was obtained from Burdick & Jackson Labs. (Muskegon, MI, U.S.A.). Ammonium acetate and polyethylene glycol (PEG-200) were purchased from J. T. Baker (Phillipsburg, NJ, U.S.A.) and Aldrich (Milwaukee, WI, U.S.A.), respectively.

Synthetic procedures

[1-^{15}N,2-^{13}C]Carbamazepine epoxide ([^{15}N,^{13}C]CBZE). [^{15}N,^{13}C]CBZ was synthesized by the sequential reaction of iminostilbene with [^{13}C]phosgene and [^{15}N]ammonia according to Osterloh and Bertilsson[12]. The epoxidation of the purified [^{15}N,^{13}C]CBZ was achieved using *m*-chloroperbenzoic acid and the product, [^{15}N,^{13}C]CBZE, was recrystallized from ethanol. Purity and identity of the synthesized compound were verified by thin-layer chromatography (TLC) and melting point analysis and further confirmed by NMR and MS[8,13]. The ^{1}H NMR (300 MHz) in deuterochloroform using tetramethylsilane as internal standard, was found to be identical to that of the authentic unlabelled compound with the exception of the amino group protons at position 1. These appeared as a doublet at δ 4.59 ($^{1}J_{H,N}$ = 90 Hz) due to the ^{15}N–H coupling. The electron impact mass spectrum was in agreement with that published earlier[8], but exhibited the ions *m/z* 254 $[M]^{+\cdot}$ and 225 $[M-CHO]^{+}$ in contrast to *m/z* 252 $[M]^{+\cdot}$ and 223 $[M-CHO]^{+}$ as seen for authentic CBZE.

[$^{2}H_4$]Carbamazepine (d_4-CBZ) and [$^{2}H_4$]carbamazepine epoxide (d_4-CBZE). These two compounds were prepared as above using [$^{2}H_4$]iminostilbene (d_4-IMS), phosgene and ammonia as starting materials. The d_4-IMS was obtained by twice heating iminostilbene for 24 h at 78°C with anhydrous ethanol-d_1 in the presence of $^{2}H_2SO_4$ ($^{2}H_2SO_4$–$C_2H_5O^{2}H$, 1:100, v/v) according to a published procedure[12]. Electron impact mass spectra of the recrystallized d_4-CBZE and d_4-CBZ showed identical isotopic composition. The compounds contained 63% of the d_4 isomer and 4% d_6, 20% d_5, 12% d_3 and 1% d_1.

Chromatography

HPLC analysis was carried out under isocratic conditions using a LKB 2150 HPLC pump combined with a LKB 2152 controller unit (LKB, Bromma, Sweden). Samples were injected via a Valco C6W manual injector (Valco Instruments, Houston, TX, U.S.A.) equipped with a 100-μl sample loop. Separations were achieved on a Spherisorb C_8 analytical column (25 cm × 4.6 mm I.D., 5 μm Phase Separation, Norwalk, CN, U.S.A.) connected to a Brownlee RP-8 guard column (1.5 cm × 3.2 mm I.D., 7 μm, Brownlee Labs., Santa Clara, CA, U.S.A.). The mobile phase was acetonitrile–0.1 *M* ammonium acetate (40:60) at a flow-rate of 1.2 ml/min.

Mass spectrometry

TSP LC–MS analysis was performed in positive ion mode with the filament off, utilizing a Vestec Model 201 dedicated thermospray masss spectrometer (Vestec, Houston, TX, U.S.A.) with a directly heated probe vaporizer[14]. Thermospray probe control and tip temperatures were 120 and 180°C, respectively, and adjusted to maintain a jet temperature of 250°C. The source block was held at 300°C. A Hewlett-Packard 59979C ChemStation™ (Palo Alto, CA, U.S.A.) data system was used to control the mass analyzer and the data acquisition in selected-ion monitoring (SIM) mode. Selected ions of a 100 ppm solution of PEG 200 in 0.1 *M* ammonium acetate were used to provide mass calibration of the data system. Ions monitoring were *m/z* 253.1, 255.1 and 257.1, corresponding to the MH^+ ions of the CBZE analytes and their d_4-labelled internal standard and *m/z* 237.1 and 241.1, corresponding to the MH^+ of CBZ and its d_4-analogue. The dwell-times were set at 350 ms/ion for CBZE analogues and at 750 ms/ion for CBZ and its internal standard.

Quantitative analysis

Sample preparation. To each 250 μl blood sample, 50 μl of each of the two methanolic internal standard solutions containing d_4-CBZE (5 μg/ml) and d_4-CBZ (25 μg/ml), respectively, was added. Following the addition of 5 ml of dichloromethane, the samples were shaken for 20 min in a horizontal shaker and centrifuged at 500 *g* for 5 min at room temperature. The organic phase was then transferred to a disposable glass tube and again to a glass storage vial using a pasteur pipet. After evaporation to dryness the vials were capped and stored at −20°C to await TSP LC–MS analysis. For the generation of standard curves, 25 μl aliquots of each of five methanolic stock solutions containing increasing amounts of [^{15}N,^{13}C]CBZE (0.5, 1.0, 2.5, 5.0 and 10.0 μg/ml), CBZE (2.5, 5.0, 12.5, 25.0 and 50.0 μg/ml) and CBZ (5.0, 10.0, 25.0, 50.0 and 100 μg/ml) were added to 250 μl of blank human blood in separate vials and processed in the same manner as the samples.

With each sample set, two 250 μl control blood samples were assayed to monitor the precision and reproducibility of the method. Stocks of these samples containing 0.10, 0.50 and 5.0 μg/ml and 0.75, 2.0 and 10.0 μg/ml of [^{15}N,^{13}C]CBZE, CBZE and CBZ, respectively, were stored at −20°C and used throughout the study.

Analysis. Chromatographic analysis was performed using 20 μl aliquots of the samples reconstituted in 100 μl of mobile phase. Individual ion intensities were integrated using standard Hewlett-Packard MSD-GC™ software. Peak areas of [^{15}N,^{13}C]CBZE were corrected for the natural abundance derived from the unlabelled CBZE in the samples. The correction factor was determined empirically by LC–MS analysis of CBZE stock-solutions.

Response ratios for each analyte relative to its internal standard were calculated and used for the generation of the standard curves or the determination of the analyte concentration in patient and control samples.

RESULTS AND DISCUSSION

Optimization of chromatographic and instrumental parameters

Previously reported HPLC methods[9,10] were modified by the incorporation of ammonium acetate into the mobile phase to allow for TSP ionization of the analytes.

As may be seen in the reconstructed ion chromatogram illustrated in Fig. 2A, the acetonitrile–0.1 *M* ammonium acetate (40:60) mobile phase employed, resulted in excellent separation of CBZE (peak 3) and CBZ (peak 4) which eluted at 4.3 min and 6.4 min, respectively. In addition to the peaks of CBZE and CBZ, two other CBZ metabolites were detected. The diol, CBZD and [^{15}N,^{13}C]CBZD, was found to elute at 2.7 min (Fig. 2A, peak 1) and could have been monitored if the corresponding MH^+ of these compounds at *m/z* 271 and 273 had been acquired. The peak eluting at 3.9 min (Fig. 2A, peak 2) was identified as 9-hydroxymethyl-10-carbamoylacrian (HMCA, Fig. 1), whose MH^+ is isobaric with that of the labelled CBZE at *m/z* 255. Under the LC conditions employed, baseline separation of these two compounds was achieved (Fig. 2B).

The TSP LC–MS spectra of CBZE and CBZ showed protonated molecular ions

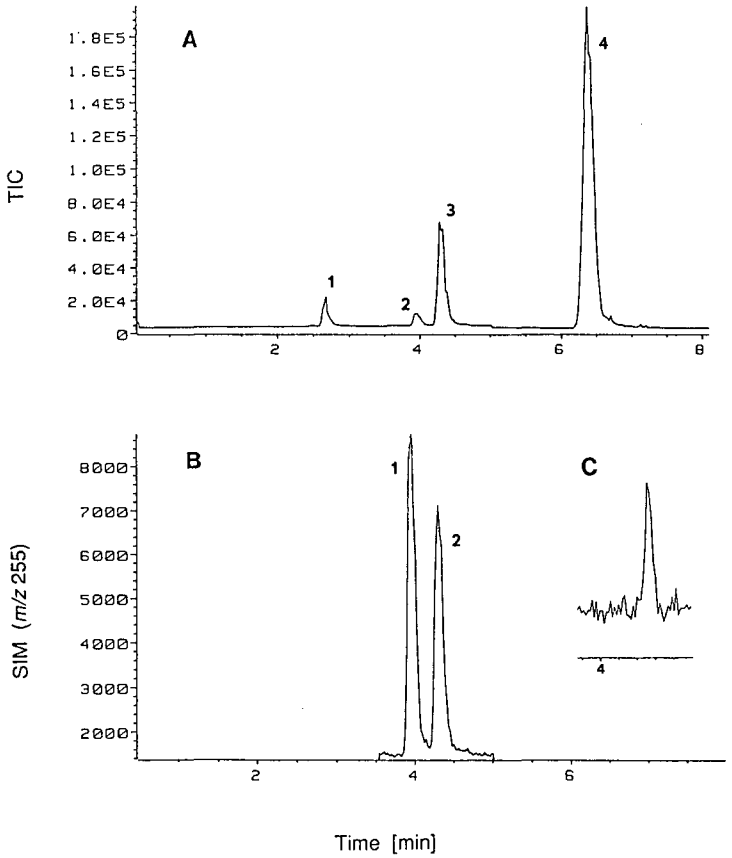

Fig. 2. TSP LC–MS ion current chromatograms from a patient blood sample. (A) Total-ion current chromatogram with the compounds being detected and the ions monitored for each peak as follows: 1 = *m/z* 271 and 273 (CBZD and [^{15}N,^{13}C]CBZD); 2 = *m/z* 255 (HMCA); 3 = *m/z* 253, 255 and 257 (CBZE, [^{15}N,^{13}C]CBZE and d_4-CBZE); 4 = *m/z* 237 and 241 (CBZ and d_4-CBZ). (B) Selected-ion current chromatogram *m/z* 255; 1 = HMCA; 2 = [^{15}N,^{13}C]CBZE at a blood concentration of 0.204 μg/ml. (C) Selected-ion current chromatogram *m/z* 255; detection of 1 ng [^{15}N,^{13}C]CBZE on-column. Signals in each chromatogram are normalized to the most intense peak.

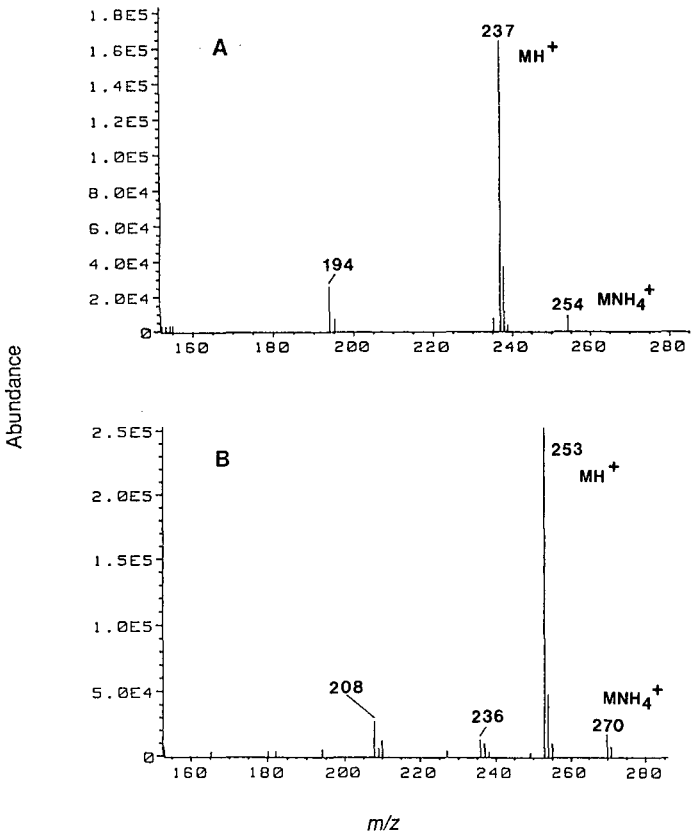

Fig. 3. TSP mass spectra of CBZ (A) and CBZE (B).

as their base peaks (Fig. 3). In addition, minor ammonium adducts were observed. Quantitative analysis was performed in the SIM mode for the protonated molecular ions. Thus, ions of *m/z* 253, 255 and 257 were monitored for the CBZE analogues in the time window between 3.5 and 5.0 min and ions of *m/z* 237 and 241 for CBZ between 5.0 and 8.0 min.

Critical TSP temperature parameters were optimized by injection of pure analytes on column. It was observed that source temperature variations over the range of 280 to 320°C did not significantly effect the TSP ionization. However, as observed by others[15], high jet temperatures resulted in pronounced instabilities of the jet leading to "spiking" in peak chromatographic profiles, while low jet temperatures yielded significant losses in sensitivity. To overcome this difficulty the peak width of the analytes were determined and dwell times chosen to enable at least 12 to 15 sampling across the peak of each ion monitored. The jet temperature was then adjusted to provide the optimal combination of sensitivity and stability. By this method the jet temperature of 250°C and dwell times of 350 and 750 ms for the CBZE and CBZ analogues, respectively, were established.

The ion chromatogram illustrated in Fig. 3C shows 1 ng of standard [^{15}N,^{13}C]CBZE on-column obtained by monitoring the MH^+ ion at a dwell time of 350 ms. The detection limit was 500 pg with a signal to noise ratio of 3:1.

Standard curves

For all the quantitative calculations peak areas of [^{15}N-^{13}C]CBZE were corrected for contributions resulting from the natural abundance of the unlabelled CBZE. Correction factors were determined empirically by the TSP LC–MS analysis of CBZE. For the generation of the standard curves, peak area ratios of analytes to internal standards were plotted against standard sample concentrations. Over the concentration ranges of 0.05–1.0 μg/ml, 0.25–5.0 μg/ml and 0.50–10.0 μg/ml for [^{15}N,^{13}C]CBZE, CBZE and CBZ, respectively, the standard curves were found to be linear with correlation coefficients greater than 0.999.

As discussed elsewhere[16,17], the detection of natural isotopic species from an analyte in the mass window of the internal standard results in standard curves which diverge from linear. In all cases presented, these isotopic contributions were found to be minor and an insignificant source of non-linearity. Of greater consequence was the observed 2.02% isotopic contribution of CBZE to the measured abundance of [^{15}N,^{13}C]CBZE at *m/z* 255. Since all of the standard solutions contained CBZE and [^{15}N,^{13}C]CBZE in the ratio of 5:1, the use of the observed peak areas in the generation of standard curves for the latter would have resulted in an approximate 10% systematic error. In the quantification of patient samples, where the ratios were as high as 40:1, the correction for isotopic contribution was found to be correspondingly more critical.

Precision and accuracy data of the assay are summarized in Table I. The intra-day variability was determined by analysis of triplicate extracts of the control samples throughout the day and was less than 1% for CBZ and CBZE, and 6% for [^{15}N,^{13}C]CBZE at a blood concentration of 100 ng/ml. The interday reproducibility showed coefficients of variation of less than 9% in all cases. Furthermore, it was found that the calculated concentrations were in good agreement with the predicted values.

TABLE I

INTRA- AND INTER-DAY VARIATIONS FOR [^{15}N,^{13}C]CBZE, CBZE AND CBZ IN HUMAN BLOOD CONTROL SAMPLES

Compound	*Nominal concentration (μg/ml)*	*Intra-day variation (n = 3)*		*Inter-day variation (n = 3)*	
		Mean (μg/ml)	*C.V. (%)*	*Mean (μg/ml)*	*C.V. (%)*
[^{15}N,^{13}C]CBZE	0.100	0.10	5.7	0.11	6.2
	0.750	0.76	3.9	0.72	7.3
CBZE	0.500	0.58	1.0	0.54	8.9
	2.000	2.05	1.0	1.98	7.7
CBZ	5.000	5.05	0.4	5.12	1.3
	10.000	10.94	0.1	10.66	5.4

CBZ, CBZE and [^{15}N-^{13}C]CBZE concentrations in patient blood samples

This method has been used to measure CBZ, CBZE and [^{15}N,^{13}C]CBZE in over 200 blood samples of children on CBZ monotherapy. The steady-state blood concentrations for CBZ and CBZE were found to be in the range of 8–12 and 1–2 μg/ml, respectively. Values for [^{15}N,^{13}C]CBZE varied in the range 50–800 ng/ml.

CONCLUSIONS

A TSP LC–MS method which allows the simultaneous quantification of [^{15}N,^{13}C]CBZE, CBZE and CBZ from blood samples after a single extraction procedure has been developed. The technique has proven to be rapid, sensitive and reliable, demonstrating little or no thermal degradation of the analytes, and unlike GC–MS methods does not require derivatization. The high specificity of LC–MS in combination with the exact control of sample recovery, using d_4-CBZE and d_4-CBZ as internal standards, provides precise and accurate determination of the analytes, with a detection limit for CBZE of 500 pg on-column. To date, this analytical procedure has been successfully utilized in the analysis of [^{15}N,^{13}C]CBZE, CBZE and CBZ in over 200 blood samples collected in single dose pharmacokinetic studies conducted in children on CBZ monotherapy.

ACKNOWLEDGEMENTS

This research was supported by research grant GM 37752 from the National Institutes of Health. We would like to thank Ms. Shannon West for her efforts in manuscript preparation and Ms. Martha Moore for her fine technical assistance.

REFERENCES

1 F. Oesch, *Arch. Toxicol.*, 60 (1987) 174.
2 L. McKauge and H. J. Tyrer, *Ther. Drug Monit.*, 3 (1981) 63.
3 S. Pynnonen, M. Sillanpaa, H. Frey and E. Sisalo, *Eur. J. Clin. Pharmacol.*, 11 (1977) 129.
4 R. E. Chambers, *J. Chromatogr.*, 154 (1978) 272.
5 C. Pantarotto, V. Crunelli, J. Lanzoni, A. Frigerio and A. Quattrone, *Anal. Biochem.*, 93 (1979) 115.
6 W. F. Trager, R. H. Levy, I. H. Patel and J. N. Neal, *Anal. Lett.*, B11(2) (1978) 119.
7 D. Alkalay, S. Carlson, S. Miotto and D. Gaudry, in W. W. Harrison (Editor), *"Simultaneous Quantification of Carbamazepine, Carbamazepine-10,11-epoxide and Carbamazepine-10,11-diol in Plasma by Gas Chromatography–Mass Spectrometry", Proceedings of the 36th ASMS Conference of Mass Spectrometry and Allied Topics, San Francisco, CA, June 5–10, 1988.*
8 K. M. Baker, A. Frigerio, P. L. Morselli and G. Pifferi, *J. Pharm. Sci.*, 62 (1973) 475.
9 A. A. Elyas, N. Ratnaraj, V. D. Goldberg and P. T. Lascelles, *J. Chromatogr.*, 231 (1982) 93.
10 N. Wad, *J. Chromatogr.*, 305 (1984) 127.
11 C. R. Blakely and M. L. Vestal, *Anal. Chem.*, 55 (1983)
12 J. Osterloh and L. Bertilsson, *Life Sci.*, 23 (1978) 83.
13 G. Bellucci, G. Berti, C. Chiappe, A. Lippi and F. Marioni, *J. Med. Chem.*, 30 (1987) 768.
14 M. L. Vestal and G. J. Fergusson, *Anal. Chem.*, 57 (1985) 2373.
15 M. S. Lant, J. Oxford and L. E. Martin, *J. Chromatogr.*, 394 (1987) 223.
16 W. A. Garland and R. P. Powell, *J. Chromatogr. Sci.*, 19 (1981) 392.
17 A. L. Yergey, N. V. Esteban and D. J. Liberato, *Biomed. Environ. Mass Spectrom.*, 14 (1987) 623.

Journal of Chromatography, 474 (1989) 231–243
Elsevier Science Publishers B.V., Amsterdam — Printed in The Netherlands

CHROM. 21 387

CHARACTERIZATION OF SOLUTION-PHASE AND GAS-PHASE REACTIONS IN ON-LINE ELECTROCHEMISTRY–THERMOSPRAY TANDEM MASS SPECTROMETRY

KEVIN J. VOLK, RICHARD A. YOST* and ANNA BRAJTER-TOTH
Department of Chemistry, University of Florida, Gainesville, FL 32611 (U.S.A.)

SUMMARY

Electrochemistry was used on-line with high-performance liquid chromatography–thermospray tandem mass spectrometry to provide insight into the solution-phase decomposition reactions of electrochemically generated oxidation products. Products formed during electrooxidation were monitored as the electrode potential was varied. The solution reactions which follow the initial electron transfer at the electrode are affected by the vaporizer tip temperature of the thermospray probe and the composition of the thermospray buffer. Either hydrolysis or ammonolysis reactions of the initial electrochemical oxidation products can occur with pH 7 ammonium acetate buffer. Both the electrochemically generated and the synthesized disulfide of 6-thiopurine decompose under thermospray conditions to produce 6-thiopurine and purine-6-sulfinate. Solution-phase studies indicate that nucleophilic and electrophilic substitution reactions with purine-6-sulfinate result in the formation of purine, adenine, and hypoxanthine. Products were identified and characterized by tandem mass spectrometry. This work shows the first example of high-performance liquid chromatography used on-line with electrochemistry to separate stable oxidation products prior to analysis by thermospray tandem mass spectrometry. In addition, solution-phase and gas-phase studies with methylamine show that the site of the nucleophilic and electrophilic reactions is probably inside the thermospray probe. Most importantly, these results also show that the on-line combination of electrochemistry with thermospray tandem mass spectrometry provides valuable information about redox and associated chemical reactions of biological molecules such as the structures of intermediates or products as well as providing insight into reaction pathways.

INTRODUCTION

Redox reactions play an important role in the metabolism and activation of xenobiotics and other substances. Because modern electrochemical methods have been shown to be useful in mimicking enzyme-catalyzed oxidation reactions[1–7], the combination of electrochemistry with mass spectrometry (MS) can provide important chemical information about intermediates and products formed in these redox reac-

0021-9673/89/$03.50

tions[8,9]. Most importantly, tandem mass spectrometry (MS–MS) can be used to confirm the presence of reaction intermediates as well as provide structural information. The driving force behind this work lies in the similarity between the biological oxidation and the electrochemical oxidation of many types of biologically important compounds such as purine drugs[10].

6-Thiopurine (6-TP) is a potent antineoplastic agent used in the treatment of several types of leukemia. However, its use has been restricted due to hepatotoxicity in some patients[11]. 6-TP is known to undergo extensive metabolism along several possible routes such as the transformation to its nucleotide[12], and nucleoside[13]. Hyslop and Jardine[11] have recently described a previously unknown oxidation pathway of 6-TP which involves activation by cytochrome P-450 with subsequent binding to protein via mixed disulfide bonds.

The electrochemical oxidation pathways of 6-TP and other structurally similar thiopurines such as 6-thioxanthine (6-TX), and 6-thioguanine (6-TG) have been extensively studied by off-line methods[1–3,14]. At low potentials, the first step in the oxidation of thiols is a one-electron process resulting in thiyl radicals followed by rapid dimerization to form disulfides. The S–S bonds of many disulfides have been shown to be unstable in acidic and basic media[2,15]. Cleavage of the S–S bond by a hydroxide ion will regenerate the parent thiol and give rise to a sulfinic acid[15–17]. The parent thiols are regeneratad in *ca.* 70% yield in this disproportionation process[15] (Fig. 1). The compound 6-thiopurine serves as an excellent model for studying the electrochemical oxidation of thiopurines because only the thiol group is involved in the oxidation process in the potential range from 0.0 to +1.1 V *vs.* Pd which is the normally accessible potential range in aqueous electrolytes. Other substituted thiopurines such as 6-TX and 6-TG behave differently electrochemically than 6-TP at high potentials of *ca.* 1.0 V. The difference in electrochemical behavior is due to the electronegative substituents which make the purine ring more vulnerable to oxidation. However, all three thiopurines are thought to undergo a one-electron oxidation at moderately low potentials to form a thiyl radical resulting in disulfide formation. This has been shown for 6-TX and 6-TG[2,3]. It is often difficult to verify this by coulometry because of the disproportionation reaction which regenerates the starting material in high yield[2]. The electrochemical oxidation products of 6-TP have been previously identified as bis(6-purinyl) disulfide, purine-6-sulfonic acid, and purine-6-sulfinic acid

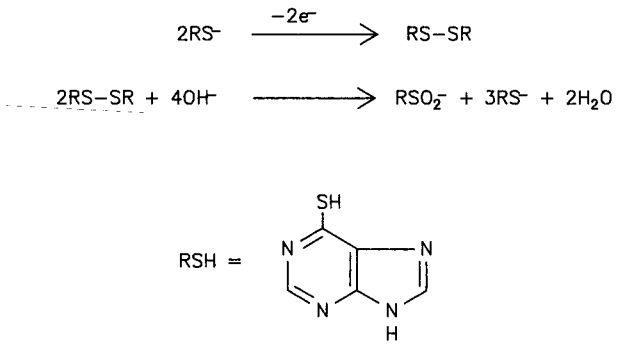

Fig. 1. Oxidation of 6-thiopurine to form 6-thiopurine disulfide, followed by disproportionation in alkaline media to form purine-6-sulfinate and the original thiol.

by comparison of the polarographic waves of electrolysis solutions with authentic standards[14].

Since the introduction of thermospray as a viable high-performance liquid chromatographic (LC)–MS interface, this technique has gained popularity as a soft ionization technique that gives primarily molecular weight information. Hambitzer and Heitbaum[18] were the first to successfully combine electrochemistry on-line with MS via a thermospray LC–MS interface. The experiments carried out by Hambitzer *et al.* demonstrated the potential for direct detection of electrochemically generated products by monitoring the formation of intact dimers and trimers upon electrooxidation of N,N dimethylaniline at a Pt electrode.

We have shown that the coupling of electrochemistry (EC) with tandem mass spectrometry via a thermospray interface (EC–thermospray MS–MS) can provide important chemical information about redox reactions of small biological molecules[8,10]. After the initial redox reaction has taken place, following chemical reactions can occur and produce a variety of products. Some of the products observed in on-line EC–TSP–MS result from unstable compounds undergoing electrophilic and nucleophilic substitution reactions with the mobile phase during the thermospray process. In this work, we show the first example of HPLC used on-line with electrochemistry to separate stable oxidation products prior to analysis by thermospray tandem mass spectrometry (EC–LC–thermospray MS–MS). In this paper, we report our attempts to characterize the chemical reactions which occur after the on-line electrooxidation of 6-thiopurine.

EXPERIMENTAL

Materials

Purine, hypoxanthine, adenine and 6-thiopurine were obtained from Sigma. Bis(6-purinyl) disulfide and sodium purine-6-sulfonate were prepared according to Doerr *et al.*[15].

HPLC procedure

Samples were analyzed by HPLC using a Microsorb (Rainin) C_{18} reversed-phase column (15 cm × 4.6 mm I.D.). All experiments were performed with a Rainin MacRabbit HPLC gradient system. The separation procedure for the oxidation products of 6-thiopurine required isocratic elution with 0.1 *M* ammonium acetate–methanol (pH 6.9) (98:2, v/v) for 9 min followed by a 2-min ramp from 2% methanol to 30% methanol with a flow-rate of 2.0 ml/min. The ammonium acetate and methanol solutions were filtered through a 0.45-μm filter before use. Samples were injected with a Rheodyne (Model 7125) injector fitted with a 20-μl loop. Details of the electrochemical cell have been described previously[8].

Mass spectrometry

The thermospray interface (Vestec) was mounted on a triple quadrupole mass spectrometer (Finnigan Model TSQ 45) equipped with an INCOS data system. Two temperatures were monitored in the experiments: the vaporizer exit temperature (tip temperature) and the source block temperature. In the tip temperature profile studies, the tip temperature was varied while the source temperature was held constant at

290°C. At a flow-rate of 2.0 ml/min, the typical operating temperatures were tip, 240°C, and source, 290°C.

Both positive ion and negative ion thermospray mass spectra were obtained by pulsed positive ion–negative ion chemical ionization (PPINICI). Typical conditions for thermospray MS were scan range m/z 120–300 in 0.3 s, electron multiplier voltage 1000 V, and preamplifier gain 10^8 VA^{-1}. The lower scan range limit of m/z 120 was normally used to avoid background interference from the ammonium acetate reagent ions. For MS–MS, the scan range and rates varied depending upon the m/z of the parent ion. Collisionally activated dissociation (CAD) studies were carried out using nitrogen as the collision gas (2 mTorr) with a collision energy of 30 eV.

RESULTS AND DISCUSSION

Identification of products by EC–thermospray MS–MS

Based on the electrochemical results, the known chemistry of 6-TP[14,18], EC–thermospray MS results with 6-TP were expected to indicate dimer formation by producing intact molecular-type ($[M+H]^+$ and $[M-H]^-$) ions of the disulfide. However, neither the disulfide nor its decomposition product, purine-6-sulfinate (Fig. 1), are observed in the EC–thermospray mass spectra. The results obtained by on-line EC–thermospray MS of 6-TP were initially confusing because of the unusual products which were detected and identified. Table I lists the ions identified in the EC–thermospray mass spectra of 6-TP. The formation of purine, adenine, and hypoxanthine (Table I) during the electrooxidation of 6-TP must clearly involve substitution reactions prior to mass analysis.

MS–MS was used to confirm the presence of purine, adenine, and hypoxanthine in the EC–thermospray mass spectra by comparing the daughter spectra of authentic standards with the daughter spectra of electrochemically generated products. The agreement between daughter ion abundances of standards and electrochemically generated products was generally ± 10% relative abundance (R.A.). The comparison of results is shown in Table II. The identification of intermediates and products in a mixture was based on their characteristic daughter spectra[19] which were obtained through the use of MS–MS as shown in Fig. 2.

TABLE I

OXIDATION PRODUCTS OF 6-THIOPURINE

Positive ions (m/z)	*Negative ions (m/z)*	*Structure correlation*
121	–	Purine $[M+H]^+$
136	134	Adenine $[M+H]^+$, $[M-H]^-$
–	194	Adenine $[M+CH_3COO]^-$
137	135	Hypoxanthine $[M-H]^-$
154	195	Hypoxanthine $[M+NH_4]^+$, $[M+CH_3COO]^-$
153	151	6-Thiopurine $[M+H]^+$, $[M-H]^-$
170	–	6-Thiopurine $[M+NH_4]^+$

TABLE II

COMPARISON OF DAUGHTER SPECTRA OF THE $[M+H]^+$ IONS OF AUTHENTIC STANDARDS WITH THOSE OF ELECTROCHEMICALLY GENERATED PRODUCTS

Compound	$[M+H]^+$ *ion*	*Authentic standard ion (% R.A.)*	*EC generated product ion (% R.A.)*
Purine	121^+	121(100), 94(35) 67(10), 52(2)	121(100), 94(36) 67(7), 52(2)
Adenine	136^+	136(100), 119(73) 94(5), 92(5)	136(100), 119(63) 94(1), 92(5)
Hypoxanthine	137^+	137(100), 119(21) 110(23), 94(7) 82(3), 55(2)	137(100), 120(5) 119(20), 110(26) 94(10), 82(3), 55(2)

Insights into the reaction pathway provided by EC–LC–thermospray MS

Although MS-MS allowed identification of purine, adenine, and hypoxanthine in the EC–thermospray mass spectra, MS–MS did not provide any information concerning the location of the reactions responsible for these products. In order to help determine whether the reactions occurred in solution prior to analysis by thermospray or during the thermospray vaporization process, HPLC was used on-line with an electrochemical cell to separate electrochemically generated products prior to analysis by thermospray MS–MS (Fig. 2). It was postulated that if the products listed in Table I were formed in solution immediately after electrooxidation, then it should be possible to correlate the retention times of these products with the retention times of the authentic standards. If, on the other hand, these products were formed later, in the thermospray probe or in the source, their retention times should instead be the same as that of the electrochemically generated disulfide which eventually leads to their formation.

Fig. 3 illustrates the LC–thermospray positive ion $[M+H]^+$ mass chromatograms of a four-component mixture of authentic purine [molecular weight (MW)

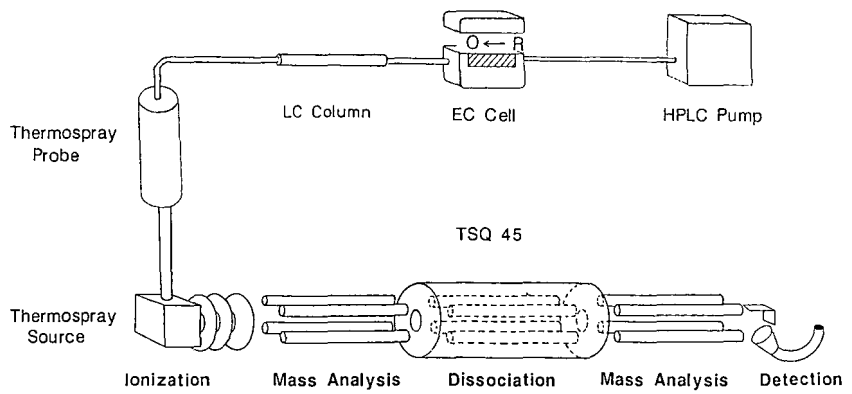

Fig. 2. On-line EC–LC–thermospray MS–MS system.

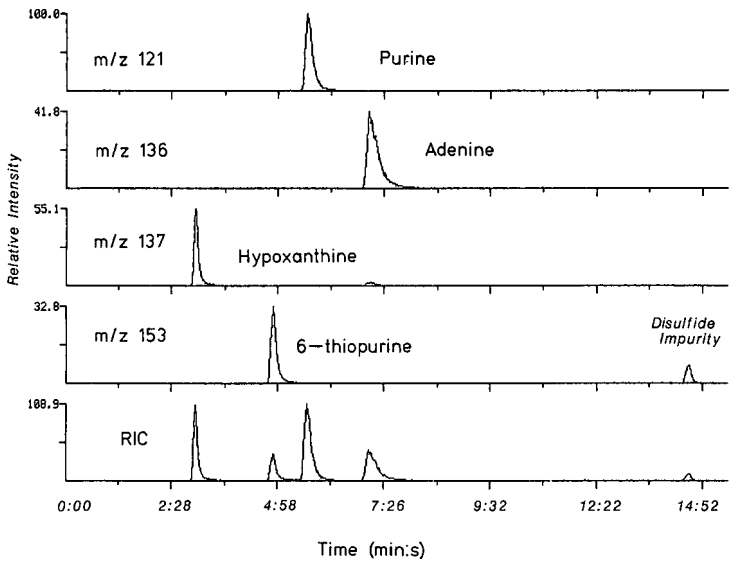

Fig. 3. HPLC–thermospray MS positive ion mass chromatograms of 4-component purine mixture. Flow-rate of 0.1 *M* ammonium acetate mobile phase 2.0 ml/min. Tip temperature 240°C, source temperature 300°C.

120], adenine (MW 135), hypoxanthine (MW 136), and 6-TP (MW 152) which are chromatographically separated in *ca.* 8 min. The small peak at *ca.* 14 min (Fig. 3) is due to trace amounts of the 6-TP disulfide, an impurity in the 6-TP standard. The retention time of this small peak at *ca.* 14 min is identical to the retention time of the synthesized disulfide (Fig. 4).

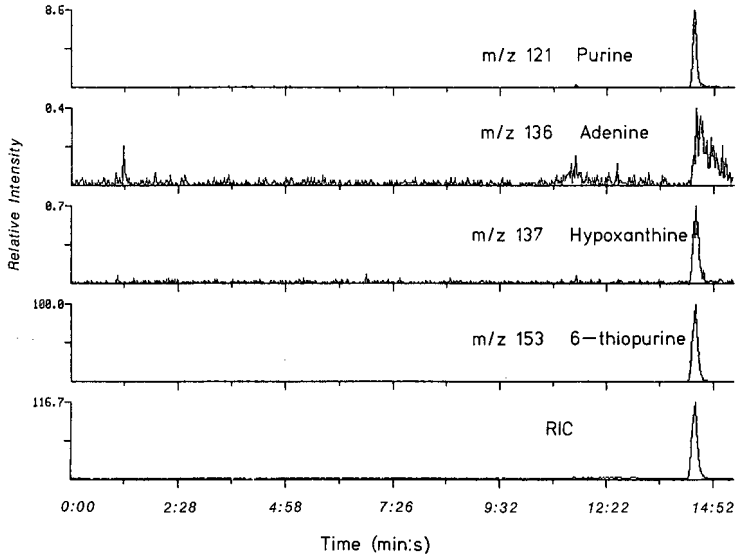

Fig. 4. HPLC–thermospray MS positive ion mass chromatograms of synthesized 6-thiopurine disulfide. Flow-rate 2.0 ml/min, tip temperature 240 °C, and source temperature 300°C.

When a sample of synthesized 6-TP disulfide is analyzed by LC–thermospray MS, decomposition reactions occur during the thermospray vaporization process which result in the formation of 6-thiopurine, adenine, hypoxanthine, and purine (Fig. 4). The LC–MS mass chromatograms of the $[M+H]^+$ ions formed during the decomposition of the authentic disulfide standard can be seen in Fig. 4. The fact that all four products originate from a single peak with a retention time of *ca.* 14 min reveals that decomposition of the disulfide occurs somewhere during the thermospray ionization process. This is clear from the comparison of the retention times of the authentic purine standards (Fig. 3) with the retention times of the decomposition products arising from the disulfide (Fig. 4).

The on-line EC–LC–thermospray MS results obtained for the electrochemical oxidation products of 6-thiopurine can be seen in Fig. 5. The positive ion mass chromatograms obtained in an EC–LC–thermospray MS experiment (Fig. 5) are in agreement, when both the retention time and relative intensity are compared, with the positive ion mass chromatograms obtained for the authentic 6-TP disulfide standard (Fig. 4). In addition to the peak corresponding to the disulfide at *ca.* 14 min in EC–LC–thermospray mass chromatograms in Fig. 5, a few smaller peaks with much shorter retention times (2 and 4 min) are also observed. Although these ions correspond to oxidation products of 6-TP, they could not be positively identified because their retention times did not match those of the available standards and their low intensities precluded the use of MS–MS for structural elucidation. The only conclusion which can be drawn is that the product at *ca.* 2 min forms only a positive ion at *m/z* 121 and the product at *ca.* 4 min forms only positive ions at *m/z* 121 and *m/z* 136.

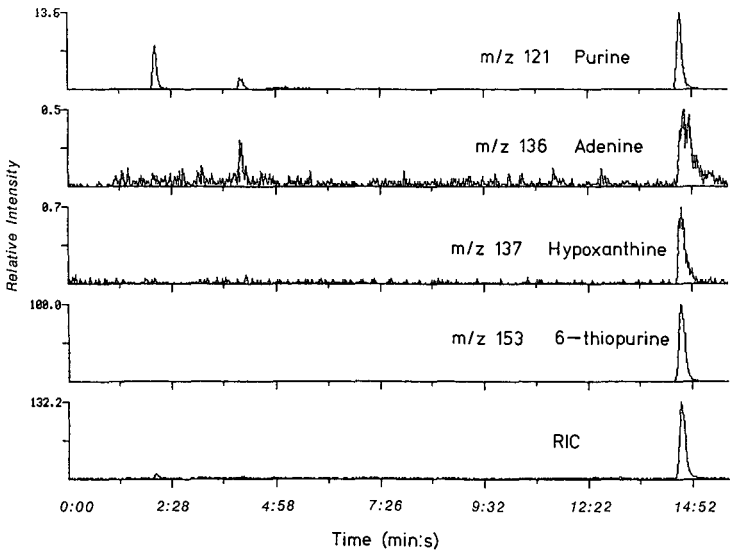

Fig. 5. EC–LC–thermospray MS positive ion mass chromatograms of the oxidation products of 6-thiopurine. Flow-rate 2.0 ml/min, tip temperature 240°C, and source temperature 300°C. Potential +0.60 V *vs.* Pd.

Tip temperature studies

Optimum thermospray interface parameters such as tip temperature are traditionally determined by maximizing the solvent-buffer ion intensities for a given flow-rate[20–22]. Using the solvent-buffer ion intensity method, a signal maximum is obtained at a tip temperature of *ca.* 240°C for a flow-rate of 2.0 ml/min. As expected, this tip temperature also produces the most intense reconstructed ion current for samples in EC–thermospray MS. However, some ions produced during the vaporization process of 6-TP oxidation products do not follow the tip temperature profile of the authentic standards. In this study, we have identified the ions which show different responses. These ions have been identified as ammonolysis products and are believed to result from purine-6-sulfinate. Purine-6-sulfinate is one of the 6-TP disulfide disproportionation products (Fig. 1). Because hydrolysis reactions of intermediates following electrochemical oxidation are well known[1], the formation of ammonolysis products under EC–thermospray MS conditions is not surprising but has only recently been reported[23–25].

We hypothesize that ammonia and water react with purine-6-sulfinate by nucleophilic substitution to form adenine and hypoxanthine (Fig. 6). Electrophilic substitution by a proton followed by elimination of SO_2 gas is responsible for the formation of purine (Fig. 6). Decomposition of purine-6-sulfinate in 98–100% formic acid to yield purine has been previously reported[15]. It is important to note that no ions corresponding to either H_2SO_2, the leaving group produced by nucleophilic substitution, or SO_2, the leaving group produced by electrophilic substitution, are observed in the thermospray mass spectra when the lower m/z scan limit is reduced from m/z 120 to m/z 25.

Fig. 7 compares the tip temperature profiles of authentic adenine and hypoxanthine with the tip temperature profiles of electrochemically generated adenine and hypoxanthine. As can be seen in Fig. 7, the profiles differ dramatically at tip temperatures lower than 240°C due to the decreased efficiency with which the product of electrochemical oxidation, postulated to purine-6-sulfinate, undergoes ammonolysis and hydrolysis reactions. The decreased intensity of products at lower tip temperatures is indicative that the reactions of the electrochemical product forming adenine and hypoxanthine are occurring inside the vaporizer probe.

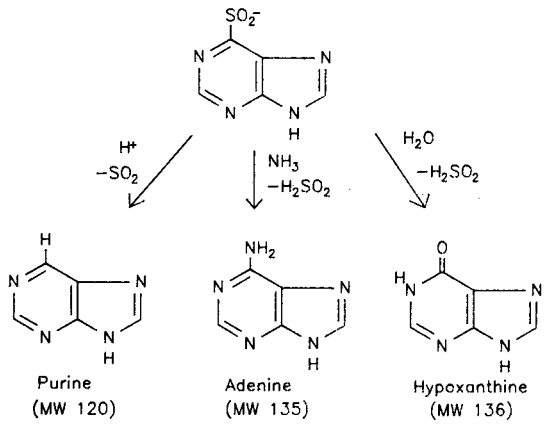

Fig. 6. Reaction pathways of purine-6-sulfinate under thermospray conditions.

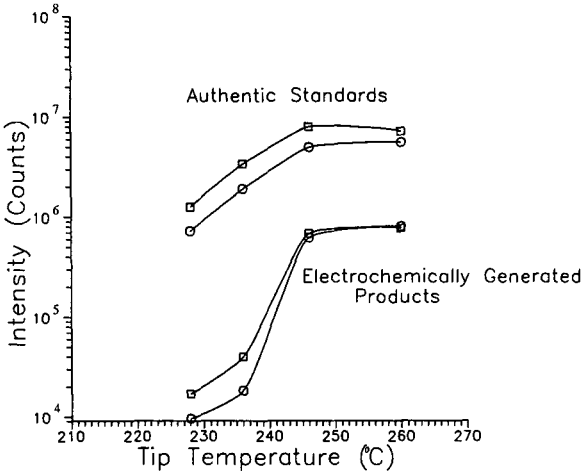

Fig. 7. EC–thermospray MS tip temperature study of hydrolysis and ammonolysis reactions with purine-6-sulfinate under thermospray conditions. (○) Hypoxanthine, (□) adenine.

Because the synthesis of sodium purine-6-sulfinate ($RSO_2^-Na^+$) using the method described by Doerr *et al.*[15] was not successful, it was not possible to analyze it under thermospray conditions to prove our hypothesis. However, a very similar compound, sodium purine-6-sulfonate ($RSO_3^-Na^+$), was prepared instead[15] and analyzed by LC–thermospray MS. Fig. 8 illustrates the LC–thermospray positive ion mass chromatograms of sodium purine-6-sulfonate. As can be seen in Fig. 8, pu-

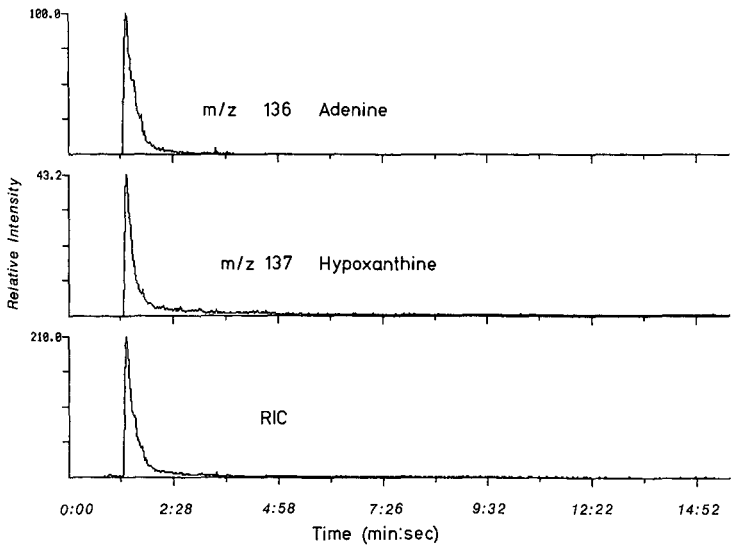

Fig. 8. LC–thermospray MS positive ion mass chromatograms of the thermospray-induced decomposition products of purine-6-sulfonate. Flow-rate 2.0 ml/min, tip temperature 240°C, and source temperature 300°C.

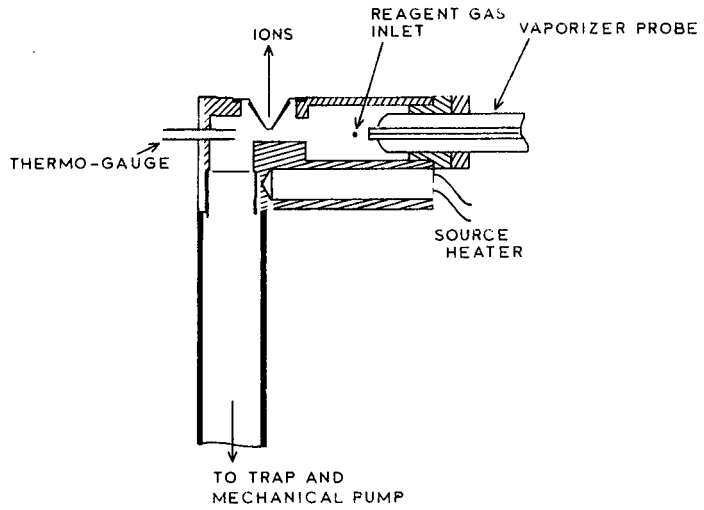

Fig. 9. Modified Vestec thermospray source. Reagent gases introduced in the orifice normally holding the discharge electrode. Source pressure monitored by replacing vapor temperature sensor with thermogauge.

rine-6-sulfonate completely decomposes during the thermospray process to produce adenine and hypoxanthine. Hydrolysis studies have shown that both purine-6-sulfinate and purine-6-sulfonate are very labile to acid resulting in the formation of hypoxanthine[15]. No ions indicative of intact purine-6-sulfonate are observed in the LC–thermospray mass spectra. It is important to point out that purine is not produced during the decomposition of sodium purine-6-sulfonate under thermospray conditions; however, purine is produced during the thermospray-induced decomposition of 6-TP disulfide which may occur via electrophilic substitution reactions with purine-6-sulfinate.

Solution-phase and gas-phase studies

These studies were performed to determine if substitution reactions such as ammonolysis and hydrolysis reactions shown for purine-6-sulfinate were occurring

TABLE III

PRODUCTS FORMED IN SOLUTION-PHASE AND GAS-PHASE STUDIES OF ELECTROOXIDATION PRODUCTS OF 6-THIOPURINE

Reagent gas added to source	*Buffer composition*	*Products*
None	0.1 *M* NH_4OOCCH_3	Purine, hypoxanthine, 6-thiopurine and adenine
None	0.1 *M* NH_4OOCCH_3-CH_3NH_2	Purine, hypoxanthine, 6-thiopurine, adenine and N6-methyladenine
CH_3NH_2	0.1 *M* NH_4OOCCH_3	Purine, hypoxanthine, 6-thiopurine and adenine
NH_3	0.1 *M* CH_3COOH	Purine, hypoxanthine, 6-thiopurine and 6-TP disulfide

inside the thermospray vaporizer probe or in the thermospray source. By modifying a standard Vestec thermospray source, we were able to introduce various reagent gases capable of acting as nucleophiles into the thermospray source (Fig. 9). The electrochemical oxidation products of 6-TP were monitored as the mobile phase composition and reagent gas were varied.

Methylamine was chosen as a model nucleophile in these experiments because its chemical properties and reactivity are similar to those of ammonia and it is not present in the normal thermospray buffer. When a mixture of 0.1 *M* methylamine (CH_3NH_2) and 0.1 *M* ammonium acetate pH 7 is used as a buffer during the electrooxidation of 6-TP, a new product, N6-methyladenine, is observed in the EC–thermospray mass spectra (Table III). N6-methyladenine is formed as a result of the electrochemically formed product undergoing a nucleophilic substitution with methylamine in analogy to the reaction with NH_3 which forms adenine (Fig. 6).

To determine if the nucleophilic reaction with methylamine can occur inside the thermospray source, methyl amine (0.4 Torr) was introduced into the thermospray source while 0.1*M* ammonium acetate was used as the buffer. Under these conditions, no gas-phase nucleophilic reactions between methylamine and the electrochemical oxidation products of 6-TP are observed. Specifically, N6-methyladenine was not detected. Hence, it appears that methylamine must be present in the buffer solution to react and form N6-methyladenine. Therefore, this reaction and other nucleophilic substitution reactions (hydrolysis, ammonolysis) probably occur inside the vaporizer probe during the thermospray vaporization process, rather than in the thermospray ion source.

Additional results supporting this conclusion were obtained using 0.1 *M* acetic acid (pH *ca.* 2.8) as the buffer while introducing ammonia (0.4 Torr) into the thermospray source. The use of acetic acid as the mobile phase was designed to control conditions so that ammonia was present only in the source and was not part of the solution phase. Under these conditions, the normal ammonolysis product, adenine, is not observed following electrooxidation of 6-thiopurine. However, hypoxanthine and purine are still observed in addition to small amounts of the intact disulfide. The inability to detect the disulfide by EC–thermospray MS at pH *ca.* 7 with the traditional ammonium acetate buffer is consistent with the disproportionation process which is favored at high pH[15]. Detection of the disulfide shows that under acidic conditions, the disproportionation process (Fig. 1) will not be favored. This supports the results obtained with methylamine and indicates that the ammonolysis reaction occurs inside the vaporizer probe.

Mass spectrometric hydrodynamic voltammograms

Typical electrochemical techniques such as cyclic voltammetry and chronocoulometry rely on monitoring current or charge as a function of potential or time. These techniques provide little chemical information about the actual molecular structures of the species which form as a result of electron transfer at the electrode surface. One of the most important uses of on-line EC–thermospray MS or EC–thermospray MS–MS is the monitoring of reactants, intermediates, and products as a function of electrode potential[8].

Fig. 10 illustrates the mass spectrometric hydrodynamic voltammograms of 6-thiopurine obtained by EC–thermospray MS. Oxidation of 6-TP begins at poten-

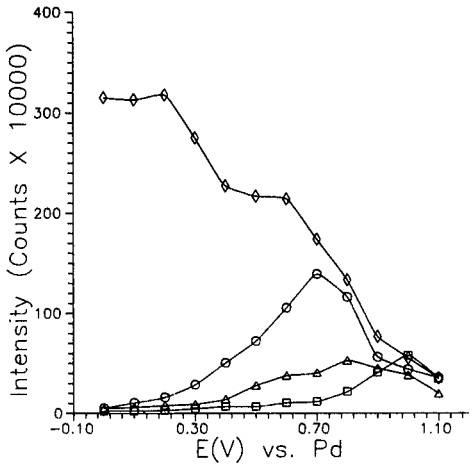

Fig. 10. MS hydrodynamic voltammograms of 6-thiopurine. Flow-rate of 0.1 *M* ammonium acetate mobile phase 2.0 ml/min. Tip temperature 240°C and source temperature 300°C. (○) Purine, *m/z* 121; (□) adenine, *m/z* 136; (△) hypoxanthine, *m/z* 137; (◇) 6-thiopurine, *m/z* 153.

tials > +0.20 V and reaches a steady-state level at potentials < +0.40 V. Steady-state behavior is expected for both reactants and products when operating in the limiting current region due to the hydrodynamic flow of reactant in the electrolysis cell. This is what is observed in HPLC with detection by electrochemistry[25]. At *ca.* +0.65 V, a second oxidation process appears to occur. This process can be followed by noting the decrease in the intensity of the $[M+H]^+$ ion of 6-TP at *m/z* 153. This second oxidation process does not favor the formation of purine. In addition, the intensities of the ions corresponding to hypoxanthine and adenine also change at potentials higher than +0.65 V. This behavior is expected if further electrochemical oxidation of 6-TP results in the formation of an intermediate which does not readily undergo the same substitution reactions or react at the same rate as the intermediate formed at lower potentials.

CONCLUSIONS

Electrochemistry has been used on-line with LC–thermospray MS–MS to provide insight into redox reactions of the purine drug 6-thiopurine. After the initial oxidation reaction of 6-TP has taken place, the disulfide which forms disproportionates in solution inside the thermospray vaporizer probe to regenerate 6-thiopurine and to form small amounts of an intermediate proposed to be purine-6-sulfinate. Neither the disulfide nor purine-6-sulfinate are detected under normal thermospray conditions. The disulfide can be detected if acetic acid is used as a mobile phase. Formation of purine-6-sulfinate was tested by synthesis of a structurally similar derivative, purine-6-sulfonate, which reacted under thermospray conditions to form the products found in EC–thermospray MS–MS. The observed products, adenine, hypoxanthine, and purine were shown to form inside the vaporizer probe by nucleophilic and electrophilic substitution reactions of purine-6-sulfinate.

In addition to the solution-phase studies, tip temperature profiles also support the disulfide disproportionation process. The LC–thermospray mass chromatograms of authentic 6-TP disulfide and the EC–LC–thermospray mass chromatograms of the electrochemically generated disulfide indicate that all decomposition products arise from a single LC peak corresponding to the retention time of 6-TP disulfide thereby supporting the hypothesis of decomposition occurring inside the vaporizer probe. This is further supported by the formation of the nucleophilic substitution product, N6-methyladenine, when methylamine is added to the thermospray buffer. Because N6-methyladenine is not detected when methylamine is added to the thermospray source, these results indicate that the site of nucleophilic and presumably electrophilic attack is within the thermospray probe.

ACKNOWLEDGEMENTS

This research was supported in part by grants from the National Institutes of Health (A.B.T.), U.S. Chemical Research Development and Engineering Center (R.A.Y., A.B.T.), the Division of Sponsored Research at the University of Florida (R.A.Y., A.B.T.), and the Interdisciplinary Center for Biotechnology Research at the University of Florida (A.B.T.). Kevin J. Volk thansk Merck-Dohme for a graduate fellowship.

REFERENCES

1 G. Dryhurst, *Electrochemistry of Biological Molecules*, Academic Press, New York, 1977.
2 K. McKenna and A. Brajter-Toth, *J. Electroanal. Chem.*, 233 (1987) 49.
3 P. J. Kraske and A. Brajter-Toth, *J. Electroanal. Chem.*, 207 (1986) 101.
4 R. N. Goyal, A. Brajter-Toth and G. Dryhurst, *J. Electroanal. Chem.*, 131 (1982) 181.
5 D. Astwood, T. Lippincott, M. Deysher, C. D'Amico, E. Szurley and A. Brajter-Toth, *J. Electroanal. Chem.*, 159 (1983) 295.
6 D. J. Miner, J. R. Rice, R. M. Riggin and P. T. Kissinger, *Anal. Chem.*, 53 (1981) 2258.
7 J. R. Rice and P. T. Kissinger, *Biochem. Biophys. Res. Commun.*, 104 (1982) 1312.
8 K. J. Volk, M. S. Lee, R. A. Yost and A. Brajter-Toth, *Anal. Chem.*, 60 (1988) 270.
9 E. G. Rogan, E. L. Cavalieri, S. R. Tibbels, P. Cremonesi, C. D. Warner, D. L. Nagel, K. B. Tomer, R. L. Cerny and M. L. Gross, *J. Am. Chem. Soc.*, 110 (1988) 4023.
10 A. Brajter-Toth, T. Peterson, K. McKenna, P. J. Kraske and K. J. Volk, in G. Dryhurst and K. Niki (Editors), *Redox Chemistry and Interficial Behavior of Biological Molecules*, Plenum Press, 1988.
11 R. M. Hyslop and I. Jardine, *J. Pharmacol. Exp. Ther.*, 218 (1981) 621.
12 R. W. Brockman, *Cancer Res.*, 23 (1963) 1191.
13 S. Zimm, G. E. Johnson, B. A. Chabner and D. G. Poplack, *Cancer Res.*, 45 (1985) 4156.
14 G. Dryhurst, *J. Electrochem. Soc.*, 116 (1969) 1097.
15 I. L. Doerr, I. Wempen, D. A. Clarke and J. J. Fox, *J. Org. Chem.*, 26 (1961) 3401.
16 E. L. Carr, G. P. Smith and G. J. Alliger, *J. Org. Chem.*, 14 (1949) 921.
17 A. J. Parker and N. Kharasch, *Chem. Rev.*, 59 (1959) 583.
18 G. Hambitzer and J. Heitbaum, *Anal. Chem.*, 58 (1986) 1067.
19 R. J. Perchalski, R. A. Yost and B. J. Wilder, *Anal. Chem.*, 54 (1982) 1466.
20 C. R. Blakley and M. L. Vestal, *Anal. Chem.*, 55 (1983) 750.
21 C. Linberg and J. J. Paulson, *J. Chromatogr.*, 394 (1987) 117.
22 R. D. Voyksner and C. A. Haney, *Anal. Chem.*, 57 (1985) 991.
23 K. J. Volk, R. A. Yost and A. Brajter-Toth, *Anal. Chem.*, (1989) in press.
24 R. A. Yost, K. J. Volk, M. S. Lee and A. Brajter-Toth, *Adv. Mass Spectrom.*, (1988) in press.
25 P. T. Kissinger and W. R. Heineman, *Laboratory Techniques in Electroanalytical Chemistry*, Marcel Dekker, New York, 1984.

Journal of Chromatography, 474 (1989) 245–256
Elsevier Science Publishers B.V., Amsterdam — Printed in The Netherlands

CHROM. 21 441

UTILITY OF SOLUTION ELECTROCHEMISTRY MASS SPECTROMETRY FOR INVESTIGATING THE FORMATION AND DETECTION OF BIOLOGICALLY IMPORTANT CONJUGATES OF ACETAMINOPHEN

T. A. GETEK*, W. A. KORFMACHER, T. A. McRAE and J. A. HINSON
National Center for Toxicological Research, Jefferson, AR 72079 (U.S.A.)

SUMMARY

On-line formation and detection of glutathione and cysteine conjugates of acetaminophen were accomplished by the interfacing of a coulometric electrochemical cell with a thermospray mass spectrometer in a flow-injection experiment using a liquid chromatographic pump. Formation of the conjugates occurred only after acetaminophen was oxidized electrochemically by a two-electron transfer to N-acetyl-*p*-benzoquinoneimine and reacted in a mixing tee with either glutathione or cysteine. The newly formed conjugate was detected by thermospray mass spectrometry by observing the $[M + H]^+$ ion for the acetaminophen–glutathione conjugate at *m/z* 457, or the $[M + H]^+$ ion for the acetaminophen–cysteine conjugate at *m/z* 271. Both the glutathione and cysteine conjugates produced a common fragment ion at *m/z* 184. The on-line reaction of glutathione and electrochemically generated N-acetyl-*p*-benzoquinoneimine was monitored at varying pH. At pH 8.5 the ion intensity for the acetaminophen–glutathione conjugate was greater than at lower pH, indicating that lower proton concentration enhanced the reaction of glutathione with N-acetyl-*p*-benzoquinoneimine. This on-line electrochemical–thermospray mass spectrometric method demonstrated that acetaminophen conjugates may be formed and detected in the time frame of 1 s.

INTRODUCTION

Thermospray mass spectrometry (TSP MS) has been an indisputable success as an interface and detection mode for high-performance liquid chromatography (HPLC) and as a soft ionization mode for non-volatile compounds. A good part of this success stems from the fact that the mobile phases used in reversed-phase HPLC, the method of choice for many of today's analyses by HPLC, usually utilize polar solvents and various salts that buffer the mobile phase. These types of polar mobile phase for reversed-phase HPLC are similar to the liquid carriers best suited for maximizing the thermospray effect. This excellent match between suitable operating conditions for reversed-phase HPLC and TSP MS is fortuitous for the viable interfacing of these two methods.

The utilization of polar solvents with various salts and buffers also allows in-

0021-9673/89/$03.50

terfacing of electrochemical methods with TSP MS. Because TSP MS is normally operated at flow-rates of 1–2 ml min^{-1}, this makes the coupling of electrochemistry (EC) with TSP MS very simple and convenient. This flow-rate also permits the thermospray mass spectrometer to be employed in the flow-injection mode. The initial development of the EC–TSP MS interface was started by Hambitzer and Heitbaum[1], and by one of the authors of this study in Marvin Vestal's laboratory[2]. Later work by Volk *et al.*[3] investigated the electrochemical oxidation of purines by tandem mass spectrometry (MS–MS) and demonstrated the utility of EC–TSP MS for studying short-lived electrochemically generated intermediates. Previous to the development of TSP MS[4], electrochemical methods were coupled to MS for purposes of detecting electrolysis products[5,6], but these products had to be gaseous in order to accommodate the mass spectrometer's vacuum environment. Only with the advent of TSP MS and its flow-injection capabilities did the EC–MS interface for directly studying nonvolatile compounds in solution on-line become feasible. In order to differentiate the EC–TSP MS interface from the EC–MS interface, which detects only volatile products, the name "solution electrochemistry mass spectrometry" (SECYMS) was given to this EC–TSP MS interface[2].

The conjugation of glutathione (GSH) to acetaminophen (APAP) has been reported by Potter and Hinson[7] to go through a two-electron oxidation step for APAP followed by reaction with GSH. Recently the enzymic reaction of the oxidized product of APAP, *i.e.* N-acetyl-*p*-benzoquinoneimine (NAPQI), and its spontaneous reaction with GSH were investigated by stopped-flow experiments[8]. The direct analysis by TSP MS of rat bile for APAP conjugates by Betowski *et al.*[9] demonstrated that the GSH conjugate may be detected as the $[M+H]^+$ ion.

As an extension of the SECYMS method, the electrochemical oxidation of APAP to NAPQI was performed on-line as a constant flow-injection experiment followed by TSP MS. After injection of GSH into the stream of NAPQI, the reaction was monitored by the thermospray mass spectrometer. Preliminary results showed that this is a very rapid (*ca.* 1 s) and simple method for forming and detecting the acetaminophen–glutathione (APAP-SG) conjugate[10]. Details of the APAP-SG formation, as well as similar experiments with APAP and cysteine (CSH) conjugation to form the acetaminophen–cysteine (APAP-SC) conjugate are reported in this paper.

EXPERIMENTAL

A diagram of the flow-injection system for forming and detecting conjugates of APAP by SECYMS is shown in Fig. 1. For the APAP-SG formation, a $3.3 \cdot 10^{-5}$ *M* APAP solution in water–methanol (90:10) containing 0.1 *M* ammonium acetate was placed in the syringe pump (ISCO LC-5000). The reciprocal pump (Waters 6000A) contained an identical solution, but without APAP. The solution containing APAP was pumped through an electrochemical coulometric guard cell (ESA, Model 5020) at various potentials as maintained by a potentiostat (ESA, Model 5100A). The potential was reported as referenced to a palladium reference electrode[11]. The potentiostat was modified so that guard cell currents could be fed to an integrator. Solutions of GSH diluted in water–methanol (90:10) containing 0.1 *M* ammonium acetate were injected into the stream of APAP by an HPLC injector (Rheodyne, Model 7125) with a 100-μl loop and reacted in a stainless-steel mixing tee with a 0.043 in. through-hole

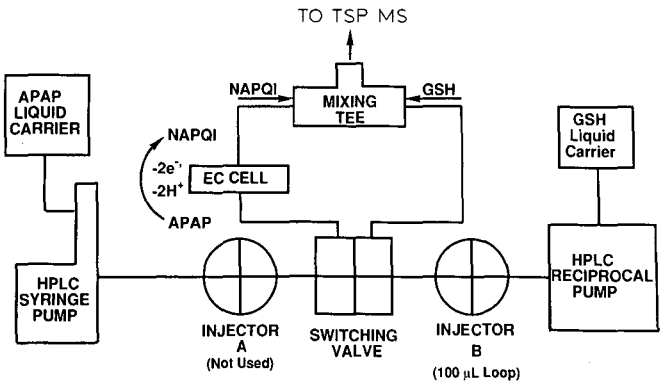

Fig. 1. Flow-injection system used to form and detect acetaminophen–glutathione conjugates by TSP MS. For the case of the cysteine conjugate, the acetaminophen solution was in the reciprocal pump and the 100-μl loop on injector A.

(Scientific Systems Inc.). The mixed streams of APAP and GSH were then directly pumped into a quadrupole mass spectrometer (Delsi R-1010C) equipped with a thermospray probe (Vestec) and thermospray source (Delsi). The vaporizer and block temperatures were maintained by a thermospray controller (Vestec). Solutions of different pH were made of ammonium acetate aqueous solutions adjusted with acetic acid for pH below neutral and ammonium hydroxide for pH > 7. For each pH evaluated, the pH for the GSH and APAP solutions, and the pH for the liquid carrier for injections were equivalent. Potentials were manually adjusted on the potentiostat (non-scanning mode). Temperature conditions for TSP MS were: vaporizer (T_1), 137°C; tip (T_2), 246°C; and block 285°C. The flow-rates for syringe and reciprocal pumps were 0.7 ml min^{-1} each; the total flow into mass spectrometer was 1.4 ml min^{-1}.

The procedure for forming CSH conjugates was identical with that used for APAP-SG, except the APAP-containing solutions were pumped by the reciprocal pump. A solution of $1.8 \cdot 10^{-4}$ *M* APAP was used to form the CSH conjugate. The concentration of cysteine injected was 1 mg ml^{-1} in a 100-μl loop. Thermospray conditions were: vaporizer (T_1), 140°C; tip (T_2), 198°C; and block, *ca.* 250°C. Flow-rates for the reciprocal and syringe pump were 0.5 ml min^{-1} each for the APAP-SC.

Cyclic voltammetry and differential pulse voltammetry utilized a BAS (Bioanalytical Systems) glassy carbon electrode as the working electrode. Waveforms were generated by a BAS-100A electroanalytical system. In both cases, potentials were referenced to an Ag/AgCl electrode, and a platinum wire was the counter electrode. The electrolyte was 0.1 *M* ammonium acetate (pH 4.5) for the APAP and APAP-SG cyclic voltammetry. The cyclic and differential pulse voltammetry study of GSH and CSH employed 0.1 *M* ammonium acetate (pH 7) as electrolyte. Differential pulse voltammetry was carried out at a scan-rate of 5 mV s^{-1} with a pulse amplitude of 50 mV. Solute concentrations were *ca.* $1 \cdot 10^{-3}$ *M*.

An authentic sample of APAP-SC was synthesized using methods similar to those previously described[7,12]. The identity of the conjugate was proven by TSP MS and proton NMR spectrometry, and the purity of the conjugate was evaluated by analytical HPLC with UV detection and with electrochemical detection. Electro-

chemical detection [13] indicated that the APAP-SC contained 4.1% cysteine. The analysis of APAP-SC by TSP MS was performed in 0.1 *M* ammonium acetate at a flow-rate of 1.0 ml min^{-1} without a chromatographic column.

All mass spectral scans in this study by TSP MS were full scan range (*ca.* 100–500 *m/z*). The term "selective ion monitoring" is used in this text to refer to the selected m/z plots after a full scan measurement.

RESULTS AND DISCUSSION

The reported electrochemical oxidation of APAP in water, which is catalyzed by H^+, is shown in Fig. 2, pathway A[14]. Cyclic voltammetry of APAP at a scan-rate of 50 mV s^{-1} gave an oxidation wave, which is indicative of the electrochemical conversion to NAPQI, at a potential of +0.58 V *vs.* Ag/AgCl. A quasireversible wave for the reduction of NAPQI to APAP was observed at *ca.* −0.08 V *vs.* Ag/AgCl. When GSH was added to APAP in a 1:1 mole ratio, the cyclic voltammogram showed an oxidation wave at +0.60 V *vs.* Ag/AgCl, but no quasireversible wave for the reduction of NAPQI back to APAP. This indicated that GSH reacted completely with the electrochemically generated NAPQI at the electrode interface and this led to no observance of the reduction of NAPQI. This reaction of NAPQI with GSH is shown in Fig. 2, pathway B.

The electrochemical study of APAP is a good candidate for the technique of SECYMS because of the electrochemical quasireversible nature of APAP[15]. As shown in Fig. 3a, when analyzed by TSP MS, APAP produced an $[M+H]^+$ ion at *m/z* 152, an $[M+NH_4]^+$ ion at *m/z* 169, and an $[M_2H]^+$ ion at *m/z* 303. Upon oxidation of APAP to NAPQI utilizing the on-line electrochemical coulometric ESA guard cell, NAPQI was detected at an applied oxidation potential of *ca.* +0.5 V. As shown in Fig. 3b, NAPQI produced an $[M+H]^+$ ion at *m/z* 150 and a fragment ion at *m/z* 108, which may be due to protonated *p*-benzoquinoneimine formed from deacetylation of APAP. A residual mass spectral peak at *m/z* 152 for the $[M+H]^+$ ion of APAP is also observed. This residual APAP $[M+H]^+$ ion is due to the electrochemical quasireversible nature of APAP[15].

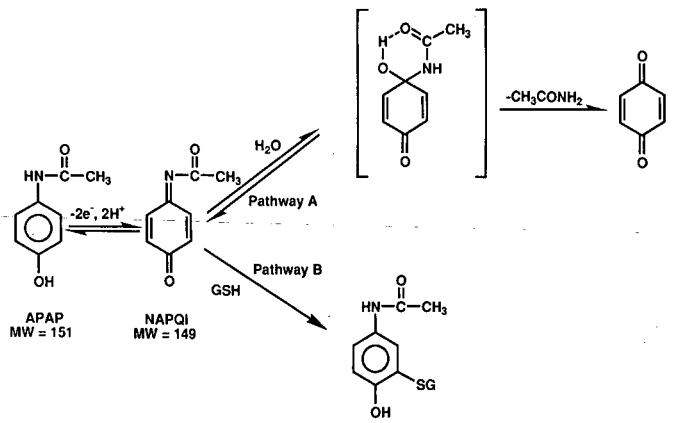

Fig. 2. Electrochemical oxidation of APAP as it occurs by pathway A in H_2O as catalyzed in acidic media (ref. 14) and by pathway B with glutathione.

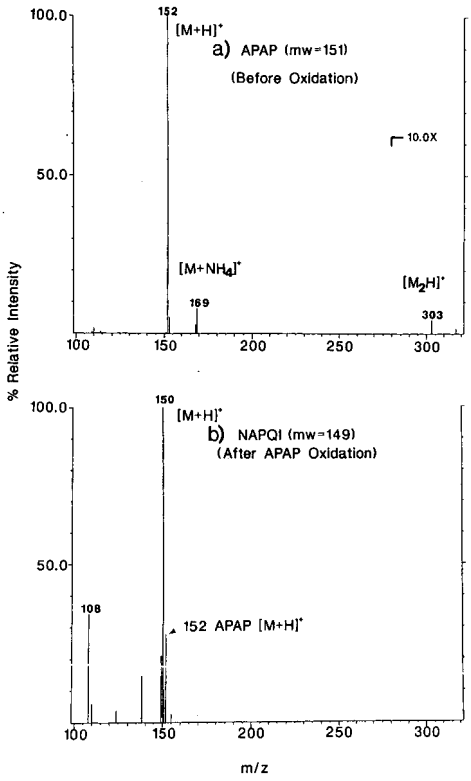

Fig. 3. TSMS of APAP in 0.1 *M* ammonium acetate obtained (a) before oxidation of APAP to NAPQI and (b) after oxidation of APAP to NAPQI at *ca.* +0.5 V. Mass spectral peaks at *m/z* 150 and 108 are indicative of NAPQI.

The TSP MS of APAP-SG has been reported, the $[M+H]^+$ ion at *m/z* 457 and a fragment ion at *m/z* 184 were observed[9]. The fragment ion corresponded to a cleavage of the GSH molecule from the APAP, leaving only a thiol attached to the APAP moiety. The thiol fragment, APAP-SH, had a much higher ion intensity than the peak intensity for the $[M+H]^+$ ion for APAP-SG.

The flow-injection arrangement in Fig. 1 was utilized to form and detect the APAP-SG conjugate on-line. At a constant flow-rate of APAP through the electrochemical cell (labeled EC cell in Fig. 1), the potential was increased by 0.05 V increments until APAP was oxidized to NAPQI. Complete oxidation of APAP in the coulometric electrochemical cell occurred at +0.2 V, as indicated by the hydrodynamic voltammogram in Fig. 4. The oxidation of APAP to NAPQI was confirmed by TSP MS. A 100-μl volume of the GSH solution was injected into the stream of NAPQI and it reacted in less than 1 s to form the APAP-SG conjugate. The time of formation was calculated from the volume inside the stainless-steel tubing after the mixing tee, and the flow-rate. The results of this reaction are illustrated in Fig. 5. Before oxidation of APAP, injection of the GSH solution produced only the $[M+H]^+$ ion for GSH at *m/z* 308 and fragment ions for GSH at *m/z* 179, 147, and 130 (Fig. 5a). When APAP was oxidized to NAPQI, and then mixed with GSH, the

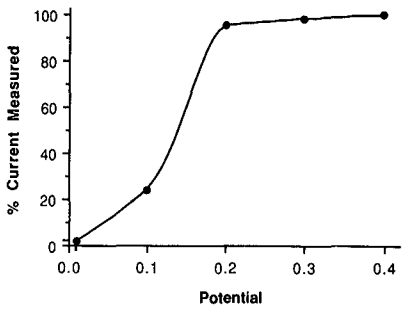

Fig. 4. Hydrodynamic voltammogram of APAP obtained by constant flow of APAP in water–methanol (90:10) containing 0.1 *M* ammonium acetate through the coulometric ESA guard cell. The potential is given in volts *vs.* reference.

APAP-SG conjugate is detected by TSP MS at *m/z* 457 for the $[M+H]^+$ ion and the corresponding fragment ion at *m/z* 184 (Fig. 5b).

The constant flow of APAP was monitored on-line by TSMS at various applied potentials. The selective ion monitoring scan of *m/z* 150 and 108, ions indicative of

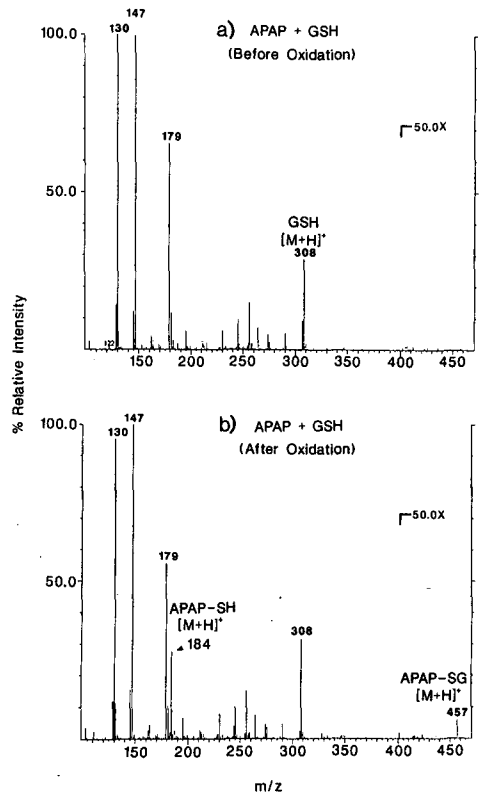

Fig. 5. TSP MS of APAP mixed with GSH acquired (a) before oxidation of APAP and (b) after oxidation of APAP. After oxidation of APAP, mass spectral peaks indicative of APAP-SG are seen for $[M+H]^+$ at *m/z* 457 and the protonated thiol fragment ion at *m/z* 184.

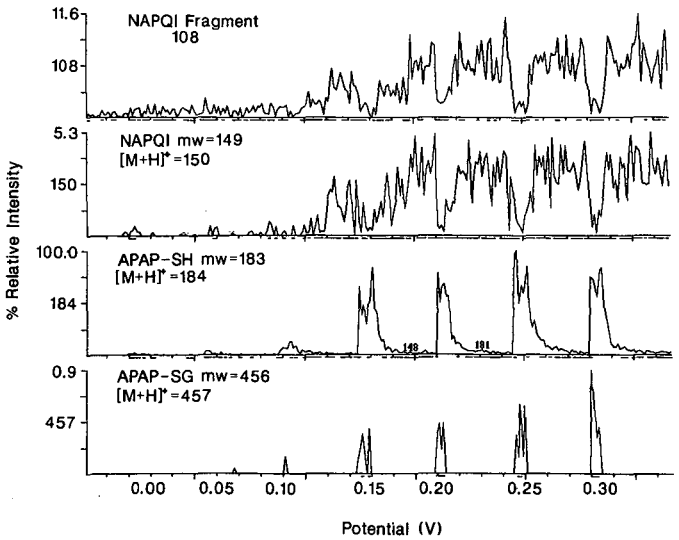

Fig. 6. Selective ion monitoring of ions indicative of NAPQI (*m/z* 150 and 108) and APAP-SG (*m/z* 457 and 184) shown at various applied potentials. Note that ions associated with APAP-SG did not appear until NAPQI was formed.

the oxidation of APAP to NAPQI, is seen in Fig. 6 as a function of potential. Initially, only background ion intensity was observed for the monitoring of *m/z* 150 and 108, but when NAPQI began to form these ion intensities increased significantly. This occurred at *ca.* +0.2 V. A point to remember is that the stream of APAP is continuously being oxidized to NAPQI at potentials greater than +0.2 V, thus the selective ion scans for *m/z* 150 and 108 appeared as a plateau above +0.2 V, and only background intensity is observed at non-oxidizing potentials. GSH was injected into this stream of constantly formed NAPQI. These injections corresponded to peaks observed in Fig. 6 for scans of *m/z* 457 and 184, ions representing the APAP-SG conjugate. A feature to note from Fig. 6 is that the conjugate was observed only after APAP was oxidized to NAPQI. The emergence of ion intensities for monitoring *m/z* 457 and 184 correlated with the growth of ion intensities for the NAPQI ions. Another feature to note is that upon injection of GSH, the peaks observed for the ions due to formation of APAP-SG correspond to the valleys in the selective ion scans for the NAPQI fragment. This feature is expected because the NAPQI is being depleted by the reaction with GSH to form the APAP-SG conjugate.

The formation of APAP-SG was evaluated at varying pH *vs.* peak area of the ion intensities. The ion intensities for the ions corresponding to APAP-SG, formed after the on-line electrolysis of APAP and injection of GSH, were determined as a function of pH as shown in Fig. 7. At a pH 8.5, the ion intensity for APAP-SG is considerably higher than at pH 4.5. It may be interpreted from Fig. 2 that at lower pH the alternative pathway for the oxidation of APAP to NAPQI, which is catalyzed by H^+ [14], to form 1,4-benzoquinone (pathway A) is competing with the GSH conjugation (pathway B). At higher proton concentrations pathway A becomes more prominent than pathway B, hence the decrease in intensities for the APAP-SG conjugate.

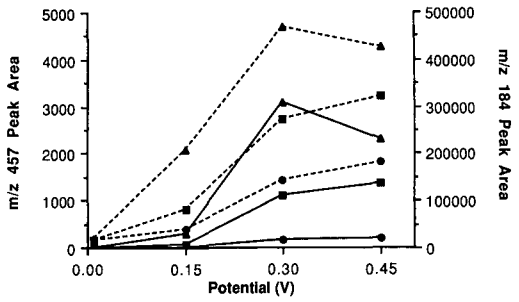

Fig. 7. Peak area of ion intensities for APAP-SG ions at m/z 457 (——) and 184 (---) formed and detected at various potentials and pH. (●) pH 4.5; (■) pH 6.0; (▲) pH 8.5.

The pH affects the potential where APAP begins to oxidize to NAPQI. At lower pH, the oxidation is more difficult, *i.e.* a higher positive potential is needed to convert APAP into NAPQI. This pH effect on oxidation has been reported for APAP[16]. Hydrodynamic voltammograms in the ESA coulometric electrochemical cell confirmed this effect of pH. This is indicated in Fig. 7 by the intensity of m/z 457 at pH 4.5 and pH 8.5. For the potential of +0.15 V, the lower pH of 4.5 produced no ion intensity for the $[M+H]^+$ ion compared with the $[M+H]^+$ ion intensity at pH 8.5 for +0.15 V.

The electrochemical cell employed in this study was a coulometric cell. If the concentration of a constant flow of solute through the electrochemical cell is known, then the number of electrons transferred during the redox event may be calculated by

$$i = (n\,F\,f\,C)/(60\text{ s min}^{-1})$$

where i is the constant current that is measured, n is the number of electrons transferred, F is Faraday's constant (96 500 A s mol^{-1}), f is the flow-rate in ml min^{-1}, and C is concentration of solute in mol ml^{-1}. For the case of APAP, the expected two-electron transfer was confirmed by the flow coulometric measurement.

The thermospray mass spectrum of an authentic sample of the cysteine conjugate of APAP is shown in Fig. 8. The $[M+H]^+$ ion for APAP-SC at m/z 271 and the protonated APAP-SH fragment ion at m/z 184 were observed. The ammoniated form of the fragment ion was also detected at m/z 201.

The APAP-SC conjugate was also electrochemically formed on-line and detected by TSP MS in a similar manner to the APAP-SG conjugate. The TSP MS of APAP before oxidation and mixing with CSH is shown in Fig. 9a. Mass spectral peaks for CSH were detected for the $[M+H]^+$ ion at m/z 122 and the $[M_2H]^+$ ion at m/z 243. Two undetermined peaks were seen at m/z 148 and m/z 273. These two undetermined peaks were also observed following injection of CSH without APAP. As shown in Fig. 9b on oxidation of APAP and mixing with CSH, two mass spectral peaks with low ion intensities were observed at m/z 184 and m/z 271. These m/z values correspond to the values indicative of the APAP-SC conjugate (Fig. 8). The selective ion scans of NAPQI, APAP-SC, and the two undetermined peaks m/z 148 and m/z 273 are shown in Fig. 10 at increasing oxidizing potentials, at 0.2 V increments. The NAPQI ion at m/z 108 behaved as described previously for the APAP-SG conjugate,

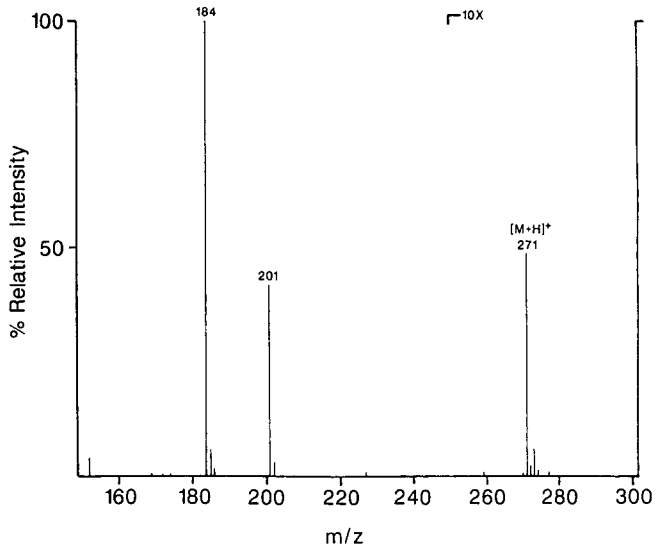

Fig. 8. Authentic sample of APAP-SC conjugate analysed by TSP MS in 0.1 *M* ammonium acetate.

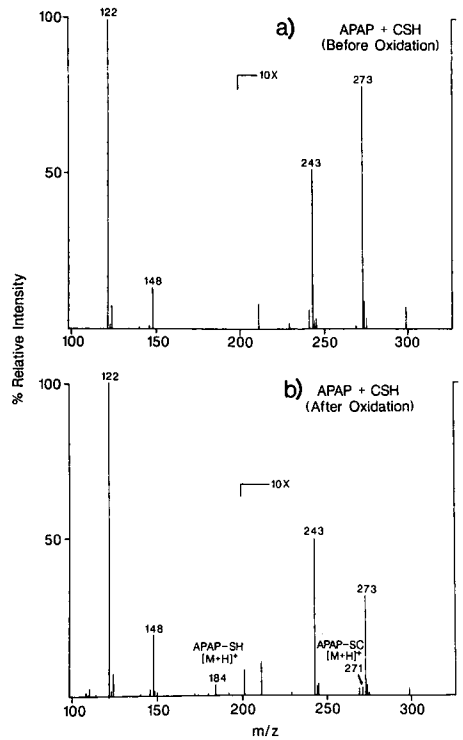

Fig. 9. TSP MS of APAP mixed with CSH acquired (a) before oxidation of APAP and (b) after oxidation of APAP. After oxidation of APAP, mass spectral peaks indicative of APAP-SC are observed for $[M + H]^+$ at m/z 271 and for the protonated thiol fragment ion at m/z 184.

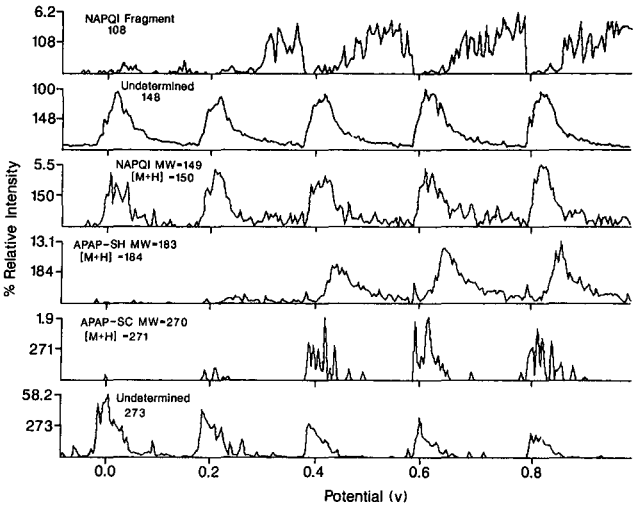

Fig. 10. Selective ion monitoring of ions indicative of NAPQI (*m/z* 150 and 108) and APAP-SC (*m/z* 271 and 184) shown at various-applied potentials. Ion intensities at *m/z* 148 and *m/z* 273 were due to undetermined ions.

but the *m/z* 150 ion intensity appeared even before APAP began to be oxidized. This ion intensity for *m/z* 150 prior to oxidation is possibly due to a sulfur isotope from the undetermined peak at *m/z* 148. This possibility is supported by the ratio of relative ion intensities (Fig. 10) for *m/z* 148 and *m/z* 150, which are 100% and 5.5%, respectively. The 100:5.5 ratio is approximately the ratio for the ^{32}S:^{34}S isotopes. The peaks corresponding to the ions associated with the APAP-SC conjugate appeared only after the APAP was electrochemically converted into NAPQI at +0.2 V. The $[M+H]^+$ ion at *m/z* 271 and the fragment at *m/z* 184 for APAP-SC appeared when 100 μl of the CSH solution was injected into the stream of NAPQI and mixed. The selective ion scan of one of the undetermined peaks in Fig. 10 demonstrated potential *vs.* ion intensity dependency; the *m/z* 273 species decreased in ion intensity at increasing oxidizing potential.

Glutathione conjugates have been succesfully observed as the $[M+H]^+$ ion by fast atom bombardment (FAB) MS for the APAP moiety[17], and FAB tandem mass spectrometry has also been reported[18]. A comparative study of TSP MS analyses of glutathione and cysteine conjugates has been carried out, and various other ionization modes in MS for these conjugates have been discussed[19]. In their comparative study, Parker *et al.*[19] noted that the ion intensities for $[M+H]^+$ ions were dependent on source conditions for these thermally labile conjugates. Optimizing the APAP-SG and APAP-SC ions for this study did require fine adjustment of the vaporizer and block temperatures, as well as the flow-rate into the mass spectrometer.

For the APAP-SG conjugate, ion intensities produced by SECYMS for the $[M+H]^+$ ion and the protonated APAP-SH fragment ion were similar to those previously reported[9]. The SECYMS of APAP-SC gave a much diminished ion intensity for the $[M+H]^+$ ion and protonated APAP-SH compared with the authentic sample. One difference for the APAP-SC conjugate *vs.* APAP-SG is that CSH was found to be

electrochemically oxidizable at a glassy carbon electrode. This oxidation occurred at a more anodic potential than that of APAP, so it did not have a direct effect on the formation of the APAP-SC conjugate. However, as pointed out in Fig. 10, one of the undetermined peaks (*m/z* 273) associated with CSH did give an indication that its ion intensity varied with electrode potential. It should be noted that the *m/z* 148 mass spectral peak also appeared in the APAP-SC authentic sample analysed by TSP MS (not shown in Fig. 8).

The electrochemistry of GSH and CSH has been studied by Thackrey and Riechel[20], who used glassy carbon electrode and mediators to enhance the electrochemistry. Cyclic voltammetry of GSH produced no discernible oxidative wave in 0.1 *M* KCl, which confirmed our observations of GSH in 0.1 *M* ammonium acetate, *i.e.* no oxidation detected by cyclic voltammetry. The reported voltammogram of CSH in 0.1 *M* KCl also indicated no oxidation[20]; however, in our experiments with differential pulse voltammetry we observed an oxidation wave at +1.45 V *vs.* Ag/AgCl in 0.1 *M* ammonium acetate without a mediator. The cyclic voltammogram of CSH gave only a rising background in 0.1 *M* ammonium acetate. Another factor that may explain the diminished ion intensities for APAP-SC by the SECYMS method compared with the authentic sample is that the rate of reaction for CSH conjugation with APAP may not be as rapid relative to GSH conjugation, which produced ion intensities similar to authentic samples reported in the literature[9].

The large ion intensities for CSH in Fig. 9, before and after oxidation of APAP, is due to the large excess of CSH used for the on-line electrochemical synthesis of APAP-SC. The mole ratio of CSH:APAP was *ca.* 20:1. The mole ratio of GSH:APAP to form the APAP-SG conjugate was *ca.* 10:1.

The study of APAP-SG and APAP-SC conjugation by SECYMS could be further enhanced by the utilization of an HPLC column between the electrochemical coulometric cell and thermospray mass spectrometer. This EC–HPLC–TSP MS experiment should be capable of separating unused reactants and multiple products, followed by characterization by TSP MS. For the example of APAP-SC, identification of *m/z* 148 and *m/z* 273 may be possible after separation by HPLC. Future studies will investigate the conjugates of *p*-aminophenol and related compounds and their electrochemical formation and detection by SECYMS.

CONCLUSION

The extension of SECYMS as a flow-injection reaction system has proved successful as a means to form on-line the GSH and CSH conjugates of APAP. The ability to generate conjugates in less than 1 s may prove invaluable in evaluating plausible conjugate formation prior to scaled-up synthesis for biochemical and animal studies. Furthermore, the electrochemical information retrieved, such as the number of electrons transferred, may enable investigators to confirm *in vivo* reaction mechanisms. An advantage for the mass spectrometrist utilizing TSMS is that a practically infinite amount of conjugates is available by this SECYMS method. This permits the optimization of the operating conditions for TSMS. These conditions may include varying the vaporizer and block temperatures along with flow-rates of liquid carriers. The SECYMS method may supply information on the chemical conditions for conjugate formation, as exemplified by the pH study of APAP-SG.

The SECYMS method is another technique that falls into the domain of spectroelectrochemistry. The coupling of mass spectrometry with electrochemistry allows the detection and characterization of reactive species, such as NAPQI, that may not be detected or characterized by any other MS method or, for that matter, any other spectroscopic technique. The simplicity and utility of SECYMS for observing redox reactions have been demonstrated by this study of on-line APAP conjugate formation.

ACKNOWLEDGEMENTS

One of us (T.A.G.) was supported in part by an appointment to the ORAU Postgraduate Research Program at the National Center for Toxicological Research, which is administered by the Oak Ridge Associated Universities through an interagency agreement between the US Department of Energy, and the US Food and Drug Administration. The authors thank Dr. A. Shaikh at the University of Arkansas at Little Rock for use of BAS-100A, and C. Hartwick for typing the manuscript.

REFERENCES

1 G. Hambitzer and J. Heitbaum, *Anal. Chem.*, 58 (1986) 1067.
2 T. Getek, *"The Development of Thermospray Mass Spectrometry Combined with Electrochemical Redox Processes"*, presented at the *34th Annual Conference on Mass Spectrometry and Allied Topics, Cincinnati, OH, June 8–13, 1986.*
3 K. Volk, M. Lee. R. Yost and A. Brajter-Toth, *Anal. Chem.*, 60 (1988) 722.
4 C. Blakley and M. Vestal, *Anal. Chem.*, 55 (1983) 750.
5 S. Bruckenstein and R. Gadde, *J. Am. Chem. Soc.*, 93 (1971) 5941.
6 O. Wolter and J. Heitbaum, *Ber. Bunsenges. Phys. Chem.*, 88 (1984) 2.
7 D. Potter and J. Hinson, *Mol. Pharmacol.*, 30 (1986) 33.
8 B. Coles, I. Wilson, P. Wardman. J. Hinson, S. Nelson and B. Ketterer, *Arch. Biochem. Biophys.*, 364 (1988) 253.
9 L. Betowski, W. Korfmacher, J. Lay, Jr., D. Potter and J. Hinson, *Biomed. Environ. Mass Spectrom.*, 14 (1987) 705.
10 T. Getek and W. Korfmacher, *"The Study of Acetaminophen Conjugate Formation by Oxidative Electrochemistry and Thermospray Mass Spectrometry"*, in *Proceedings of the 36th ASMS Conference on Mass Spectrometry and Allied Topics, San Francisco, CA, June 5–10, 1988.*
11 ESA Model 5100A Coulochem Detector Instruction Manual, Bedford, MA, 1987.
12 T. McRae, K. Furuhama, D. Roberts, T. Getek and J. Hinson, to be presented at the *28th Annual Meeting of the Society of Toxicology, Atlanta, GA, 1989.*
13 G. Carro-Ciampi, P. Hunt, C. Turner and P. Wells, *J. Pharm. Meth.*, 19 (1988) 75.
14 J. Van Benshoten, J. Lewis, W. Heineman, D. Roston and P. Kissinger, *J. Chem. Educ.*, 60 (1983) 772.
15 T. Getek, *Diss. Abstr. Int. B*, 48 (1988) 2951.
16 D. Miner, J. Rice, R. Riggin and P. Kissinger, *Anal. Chem.*, 53 (1981) 2258.
17 J. Lay, Jr., D. Potter and J. Hinson, *Biomed. Environ. Mass Spectrom.*, 14 (1987) 517.
18 P. Haroldsen, M. Reilly, H. Hughes, S. Gaskell and C. Porter, *Biomed. Environ. Mass Spectrom.*, 15 (1988) 615.
19 C. Parker, J. deWit, R. Smith, M. Gopinathan, O. Hernandez, K. Tomer, C. Vestal, J. Sanders and J., Bend, *Biomed. Environ. Mass Spectrom.*, 15 (1988) 623.
20 R. Thackrey and T. Riechel, *J. Electroanal. Chem.*, 245 (1988) 131.

Journal of Chromatography, 474 (1989) 257–263
Elsevier Science Publishers B.V., Amsterdam — Printed in The Netherlands

CHROM. 21 390

COUPLED COLUMN CHROMATOGRAPHY–MASS SPECTROMETRY

THERMOSPRAY LIQUID CHROMATOGRAPHIC–MASS SPECTROMETRIC AND LIQUID CHROMATOGRAPHIC–TANDEM MASS SPECTROMETRIC ANALYSIS OF METOPROLOL ENANTIOMERS IN PLASMA USING PHASE-SYSTEM SWITCHING

A. WALHAGEN*
Technical Analytical Chemistry, University of Lund, P.O. Box 124, S-221 00 Lund (Sweden)
L.-E. EDHOLM
Bioanalytical Laboratory, AB Draco (Subsidiary of AB Astra), P.O. Box 24, S-221 00 Lund (Sweden)
and
C. E. M. HEEREMANS, R. A. M. VAN DER HOEVEN, W. M. A. NIESSEN, U. R. TJADEN and J. VAN DER GREEF
Division of Analytical Chemistry, Centre for Bio-Pharmaceutical Sciences, P.O. Box 9502, 2300 RA Leiden (The Netherlands)

SUMMARY

The applicability of phase-system switching using thermospray tandem mass spectrometry is demonstrated for the bioanalysis of the enantiomers of the betablocker metoprolol. Independent optimization of the chromatography, using an α_1-acid glycoprotein chiral stationary phase, and the mass spectrometric detection system is realized. By utilizing peak compression, 10 ng (37 pmol) of each enantiomer is easily detected in standard solutions. In plasma samples, with use of tandem mass spectrometry for additional selectivity, levels of 61 ng/ml (230 nmol/l) can be measured by using [$^2H_6$]metoprolol as internal standard.

INTRODUCTION

Stereochemical aspects are of growing importance in the development of drugs, since the pharmacological activity often resides in only one of the enantiomers[1]. As the awareness of the pharmacological and pharmacokinetic differences of enantiomers increases, there is a growing need for sensitive and selective bioanalytical methods for the determination of enantiomeric drugs in biological matrices[2]. The technique with the greatest potential for the separation of enantiomers is column liquid chromatography (LC).

Separation can be performed either directly or indirectly. Direct separation is to be preferred, and a number of chromatographic systems have been developed utilizing either chemically bonded chiral stationary phases or a chiral phases with a chiral mobile phase. Most of the systems, however, have only been applied to relatively

0021-9673/89/$03.50

uncomplicated samples at high concentrations. Application to bioanalytical work at low concentrations will not be straightforward and a number of problems can be foreseen.

In a recent paper[2], the use of coupled column chromatography (CCC) and liquid chromatography–mass spectrometry (LC–MS) has been discussed as a way to overcome some of these problems. With CCC, selective on-line sample work-up can be performed, and if combined with a heart-cutting technique, excellent selectivity can be obtained. Further work to explore the use of CCC in separation and determination of enantiomers has focussed on applications of immobilized protein phases[3], in order to extend their usage to bioanalytical work. It was shown that CCC can be used to increase the overall selectivity and the often low efficiency obtained on this type of phase. Examples were given of the separation and determination of some selected drugs in plasma, among them the beta-blocker metoprolol[4].

As was discussed earlier[2], it is often necessary to use an internal standard in bioanalytical work, but finding a suitable standard can be very difficult. When a mass spectrometer is used as a detector, this problem is less complicated because isotopically labelled internal standards can be used.

Chromatography with α_1-acid glycoprotein chiral stationary phases is usually performed with a mobile phase of aqueous phosphate buffer, which is not compatible with on-line LC–MS. Therefore, a special application of coupled column chromatography, called phase-system switching (PSS)[5], is used to perform the analysis. PSS has been developed to solve problems of mobile phase incompatibilities in LC–MS target compound analysis[6,7]. By using valve-switching techniques, enantiomers can be successively heart-cut from the chromatogram developed on the chiral column and trapped on two short trapping columns, which are washed with water to remove residual buffer constituents. In the next step the enantiomers are eluted from the trapping columns with a solvent suitable for the applied LC–MS interface, and mass analyzed.

In this paper metoprolol (Fig. 1) has been used as a model substance to demonstrate the potential of the PSS approach, in combination with chiral separation by thermospray LC–MS or LC–MS–MS. The analysis of metoprolol enantiomers in plasma was carried out using deuterium-labelled metoprolol as internal standard.

EXPERIMENTAL

Equipment

A schematic diagram of the chromatographic system is given in Fig. 2. The system consists of two type 2150 LC pumps (LKB, Bromma, Sweden), a Model

Metoprolol

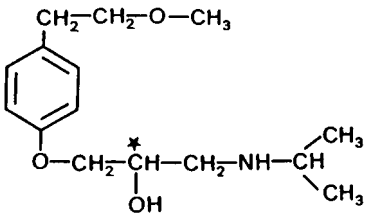

Fig. 1. Structural formula of metoprolol.

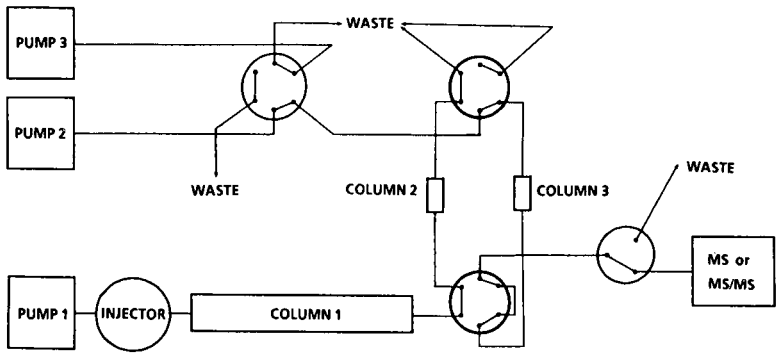

Fig. 2. Schematic diagram of the experimental setup.

SP-8700 LC pump (Spectra Physics, San José, CA, U.S.A.), a Model 7125 injection valve (Rheodyne, Berkeley, CA, U.S.A.), an MUST valve-switching unit (Spark Holland, Emmen, The Netherlands) and a Model 7010 switching valve (Rheodyne). UV detection at 254 nm was performed using a type 440 UV detector (Waters Assoc., Milford, MA, U.S.A.) coupled directly to the chiral column. Combined LC–MS was performed with a Finnigan MAT TSQ-70 triple quadrupole mass spectrometer equipped with a thermospray interface (Finnigan MAT, San José, CA, U.S.A.). Vaporizer temperature and repeller voltage were optimized under current conditions, resulting in values of 130°C and 50 V, respectively. The source block temperature was kept at 200°C. In the MS–MS experiments air was used as collision gas at a pressure of 0.05 Pa. The optimized collision energy was 30 V.

Materials

Racemic metoprolol {1-isopropylamino-3-[4-(2-methoxyethyl)phenoxy]-2-propanol}, $^2H_6$-labelled metoprolol and *S*-(−)-metoprolol were kindly supplied by Hässle AB (subsidiary of Astra, Gothenburg, Sweden). Sodium dihydrogenphosphate monohydrate, disodium hydrogenphosphate dihydrate and 2-propanol were of analytical reagent grade and obtained from E. Merck (Darmstadt, F.R.G.). HPLC-grade methanol and acetonitrile were obtained from Rathburn Chemical (Walkerburn, U.K.). Water was purified with a Milli-Q system (Millipore, Bedford, MA, U.S.A.). Bond Elut C_{18} was obtained from Analytichem International (Harbor City, CA, U.S.A.).

The α_1-acid glycoprotein column (100 mm × 4 mm I.D.) was obtained from ChromTech (Stockholm, Sweden). The trapping columns were Guard-Pak Bondapak C_{18} cartridges (4 mm × 5 mm I.D.) (Waters Assoc.).

Mobile phase 1, used in the chiral separation, was 0.25% 2-propanol in 20 m*M* phosphate buffer of pH 7 and the flow-rate was 0.8 ml/min. Mobile phase 2, used for desorption and thermospray LC–MS analysis, was 20% methanol in 50 m*M* ammonium acetate; the flow-rate was 1.5 ml/min. Washing of the trapping columns was performed with 1 ml/min of water.

Sample pre-treatment

Plasma samples were pre-treated using Bond Elut C_{18} columns (capacity 1 ml)

according to ref. 8. Each column was conditioned with 2 × 1 ml of acetonitrile and 2 × 1 ml of water. To 1 ml of plasma was added 100 μl of 1.8 μg/ml (6.4 μ*M*) internal standard solution. The sample was drawn through the column by suction. After washing the column with two 0.5 ml volumes of 10% acetonitrile in water the metoprolol-containing fraction was eluted with 500 μl of 50% acetonitrile in 0.1 *M* HCl into a test tube. After evaporating the eluate under a stream of nitrogen the residue was dissolved in 280 μl of mobile phase 1. The injection volume was 130 μl.

RESULTS AND DISCUSSION

System description

A schematic diagram of the PSS system is shown in Fig. 2. The procedure is as follows: the pre-treated samples are injected on to the α_1-acid glycoprotein column (column 1). The first-eluting enantiomer, (+)-metoprolol, is collected on the first trapping column (column 2) and the other enantiomer is collected on column 3. (The retention time windows, setting the volumes that must be switched to the two trapping columns, are determined daily in a separate experiment using a UV detector coupled directly to the outlet of the chiral column). The two trapping columns are then washed with water to remove residual buffer salts, and the metoprolol enantiomers are subsequently eluted and introduced into the mass spectrometer. A three-port valve is placed between the valve-switching unit and the thermospray interface in order to discard water containing the phosphate buffer from the washing step. If this latter step is omitted, the thermospray interface capillary is frequently clogged by buffer salts.

In the development of phase-system switching several aspects have to be dealt with. Baseline separation of the two enantiomers on the chiral column is essential in order to enable quantitative heart-cutting from the developing chromatogram. Trapping columns must be selected that have sufficient sample capacity and sufficiently high capacity ratios for the metoprolol enantiomers both in the mobile phase of the chiral column and in water, which is used for removal of the residual phosphate buffer in the washing step. Furthermore, the enantiomers should have low capacity ratios in the desorbing eluent. Ideally, the compound of interest is adsorbed on top of the trapping column and rapidly desorbed in the backflush mode in a sharp band. In the present case it appears that metoprolol is distributed over the trapping column during adsorption and washing. Thus the washing should be kept to a minimum. Without washing of the trapping columns, frequent clogging of the thermospray interface capillary occurs. When the trapping columns are washed with water for 30 s at a flow-rate of 1 ml/min, clogging of the thermospray interface capillary is no longer observed and stable ionization conditions can be achieved. The dimensions of the trapping columns are also important in optimizing the peak compression. Optimization of the system in this respect has not been studied here.

Liquid chromatography–mass spectrometry

Under the present conditions an intense peak at $m/z = 268$ for the protonated metoprolol molecule is observed in thermospray buffer ionization mode (Fig. 3). Hardly any fragmentation occurs. Full-scan mass spectra with good signal-to-noise ratios can be obtained with amounts as low as 4 ng of metoprolol, injected in the column-bypass mode.

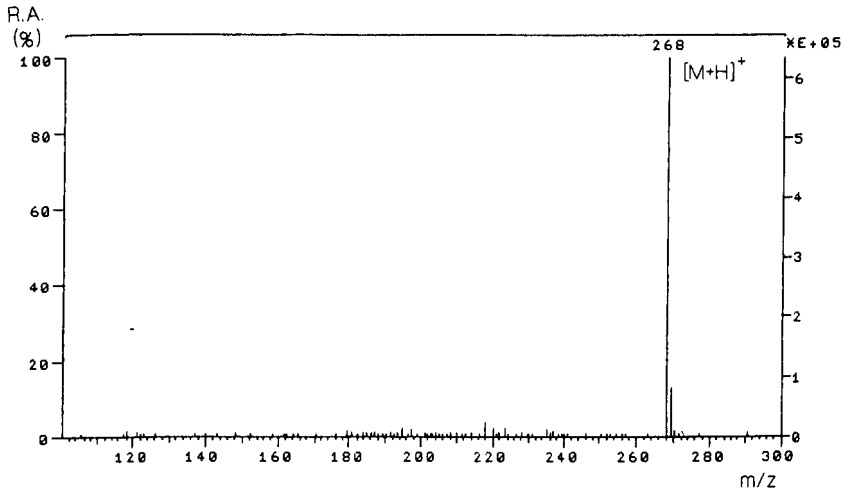

Fig. 3. Thermospray mass spectrum of metoprolol. For conditions see text. Right-hand side: absolute intensity in arbitrary units.

The successful performance of the valve-switching system is demonstrated in Fig. 4. The system shows good performance with respect to the separation of the two enantiomers, the quantitative collection of both enantiomers, and the mass analysis of them after phase-system switching from the LC–MS-incompatible mobile phase, containing phosphate buffer, to an ammonium acetate buffer system, as frequently used in thermospray LC–MS. Equal peak areas were obtained for the two enantiomers using the racemate standard solution containing 29 ng (110 pmol) of metoprolol [14.5 ng (55 pmol) of each enantiomer].

Considerable peak compression is evident upon comparison of the peak width obtained with UV detection directly after chiral separation on one hand and the peak

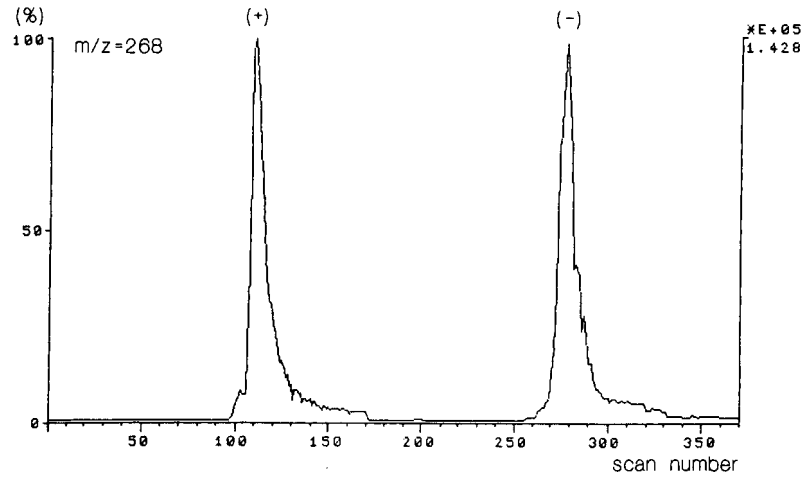

Fig. 4. Mass chromatogram after PSS for the racemic mixture; each peak corresponds to 18 ng. For conditions see text. Right-hand side: absolute intensity in arbitrary units.

width after PSS and LC–MS analysis at the other. The peak width is decreased by a factor of *ca.* 5 by applying the PSS approach.

A drawback of the PSS approach in combination with the thermospray interface in this case appears to be the increase in the background ion current which results from valve switching. Before switching the valves in the desorption mode no liquid is entering the thermospray interface. Upon switching, when introduction of liquid into the interface is resumed the thermospray conditions need some time to stabilize, resulting in baseline disturbances at all m/z ratios. As a result the mass chromatograms of blank samples show a signal. This is a problem for compounds eluting directly from the trapping column, which is in fact the most favourable situation with respect to peak compression. There are several ways to overcome this problem. By using either a more hydrophobic trapping column or a weaker eluting solvent (or both) some retention of the compound of interest will be obtained on the trapping column, resulting in some delay between the solvent front causing the baseline disturbance and the compound of interest. Another approach is the use of a second column between the trapping column and the LC–MS interface to achieve a similar effect. However, both approaches will influence the peak shape and result in less peak compression. These two approaches have therefore not been investigated extensively.

Liquid chromatography–tandem mass spectrometry

Another solution to the problem of baseline disturbance due to valve switching is the use of MS–MS. The signal in MS–MS will be less subject to disturbances due to changes in mobile phase composition and flow-rate occurring in the ion source, because a selective reaction in the collision chamber is monitored. Because the use of MS–MS circumvents the most significant disadvantages of the other solutions mentioned above, and even adds selectivity in the bioanalytical determination, its applicability has been investigated.

The daughter spectra of protonated metoprolol ($m/z=268$) show structurally informative fragmentation, *e.g.*, peaks at $m/z=72$, 98 and 116, corresponding to neutral losses of 196, 170 and 152 amu, respectively. Similar neutral losses are also observed in the daughter spectrum of protonated [$^2H_6$]metoprolol. Since the enantiomers and internal standards (the deuterium labels remain incorporated in the fragment ions) show an equal neutral loss, the neutral loss scan mode can be used to detect these compounds with enhanced selectivity. The neutral loss of 152 a.m.u. corresponding to the loss of 4-(2-methoxyethyl)phenol, is selected as a probe in the analysis of the metoprolol enantiomers in plasma. Fig. 5 shows the MS–MS mass chromatograms of both metoprolol and the deuterated internal standard as obtained after injection of a plasma sample spiked with 0.37 μg/ml (1.4 μmol/l) of racemic metoprolol and 0.18 μg/ml of internal standard, which corresponds to an injected amount of 86 ng (320 pmol) of each enantiomer (and 46 ng of each deuterated enantiomer). The ratio between the peak areas from the internal standard and metoprolol itself is the same for both enantiomers, even when their areas are not the same (probably due to either a less favourable setting of the retention time window in this particular experiment or differences in desorption characteristics). Thus, it is shown that the internal standard method compensates for variations in thermospray MS–MS conditions. Mass chromatograms of blank plasma samples are free of erroneous signals. The lowest detectable plasma level was 70 ng/ml of racemic metoprolol using an internal standard concentration of 100 ng/ml.

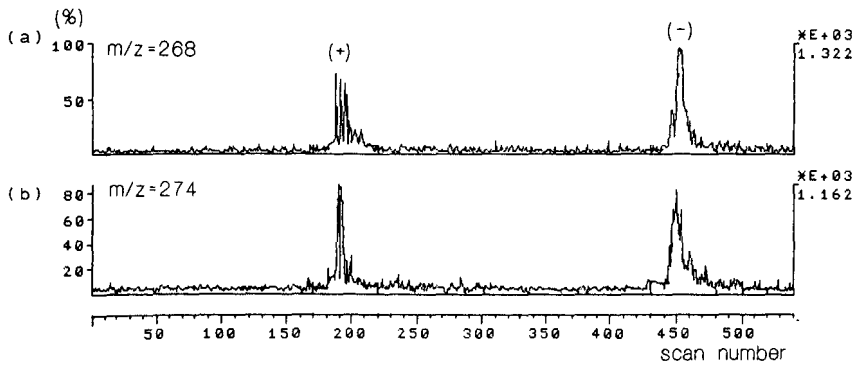

Fig. 5. MS–MS (neutral loss mode) mass chromatograms of (a) metoprolol enantiomers (following the reaction $m/z = 268 \rightarrow m/z = 116$) and (b) $^2H_6$-labelled internal standard ($m/z = 274 \rightarrow m/z = 122$) in plasma. Right-hand side: absolute intensity in arbitrary units.

CONCLUSION

The PSS approach coupled to MS, developed for target compound analysis, increases the possibility of determination of enantiomeric compounds, as shown by using metoprolol as an example. The benefit of using MS is that isotopically labelled internal standards can be used, selectivity can be tuned and, if necessary, identification can be performed. Enhanced selectivity in bioanalytical applications can be achieved by utilizing MS–MS.

REFERENCES

1 E. J. Ariens, *Eur. J. Clin. Pharmacol.*, 26 (1984) 663.
2 L.-E. Edholm, C. Lindberg, J. Paulson and A. Walhagen, *J. Chromatogr.*, 424 (1988) 61.
3 A. Walhagen and L.-E. Edholm, presented at *the 12th International Symposium on Column Liquid Chromatography, Washington, June 19–24, 1988.*
4 A. Walhagen and L.-E. Edholm, *J. Chromatogr.*, 473 (1989) 371.
5 J. van der Greef, W. M. A. Niessen and U. R. Tjaden, presented at *the International Symposium on Pharmaceutical and Biomedical Analysis, Barcelona, September 23–25, 1987.*
6 J. van der Greef, W. M. A. Niessen and U. R. Tjaden, *J. Pharm. Biomed. Anal.*, 6 (1988) 565.
7 E. R. Verheij, H. J. E. M. Reeuwijk, G. F LaVos, W. M. A. Niessen, U. R. Tjaden and J. van der Greef, *Biomed. Environ. Mass Spectrom.*, 16 (1988) 393.
8 P. M. Harrison, A. M. Tonkin and A. J. McLean, *J. Chromatogr.*, 339 (1985) 429.

Journal of Chromatography, 474 (1989) 265–273
Elsevier Science Publishers B.V., Amsterdam — Printed in The Netherlands

CHROM. 21 205

LIQUID CHROMATOGRAPHY–MASS SPECTROMETRY OF TRACE COMPOUNDS WITH A MOVING-BELT INTERFACE AND MULTI-DIMENSIONAL CHROMATOGRAPHY

WIM LUIJTEN*, GÉRARD DAMIEN and JOSETTE CAPART
Technologie Servier, 27 rue Eugène Vignat, P.O. Box 1749, 45007 Orléans Cédex 01 (France)

SUMMARY

A high-performance liquid chromatographic method with on-line mass spectrometric detection is described for the structural analysis of a number of synthetic impurities, present at trace levels in almitrine. To obtain mass spectra with various ionization methods and high-resolution mass measurements, a moving-belt liquid chromatograph–mass spectrometer interface is used. A two-column switching system allows the injection of large amounts of almitrine, from which the trace compounds are trapped on a second column, while discarding the major component. This permits the introduction of the impurities into the mass spectrometer by elution of the second column, without the risk of introducing too large an amount of the major compound into the mass spectrometer. The mass spectra thus obtained are of sufficient quality to permit a correct structural assignement of the impurities.

INTRODUCTION

The physico-chemical characterization of an active compound in a drug includes the structural identification of synthetic impurities. As the major part of the chromatographic separations is performed with liquid chromatography, combined liquid chromatography–mass spectrometry (LC–MS) is often the method of choice for a first structural determination of these impurities.

The amount of synthetic impurities in a compound used as a drug is often very low, usually of the order of 0.01–0.5%. As it is undesirable to introduce large amounts of the major component into the LC–MS system, column-switching techniques can be used effectively to separate and accumulate sufficient amounts of minor constituents on a second column[1–5]. The moving-belt interface offers the advantage that the mass spectrometric conditions are much less influenced by changes in flow and/or solvent composition than, for instance, the thermospray interface[6–10].

Generally, in handling problems of structural identification of unknown compounds ionization by electron impact (EI) is often the first technique to be used, because in this mode the fragmentation pattern provides the major part of the structural information. At some stage chemical ionization and/or fast atom bombardment can be used to acquire information on molecular weight. The moving-belt LC–MS

0021-9673/89/$03.50

interface in combination with a double-focusing mass spectrometer offers the advantage of a variety of ionization methods which can be used[11–15], with the possibility of performing high-resolution measurements for accurate mass determinations[16].

During an analysis of almitrine (Vectarion)[17–19], reversed-phase LC was used to separate a number of minor impurities (<0.1%) from the main component. To permit structural analysis of these compounds by mass spectrometry, a two-dimensional LC system was used, allowing the injection of large amounts of the compound without disturbing the performance of the moving-belt LC–MS system.

The first column was used to discard the major part of the main compound (S 2620) while the second column in the LC system was used to collect, by repeated injections, sufficient amounts of the impurities. On elution of the second column, EI and chemical ionization (CI) were used for structural analysis. The chromatographic separation on the two columns was monitored by two UV detectors in series with the LC system.

EXPERIMENTAL

Chromatography

LC was performed with two Waters 590 solvent delivery systems and a Rheodyne 7125 injection valve. The two columns were of stainless steel with Nucleosil $5C_{18}$ (150 × 4.7 mm I.D., first column) and Nucleosil $3C_{18}$ stationary phases (70 × 4.7 mm I.D., second column). The mobile phase for both columns was methanol–water–trifluoroacetic acid (60:40:0.1, v/v/v), at a flow-rate of 1.0 ml/min in the first stage of the analysis (elution of the first column) and 0.5 ml/min for the subsequent elution of the second column, on-line with the mass spectrometer. The switching between the various elution modes was made by three- and six-way valves (Chromatem SSI, Rheodyne 7000). The elution of the columns was monitored by (1) a Waters M 440 and (2) a Shimadzu SPD-6A variable-wavelength UV detector set at 254 nm.

Moving-belt LC–MS system

A VG Analytical LC moving-belt interface equipped with a spray deposition probe and a Kapton belt was coupled to a VG Analytical 70-250 S double-focusing mass spectrometer. The interface conditions were a spray probe temperature of 280°C, auxiliary gas (nitrogen) at 70 kPa and a belt speed of 0.8 cm/s.

The EI mass spectra were taken at 70 eV ionization energy and 0.1 mA ionization current. The CI mass spectra were obtained with an ionization energy of 125 eV and an emision current of 1.0 mA. The source temperatures were 180 and 140°C in the EI and CI mode, respectively. The mass range was 600–60 amu at a scan speed of 1.0 s/decade. The CI reagent gas was ammonia at approximately 0.5 Torr ion source pressure. High-resolution mass measurements were performed at a resolving power of 7500.

RESULTS AND DISCUSSION

Fig. 1 shows the LC–UV analysis of almitrine obtained after an injection of 100 μg on to a one-column system. In addition to the main compound (S 2620), there are six impurities, present at levels varying from 0.1 to 0.01%. Based on LC analyses of

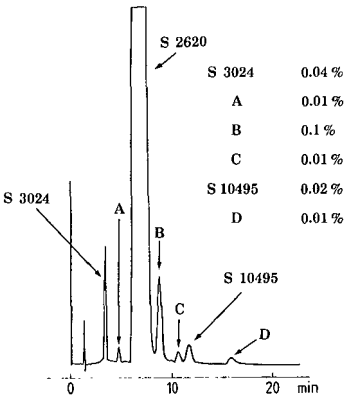

Fig. 1. Liquid chromatogram (UV, 254 nm) showing S 2620 and six minor impurities.

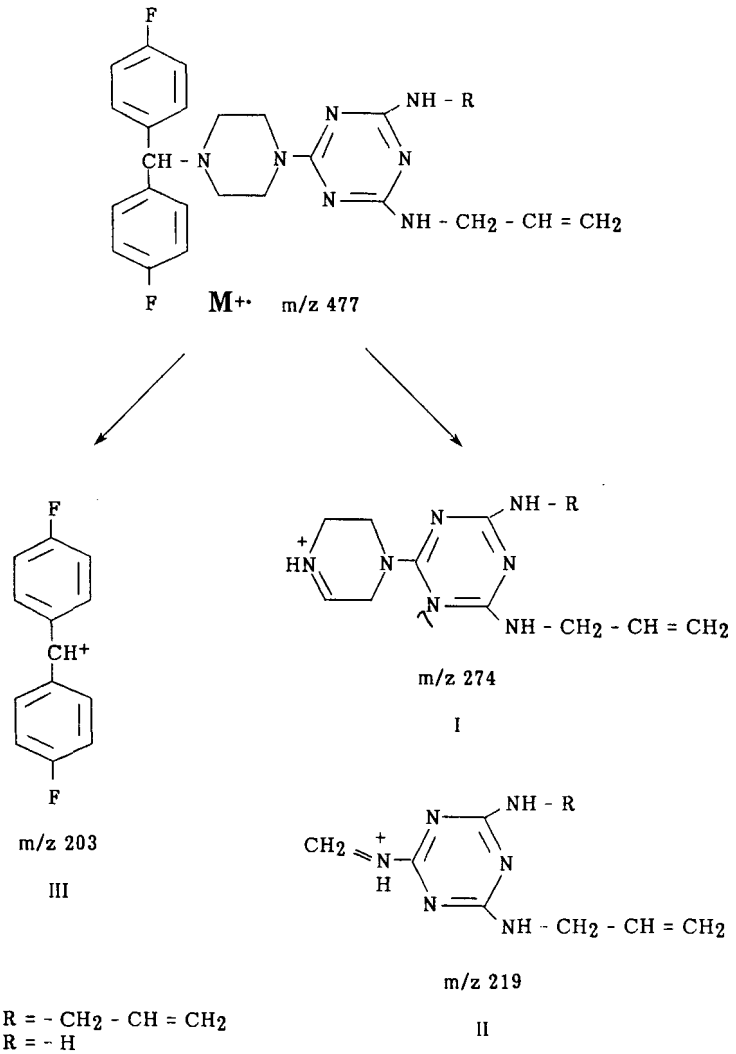

S 2620 R = - CH_2 - CH = CH_2
S 3024 R = - H
S 10495 ortho para isomer of S 2620

Scheme 1. Structure and fragmentations (EI) of almitrine (S 2620) and two known impurities. *m/z* values for S 2620.

some reference compounds, the structures of two of the impurities were known (Scheme 1). On-line LC–MS analysis showed that, in order to obtain mass spectra of sufficient quality to permit structural identification (*i.e.*, EI, CI and high-resolution spectra), an injection of at least 500 μg of almitrine was necessary. As it is impossible to introduce 500 μg of a compound into the mass spectrometer, a column-switching procedure was set up to discard the major part of the principal component eluting from the first column, while trapping the minor compounds on the second column for later LC–MS analysis.

Switching technique

Before performing the actual injection, the first column is conditioned with the elution solvent system, while the second column is flushed with water (Scheme 2, 1). After the injection the minor components (as indicated by the first UV detector) are concentrated on to the head of the second column, while diluting the elution solvent with water, to diminish its eluting capacity (2).

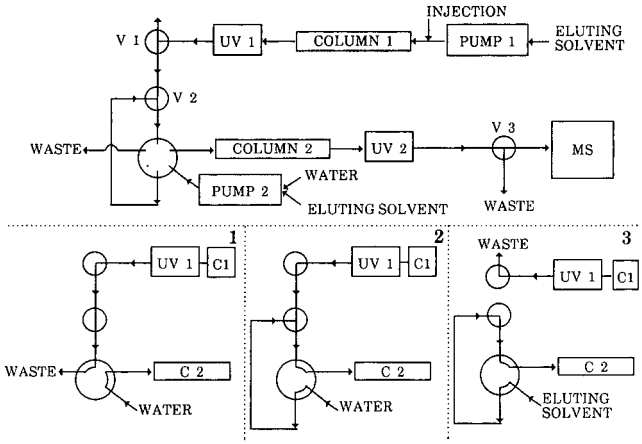

Scheme 2. Overall schematic view of the two-dimensional LC system. (1) Initial conditioning and disposal of major compound; (2) concentration of impurities on the second column; (3) elution of the second column.

When the major compound (S 2620) starts to elute from the first column, the system is switched to its first configuration (1), *i.e.*, the compound is led to waste while the second column is flushed with water. After elution of the main component, the system is switched back to the second configuration to trap the impurities eluting after S 2620.

The third configuration is used to elute the compounds which are trapped and concentrated on the second column, and to feed them through the LC–MS interface into the mass spectrometer. The first column remains under eluting conditions (3). The elution process can be monitored by the second UV detector. In the event that it is undesirable to lead the eluted compounds into the MS, a valve can be used to divert the eluate to waste.

Compound A

The mass spectrum of compound A, obtained after four injections of 500 μg, is similar to that of S 2620 (Table II), but with two differences: the molecular ion has shifted to *m/z* 489 and the *m/z* 203 ion, $[(F - C_6H_4)_2 - CH]^+$ (Scheme 1, fragment III), can now be found at *m/z* 215. The molecular ion was confirmed to be at *m/z* 489 from the CI/NH_3 mass spectrum (MH^+, *m/z* 490). High-resolution mass measurement showed the mass of the molecular ion to be 489.2676 ($C_{27}H_{32}N_7FO$ requires 489.2652), while the accurate mass for the fragment at *m/z* 215 was 215.0873 ($C_{14}H_{12}FO$ requires 215.0872). The conclusion is therefore that in compound A one of the two fluorine atoms on the diphenylmethyl moiety has been replaced by OCH_3.

Compound B

Whereas the LC–MS analysis of compound A was relatively easy, as it eluted before the main compound, the trapping of compound B, eluting just after S 2620, was more difficult because of the large amount of S 2620 eluting just before compound B. The UV trace shows the result of the elution of the second column after a single injection of 0.5 mg of almitrine (Fig. 2). The presence of S 2620 shows that this compound undergoes tailing to some extent when injected in these amounts. However, the impurity B/S 2620 ratio has increased sufficiently to obtain an interpretable mass spectrum (Fig. 3).

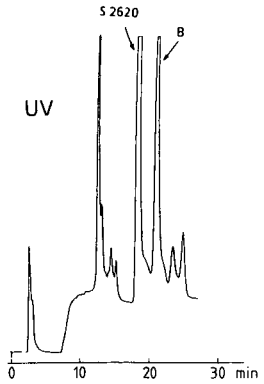

Fig. 2. Liquid chromatogram (UV, 254 nm) obtained after trapping of compound B and elution of the second column.

The fragments corresponding to the bisallylaminotriazine part of the molecule (*m/z* 477, 274, 219) (Scheme 1) are all shifted two mass units upwards, which led us to suspect that one of the allylamino groups is replaced by a propylamine. CI/NH_3 mass spectral analysis produced a protonated molecule at *m/z* 480, thus confirming a molecular weight of 479. The presence of one allylamino and one propylamino group was shown by high-resolution mass measurements of the molecular ion and the major fragments (Table I).

The chromatographic separation is satisfactory, as indicated by the ion chromatogram traces (Fig. 4). Synthesis of a reference compound confirmed that the identification of compound B was correct.

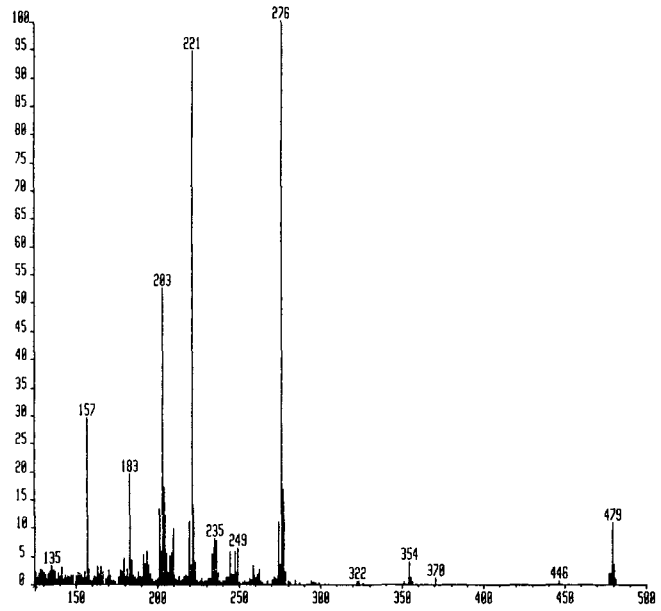

Fig. 3. Mass spectrum (EI, 70 eV) of compound B.

Compound C

Impurity C represents only 0.01% in the initial compound. Consequently, only one injection of 0.5 mg is insufficient to produce a reliable mass spectrum. Therefore, four repeated injections were made, while trapping the impurity C and S 10495 (which has a known structure) on the second column. Once again there is an important amount of S 2620 present owing to tailing of the major compound (Fig. 5).

The mass spectra of S 2620, impurity C and S 10495 are virtually identical (Table II), so that impurity C can be identificed as another isomer of S 2620. By synthesis the compound was confirmed to be the *meta–para* isomer of S 2620. No loss of chromatographic integrity was observed, as indicated by comparison of the UV and reconstructed ion chromatogram traces (Fig. 6).

Finally, peak D, isolated via a slightly modified procedure because of the longer retention time, produced a mass spectrum which again showed only minor differences

TABLE I

HIGH RESOLUTION MASS MEASUREMENT OF COMPOUND B

Found	*Theoretical*		*Deviation (ppm)*
479.2600	$C_{26}H_{31}N_7F_2$	= 479.2609	−1.9
276.1931	$C_{13}H_{22}N_7$	= 276.1937	−2.2
221.1521	$C_{10}H_{17}N_6$	= 221.1514	3.2
203.0663	$C_{13}H_9F_2$	= 203.0672	−4.4

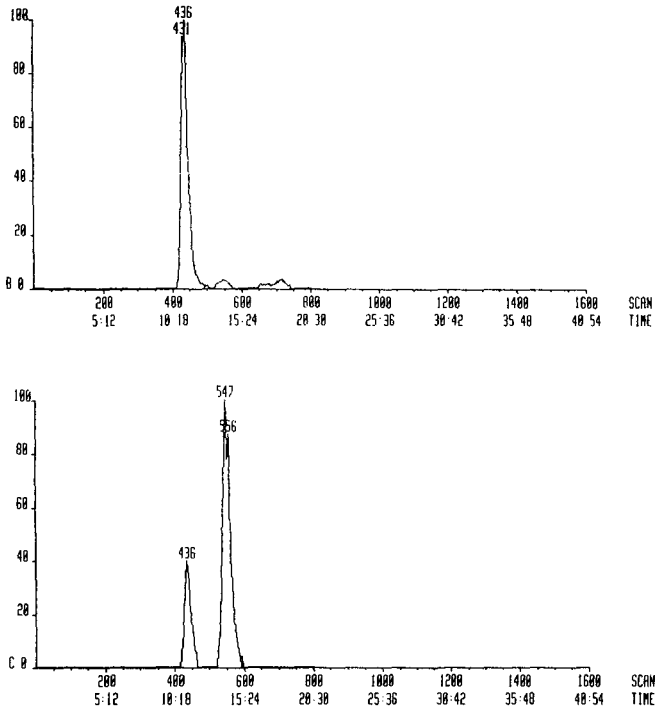

Fig. 4. Reconstructed ion chromatogram of *m/z* 477 (top) and *m/z* 479 (bottom) of compounds B and S 2620.

in the relative abundances of the molecular ion and the important fragments found in the mass spectrum of S 2620 (Table II). Synthesis of some reference compounds identified compound D as another isomer of S 2620, having the two fluorine atoms at the *ortho* and *meta* positions.

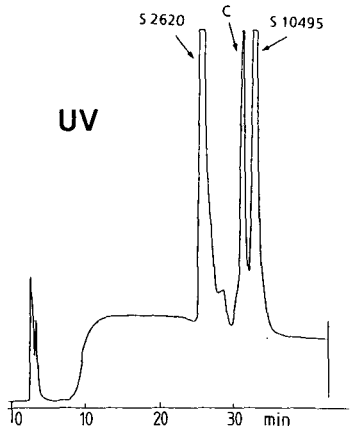

Fig. 5. Liquid chromatogram (UV, 254 nm) obtained after trapping of compounds C and S 10495 and elution of the second column.

TABLE II

MASS SPECTRA (EI, 70 eV) OF S 2620 AND IMPURITIES

Compound	$[M]^{+\cdot}$	*Fragments (Scheme 1)*		
		I	*II*	*III*
S 2620	477 (10)	274 (95)	219 (100)	203 (45)
S 3024	437 (10)	234 (60)	179 (100)	203 (50)
A	489 (15)	274 (70)	219 (100)	215 (90)
B	479 (15)	276 (100)	221 (95)	203 (55)
C	477 (15)	274 (100)	219 (100)	203 (40)
S 10495	477 (20)	274 (90)	219 (100)	203 (40)
D	477 (25)	274 (100)	219 (100)	203 (65)

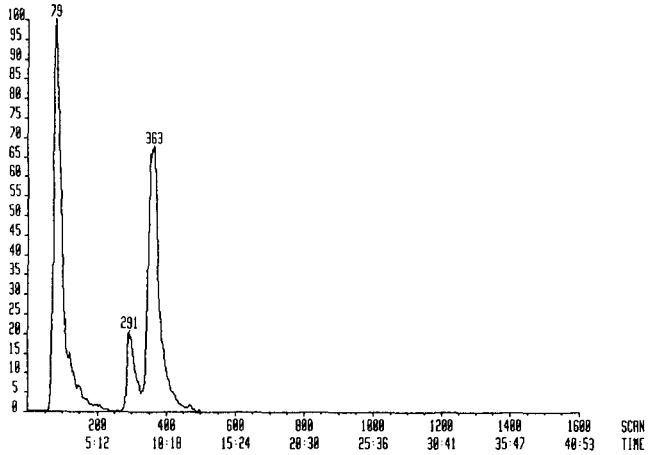

Fig. 6. Reconstructed total ion chromatogram of compounds S 2620, C and S 10495.

CONCLUSION

The method has proved itself useful in the structural analysis of unknown compounds present at trace levels in a major component. The advantage of the moving-belt LC–MS interface in this particular instance has been the possibility of using different ionization techniques (EI and CI) to assist in the structural determination of unknown compounds during on-line LC–MS.

Another useful application that has been tested is to use the two-column LC system to change the elution solvent to make it more compatible with the LC–MS system, such as removal of (phosphate) buffers and avoiding excess amounts of water[20,21].

REFERENCES

1 J. F. K. Huber, R. van der Linden, E. Ecker and M. Oreans, *J. Chromatogr.*, 83 (1973) 267.
2 F. Erni, H. P. Keller, C. Morin and M. Schmitt, *J. Chromatogr.*, 204 (1981) 65.
3 C. C. Honegger, W. Krenger, H. Langemann and A. Kempf, *J. Chromatogr.*, 381 (1986) 249.
4 C. Rodriguez, N. Bertrand, C. Julien, G. Cuisinaud and J. Sassard, *Int. J. Environ. Anal. Chem.*, 25 (1986) 235.
5 L. C. Verhagen, J. Strating and U. R. Tjaden, *J. Chromatogr.*, 393 (1987) 85.
6 T. R. Covey, J. B. Crowther, E. A. Dewey and J. D. Henion, *Anal. Chem.*, 57 (1985) 474.
7 R. D. Voyksner and C. A. Haney, *Anal. Chem.*, 57 (1985) 991.
8 I. G. Beattie, D. E. Games, J. R. Startin and J. Gilbert, *Biomed. Mass Spectrom.*, 12 (1985) 616.
9 D. J. Liberato and A. L. Yergey, *Anal. Chem.*, 58 (1986) 6.
10 C. Lindberg and J. Paulson, *J. Chromatogr.*, 394 (1987) 117.
11 T. P. Fan, E. D. Hardin and M. L. Vestal, *Anal. Chem.*, 56 (1984) 1870.
12 J. van der Greef, A. C. Tas, M. C. ten Noever de Brauw, M. Höhn, G. Meijerhoff and U. Rapp. *J. Chromatogr.*, 323 (1985) 81.
13 J. G. Stroh, J. C. Cook, R. M. Milberg, L. Brayton, T. Kihara, Z. Huang, K. L. Rinehart, Jr. and I. A. S. Lewis, *Anal. Chem.*, 57 (1985) 985.
14 J. G. Stroh, K. L. Rinehart, Jr., J. C. Cook, M. Suzuki and T. Arai, *J. Am. Chem. Soc.*, 108 (1986) 858.
15 W. Luijten, G. Damien, B. Marchand and J. Capart, *Biomed. Environ. Mass Spectrom.*, 16 (1988) 93.
16 J. van der Greef, A. C. Tas, L. M. Nijssen, J. Jetten and M. Höhn, *J. Chromatogr.*, 394 (1987) 77.
17 Y. Castaing, G. Manier, N. Varene and H. Guenard, *Bull. Eur. Physiopath. Resp.*, 17 (1981) 917.
18 G. Simmoneau, A. Denjean, B. Raffestin, O. Meyniard, S. Laurent, M. Meignan and A. Harf, *Am. Rev. Respir. Dis.*, 123 (1981) 88.
19 F. Arnaud, A. Bertrand, J. Charpin, J. Chrétien, G. Decroix, F. Guerrin, J. C. Kalb, J. Lissac, F. B. Michel, P. Moere, B. Paramelle, R. Pariente, M. Perrin-Fayole, J. Rochemaure and C. Voisin, *Bull. Eur. Physiopath. Resp.*, 18 (1982) 373.
20 G. M. Kresbach, T. R. Baker, R. J. Nelson, J. Wronka, B. L. Karger and P. Vouros, *J. Chromatogr.*, 394 (1987) 89.
21 C. Lindberg, J. Paulson and S. Edsbäcker, *Biomed. Environ. Mass Spectrom.*, 14 (1987) 535.

Journal of Chromatography, 474 (1989) 275–283
Elsevier Science Publishers B.V., Amsterdam — Printed in The Netherlands

CHROM. 21 376

BELT-SPEED PROGRAMMING, A NEW TECHNIQUE FOR PEAK COMPRESSION IN LIQUID CHROMATOGRAPHY–MASS SPECTROMETRY AND SUPERCRITICAL-FLUID CHROMATOGRAPHY–MASS SPECTROMETRY WITH MOVING-BELT INTERFACES

E. R. VERHEIJ

Division of Analytical Chemistry, Center for Bio-Pharmaceutical Sciences, Gorlaeus Laboratories, P.O. Box 9502, 2300 RA Leiden, (The Netherlands) and TNO-CIVO Institutes, P.O. Box 360, 3700 AJ Zeist (The Netherlands)

G. F. LA VOS

TNO-CIVO Institutes, P.O. Box 360, 3700 AJ Zeist (The Netherlands)

W. M. A. NIESSEN* and U. R. TJADEN

Division of Analytical Chemistry, Center for Bio-Pharmaceutical Sciences, Gorlaeus Laboratories, P.O. Box 9502, 2300 RA Leiden, (The Netherlands)

and

J. VAN DER GREEF

Division of Analytical Chemistry, Center for Bio-Pharmaceutical Sciences, Gorlaeus Laboratories, P.O. Box 9502, 2300 RA Leiden, (The Netherlands) and TNO-CIVO Institutes, P.O. Box 360, 3700 AJ Zeist (The Netherlands)

SUMMARY

The mass spectrometer is a mass-flow-sensitive detector. Improvement of the detection limit in target compound analysis can be obtained by increasing the analyte mass-flow into the spectrometer. This can be achieved by applying peak compression methods. Belt-speed programming is a peak compression method that can be applied with the moving-belt interface for liquid chromatography–mass spectrometry. Peak compression is obtained by increasing the belt speed after the deposition of a chromatographic peak on to the belt. This paper describes preliminary results of belt-speed programming in both liquid chromatography–mass spectrometry and supercritical-fluid chromatography–mass spectrometry, with the latter case being the most effective. At present, the gain in mass flow is limited by the belt speed range available with the interface and by the inefficiency of the thermal desorption process.

INTRODUCTION

Although combined liquid chromatography–mass spectrometry (LC–MS) is nowadays used on a routine basis, it still lacks the sensitivity normally achived in combined gas chromatography–mass spectrometry (GC–MS). In general, the detection limits in LC–MS are in the picogram to nanogram range, depending on the type of analyte, the instrumentation and the operating conditions[1]. Optimization of experimental parameters does not often result in sufficiently low detection limits. Therefore,

0021-9673/89/$03.50

other ways of improving the detection limits in target compound analysis are investigated.

Because the mass spectrometer is a mass-flow-sensitive detector, an improvement in detection limits can be obtained by means of an increase in the mass flow. One of the methods applicable in this respect is the phase-system switching (PSS) approach, which was introduced for the post-chromatographic elimination of non-volatile additives in mobile phases[2,3]. In applying the PSS method it is possible to obtain an increased mass-flow as a result of peak compression effects[4].

In this paper another method for increasing the mass-flow to the mass spectrometer is presented, the so-called belt-speed programming (BSP). In contrast to PSS this method can only be used with a moving-belt interface. In BSP the chromatographic peak of interest is deposited or collected on the belt at a very low belt speed, while the actual mass analysis is performed at high belt speed. After collection of the peak on the belt the belt speed is increased, resulting in an increased mass-flow. The BSP method can be applied in LC–MS, and also in combined supercritical-fluid chromatography–mass spectrometry (SFC–MS). Results from both LC–MS and packed-column SFC–MS are reported here.

THEORETICAL

In the discussion on the theoretical aspects of BSP a Gaussian peak shape has been assumed, despite the fact that the usual peak asymmetry of real LC peaks will also influence the peak heights and thereby the detection limits. A chromatographic peak can be characterized by the peak S.D. σ_v, the concentration of the analyte at the peak maximum C_{max}, and the retention volume V_r. Furthermore, it has been assumed that the moving-belt interface does not cause any additional band-broadening[5,6].

In a mass-flow-sensitive detector the signal is directly proportional to the mass-flow, which can be expressed as:

$$dm/dt = C(t)F$$

in which $C(t)$ is the concentration at the end of the column and F is the flow-rate. At the peak maximum, $C(t)$ is equal to the maximum concentration C_{max}. The moving-belt interface is based on solvent removal. Therefore, C_{max} is ill-defined and difficult to use in this case. The use of the peak standard deviation instead of C_{max} is very attractive and valid because of the inverse relation with C_{max}.

The initial σ_v (in units of volume) is transformed by the flow-rate F to σ_t (in units of time) at the outlet of the chromatographic system:

$$\sigma_t = \frac{\sigma_v}{F}$$

Deposition of the peak on the belt moving at a certain speed v_1 and the subsequent evaporation of the solvent gives a σ_z (in units of length):

$$\sigma_z = \sigma_t v_1 = \sigma_v \frac{v_1}{F}$$

If the analyte on the belt is introduced into the spectrometer without changing the belt speed v_1, the σ_t is:

$$\sigma_{t,MS} = \frac{\sigma_z}{v_1} = \sigma_t = \frac{\sigma_v}{F}$$

If, however, the belt speed is increased to v_2 prior to introduction of the analyte into the MS, the σ_t becomes:

$$\sigma_{t,MS} = \frac{\sigma_z}{v_2} = \sigma_t = \frac{v_1}{v_2} = \sigma_v \frac{v_1}{v_2 F}$$

It can be seen that the effect of the belt-speed programming is a reduction of the peak standard deviation. As a result of the inverse relationship between C_{max} and σ this leads to an increase of the mass flow.

EXPERIMENTAL

Liquid chromatography

The HPLC system consisted of a Model 2150 HPLC pump (LKB, Bromma, Sweden) and a Model 7125 injector (Rheodyne, Berkeley, CA, U.S.A.), and was used in flow injection mode, *i.e.* direct injection in a liquid stream without a chromatographic column. The mobile phase was analytical grade methanol (Merck, Darmstadt, F.R.G.) with a flow-rate of 0.2 ml/min unless stated otherwise. Cholesterol (30 ng) was used as a test compound by injecting 20 μl of a solution containing 1.5 ng/μl of cholesterol. The solvent was deposited on the belt with the standard deposition needle.

Two series of experiments were performed, *i.e.* reference measurements at a constant belt speed for depositing and mass analysis, and the actual BSP measurements.

Supercritical-fluid chromatography

The laboratory-built SFC system consisted of slightly modified commercially available modules. A detailed description of the SFC instrument is given elsewhere[7]. SFC was performed with a Rosil C_{18} packed column (150 mm × 4.6 mm I.D., 8-μm packing) and a mobile phase consisting of carbon dioxide modified with 2% analytical grade methanol (Merck) at a flow-rate of 2 ml/min unless stated otherwise. Diuron (62.5 ng) was used as a test compound by injecting 5 μl of a solution containing 12.5 ng/μl of diuron. A crimped stainless-steel capillary was used as a restrictor for the SFC system and as a spray device for mobile phase deposition. Freezing of the restrictor owing to expansion of the supercritical fluid is prevented by installing a small heating element at the tip[8].

Two series of experiments were performed, *i.e.* reference measurements at a constant belt speed for depositing and mass analysis, and the actual BSP measurements.

Mass spectrometry

The system used was a H-SQ 30 Hybrid (BEQQ) mass spectrometer (Finnigan MAT, Bremen, F.R.G.) linked to a SS-300 data system and equipped with a moving-belt interface (Finnigan MAT). The source temperature was 200°C.

The control electronics of the moving-belt interface used in this study only supports belt speeds between 2.0 and 4.5 cm/s. Theoretically this will give a maximal gain in mass flow of a factor of 2.2, which for validation of the BSP method is rather low. Therefore, it was desirable to increase the belt-speed range available on the moving-belt interface. By installing a variable resistor in the belt-speed control electronics, the belt speed could be regulated continuously between 1.0 and 4.5 cm/s.

For the HPLC experiments with cholesterol the spectrometer was operated in electron impact mode (EI, 70 eV). The operating conditions of the moving-belt interface were: solvent evaporator temperature, 150°C; sample evaporator setting, 5.

For the SFC experiments with diuron the spectrometer was operated in EI mode 70 eV). The operating conditions of the moving belt interface were: solvent evaporator temperature, 60°C; sample evaporator setting, 5.

Detection was performed in both cases in MID mode (resolution 1000), on masses *m/z* 368 and *m/z* 386 for cholesterol or *m/z* 232 for diuron.

Data evaluation

For the interpretation of the results, $\sigma_{t,MS}$ values are approximated by means of the area method:

$$\sigma_{t,MS} = \frac{A}{h\sqrt{2\pi}}$$

where *A and h* are the peak area and the peak height, respectively[9]. The accuracy of this approximation depends on peak asymmetry[9], but is nevertheless satisfactory for this study.

For the evaluation of the BSP results, the ratios of the peak areas, the peak heights and the peak S.D. as obtained with and without BSP are compared with the ratio of the belt speeds used in BSP. Theoretically a ratio of peak areas of 1.0 is expected, while the ratio of peak heights with and without BSP is equal to the ratio of the belt speeds v_2 and v_1 in BSP, and the ratio of peak S.D. with and without BSP is equal to the ratio of the belt speeds v_1 and v_2.

RESULTS AND DISCUSSION

Moving-belt interface characteristics

By calibration of the belt speed it was found that the actual belt speed can be regulated between 0.6 to 3.9 cm/s instead of the indicated 1.0–4.5 cm/s. Since belt speeds in the range 0.6–1 cm/s frequently lead to irregular belt speeds and even stopping of the belt, because the drive mechanism was not designed for such low belt speeds, those belt speeds cannot be used reliably. Actual belt speeds will be indicated in the text from now on.

The deposition of a typical reversed-phase mobile phase, *e.g.* 50% methanol in water, with a flow-rate of 0.6-1.0 ml/min on a moving-belt running at a low belt speed,

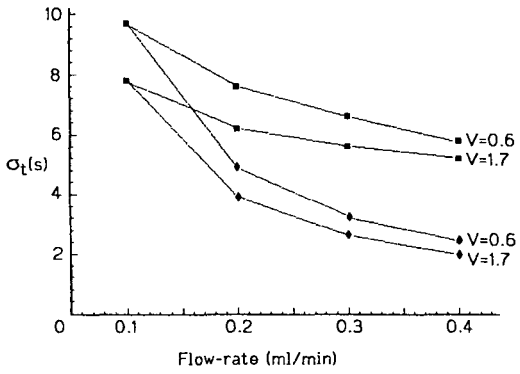

Fig. 1. Influence of the flow-rate on the peak S.D. (σ_t) at belt speeds of 0.6 and 1.7 cm/s, with (■) the experimental and (◆) the theoretical values, as calculated from the peak S.D. at a flow-rate of 0.1 ml/min.

will give problems with respect to the evaporation of the mobile phase and will often lead to a deteriorated peak shape. For BSP the belt speed for deposition will preferably be in the range 0.6–1.5 cm/s. In order to study the influence of the flow-rate on the peak S.D. at low belt speeds the flow-rate was varied in the range 0.1–0.4 ml/min at belt speeds of 0.6 and 1.7 cm/s, with a solvent evaporator temperature of 100°C. Fig. 1. shows the experimental and theoretical curves for these experiments. The results indicate that a high flow-rate, relative to the belt speed, causes significant additional band-broadening, which is probably due to a reduced storage capacity of the belt, resulting in severe back-mixing at the deposition needle. It has been observed that this back-mixing effect is negligible when a spray deposition device is used instead of the needle deposition device[10].

Another important factor determining the interface performance is the desorption of the analyte as a function of the belt speed at a given flow-rate and sample evaporator setting. As a measure of the desorption efficiency, the peak heights and areas as calculated by the data system were used. The result of these experiments, shown in Fig. 2, agrees with theory. There is an almost linear relationship, with a negative slope, between belt speed and the mass flow entering the ion source. These results seem to be unfavourable for a successful application of the BSP method.

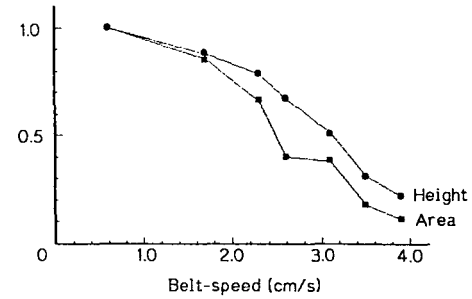

Fig. 2. Normalized (■) peak area and (●) peak height for cholesterol (*m/z* 386) as a function of the belt speed (methanol, flow-rate 0.6 ml/min, sample evaporator setting 5, and solvent evaporator temperature 100°C).

Belt-speed programming

In order to accomplish a successful BSP experiment three important parameters have to be known: (1) the retention time of the compound; (2) the width (in units of time) of the chromatographic peak; (3) the transport time of the chromatographic peak to the mass spectrometer at the deposition belt speed. Proper collection of peaks is possible only when the total peak width is smaller then the tranport time of the chromatographic peak. Otherwise, the front of the peak will enter the spectrometer before belt-speed programming is applied.

Demonstrating BSP in combination with HPLC and SFC, Figs. 3 and 4 show the mass chromatograms that have been obtained with either a constant belt speed or BSP for HPLC and SFC, respectively. The improvements in peak heights and peak S.D. obtained with BSP in LC and in SFC are summarized in Table I and II.

By comparing the ratio of belt speeds (v_2/v_1) with that of peak S.D. (σ_1/σ_2), the conclusion can be drawn that, with respect to peak S.D., experimental values in BSP agree with the theory described above. With respect to peak heights, the agreement between theoretical and experimental values is less accurate. The deviations observed can be attributed to a decrease of the desorption efficiency at higher belt speeds (see below). This can be concluded from the fact that the observed ratios of peak areas (A_2/A_1) lie between 0.6 and 0.7, whereas theoretically, a value of 1.0 is predicted: a signal loss of *ca.* 30% is occurring. Correcting the observed peak heights for this loss [see column $(h_2/h_1)_{corr}$ in Tables I and, II], assuming a linear relation between peak height and area, yields ratios of peak heights that are almost identical with the ratios of peak S.D.

Signal losses of *ca.* 80% are observed at high belt speeds (*i.e.* 4.0 cm/s), when the influence of the belt speed on the signal at a constant flow-rate and a constant sample

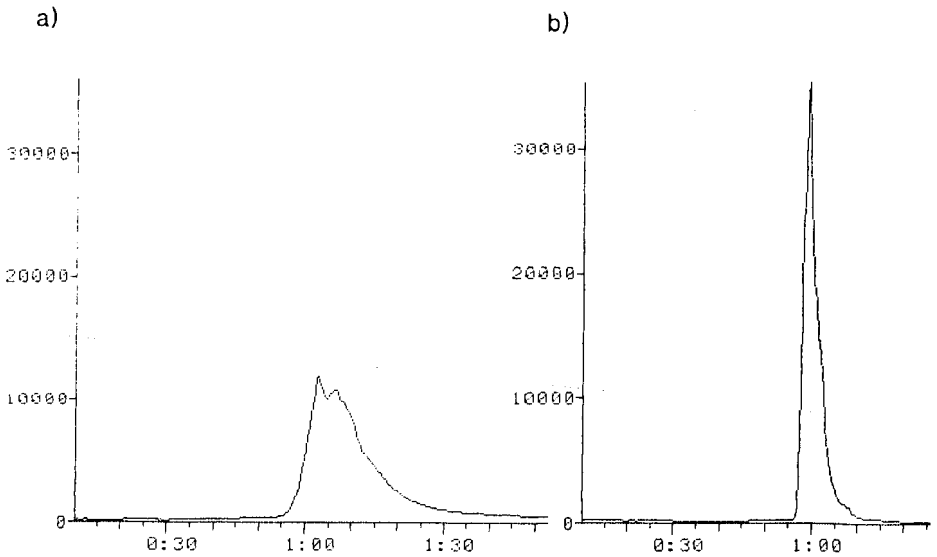

Fig. 3. Mass chromatograms from LC/MS of cholesterol (*m/z* 386). (a) Normal operation with belt speed 1.2 cm/s; (b) belt-speed programming with deposition rate 1.2 cm/s and desorption rate 4.0 cm/s.

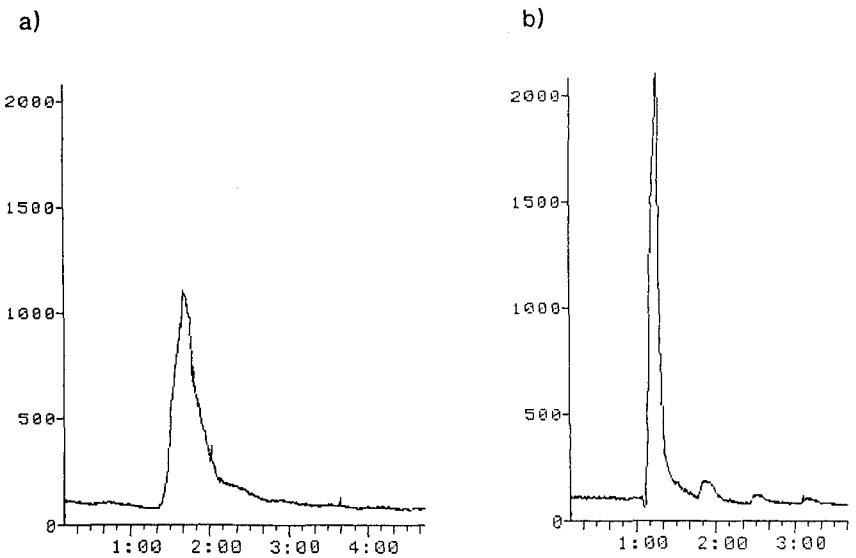

Fig. 4. Mass chromatograms from SFC–MS of diuron (m/z 232). (a) Normal operation with belt speed 3.6 cm/s; (b) belt-speed programming with deposition rate 1.2 cm/s and desorption rate 3.6 cm/s.

evaporator temperature is studied. This signal loss at higher belt speed can be attributed to a decreased desorption efficiency. The chromatographic peak is spread over a rather large belt area containing, relatively, more active sites on the belt material. In order to minimize these losses it is necessary to apply higher sample evaporator temperatures. However, higher sample evaporator temperatures cannot be used at low belt speeds, because they lead to destruction of the belt. As a result the BSP experiments are performed at values of the sample evaporator temperature that are lower than the optimum values at the belt speed of desorption. Owing to a long response time of the sample evaporation heater, there was no improvement when the

TABLE I
SUMMARY OF THE RESULTS OF BSP IN COMBINATION WITH HPLC

v (cm/s)	Area ($/10^5$)	Height ($/10^4$)	σ(s)
1.2	1.6	1.2	5.6
1.2–>4.0	1.3	3.2	1.4
1.7	2.1	1.7	4.9
1.7–>4.0	1.3	3.0	1.7

v_1–>v_2 (cm/s)	v_2/v_1	A_2/A_1	h_2/h_1	σ_1/σ_2	$(h_2/h_1)_{corr}$
1.2–>4.0	3.3	0.7	2.8	4.0	4.0
1.7–>4.0	2.4	0.6	1.8	2.9	3.0

TABLE II
SUMMARY OF THE RESULTS OF BSP IN COMBINATION WITH SFC

v (cm/s)	Area ($/10^4$)	Height ($/10^3$)	σ(s)
3.6	2.1	1.1	8.1
1.2–>3.6	1.5	2.0	2.9

v_1–>v_2 (cm/s)	v_2/v_1	A_2/A_1	h_2/h_1	σ_1/σ_2	$(h_2/h_1)_{corr}$
1.2–>3.6	3.0	0.7	1.9	2.8	2.7

sample evaporator setting was changed to higher values at the same time as the change in belt speed. The losses due to insufficient desorption are less in BSP than in an experiment with constant belt speed. The main difference between BSP and the constant speed experiment (as described above) is that in the latter the chromatographic peak is spread over a rather large belt area, while in BSP it is deposited on only a small area of the belt, containing fewer active sites.

Another unsolved limitation is the belt-speed range supported by the moving-belt interface. The maximum gain in mass flow that can be obtained is about a factor of 4 when the desorption is complete. Increasing this gain requires a wider range of belt speed, *i.e.* 0.5–10.0 cm/s. A belt speed of 10.0 cm/s can be used successfully only when the desorption process is significantly improved. Also the belt speed at the lower end is of great importance because it not only effects the gain in mass-flow but also the maximum time for peak collection, which at present is *ca.* 60 s. At this point it is interesting to compare results from HPLC and SFC. As a result of the differences in the volatilities of the mobile phases, the flow-rate and the peak deposition belt speed are strongly related in HPLC, whereas this is not the case in SFC. Very low deposition belt speeds are only interesting in the case of SFC. It should even be possible, at low modifier contents of the supercritical mobile phase, to collect the chromatographic peak in SFC with zero belt speed. Assuming that it is possible to collect a chromatographic peak with a total width of 20 s on 1 cm of the belt, desorption and introduction into the spectrometer at a belt speed of 5.0 cm/s will result in a peak width of 20 ms in the spectrometer. In terms of mass flow this example represents a gain of 100. As indicated above, other means of desorption than presently available on the interface are necessary to perform an experiment with zero belt speed.

A factor of great importance for quantitative analysis is the reproducibility and linearity of the BSP method. The variance in peak height and area between repeated experiments are comparable with those obtained under normal operation of the moving-belt interface. The linearity of the method has not yet been investigated, but it is expected to be similar to that of normal operation of the moving-belt interface[12].

CONCLUSION

It is demonstrated that belt-speed programming is capable of improving the sensitivity in LC–MS and SFC–MS, although the gain is not as great as expected

theoretically. The major reasons are the incomplete desorption of the compound at low sample evaporator temperatures and the slow response of the sample evaporator to a change in the settings. For useful application of BSP, a desorption method with an instantaneous response to a change in the desired desorption power is required. Laser desorption and fast atom bombardment are two techniques that meet this requirement.

Another conclusion is that with the available moving-belt interface the gain in mass flow is limited because of the limited belt-speed range. This is true even if the moving-belt interface is adapted to support very low (*ca.* 0.5 cm/s or less) and high (greater than 5.0 cm–s) belt speeds. This is especially the case for BSP in combination with HPLC because the flow-rates in conventional HPLC are incompatible with very low belt speeds. For SFC, such a limitation is not present and consequently a large gain in mass flow can be obtained with BSP.

ACKNOWLEDGEMENT

Mr. M. A. G. de Kraa is thanked for his technical assistance in the BSP experiments with SFC.

REFERENCES

1 T. R. Covey, E. D. Lee, A. P. Bruins and J. D. Henion, *Anal. Chem.*, 58 (1986) 1451A.
2 J. van der Greef, W. M. A. Niessen and U. R. Tjaden, *J. Pharm. Biomed. Anal.*, 6 (1988) 565.
3 E. R. Verheij, H. J. E. M. Reeuwijk, G. F. la Vos, W. M. A. Niessen, U. R. Tjaden and J. van der Greef, *Biomed. Environ. Mass Spectrom.*, 16 (1988) 393.
4 E. R. Verheij, G. F. la Vos, W. M. A. Niessen, U. R. Tjaden and J. van der Greef, in preparation.
5 E. P. Lankmayr, M. J. Hayes, B. L. Karger, P. Vouros and J. M. McGuire, *Int. J. Mass. Spectrom. Ion Phys.*, 46 (1983) 177.
6 D. E. Games, M. J. Hewlins, S. A. Westwood and D. J. Morgan, *J. Chromatogr.*, 250 (1982) 62.
7 W. M. A. Niessen, P. J. M. Bergers, U. R. Tjaden and J. van der Greef, *J. Chromatogr.*, 454 (1988) 243.
8 A. J. Berry, D. E. Games and J. R. Perkins, *J. Chromatogr.*, 363 (1986) 147.
9 J. J. Kirkland, W. W. Yau, H. J. Stoklosa and C. H. Dilks, Jr., *J. Chromatogr. Sci.*, 15 (1977) 303.
10 M. J. Hayes, E. P. Lankmayer, P. Vouros, B. L. Karger and J. M. McGuire, *Anal. Chem.*, 55 (1983) 1745.
11 J. van der Greef, A. C. Tas, M. C. ten Noever de Brauw, M. Höhn, G. Meyerhoff and U. Rapp, *J. Chromatogr.*, 323 (1985) 81.
12 L. E. Martin, J. Oxford and R. J. N. Tanner, *J. Chromatogr.*, 251 (1982) 215.

Journal of Chromatography, 474 (1989) 285–300
Elsevier Science Publishers B.V., Amsterdam — Printed in The Netherlands

CHROM. 21 400

DEVELOPMENTS OF MICRO LIQUID CHROMATOGRAPHY–MASS SPECTROMETRY WITH GRADIENT ELUTION

IMPROVEMENTS TO OBTAIN LESS THERMAL DECOMPOSITION OF LABILE COMPOUNDS

GUNNAR STENHAGEN* and HANS ALBORN
Department of Chemical Ecology, University of Göteborg, Kärragatan 6, S-431 53 Mölndal (Sweden)

SUMMARY

Fused-silica columns (I.D. 0.22 mm) packed with ordinary small particle liquid chromatographic material were used in direct connection to an electron impact ion source. The electrostatic field between the column end and an extraction–focusing plate, located close to the ion source inlet, was used for nebulization of the solvent. The ion source was modified to obtain higher efficiency and to reduce the thermal decomposition of labile compounds. A system for micro flow gradients (less than 2 μl/min) has been developed. The flow of a pumping medium (glycerol) is divided into two parallel streams and the flow distribution is controlled using the temperature dependence of the viscosity. The glycerol flow is changed by two "media converters" to the chromatographic solvents. Applications of micro liquid chromatography–mass spectrometry are shown for a plant allelochemical, dhurrin, obtained from Sorghum leaf extract. Mass spectra of glucose, sucrose, neral, geranial, chlorsulphuron, myoinositol, 3,5-dinitrobenzoic acid, amitriptyline, 10-hydroxyamitriptyline and omeprazole after liquid chromatography are shown.

INTRODUCTION

The main difficulties involved in coupling liquid chromatography (LC) with mass spectrometry (MS) are much the same as the difficulties of combining packed gas chromatography (GC) with MS: the two techniques operate at pressures which differ by several orders of magnitude. In LC–MS, the problem is even more complicated, since the chromatograph works in the liquid state and the mass spectrometer in the vapour state.

An important consideration in an LC–MS interface is the maintenance of high chromatographic performance. From a chromatographic point of view, freedom to select mobile phases and additives, possibility of gradient elution, no loss of resolution caused by the interface, high linear dynamic range, low detection limits, and high-molecular-weight detection capabilities are important factors for an effective LC–MS system. The LC–MS system is a particularly useful tool for the identification

0021-9673/89/$03.50

of thermolabile allelochemicals, especially when informative mass spectra of the separated components can also be obtained. The implications of narrow-bore packed columns (*e.g.*, micro-packed fused-silica columns) for LC–MS become apparent when one considers the low flow-rate relative to normal-bore columns. This is because, for the same velocity, the flow-rate is proportional to the square of the column diameter. A 0.2 mm I.D. column operates at liquid flow-rates approaching 1 μl/min, corresponding to gas flows of *ca.* 1 ml/min. This gas flow-rate is equivalent to that found in capillary GC–MS and, as a result, the fused-silica micro-packed columns can be attached directly into the mass spectrometer ion source for electron impact (EI) ionization.

The LC–MS system discussed here was first presented at the Montreux meeting in 1984[1], and the first version of the gradient system was presented at the following Montreux meeting in 1986[2].

EXPERIMENTAL

The micro-packed fused-silica LC column

The column which is used in the LC–MS system is prepared by packing fused-silica tubing of 200–500 mm length and 0.2 mm I.D. with 3- or 5-μm liquid chromatography (HPLC) packing material[1]. Special attention has to be paid to the design of the column end[2]. The best performance, so far, is obtained when a small silica tube is placed at the end of the column. This tube is filled with coarser packing material (10–50 μm) and its purpose is to support the column bed and to provide an effective spray of the effluent into the ion source via a small and distinct nebulization point.

Coupling to the ion source

The column, which is mounted on a support for easy handling, is simply led (through a valve) into the ion source. The tip of the column terminates just in front of a 1-mm diameter hole in an extraction–focusing plate (EF plate) which is placed 1.5 mm in front of the inlet hole in the ion source block (Fig. 1). The inlet hole is 10 mm wide except for the entrance, where the diameter is 4 mm. Nebulization is governed mainly by the electrostatic field between the column tip and the EF plate, causing the

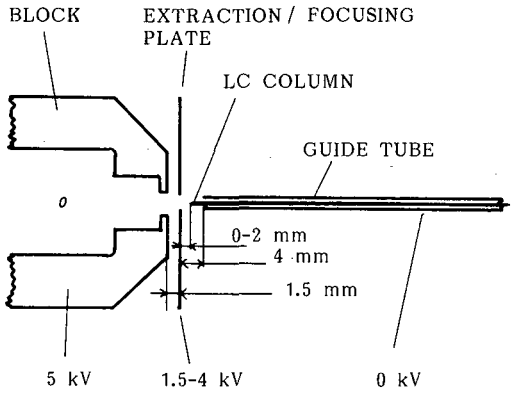

Fig. 1. Schematic diagram of the ion source–micro column connection.

eluate from the column to leave the tip as very small droplets. This is due to two main effects caused by the electrostatic field: (1) the surface tension of the solvent is decreased, and (2) the formed droplets are polarized as the distribution of charges at their surface is changed. The polarized droplets are drawn out by the field between the tip and the EF plate and focused by the field between the plate and the ion source block.

The distance between the column tip and the electron beam inside the ionization chamber of the source has to be short, otherwise the sample molecule may possibly hit the hot walls of the ion source block on its way into the ionization chamber. To avoid this, the EF plate was included between the tip and the block. The distance between the tip and the plate is critical, as shown by Fig. 2. The same sample amount was injected and all other conditions were the same except for the distances, which were 0.0 mm and 1.0 mm, respectively. In the latter case the signal-to-noise ratio was increased by a factor of at least five.

Fig. 3 shows the effect of the EF plate potential on peak height. The same amounts of sucrose were injected at different potentials between 1200 and 3100 V on a reversed-phase system with the mobile phase consisting of methanol–water (80:20). The best response was obtained at 1800 V.

Another important observation was that no heating is needed for the nebulizaiton of the solvent. With the new design of the ion source inlet, the nebulization of the solvent and the ionization of the molecules are processes independent of each other.

Injection of samples

The injection of sample on to the column is made with a syringe-loaded microsample injector (Rheodyne 7520) utilizing a pulsatile injection method for each sam-

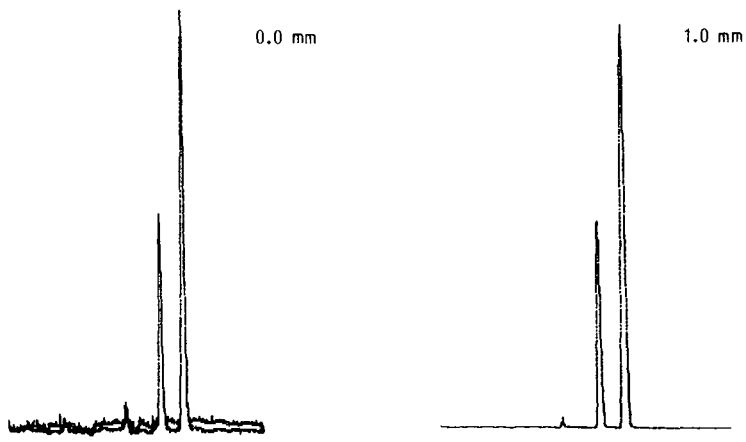

Fig. 2. Effect of the distance between the column tip and the extraction–focusing plate. Column: 25 cm × 0.22 mm I.D., 3-μm Nucleosil C_{18}. Mobile phase: methanol–water (80:20). Injection: 2 ng toluene and 4 ng *m*-xylene.

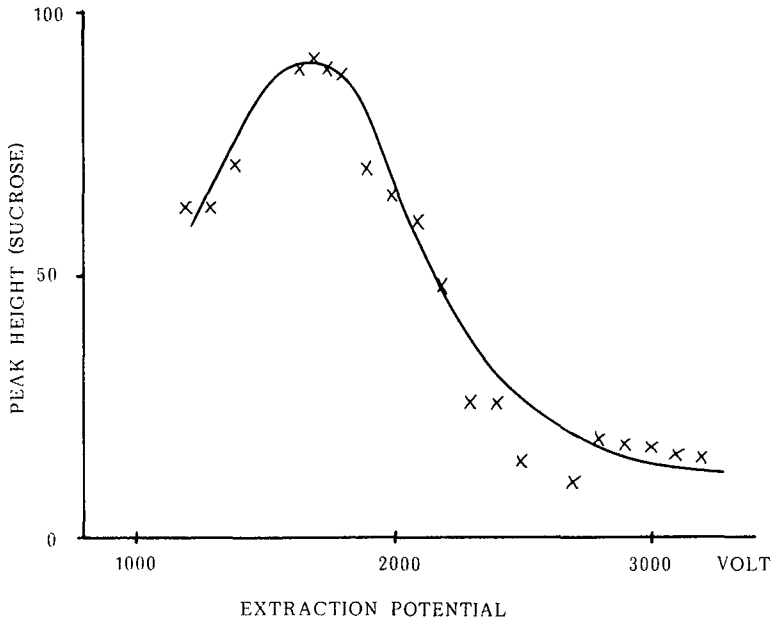

Fig. 3. Effect of the extraction–focusing plate potential on peak height. Peak height (mm) of sucrose (100 ng injections) at different plate potentials.

ple[1]. The sample chamber of the rotor is turned to the inject position for only a few seconds. The configuration of the rotor gives sharp "cuts" of the injected volume, and this is important for the utilization of the high separation efficiencies of the micro-packed columns. An important consideration, when a micro system is used, is to avoid the extra band broadening effects of, *e.g.*, "dead volumes" in the connections of the column. Therefore the column is connected directly to the injector and the ion source block.

Solvent delivery system

An ordinary LC solvent pump is used in the system, and has the ability to work in a constant pressure mode. However, it would be easier to obtain the optimal flow-rate and to predict the retention if a constant flow pump was available for these particular flow-rates, around 1 μl/min.

Gradient system

With a gradient system utilizing the flow properties of a liquid, a practical gradient elution with such low flow-rates (1–2 μl/min) is possible (Fig. 4). If the flow is divided into two parallel tubes which are connected at the ends, the pressure drop is the same for both tubes and the flow distribution between the tubes can be controlled by changing the viscosity of the flowing media. The viscosity of, *e.g.*, glycerol is highly dependent on temperature and, therefore, by temperature programming of the tubes it is possible to obtain a solvent gradient.

The greatest difficulty in the construction of the gradient system has been the

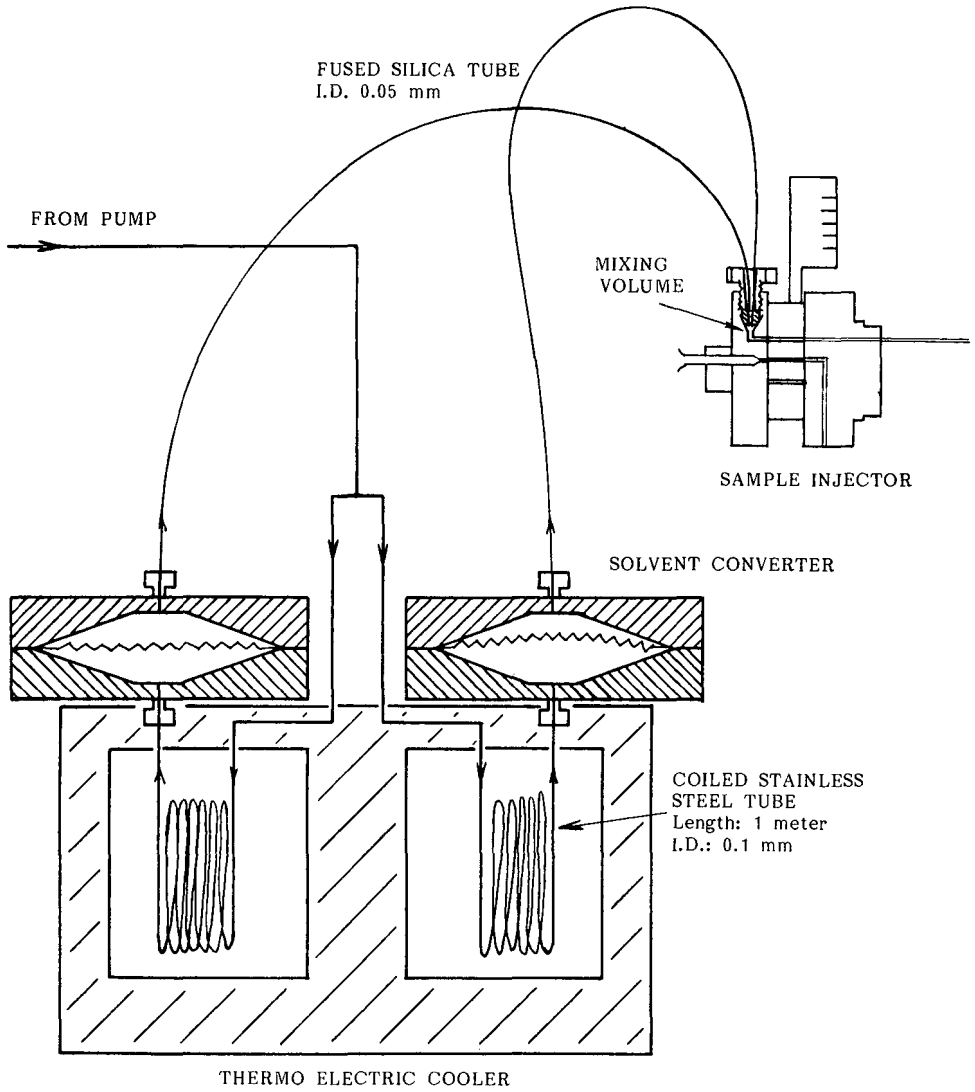

Fig. 4. Schematic diagram of the gradient system.

design of the device which converts the flow of glycerol to the same flow of LC solvent. The divider which separates the LC solvents from the pumping media must be flexible, inert and non-penetrable. After testing several designs and materials for the "solvent converter", we finally chose a divider made of thin, checkered, soft copper sheet. This membrane is placed between strong flanges of stainless steel. The solvent volume of each "converter" is 17 ml, which is sufficient for more than 200 hours of operation. The solvents are led through 50 μm I.D. fused-silica tubes of 50 cm length to a small mixing volume (1 μl) at the LC injector inlet.

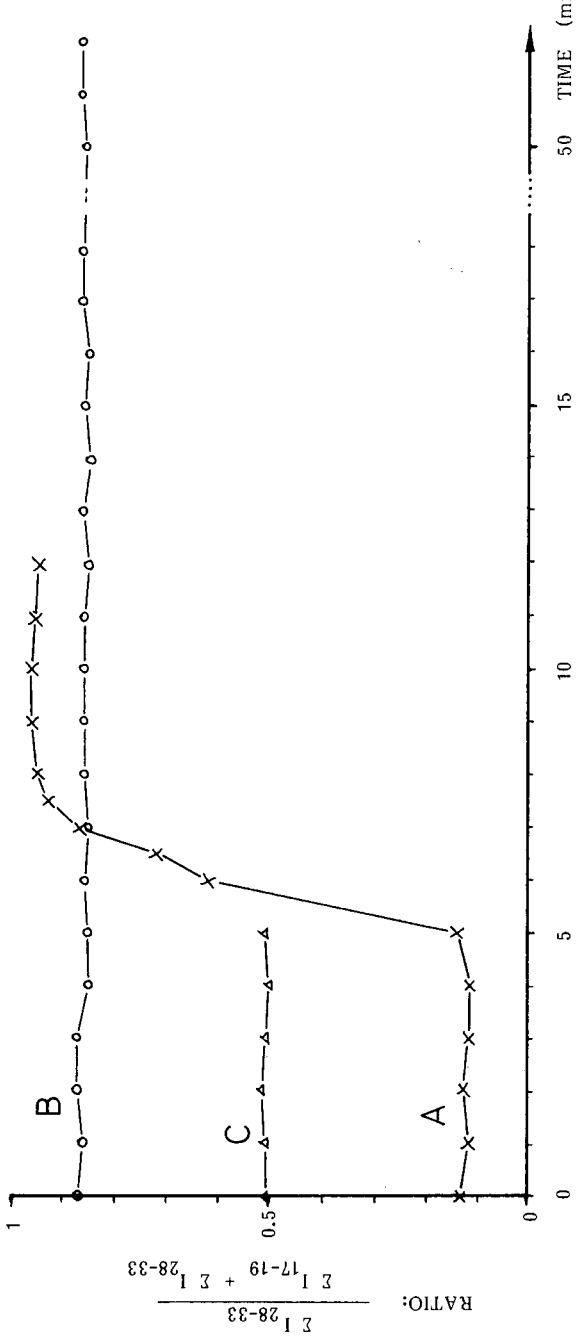

Fig. 5. Time diagram of solvent composition. Curve A: a rapid change from 14 to 95% of methanol in water. Curve B: constant setting at 86% during a period of 1 h. Curve C: constant setting at 50%. For method of obtaining solvent ratio see text.

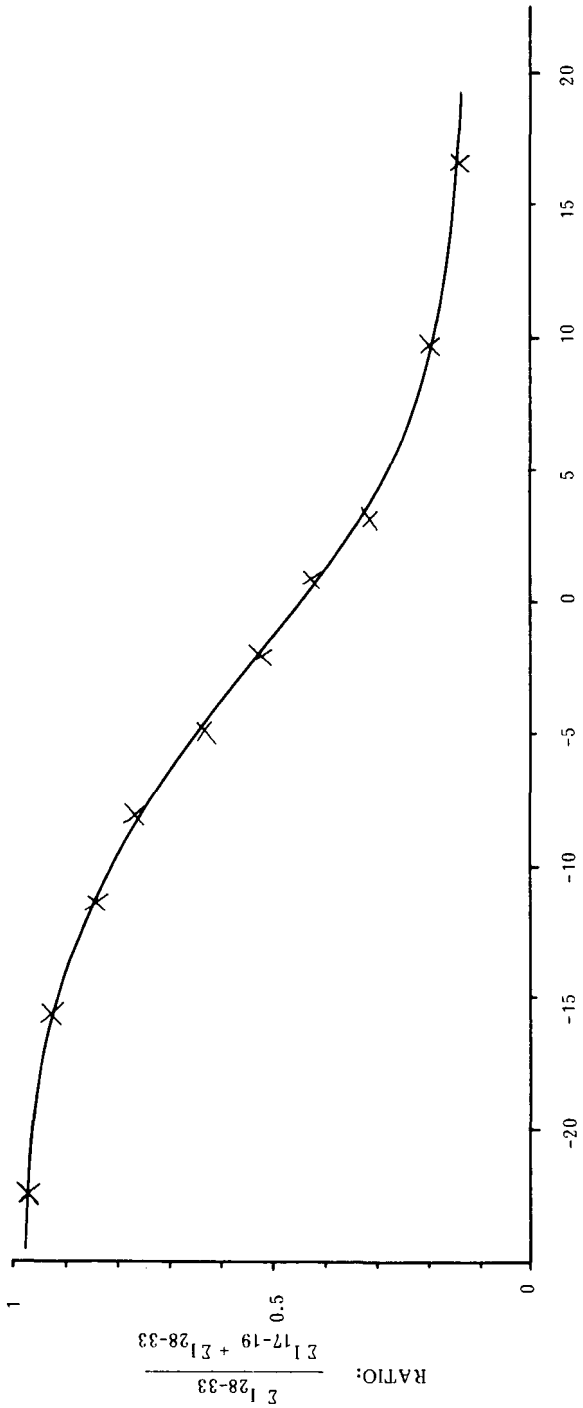

Fig. 6. Solvent composition (methanol–water) as a function of the tube temperature difference. For explanation of y axis see text.

The viscosity of glycerol is highly dependent on the temperature, especially in the lower temperature range. If the temperature is changed from −8 to +8°C the viscosity changes from 4500 to 18 000 cP. To be able to work with temperatures below ambient, this being needed to obtain a wide composition range, a thermoelectric cooler is used. The tubes inside the cooler can be heated by an electric current led directly through each tube. The electric power input for heating of the tubes matches the heat pumping of the cooler, and that power can be directed to the tubes as desired. Because the tubes are air-cooled their temperatures can be changed rapidly.

Curve A in Fig. 5 shows the result of a rapid change from 14% to 95% methanol in water. The composition of the solvent is measured by its mass spectrum and calculated in the following way: the sum of the peak intensity values for methanol (*m/z* 28–33) is devided by the sum of the intensities for water (*m/z* 17–19) plus the sum for methanol. The elution time for an unretained sample (t_0) is 4.0 min, and the new solvent composition reaches the column after 1 min. The final composition (95%) elutes from the column after less than 8 min. Measurements at a constant setting of

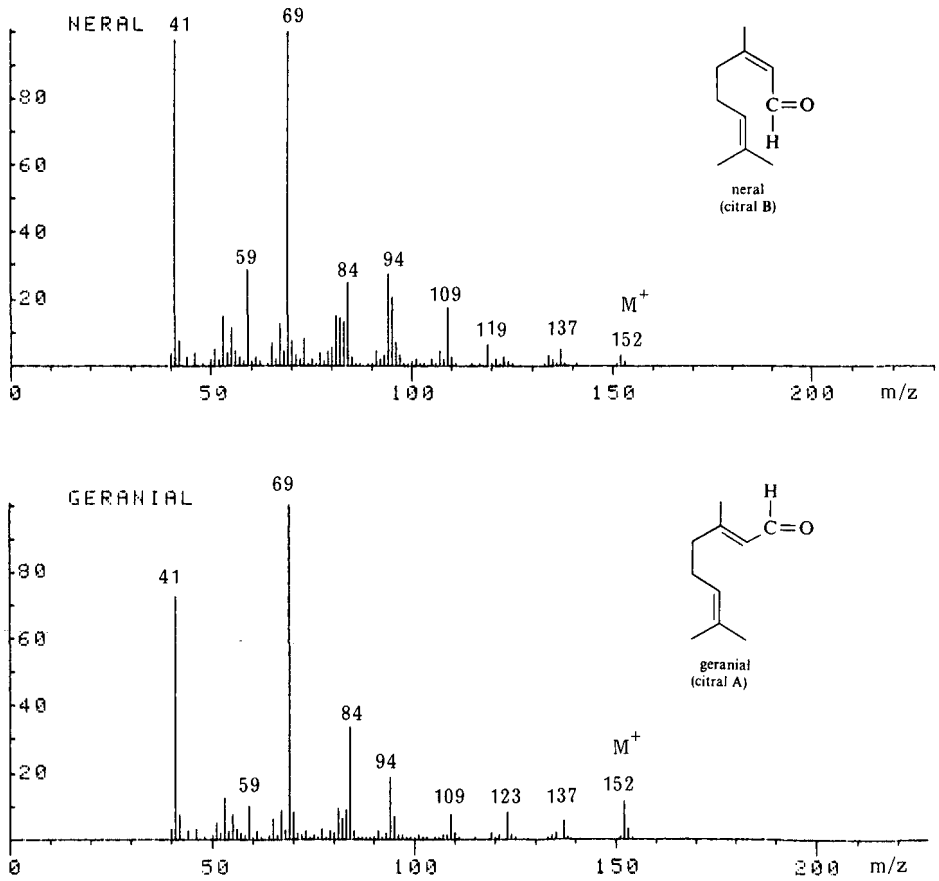

Fig. 7. Mass spectra of neral (above) and geranial. Ion source temperature 110°C.

methanol–water (86:14) during operation for 1 h are shown in Fig. 5, curve B, providing a standard deviation of 1%. The same tendency is shown for the 50% setting, curve C. Fig. 6 shows the solvent composition as a function of tube temperature difference. The differential temperature measurements were made with a digital thermometer (Fluke 52) using thermocouples attached to the tubes. The solvent composition was calculated by its mass spectrum, as above. The mean value of three spectra for each temperature difference are plotted. The curves can be used to calculate the solvent composition when the temperatures of the tubes are known. However, a more accurate determination of the solvent composition can be made by using its actual mass spectrum.

Measurements of the capacity ratio (k') at constant solvent composition for the injections of a solution of aromatics during a period of 3 h gave the following results: for benzene, mean k' 0.54 with standard deviation (S.D.) of 0.002; for toluene, mean k' 0.572, S.D. 0.004; and for *m*-xylene, mean k' 0.612 with S.D. 0.006.

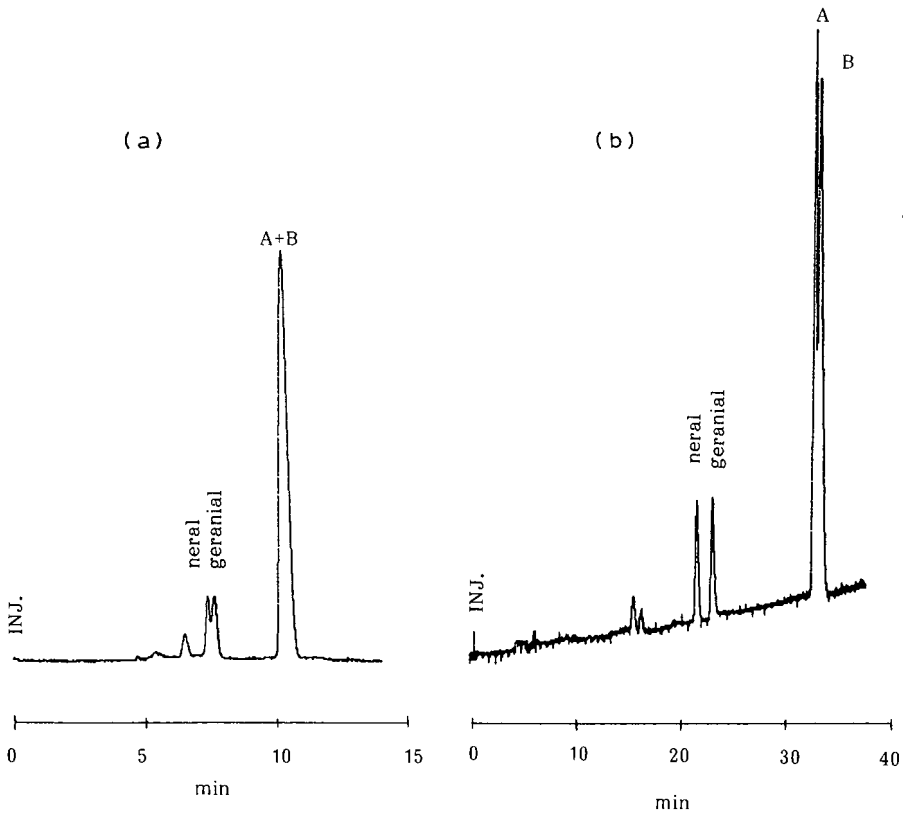

Fig. 8. Liquid chromatograms of a methanol–water (50:50) solution of citral. (a) Isocratic, methanol–water (85:15). (b) Gradient of methanol–water from 60:40 to 90:10 in 40 min. Column: 25 cm × 0.22 mm I.D., 3-μm Nucleosil C_{18}. Detection: total ion current (ions of m/z <40 suppressed).

RESULTS

LC–MS analysis of citral

Citral is a mixture of two components, neral (3,7-dimethyl-2-*trans*, 6-octadien-1-al) and geranial (3,7-dimethyl-2-*cis*, 6-octadien-1-al), which were once difficult to separate. Citral has been found to be a widespread trigger of behaviour in insects. Fig. 7 shows mass spectra of neral and geranial after LC. Like other mass spectra obtained from volatile and less volatile compounds, they are similar to ordinary EI spectra and therefore, may be interpreted by comparison with normal reference spectra.

Repeated injections of citral dissolved in methanol–water (50:50) showed that the amounts of neral and geranial decrease gradually and new peaks appear in the chromatograms. As shown by Fig. 8, the components were difficult to separate with an isocratic reversed-phase system (C_{18}) and, therefore, were used as test substances for the gradient system. With a methanol–water gradient composition from 60:40 to 90:10, the two compounds are separated, not completely, but sufficiently to give mass spectra of the individual compounds, as shown in Fig. 9. The peak at *m/z* 198 is the molecular ion peak; the strong *m/z* 69 peak indicates an acyclic monoterpenoid and arises by loss of the terminal isopentenyl group. The identification has not yet been

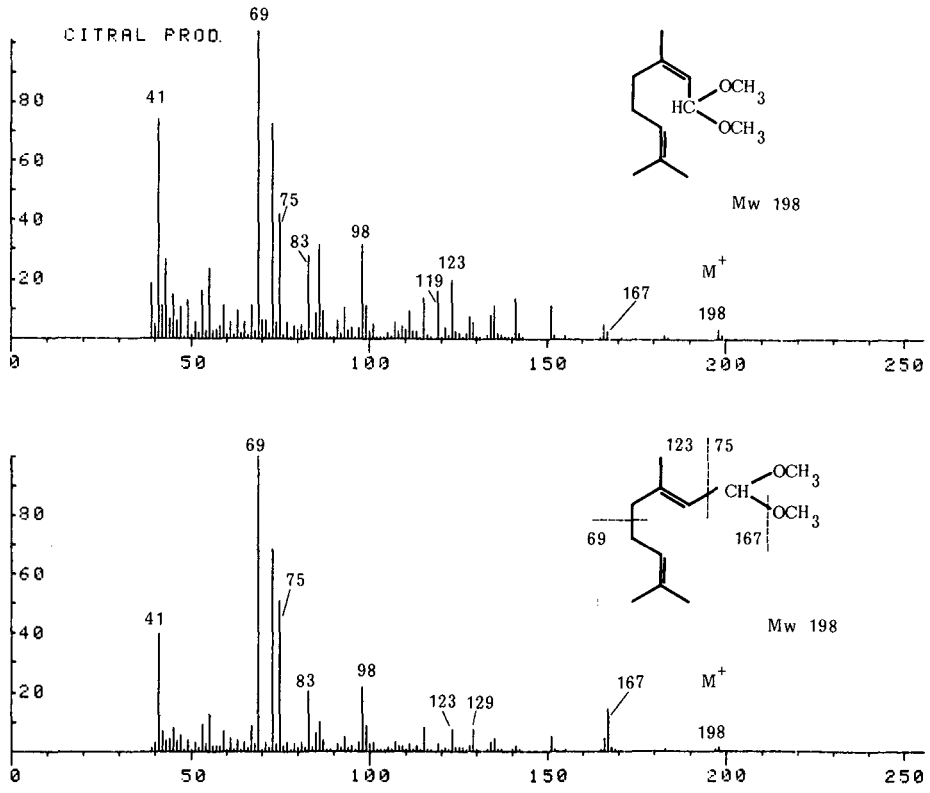

Fig. 9. Mass spectra of nerylacetal (above) and geranyl-acetal. Ion source temperature 110°C.

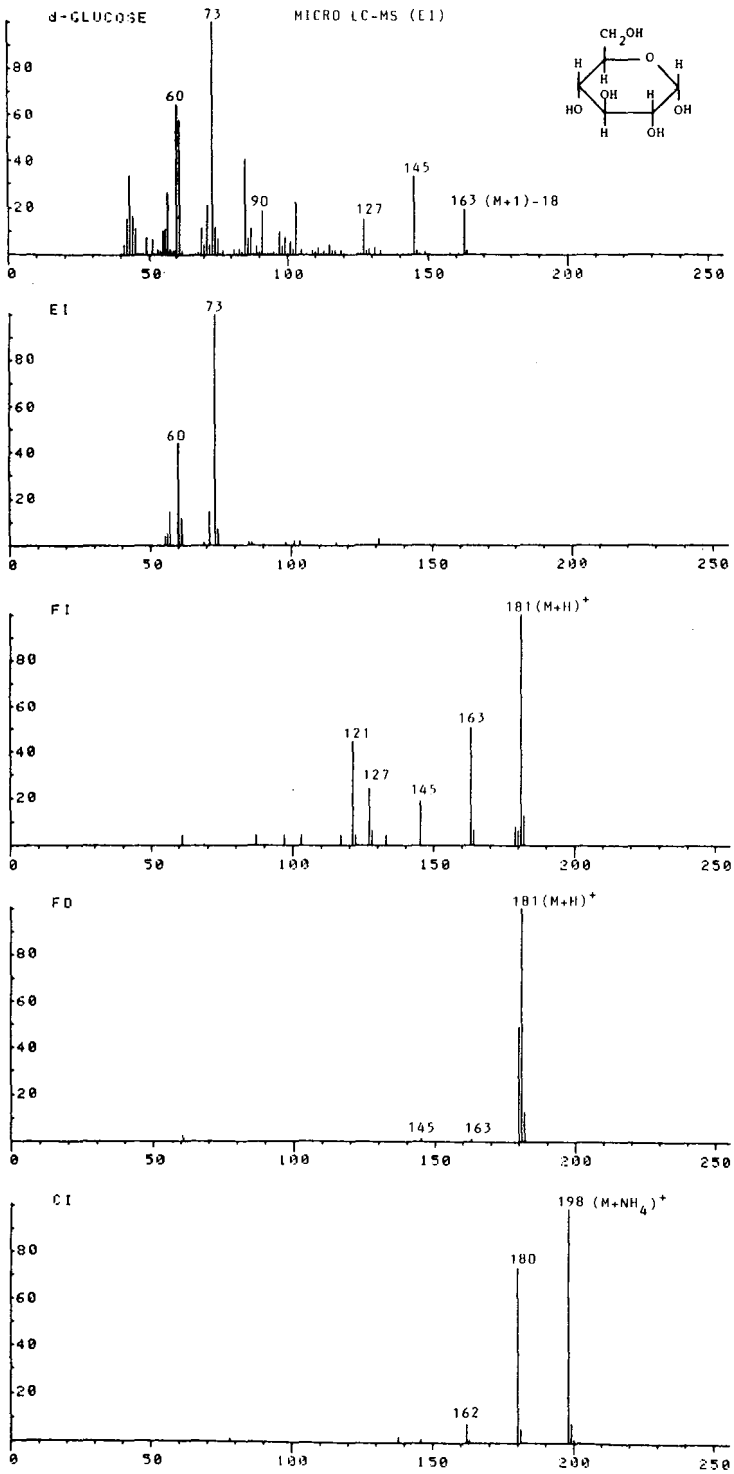

Fig. 10. Micro LC–MS, electron impact (70 eV), field ionization (FI), field desorption (FD) and ammonia chemical ionization (CI NH_4) spectra of D-glucose.

confirmed, but the mass spectra give strong evidence of acetal formation of the two components, *e.g.*, as shown by the peak at *m/z* 75.

Saccharides

A comparison can be made in Fig. 10 between the mass spectra of glucose obtained by using five different MS techniques: micro LC–MS, EI, field ionization (FI), field desorption (FD) and chemical ionization (CI)[3]. Although the spectrum from micro LC–MS shows no molecular ions, it gives structural information from the fragmentation pattern.

The sucrose spectrum obtained after modification of the LC column coupling to the ion source is shown in Fig. 11 (B). It is similar to the spectrum of Fig. 1(A) except for the peak at *m/z* 311 [(M + 1) − 32], which is about three times as intense owing to the decreased thermal degradation.

LC mass spectrum of dhurrin

One major peak in the chromatogram of a leaf extract (from sorghum cultivars susceptible to insect pests) was elucidated by the LC–MS system. The fraction was collected from an analytical LC system and injected on to the micro-LC column, giving a sharp peak. By its mass spectrum, which is shown in Fig. 12, the fraction was identified as dhurrin, a cyanogenic glucoside previously found in sorghum. The peak at *m/z* 311 is the molecular ion. The mass spectrum also shows typical glucose peaks at *m/z* 60, 61, 73, 91, 127, 145 and 163. There are two alternative ways of breaking the glucosidic bond, which give the peaks at *m/z* 149 and 132. In the spectrum, the *m/z* 132 peak dominates that at *m/z* 149, probably because of the nitrile group attached to the same carbon atom as the sugar.

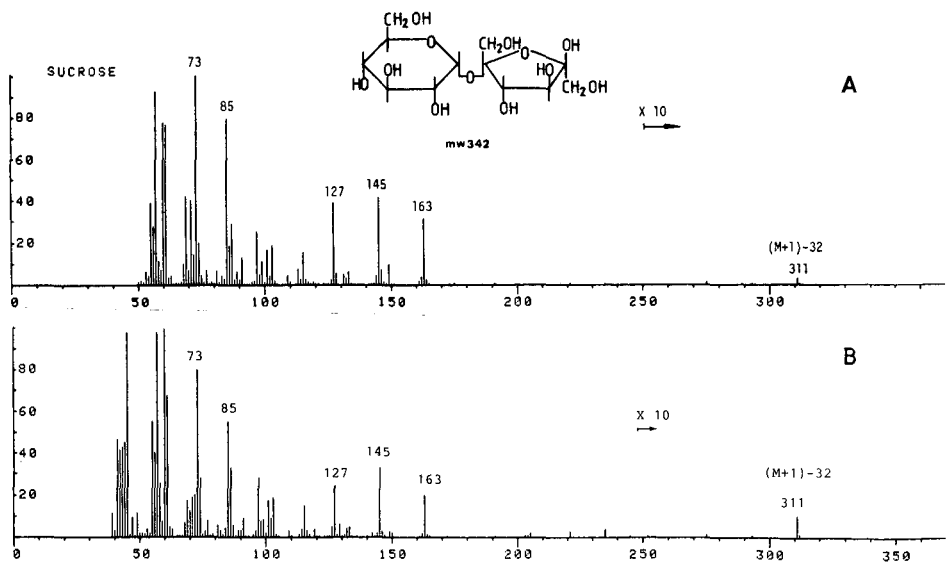

Fig. 11. Mass spectra of sucrose before (A) and after (B) the modification. Ion source temperature: 180°C.

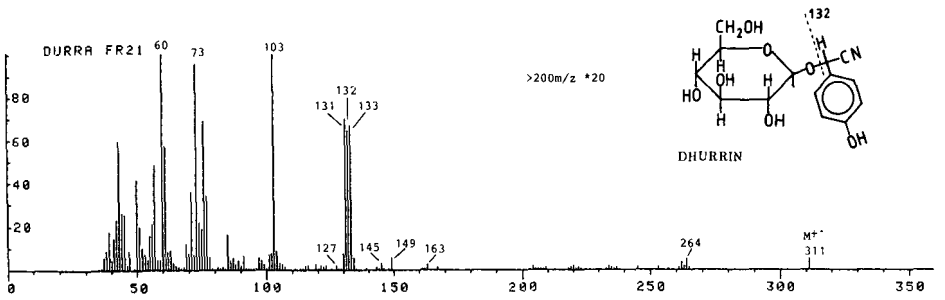

Fig. 12. Mass spectrum of dhurrin obtained from Sorghum leaf extract. Ion source temperature: 140°C.

Mass spectra of some other thermolabile compounds after LC

Chlorsulphuron, a sulphonylurea herbicide, gave at 110°C ion source temperature the mass spectrum shown in Fig. 13. The molecular ion at *m/z* 357 is present. A peak at *m/z* 321, due to loss of hydrogen chloride, and a number of other structurally useful fragments of the molecule are observed. At ion source temperatures above 200°C all information in the high mass region is lost. A chemical ionization mass spectrum of chlorsulphuron is given in ref. 6.

The mass spectrum of myoinositol can be seen in Fig. 14. No molecular ion peak is present, but a small M + 1 peak exists at *m/z* 181. The peak at *m/z* 163 is formed by the loss of water from the protonated molecular ion.

The mass spectrum of 3,5-dinitrobenzoic acid is shown in Fig. 15. The molecular ion peak (*m/z* 212) is the most abundant in the spectrum. The peak at *m/z* 182 (M − 30) corresponds to the loss of nitric oxide, and other large peaks are due to elimination of the nitro groups, *viz.* *m/z* 155 and 120.

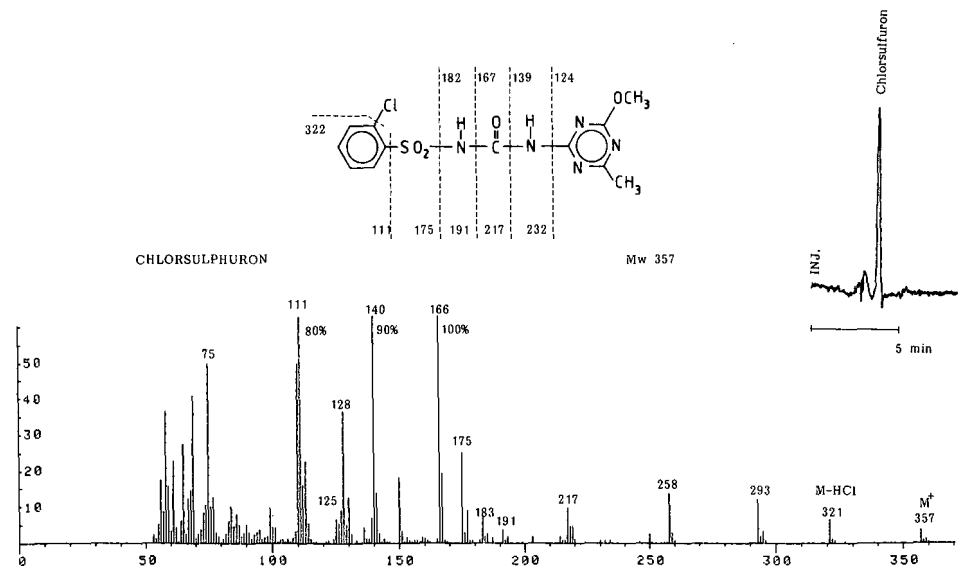

Fig. 13. Mass spectrum of chlorsulphuron. Ion source temperature: 110°C. The total ion current trace (ions of *m/z* <40 suppressed) of 50 ng chlorsulphuron injected on column is shown to the right.

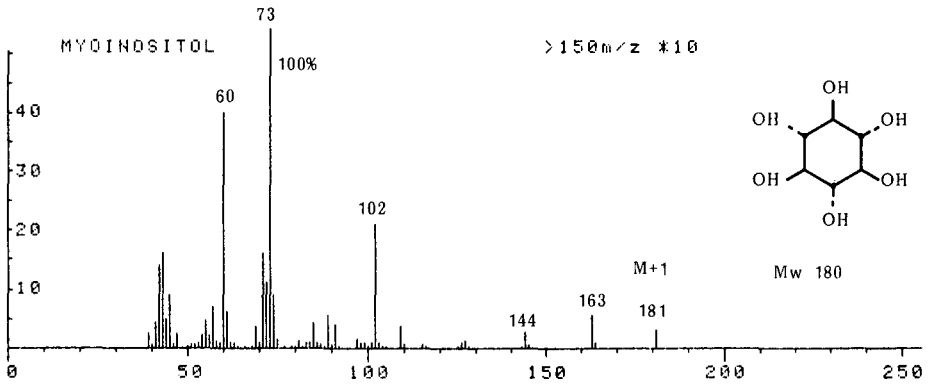

Fig. 14. Mass spectrum of myoinositol. Ion source temperature: 165°C.

The mass spectra in Fig. 16 of amitriptyline (an antidepressive drug) and 10-hydroxyamitriptyline (a metabolite) are both dominated by a very intense immonium ion peak at *m/z* 58. The spectra show molecular ion peaks at *m/z* 277 and 293. Hydroxyamitriptyline gives a peak at *m/z* 276 probably due to loss of water from the protonated molecular ion (M + 1 − H_2O). The fragmentation patterns in the middle region, which are almost the same for the two compounds, are not yet fully interpreted. However, the LC–MS method could give structurally important information in addition to the acetylation or chemical ionization MS techniques used[7].

Fig. 17 shows a mass spectrum of omeprazole in comparison with a direct (in-beam) EI spectrum. The molecular ion peak is present at *m/z* 347 in both spectra. The *m/z* 329 peak in the mass spectrum is due to the loss of oxygen. The fragment at *m/z* 150 corresponds to the protonated fragment at *m/z* 151, which is the base peak in the mass spectrum.

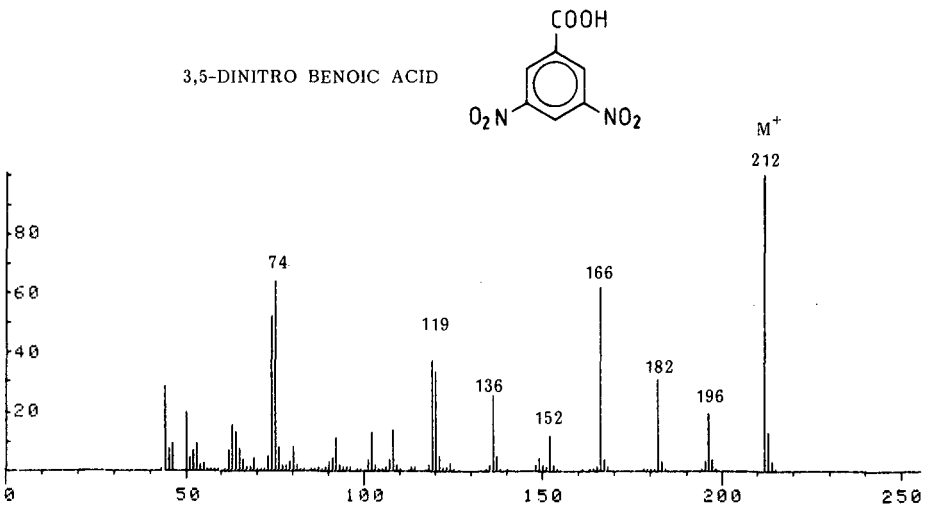

Fig. 15. Mass spectrum of 3,5-dinitrobenzoic acid. Ion source temperature: 210°C.

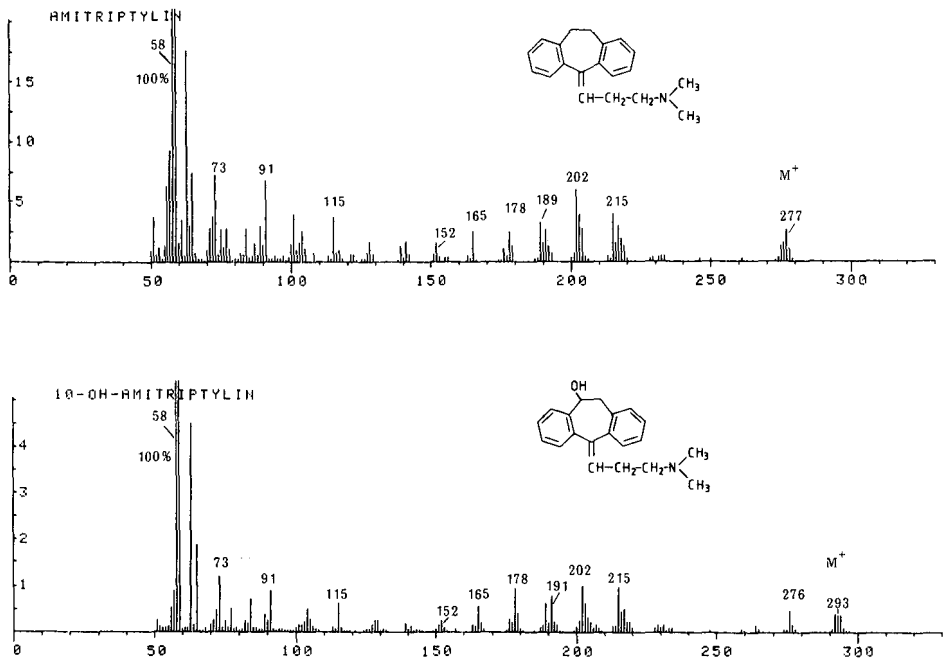

Fig. 16. Mass spectra of amitriptyline (above) and 10-hydroxyamitriptyline. Ion source temperature: 150°C.

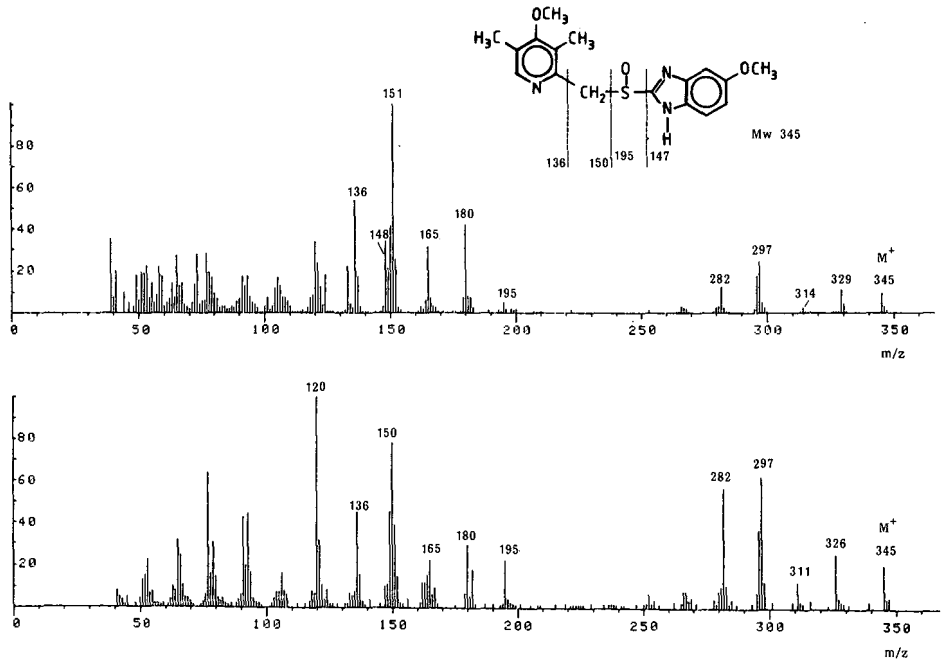

Fig. 17. Mass spectra of omeprazole. Above: mass spectrum at 165°C ion source temperature. Below: direct in-beam EI spectrum (70 eV) at 200°C.

CONCLUSION

The key point in the connection of the micro LC column to the electron impact ion source of the mass spectrometer is the behaviour of the spray into the source. With careful design of the column tip, the correct geometric distances between the ion source inlet parts and the column tip, and good control of the electrical potential between the focusing plate and ion source, it is possible to obtain stable nebulization of the effluent, even at low ion source temperature. Thus advantage can be taken of both the high performance[8,9] of the packed capillary LC column and the possibility of obtaining informative mass spectra. The gradient gives the micro LC technique the same ability for separation of complex samples as ordinary LC methods. The combination of micro LC with the mass spectrometer also gives a powerful tool for the identification of the separated substances.

The LC–MS system has already proved its usefulness in our work with biologically active compounds, *e.g.*, with allelochemicals. As the specific plant allelochemicals and their actions are identified, it will be easier to incorporate the ability to produce the desired chemicals into the plant of interest. Furthermore, suspected new components emerging from the consumed parts of the plant during the plant breeding programme will be more quickly recognized and identified.

REFERENCES

1 H. Alborn and G. Stenhagen, *J. Chromatogr.*, 323 (1985) 47–66.
2 H. Alborn and G. Stenhagen, *J. Chromatogr.*, 394 (1987) 35–49.
3 L. Lundgren, G. Norelius and G. Stenhagen, *Hereditas*, 97 (1982) 115–122.
4 H. Alborn, G. Stenhagen and K. Leuschner, in press.
5 T. Radford and D. C. Dejonh, in G. R. Waller and O. C. Dermer (Editors), *Biochemical Applications of Mass Spectrometry*, Vol. 2, Wiley, New York, 1980, pp. 266–272.
6 A. C. Barefoot and R. W. Reiser, *J. Chromatogr.*, 398 (1987) 217–226.
7 R. Ishida, T. Ozaki, H. Uchida and T. Irikura, *J. Chromatogr.*, 305 (1984) 73–82.
8 G. Crescentini, F. Bruner, F. Mangani and G. Yafeng, *Anal. Chem.*, 60 (1988) 1659–1662.
9 K.-E. Karlsson and M. Novotny, *Anal. Chem.*, 60 (1988) 1662–1665.

Journal of Chromatography, 474 (1989) 301–316
Elsevier Science Publishers B.V., Amsterdam — Printed in The Netherlands

CHROM. 21 448

COMPARISON OF OPEN-TUBULAR LIQUID CHROMATOGRAPHY–MASS SPECTROMETRY AND DIRECT LIQUID INTRODUCTION LIQUID CHROMATOGRAPHY–MASS SPECTROMETRY FOR THE ANALYSIS OF METRIBUZIN AND ITS METABOLITES IN PLANT TISSUE AND WATER SAMPLES

B. H. ESCOFFIER[a], C. E. PARKER*, T. C. MESTER[b] and J. S. M. DEWIT[c]
Laboratory of Molecular Biophysics, N.I.E.H.S., Research Triangle Park, NC 27709 (U.S.A.)
F. T. CORBIN
Crop Science Department, North Carolina State University, Raleigh, NC 27695 (U.S.A.)
J. W. JORGENSEN
Department of Chemistry, University of North Carolina at Chapel Hill, Chapel Hill, NC 27514 (U.S.A.)
and
K. B. TOMER
Laboratory of Molecular Biophysics, N.I.E.H.S., Research Triangle Park, NC 27709 (U.S.A.)

SUMMARY

Direct liquid introduction (DLI) and open-tubular liquid chromatography–mass spectrometry (OTLC–MS) have been evaluated for the analysis of metribuzin and its metabolites in water and soybean samples. To improve sensitivity and column performance, a column-switching procedure was developed for on-line analyte preconcentration and sample cleanup in DLI LC–MS. To reduce the amount of sample needed for OTLC–MS injection, a "dip" technique analogous to on-column injection in high-resolution gas chromatography (HRGC)–MS was used. Although OTLC was more sensitive than DLI for mixtures of pure standards, severe matrix effects were encountered when plant and water samples were analyzed by this technique. DLI LC–MS was more successful than OTLC–MS for environmental samples due to both the inherent loading capacity of the larger column and the use of the preconcentration/cleanup injection technique.

INTRODUCTION

Metribuzin (MZN) is a 1,2,4-triazine herbicide which has been widely used on foodcrops, including soybeans, tomatoes, and sugarcane. Differences in crop tolerance to this herbicide has led to studies of its metabolism. Three major metabolites are

[a] Present address: Groupement de Recherches de Lacq, D.A.A., 64170 Artix, France.
[b] Present address: Landis Associates, Placerville, CA 95667, U.S.A.
[c] Present address: Tennessee Eastman Co., Kingsport, TN 37662, U.S.A..

0021-9673/89/$03.50

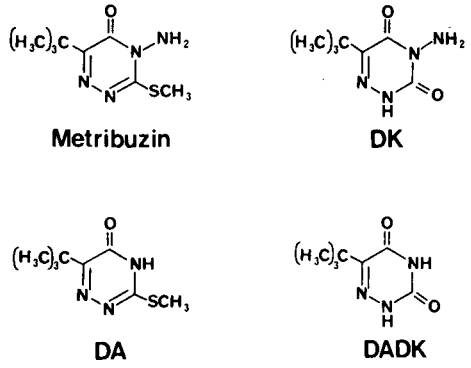

Fig. 1. Reported structures for metribuzin, DK, DA, and DADK.

presently known: deaminated metribuzin (DA); diketometribuzin (DK) and deaminated diketometribuzin (DADK)[1–4] (see Fig. 1). Metabolism of these compounds via glucoside and glutathione conjugation has also been studied[5,6]. Concern over this herbicide entering the food chain through the ingestion of residues on crops has led to its study in crops, food, milk and tobacco[7–10]. Another area of concern is the effect on subsequent crops through soil residues[11–13] and on the environment through runoff and groundwater contamination[14–23]. MZN has been placed on the U.S. Environmental Protection Agency (E.P.A.) list of cancer-suspect agents[24].

In this paper, we compare two liquid chromatography–mass spectrometry (LC–MS) techniques (direct liquid introduction, DLI LC–MS, and open-tubular liquid chromatography, OTLC–MS) for the analysis of metribuzin (MZN) and its major metabolites in plant tissues and water samples. These two LC–MS techniques are evaluated as confirmatory techniques when the presence of these metabolites is indicated by other, less-selective, detectors.

MATERIALS AND METHODS

Equipment

OTLC

The chromatographic system used in this work has previously been described[25,26]. A 10-μm I.D. fused-silica column, approximately 1.5 m in length, coated with OV-17-V was used[27,28]. The mobile phase used was methanol–water (10:90) at a flow-rate of 50 nl/min. The OTLC–MS interface used in these experiments has been described previously[26]. The interface tip temperature was 270°C.

"Minibore" HPLC

The HPLC system used for the "minibore" separations consisted of two Gilson Model 302 pumps (Gilson Medical Electronics, Middleton, WI, U.S.A.), a Gilson Model 802B manometric module, a Gilson gradient controller, and a Waters 440 UV detector (Waters Assoc., Milford, MA, U.S.A.). One Rheodyne Model 7125 injector

(Rheodyne, Cotati, CA, U.S.A.), equipped with a 1-ml loop, was placed between the column and the mass spectrometer, and was used for the introduction of a tuning solution. Two Rheodyne Model 7010 injectors were used in the sample preconcentration system, which will be described below. A DuPont Zorbax C_{18} column (Dupont Instruments, Analytical Division, Wilmington, DE, U.S.A.), 2 mm I.D., packed by Alltech Assoc. (Deerfield, IL, U.S.A.), was used for the separations. The flow-rate used was 0.2 ml/min. The solvent was methanol–water (50:50). The DLI interface was purchased from Hewlett-Packard (Palo Alto, CA, U.S.A.).

Radiochemical analysis

For the experiments involving radiochemical detection, a Flo-one radiodetector (Radiomatic Instr. and Chemical, Tampa, FL, U.S.A.), operated in the ^{14}C mode, was used. The effluent from the Waters 440 UV detector was sent into the Flo-one detector, where Hydrofluor scintillation fluid (National Diagnostics, Manville, NJ, U.S.A.) was added.

Mass spectrometry

The mass spectrometer used was a Finnigan 3300 chemical ionization mass spectrometer (Finnigan-MAT, San Jose, CA, U.S.A.), previously modified for negative ion detection[29], and DLI[30,31] and OTLC[26] probe introduction.

Samples and solvents

The metribuzin standard was obtained from the E.P.A. repository (Environmental Protection Agency, Research Triangle Park, NC, U.S.A.). Standards of the three metribuzin metabolites were obtained as a gift from Mobay (St. Louis, MO, U.S.A.).

The solvents used (HPLC-grade methanol and acetonitrile) were from Fisher Scientific (Fairlawn, NJ, U.S.A.). The water used was Millipore "Milli-Q/Milli-Rho" water (Millipore, Bedford, MA, U.S.A.).

Water samples

Water samples were collected from a lake on the N.I.E.H.S. site. Known amounts of a mixture of MZN, DA, DK and DADK were added to the lakewater to produce the spiked sample. Both the spiked and control water samples were then filtered through a Millipore HA filter (0.45 μm). For OTLC–MS analysis, 2.5-ml samples of spiked and of unspiked lakewater were freeze-dried and taken up in 10 μl methanol–water (10:90).

Plant samples

Plant culture. Three tetraploid (MZN-tolerant) soybean[5] or diploid (MZN-sensitive) soybean seeds (var. Coker 156) were planted 2 cm deep in sand in 7 cm diameter styrofoam cups. The cups were watered to field capacity and kept moist with half-strength Hoagland's solution[32] at pH 6.5. The cups were placed on a growth table for germination at ambient temperature with a fluorescent light intensity of 1500 footcandles at plant height with 14-h days. After 4 days, the seedlings had emerged. The sand was removed by washing. Seedlings selected for uniformity were placed two per flask in 250-ml Erlenmeyer flasks containing 240 ml half-strength Hoagland's

solution at pH 6.5. The flasks were wrapped in aluminum foil, and replaced on the growth table in a completely-randomized block design. At least once per day during the growth period, the volume of Hoagland's solution was measured and replaced to 200 ml.

Chemical treatment. Diploid and tetraploid seeds were treated identically. The treatments consisted of: (1) [^{14}C]carbonyl-labeled metribuzin with 4.44 mCi/mole specific activity and a purity of 98% was applied at a rate of 0.2 μCi per flask in 0.5 ml methanol to give a final concentration of 0.04 ppm in the nutrient solution; (2) unlabeled metribuzin in 0.5 ml methanol was added to the flasks to give a final solution concentration of 0.04 ppm; and (3) 0.5 ml methanol was added to the control flasks.

Chemical extraction. The two seedlings per flask were treated as a composite sample. The plants were divided into shoots and roots immediately below the cotyledonary node. Fresh weights were recorded. The shoots were homogenized in 30 ml of methanol, and the homogenates were filtered through a Buchner funnel under vacuum and washed with several volumes of methanol. The filtrates were collected and evaporated to dryness in a rotary evaporator. The extracts were resuspended in 2 ml chloroform, followed by 3 ml of methanol and refrigerated until analysis.

Sample preparation. Before LC/MS analysis, the final extracts were dried *in vacuo* and resuspended in 1 ml methanol. For DLI analysis, 100 μl of an extract was dissolved in 2.4 ml water and eluted onto the minibore column using the preconcentration/cleanup system described below. A Millipore Millex-HV (25 mm) filter was used while injecting.

For OTLC analysis, 720 μl of the 1-ml plant extract was passed through a Waters C_{18} Sep-pak, and eluted with an additional 2.5 ml methanol. The eluent was evaporated to 500 μl under nitrogen and centrifuged at 16 000 *g* for 10 min. The pellet was discarded, the supernatant was evaporated to 100 μl and centrifuged again. This was repeated for 50-μl and 20-μl volumes. The supernant was evaporated under nitrogen, resuspended in 30 μl water–methanol (90:10), and recentrifuged. The supernatant was evaporated, taken up in 10 μl water–methanol (90:10), and recentrifuged. The sample was then ready for analysis using the "dip" injection technique described below.

For radiochemical detection, the extracts from the plants which had been treated with the ^{14}C-labeled metribuzin were evaporated under nitrogen, and taken up in 1 ml methanol. A 300-μl aliquot of each sample was evaporated to 100 μl and then water (2.4 ml) was added. The extract was loaded onto the minibore column using a Millex-HV filter and the precolumn cartridge system as described below.

RESULTS AND DISCUSSION

Comparison of spectra and sensitivities (standards)

As can be seen in Figs. 2 and 3, the elution order of the compounds is different on the C_{18} minibore column and the OV-17-V OTLC column. All four of the metabolites could be separated on the DuPont Zorbax C_{18} column; three could be separated by OTLC on the OV-17-V column. The fourth compound (DADK) exhibits very low sensitivity, however, which would limit its detectability in either LC–MS mode (Table I). The detection limits of MZN, DA and DK under negative ion conditions were 10–30 pg in OTLC and 2–5 ng by DLI (Table I). Triplicate injections of MZN by

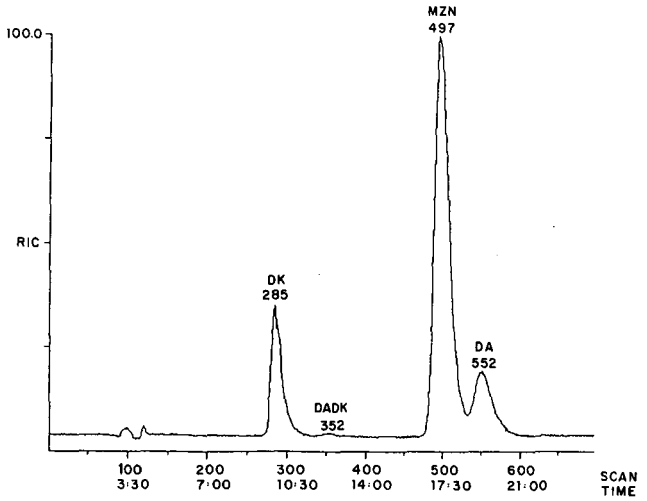

Fig. 2. Total ion chromatogram (TIC) trace for a mixture of standards by DLI LC–MS [multiple ion detection (MID), NCI]. Amounts injected were 250, 250, 250 and 500 ng of DA, DADK, DK and MZN, respectively. Time in min:s.

OTLC down to the 20 pg level are shown in Fig. 4. Since negative ion sensitivities were better than positive ion sensitivities, negative ion detection was used for the lakewater and soybean samples.

The positive and negative ion spectra obtained by OTLC–MS which uses a heated interface were essentially identical to those obtained by DLI, where the interface is cooled (Table II). No additional fragmentation was observed in OTLC–MS, thus there is no evidence of thermal degradation of these compounds.

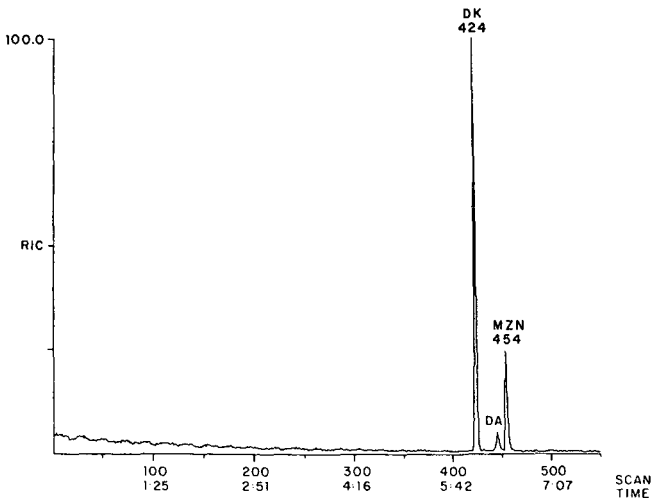

Fig. 3. Total ion chromatogram (TIC) trace for a mixture of standards by OTLC–MS (MID, NCI). Amounts injected were 200 pg each of DA, DADK, DK, and MZN.

TABLE I

DETECTION LIMITS BY MID, NEGATIVE ION MODE

Solvent, methanol–water (50:50). The compounds exhibit *ca.* 2 orders of magnitude less sensitivity in the positive ion mode, with the exception of DADK, for which the sensitivities are approximately equal.

	Selected mass (m/z)	*Detection limits (pg)*		*Relative sensitivity OTLC/DLI*
		DLI	*OTLC*	
MZN	198	2000	10	200
DA	184	5000	30	170
DK	168	5000	20	250
DADK	168	100 000	1000	100

For on-line injection of standards, the OTLC system has a sensitivity advantage of *ca.* 200:1. This can be partly explained by the absence of a solvent stream split in OTLC, and partly by the greatly reduced peak width in OTLC, leading to a higher mass flow per scan. Also, in DLI some of the sample may be lost with the solvent as the source pressure is adjusted by moving the probe inside the desolvation chamber.

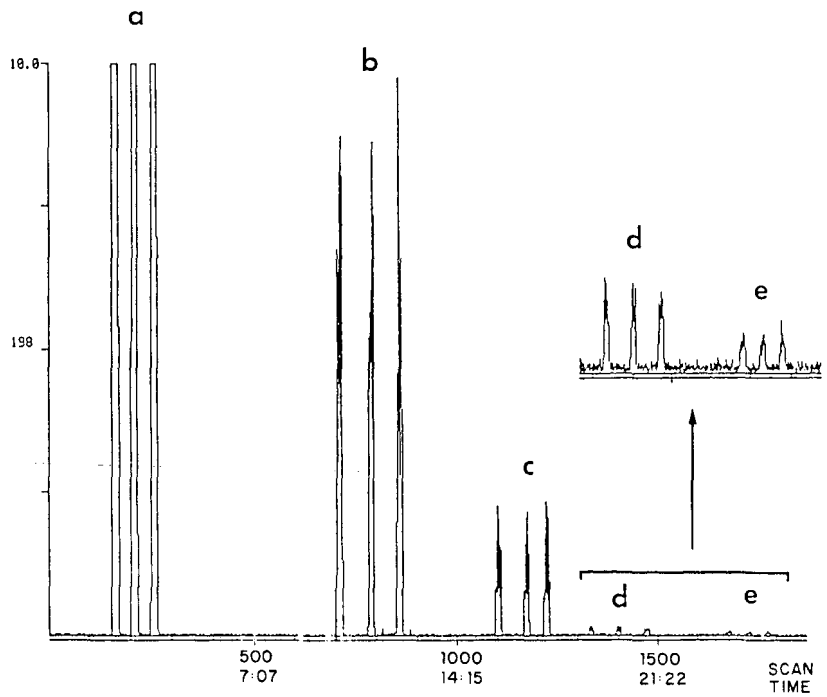

Fig. 4. OTLC–MS detection limit for MZN by MID-NCI. Triplicate injections of (a) 2 ng, (b) 400 pg, (c) 200 pg, (d) 40 pg, and (e) 20 pg MZN.

TABLE II
POSITIVE AND NEGATIVE DLI MASS SPECTRA OF METRIBUZIN AND METABOLITES
PCI = Positive ion chemical ionization; NCI = negative ion chemical ionization; RA = relative abundance.

Compound	*Mol. wt.*	*DLI-PCI-MS*			*DLI-NCI-MS*		
		m/z	*% RA*	*Proposed ID*[a]	*m/z*	*% RA*	*Proposed ID*[a]
Metribuzin	214	215	100.0	$[M+H]^+$	198	100.0	$[M-NH_2]^-$
		200	18.5	$[M-NH_2+2H]^+$	184	7.0	
		169	11.4	$[M+H-SCH_2]^+$	152	4.6	
		154	14.2	$[M-NH_2+2H-SCH_2]$			
DA	199	200	100.0	$[M+H]^+$	184	100.0	$[M-CH_3]^-$
		154	45.1	$[M+H-SCH_2]^+$			
DK	184	185	100.0	$[M+H]^+$	168	100.0	$[M-NH_2]^-$
		170	42.0	$[M-NH_2+2H]^+$			
DADK	169	170	100.0	$[M+H]^+$	168	100.0	$[M-H]^-$

[a] The proposed identifications are based only on nominal mass values.

Environmental applications

The levels of MZN and its metabolites expected to be found in treated soybean plants and in runoff studies are sufficiently low that, even with the low detection limits achieved by LC–MS, sample extracts have to be concentrated prior to analysis. This preconcentration can be done in two ways, either on-column or by solvent removal prior to injection.

Concentration/injection technique—DLI. Direct injection of the soybean plant extract onto the minibore HPLC column led to rapid degradation of column performance. Changes in the elution order of DA and MZN in soybean extracts and lakewater samples were sometimes observed. Similar effects were observed in earlier HPLC studies on these metabolites[33,34].

To avoid these matrix effects, and to improve the on-column detection limits for these compounds, a column switching technique was developed. This system is shown in Fig. 5 where two pumps delivered different mobile phases at different flow-rates to different column combinations (pump A: 100% water at 0.8 ml/min; pump B: methanol–water (50:50) at 0.2 ml/min). A Waters Guard-Pak Resolve C_{18} cartridge was used for sample preconcentration and cleanup, and a DuPont Zorbax minibore column was used for the separation. In addition to the requirements for standard HPLC work, the use of a preconcentration/cleanup system in DLI LC–MS required that constant flow be maintained to the mass spectrometer to avoid loss of the DLI jet. The procedure used is as follows (refer to Fig. 5):

(1) Loading configuration: a 2.5-ml loop was filled with the solution to be analyzed. Pump A (weak solvent) and pump B (stronger solvent) flow into the cartridge and the analytical columns, respectively. In this reversed-phase system, the weak solvent used was water (more polar), and the stronger solvent used was methanol–water (50:50) (less polar).

(2) Concentrating configuration and front-flushing: the injection valve was turned so that pump A (weak solvent) flowed through the cartridge, concentrating the

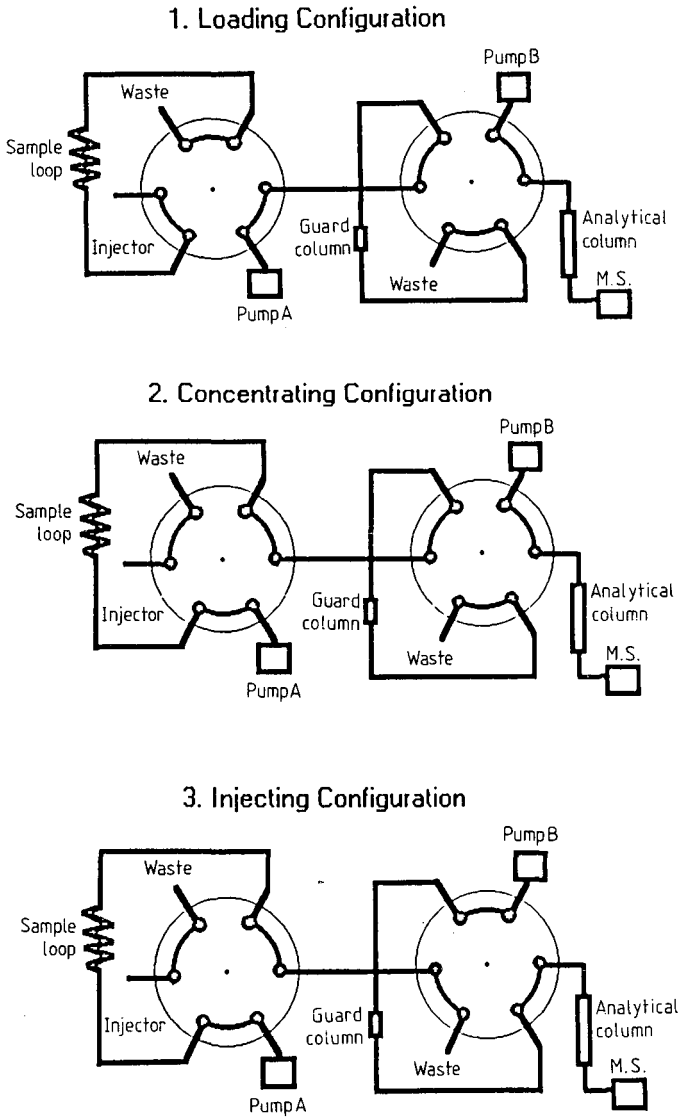

Fig. 5. On-line preconcentration/cleanup system for DLI LC–MS.

compounds of interest on the cartridge, and flushing away the more polar constituants of the matrix. The flow-rate of pump A was not restricted by the limitations of the analytical (minibore) column, so higher flow-rates could be used. Thus analysis time was reduced by reducing sample preconcentration time.

(3) Injecting configuration: after 5 min, the switching valve was turned so that the cartridge was now on-line with the analytical column. At this point the preconcentrated analytes were eluted onto the analytical column by the stronger mobile phase from pump B.

(4) Backflushing: After an additional 2 min, the two valves were turned back to the loading configuration. At this point, the position of a low-pressure three-way valve on the solvent inlet line of pump A was changed to introduce 100% methanol into the pump instead of the weak solvent, water. At this time, any less-polar compounds which may have been adsorbed onto the cartridge could be removed while the separation was accomplished on the analytical column. Approximately 10 min before the end of the run (the run duration here was approximately 30 min), the three-way valve was turned back to the weaker solvent, here 100% water.

This sequence of operations permitted the "injection" of 2.5 ml of lakewater (or 100 μl of plant extract dissolved in 2.4 ml of deionized water) onto the minibore column without loss of the analytes during the preconcentration step, without loss of resolution, and without degradation of column performance over a series of analyses.

This preconcentration/clean-up technique was equally applicable to UV or radiochromatographic detection, and should prove useful for the analysis of pesticides and other analytes for which precolumn cartridges sufficiently selective for the compounds of interest can be found. Similar column switching schemes have been used for problems as diverse as the analysis of impurities in gasoline[35] or drugs in biological fluids[36]. Recently, an off-line preconcentration/cleanup scheme was reported for a variety of pesticides prior to thermospray LC–MS analysis[37,38]. The on-line scheme described here should also be applicable to these and other pesticides and to this type of LC–MS analysis. This injection technique can be used for sample cleanup even if preconcentration is unnecesary, and could be automated if desired.

Injection technique—OTLC. The original injection system[25,26] required *ca.* 200 μl of sample solution in order to make an injection of *ca.* 1 nl. For situations where the sample volume is limited, a "dip" technique, analogous to on-column injection in capillary GC–MS, was developed in which the vacuum in the mass spectrometer was used to pull a known volume (*ca.* 1 nl) into the OTLC column. In this new technique, only 2–10 μl were needed to per injection. A brief description follows (refer to Fig. 6): the Valco four-port injection valve was turned to the "load" position to stop the mobile phase flow. The column was then disconnected from the "tee" and the end was dipped into the sample solution. At this time the analyte solution was drawn into the column by the pressure differential. After an appropriate injection time, typically 8–10 min, the column was reconnected to the "tee", the waste valve was opened, and the Valco valve is turned so that the pressurized mobile phase rinses the outer part of the column tip. After about 5–10 s, the waste valve is closed again, and the chromatographic process begins.

The amount of sample entering the column during this "dip" procedure was a function of the sample viscosity, the mobile phase viscosity, and the column taper. The amount of sample injected can be determined experimentally by measuring the response from different timed injections of a solution of known detector response and making a calibration curve. The amount can also be determined by measuring (with an optical microscope) the movement of the sample meniscus as a function of time and calculating the volume from the inner diameter of the column. Fig. 7 shows a loading curve determined for methanol–water (10:90). This figure shows no apparent movement for about 300 s, and the rate gradually increases until *ca.* 500 s. After this initial lag phase, the linear velocity throughout the column was constant.

Comparison of DLI and OTLC–MS results. A chromatogram of a diploid

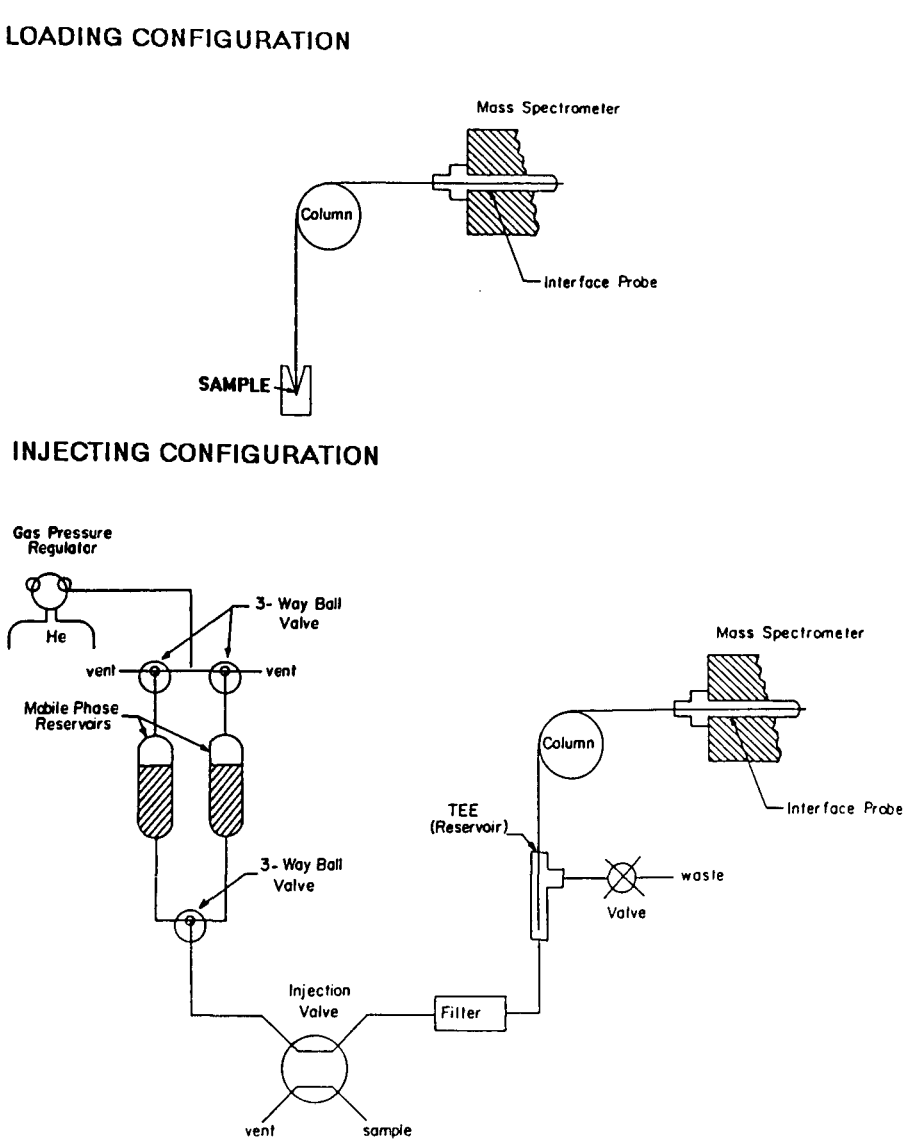

Fig. 6. Loading and injection system for OTLC–MS.

soybean shoot extract run using DLI LC–MS and the preconcentration technique is shown in Fig. 8. A DLI LC–MS chromatogram of a 2.5-ml lakewater sample spiked with 25 ng DA, DK and DADK, and 50 ng MZN [10, 10, 10 and 20 ppb (μg/l), respectively] is shown in Fig. 9.

There was very little chemical noise in the DLI chromatograms of the lakewater extracts, so the detection limits (for the amount of material reaching the source) were the same as those determined by injection of pure compounds. For the soybean extracts, the estimated source detection limits for DA and MZN were effectively the

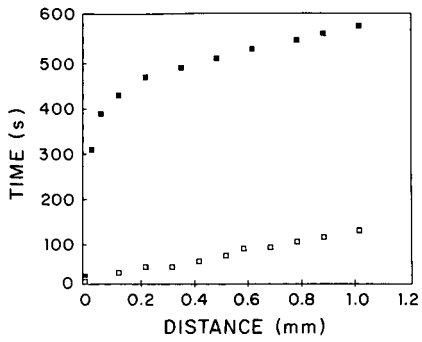

Fig. 7. OTLC solvent flow-rate, loaded by the "dip" technique. (■) = Near column entrance; (□) = in interior of column.

same as those calculated for the standard solutions. The detection limits for DK and DADK, however, were somewhat poorer in the soybean extracts due to chemical noise from other components in the matrix.

The chromatogram obtained on a diploid soybean shoot extract by OTLC–MS is shown in Fig. 10 (the DLI LC–MS results from this same extract were shown in Fig. 8). The sensitivities of both OTLC and DLI LC–MS were sufficient to allow detection in extracts of soybean plants which had been treated with 0.04 ppm MZN in the culture medium. Due to the limited injection volume of OTLC, however, the plant extract had to be concentrated by a factor of almost 100 compared to DLI before the metabolites could be detected. The plant matrix had a deleterious effect on the performance of the OTLC–MS system even with only *ca.* 0.1 nl of the concentrate injected. The matrix also

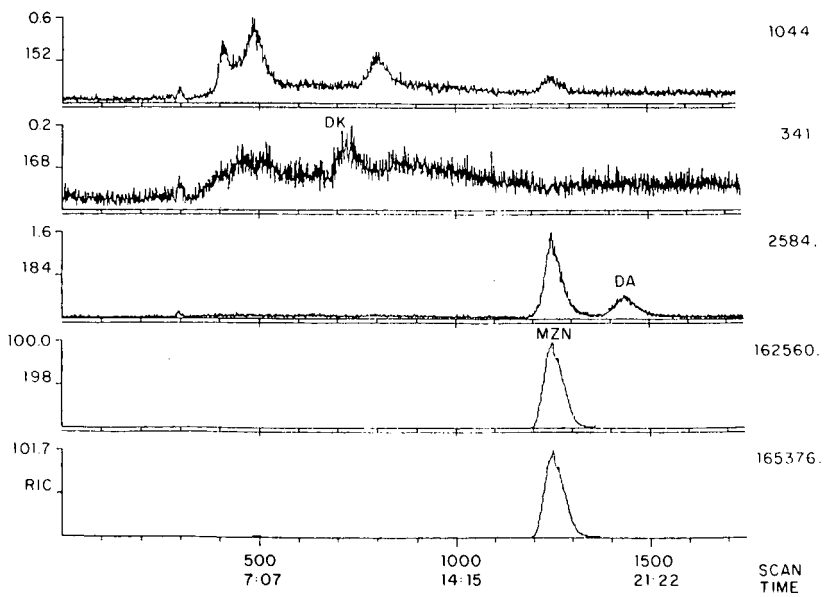

Fig. 8. Selected ion traces for a soybean shoot extract by DLI LC–MS (MID, NCI). 100 μl of 1 ml total extract injected.

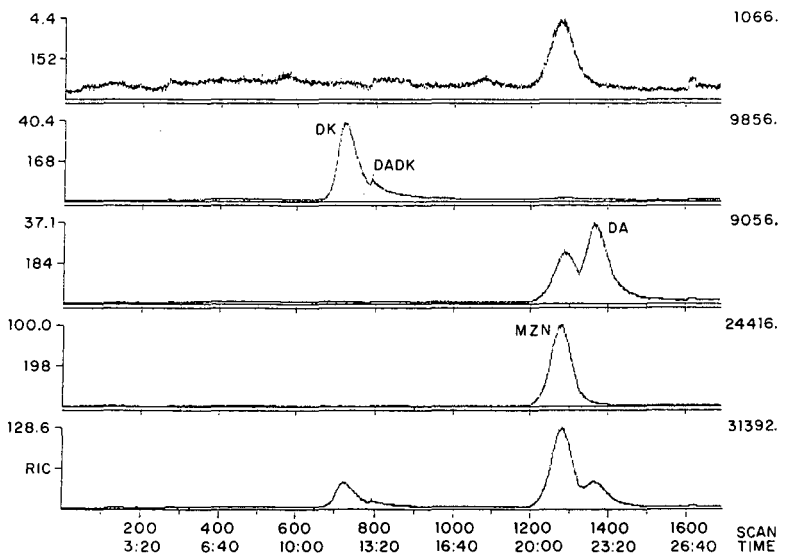

Fig. 9. Selected ion traces by DLI LC–MS (MID, NCI) for a lakewater extract spiked with DA, DADK, DK and MZN at the 10-, 10-, 10- and 20-ppb level, respectively. Results shown are for an injection of 2.5 ml of lakewater using the preconcentration/cleanup system.

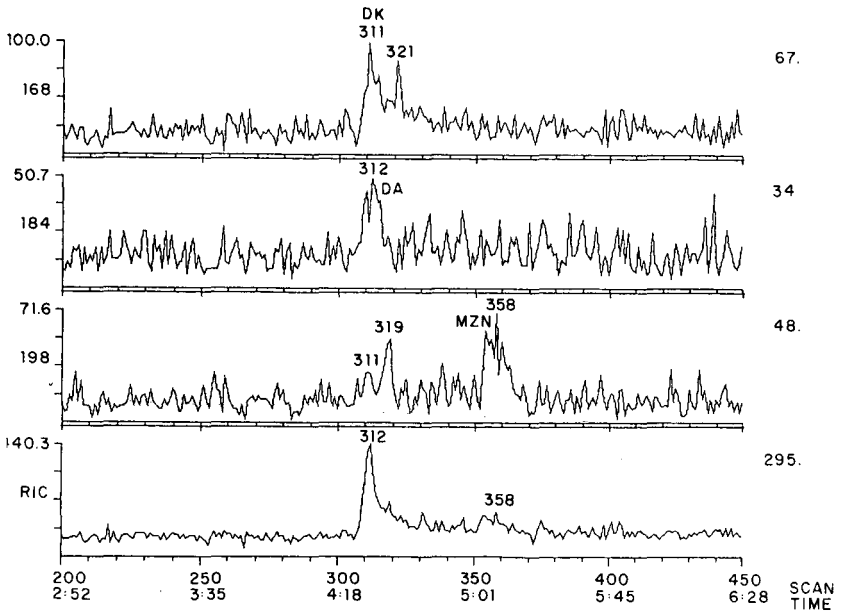

Fig. 10. Selected ion traces by OTLC–MS (MID, NCI) for the same soybean shoot extract shown in Fig. 8. Approximately 0.1 nl was injected, which corresponds to *ca.* 7.2 nl of the original 1-ml extract.

caused a shift in the retention time of DA so that it coeluted with DK in the plant sample.

Problems of column plugging occurred in the OTLC–MS analysis of the lakewater extracts (possibly due to high concentrations of inorganic salts) so no chromatograms could be obtained. Similar problems of plugging due to inorganic salts have been observed in thermospray, which also uses a heated vaporizer.

One would have expected that the sample preconcentration and the relative sensitivity advantage of OTLC over DLI would have partially compensated for the small injection volume of OTLC and would have resulted in a better response for OTLC than was observed (Table III). DLI, however, gave a much better response than did OTLC. It is possible that some of the analyte may have been lost during the extensive sample concentration process used for the OTLC samples. Matrix effects appeared to be more severe than in conventional HPLC and precluded a larger OTLC injection. Matrix effects are reduced in DLI LC–MS both by the inherent sample loading characteristics of the larger column, and by the injection system developed for on-line sample concentration and cleanup which could be used for DLI and not for OTLC.

Comparison of UV, radiochemical, and MS results. In the UV chromatogram shown in Fig. 11, the peak corresponding to the retention time of DA resulted from a component of the matrix. This and other matrix components precluded the use of UV detection for such low levels of metabolites.

The major metabolite detected by both LC–MS techniques in both diploid and tetraploid soybeans was DA. A trace of DK was also detected. The pattern of known metabolites found by LC–MS was confirmed by radiochemical detection on extracts of soybean plants treated with labeled MZN.

No consistent differences in the ratio of DA and MZN between diploid (MZN-sensitive) and tetraploid (MZN-tolerant) soybeans could be detected by DLI LC–MS, mainly due to the lack of suitable internal standards for quantitation. The major differences appared to be in the late-eluting metabolites, detected by radiochemical detection. These metabolites did not show masses characteristic of the previously-identified metabolites. The structures of these metabolites have not been determined and are the subject of continuing investigation.

TABLE III
SAMPLE LOADING COMPARISON

	DLI	*OTLC*
Volume injected	100 μl[a]	0.1 nl
Split ratio (%) (% to mass spectrometer)	<20%	100
Actual volume to mass spectrometer	20 μl[a]	0.1 nl
Relative volume to mass spectrometer	200 000:1	
Relative amount of analyte to mass spectrometer	3000:1	
Relative sensitivity	1:200	
Relative response expected	15:1	

[a] With on-line preconcentration/clean-up system.

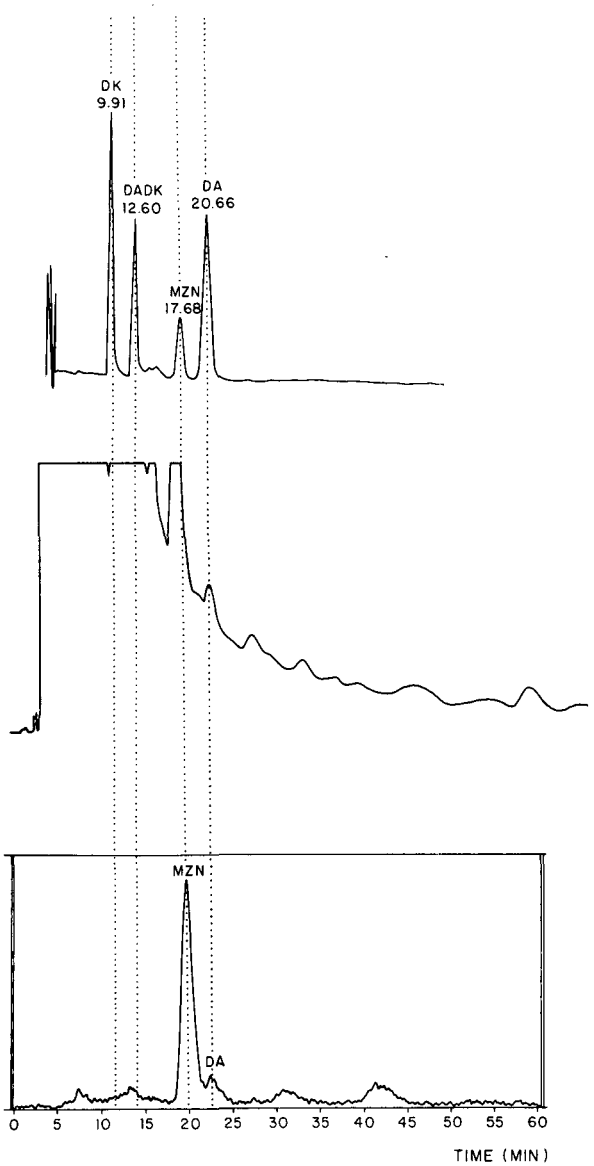

Fig. 11. A comparison of UV and radiochemical detection for the analysis of MZN and its three metabolites in soybean shoot samples. The concentrations used for the standard mixture were 250, 250, 250, and 500 ng of DA, DADK, DK, and MZN injected, respectively (detector sensitivity, 0.2 A); the UV and radiochromatograms were done on 300 μl of a 1-ml extract.

CONCLUSIONS

Several properties of OTLC–MS make it appear attractive for the analysis of environmental samples. One of these advantages is the very small amount of sample required per analysis through the use of the "dip" injection technique as demonstrated

in this paper. Compared to DLI, the OTLC interface requires no sample split, so all of the injected sample goes to the MS source. This should give better on-column detection limits. Another advantage of OTLC is better chromatographic resolution, resulting in shorter analysis times for a given separation and narrower peaks. The narrow peak width gives a higher mass flow to the MS source than do wider peaks. This should also increase the sensitivity of OTLC over DLI. Another advantage over DLI is that less mobile phase enters the MS source, so electron impact ionization is possible, and, in reversed-phase systems, less water enters the source, resulting in longer filament lifetimes.

One disadvantage of OTLC is lack of a commercial source of columns or interface probes. More important, for environmental samples (or other samples with difficult matrices), OTLC columns may be more sensitive to matrix effects, especially if extensive preconcentration of the sample is required. These matrix effects can dramatically reduce the column efficiency and chromatographic resolution. Plugging of the OTLC column and/or interface may result from matrix components or analyte solubilities; in addition, some "shedding" from the in-line filter used to protect the column may occur[39]. In the taper-type interface like that used here, when the column is plugged, the taper has to be reformed. The OTLC column can easily be overloaded and the OTLC–MS system has a low dynamic range. Successful OTLC–MS analysis requires that the amount injected onto the OTLC column be detectable by the MS. While small injection volumes (*ca.* 1 nl) mean that many analyses can be performed on a few microliter of sample, these small injection volumes also limit the amount of analyte entering the MS source. Solubility of the analyte in the mobile phase also can be a limiting factor.

Some of the problems in OTLC–MS of environmental samples could possibly have been overcome by extensive off-line sample concentration and cleanup (*e.g.*, desalting, in the case of the lakewater samples). The purpose of the present study, however, was to evaluate OTLC–MS and DLI LC–MS for the analysis of crude extracts so these additional cleanup procedures were not included. Some of the difficulties encountered in the analysis of crude extracts may be mitigated by the use of packed capillary LC columns, which are presently under development.

The preconcentration/cleanup technique, which cannot be used with the small volumes and flow-rates of OTLC, and the inherent sample loading capacities of minibore and larger columns, can combine to give DLI LC–MS an advantage over OTLC–MS for the analysis of environmental samples. MZN and its metabolites could be detected in treated soybean tissue and in lakewater at the ppb level by DLI LC–MS. Quantitation by either LC–MS technique would require coinjection of a suitable internal standard to compensate for sensitivity changes in the MS source. Without internal standards, LC–MS can be used for confirmation of the identity of suspected metabolites detected by other less-selective techniques, and the identification of new metabolites, but is less well-suited to quantification.

REFERENCES

1 R. R. Gronberg, D. R. Flint, H. R. Shaw and R. A. Robinson, *Report No. 29800*, Research and Development Department, Mobay Corp., St. Louis, MO. Agricultural Chemicals Division, Stillwell, KA, 1971.

2 D. D. Church, R. R. Gronberg and D. R. Flint, unpublished results, 1972.

3 B. E. Pape and M. J. Zabik, *J. Agric. Food Chem.*, 20 (1972) 72.
4 P. W. Albro, C. E. Parker, G. D. Marbury, O. Hernandez and F. T. Corbin, *Appl. Spectrosc.*, 38 (1984) 556.
5 E. O. Abusteit, F. T. Corbin, D. P. Schmitt, J. W. Burton, A. D. Worsham and L. Thompson, Jr., *Weed Sci.*, 33 (1985) 618.
6 D. S. Frear, H. R. Swanson and E. R. Mansager, *Pestic. Biochem. Physiol.*, 23 (1985) 56.
7 T. Zlatev and D. Stoichev, *Khranitelnoprom. Nauka*, 2 (1986) 42.
8 J. Kovac, J. Tekel and K. Kurucova, *Z. Lebensm.-Unters. Forsch.*, 184 (1987) 96.
9 H. J. Stan and D. Mrowetz, *J. Chromatogr.*, 279 (1983) 173.
10 M. Eichner and R. Renner, *Z. Lebnm.-Unters.-Forsch.*, 170 (1980) 1.
11 A. Andersson and B. Ohlin, *Vaar Foeda*, 38 (1986) 79.
12 L. Stalder and W. Pestemer, *Weed Res.*, 20 (1980) 341.
13 W. Pestemer, L. Stalder and B. Eckert, *Weed Res.*, 20 (1980) 349.
14 K. A. Krieger, D. B. Baker and J. W. Kramer, *Arch. Environ. Contam. Toxicol.*, 17 (1988) 299.
15 H. Geyer, G. Politzki and D. Freitag, *Chemosphere*, 13 (1984) 269.
16 Y. Nishiuchi, *Suisan Zoshoku*, 30 (1982) 158.
17 M. Grandet, L. Weil, K. E. Quentin, *Z. Wasser Abwasser Forsch.*, 21 (1988) 21.
18 D. Freitag, L. Ballhorn, H. Geyer and F. Korte, *Chemosphere*, 14 (1985) 1589.
19 J. W. Kramer and D.B. Baker, *ASTM Spec. Tech. Publ.*, 867 (1985) 116.
20 D. F. Brown, L. M. McDonough, D. K. McCool and R. I. Papendick, *J. Agric. Food Chem.*, 32 (1984) 195.
21 A. Kettrup, W. Maasfeld, D. Dubisch and U. Kampschultze, *Pergamon Ser. Environ. Sci.*, 7 (1982) 231.
22 T. A. Presley and J. E. Longbottom, *EPA Report, EPA-600/4-82-013, Gov. Rep. Announce Index*, 82 (1982) 1544.
23 I. A. Shevchuk, Y. G. Dubchenko, V. V. Kucherenko and Z. Gulahmad, *Ukr. Khim. Zh.* 53 (1987) 732.
24 *E.P.A. Chemical Information Factsheet for Metribuzin, Factsheet No. 53*, Office of Pesticide Programs, E.P.A. Registration Division, Washington, DC, June 30, 1985, p. 5.
25 E. J. Guthrie and J. W. Jorgenson, *Anal. Chem.*, 56 (1984) 483.
26 J. S. M. de Wit, C. E. Parker, K. B. Tomer and J. W. Jorgenson, *Anal. Chem.*, 59 (1987) 2400.
27 P. R. Dluzneski and J. W. Jorgenson, *J. High Resolut. Chromatogr. Chromatogr. Commun.*, 11 (1988) 332.
28 P. R. Dluzneski, *Ph. D. Thesis*, University of North Carolina at Chapel Hill, 1987.
29 M. Friesen, *Ph. D. Thesis*, Kansas State University, Manhattan, KA, 1977.
30 C. E. Parker, R. D. Voyksner, Y. Tondeur, J. D. Henion, J. R. Hass and J. Yinon, *J. Forensic Sci.*, 27 (1982) 495.
31 C. E. Parker, C. A. Haney and J. R. Hass, *J. Chromatogr.*, 237 (1982) 233.
32 D. R. Hoagland and D. I. Arnon, *California Expt. Station Circular 347*, University of California at Davis, Davis, CA, 1950, 32 pp.
33 C. E. Parker, G. Degen, E. O. Abusteit and F. T. Corbin, *J. Liq. Chromatogr.*, 6 (1983) 725.
34 C. E. Parker, A. V. Geeson, D. E. Games, E. D. Ramsey, E. O. Abusteit, F. T. Corbin and K. B. Tomer, *J. Chromatogr.*, 438 (1988) 359.
35 R. C. Ludwig and R. Eksteen, *LC·GC Mag. Liq. Gas Chromatogr.*, 6 (1988) 250.
36 J. W. Veals and C. C. Lin, *Am. Lab. (Fairfield, Conn.)*, 4 (1988) 42.
37 T. A. Bellar and W. L. Budde, presented at the *35th Annual Conference on Mass Spectrometry and Allied Topics, Denver, May 24–29, 1987*, Abstract p. 1072.
38 G. A. Junk and J. J. Richard, *Anal. Chem.*, 60 (1988) 451.
39 J. A. Poppiti, personal communication.

Journal of Chromatography, 474 (1989) 317–327
Elsevier Science Publishers B.V., Amsterdam — Printed in The Netherlands

CHROM. 21 343

LIQUID CHROMATOGRAPHIC–MASS SPECTROMETRIC STUDIES ON RIFAMYCIN ANTIBIOTICS

K. VÉKEY*, D. M. F. EDWARDS and L. F. ZERILLI
Lepetit Research Center of the Merrell-Dow Research Institute, Via R. Lepetit 34, 21040 Gerenzano (Italy)

SUMMARY

The use of a direct liquid introduction type liquid chromatographic–mass spectrometric interface to study highly thermally labile rifamycin antibiotics is described. Using negative ionization, abundant molecular ions were observed, and the spectra also contained structurally significant fragments. Variation of the high-performance liquid chromatographic parameters did not change the spectra, thus making it easy to change chromatographic conditions. In quantitative studies, a surprising correlation was found, indicating that the mass spectrometric signal was proportional to the square of the sample concentration.

INTRODUCTION

Rifamycins are a well known family of antibiotics obtained by fermentation and successive chemical modification. The most widely used member of this group is rifampicin; there are also some important new derivatives, such as rifapentine (Fig. 1). Their activity against both Gram-positive and Gram-negative bacteria, and in particular *Mycobacterium tuberculosis*, makes some of these antibiotics widely employed in therapy. Recently, interesting activity has been observed against *Mycobacterium avium* complex, the causative agent of an infection common in patients with autoimmune deficiency syndrome (AIDS).

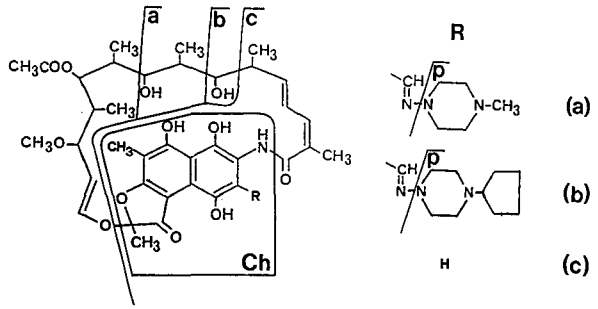

Fig. 1. Structure and main fragmentations of (a) rifampicin, (b) rifapentine and (c) rifamycin SV. a, b, c, p and Ch indicate main fragmentation processes (see also Figs. 2, 3 and 5).

0021-9673/89/$03.50

Mass spectrometric studies of these antibiotics are hindered by their thermal lability. Electron impact (EI) using direct inlet[1–5] gave useful results but also indicated serious limitations. Whereas certain rifamycins give interpretable EI spectra on some mass spectrometers, there are many cases where extensive thermal decomposition occurs, resulting in spectra which may not only lack the molecular ion, but which also depend strongly on the instrument used. Structurally significant ions may be absent, and in some cases the spectra show peaks at every mass unit, with rapidly decreasing abundance towards higher masses. Our preliminary studies indicate that the same is true for chemical ionization using direct inlet. Rifamycins were also studied by other ionization methods. Field desorption[5,6] gives the molecular weight but little structural information. Laser desorption[7] and fast atom bombardment[8] have recently been used, giving promising results.

In our laboratory, a direct liquid introduction (DLI) type liquid chromatography–mass spectrometric (LC–MS) connection is used, and has proved very useful for studying thermally labile compounds, even if chromatographic separation is not required[9,10]. Contrary to some comments in the literature[11] this method is suitable for the study of non-volatile compounds, as also illustrated by this report. In DLI (for reviews see refs. 9, 12 and 13), liquid flows at 10–50 μl/min through a *ca.* 5 μm diameter orifice diaphragm, forming a liquid jet. The jet very soon breaks up into small droplets, from which the solvent evaporates. This process requires heating: not to warm up the liquid, but to stop it from freezing due to fast evaporation. The only part of the instrument where thermal decomposition is likely is the ion source. Even here the sample molecules normally should not make contact with the walls of the source, only with the reagent gas (in low vacuum). This provides a less efficient heat transfer, and only for a few milliseconds. However, some of the sample molecules may (temporarily) be adsorbed on the walls, especially if the jet is bent, and this may lead to thermal decomposition[14]. It is also worth mentioning that solutes of low volatility are probably not evaporated in this process, but evaporation of volatile solvents from the droplets may leave them in the gas phase.

In the present work, MS characteristics and optimization of experimental conditions to study rifamycins are discussed. The main purpose is partly to use DLI as a sample introduction method for these thermally labile compounds and partly to establish LC–MS conditions to analyse various derivatives, metabolites and impurities. The study focuses principally on the behaviour of rifapentine. Our experience with rifampicin, rifamycin SV (Fig. 1) and various other derivatives indicates that these results can be generalized for most rifamycins.

EXPERIMENTAL

Samples

Rifapentine, rifampicin and rifamycin SV Lepetit analytical reference substances were used. Unless otherwise indicated, 50 μg of sample dissolved in 10 μl of methanol was injected on to the HPLC column. As rifamycins slowly decompose in solution, fresh stock solutions were prepared each day.

Liquid chromatographic–mass spectrometric system

An HP-1090 HPLC system was connected to an HP-5985B quadrupole mass

spectrometer system of 1000 dalton mass range using a direct liquid introduction interface (5 μm orifice water-cooled stainless-steel diaphragm). Unless otherwise stated, methanol was used as the mobile phase at 1 ml min^{-1} flow-rate with a Hewlett-Packard Hypersil C_{18} column (100 × 4.6 mm) with the addition of a precolumn. The eluate from the column passed through a Perkin Elmer LC-15 UV detector (254 nm) and a 5-μm filter frit before entering the mass spectrometer. The mass spectrometer was used in chemical ionization mode; the ion source pressure was *ca.* 1 Torr (measured in the otherwise unused gas chromatographic transfer line of the HP-5985B system) and the ion source temperature was 250°C. The LC eluent was used as reagent gas.

RESULTS AND DISCUSSION

Mass spectral characteristics

Positive chemical ionization of rifamycins using DLI gives protonated molecular ions and some structurally characteristic fragments (Fig. 2). The main fragment ions are analogous to those described previously[1,2] but, as the molecular ion is clearly identifiable, this method is a significant improvement over direct inlet methods. However, sensitivity is poor, and due to a high background, fragment ions are difficult to identify below *m/z* 300.

Negative ionization with DLI (Fig. 3) also gives abundant molecular ions together with some fragments. The sensitivity is 100–1000 times better than in positive ionization, background ions are smaller, so lower mass fragments can also be studied. For these reasons, negative ionization proved more suitable than positive ionization for the analysis of rifamycins, and only the former has been studied in detail.

In negative ionization, $M^{-\cdot}$ is formed with high abundance, indicating an electron attachment process and a correspondingly high electron affinity for rifamycins. This also suggests that the eluent acts as a moderator gas. It is interesting to note that $[M-H]^-$ type ions, which are more usually encountered in negative chemical

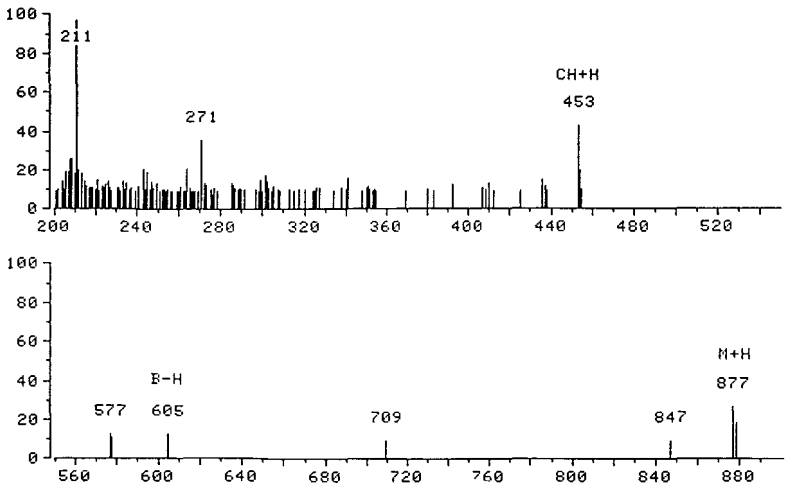

Fig. 2. Positive ion DLI spectrum of rifapentine.

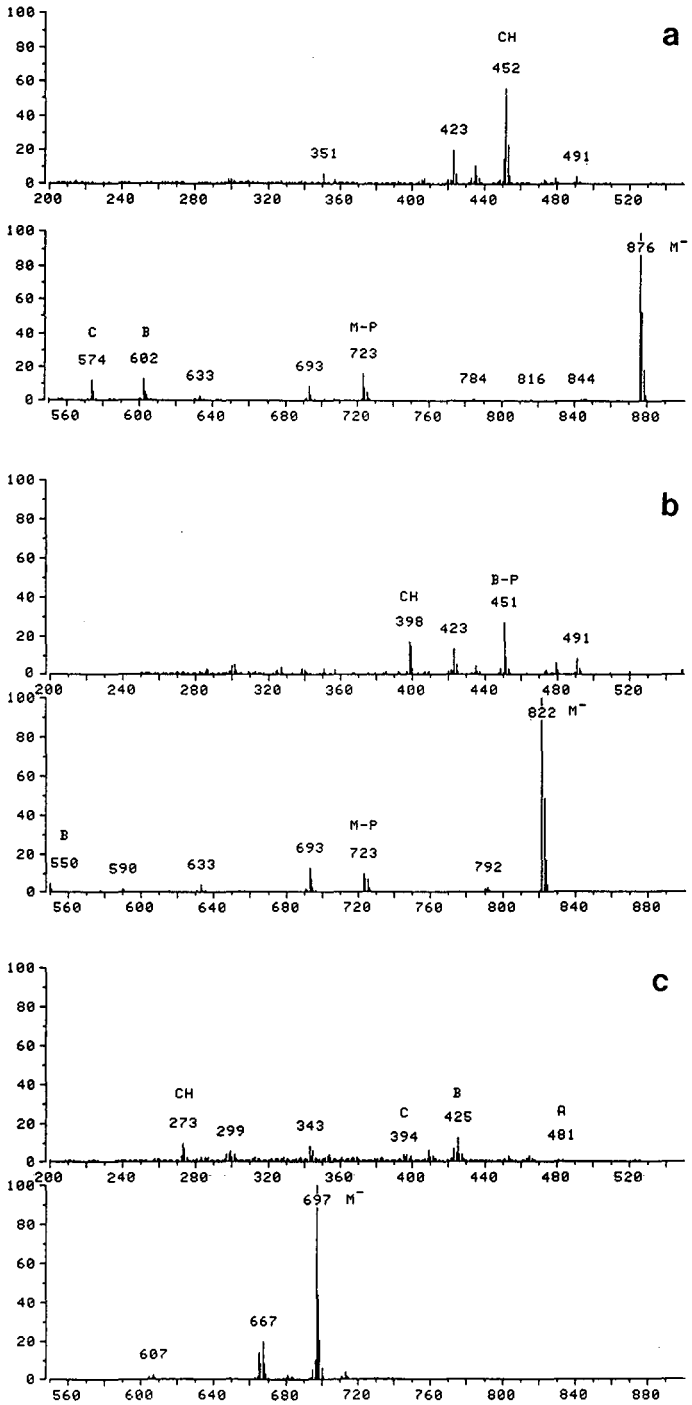

Fig. 3. Typical negative ion DLI spectra of (a) rifapentine, (b) rifampicin and (c) rifamycin SV obtained at the top of the molecular ion chromatograms.

ionization, are absent in the spectra of rifamycins. Recently, use of chlorine-containing additives in the mobile phase was suggested to increase sensitivity in negative ionization DLI[15]. In the case of rifamycins it has an opposite effect: even traces of chlorine-containing solvents reduce the abundance of rifamycin-related ions by several orders of magnitude, probably by quenching the supply of low velocity electrons necessary for electron attachment. This finding suggests that halogen-containing additives should generally be avoided if negative ionization occurs by electron attachment.

In the spectra of rifamycins (Fig. 3) there are a number of significant fragment ions. One of the most abundant is the so-called "chromophoric" ion[1,2] (denoted Ch in Fig. 1, *m/z* 452 for rifapentine, *m/z* 398 for rifampicin, *m/z* 273 for rifamycin SV). There are small but significant fragments characteristic of a, b and c type cleavages first noticed in electron impact studies[1,2] (Fig. 1); these give information about the "ansa" part of the molecule (the saturated part of the macrocycle). There is fragmentation at the piperazino ring in rifampicin and rifapentine (p in Fig. 1), which has not been reported previously, and there are losses of small molecules such as CH_2O, CH_3OH and CH_3COOH from various ions listed above. Fragmentations such as these can be helpful in determination of the structure of synthetic modifications of known rifamycins. There is also an abundant ion at *m/z* 150, not previously observed, present in the spectra of all derivatives studied. This might originate from the ansa chain, though we could not locate which part. As the abundance of *m/z* 150 is very variable, partly due to thermal decomposition, it was decided to show spectra above *m/z* 200 in Figs. 2, 3 and 5.

Thermal decomposition and reproducibility

There are several features in the behaviour of rifamycins suggesting that thermal decomposition occurs to some degree under DLI conditions. In the case of rifapentine, for example, the chromatographic response obtained at the UV detector comprised

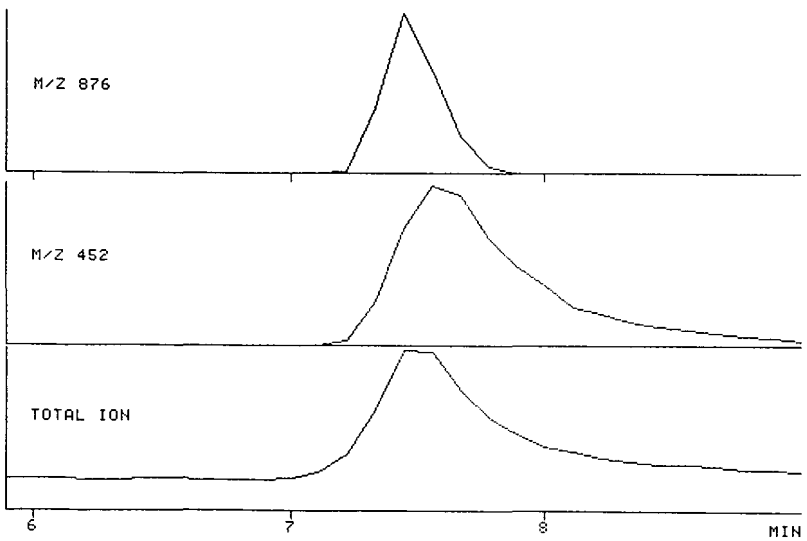

Fig. 4. Ion chromatograms of rifapentine in negative ion DLI LC–MS.

a symmetrical peak *ca.* 14 s wide at half height. The ion chromatogram of the negative molecular ion was likewise fairly symmetrical (Fig. 4) with a similar half-width. The total ion chromatogram and ion chromatograms of several fragment ions (*e.g.*, *m/z* 452), on the other hand, were about twice as wide (Fig. 4), showing significant tailing. As the residence time of gases in the source is in the order of 0.01–0.1 s, this can be explained easily only by an adsorption/desorption process. Such a process could occur either on the hot walls of the source or, perhaps, on the diaphragm, desorption occurring with thermal decomposition. Using the different time behaviour of the various peaks, it is possible to deconvolute them to obtain spectra for two main

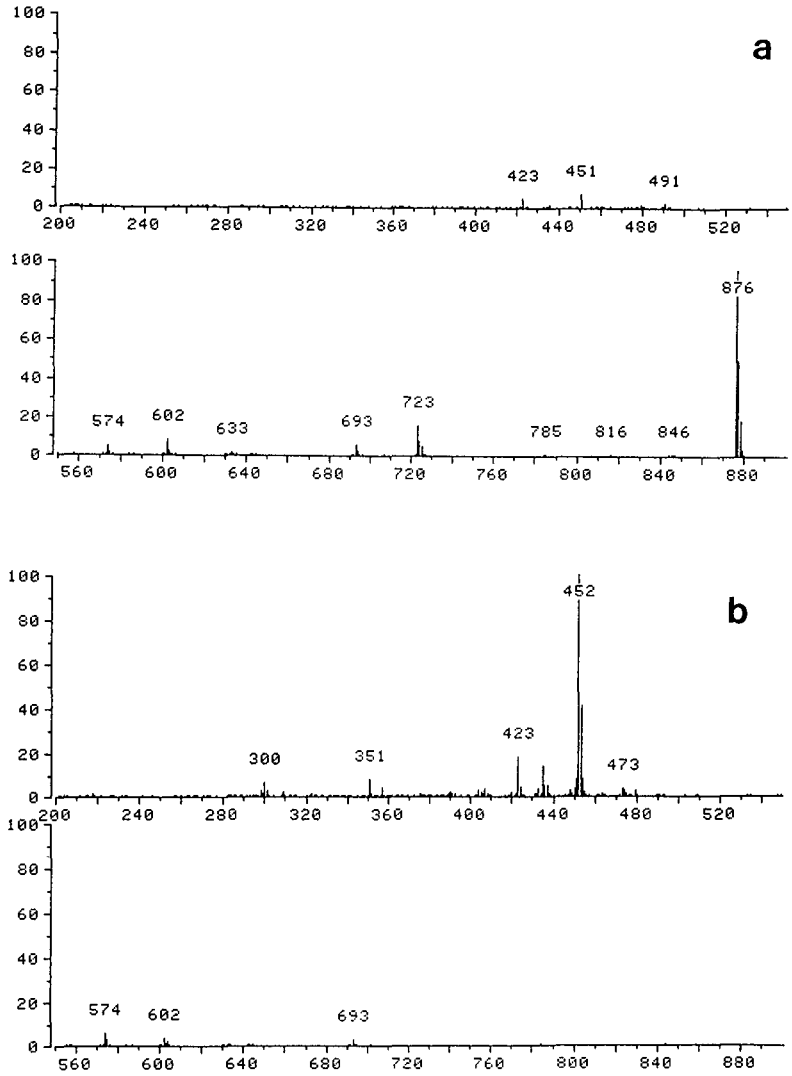

Fig. 5. Deconvoluted negative ion DLI spectra of rifapentine pure electron attachment spectrum of (a) rifapentine; (b) spectrum of the main thermal decomposition product.

components, as shown in Fig. 5. It is worth noting that the ion at *m/z* 452, probably the structurally most useful ion indicating the "chromophore" of rifamycins[1,2], seems to arise from thermal decomposition. This ion is absent in the deconvoluted "pure electron capture" spectrum of rifapentine (Fig. 5a), while there is a small but significant ion at *m/z* 451. This might be interpreted as thermal decomposition to produce a molecule which in turn gives an odd electron ion, while fragmentation following electron capture might produce an even electron ion of similar structure.

Temperature dependence of the spectra has been studied between 150 and 300°C. As might be expected, the abundance of most fragments relative to the molecular ion is higher at higher source temperatures. While this increase is moderate for most fragments, the abundance of *m/z* 452 increases about 100–1000 fold. This is in accordance with its formation by thermal decomposition. As the diaphragm is water cooled (and therefore its temperature is constant), this large variation suggests that thermal decomposition occurs on the walls of the ion source. This is further supported by the observation that, if the jet through the diaphragm is bent, so that the liquid may hit the walls of the source before complete evaporation, the intensity of the molecular ion decreases dramatically, while that of *m/z* 452 does not change significantly.

Optimum ion source temperature depends on various factors, such as contamination in the ion source and type of information sought. In general, lower source temperatures are preferred if detection of the molecular ion is desired, whereas at higher temperatures fragment ions have higher abundance. However, below about 200°C, buildup of contaminants in the ion source and incomplete evaporation of the droplets produced by the liquid jet result in low sensitivity and unstable operation of the instrument.

Because many parameters affect thermal decomposition processes, care should be taken not to change instrumental conditions during a set of experiments. When spectra taken at the top of a chromatographic peak are compared, the short term reproducibility (within a few hours or a day) is good, about 10–20% (relative). It is not significantly worse than long term or interlaboratory reproducibility of mass spectra in general, when no special care is taken. Long term reproducibility (within a few months, during which period the ion source is cleaned) is much worse. Ions which are supposed to be formed following ionization (*e.g.*, those at *m/z* 723 and 693), and which are seen in the "deconvoluted" spectrum of rifapentine in Fig. 5a, could be reproduced well (20%). The relative abundance of the ion at *m/z* 452, which is thought to be formed by a thermal decomposition process, varies widely (by a factor of 100) even if the source is kept at constant temperature. The abundance of other peaks, which could be formed partly by thermal decomposition and partly following ionization (most other peaks including b and c) vary usually within a factor of two or three. When the spectra were studied throughout the elution time, they could be deconvoluted as shown in Fig. 5. In contrast to spectra taken at the top of the chromatographic peak, the long term reproducibility of these "deconvoluted" spectra is good, *ca.* 20–30%.

Apart from the source temperature, the most important parameters affecting thermal decomposition seem to be the condition (probably the catalytic effect) of the ion source and the quality of the liquid jet. A clean ion source with a straight liquid jet gives practically no thermal decomposition, and the spectrum obtained at the top of the chromatographic peak is practically the same as the "deconvoluted" spectrum shown in Fig. 5a. On the other hand, spectra obtained with a very dirty ion source may

be dominated by decomposition products, even with a straight jet. The relative abundance of the molecular ion may drop below 1% if a dirty source is used with a bent jet.

Quantitative studies

To extend LC–MS analysis to quantitative or semi-quantitative determination of rifamycin derivatives, the relationship between the sample amount injected and the MS signal was studied. Surprisingly, instead of a linear response, a quadratic relationship was observed. This is shown in Fig. 6 using a double logarithmic scale. The range of sample amount extended from about 2 to 100 nmol of rifapentine injected, and the signals at the maximum of the ion chromatograms were recorded. The low end of this range corresponded to the appearance of rifapentine-related signals (using full scans), while at high levels the HPLC peak (as observed on the UV trace) started to broaden significantly. As we are not aware of previous observation of a quadratic response in LC–MS, the instrument performance was checked thoroughly, as follows.

(1) The response of the LC–MS system was checked using two standards: the $[M-H]^-$ ion of hydroquinone and the M^- ion of nitrobenzene (these ions represent over 70% of the total ion current in the respective spectra), in the same molar concentration range. The response of the mass spectrometer was found to be linear within a factor of 1.5; the data for nitrobenzene are shown in Fig. 6. The response for some other classes of antibiotics were also checked, and approximately linear relationships were found.

(2) For rifapentine, both the molecular ion and the chromophoric ion at m/z 452 showed a quadratic response (Fig. 6). This was reproduced on several occasions, even when the ratio between the molecular ion and m/z 452 differed by a factor of 10–100 (due to varying conditions of the ion source and the liquid jet, as described above).

(3) While the MS signal showed a quadratic relationship with the amount of rifapentine, the UV trace showed the expected linear response. (At high levels slight deviations from linearity and quadraticity were observed, owing to peak broadening.)

(4) Beside rifapentine, some other rifamycins were also checked, and similar quadratic relationships were found.

The observed quadratic relationship between amount of rifamycin and mass spectrometer response suggests that interaction between two rifamycin molecules is necessary for the ionization process. However, in the range studied there are *ca.* 10^5 to 10^6 solvent molecules for each rifamycin molecule present, even at the top of the chromatographic peak! This makes intermolecular interactions in the gas phase unlikely. In the DLI process, however, small droplets are formed, from which the solvent evaporates. In the process the liquid phase becomes more concentrated. This might explain the interaction of two sample molecules. Solute clustering in solution or enhanced surface concentrations might also be involved. It is not possible at present to offer a detailed explanation of this unexpected relationship.

Effect of HPLC conditions on mass spectra

As discussed above, the molecular ion is probably formed by electron attachment, where the solvent used in HPLC acts as a moderator gas by thermalizing electrons. In accordance with this mechanism, changes of solvent do not significantly alter either the relative ion abundances or the sensitivity for rifamycins. Various

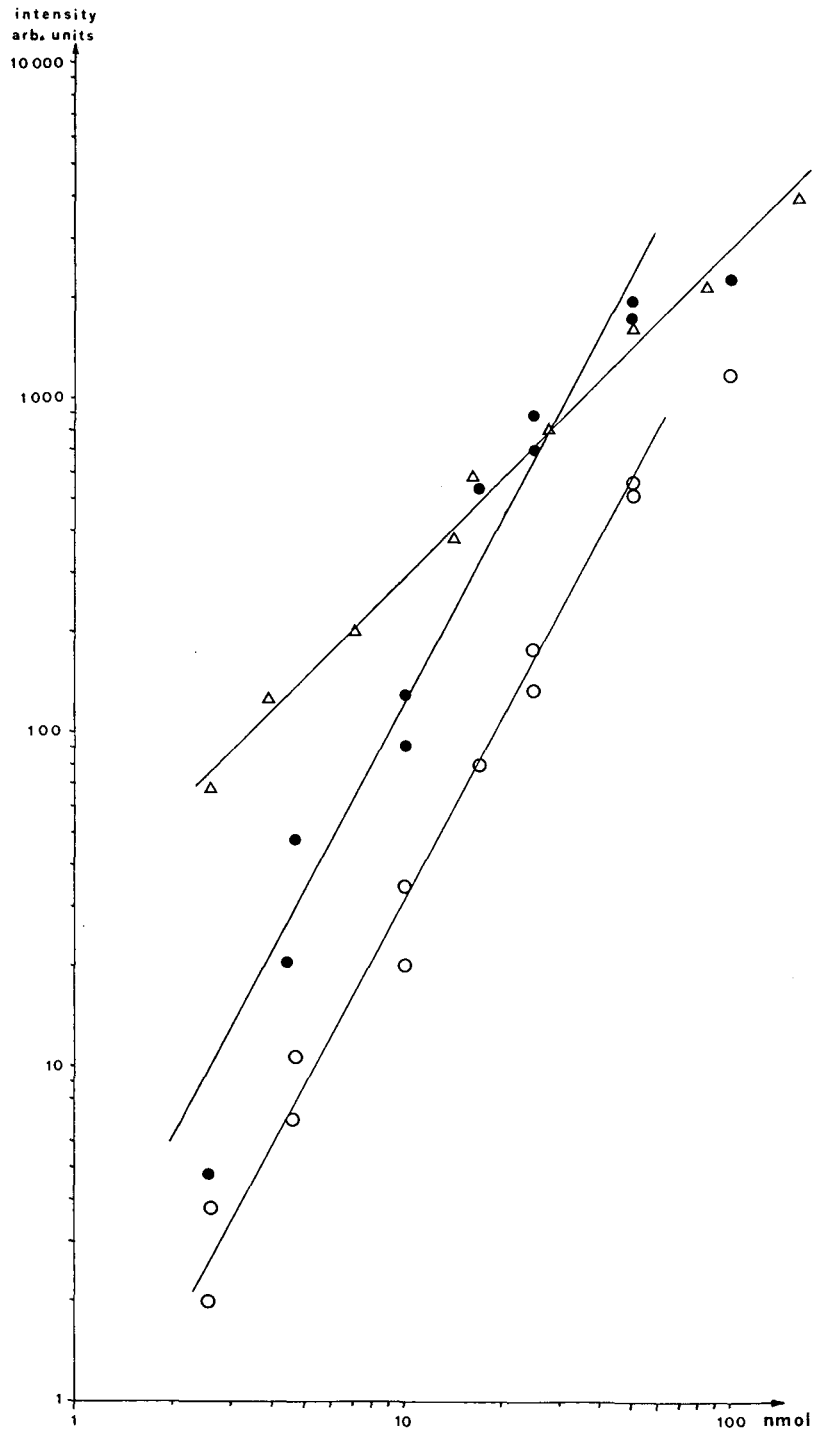

Fig. 6. Correlation between the mass spectrometric signal and the sample amount injected on to the HPLC column, shown on a double logarithmic scale. Negative ionization DLI LC–MS. Molecular ion (*m/z* 876) of (●) rifapentine; *m/z* 452 of (○) rifapentine; molecular ion (*m/z* 123) of (△) nitrobenzene.

combinations of water, methanol, acetonitrile and toluene were used as eluents, and only differences in the low mass solvent clusters were observed, usually below m/z 100. The addition of volatile acids (*e.g.*, CH_3COOH) or ammonium formate buffers with pH from 4.3 to 8.0 also did not change the spectra significantly. However, as a general restriction when using a DLI interface, non-volatile buffers cannot be used. For reasons discussed above, halogen-containing additives should be avoided.

The flow-rate in HPLC may be varied between *ca.* 0.5 and 2 ml/min without significant effect on the spectra. However, when the flow-rate is altered the pressure in the ion source may also change. If it becomes too high (*ca.* 2 Torr in our instrument) sensitivity may drop significantly, probably due to scattering in the analyser region. In such a case it is necessary to lower the amount of liquid getting into the ion source by shortening the liquid jet.

CONCLUSION

A DLI type LC–MS interface using negative ionization gave very good results for rifamycin antibiotics. This demonstrates that DLI is very useful for studying non-volatile and thermally labile compounds. Beside an abundant molecular ion the spectra show various fragments suitable for structural characterization of rifamycins.

Changes in the spectra during a chromatographic peak, temperature dependence and long term reproducibility of the spectra suggest that a structurally important fragment, the so-called chromophoric ion, is formed by thermal decomposition. This specific process, however, may not always occur, *e.g.*, when the ion source is properly cleaned. As the chromophoric ion gives valuable structural information, the ironic consequence is that sometimes a dirty source is a desirable feature!

Short term reproducibility is reasonable (*ca.* 20%), but over a longer period the relative abundance of the chromophoric ion may change over two orders of magnitude. To obtain comparable mass spectra of rifamycins, it is suggested that at the beginning of each day a standard (*e.g.*, rifampicin) should be used to determine the extent of thermal decompositions, and the unknown rifamycin spectra should be compared with the spectrum of this standard.

Chromatographic conditions do not seem to affect the mass spectra significantly, making it easy to change solvents or pH or to use gradient methods. The only real restriction is that non-volatile buffers cannot be used. However, the unexpected quadratic relationship found between the MS signal and the sample amount injected makes quantitative analysis and trace determination of rifamycins difficult.

REFERENCES

1 L. F. Zerilli and G. G. Gallo, *Comm. Eur. Communities [Rep.] EUR*, 4675, 1971, 217–235.
2 L. F. Zerilli, M. Landi, N. Rimorini and G. G. Gallo, *Ann. Chim. (Rome)*, 64 (1974) 199.
3 Wang Cong-hui, Cao Kai-Xing, Wang Yao-Xin and Cui Jiau-min, *Kanshengsu*, 8 (1983) 224.
4 A. Vigevani, M. Ballabio, B. Gioia, L. Marsili, S. Vioglio and G. Franceschi, *J. Antibiot.*, 38 (1985) 1799.
5 A. Vigevani, E. Arlandini, M. Ballabio, G. Franceschi, B. Gioia and S. Vioglio, *Farmaco (Ed. Prat.)*, 40 (1985) 131.
6 L. F. Zerilli, M. Landi, G. C. Gallo, K. H. Maurer and U. Rapp, *Biomed. Mass Spectrom.*, 2 (1975) 307.
7 P. Bravo, B. Cavalleri, L. F. Zerilli, A. M. Maccioni, P. Traldi, W. Cecchetti and P. Polloni, *Biomed. Environ. Mass Spectrom.*, in press.
8 K. Vékey, in preparation.

9 K. Vékey, D. M. Edwards and L. F. Zerilli, *J. Chromatogr.*, 488 (1989) 73.
10 D. J. Dixon, *Analusis*, 10 (1982) 343.
11 M. L. Vestal, *Life Sci. Res. Rep.*, 33 (1986) 613.
12 W. M. A. Niessen, *Chromatographia*, 21 (1986) 277.
13 W. M. A. Niessen, *Chromatographia*, 21 (1986) 342.
14 P. J. Arpino, P. Krien, S. Vajta and G. Devant, *J. Chromatogr.*, 203 (1981) 117.
15 R. B. Geerdink, F. A. Maris, G. J. de Jong, R. W. Frei and U. A. Th. Brinkman, *J. Chromatogr.*, 394 (1987) 51.

Journal of Chromatography, 474 (1989) 329–333
Elsevier Science Publishers B.V., Amsterdam — Printed in The Netherlands

CHROM. 21 398

IDENTIFICATION OF NICOTINE BIOSYNTHETIC INTERMEDIATES IN TOBACCO ROOTS BY LIQUID CHROMATOGRAPHY–MASS SPECTROMETRY

HENRY L. CHUNG* and DENISE E. BLUME
R. J. Reynolds Tobacco Company, Bowman Gray Technical Center, Winston-Salem, NC 27102 (U.S.A.)

SUMMARY

The occurrence of two nicotine biosynthetic intermediates, putrescine (1,4-diaminobutane) and N-methylputrescine (N-methyl-1,4-diaminobutane), within tobacco roots has been confirmed by combined liquid chromatography–mass spectrometry. Perchloric acid extracts of tobacco roots were derivatized with benzoyl chloride. High-performance liquid chromatography was used to separate polyamines. Compounds resolved by isocratic elution on a reversed-phase C_{18} column were detected by UV absorbance at 254 nm. Column effluents were transferred to the mass spectrometer by a direct liquid introduction interface. Putrescine and N-methylputrescine were identified by selected ion monitoring of ions at m/z 297 and 311, respectively in the positive ion chemical ionization mode. Identification of N-methylputrescine within tobacco roots strengthens the proposed biosynthetic pathway for nicotine.

INTRODUCTION

The biosynthesis of nicotine within *Nicotiana* species has been studied extensively and precursors for both the pyridine and pyrrolidine rings of nicotine have been determined from research with labeled precursors[1,2]. There is considerable evidence that the biosynthesis of the N-methylpyrrolidine ring involves the conversion of putrescine to N-methylputrescine and subsequent oxidation of N-methylputrescine to 4-methylaminobutanal (Fig. 1).

Mizusaki *et al.*[2] reported that a putrescine N-methyltransferase enzyme from tobacco roots catalyzed the conversion of putrescine to N-methylputrescine. They also showed that N-methylputrescine oxidase from tobacco roots converted N-methylputrescine into 4-methylaminobutanal[3]. Saunders and Bush[4] have studied the activities of both enzymes in extracts of burley tobaccos differing in nicotine content. Feth *et al.*[5] utilized high-performance liquid chromatography (HPLC) to assay putrescine N-methyltransferase in roots of *Nicotiana tabacum*. Feth *et al.*[6] have also utilized HPLC to assay N-methylputrescine oxidase in tobacco roots and tissue cultures. These reports, coupled with tracer studies, strengthen the view that

0021-9673/89/$03.50

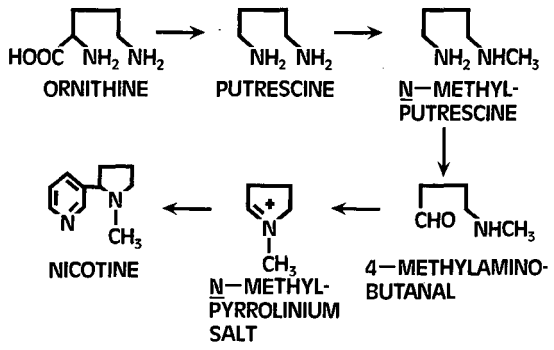

Fig. 1. Biosynthetic pathway of N-methylpyrrolidine ring of nicotine.

N-methylputrescine is involved in nicotine biosynthesis; however, this compound has not yet been reported to occur in tobacco roots. One reason for this may be that the compound is readily utilized for nicotine and does not accumulate within tobacco roots under normal growing conditions.

During investigation of nicotine biosynthesis in stressed tobacco, HPLC profiles of polyamines revealed a compound which co-eluted with authentic N-methylputrescine. A liquid chromatography–mass spectrometry (LC–MS) technique[7] was used to confirm the occurrence of N-methylputrescine in tobacco roots. This report presents our findings on the occurrence of N-methylputrescine in tobacco roots.

EXPERIMENTAL

Chemicals and plant materials

The hydrochloride salt of putrescine and benzoyl chloride were obtained from Sigma (St. Louis, MO, U.S.A.). N-Methylputrescine dihydrochloride was generously provided by Dr. E. Leete of the University of Minnesota. All other chemicals and solvents were of reagent grade or higher.

Seeds of *Nicotiana rustica* var. *pumila* were sown in vermiculite and maintained in an environmentally-controlled chamber at 26°C under a 16-h photoperiod. Three to four weeks after seeding, plants were transferred to nutrient jars containing 3/4 strength Hoagland's solution. Plants with seven or eight leaves were decapitated at the fourth leaf and roots collected at various time intervals after decapitation.

Benzoylation

The procedure for extraction and benzoylation of tobacco roots followed Flores and Galston[8] with slight modifications. Plant root (1 g) was homogenized in 7% perchloric acid and centrifuged. An aliquot of the supernatant (250 μl) was added to 1 ml of 2 *N* sodium hydroxide. A volume of 10 μl of benzoyl chloride was added and the tubes vortexed for at least 30 s to ensure a homogeneous suspension of benzoyl chloride. The benzoylation reaction was carried out for 20 min in a hood at room temperature. A volume of 1 ml of saturated sodium chloride was added, followed by 2 ml of diethyl ether. After centrifugation at 5000 *g* for 2 min, 1 ml of the ether phase

was collected and evaporated to dryness under a stream of dry air. Benzoylamines were dissolved in 0.25 ml of acetonitrile prior to LC–MS identification.

LC–MS analysis

LC was performed with a Waters Assoc. system equipped with two Model 6000A pumps, Model 720 system controller, Model 710B automatic injection system. The column was a Micromeritics C_{18} column, particle size 7.5 μm, 30 cm × 5 mm I.D. (Micromeritics, Norcross, GA, U.S.A.). The solvent was 50% acetonitrile in water maintained at a flow-rate of 1.0 ml/min for 15 min. After elution of the polyamines, the solvent was increased to 100% acetonitrile to remove other derivatized components present in the crude extracts. Typically, 50-μl aliquots of each sample were injected into the HPLC. Standards of authentic polyamines were used for confirmation. The HPLC effluent from the UV detector was passed through a Hewlett-Packard direct liquid introduction (DLI) LC–MS interface (Hewlett-Packard, Palo Alto, CA, U.S.A.). The splitting ratio was 1:99 resulting in a transfer of 0.5 μl of the HPLC effluent to the mass spectrometer. The mass spectrometer was a Hewlett-Packard 5985B GC–MS system. The instrument was scanned at 1 s per scan from 100 to 450 a.m.u. in the positive ion chemical ionization (PICI) mode. The mass spectrometer was operated at a source pressure of 0.5 Torr, a source temperature of 200°C, an electron energy of 230 eV, an emission current of 300 μA, and an electron multiplier of 1800 V.

RESULTS AND DISCUSSION

HPLC profiles of polyamine from roots of tobacco showed the presence of putrescine. In addition, a compound which co-eluted with authentic N-methyl-putrescine was detected. Since putrescine has already been identified as a component of tobacco roots[9], and our HPLC profiles indicated that it was present in our samples, we chose first to test the LC–MS capability by analyzing benzoylated root extracts for putrescine.

Since no peaks could be detected at the elution time for putrescine or N-methylputrescine in the total ion monitoring of a tobacco root extract, the sample was scanned by selected ion monitoring. Fig. 2 indicates a peak with a protonated molecular ion at m/z 297 which matched the elution time for benzoylated putrescine. It appears that putrescine is derivatized with two benzoyl groups. There was no indication of substitution by only one benzoyl group. Fig. 3 shows the PICI mass

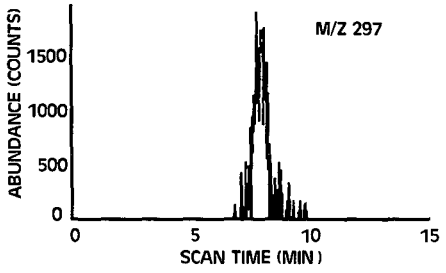

Fig. 2. Selected ion chromatogram of benzoylated putrescine from a tobacco root extract.

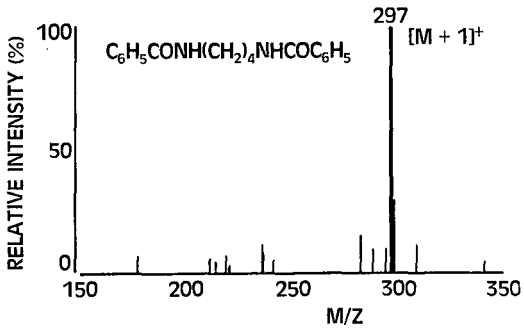

Fig. 3. PICI mass spectrum of benzoylated putrescine.

spectrum of the derivatized putrescine and its chemical formula. LC–MS analysis of authentic putrescine confirmed the ion monitoring patterns shown in the tobacco extracts.

Tobacco root extracts were subsequently scanned for the presence of N-methylputrescine by selected ion monitoring. Fig. 4 shows that monitoring with an ion at m/z 311 revealed a peak matching the elution time for authentic derivatized N-methylputrescine. A PICI mass spectrum of the sample compound is shown in Fig. 5. The

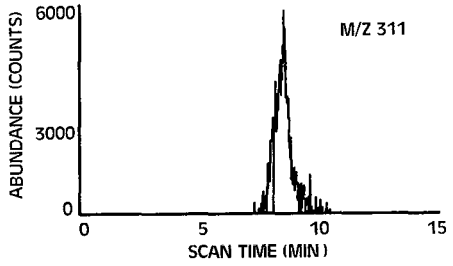

Fig. 4. Selected ion chromatogram of benzoylated N-methylputrescine from a tobacco root extract.

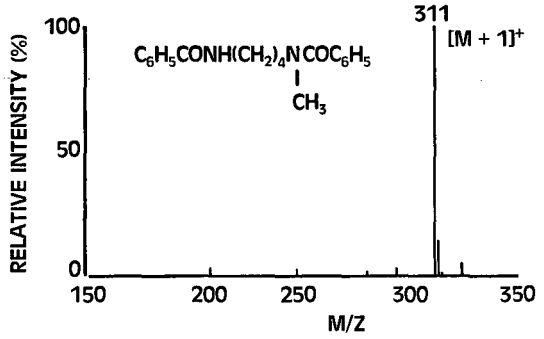

Fig. 5. PICI mass spectrum of benzoylated N-methylputrescine.

compound showed a protonated molecular ion at m/z 311, indicating the presence of two benzoyl groups. There was no indication of the presence of N,N-dimethylputrescine in extracts of tobacco roots.

Although the mass spectrometer is less sensitive than the UV detector due to the 1:99 splitting ratio, it remains the most selective among the LC detectors. We were unable to analyze underivatized samples because the acetonitrile solvent interfered with spectral analyses for N-methylputrescine. Apparently, acetonitrile and water solvate to form an adduct having an isotopic mass the same as the underivatized N-methylputrescine.

The sensitivity of the LC–MS system was adequate to confirm the presence of putrescine and N-methylputrescine in tobacco roots. This evidence strengthens the proposed root locale for nicotine biosynthesis.

CONCLUSIONS

Confirmation of the presence of putrescine and N-methylputrescine in tobacco roots in this report strengthen the proposed pathway for the synthesis of the pyrrolidine ring of nicotine. It is anticipated that LC–MS techniques can be further utilized to confirm and localize other nicotine biosynthetic intermediates.

REFERENCES

1 E. Leete, *Alkaloids: Chemical and Biological Perspectives*, Wiley, New York, 1983.
2 S. Mizusaki, Y. Tanabe, M. Noguchi and E. Tamaki, *Plant Cell Physiol.*, 12 (1971) 633.
3 S. Mizusaki, Y. Tanabe, M. Noguchi and E. Tamaki, *Phytochemistry*, 11 (1972) 2757.
4 J. Saunders and L. Bush, *Plant Physiol.*, 64 (1979) 236.
5 F. Feth, H.-A. Arfmann, V. Wray and K. G. Wagner, *Phytochemistry*, 24 (1985) 921.
6 F. Feth, V. Wray and K. G. Wagner, *Phytochemistry*, 24 (1985) 1653.
7 C. G. Edmonds, J. A. McCloskey and V. A. Edmonds, *Biomed. Mass Spectrom.*, 10 (1983) 237.
8 H. Flores and A. Galston, *Plant Physiol.*, 69 (1982) 701.
9 J. Madsen, S. Gay and L. Bush, *The 37th Tob. Chem. Res. Conf., Washington, DC, October 10–13, 1983.*

Journal of Chromatography, 474 (1989) 335–343
Elsevier Science Publishers B.V., Amsterdam — Printed in The Netherlands

CHROM. 21 460

CORONA DISCHARGE IONIZATION LIQUID CHROMATOGRAPHY–MASS SPECTROMETRY INTERFACE FOR TARGET COMPOUND ANALYSES

FRANCIS S. PULLEN*,[a] and DAVID S. ASHTON
Welcome Research Laboratories, Langley Court, Beckenham, Kent, BR3 3BS (U.K.)
and
MICHAEL A. BALDWIN
School of Pharmacy, Brunswick Square, London, WC1N 1AX (U.K.)

SUMMARY

The design and construction of a dedicated liquid chromatography–mass spectrometry instrument for detecting and assaying trace-level target compounds are described. It employs a microbore high-performance liquid chromatograph interfaced directly to a point-to-point high voltage corona discharge ionization source with a quadrupole mass analyser. Applications are described using reversed-phase chromatography for the detection of route-specific impurities in formulated medicinal preparations at the 5 ppb level for patent protection, and for the detection of biogenic amines in blood plasma without derivatization.

INTRODUCTION

Mass spectrometry (MS) is an analytical technique of the highest specificity and sensitivity, but it is generally unsatisfactory for the analysis of mixtures or for the detection of target compounds in mixtures, owing to the complexity of the spectral data for each component. This problem was tackled effectively in the 1960s for volatile compounds by the coupling of gas chromatography (GC) with MS, allowing MS analysis of each component in a mixture. The newly developed soft ionization techniques have simplified the spectra and concentrated the signal for each component into a pseudomolecular ion, thereby increasing sensitivity. Liquid chromatography has long been an important separative method, but it was through the development of high-performance liquid chromatography (HPLC) that it came to rival GC in terms of speed and resolution. HPLC also has a substantial advantage over GC in being able to handle polar, involatile and thermally unstable materials without derivatization.

Unfortunately there is a basic incompatibility between HPLC and MS in that

[a] Present address: Pfizer Ltd., Central Research, Sandwich, Kent, CT13 9NJ, U.K.

0021-9673/89/$03.50

one operates in the condensed liquid phase and the other at high vacuum. For HPLC the ideal interface should not restrict the solvent systems, the use of buffers, or the solvent flow-rate, and it should not impair chromatographic integrity. It should be capable of the efficient transfer of the entire chromatographic eluent for compounds that vary widely in polarity, volatility and stability. From the MS point of view the interface should not restrict the method of ionization, and electron impact (EI), chemical ionization (CI), fast atom bombardment (FAB), etc. should be operable in both positive and negative ion modes. The solvent must not impair the high vacuum requirement in critical regions or cause maintenance problems or loss of sensitivity. The mode of scanning the mass spectrometer should not be restricted, *i.e.* full scans, single ion monitoring, linked scans and other tandem modes should all be available[1–6].

Following pioneering work by Tal'roze[7], many approaches have been adopted to the solution of these problems but none meets all of the requirements specified above. The early use of direct liquid introduction (DLI) into the ion source resulted in high pressures, even with the low flow-rates achieved by 1:1000 splitting of the eluent, and only CI was possible, with the solvent acting as the reagent gas[8]. This compromised both the HPLC and the MS operations as only a limited range of solvents was acceptable. The transport interface (moving belt) also relied on a volatile solvent system but it allowed a range of ionization techniques to be employed[9]. Early versions were ineffective for reversed-phase chromatography and involatile compounds, but more recently FAB has been added to the range of ionization techniques applicable[10].

Thermospray is currently the most widely used technique[11]. This development from DLI, in which most of the solvent is pumped away leaving ionized solute, enjoys the advantages of not requiring solvent splitting for conventional flow-rates of 1 cm^3/min and being able to handle reversed-phase chromatography with high aqueous phase solvents, buffers and polar solutes. However, for the analysis of non-polar compounds a secondary ionization method, such as corona discharge, is required. Continuous-flow FAB offers exceptional promise for the analysis of involatiles[12,13], but the very low flow-rates of < 10 μl/min make direct interfacing to standard analytical columns difficult, and although packed fused-silica microbore columns can be directly coupled to mass spectrometers[14], the technical problems associated with handling these miniature LC systems makes them undesirable for routine use. Ionization has also been achieved at atmospheric pressure using radioactive decay[15], corona discharge[16], thermospray[17], and ion spray[18,19]. This eliminates the problem of pumping away the solvent, but still requires the efficient transfer of the ions into the mass spectrometer. The monodispersed aerosol generation interface combining HPLC and MS (MAGIC)[20], which allows both EI and CI data to be obtained, gives spectra that can be subjected to library search and is therefore suited to the identification of unknown compounds.

In the present study it was desired to construct an instrument that would provide high sensitivity detection and assaying of known target compounds at trace levels in pharmaceutical formulations and in biological fluids, often for screening with a minimum of sample work-up and without derivatization. The target compounds could vary widely in terms of polarity and volatility and would not necessarily be amenable to thermospray. It was decided that microbore HPLC at 50–100 μl/min

flow-rates using a DLI interface with corona discharge would best meet these requirements, giving soft ionization with little or no fragmentation and therefore being ideal for single or multiple ion monitoring.

DESIGN AND CONSTRUCTION

The corona discharge LC–MS system was designed to be flexible. Variable dimensions in the ion source were the electrode gap, the position of the nebulizer with respect to this, the ion exit aperture and the distance between it and the entrance to the quadrupole analyser. The dimensions given in this section were found to give optimum performance with the initial design, and these were used for the two studies below. Subsequent changes to the pumping improved the performance as detailed later.

The instrument has two vacuum housings connected only by a 0.3-mm diameter aperture. The ion source housing is pumped by a 2000 l/s diffusion pump giving a pressure of $1\text{–}5{\cdot}10^{-4}$ Torr at a solvent flow-rate of 100 μl/min. There is no direct measurement of the pressure within the ion chamber but it is calculated to be *ca.* 10 Torr. The analyser region is pumped by an Edwards EO4 diffusion pump (70 l/s) and cold trap, which maintains a pressure of $1{\cdot}10^{-5}$ Torr. The gas-tight ion chamber in Fig. 1 is a high-grade non-magnetic stainless-steel block with a cylindrical cavity, 38 mm diameter × 24 mm deep with a 2 mm diameter ion exit aperture. The corona electrodes are pointed stainless-steel rods with a diameter of 1 mm, mounted on either side of the chamber, one being electrically insulated. The electrode gap was optimized at 14 mm. The LC eluent is introduced into a nebulizer consisting of a fused-silica tube carrying the liquid, surrounded by a larger bore silica tube through which heated nitrogen gas is blown. The outer tube extends slightly beyond the inner tube, preventing drops formation and ensuring spray formulation. The nebulizer is mounted through the wall of the ion chamber and extends in by *ca.* 10 mm, from where the spray is directed into the electrode gap. As reported by others[21], experiments without the nebulizer suffered from pulsing due to drop formation. The ion chamber can be

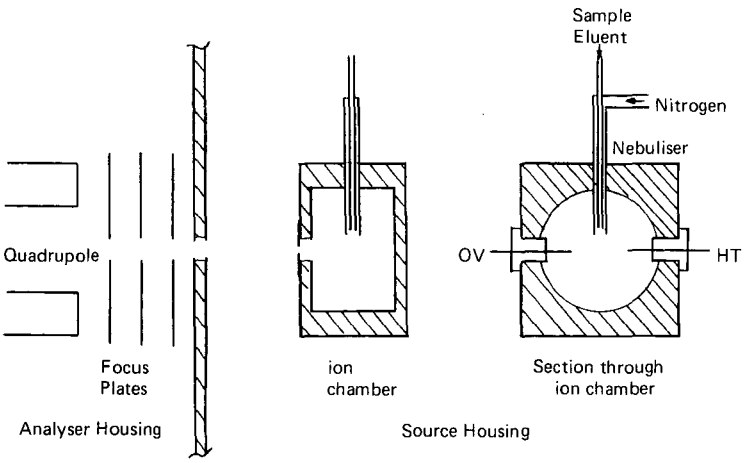

Fig. 1. Schematic diagram of the ion source.

moved to vary the distance between the ion exit aperture and the analyser entrance aperture, which was optimized at 14 mm. The chamber support assembly provides electrical isolation and ensures precise alignment of these two apertures with the focus plates and the quadrupole analyser.

In the experiments described here the chamber was held at ground potential, although later experiments with a small positive potential showed enhanced sensitivity due to the improvement in ion abstraction efficiency, 70 V giving a two-fold increase in signal strength. The corona is struck by applying 5 kV to the insulated electrode, giving a corona current of 300 μA under normal operating conditions. As reported before[22], the relationship between current and voltage is non-linear, and higher voltages give significantly higher currents, but 5kV was adopted as it gives reliable operation without electrical breakdown. The position and influence of the negative glow region of the corona is crucial in maximizing the positive ion current detected. Ions passing through the small aperture into the analyser region are focused into the quadrupole by a three-element lens, the grounded aperture being the first element. The centre element is held at $-$ 70 V and the third element is at $-$10 V, the same as the bias on the quadrupole. The quadrupole in the experiments described here was a VG QXK400, mass range 0–400 a.m.u.

CHROMATOGRAPHY

Most HPLC analyses in the pharmaceutical industry are carried out under reversed-phase conditions with solvent systems such as methanol–water or acetonitrile–water, often with buffers. Here two different methanol–water systems were used, in one case with buffers. The equipment comprised a DuPont 8800 pump with a Chrompak 25 cm $\times$ 1.35 mm I.D. CP-Spher-C_{18} 8-μm column. Samples were introduced through a Rheodyne 7520 microinjection valve using either a 1-μl or a 5-μl loop. The flow-rate was 100 μl/min, and the column eluent flowed through a micro UV cell (8 μl) before introduction into the mass spectrometer. A series of compounds was examined to evaluate the chromatographic integrity of the LC–MS system, and no measurable broadening of mass spectral peaks was observed when compared with the UV signal. Separations were carried out at 22°C, and UV absorption was measured at 280 nm using a DuPont 852 UV detector.

PATENT PROTECTION—IMPURITIES IN TRIMETHOPRIM

The financial investment required to successfully produce a new medicinal agent is very high, and companies protect this investment through the medium of patents. It may be possible to prove that a competitor's product infringes patents that protect manufacturing methods by detecting route-specific trace impurities, *i.e.* starting materials, intermediates or side-products[23]. Preparation of trimethoprim (TMP) (**1**)[24], an important antibacterial agent, by the so-called anilino route gives rise to the impurity TAA, β-anilino-α-(3,4,5-trimethoxybenzyl)acrylonitrile (**2**), whereas an alternative route can give the benzal impurity, β-methoxy-α-(3,4,5-trimethoxybenzylidene)propionitrile (**3**).

The calibration curves illustrated in Fig. 2 were constructed for TAA and benzal. For both compounds these show linear responses for protonated molecular ion

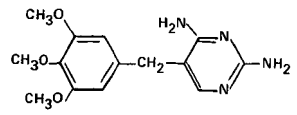

Trimethoprim (1)

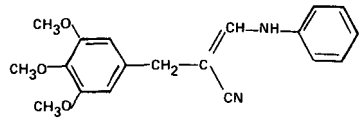

TAA (2)

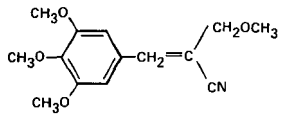

Benzal (3)

current *versus* amount on column over the range 50–750 pg (absolute measurements, with no internal standards), and 50 pg (150–200 fmol) represents the lower limit of detection as the signal-to-noise ratio was reduced to 2:1. This represents a substantial increase in sensitivity compared with UV detection, for which the lower limit was 1 ng injected on column. TMP is usually formulated with sulphamethoxazole as Co-trimoxazole. For the analysis of Co-trimoxazole tablets an initial solvent extraction was carried out to remove the bulk of the TMP and the sulphamethoxazole, and 6.5 g of crushed Co-trimoxazole tablets containing 1 g of TMP were shaken with 20 cm^3 of

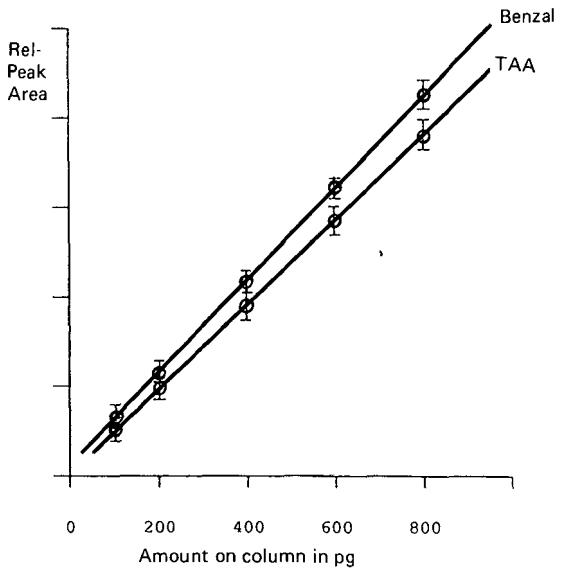

Fig. 2. Calibration plots for TAA and benzal.

dichloroethane for 10 min. The supernatant liquid was filtered off and reduced almost to dryness in a stream of dry nitrogen. Methanol (100 μl) was added and 1 μl was injected into the chromatograph. The signals were monitored at *m/z* 264 (benzal), 291 (TMP) and 235 (TAA). The traces are shown in Fig. 3.

Despite the extraction the strongest signal was observed for TMP at a retention time of 9 min, and this was also seen by the UV detector at 280 nm. The retention times for TAA and benzal are 12 and 14 min. A peak was observed for TAA but not for benzal, confirming that the preparation employed the anilino route. It is noteworthy that the UV trace does not show a peak for TAA, and indeed a weak peak would be obscured by the tailing of the TMP peak. Multiple ion monitoring by MS eliminates such interferences. This experiment was designed to confirm the presence or absence of target compounds and was not an accurate assay as no internal standards were employed. However, reference to the calibration curve indicated that *ca.* 220 pg of TAA were injected, being 1% of the total sample, therefore *ca.* 22 ng of TAA had been extracted from the 6.5 g of tablets. Separate experiments have shown the extraction to be *ca.* 70% efficient for TAA, so this shows the detection of TAA in formulated TMP preparations at a level down to *ca.*5 ppb. This gives a rapid and sensitive method of screening pharmaceutical products for known route-specific impurities.

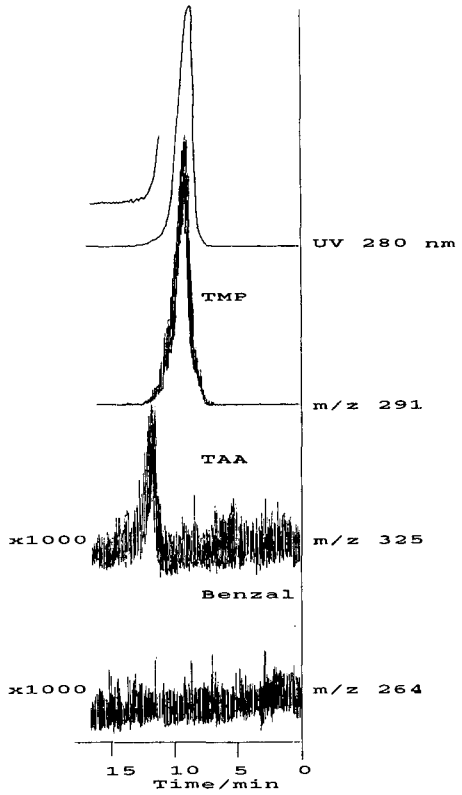

Fig. 3. Multiple ion monitoring traces dor Co-trimoxazole extracts.

BIOGENIC AMINES IN BLOOD PLASMA

The function of adrenaline and noradrenaline as chemical mediators of most of the postganglionic fibres of the sympathetic division of the autonomic nervous system is well known[25]. O-Methylation is an important metabolic pathway for catecholamine hormones[26], O-methyl transferase being the primary enzyme that inactivates circulating and possible locally released catecholamines. Detection and quantitation of adrenaline and metanephrine in tissue, blood plasma and urine are important for recognizing pheochromocytoma and also as a reflection of adrenergic and adrenomedullary stimulation[27]. GC–MS is effective for such assays but derivatization is necessary to aid volatility and thermal stability[27–29]. HPLC with electrochemical detection gives high sensitivity but it lacks the specificity of MS[30–32]. Consequently an LC–MS method is being developed.

The amines were extracted from 5 cm^3 samples of rat plasma by a published method[33], using an alumina column (Bondulate). They were absorbed onto the column from alkaline buffered plasma (pH 8.6) and after the column had been washed they were desorbed with 0.5 *M* acetic acid. The volume was reduced under vacuum to 10 μl and 5 μl were injected on column. The solvent system was methanol–0.1 *M* sodium orthophosphate–0.05 *M* citric acid (40:20:40). The sample HPLC column was used as in the previous experiment. Multiple ion monitoring was carried out at *m/z* 184 and 198 for the protonated molecular ions of adrenaline and metanephrine respectively. The traces are shown in Fig. 4 for the analysis of the plasma of two rates.

Calibration curves showed that adrenaline and metanephrine gave linear responses for ion current *versus* amount injected, and they could be detected down to a level of 100 pg (S/N = 2:1), whereas UV detection gave a lower limit of 10 ng from blood plasma. The extract from a healthy rat (A) gave a signal for adrenaline corresponding to 250 pg on column, which, assuming 100% efficiency of extraction, is 100

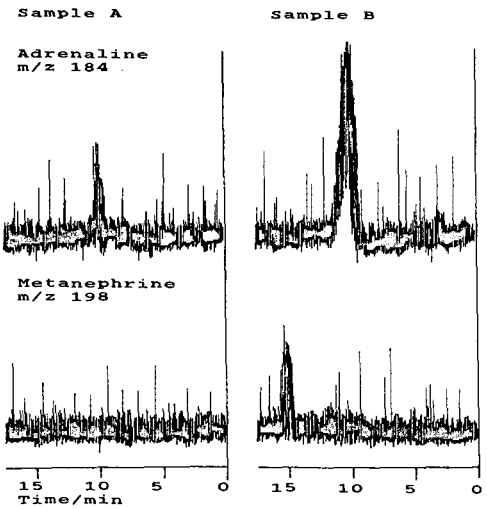

Fig. 4. Multiple ion monitoring traces for extracts from rat serum.

pg/cm^3 in plasma; there was no detectable signal for metanephrine. The extract from a hypertensive rat (B) showed an increase in adrenaline to 250 pg/cm^3 and metanephrine was detected at 80 pg/cm^3. These results may be subject to the well-known errors associated with assays carried out without internal standards, and a suitable standard is now being developed. However, these preliminary data agree well with observations by GC–MS and HPLC with electrochemical detection and they demonstrate the sensitivity attainable with a relatively simple extraction procedure and without derivatization.

IMPROVEMENTS AND MODIFICATIONS

A programme of modifications and improvements was carried out to further enhance the performance, the most important being to optimize ion transfer from the ion chamber to the analyser. The pumping of the analyser region was up-rated with the replacement of the original 70 l/s diffusion pump by a 700 l/s Edwards Diffstak. This reduced the analyser pressure from $1{\cdot}10^{-5}$ to $1{\cdot}10^{-6}$ Torr and increased the detected ion current for 100 pg of TAA by a factor of 1.7 as losses due to ion–molecule collisions were reduced.

The improved pumping also allowed better ion transmission to be achieved by increasing the size of the analyser entrance aperture from 0.3 to 0.9 mm, giving a nine-fold increase area, the signal for 100 pg of TAA increasing by a factor of 7. It is believed that further improvements to the pumping in the region of these apertures will provide a further sensitivity gain. The original quadrupole analyser had a very limited mass range, restricting the applications of the instrument. It is now being replaced by a VG 12/12 with a mass range of 2000 a.m.u. Finally, a computer-based control and data acquisition system is being installed.

CONCLUSIONS

The LC–MS system described has been demonstrated to provide high sensitivity specific detection and assay of target compounds in complex mixtures with the minimum of sample work-up. Unlike earlier corona sources with point-to-plane discharges, this source uses a precisely controlled point-to-point discharge that allows the region of maximum ion generation to be focussed coaxially with the ion slit and the quadrupole analyser. The use of corona discharge provides a soft ionization method that gives strong protonated molecular ions for both polar and non-polar compounds with little fragmentation, ideal for single or multiple ion monitoring. It can cope with normal or reversed-phase chromatography, with or without added buffers, and although not reported here it is amenable to gradient operation. As well as the studies reported above, the instrument has been used equally effectively for aromatic hydrocarbons and peptides, showing the wide range of compound polarities amenable to analysis.

REFERENCES

1 W. H. McFadden, *J. Chromatogr. Sci.*, 18 (1980) 97.
2 P. J. Arpino, *Trends Anal. Chem.*, 1 (1982) 154.
3 F. Ernie, *J. Chromatogr.*, 251 (1982) 141.

4 M. L. Vestal, *Mass Spectrom. Rev.*, 2 (1983) 447.
5 M. L. Vestal, *Science*, 226 (1984) 275.
6 D. E. Games, in J. F. J. Todd, *Advances in Mass Spectrometry 1985*, Wiley, Chichester, 1986, p. 323.
7 V. L. Tal'roze, V. E. Skurat and G. P. Karpov, *J. Phys. Chem. (Moscow)*, 43 (1969) 241.
8 P. J. Arpino, M. A. Baldwin and F. W. McLafferty, *Biomed. Mass Spectrom.*, 1 (1974) 80.
9 W. H. McFadden, H. L. Schwartz and S. Evans, *J. Chromatogr.*, 122 (1976) 389.
10 J. G. Stroh, J. C. Cook, R. M. Milberg, L. Brayton, T. Kihara, Z. Huang, K. L. Rinehart Jnr. and I. A. S. Lewis, *Anal. Chem.*, 57 (1985) 985.
11 C. R. Blakley, J. J. Carmody and M. L. Vestal, *Anal. Chem.*, 52 (1980) 1636.
12 Y. Ito, T. Takeuchi, D. Ishi and M. J. Goto, *J. Chromatogr.*, 346 (1985) 161.
13 R. M. Caprioli, T. Fan and J. S. Cottrell, *Anal. Chem.*, 58 (1986) 2949.
14 H. Alborn and G. Stenhagen, *J. Chromatogr.*, 323 (1985) 47.
15 D. I. Carroll, I. Didzic, R. N. Stillwell, M. G. Horning and E. C. Horning, *Anal. Chem.*, 45 (1973) 936.
16 D. I. Carroll, I. Didzic, R. N. Stillwell, K. D. Haegle and E. C. Horning, *Anal. Chem.* 47 (1975) 2369.
17 T. R. Covey, A. P. Bruins and J. D. Henion, *Org. Mass. Spectrom.*, 23 (1988) 178.
18 B. A. Thomson, J. V. Iribane and P. J. Dziedzic, *Anal. Chem.*, 54 (1982) 2219.
19 A. P. Bruins, T. R. Covey and J. D. Henion, *Anal. Chem.*, 59 (1987) 2642.
20 R. C. Willoughby and R. F. Browner, *Anal. Chem.*, 56 (1984) 2626.
21 K. Kambara, *Anal. Chem.* 54 (1982) 143.
22 K. Matsumoto, K. Yasudo and S. Tsuge, *Org. Mass Spectrom.*, 20 (1985) 243.
23 H. Brett, *The Patents Act 1977. An Introductory Guide*, ESC Publishing, London, 1978.
24 Trimethoprim Patent Registration Number 875562 Drug Registration patent Great Britain, 1978.
25 M. Gordon, *Psychopharmacological Agents*, Vol. 1, Academic Press, London, 1964.
26 J. Axelrod, *Science (Washington DC)*, 126 (1957) 400.
27 D. Robertson, E. C. Heath, F. C. Falkner, R. E. Hill, G. M. Brillis and J. T. Watson, *Biomed. Mass Spectrom.*, 5 (1978) 704.
28 M. Donike, *Chromatographia*, 7 (1974) 651.
29 J. T. Martin, J. D. Barchas and K. F. Faull, *Anal. Chem.*, 54 (1982) 1806.
30 E. Kempf and P. Mandel, *Anal. Biochem.*, 112 (1981) 223.
31 C. Hansson, G. Agrup, H. Rorsman, A. M. Rossengren and E. Rossengren, *J. Chromatogr.*, 162 (1979) 7.
32 F. Smedes, J. C. Kraak and H. Poppe, *J. Chromatogr.*, 231 (1982) 25.
33 I. V. Mefford, *J. Neurosci. Methods*, 3 (1981) 207.

END OF SYMPOSIUM PAPERS

PUBLICATION SCHEDULE FOR 1989

Journal of Chromatography and Journal of Chromatography, Biomedical Applications

MONTH	J	F	M	A	M	J	J	A	S	
Journal of Chromatography	461 462 463/1	463/2 464/1	464/2 465/1 465/2	466 467/1 467/2	468 469 470/1 470/2	471 472/1 472/2 473/1	473/2 474/1 474/2 475	476 477/1 477/2		The publication schedule for further issues will be published later
Bibliography Section		486/1		486/2		486/3		486/4		
Biomedical Applications	487/1	487/2	488/1 488/2	489/1 489/2	490/1 490/2	491/1	491/2	492 493/1	493/2	

INFORMATION FOR AUTHORS

(Detailed *Instructions to Authors* were published in Vol. 445, pp. 453–456. A free reprint can be obtained by application to the publisher, Elsevier Science Publishers B.V., P.O. Box 330, 1000 AH Amsterdam, The Netherlands.)

Types of Contributions. The following types of papers are published in the *Journal of Chromatography* and the section on *Biomedical Applications*: Regular research papers (Full-length papers), Notes, Review articles and Letters to the Editor. Notes are usually descriptions of short investigations and reflect the same quality of research as Full-length papers, but should preferably not exceed six printed pages. Letters to the Editor can comment on (parts of) previously published articles, or they can report minor technical improvements of previously published procedures; they should preferably not exceed two printed pages. For review articles, see inside front cover under Submission of Papers.

Submission. Every paper must be accompanied by a letter from the senior author, stating that he is submitting the paper for publication in the *Journal of Chromatography*. Please do not send a letter signed by the director of the institute or the professor unless he is one of the authors.

Manuscripts. Manuscripts should be typed in double spacing on consecutively numbered pages of uniform size. The manuscript should be preceded by a sheet of manuscript paper carrying the title of the paper and the name and full postal address of the person to whom the proofs are to be sent. Authors of papers in French or German are requested to supply an English translation of the title of the paper. As a rule, papers should be divided into sections, headed by a caption (*e.g.*, Summary, Introduction, Experimental, Results, Discussion, etc.). All illustrations, photographs, tables, etc., should be on separate sheets.

Introduction. Every paper must have a concise introduction mentioning what has been done before on the topic described, and stating clearly what is new in the paper now submitted.

Summary. Full-length papers and Review articles should have a summary of 50–100 words which clearly and briefly indicates what is new, different and significant. In the case of French or German articles an additional summary in English, headed by an English translation of the title, should also be provided. (Notes and Letters to the Editor are published without a summary.)

Illustrations. The figures should be submitted in a form suitable for reproduction, drawn in Indian ink on drawing or tracing paper. Each illustration should have a legend, all the *legends* being typed (with double spacing) together on a *separate sheet*. If structures are given in the text, the original drawings should be supplied. Coloured illustrations are reproduced at the author's expense, the cost being determined by the number of pages and by the number of colours needed. The written permission of the author and publisher must be obtained for the use of any figure already published. Its source must be indicated in the legend.

References. References should be numbered in the order in which they are cited in the text, and listed in numerical sequence on a separate sheet at the end of the article. Please check a recent issue for the layout of the reference list. Abbreviations for the titles of journals should follow the system used by *Chemical Abstracts*. Articles not yet published should be given as "in press" (journal should be specified), "submitted for publication" (journal should be specified), "in preparation" or "personal communication".

Dispatch. Before sending the manuscript to the Editor please check that the envelope contains three copies of the paper complete with references, legends and figures. One of the sets of figures must be the originals suitable for direct reproduction. Please also ensure that permission to publish has been obtained from your institute.

Proofs. One set of proofs will be sent to the author to be carefully checked for printer's errors. Corrections must be restricted to instances in which the proof is at variance with the manuscript. "Extra corrections" will be inserted at the author's expense.

Reprints. Fifty reprints of Full-length papers, Notes and Letters to the Editor will be supplied free of charge. Additional reprints can be ordered by the authors. An order form containing price quotations will be sent to the authors together with the proofs of their article.

Advertisements. Advertisement rates are available from the publisher on request. The Editors of the journal accept no responsibility for the contents of the advertisements.